

WL-TR-91-2111

AD-A247 464



DTIC
S ELECTE D
MAR 13 1992
C

2



LUBRICANT EVALUATION AND PERFORMANCE II

Costandy S. Saba, et al.
University of Dayton Research Institute
300 College Park
Dayton, Ohio 45469

January 1992

Interim Report For Period July 1988 - December 1990

APPROVED FOR PUBLIC RELEASE; DISTRIBUTION UNLIMITED

AERO PROPULSION AND POWER DIRECTORATE
WRIGHT LABORATORY
AIR FORCE SYSTEMS COMMAND
WRIGHT-PATTERSON AIR FORCE BASE, OHIO 45433-6563

92-06511



NOTICE

When government drawings, specifications, or other data are used for any purpose other than in connection with a definitely government-related procurement, the United States Government incurs no responsibility or any obligation whatsoever. The fact that the government may have formulated or in any way supplied the said drawings, specifications, or other data is not to be regarded by implication, or otherwise in any manner construed, as licensing the holder or any other person or corporation, or as conveying any rights or permission to manufacture, use, or sell any patented invention that may in any way be related thereto.

This report is releasable to the National Technical Information Service (NTIS). At NTIS, it will be available to the general public, including foreign nations.

This technical report has been reviewed and is approved for publication.

Lynne M. Nelson

LYNNE M. NELSON, Project Monitor
Lubrication Branch
Fuels and Lubrication Division
Aero Propulsion and Power Directorate

Ronald D. Dayton

RONALD D. DAYTON, Chief
Lubrication Branch
Fuels and Lubrication Division
Aero Propulsion and Power Directorate

Donn M. Storch

DONN M. STORCH, Major, USAF
Acting Chief
Fuels and Lubrication Division
Aero Propulsion and Power Directorate

If your address has changed, if you wish to be removed from our mailing list, or if the addressee is no longer employed by your organization, please notify WL/POSL, Wright-Patterson AFB OH 45433-6563 to help us maintain a current mailing list.

Copies of this report should not be returned unless return is required by security considerations, contractual obligations, or notice on a specific document.

REPORT DOCUMENTATION PAGE				Form Approved OMB No. 0704-0188	
1a. REPORT SECURITY CLASSIFICATION UNCLASSIFIED			1b. RESTRICTIVE MARKINGS None		
2a. SECURITY CLASSIFICATION AUTHORITY N/A			3. DISTRIBUTION / AVAILABILITY OF REPORT Approved for Public Release; Distribution Unlimited		
2b. DECLASSIFICATION / DOWNGRADING SCHEDULE N/A					
4. PERFORMING ORGANIZATION REPORT NUMBER(S) UDR-TR-91-53			5. MONITORING ORGANIZATION REPORT NUMBER(S) WL-TR-91-2111		
6a. NAME OF PERFORMING ORGANIZATION University of Dayton Research Institute		6b. OFFICE SYMBOL (if applicable)	7a. NAME OF MONITORING ORGANIZATION Aero Propulsion and Power Directorate(WL/POSL) Wright Laboratory		
6c. ADDRESS (City, State, and ZIP Code) 300 College Park Dayton, Ohio 45469			7b. ADDRESS (City, State, and ZIP Code) Wright-Patterson AFB, OH 45433-6563		
8a. NAME OF FUNDING / SPONSORING ORGANIZATION		8b. OFFICE SYMBOL (if applicable) WL/POSL	9. PROCUREMENT INSTRUMENT IDENTIFICATION NUMBER F33615-88-C-2817		
8c. ADDRESS (City, State, and ZIP Code) Wright-Patterson AFB OH 45433-6563			10. SOURCE OF FUNDING NUMBERS		
			PROGRAM ELEMENT NO. 62203F	PROJECT NO. 3048	TASK NO. 06
11. TITLE (Include Security Classification) Lubricant Evaluation and Performance II					
12. PERSONAL AUTHOR(S) Saba, C.S., Keller, M.A., Smith, H.A., Kauffman, R.E., Toth, D.K., Allen, J.S., Strunks, G.A., Byrd, R.J. and Baker, K.N.					
13a. TYPE OF REPORT Interim		13b. TIME COVERED FROM Jul 88 to Dec 90		14. DATE OF REPORT (Year, Month, Day) January 1992	
15. PAGE COUNT 576					
16. SUPPLEMENTARY NOTATION					
17. COSATI CODES			18. SUBJECT TERMS (Continue on reverse if necessary and identify by block number) High Temperature Lubricant Stability, Deposition, Foaming, Wear, Lubricant Monitoring		
FIELD	GROUP	SUB-GROUP			
11	08				
14	02				
19. ABSTRACT (Continue on reverse if necessary and identify by block number) The development of improved methods is described for defining, measuring and assessing high temperature (500-750°F) lubricants for use in advanced aircraft turbine engines and the development of improved techniques for lubricant monitoring and lubricant condition monitoring for advanced lubricating fluids. Arrhenius plots were developed for describing the effective life of candidate 4 cSt lubricants, polyphenyl ethers and other experimental fluids as a function of time and temperature for selected limiting values of changes in physical and chemical properties. Significant improvement in AE spectrometer sensitivity for analyzing wear metal was made. An in-line magnetic wear monitor was evaluated for possible application as condition monitoring device for oil systems. Fluorescence, UV, dielectric constant, voltammetric and thermal analysis techniques were developed and evaluated as high temperature lubricant monitoring devices. The tribological behavior of high temperature candidate fluids were evaluated and compared in the boundary lubrication regime using sliding four-ball test and various steel and ceramic specimens.					
20. DISTRIBUTION / AVAILABILITY OF ABSTRACT <input checked="" type="checkbox"/> UNCLASSIFIED/UNLIMITED <input type="checkbox"/> SAME AS RPT. <input type="checkbox"/> DTIC USERS				21. ABSTRACT SECURITY CLASSIFICATION UNCLASSIFIED	
22a. NAME OF RESPONSIBLE INDIVIDUAL L.M. NELSON				22b. TELEPHONE (Include Area Code) (513)-255-3100	
				22c. OFFICE SYMBOL WL/POSL	

FOREWORD

This report describes the research conducted by personnel of the University of Dayton Research Institute on Contract No. F33615-88-C-2817. The work was conducted at the Aero Propulsion and Power Directorate, Wright Laboratory, Air Force Systems Command, Wright-Patterson AFB, Ohio.

The work was accomplished under Project 3048, Task, 304806, Work Unit 30480648, Lubricant Evaluation and Performance II, with Mrs. Lynne Nelson as the project monitor.

The work reported herein was performed during July 1988 to December 1990.

Accession For	
NTIS	<input checked="" type="checkbox"/>
DTIC Tab	<input type="checkbox"/>
Unref. Index	<input type="checkbox"/>
Justification	
By	
Distribution	
Approved by GPOSS	
Availability or	
Dist	Special
A-1	

TABLE OF CONTENTS

SECTION	PAGE
I INTRODUCTION	1
II DEVELOPMENT OF IMPROVED METHODS FOR MEASURING LUBRICANT PERFORMANCE	5
1. LUBRICANT OXIDATIVE STABILITY OF ESTER BASE FLUIDS	3
a. Introduction	3
b. Test Apparatus and Test Procedure	3
c. Test Lubricants and Test Conditions	3
d. Results and Discussion	4
e. Summary	9
2. LUBRICANT CORROSION AND OXIDATION STABILITY OF HIGH TEMPERATURE FLUIDS	9
a. Stability Testing of Fresh Polyphenyl Ethers	9
(1) Introduction	9
(2) Test Apparatus and Test Procedure	10
(3) Test Lubricants and Test Conditions	10
(4) Arrhenius Plot Development	10
(5) Stability Testing of Fresh Polyphenyl Ethers	12
(6) Summary	32
b. Lubricant Analysis of Polyphenyl Ethers	33
(1) Introduction	33
(2) ¹¹⁹ Sn Mossbauer Analysis of Oxidized O-67-1	33
(3) GPC Analysis of TEL-8039 and TEL-8040	34
(4) GPC Area Summation of Oxidized PPEs	34
c. Vapor Phase Corrosion of O-67-1	36

TABLE OF CONTENTS (CONTINUED)

SECTION	PAGE
II	
d. Vapor Phase Corrosion of O-77-6 Fluid	41
(1) Introduction	41
(2) Test Data	42
(3) XPS Analyses of Stains/Deposits on Specimens	42
(4) O-77-6 Condensate	-44
(5) Summary	47
e. Used Polyphenyl Ether Lubricants	47
(1) Corrosion and Oxidation of Used Polyphenyl Ether Lubricants	47
(2) Effect of Filtration on Corrosion and Oxidation Stability of Used Polyphenyl Ether Lubricants	53
(3) Effect of Four-Ball Wear Test Parameters on the Corrosion and Oxidation Stability of MIL-L-87100 Lubricant	59
(a) Corrosion and Oxidation Testing of Four-Ball Test Fluids	59
(b) Oxidation of O-67-1 during Four-Ball Testing	60
(c) Effect of Four-Ball Testing on Additive A in O-67-1	62
(d) Oxidative Stability of Friction Polymer	66
(4) Effect of Diluents on Polyphenyl Ether Fluid Stability	69
(5) Summary	75
f. Non-Polyphenyl Ether Based Experimental Fluids	78
(1) Corrosion and Oxidation Testing of TEL-9050 and TEL-9071	78

TABLE OF CONTENTS (CONTINUED)

SECTION		PAGE
II	(2) Corrosion and Oxidation Testing of TEL-90024	81
	(3) Vapor Phase Corrosion of TEL-9071	89
	(a) Introduction	89
	(b) Viscosity Test Data	90
	(c) Thermal Gravimetric Analyses	92
	(d) Total Acid Number Test Data	92
	(e) Fluoride Test Data	94
	(f) Weight Changes of Test Washers	94
	(g) X-Ray Photoelectron Spectroscopic Analysis of Test Washers	95
	(h) Scanning Electron Microscopic/Energy Dispersive Spectroscopic Analyses of Test Washers	98
	(i) EDS Analyses of Glass Deposits	101
	(j) Analysis of Condensate	101
	(4) Summary	101
3.	LUBRICANT DEPOSITION STUDIES	103
	a. AFAPL Static Coker	103
	(1) Introduction	103
	(2) Apparatus and Test Procedures	103
	(3) Test Lubricants	103

TABLE OF CONTENTS (CONTINUED)

SECTION		PAGE
II	(4) Results and Discussion	105
	(a) Initial Studies of Optimum Sample Size on Polyphenyl Ether Fluid O-77-6	105
	(b) Programmable Temperature Controller Studies	107
	(c) Initial Programmable Temperature Studies of O-67-1 Using Shim Stock Test Specimens	108
	(d) Initial Programmable Temperature Studies of New and Stressed O-67-1 Lubricant Using 0.005 Inch T302 Stainless Steel Specimens	110
	(e) Effects of Test Temperature, Test Time and C&O Stressing on AFAPL Static Coker Deposits	114
	(f) AFAPL Static Coker Deposits of Engine Stressed MIL-L-87100 Lubricant	119
	(g) Study of Test Specimen Material on Coking Characteristics of Polyphenyl Ether Fluids	122
	(h) Volatilization Study of Lubricant O-67-1	122
	(i) Comparison of 5P4E and 6P5E Polyphenyl Ether Coking Characteristics Using the AFAPL Static Coker	126
	(j) AFAPL Static Coker Studies of Non-Polyphenyl Ether Base Fluids	126
	(k) Summary	126
	b. Micro Carbon Residue Tester (MCRT)	129
	(1) Introduction	129
	(2) Apparatus and Procedure	129
	(3) Test Lubricants	129

TABLE OF CONTENTS (CONTINUED)

SECTION	PAGE
II	
(4) Results and Discussion	130
(a) Investigation of Temperature Uniformity of MCRT Ovens and the Reproducibility of Data from the Two Units	130
(b) MCRT Testing of New and Stressed 5P4E Fluids Using Short and Tall Vials, Various Temperatures and Melting Point Determination of Deposits	135
(c) Effect of Sample Size on MCRT Deposits	145
(d) Effect of Test Vial Material on MCRT Deposits	148
(e) MCRT Coking Study of Unfiltered and Filtered Used MIL-L-87100 Lubricant	148
(f) Effect of Four-Ball Wear Testing and Four-Ball Test Specimen Material on MCRT Deposits	150
(g) Variable Temperature and Testing Time Study	157
(h) Argon Versus Air MCRT Deposit Study	159
(i) MCRT Residue Studies of Various High Temperature Lubricants and Experimental Fluids	161
(j) Correlation of MCRT and AFAPL Static Coker Test Data	161
(k) Summary	164
4. LUBRICANT FOAMING STUDY	165
a. Introduction	165
b. Test Apparatus and Procedure	166
c. Test Lubricants	166

TABLE OF CONTENTS (CONTINUED)

SECTION		PAGE
II	d. Results and Discussion	167
	(1) Low Temperature Testing of Polyphenyl Ether Fluids	167
	(2) High Temperature Testing of New O-67-1 and TEL-90018	171
	(3) High Temperature Testing of C&O and Engine Stressed MIL-L-87100 Fluids	173
	(4) Foaming Characteristics of Non-Polyphenyl Ether High Temperature Fluids	177
	(5) Foaming Characteristics of Three MIL-L-7808 Type Lubricants	177
	e. Summary	180
	5. VISCOMETER EVALUATION	180
	a. Introduction	180
	b. Results and Discussion	181
	c. Summary	183
III	DEVELOPMENT OF IMPROVED LUBRICATION SYSTEM HEALTH MONITORING TECHNIQUES	185
	1. Ferrosan as an In-Line Magnetic Wear Debris Monitor for Lubrication Systems	185
	a. Introduction	185
	b. Theory	187
	c. Experimental	188
	(1) Apparatus	188
	(2) Procedure	188
	d. Results and Discussion	191
	(1) Effect of Particle Size on Ferrosan Response	191

TABLE OF CONTENTS (CONTINUED)

SECTION		PAGE
III	(2) Effect of Particle Concentration on Ferrosan Sensitivity	191
	(3) Effect of Temperature on Ferrosan Response	196
	(4) Effect of Oil Velocity on the Ferrosan Response	196
	(5) Effect of Concentration, Flow Rate and Noise on a New Ferrosan Detector	200
	(6) Repeatability	202
	(7) Detection of Steel Wear Debris from a Pin-on-Disk Wear Test	210
	(8) Detection of Real Wear Debris	210
	e. Conclusions	214
2.	Improving Sample Introduction for Total Wear Metal Determination by Atomic Emission Spectroscopy	219
3.	Ferrographic Analysis of High Temperature Fluids	219
	a. Introduction	219
	b. Test Apparatus and Procedure	220
	c. Results and Discussion	221
	(1) Initial Ferrograph study of O-77-6	221
	(2) Variable Oil/Fixer Ratio Study	222
	(3) Effect of Varying Wear Test Parameters on Subsequent Ferrograph Analyses of O-67-1 Lubricant Wear Test Samples	225
	(4) Analytical Ferrographic Analysis of a Rolling Four-Ball Wear Test Sample of O-67-1 Lubricant	228
	(5) Effect of Oxidative Stressing of Four-Ball Wear Test Samples of O-67-1 Lubricant on Analytical Ferrograph Data	228

TABLE OF CONTENTS (CONTINUED)

SECTION		PAGE
III	(6) Effect of Filtration on Analytical Ferrograph Data	230
	(7) Analytical Ferrographic Analysis of Engine Stressed O-67-1 Lubricant	232
	(8) Summary	232
IV	CANDIDATE HIGH TEMPERATURE LUBRICANT DIAGNOSTIC DEVICES	235
	1. Introduction	235
	2. Fluorescence Spectroscopic Characteristics of Stressed PPEs	235
	a. Introduction	235
	b. Description of Fluorescence Phenomenon and Instrumentation	236
	c. Experimental	237
	d. Fluorescence Excitation/Emission Characteristics of Stressed PPEs	238
	e. Concentration/Emission Intensity Relationships	238
	f. Emission Intensity of Oxidized PPEs	242
	g. Quantitative Fluorescence Measurements on Neat Polyphenyl Ethers	244
	(1) Fluorescence Measurements on Thick PPE Films	244
	(2) Fluorescence Measurements on Thin PPE Films	246
	(3) Fluorescence Measurements on Very Thin PPE Films	246
	h. Conclusions	249
	3. Dielectric Constant (DC) Measurements at Extended Cell Temperatures	249
	a. Introduction	249
	b. DC Readings of Fresh PPEs at Various Temperatures	250

TABLE OF CONTENTS (CONTINUED)

SECTION		PAGE
IV	c. DC Readings of Stressed PPEs at Different Cell Temperatures	252
	d. DC Readings of MIL-L-7808 Oils at Different Cell Temperatures	252
	e. Conclusions	254
4.	Thermal Analysis	257
	a. Introduction	257
	b. Sealed-Pan DSC	257
	c. Thermogravimetric Analysis	263
	d. High Pressure DSC	265
	e. Summary	268
5.	Spectrometric Techniques	268
	a. Introduction	268
	b. Fourier Transform Infrared Spectroscopy	268
	c. Ultraviolet-Visible Spectrophotometry with Solvent Dilution	270
	d. Ultraviolet-Visible Spectrophotometry without Solvent Dilution	276
	e. UV Thermal Analytical Technique	281
	f. Summary	284
6.	Electrochemical Technique	285
	a. Introduction	285
	b. Literature Search	285
	c. Cyclic Voltammograph Optimization	286
	d. Effects of Sample Preparation	286
	e. Effects of Electrode Design	290
	f. Summary	296

TABLE OF CONTENTS (CONTINUED)

SECTION		PAGE
V	LUBRICANT LOAD CARRYING CAPABILITY TEST ASSESSMENT	297
VI	TRIBOLOGICAL EVALUATION OF CANDIDATE FLUIDS	299
	1. Introduction	299
	2. Apparatus	303
	3. Four-Ball Wear Model	305
	a. Background	305
	b. Four-Ball Geometry	305
	c. Scar Chord	307
	d. Derivation of Scar Equation	312
	e. Relationship Between Alpha and the Scar Dimensions	316
	f. Alpha as a Function of k	316
	g. Upper and Lower Ball Wear Volume	319
	h. Lower Ball Scar Shape	325
	4. Effect of Oil, Specimens and Experimental Conditions on Wear Scar	328
	a. Length-Width Relationship	328
	b. Comparison of Oils and Specimen Materials	349
	c. Surface Analysis of Wear Scar	363
	d. Introduction of Gas into the Four-Ball Test Cup	378
	e. Testing of Diluted PPE	382
	f. Testing of Stressed PPE	386
	g. Temperature Study at the Ball Contact Zone	391
	h. Summary	394
VI	5. Analysis of Friction Polymer from Four-Ball Testing of Polyphenyl Ether	396
	a. Background	396

TABLE OF CONTENTS (CONCLUDED)

SECTION	PAGE
b. Quantitation of FP in Four-Ball Testing of O-67-1	397
c. Iron Content in FP from O-67-1	397
(1) Quantitative Analysis of Iron in FP	400
(2) Qualitative Analysis of Iron in FP	400
d. Analysis of the Organic Fraction of FP	404
(1) Elemental Analysis	404
(2) FTIR Analysis	408
e. Spectrometric Analysis of Wear Deposits	408
(1) Introduction	408
(2) X-Ray Fluorescence Analyses	413
(3) SEM/EDS Analyses	413
f. Analysis of Debris in Engine Tested PPEs	416
(1) Percent Filterable Insolubles	416
(2) FTIR Analysis	418
(3) DSC Analysis	418
g. Conclusions	418
APPENDIX A Lubricant Performance Test Data	423
APPENDIX B Improving Sample Introduction for Total Wear Metal Determination by Atomic Emission Spectroscopy	505
APPENDIX C Determination of the Alpha Parameter by the Lower Ball Wear Scar	522
REFERENCES	534

LIST OF ILLUSTRATIONS

FIGURE		PAGE
1.	Squires Oxidative Stability of Various 4 cSt Fluids at 210°C	5
2.	Squires Oxidative Stability of Various 4 cSt Fluids at 215°C	7
3.	Squires Oxidative Stability of TEL-90087 at 210°C and 225°C	8
4.	Effect of Temperature on Lubricant Life Using Corrosion and Oxidation Testing and a 15% Viscosity Increase Limit (40°C) for High Temperature Fluids	16
5.	Effect of Temperature on Lubricant Life Using Corrosion and Oxidation Testing and a 25% Viscosity Increase Limit (40°C) for High Temperature Fluids	17
6.	Effect of Temperature on Lubricant Life Using Corrosion and Oxidation Testing and a 35% Viscosity Increase Limit (40°C) for High Temperature Fluids	18
7.	Effect of Temperature on Lubricant Life Using Corrosion and Oxidation Testing and a 5% Viscosity Increase Limit (100°C) for High Temperature Fluids	19
8.	Effect of Temperature on Lubricant Life Using Corrosion and Oxidation Testing and a 10% Viscosity Increase Limit (100°C) for High Temperature Fluids	20
9.	Effect of Temperature on Lubricant Life Using Corrosion and Oxidation Testing and a 15% Viscosity Increase Limit (100°C) for High Temperature Fluids	21
10.	Viscosity Increase vs. Test Time of O-67-1 After C&O at 320°C with and without Condensate Return	23
11.	40°C Viscosity Change During Corrosion and Oxidation Testing of O-67-1 at 320°C Using D 4871 Tubes, 10 L/H Airflow (Both Moist and Dry) and Intermediate Sampling	25
12.	40°C Viscosity Change During Corrosion and Oxidation Testing of TEL-90028 Using D 4871 Tubes, 10 L/H Airflow and Intermediate Sampling	25
13.	¹¹⁹ Sn Mossbauer Spectra of the 24, 120 and 240 Hour Samples from the Corrosion and Oxidation Test of O-67-1 at 320°C	35

LIST OF ILLUSTRATIONS (CONTINUED)

FIGURE		PAGE
14.	Gel Permeation Chromatograms of Corrosion and Oxidation Tested O-67-1 and TEL-8039 at 320°C	37
15.	High Molecular Weight Oxidation Product Concentration, as determined by GPC Area Summation, in O-67-1 and TEL-8039 During Corrosion and Oxidation Testing at 320°C	38
16.	High Molecular Weight Oxidation Product Concentration Versus 40°C Kinematic Viscosity of O-67-1 and TEL-8039 from Corrosion and Oxidation Testing at 320°C	39
17.	High Molecular Weight Oxidation Product Concentration Versus 100°C Kinematic Viscosity of O-67-1 and TEL-8039 from Corrosion and Oxidation Testing at 320°C	40
18.	Gas Chromatogram of O-77-6 Condensate Collected After 24 Hours of Stressing at 300°C without Specimens Present	46
19.	Changes in 40°C Viscosity of Engine Stressed Polyphenyl Ether 5P4E Lubricant During Corrosion and Oxidation Testing at 320°C	50
20.	Changes in 100°C Viscosity of Engine Stressed Polyphenyl Ether 5P4E Lubricant During Corrosion and Oxidation Testing at 320°C	51
21.	Variation of Viscosity and Sn with Time in TEL-9070 Series of Engine Test Samples	52
22.	Viscosity @ 40°C for Fresh O-67-1 and Effect of Subsequent Wear or Engine Testing, 48 Hour C&O at 320°C, and 3 Micron Filtering on CB-1, TEL-9030 and TEL-9040 Viscosity	55
23.	Viscosity @ 40°C for Fresh O-67-1 and Effect of Subsequent Engine Testing, 48 Hour C&O at 320°C, and 3 Micron Filtration on CB-2 and CB-3 Viscosity	56
24.	Sn Level of Fresh O-67-1 and Effect of Subsequent Engine Testing, 48 Hour C&O at 320°C and 3-Micron Filtering on Sn Levels of CB-2 and CB-3	57
25.	Sn Level of Fresh O-67-1 and Effect of Wear or Engine Testing on CB-1, TEL-9030 and TEL-9040	58

LIST OF ILLUSTRATIONS (CONTINUED)

FIGURE		PAGE
26.	Change in Additive A Concentration During Four-Ball Testing of O-67-1 at 150°C, 145 N Load and 52100 Bearings	64
27.	DSC and TGA Thermograms of Friction Polymer from Four Ball Test #426 (DSC and TGA Conditions: 5°C/Minute to 400°C, Air, 2.0 mg Sample)	67
28.	DSC Thermograms of Friction Polymer from Four Ball Tests of O-67-1 at Various Temperatures	70
29.	Plots of Oil Temperature vs. Time During Corrosion-Oxidation Testing Showing, a) the Difference Between O-67-1 and Additive A Contaminated O-77-6 without Silver Coupons, b) Same as a but with Silver Coupons Added to Test, and c) the Difference Between O-77-6 Diluted Fluids	72
30.	Effect of Solvent Dilution on 5P4E Fluids O-77-6 and O-67-1 Subjected to Corrosion and Oxidation Testing for 48 Hours at 320°C Using Squires Tubes and 10 L/H Airflow	73
31.	40°C Viscosity Change During Corrosion and Oxidation Testing of TEL-90059 and TEL-90024 Using D 4871 Tubes, Intermediate Sampling and 10 L/H Airflow. Filled Circle Represents New Data	85
32.	40°C Viscosity Change During Corrosion and Oxidation Testing of TEL-90063 Fluid Using D 4871 Tubes, Intermediate Sampling and 10 L/H Airflow	88
33.	TAN Increase During Corrosion and Oxidation Testing of TEL-90063 Fluid Using D 4871 Tubes, Intermediate Sampling and 10 L/H Airflow	88
34.	TGA Weight Percent Remaining Versus Temperature Profile (Nitrogen Atmosphere, 10 mg Samples) for Fresh and 48 Hour Stressed (320°C, 10 L/H) TEL-9071 Fluids (Sample Size = 10 mg; Heating Rate Rate = 20°C/min)	93
35.	Crater Produced in the Deposit on the 320°C C&O Test, Vapor Phase Silver Specimen	99
36.	EDS Spectra of Top and Bottom Layers of Deposit on the 320°C C&O Test, Vapor Phase Silver Specimen	100

LIST OF ILLUSTRATIONS (CONTINUED)

FIGURE		PAGE
37.	Effect of Sample Size on AFAPL Static Coker Deposits at 375°C, 3 Hour Test Time, Shim Stock Test Specimen and Lubricant O-77-6	106
38.	Correlation Between AFAPL Static Coker Controller Temperature and Test Surface Temperature	109
39.	Effect of Test Time on Static Coker Deposits of O-77-6 after 120 h C&O Stressing at 290°C Using 425°C Test Temperature	116
40.	Volatilization Rate of O-67-1 at Various Test Temperatures Using Static Coker with SS-302 Specimens	125
41.	Correlation of MCRT Displayed Temperature and Average Cell Temperature	133
42.	Correlation Between Cell Deposits (O) and Measured Cell Position Temperatures () for MCRT Testing of Lubricant O-86-2 at 275°C MCRT Displayed Temperature and 30 Hours Test Period	134
43.	MCRT Residue of the 240 h, 320°C C/O Test Sample of Lubricant O-67-1 after Various Test Hours (350°C MCRT Displayed Temperature; 362°C Average Cell Temperature, Tall Vials)	140
44.	Effect of Temperature on MCRT Residue Using Tall vs. Short Vials for Lubricant O-67-1	143
45.	Effect of Temperature on MCRT Residue Using Tall vs. Short Vials for Lubricant O-77-6	144
46.	Effect of Sample Size on MCRT Residue at 400°C Using 3.5 cm Vials and 30 Hour Test	147
47.	The Effect of Vial Material and Temperature on MCRT Percent Residue for O-77-6 and O-67-1	149
48.	The Effect of Wear Metal Generated from Four-Ball Wear Tests Using Different Temperatures and Loads on MCRT Percent Residue for O-67-1	154
49.	Effect of Test Time on Coking Tendency of O-77-6 Using MCRT at Various Temperatures and 7.5 cm Pyrex Vials	158
50.	Sensor Frequency Versus Time	186

LIST OF ILLUSTRATIONS (CONTINUED)

FIGURE		PAGE
51.	Microfiltration Test Rig Equipped with Ferroskan Sensor	189
52.	Ferroskan Sensor Readout of FE1 and FE2 Versus Concentration of Various Sizes of Fe Particles in MIL-L-7808. Conditions: 1.3 m/s Oil Velocity; 77°C Oil Temperature	192
53.	Ferroskan Readout of FE1 and FE2 Versus Concentration of Various Sizes of Fe Particles Added Sequentially. Conditions: 1.3 m/s Oil Velocity; 77°C Oil Temperature	193
54.	Sensitivities of Ferroskan Sensor in Hz/s/ppm Versus Fe Particle Size from Various Experiments	194
55.	Sensitivities of Ferroskan Sensor in Hz/s/ppm Versus Fe Particle Size from Sequential Addition	195
56.	Real Time Data of FE1 and FE Versus Elapsed Time for Various Fe Particles Added Sequentially	197
57.	Effect of Temperature Rise on Ferroskan Output. Conditions: 1.3 m/s Oil Velocity; 10 ppm Concentration of <3 Micron Fe Particles	198
58.	Effect of Oil Flow Rate on Ferroskan Output. Conditions: 77°C Oil Temperature, 51.5 ppm Concentration of 0 to >45 Micron Fe Particles	198
59.	Ferroskan Real Time Data During the 0-10 Micron Fe Powder Addition	201
60.	Effect of Concentration on Sensor Readout During the Sequential Addition of 0-10 Micron Fe Powder	203
61.	Ferroskan Readout per ppm as a Function of Concentration After Each Addition of 0-10 Micron Fe Powder	204
62.	Effect of Flow Rate on Ferroskan Readings Using 0-10 Micron Fe Powder at 158.3 ppm	205
63.	Ferroskan Real Time Data During the 0-10 Micron Fe Powder Addition	206

LIST OF ILLUSTRATIONS (CONTINUED)

FIGURE		PAGE
64.	Comparative Curves Illustrating the Repeatability of Two Identical Experiments Showing the Ferroskan Response as a Function of Concentration for Fe Particles of Less than 10 Micron	206
65.	Ferroskan Readout per ppm as a Function of each Addition of 0-10 Micron Fe Powder	208
66.	Ferroskan Real Time Data for Steel Wear Debris Generated from a Pin-on-Disk Wear Test Device	211
67.	Ferroskan Response for Two Ranges of Particle Sizes, FE1 and FE2 as a Function of Concentration Using Steel Particles from a Wear Test	212
68.	Ferroskan Response per ppm as a Function of Each Addition Using Steel Particles from a Wear Test	213
69.	Ferroskan Real Time Data for Wear Debris Isolated from Gas Turbine Engine Used Oil Samples	215
70.	Ferroskan Response as a Function of Fe Concentration for Two Ranges of Particle Sizes Using Wear from Gas Turbine Engine Used Oils	216
71.	Ferroskan Response per ppm as a Function of Addition Number for Wear Debris from Gas Turbine Engines	217
72.	Fluorescence Intensity as a Function of Concentration of O-67-1 Stressed at 320°C for 240 Hours in the Corrosion and Oxidation Test. (Excitation/Emission Wavelengths of 400/454 nm)	241
73.	Relationship of Fluorescence Intensity to Viscosity Increase for PPEs from C&O Testing at 320°C (Excitation/Emission Wavelengths of 340/365 nm and 400/454 nm)	243
74.	Fluorescence Intensity of Thick Films of PPEs from the Corrosion and Oxidation Test at 320°C (Excitation/Emission Wavelengths of 396/454 nm)	245
75.	Fluorescence Intensity of Thin Films of PPEs from the Corrosion and Oxidation Test at 320°C (Excitation/Emission Wavelengths of 450/520 nm)	247
76.	Fluorescence Intensity of Very Thin Films of PPEs from the Corrosion and Oxidation Test at 320°C (Excitation/Emission Wavelengths of 450/520 nm)	248

LIST OF ILLUSTRATIONS (CONTINUED)

FIGURE		PAGE
77.	Relationship of Dielectric Constant to Temperature for a MIL-L-7808 (O-79-17) and a PPE (O-77-6) Lubricant	251
78.	Dielectric Constant Readings at 30°C and 50°C of a PPE (O-67-1) from the Corrosion and Oxidation Test at 320°C	253
79.	Dielectric Constant Readings at 30°C and 50°C for a MIL-L-7808 (O-79-17) Lubricant from the Squires Confined Heat Test and Squires Oxidative Test at 190°C	255
80.	Dielectric Constant Readings at 50°C for MIL-L-7808 Lubricants from the Squires Oxidative Test at 190°C	256
81.	Sealed Pan-DSC Thermograms (200-500°C, 20°C/Minute Heating Rate) of the Fresh O-77-6 Polyphenyl Ether Basestock and the Fresh and 24 Hour 320°C Stressed O-67-1 Polyphenyl Ether Oils	259
82.	Sealed Pan-DSC Thermograms (200-500°C, 20°C/Minute Heating Rate) of the 24, 72, 120 and 192 Hour 320°C Stressed O-67-1 Polyphenyl Ether Oils	261
83.	Sealed Pan-DSC Thermograms (200-500°C, 20°C/Minute Heating Rate) of the 192 Hour 320°C Stressed O-67-1 oil Using 0.2 and 2.0 µL Sample Sizes	262
84.	TGA Thermograms (25-400°C, 25°C/Minute Heating Rate) of the 24 and 192 Hour 320°C Stressed O-67-1 Polyphenyl Ether Oils	264
85.	HP-DSC Thermograms Produced by the Fresh and Stressed (24 and 120 Hours at 320°C) O-67-1 Polyphenyl Ether Oils	266
86.	HP-DSC Thermogram Produced by the 240 Hour Stressed (320°C) O-67-1 Polyphenyl Ether Oil	267
87.	HP-DSC Thermogram (25-475°C, Ramp Rate of 25°C/min) of Fresh and Stressed (24, 120 and 240 h at 320°C) O-67-1 Lubricants (Sample Size 6 mg)	269
88.	FTIR Spectra (4000-400 cm ⁻¹) of the 24 and 240 Hour 320°C Stressed O-67-1 Polyphenyl Ether Oils	271
89.	UV-VIS Spectra (400-200 nm) of the Fresh and 24-240 Hour 320°C Stressed O-67-1 Oils in 1,2-Dichloroethane	273

LIST OF ILLUSTRATIONS (CONTINUED)

FIGURE		PAGE
90.	Absorbance at 320 nm and % Viscosity Change at 40°C Versus Stressing Time at 320°C for O-67-1 Polyphenyl Ether Oil	274
91.	UV-VIS Spectra (500-200 nm) of the Badly Degraded O-77-6 Oil and the 48 Hour 320°C Stressed O-67-1 Polyphenyl Ether Oil	275
92.	UV-VIS Spectra (400-300 nm) of the 24 and 192 Hour 330°C Stressed TEL-8039 and the 48 Hour 320°C Stressed O-67-1 Polyphenyl Ether Oils	277
93.	Absorbance Spectra of Fresh and Stressed (24-240 Hours at 320°C) O-67-1 and Used (TEL-9028, TEL-9029 and TEL-9030) Polyphenyl Ether Oils	278
94.	UV Spectra of Fresh and Stressed (300°C, 320-400 nm UV Light for 5 h) O-77-6 Polyphenyl Ether Fluids	283
95.	Cyclic Voltammograms of Fresh and Stressed (360 h at 175°C) O-85-1 4 cst Oils Diluted in Isobutyl Acetate (without Electrolyte) Using the Pt-10 Electrode and a +60 to -60 V Scan Range	288
96.	First and Second Reduction Scan Voltammograms of Fresh and Stressed (120 and 240 h at 305°C) O-67-1 Polyphenyl Ether Oils Diluted in Isobutyl Acetate (without Electrolyte) Using the Pt-10 Electrode and a +60 to -60 V Scan Range	289
97.	Cyclic Voltammograms of Solventless Fresh and Stressed (360 h at 175°C) O-85-1 Oils Using the Pt-10 and Pt-25 Electrodes, a Voltage Scanning Range of +60 to -60 V, and an Analysis Temperature of 175°C	291
98.	Cyclic Voltammograms of Solventless Fresh and Stressed (360 h at 175°C) O-85-1 Oils Using the Au-12.5, Pt-10, and W-10 Electrodes, a Voltage Scanning Range of +60 to -60 V, and an Analysis Temperature of 175°C	294

LIST OF ILLUSTRATIONS (CONTINUED)

FIGURE		PAGE
99.	Cyclic Voltammograms of Solventless Fresh and Stressed (168 h at 305°C) O-67-1 Polyphenyl Ether Oils Using the Au-12.5 and W-10 Electrodes, a Voltage Scanning Range of +60 to -60 V, and an Analysis Temperature of 275°C	295
100.	Gear Test Configuration Using the Falex Multispecimen Wear Test Machine	297
101.	Four-Ball Configuration	300
102.	Non-Circular Lower Ball Wear Scars Formed on 52100 Steel Specimens by Lubrication with Polyphenyl Ether (48X Actual Size)	302
103.	Falex Four-Ball Wear Test Machine Showing Spindle, Test Cup, Heater and LVDT	304
104.	Upper Ball and One Lower Ball, Before and After Wear, Corresponding to the (a) Bos Model and (b) Actual Geometry	306
105.	Four-Ball Configuration and Nomenclature for the Upper Ball and One Lower Ball, Before and After Wear	308
106.	Ball Displacement Caused by Elastic Deformation	310
107.	Relationship Between Upper Ball Displacement and Chord Length (Theoretical and Experimental)	311
108.	Two Possible Scar Surfaces, s_3 , Assuming the Scar Profile can be Approximated with a Circular Arc; (a) s_3 Centered on the Same Side of Contact as the Upper Ball and (b) s_3 Centered on the Same Side of Contact as the Lower Ball	313
109.	Scar Profiles from a 20-hour Test of O-67-1 at 150°C (1200 RPM, 145-N Load, 52100 Balls). Upper Ball Profile is Inverted to Illustrate the Similarity of Mating Surfaces. Profile Made with the Grain of the Lower Ball is Included as an Example of how a Circular Arc May Average the Roughness	314
110.	Cross-Sectional Areas of the Upper and Lower Balls at the Mid-Point of the Chord Length	317
111.	Relationship Between Scar Length, Width, and Alpha	318

LIST OF ILLUSTRATIONS (CONTINUED)

FIGURE		PAGE
112.	Relationship Between Upper Ball Displacement and Alpha for Given Lubricant and Test Conditions Compared to the Curve Representing Equal Upper Ball and Total Lower Ball Wear Volumes	320
113.	Wear Volume History of a 20-Hour Test of O-67-1 at 150°C (1200 RPM, 145-N Load, 52100 Balls) Generated from the LVDT Data and the Linear Variation on Alpha Shown in Figure 112	321
114.	Slices of Upper and Lower Ball Wear Volumes	323
115.	Sensitivity of Volume Calculations to the Alpha Parameter	324
116.	Scar Shape Predicted by the Geometric Analysis of the Four-Ball Configuration for a 2.000-mm Chord Length and a 1.625-mm Elliptical Width (giving an alpha of 0.662)	326
117.	Lower Ball Scar Shapes for Alpha Values of (a) 1 (circular scar), (b) 0.33 (elliptical scar), and (c) 0 (no scar)	327
118.	Three Wear Regions of the Sliding Four-Ball Test Represented by the Upper Ball Position Versus Time for an Ester-Based Lubricant	330
119.	Chord Length Calculated from LVDT Data Versus Time for Two 20-Hour Tests Run Under Identical Conditions	332
120.	Chord Length Versus Time for a Series of Discrete Tests. (Data Shown in Figure 119 is Included for Comparison)	333
121.	Elliptical Width Versus Chord Length for an Ester-Based Lubricant. Discrete Tests Ranged from 10 Minutes to 30 Hours in Duration	335
122.	Elliptical Width Versus Chord Length for PPE-Based Lubricant. Discrete Tests Ranged from 15 Minutes to 30 Hours in Duration	336
123.	Variation of the Alpha Parameter as a Function of the Width to Length Ratio	337

LIST OF ILLUSTRATIONS (CONTINUED)

FIGURE		PAGE
124.	Elliptical Width Versus Chord Length for PPE-Based Lubricant at 250°C (Width-Length Relationship Constructed Using Two 3-Hour Tests and Two 20-Hour Tests)	339
125.	Elliptical Width Versus Chord Length for PPE-Based Lubricant at 75°C (Width-Length Relationship Constructed Using Two 3-Hour Tests and Two 20-Hour Tests)	340
126.	Time Basis Illustration of Wear Volume for PPE-Based Lubricant with Linear Regressions of Discrete Tests	342
127.	Time Basis Illustration of Wear Volume for PPE-Based Lubricant Calculated from LVDT Data. Linear Regressions from Measurements of Discrete Tests (Figure 126) are Shown by the Solid Lines	343
128.	Parameter Basis Illustration of Wear Volume for PPE-Based Lubricant with Linear Regressions of Discrete Tests	345
129.	Parameter Basis Illustration of Wear Volume for PPE-Based Lubricant Calculated from LVDT Data. Linear Regressions from Measurements of Discrete Tests (Figure 128) are Shown by the Solid Lines	346
130.	Parameter Basis Illustration of Total Lower Ball Wear Volume for PPE-Based Lubricant Calculated from LVDT Data and from Discrete Tests	347
131.	Parameter Basis Illustration of Upper Ball Wear Volume for PPE-Based Lubricant Calculated from LVDT Data and from Discrete Tests	348
132.	Lower Ball Scar Formed on 52100 Steel Specimen at 315°C (47X Actual Size)	350
133.	Hardness as a Function of Temperature for Three Bearing Steels (from Ref. 27)	350
134.	Wear Comparison of Various High-Temperature Fluids Based on the Scar Sizes of 52100 Steel Balls Run at 150°C	352
135.	Wear Comparison of Various High-Temperature Fluids Based on the Scar Sizes of 52100 Steel Balls at 250°C	353

LIST OF ILLUSTRATIONS (CONTINUED)

FIGURE		PAGE
136.	Wear Comparison of Various High-Temperature Fluids Based on the Scar Volumes of 52100 Steel Balls at 150°C	355
137.	Wear Comparison of Various High-Temperature Fluids Based on the Scar Volumes of 52100 Steel Balls at 250°C	356
138.	Wear Comparison of Various High-Temperature Fluids Based on the Scar Sizes of M-50 Steel Balls at 150°C	358
139.	Wear Comparison of Various High-Temperature Fluids Based on the Scar Sizes of M-50 Steel Balls at 250°C	359
140.	Wear Comparison of Various High-Temperature Fluids Based on the Scar Volumes of M-50 Steel Balls at 150°C	360
141.	Wear Comparison of Various High-Temperature Fluids Based on the Scar Volumes of M-50 Steel Balls at 250°C	361
142.	SEM Microphotographs and EDS Elemental Analyses of Wear Scars Produced on Bottom Balls During O-67-1 Four-Ball Tests with M50 and 52100 Steel at 150°C	365
143.	AES Depth Profiles (5 nm/minute) of Wear Scars Produced on Bottom and Top Balls During O-67-1 Four-Ball Test with 52100 Steel at 150°C	366
144.	AES Depth Profiles (5 nm/minute) of Wear Scars Produced on Bottom and Top Balls During O-67-1 Four-Ball Test with M-50 Steel at 150°C	367
145.	AES Depth Profiles (5 nm/minute) of Wear Scars Produced on the Top and Bottom Balls During O-67-1 Four-Ball Wear Test with 52100 Steel at 315°C	369
146.	Wear Rate Comparison Between Tests of 52100 Balls Lubricated with PPE at 150°C and 315°C Represented by the Upper Ball Travel (LVDT Data)	370
147.	AES Depth Profiles (5 nm/minute) of Wear Scars Produced on the Top and Bottom Balls During O-67-1 Four-Ball Wear Test with M-50 Steel at 315°C	371
148.	Wear Rate Comparison Between Tests of M-50 Balls Lubricated with PPE at 150°C and 315°C Represented by the Upper Ball Travel (LVDT Data)	372

LIST OF ILLUSTRATIONS (CONTINUED)

FIGURE		PAGE
149.	Material Comparison Based on the Scar Sizes of Balls Lubricated with PPE at 150°C	374
150.	Material Comparison Based on the Scar Volumes of Balls Lubricated with PPE at 150°C	375
151.	Lower Ball Scars Formed on M-50 Steel Specimens Lubricated with Polyphenyl Ether (38X Actual Size)	377
152.	Wear Rate Comparison Between Tests of M-50 Balls Lubricated with PPE Under Identical Conditions Represented by the Upper Ball Travel (LVDT Data)	379
153.	AES Depth Profiles (5 nm/min) of Wear Scars Produced on the Top and Bottom Balls During O-67-1 Four-Ball Wear Test with M-50 Steel at 315°C and Excess Air	383
154.	Comparison of PPE to PPE Diluted with 25% TCE at Various Temperatures Based on the Scar Sizes of 52100 Steel Balls	384
155.	Comparison of PPE to PPE Diluted with 25% TCE at Various Temperatures Based on the Scar Volumes of 52100 Steel Balls	385
156.	AES Depth Profiles (5 nm/minute) of Wear Scars Produced on the Top and Bottom Balls During O-77-6 Four-Ball Wear Test with 52100 Steel at 150°C	387
157.	AES Depth Profiles (5 nm/minute) of Wear Scars Produced on the Top and Bottom Balls During TCE-Diluted O-77-6 Four-Ball Wear Test with 52100 Steel at 150°C	388
158.	Comparison of Various Stressed Samples of PPE Based on the Scar Size of 52100 Steel Balls at 150°C	389
159.	Comparison of Various Stressed Samples of PPE Based on the Scar Volumes of 52100 Steel Balls at 150°C	390
160.	Variation of Scar Sizes from Identical Tests of O-67-1 on 52100 Steel Balls at 150°C	392
161.	Variation of Scar Volumes from Identical Tests of O-67-1 on 52100 Steel Balls at 150°C	393

LIST OF ILLUSTRATIONS (CONTINUED)

FIGURE		PAGE
162.	Temperature Variation Within the Four-Ball Test Cup	395
163.	Percent Friction Polymer, as Trichloroethylene Insolubles, from Four-Ball Testing of O-67-1 at 150°C, 145 N Load, 52100 Bearings	399
164.	⁵⁷ Fe Mossbauer Spectra of Friction Polymer from Four-Ball Testing of O-67-1 at 145 N Load	405
165.	⁵⁷ Fe Mossbauer Spectra of Friction Polymer from Four-Ball Testing of O-67-1 at 145 N Load	406
166.	FTIR Spectra of Friction Polymer from Four-Ball Testing of O-67-1 at 150°C and 145 N Load	410
167.	FTIR Spectra of Friction Polymer from Four-Ball Testing of O-67-1 at 250°C and 145 N Load	411
168.	FTIR Spectra of Friction Polymer from Four-Ball Testing of O-67-1 at 315°C and 145 N Load	412
169.	X-Ray Fluorescence Spectra of the O-67-1 Wear Debris Collected on the Entry and Exit Areas of a Ferrographic Slide	414
170.	EDS Elemental Analyses of the O-67-1 Wear Debris Collected on the Entry and Exit Areas of a Ferrographic Slide	415
171.	FTIR Spectrum of Isolated Debris from Engine Stressed PPE (TEL-9070-18)	419
172.	FTIR Spectrum of Carbon Seal Deposits from Engine Tested PPE (J58 FX-111 89)	420
173.	DSC Thermograms of Isolated Debris from Engine Stressed PPE Lubricants TEL-9030 and TEL-9040 (DSC Conditions: Ambient to 400°C at 20°C/Minute, Hold 20 Minutes)	421
B-1.	Calibration Curve for Fe Using 25 L of Dissolved Organo-Metallic Single Element Standard, Ashing for 6 min. at 450°C in Air	509
B-2.	Effect of Sample Size on Emission Signal at Various Concentrations of Fe Organo-Metallic Standard Using 0.82 mm Deep Cup-Tip Electrodes	510

LIST OF ILLUSTRATIONS (CONCLUDED)

FIGURE		PAGE
B-3.	Effect of Ashing in Air Versus Argon on Emission Intensity for Fe Organo-Metallic Standards Using 0.82 mm Cup-Tip Electrodes	513
B-4.	Effect of Exposure Time on Particle Analysis Using Various Sizes of Fe Powder	516
C-1.	Evolution of a Lower Ball Wear Scar into an Equivalent Ellipse	524
C-2.	Equation of an Ellipse Solved in Terms of Width	525
C-3.	Width and Length Measurements (x_i , y_i) Taken on an Odd-Shaped Lower Ball Wear Scar	526
C-4.	Measurements Taken on Various Scar Sections	527

LIST OF TABLES

TABLE		PAGE
1.	DESCRIPTION OF ESTER BASE FLUIDS USED IN OXIDATIVE STABILITY	4
2.	DESCRIPTION OF TEST FLUIDS FOR LUBRICANT CORROSION AND OXIDATIVE STABILITY STUDY OF HIGH TEMPERATURE FLUIDS	11
3.	EFFECTIVE LUBRICANT LIFE OF O-77-6 AND TEL-8092 USING CORROSION AND OXIDATION TESTING, D 4871 TUBES, INTERMEDIATE SAMPLING AND 10 L/H AIRFLOW	14
4.	CORROSION AND OXIDATION TEST DATA FOR LUBRICANTS TEL-8092 AND O-67-1 AT 320°C USING 10 L/H AIRFLOW, 100 ML SAMPLE, D 4871 TUBES AND INTERMEDIATE SAMPLING	22
5.	CORROSION AND OXIDATION TEST DATA FOR LUBRICANTS TEL-90028 AND O-67-1 AT 320°C USING 10 L/H AIRFLOW, 100 ML SAMPLE AND D 4871 TUBES	26
6.	CORROSION AND OXIDATION DATA FOR LUBRICANTS TEL-8039 AND TEL-8085 AT 320°C, USING D 4871 TUBES AND INTERMEDIATE SAMPLING	28
7.	CORROSION AND OXIDATION DATA FOR LUBRICANTS TEL-8040 AND TEL-8087 @ 320°C, USING D 4871 TUBES AND INTERMEDIATE SAMPLING	29
8.	COMPARISON OF CORROSION AND OXIDATION TEST DATA FOR LUBRICANTS TEL-8039 AND TEL-8085 AT 330°C, D 4871 TUBES, INTERMEDIATE SAMPLING, 10 L/H AIRFLOW	30
9.	CORROSION AND OXIDATION DATA FOR LUBRICANTS TEL-8085 TEL-8087 AND TEL-8092 AT 340°C, D 4871 TUBES, INTERMEDIATE SAMPLING, 10 L/H AIRFLOW	31
10.	CORROSION AND OXIDATION TEST DATA FOR FLUID TEL-8087, 320°C, 10 L/H AIRFLOW, INTERMEDIATE SAMPLING AND USING MOIST (SATURATED) AIR	32
11.	TEST DATA FOR O-67-1 LUBRICANT STRESSED 48 HOURS AT 320°C WITH AND WITHOUT LIQUID AND VAPOR PHASE CORROSION SPECIMENS	41
12.	TEST DATA FOR O-77-6 FLUID STRESSED 48 HOURS AT 300°C WITH AND WITHOUT METAL SPECIMENS	43
13.	XPS ELEMENTAL ANALYSES OF DEPOSITION ON MILD STEEL AND SILVER SPECIMENS AND FRESH O-77-6	43

LIST OF TABLES (CONTINUED)

TABLE	PAGE
14. COMPOSITIONAL DATA FOR O-77-6 CONDENSATES OBTAINED AT 24 AND 48 HOURS WITH AND WITHOUT METAL AND ALLOY SPECIMENS	45
15. SUMMARY OF CORROSION AND OXIDATION TEST DATA FOR NEW AND FIELD STRESSED POLYPHENYL ETHER LUBRICANT SAMPLES (48 HOUR INTERMEDIATE TEST SAMPLES, 320°C, 10 L/H AIRFLOW)	48
16. EFFECT OF 3 MICRON FILTERABLE SOLIDS ON LUBRICANT STABILITY OF WEAR TESTED AND ENGINE TESTED MIL-L-87100 TYPE LUBRICANT	54
17. CORROSION AND OXIDATION TEST DATA AT 320°C FOR LUBRICANT O-67-1 AFTER FOUR-BALL WEAR TESTING AT VARIOUS TEMPERATURES AND LOADINGS, 1200 RPM AND 3 HOUR TEST TIME (1 HOUR FOR TEST # 362)	61
18. GPC ANALYSIS OF FOUR-BALL TESTED O-67-1 LUBRICANTS	63
19. EFFECT OF 150°C OVEN STRESSING ON VARIOUS FOUR-BALL TESTED O-67-1 LUBRICANTS	65
20. DSC AND TGA DATA FOR FRICTION POLYMER FROM FOUR-BALL TESTED O-67-1 LUBRICANT	68
21. EFFECT OF DILUTION ON CORROSION-OXIDATION OF O-67-1 AND O-77-6 AT 320°C USING SQUIRES TUBES, 25 ML SAMPLES AND 10 L/H AIRFLOW (48 H)	74
22. VISCOSITY INCREASE OF STRESSED TEL-9050	76
23. TOTAL ACID NUMBERS OF NEW AND STRESSED TEL-9050	77
24. CORROSION MEASUREMENTS OF STRESSED TEL-9050	78
25. SILVER METAL CONCENTRATION OF STRESSED TEL-9050	79
26. SILICON CONTENT OF STRESSED TEL-9050	79
27. DEPOSIT FORMATION DURING C&O TESTING OF TEL-9050	80
28. MOISTURE CONTENT OF TEL-9050	81
29. CORROSION-OXIDATION TEST DATA FOR LUBRICANT TEL-90024 AT 320°C USING 10 L/H AIRFLOW, 100 ML SAMPLE AND D 4871 TUBES	82

LIST OF TABLES (CONTINUED)

TABLE		PAGE
30.	TEST DATA FOR TEL-90024 LUBRICANT STRESSED 48 HOURS AT 300°C USING LIQUID AND VAPOR CORROSION TEST SPECIMENS	83
31.	CORROSION AND OXIDATION OF TEL-90059 AT 310°C AND 320°C USING D 4871 TUBES, INTERMEDIATE SAMPLING and 10 L/H AIRFLOW	84
32.	CORROSION AND OXIDATION OF TEL-90063 AT THREE TEST TEMPERATURES USING D 4871 TUBES, INTERMEDIATE SAMPLING AND 10 L/H AIRFLOW	87
33.	PWMA ANALYSIS OF TRACE METALS IN TEL-90063 AT DIFFERENT CORROSION AND OXIDATION STRESSING TIMES AND TEMPERATURES	89
34.	TEST DATA FOR FRESH AND STRESSED TEL-9071 FLUIDS USING LIQUID AND VAPOR CORROSION TEST SPECIMENS	91
35.	XPS ELEMENTAL ANALYSES OF STAINS/DEPOSITS PRESENT ON MILD STEEL AND SILVER SPECIMENS	97
36.	XPS ELEMENTAL RATIOS OF STAINS/DEPOSITS PRESENT ON MILD STEEL AND SILVER SPECIMENS	97
37.	DESCRIPTION OF TEST FLUIDS USED IN STATIC COKING STUDY	104
38.	AFAPL STATIC COKER DATA FOR FLUID O-77-6 AT 375°C, 3 HOURS TEST TIME USING SHIM STOCK TEST SPECIMENS	105
39.	CORRELATION BETWEEN AFAPL STATIC COKER CONTROLLER TEMPERATURE AND MEASURED COKER SURFACE TEMPERATURE	108
40.	EFFECT OF TEST TEMPERATURE ON SHIM STOCK AND STAINLESS STEEL TEST SPECIMEN DEPOSITS AFTER THREE TEST HOURS WITH AND WITHOUT TEST SAMPLE AND USING TEMPERATURE PROGRAMMING	111
41.	EFFECT OF SAMPLE SIZE ON AFAPL COKING VALUES (NEW O-67-1, 168 HOUR 320°C C&O SAMPLE, COKING TEMPERATURE OF 375°C FOR THREE TEST HOURS AND 0.005 INCH STAINLESS STEEL SPECIMENS)	112
42.	AFAPL STATIC COKER TEST DATA USING STAINLESS STEEL TEST SPECIMENS, 375°C COKING TEMPERATURE WITH AND WITHOUT TEMPERATURE RAMPING	113

LIST OF TABLES (CONTINUED)

TABLE	PAGE
43. EFFECT OF TEST TIME AND TEMPERATURE ON DEPOSITS FOR NEW O-77-6	114
44. EFFECT OF TEST TEMPERATURE ON C&O 120 H, 290°C STRESSED O-77-6 STATIC COKER DEPOSITS USING 3 HOUR TEST TIME	115
45. EFFECT OF TEST TIME ON STATIC COKER DEPOSITS OF O-77-6 (120 HOUR C&O AT 290°C) USING STAINLESS STEEL SPECIMENS, 0.5 ML SAMPLE AND 425°C TEST SURFACE TEMPERATURE	118
46. EFFECT OF TEST TIME AND TEMPERATURE ON NEW O-67-1 STATIC COKER DEPOSITS	118
47. EFFECT OF TEST TEMPERATURE ON O-67-1 (240 HOUR C&O AT 320°C USING 3 HOUR TEST TIME AND 0.5 GRAM SAMPLE) STATIC COKER DEPOSITS	119
48. AFAPL STATIC COKER TEST DATA FOR THREE MICRON FILTERED AND UNFILTERED FOUR-BALL WEAR O-67-1 FLUID BEFORE AND AFTER C&O TESTING (0.5 GRAM SAMPLE, 3 HOUR TEST TIME, TEMPERATURE PROGRAMMING AND STAINLESS STEEL TEST SPECIMENS)	120
49. AFAPL STATIC COKER TEST DATA FOR ENGINE STRESSED MIL-L-87100 LUBRICANT USING A 375°C COKING TEMPERATURE, 0.5 GRAM SAMPLE, 3 HOUR TEST TIME, TEMPERATURE PROGRAMMING AND STAINLESS STEEL TEST SPECIMENS	121
50. EFFECT OF TEST SPECIMEN MATERIAL ON STATIC COKER DEPOSITS AT 375°C USING 0.5 ML SAMPLES AND 3 HOUR TEST TIME	123
51. VOLATILIZATION RATE AND DEPOSIT AMOUNTS OF O-67-1 USING STATIC COKER AT VARIOUS TEMPERATURES	124
52. AFAPL STATIC COKER DEPOSITS FOR O-67-1 AND TEL-90028 (375°C, 3 TEST HOURS, SS-302 SPECIMENS AND TEMPERATURE PROGRAMMING)	126
53. AFAPL STATIC COKER DEPOSITION DATA ON NON-POLYPHENYL ETHER FLUIDS USING 0.5 GRAM SAMPLES, SS-302 TEST SPECIMENS AND TEMPERATURE PROGRAMMING	127

LIST OF TABLES (CONTINUED)

TABLE		PAGE
54.	DESCRIPTION OF TEST FLUIDS USED ON MCRT COKING STUDY	131
55.	UNIFORMITY OF TEMPERATURE WITHIN MICRO CARBON RESIDUE TESTERS (MCRT)	132
56.	CORRELATION OF MICRO CARBON RESIDUE TESTERS NO. 1 AND NO. 2 AT VARIOUS TEMPERATURES AND 30 H TEST DURATIONS FOR LUBRICANT O-86-2	136
57.	PERCENT WEIGHT MICRO CARBON RESIDUE TESTER (MCRT) VALUES USING 35 MM AND 76 MM HEIGHT SAMPLE VIALS FOR NEW AND STRESSED O-67-1 FLUID (30 HOUR TEST TIME)	137
58.	MELTING POINT VALUES OF MCRT DEPOSITS	139
59.	DESCRIPTION OF MCRT DEPOSITS USING 35 MM AND 76 MM HEIGHT SAMPLE VIALS FOR NEW AND STRESSED O-67-1 FLUID (30 HOUR TEST TIME)	139
60.	EFFECT OF TEST TIME ON THE MCRT RESIDUE VALUE OF THE 240 HOUR, 320°C C&O STRESSED LUBRICANT AT 350°C MCRT DISPLAYED TEMPERATURE	141
61.	EFFECT OF TEMPERATURE ON MCRT DEPOSITS USING 30 HOUR TEST TIME AND 0.5 GRAM SAMPLE SIZE	142
62.	EFFECT OF SAMPLE SIZE ON MCRT RESIDUE AT 400°C USING 3.5 CENTIMETER VIALS AND 30 HOUR TEST TIME	146
63.	MCRT DEPOSIT VALUES FOR MIL-L-87100 LUBRICANT FROM OPERATIONAL ENGINES INCLUDING INITIAL IRON AND TIN CONTENT	151
64.	MCRT DEPOSIT VALUES FOR FOUR-BALL WEAR TEST SAMPLES AT 400°C TEST TEMPERATURE AND 30 TEST HOURS	152
65.	EFFECT OF FOUR-BALL WEAR TESTING ON MCRT RESIDUE USING 30 HOUR TEST, 0.5 GRAM SAMPLE AND 3.5 CM VIALS	153
66.	FOUR-BALL WEAR TEST DATA AND MCRT RESULTS FOR O-67-1 AND TEL-90024 LUBRICANTS USING Si ₃ N ₄ , 52100 STEEL, M50 STEEL AND BRASS WEAR TEST BALLS	156
67.	COMPARISON OF 30 HOUR, 400°C MCRT DATA USING AIR AND ARGON FOR VARIOUS TEST FLUIDS	160

LIST OF TABLES (CONTINUED)

TABLE		PAGE
68.	MCRT RESIDUE VALUES OF VARIOUS HIGH-TEMPERATURE LUBRICANTS AND EXPERIMENTAL FLUIDS (400°C, 0.5 G SAMPLE, 3.5 CM VIALS, 30 TEST HOURS)	162
69.	CORRELATION OF MCRT AND AFAPL STATIC COKER DEPOSIT VALUES	163
70.	LUBRICANTS AND FLUIDS USED FOR FOAMING STUDY	167
71.	FOAMING CHARACTERISTICS OF 5P4E FLUID O-77-6 USING 200 ML SAMPLE	168
72.	SMALL VOLUME FOAM TESTING OF FLUID O-77-6 AT 80°C AND 100°C USING A 3/16" DIAMETER 5 MICRON PORE SPARGER AND AN ASTM DIFFUSER STONE	169
73.	EFFECT OF INCREASING (LOW TO HIGH) AERATION RATE ON FOAMING/AERATION CHARACTERISTICS OF 5P4E FLUID O-77-6 AT 80°C USING ASTM DIFFUSER STONE AND 25 ML SAMPLE	171
74.	LUBRICANT O-67-1 FOAMING CHARACTERISTICS AT 200°C (200 ML SAMPLE AND 13/16 INCH DIAMETER 5 MICRON SPARGER)	172
75.	LUBRICANT O-67-1 FOAMING CHARACTERISTICS AT 200°C (25 ML SAMPLE AND 5 MICRON METAL SPARGERS)	172
76.	FOAMING CHARACTERISTICS OF TEL-90018 AT 200°C USING 25 ML SAMPLE AND 13/16" 5 MICRON SPARGER	173
77.	FOAMING CHARACTERISTICS OF CORROSION AND OXIDATION STRESSED O-67-1 LUBRICANT AT 200°C USING A 13/16 INCH 5 MICRON SPARGER AND 25 ML SAMPLE	174
78.	FOAMING CHARACTERISTICS OF ENGINE STRESSED MIL-L-87100 SAMPLES AT 200°C (25 ML SAMPLE AND 13/16 INCH 5 MICRON SPARGER)	175
79.	FOAMING CHARACTERISTICS OF TEL-9050, TEL-90001 AND TEL-90024 EXPERIMENTAL FLUIDS AT 200°C USING A 25 ML SAMPLE AND A 13/16 INCH DIAMETER 5 MICRON PORE SIZE SPARGER	178
80.	STATIC FOAM TEST DATA FOR THREE MIL-L-7808 LUBRICANTS USING FEDERAL TEST METHOD STANDARD 791, METHOD 3213 AND THE SMALL VOLUME (25 ML) FOAM TEST	179

LIST OF TABLES (CONTINUED)

TABLE	PAGE
81. VISCOSITY OF O-77-6 USING ROUTINE, SEMI-MICRO AND EXTRA LOW CHARGE VISCOMETERS	182
82. VARIOUS SIZES OF FE POWDER PRODUCED BY SIEVING A COMMERCIAL FE POWDER HAVING AN AVERAGE PARTICLE SIZE OF 1-5 MICRONS	190
83. FERROSCAN READINGS FOR 0-10 MICRON FE POWDER	200
84. FERROSCAN READINGS FOR 0-10 MICRON FE POWDER USING THE NEW DETECTOR	207
85. FERROSCAN RESPONSE PER UNIT CONCENTRATION FOR FE 0-10 MICRON AT CONCENTRATION BELOW 160 PPM	209
86. COMPARATIVE DATA FROM TWO EXPERIMENTS USING SLOPES AND FERROSCAN RESPONSE PER PPM FE FOR 0-10 MICRON	209
87. INITIAL ANALYTICAL FERROGRAPH DATA FOR VARIOUS POLYPHENYL ETHER FLUIDS	221
88. IDENTIFICATION OF SAMPLES USED IN ANALYTICAL FERROGRAPHY STUDY INCLUDING DESCRIPTION OF FERROGRAM DEBRIS	223
89. ANALYTICAL FERROGRAPH DATA FOR DOD-L-85734(AS) FLUIDS AND O-77-6 FLUID AFTER FOUR-BALL WEAR TESTING	224
90. ANALYTICAL FERROGRAPH DATA FOR O-67-1 FOUR-BALL WEAR TEST SAMPLES USING VARIOUS TEST TEMPERATURES AND LOADINGS. (1200 RPM AND THREE TEST HOURS UNLESS SHOWN)	226
91. EFFECT OF OXIDATIVE STRESSING OF FOUR-BALL WEAR TEST SAMPLES OF O-67-1 LUBRICANT ON ANALYTICAL FERROGRAPH DATA	229
92. EFFECT OF 3 MICRON FILTRATION ON ANALYTICAL FERROGRAPH DATA FOR C&O STRESSED AND UNSTRESSED CB-1 SAMPLE (FOUR-BALL WEAR TEST SAMPLE OF O-67-1)	231
93. ANALYTICAL FERROGRAPH DATA FOR ENGINE STRESSED O-67-1 SAMPLES	233
94. FLUORESCENCE EMISSION MAXIMA OF OXIDIZED PPE LUBRICANTS	239

LIST OF TABLES (CONTINUED)

TABLE		PAGE
95.	UPPER CONCENTRATION LIMITS FOR FLUORESCENCE OF OXIDIZED PPES	242
96.	UV ANALYSES OF FRESH AND STRESSED O-67-1 OILS	280
97.	VARIATION IN THE ALPHA PARAMETER FOR VARIOUS TEST TIMES	329
98.	VARIATION IN THE ALPHA PARAMETERS AND TOTAL WEAR VOLUME FOR VARIOUS OILS	354
99.	FRICTION POLYMER CONTENT IN VARIOUS FOUR-BALL TESTED O-67-1 LUBRICANTS	398
100.	TOTAL IRON IN FRICTION POLYMER FROM VARIOUS FOUR-BALL TESTED O-67-1 LUBRICANTS	401
101.	TOTAL IRON IN FP BY ADM-AA AND ASHING-AA	402
102.	QUALITATIVE IRON ANALYSIS OF FP USING EXTRACTION TECHNIQUES	402
103.	⁵⁷ FE MOSSBAUER PARAMETERS FROM FIVE FP SAMPLES	407
104.	ELEMENTAL ANALYSIS OF FP FROM VARIOUS FOUR-BALL TESTS	409
105.	% TRICHLOROETHYLENE INSOLUBLES IN VARIOUS ENGINE STRESSED PPE LUBRICANTS	417
A-1.	CORROSION AND OXIDATION DATA FOR TEL-9028, TEL-9029 TEL-9030, TEL-9038, TEL-9039 AND 9040 LUBRICANTS (320°C, D 4871 TUBES, 10 L/H AIRFLOW)	424
A-2.	CORROSION AND OXIDATION TEST DATA FOR LUBRICANTS O-67-1, CB-1, TEL-9030 AND TEL-9040 (BEFORE AND AFTER 3 MICRON FILTERING) AT 320°C USING SQUIRES TUBES AND 25 ML SAMPLES	426
A-3.	SQUIRES OXIDATIVE TEST DATA	428
A-4.	CORROSION AND OXIDATION TEST DATA	433
A-5.	AFAPL STATIC COKER TEST DATA	484
A-6.	MCRT COKING TEST DATA	495
A-7.	LUBRICANT FOAMING TEST DATA	500

LIST OF TABLES (CONCLUDED)

TABLE		PAGE
B-1.	EFFECT OF SPARK DISCHARGE INTENSITY, ANALYTICAL GAP DISTANCE AND EXHAUST FLOW FOR 100 PPM FE STANDARDS	512
B-2.	EFFECT OF BOTTOM ELECTRODE GEOMETRY ON SIGNAL INTENSITY USING 5 L SAMPLES	514
B-3.	COMPARISON OF FE SIGNAL INTENSITY USING RDE VERSUS PSE METHOD	517
B-4.	RESULTS OBTAINED BY AA-ADM AND PWMA SHOWING IMPROVED PARTICLE DETECTION OF LARGE PARTICLES USING PSE VERSUS RDE TECHNIQUE FOR ACTUAL OPERATING ENGINE SAMPLES	520
C-1.	PROFILED ALPHA PARAMETER COMPARED TO CALCULATED ALPHA PARAMETER FOR FOUR-BALL TESTS OF O-67-1 ON 52100 BALLS AT 150°C (145 N, 1200 RPM)	532

SECTION I

INTRODUCTION

Fluid lubricants capable of superior performance in advanced aircraft turbine engine environments at temperatures from 500-750^oF are required by the United States Air Force to improve their propulsion capabilities. Lubricant requirements include thermal-oxidative stability within engine oil system environment, compatibility with various engine materials and satisfactory tribological performance.

This work describes the first half of research conducted for developing improved methods for measuring lubricant performance. These methods will be used to predict performance of selected high temperature candidate fluids. The work also includes the development of lubrication system monitors for assessing condition of engine health, development of techniques satisfactory for monitoring lubricant condition and evaluation of candidate fluids tribological behavior. Methods developed in this work are applicable to potential high temperature turbine engine candidate fluids including polyphenyl ethers, c-ethers, perfluoroalkyl ethers, other proprietary experimental fluids and additive modified versions of such fluids.

SECTION II

DEVELOPMENT OF IMPROVED METHODS FOR MEASURING LUBRICANT PERFORMANCE

1. LUBRICANT OXIDATIVE STABILITY OF ESTER BASE FLUIDS

a. Introduction

The objective of this phase of the program was to investigate the oxidative stability of 4 centistoke (cSt) turbine engine lubricants as it relates to temperature and determine the fluid stability in terms of effective lubricant life based upon limiting values of physical properties. Viscosity, acidity, volatility, electrochemical characteristics and composition were the properties determined after the oxidative stressing of the lubricant with only viscosity, acidity and volatility measurements being used for determining lubricant effective life.

b. Test Apparatus and Test Procedure

Both the test apparatus and test procedure have been described previously¹ and remained unchanged during this investigation. The test apparatus consists primarily of an oxidation tube for the oil sample, a heating bath containing polyphenyl ether and an air tube that allows air to bubble through the oil sample during the test. The test is essentially an oxidation test similar in some respects to many other oxidation tests.

c. Test Lubricants and Test Conditions

A total of seven lubricants were studied during this phase of the program and are described in Table 1. Test conditions ranged from 210° to 225°C test temperatures and test durations to 196 hours. Testing was terminated after severe degradation or after very high lubricant loss had occurred.

TABLE 1

DESCRIPTION OF ESTER BASE FLUIDS USED IN OXIDATIVE STABILITY

Test Fluid	Description	Viscosity, cSt at 100°C
O-85-1	Candidate Lubricant	4.04
TEL-8103	Candidate Lubricant	4.00
TEL-9022	Different Lot of O-85-1	4.04
TEL-9031	Different Lot of O-85-1	4.01
TEL-9076	Candidate Lubricant	4.04
TEL-90003	Candidate Lubricant	3.94
TEL-90087	Different Lot of TEL-90003	4.02
O-90-6	Different Lot of O-85-1	4.01

d. Results and Discussion

The oxidative stabilities of six lubricants tested at 210°C are shown graphically in Figure 1. With respect to change in viscosity the four fluids O-85-1, TEL-9076, TEL-8103 and TEL-9022 show relatively close and good stability for the test durations shown. Lubricant TEL-90087 shows about two times the rate of viscosity increase as the other four fluids but does not show a distinct "breakpoint." Lubricant TEL-9031 shows similar stability to lubricants O-85-1 and TEL-9022 for the first 75 test hours. This should be expected since TEL-9031 is a different lot of O-85-1. However, after 75 test hours TEL-9031 shows severe degradation which cannot be explained at this time.

Five of six lubricants shown in Figure 1 have small increases in the total acid numbers (TAN) with values of 3 or below after 200 test hours. Again, lubricant TEL-9031 appeared similar to the other five up to 75 test hours after which the lubricant "broke" and showed a very rapid increase in TAN. The small increase in TAN for the five lubricants indicates that a part of the viscosity increase of these fluids is due to selective volatilization

Lubricants at 210°C

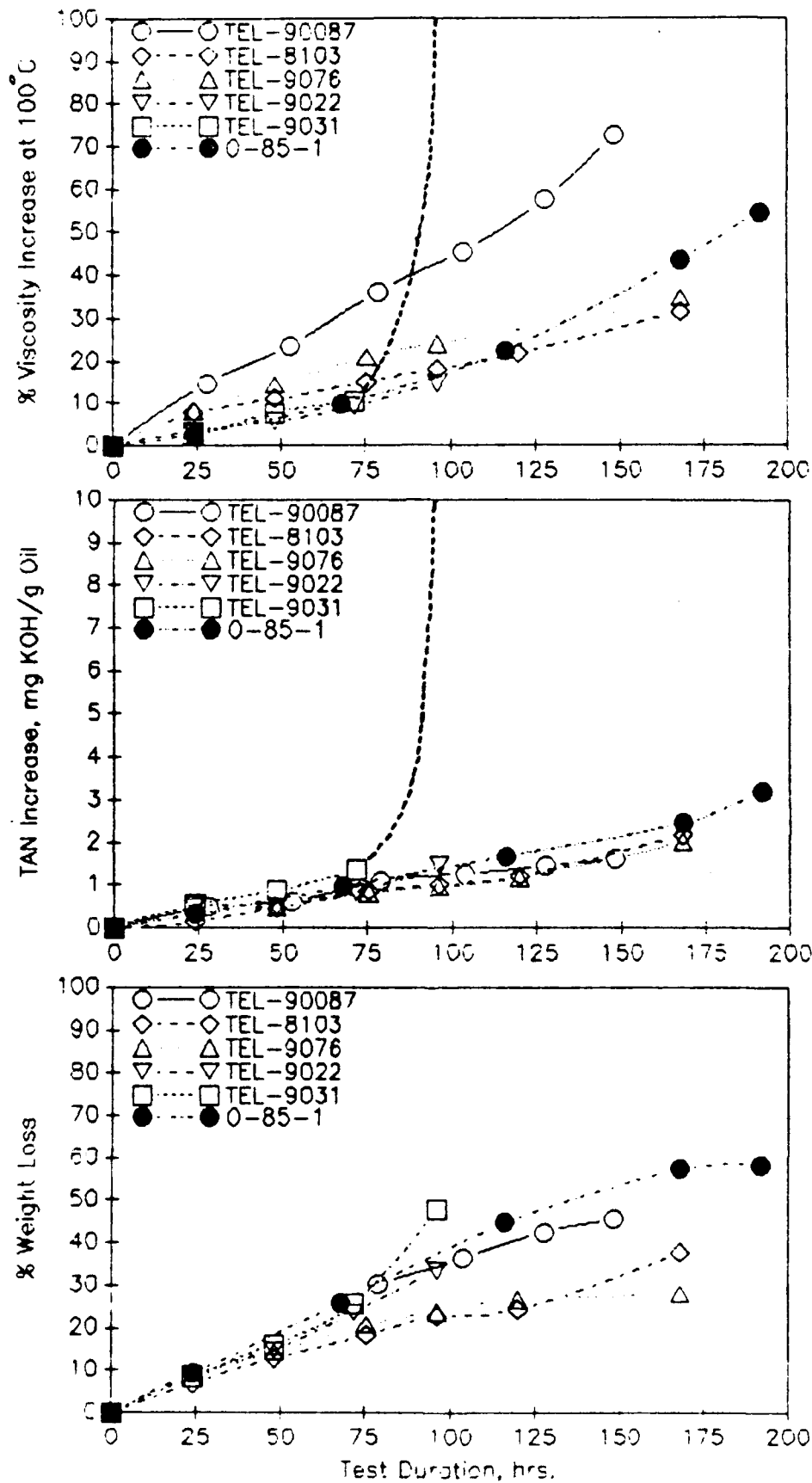


Figure 1. Squires Oxidative Stability of Various 4 cSt Fluids at 210°C

of the lighter basestock esters and is not due completely to oxidative degradation.

The percent weight losses for the various lubricants shown in Figure 1 are more scattered than either changes in viscosity or TAN especially above 75 test hours. The data show that lubricants TEL-9076 and TEL-8103 are similar and have the lowest weight loss. Lubricants O-85-1 and TEL-90087 have a greater weight loss than the above two lubricants but show a decrease in the rate of volatility which approaches a zero rate loss above 150 test hours. Lubricant TEL-9031 shows a very rapid increase in volatility above 75 test hours which is consistent with the viscosity and TAN data. Although the test data show a definite difference in volatility loss of the two groups of fluids (TEL-9076, TEL-8103 and O-85-1, TEL-90087), volatility weight loss measurements are more affected by slight differences in composition and test conditions than either viscosity changes or TAN changes. Weight loss during stability testing can be affected by small differences in basestock composition, condensate return, and test procedures such as cooling and cleaning the post test tubes when using an oil heating bath. This may be more pronounced for oxidative stability tests which require only 50 mL of test sample than the 200-mL test.

Oxidative stability data obtained at 215°C for four lubricants are shown in Figure 2. The three lubricants O-85-1, TEL-8103 and TEL-9076 show good and very similar viscosity and TAN changes. Lubricant TEL-90003 showed a continuous rapid rate of viscosity increase and a rapid increase in TAN after 75 test hours. The volatility differences between O-85-1, TEL-8103 and TEL-9076 were about the same as shown by the 210°C test data.

The oxidative stability data of TEL-90087 which have been obtained at 210°C and 225°C are shown in Figure 3. This fluid shows very good stability

SQUIRE'S OXIDATIVE @ 215 °C

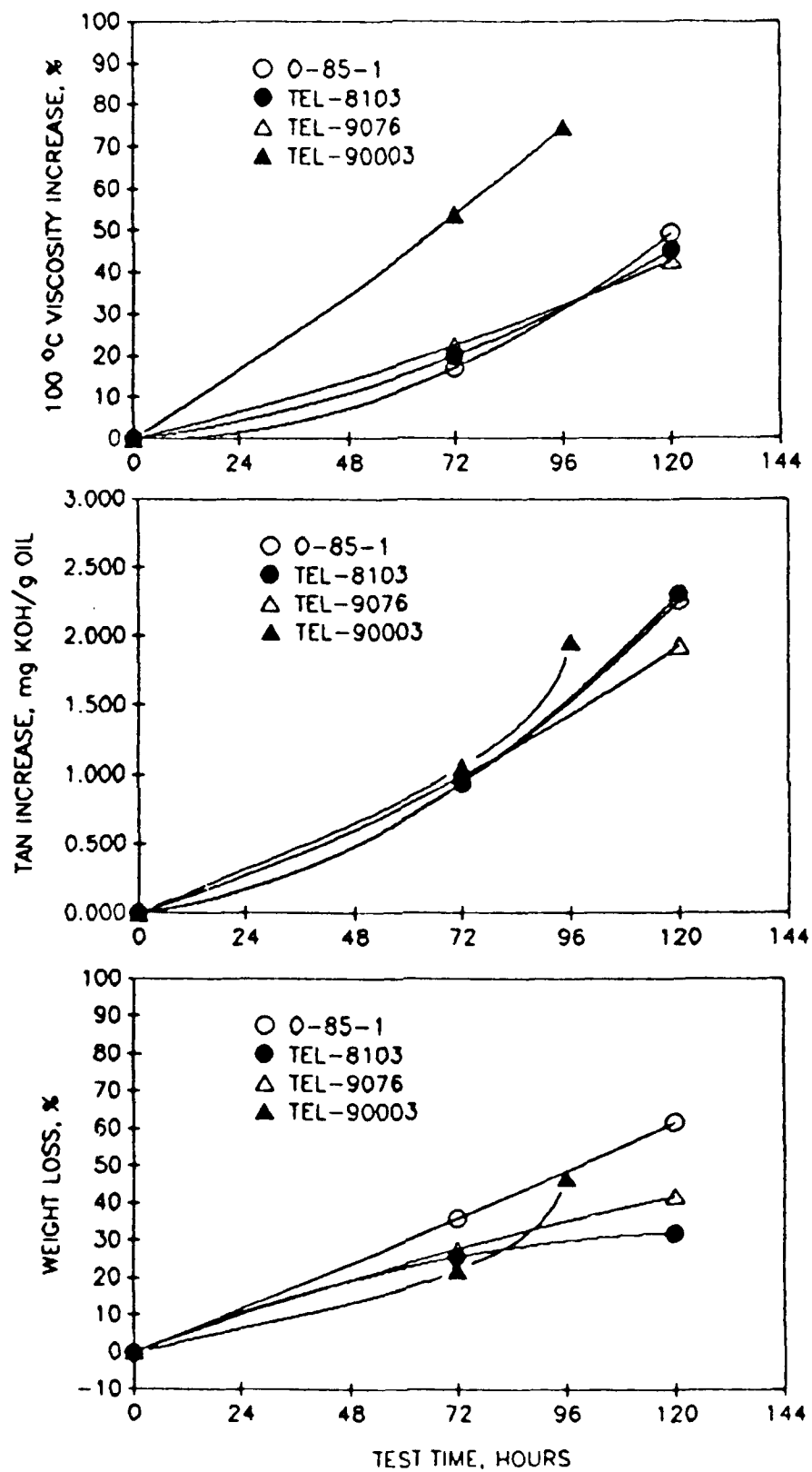


Figure 2. Squires Oxidative Stability of Various 4 cSt Fluids at 215°C

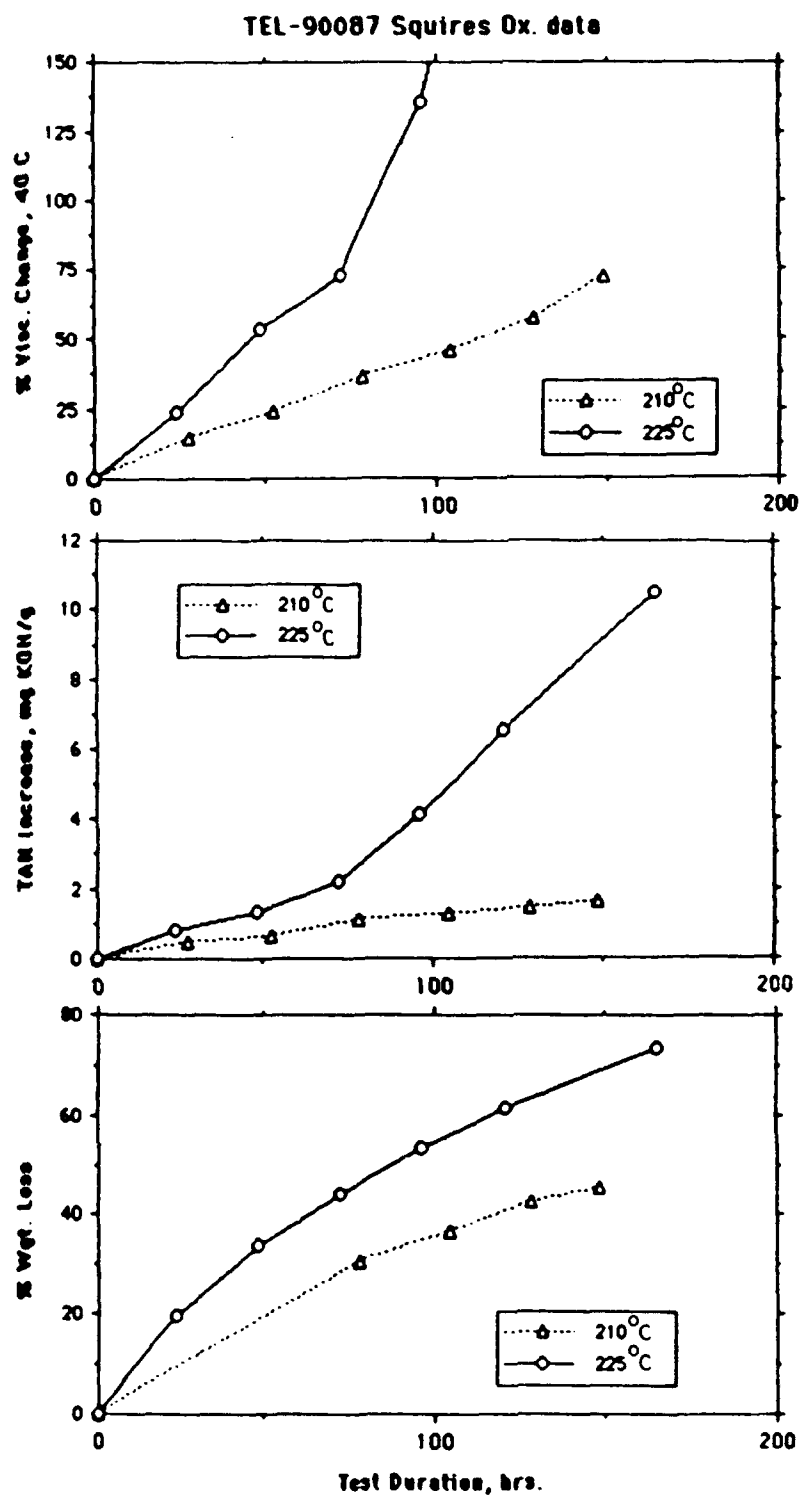


Figure 3. Squires Oxidative Stability of TEL-90087 at 210°C and 225°C

and additional testing will be conducted for the development of Arrhenius plots. The Squires oxidative data for MIL-L-7808 lubricants tested to date are listed in Appendix A.

e. Summary

The oxidative stabilities of several 4 cSt ester base candidate lubricants have been determined using the "Squires" oxidation test. With the exception of TEL-9031 and TEL-90003, the fluids showed superior oxidative stability to other ester base lubricants such as MIL-L-7808 and MIL-L-23699.

Lubricant TEL-9031 did not display the expected good oxidative stability as this fluid is a different lot of lubricant O-85-1 which has very good stability. Additional studies of TEL-9031 should be considered for identifying the reason or reasons for the poorer stability of this fluid. This information would assist in the establishing specification limits for the new 4 cSt fluids and would reduce the possibility of a problem occurring with "lot to lot" productions of these fluids.

2. LUBRICANT CORROSION AND OXIDATION STABILITY OF HIGH TEMPERATURE FLUIDS

a. Stability Testing of Fresh Polyphenyl Ethers

(1) Introduction

Polyphenyl ethers and other experimental high temperature fluids were studied with respect to their corrosion and oxidative stability and the effects of viscosity diluents on the corrosion characteristics and stability of these fluids. These investigations and evaluations included new and fresh fluids for determining their potential as high temperature lubricants, engine stressed fluids for identifying modes and degree of degradation for the development of specification tests and test limits and wear test samples for determining the effects of wear debris on fluid stability. Arrhenius curves describing effective lubricant life as a function of temperature were

developed using changes in various chemical and physical properties as limiting life values criteria for selected new fluids.

(2) Test Apparatus and Test Procedure

The test apparatus and procedures used to evaluate the high temperature fluids have been described in an earlier report.² Modifications to these procedures include testing using no condensate return and water saturated air.

(3) Test Lubricants and Test Conditions

A description of the test fluids studied under this phase of the program is given in Table 2. Normal testing of the fluids was initiated at 320°C with intermediate sampling and test times up to 264 hours. Fluids showing good stability at 320°C were evaluated at other temperatures.

(4) Arrhenius Plot Development

During this interim contract period, a new format has been adopted for the preparation and presentation of Arrhenius curves showing effective lubricant life as a function of temperature. The data points taken at selected limiting values along experimental curves are now plotted by a computer plotting package which produces more appealing graphs and computed least squares line equations. The constants from the line can lead to more accurate predictions of lubricant life at various temperatures.

Two useful formulas can be derived quite easily. With the X axis defined as temperature $1/K \times 10^3$ and Y axis as the logarithm of time, an equation for the least squares line is the slope/intercept equation:

$$\log Y = a + b X$$

where $X = 10^3/K$ or $10^3/(273.15 + ^\circ C)$ and $Y = \text{time } t$.

TABLE 2

DESCRIPTION OF TEST FLUIDS FOR LUBRICANT CORROSION
AND OXIDATIVE STABILITY STUDY OF HIGH TEMPERATURE FLUIDS

Test Lubricant	Description	Viscosity, cSt	
		40°C	100°C
O-77-6	Basestock for MIL-L-87100 Oil O-67-1	280.4	12.52
O-67-1	MIL-L-87100 Oil (5P4E)	280.3	12.61
TEL-8039	Experimental Fluid	291.2	12.77
TEL-8040	Experimental Fluid	287.9	12.79
TEL-8085	Different Lot of TEL-8039	287.3	12.76
TEL-8087	Different Lot of TEL-8040	280.5	12.58
TEL-8092	New Formulation of O-67-1 Oil	280.3	12.55
TEL-9028	Used MIL-L-87100	298.0 ¹	12.95 ¹
TEL-9029	Used MIL-L-87100	284.9	12.71
TEL-9030	Used MIL-L-87100	283.7	12.75
TEL-9038	Used MIL-L-87100	288.4	12.75
TEL-9039	Used MIL-L-87100	298.1 ²	12.92 ²
TEL-9040	Used MIL-L-87100	293.7	12.84
TEL-9050	Experimental Fluid	214.3	10.88
TEL-9069 ³	Series of Used MIL-L-87100 Samples	-	-
TEL-9070 ³	Series of Used MIL-L-87100 Samples	-	-
TEL-9071	Different Sample of TEL-9050	212.5	-
TEL-90001	Experimental Fluid	235.4	16.25
TEL-90018	Polyphenyl Ether (6P5E)	1454.2	-
TEL-90024	Inhibited TEL-9071 Fluid	195.4	10.66
TEL-90025	Used MIL-L-87100 Fluid	288.3	12.87
TEL-90026	Used MIL-L-87100 Fluid	289.3	12.75
TEL-90028	Inhibited TEL-90018 Fluid	1468.4	26.98
TEL-90059	Different Batch of TEL-90024	195.4	10.66
TEL-90063	Experimental Fluid	215.4	10.81
CB-1	Blend of Four-Ball Wear Tests ⁴	290.2	12.85
CB-2	Blend of TEL-9069 Samples (5,6,&7)	285.8	-
CB-3	Blend of TEL-9070 Samples (18 & 19)	294.7	-
WT 359	Wear Tested O-67-1 Fluid ⁵		
WT 362	Wear Tested O-67-1 Fluid ⁵		
WT 382	Wear Tested O-67-1 Fluid ⁵		
WT 386	Wear Tested O-67-1 Fluid ⁵		
WT 388	Wear Tested O-67-1 Fluid ⁵		
WT 401	Wear Tested O-67-1 Fluid ⁵		

¹After removal of 15% tetrachloroethylene

²After removal of 1.9% trichloroethylene

³Series of small SOAP samples taken from engines
at different operating times

⁴Residual sample of wear tests No. 369, 371 and 397 of O-67-1

⁵Refer to Section VI for details of wear tests

From this equation we can derive exact expressions to find the effective lubricant life knowing the temperature where:

$$t = \text{antilog} [a + b (10^3 / (273.15 + ^\circ\text{C}))] = 10^{[a + b (10^3 / (273.15 + ^\circ\text{C}))]}$$

or the temperature knowing the effective lubricant life where:

$$^\circ\text{C} = b(10^3) / (\log t - a) - 273.15$$

For example, suppose we wish to find the effective life of TEL-8092 at 350°C based upon the 25% viscosity limit (Table 3). The answer is:

$$t = 10^{[-12.08 + 8.37 (10^3 / (273.15 + 350))]} = 10^{+1.35} = 22.5 \text{ hours.}$$

Of course, one can still read the approximate value from the plot after simply converting degrees Celsius to degrees Kelvin.

One vision of the new Arrhenius plot format is to tabulate the constants a and b for lubricants based on limiting values for viscosity change, TAN increase, and weight loss. These constants could then be published or incorporated into a data base containing the necessary equations so that one could theoretically type in the desired temperature of the oil, oil property and limiting value and the effective lubricant life would be computed automatically. Appendix A lists the C&O data used for Arrhenius plots development.

(5) Stability Testing of Fresh Polyphenyl Ethers

Arrhenius plots have been developed for basestock fluid O-77-6 and formulated lubricant TEL-8092 which consist of O-77-6 basestock and 75%

relative Additive A concentration of O-67-1. These plots were developed for 15%, 25% and 35% 40°C viscosity changes and for 5%, 10% and 15% 100°C viscosity changes. No Arrhenius plots were developed for total acid number (TAN) increases or volatility loss which was done for the 4 cSt ester base oils. This is due to very low TAN increases and low volatility losses of polyphenyl ether lubricants at test temperatures up to 340°C. The Arrhenius curves are shown in Figures 4 through 9 with the test data from which these plots were made and the constants a and b from the least squares equation $\log Y = a + bX$ being summarized in Table 3. The Arrhenius plots in Figures 4 through 9 and the data in Table 3 show that the inhibited lubricant has very good oxidative stability up to and even above 325°C which is much superior to the basestock alone. These figures also show that the effective life measured by a 15%, 40°C viscosity increase is very close to the effective life measured by a 5%, 100°C viscosity increase. Likewise, the effective lubricant lives determined by the 25%, 40°C and 10%, 100°C and by the 35% 40°C and 15%, 100°C viscosities changes are also very similar.

Corrosion and oxidation test data obtained on TEL-8092 which is a fresh formulation of the MIL-L-87100 oil O-67-1 are given in Table 4 along with the test data obtained on O-67-1 for comparison.

TABLE 3

EFFECTIVE LUBRICANT LIFE OF O-77-6 AND TEL-8092
USING CORROSION AND OXIDATION TESTING, D 4871 TUBES,
INTERMEDIATE SAMPLING, AND 10 L/H AIRFLOW

15% Viscosity Limit at 40°C

Test Hours	Fluid O-77-6	Fluid TEL-8092
290	53	-
300	26	-
310	16	-
320	-	67
330	-	38
340	-	21
a*	-13.47	-13.61
b*	8.55	9.16

25% Viscosity Limit at 40°C

Test Hours	Fluid O-77-6	Fluid TEL-8092
290	70	-
300	35	-
310	22	-
320	-	104
330	-	66
340	-	36
a*	-12.84	-12.08
b*	8.26	8.36

*Constants for Equation $\log Y = a + bX$ where $Y = \text{time}$, $X = \text{temperature}$

35% Viscosity Limit at 40°C

Test Hours	Fluid O-77-6	Fluid TEL-8092
290	89	-
300	47	-
310	27	-
320	-	140
330	-	90
340	-	48
a	-13.16	-12.07
b	8.51	8.44

TABLE 3 (CONCLUDED)

5% Viscosity Limit at 100°C

Test Hours	Fluid O-77-6	Fluid TEL-8092
290	42	-
300	23	-
310	14	-
320	-	36
330	-	24
340	-	15
a	-12.30	-10.09
b	7.84	6.91

10% Viscosity Limit at 100°C

Test Hours	Fluid O-77-6	Fluid TEL-8092
290	68	-
300	36	-
310	22	-
320	-	76
330	-	57
340	-	28
a	-12.48	-11.3
b	8.0	7.86

15% Viscosity Limit at 100°C

Test Hours	Fluid O-77-6	Fluid TEL-8092
290	89	-
300	47	-
310	29	-
320	-	130
330	-	86
340	-	48
a	-12.27	-11.12
b	8.00	7.86

15 % Viscosity Limit at 40°C

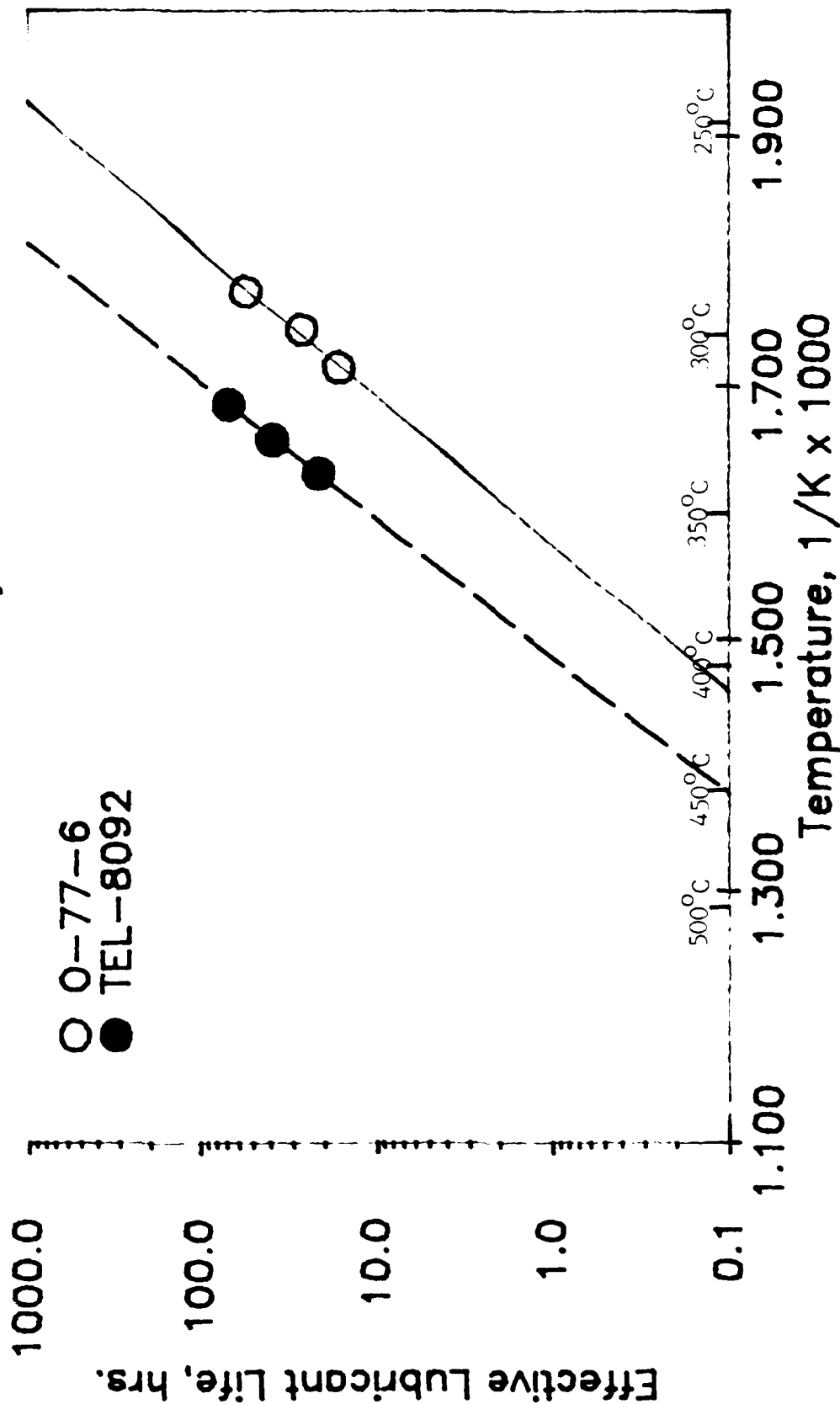


Figure 4. Effect of Temperature on Lubricant Life Using Corrosion and Oxidation Testing and a 15% Viscosity Increase Limit (40°C) for High Temperature Fluids

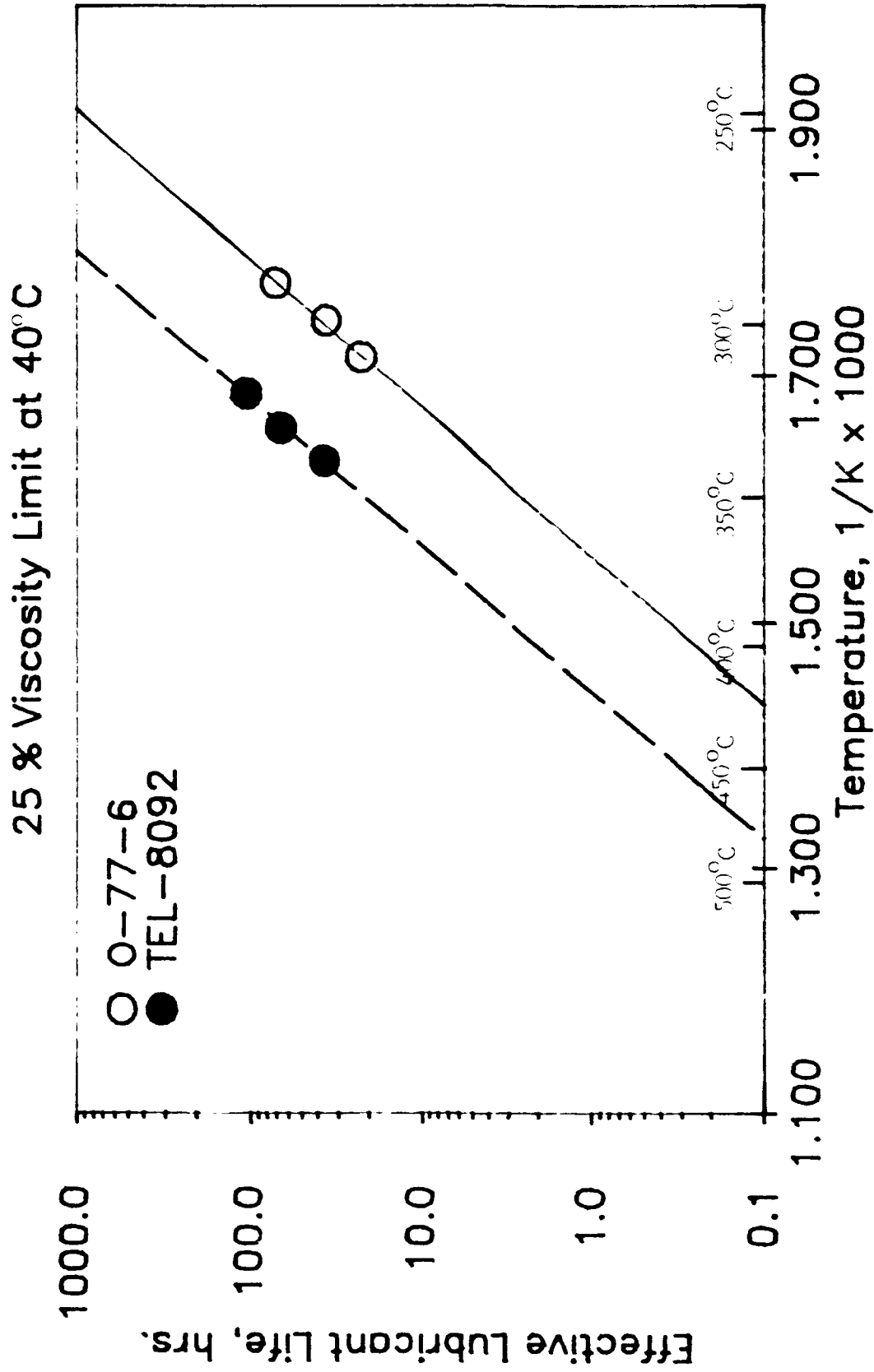


Figure 5. Effect of Temperature on Lubricant Life Using Corrosion and Oxidation Testing and a 25% Viscosity Increase Limit (40°C) for High Temperature Fluids

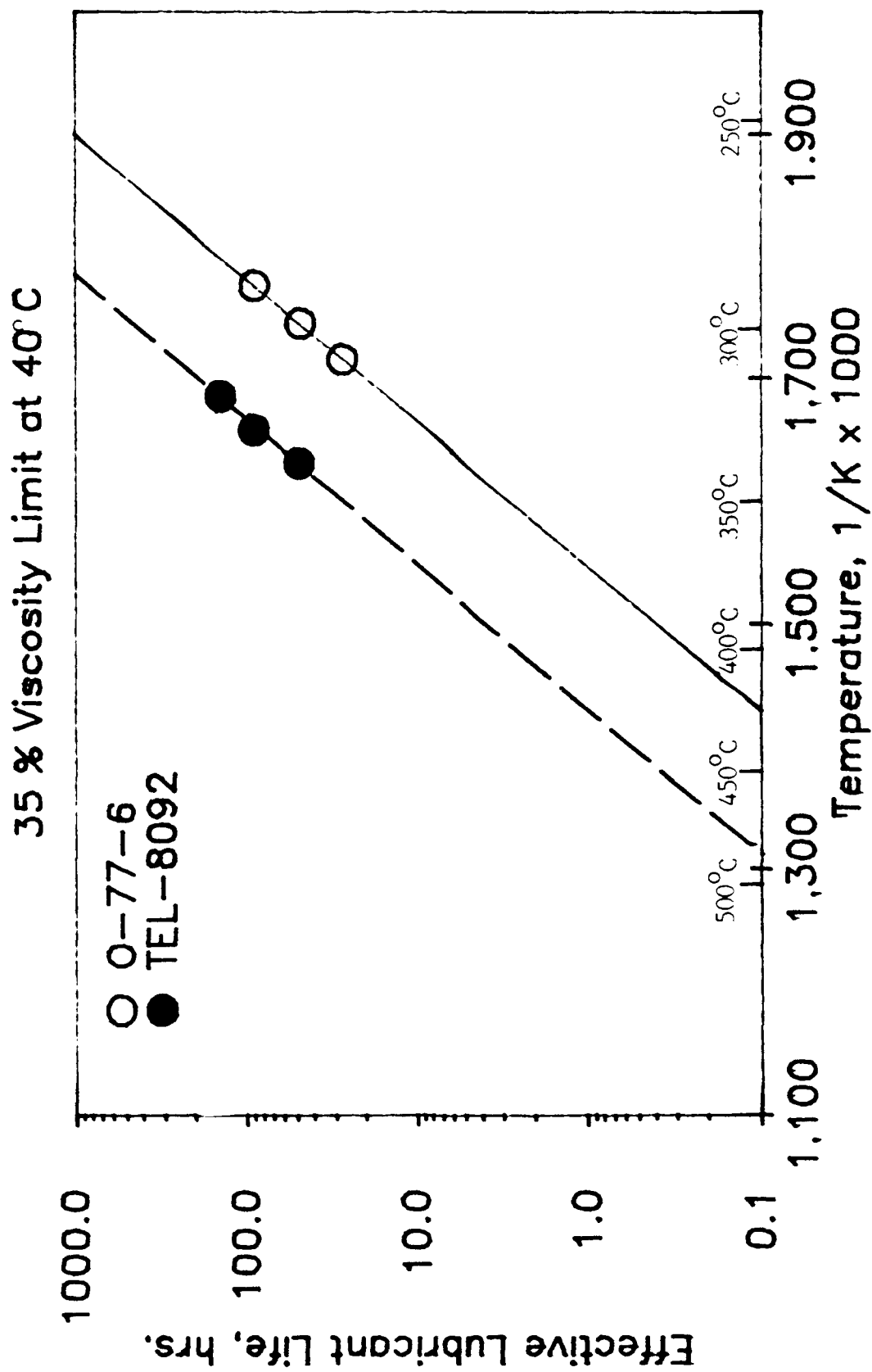


Figure 6. Effect of Temperature on Lubricant Life Using Corrosion and Oxidation Testing and a 35% Viscosity Increase Limit (40°C) for High Temperature Fluids

5 % Viscosity Limit at 100°C

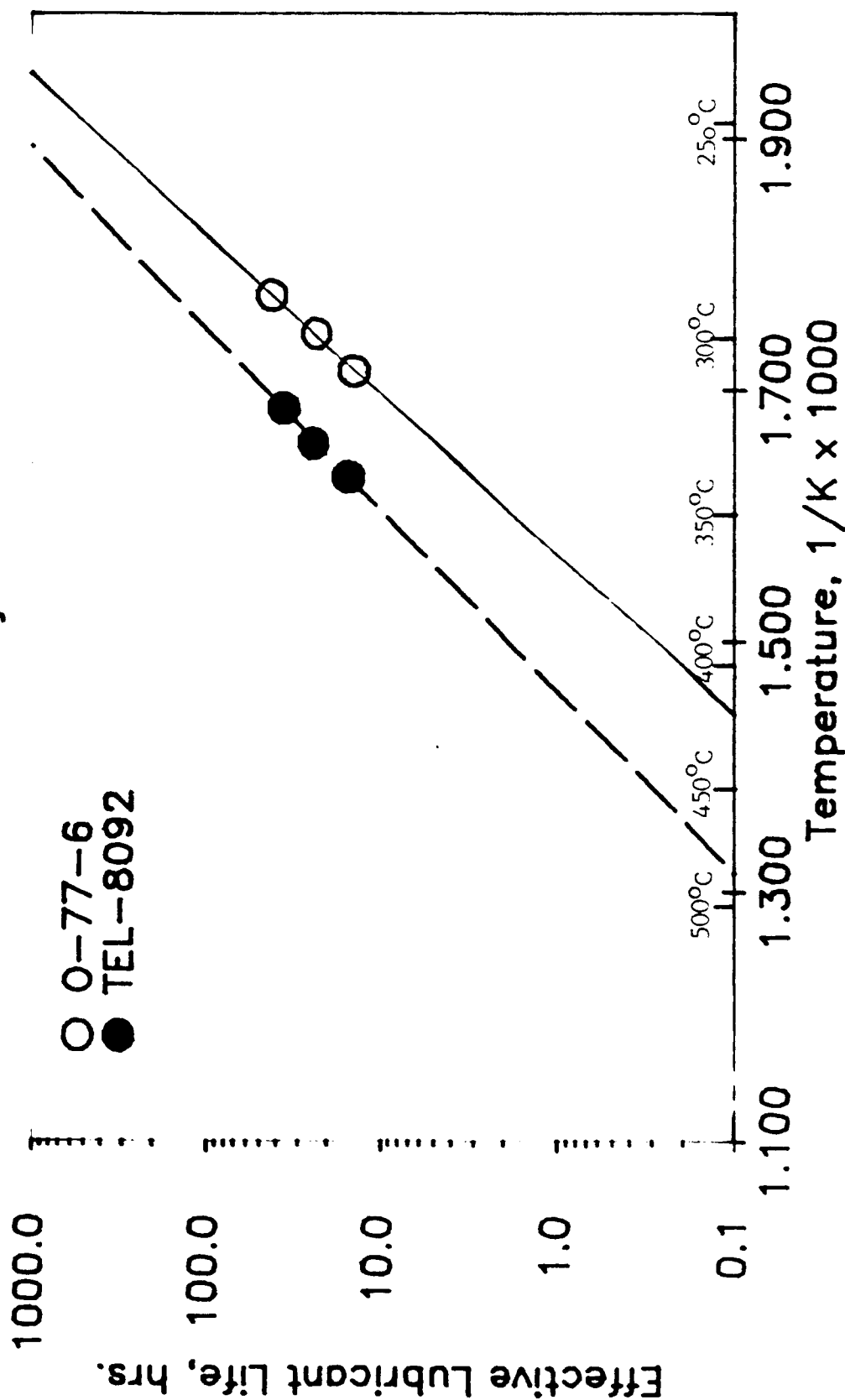


Figure 7. Effect of Temperature on Lubricant Life Using Corrosion and Oxidation Testing and a 5% Viscosity Increase Limit (100°C) for High Temperature Fluids

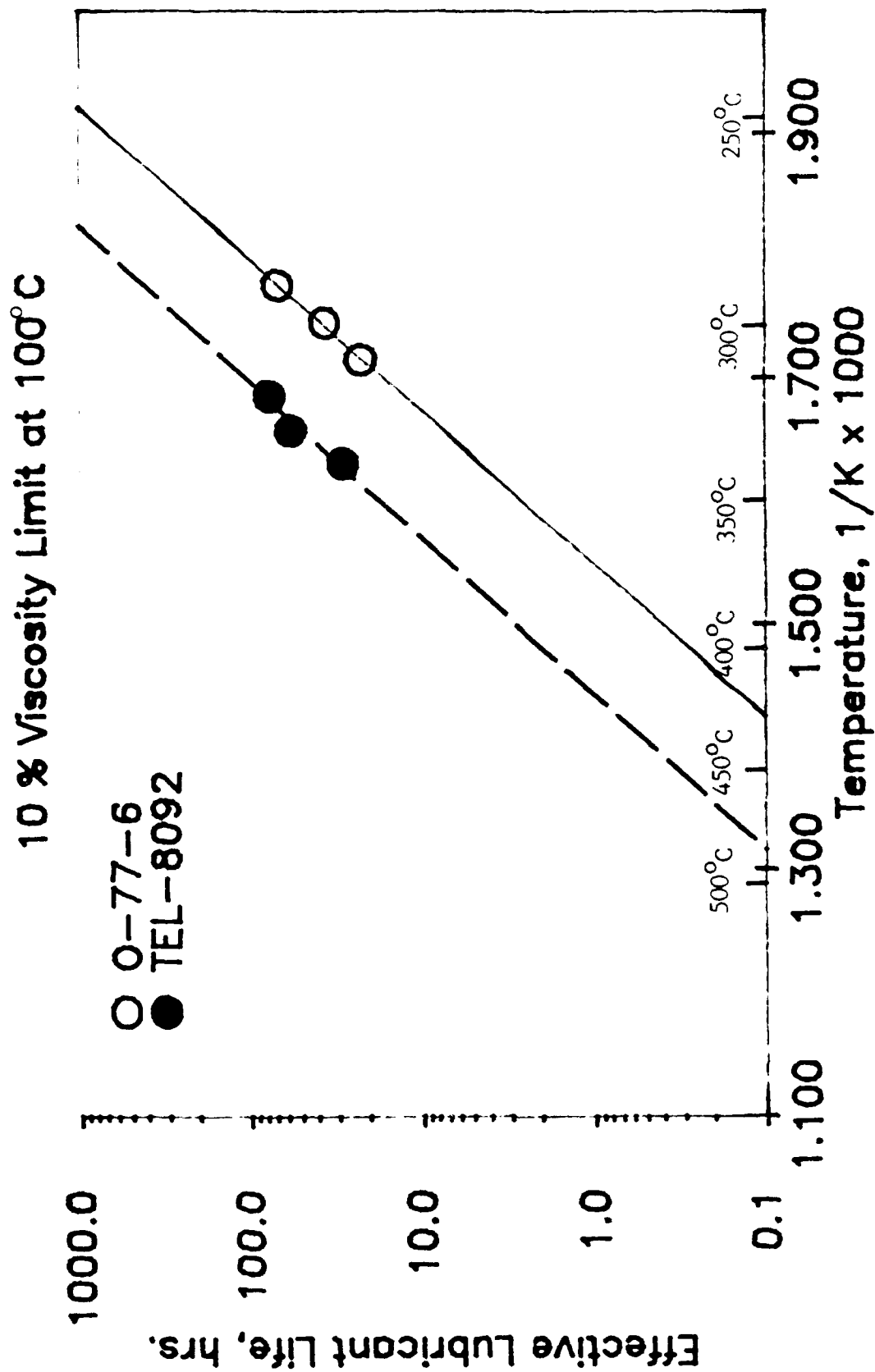


Figure 8. Effect of Temperature on Lubricant Life Using Corrosion and Oxidation Testing and a 10% Viscosity Increase Limit (100°C) for High Temperature Fluids

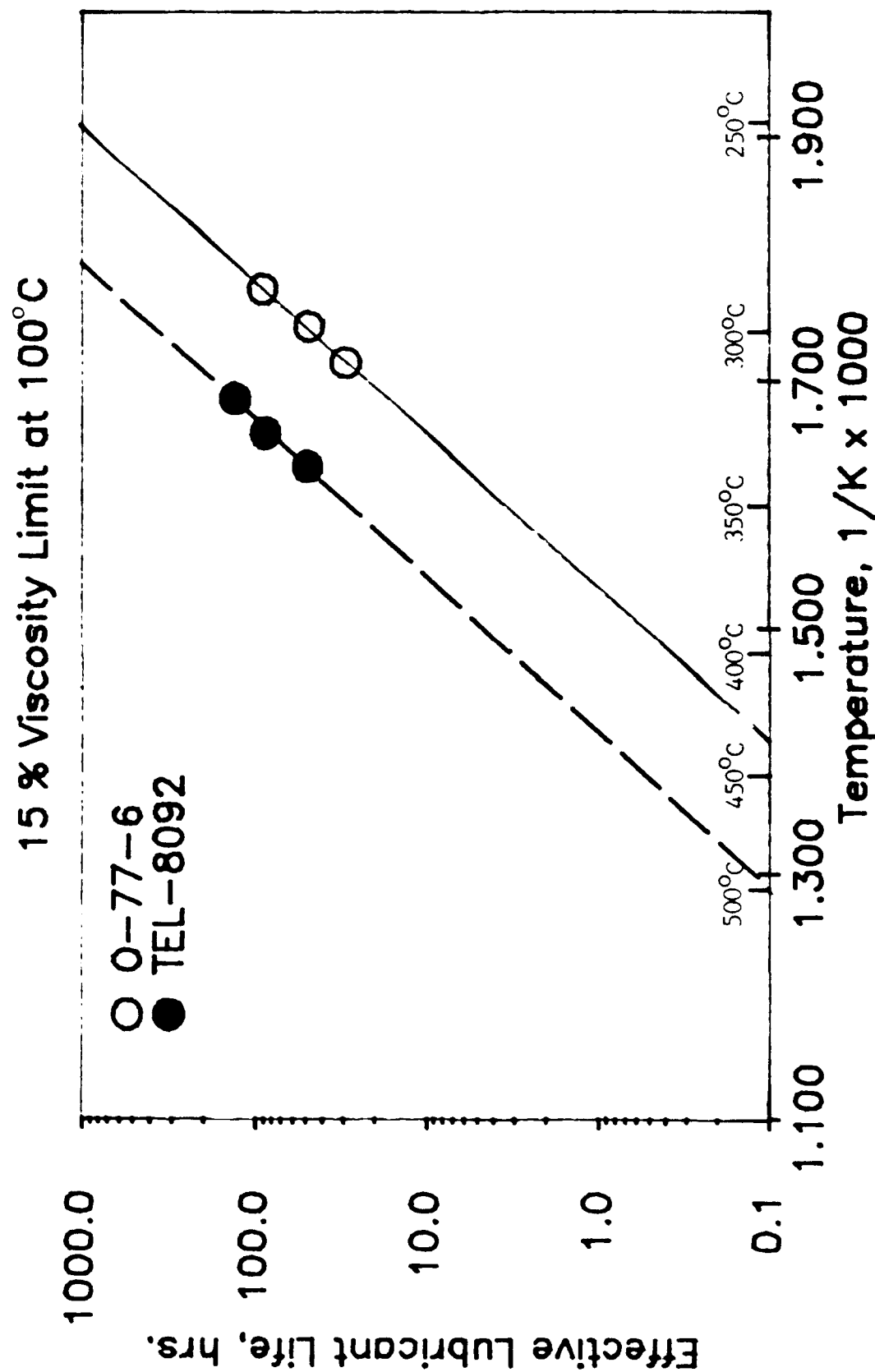


Figure 9. Effect of Temperature on Lubricant Life Using Corrosion and Oxidation Testing and a 15% Viscosity Increase Limit (100°C) for High Temperature Fluids

TABLE 4

CORROSION AND OXIDATION TEST DATA FOR LUBRICANTS
 TEL-8092 AND O-67-1 AT 320°C USING 10 L/H AIRFLOW
 100 ML SAMPLE, D 4871 TUBES AND INTERMEDIATE SAMPLING

Test Hours	Lubricant TEL-8092				O-67-1			
	Vis., 40°C	% Chg 40°C	Vis., 100°C	% Chg 100°C	Vis., 40°C	% Chg 40°C	Vis., 100°C	% Chg 100°C
0	280.3	-	12.55	-	280.4	-	12.61	-
24	312.2	11.4	13.21	5.3	308.5	9.9	13.11	4.0
48	331.3	18.2	13.59	8.3	322.0	14.7	13.42	6.4
72	356.1	27.0	14.11	12.4	337.7	20.3	13.68	8.5
96 ²	385.5	37.5	14.63	16.0	353.0	25.7	13.97	10.8
120 ²	431.6	54.0	15.35	22.0	419.2 ^{1,2}	49.3	15.1	19.8

¹168 Test Hours

²Corrosion values all less than 0.1 mg/cm² for all metals

The data in Table 4 show that lubricant TEL-8092 has very good oxidative stability with the stability being only slightly lower than fluid O-67-1. This is most probably due to test repeatability and different additive content between the two fluids.

Lubricant O-67-1 was stressed using the normal corrosion-oxidation test at 320°C without condensate return. The test was run for 264 hours in D 4871 tubes with 100 mL sample size and intermediate sampling. The condensate was collected and analyzed using gas chromatography/mass spectrometry (GC/MS) with the results to be discussed later. Viscosity measurement at 40°C indicated that the condensate is 13% lower than the viscosity of fresh O-67-1 yielding a value of 243.2 cSt. Figure 10 gives a comparison of the O-67-1 C&O tests at 320°C with and without condensate return. These data indicate that the loss of volatiles from the lubricant improves the oxidative stability of O-67-1 as measured by viscosity increase. No corrosion was observed on any of the specimens.

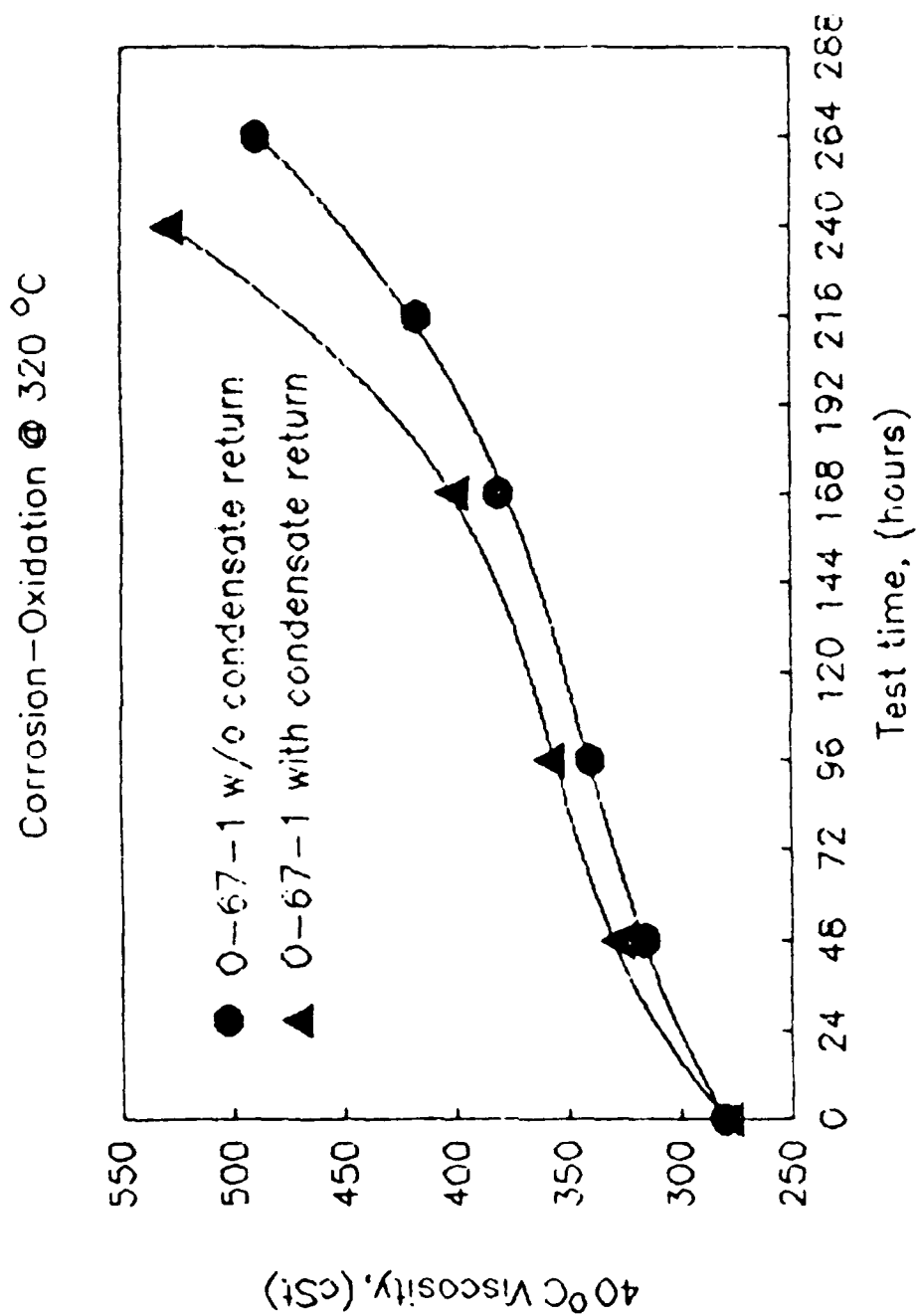


Figure 10. Viscosity Increase vs. Test Time of O-67-1 After C&O at 320°C with and without Condensate Return

Corrosion and oxidation testing of the 5P4E lubricant O-67-1 was conducted using D 4871 tubes, intermediate sampling and 10 L/h moist air flow (saturated at 20°C) at a temperature of 320°C. The data are plotted in Figure 11 along with corrosion and oxidation results of an identical test of O-67-1 using dry air. During the test, water dripped from the condenser onto the hot lubricant and hot glass surfaces causing the oil to sputter on the side of the tube. As a result heavy varnish and coke were observed on the blower tube and tube wall. Also black coke was observed on the inside of the blower tube. Figure 11 shows that the presence of water in the oxidizing air decreases the oxidation stability of the lubricant dramatically. It is interesting to note that the two curves are almost identical up to the 24 hour time point. It is highly probable that after 24 hours sufficient water had accumulated on the condenser that it started to drip into the oil. Significant corrosion of the silver metal specimen was also observed while none was observed using dry air. This indicates that water (vapor or liquid) significantly decreases the stability of O-67-1.

Corrosion and oxidation testing was conducted on polyphenyl ether lubricant TEL-90028 which is a 6P5E formulated fluid. Testing was conducted at 310°C and 320°C using 10 L/h airflow, 100 mL sample and D 4871 tubes. Table 5 gives the 320°C corrosion and oxidation test data for the lubricant TEL-90028 and for the MIL-L-87100 lubricant O-67-1 for comparative purposes.

O-67-1 air/moist air C & O test

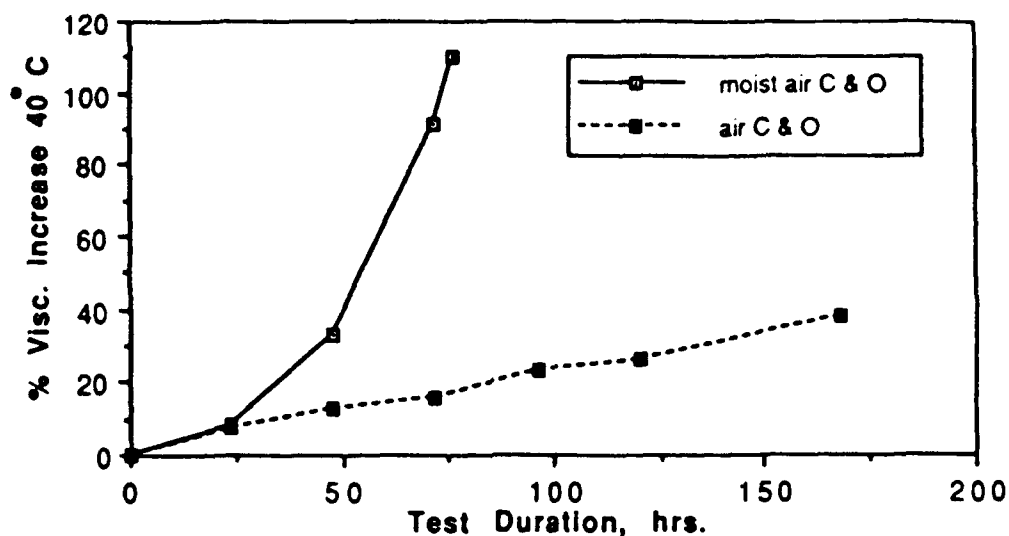


Figure 11. 40°C Viscosity Change During Corrosion and Oxidation Testing of O-67-1 at 320°C Using D 4871 Tubes, 10 L/H Airflow (Both Moist and Dry) and Intermediate Sampling.

TEL-90028 C & O Test

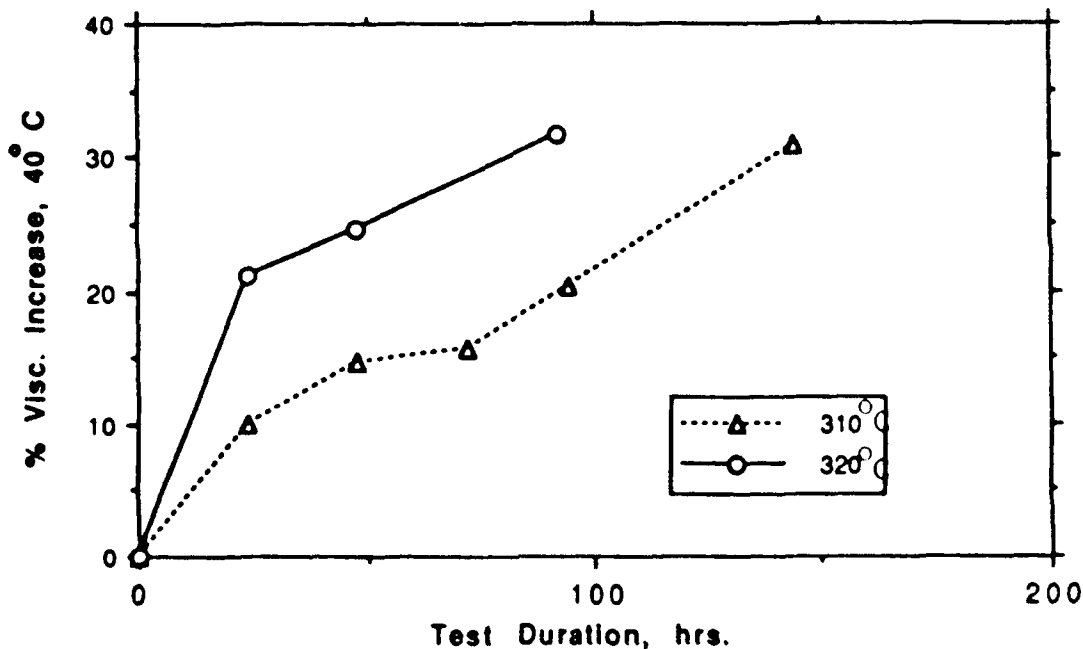


Figure 12. 40°C Viscosity Change During Corrosion and Oxidation Testing of TEL-90028 Using D 4871 Tubes, 10 L/H Airflow and Intermediate Sampling.

TABLE 5

CORROSION AND OXIDATION TEST DATA FOR LUBRICANTS
TEL-90028 AND O-67-1 AT 320°C USING 10 L/H
AIRFLOW, 100 ML SAMPLE AND D 4871 TUBES

Test Time Hours	Lubricant			
	O-67-1		TEL-90028	
	Visc., 40°C	% Visc., Chg 40°C	Visc., 40°C	% Visc. Chg 40°C
0	280.4	-	1468.4	-
24	308.5	9.9	-	- (9.9)*
48	322.0	14.7	1780.3	21.2 (14.6)*
72	337.7	20.3	1827.6	24.5 (15.7)*
96	352.0	25.7	1934.6	31.7 (20.4)*

*Data for 310°C Test Temperature

No significant corrosion (all values were less than 0.1 mg/cm²) occurred for any metal coupon for either of the two lubricants. Figure 12 shows the change in 40°C viscosity during the corrosion and oxidation testing of TEL-90028 at 310°C and 320°C which shows a significant increase in viscosity change between 320°C and 310°C (approximately 50 hour life versus 125 hour life using a 25% viscosity increase limit). Although the 6P5E based lubricant showed good stability, it does not provide improvement over the MIL-L-87100 lubricants. Also the 6P5E fluids have higher initial viscosities than the 5P4E fluids.

Experimental 5P4E inhibited lubricants TEL-8039 and TEL-8040 were investigated by C&O testing at 320°C using D 4871 tubes and intermediate sampling with the test data being previously reported.² This data showed that these two fluids possessed improved oxidative stability when compared to TEL-8092 and O-67-1 (MIL-L-87100) lubricants. Due to insufficient quantities of these fluids, new samples were obtained for additional testing and coded

TEL-8085 (same formulation as TEL-8039) and TEL-8087 (same formulation as TEL-8040). Tables 6 and 7 show comparative 320°C C&O test data for these fluids. Little difference is shown in the oxidative stability of the different lots of the same fluid. Neither of the four fluids showed significant corrosion for any of the metal corrosion test specimens. However, testing at 330°C showed a much greater stability for fluid TEL-8085 than for fluid TEL-8039 as is shown in Table 8. Corrosion and oxidation test data obtained at 340°C for fluids TEL-8085 and TEL-8087 are given in Table 9 along with equivalent test data for the TEL-8092 lubricant. These data show that the oxidative stability of TEL-8085 and TEL-8087 is approximately twice that of TEL-8092. Samples TEL-8039, TEL-8040, TEL-8085 and TEL-8087 became cloudy upon storage and after being exposed to air. Subsequent investigation identified this cloudiness was due to absorption of moisture from the air. This also caused precipitation of material from the samples after various time periods. During the 340°C C&O testing considerable sludge developed in the post test TEL-8085 fluid and in the post test TEL-8087 fluid after cooling and standing a few days.

Corrosion and oxidation testing of TEL-8087 at 320°C using a D 4871 tube with intermediate sampling was conducted using moist (saturated) air with the test data being given in Table 10.

TABLE 6

CORROSION AND OXIDATION DATA FOR
LUBRICANTS TEL-8039 AND TEL-8085
@ 320°C, USING D 4871 TUBES AND
INTERMEDIATE SAMPLING

Lubricant	Test Hours	Viscosity @ 40°C, cSt	Viscosity Chg @ 40°C, %	Viscosity @ 100°C, cSt	Viscosity Chg @ 100°C, %		
TEL-8039	0	291.2	-	12.77	-		
	144	334.4	14.8	13.49	5.6		
	240	362.5	24.5	13.92	9.0		
	336	393.9	35.3	14.53	13.8		
	408	421.7	44.8	14.95	17.1		
TEL-8085	0	287.3	-	12.76	-		
	120	337.5	17.5	13.62	6.7		
	218	362.7	26.2	14.01	9.8		
	288	383.0	33.3	14.41	12.9		
	337	399.1	38.9	14.61	14.5		
Corrosion Data, mg/cm ²							
Lubricant	Test Hours	Aluminum	Silver	Mild Steel	M-50 Steel	Waspaloy	Titanium
TEL-8039	408	-0.02	-0.04	+0.16	+0.04	-0.04	0.00
TEL-8085	337	+0.18	+0.18	+0.34	+0.24	+0.18	+0.20

TABLE 7

CORROSION AND OXIDATION DATA FOR
LUBRICANTS TEL-8040 AND TEL-8087
@ 320°C, USING D 4871 TUBES
AND INTERMEDIATE SAMPLING

Lubricant	Test Hours	Viscosity @ 40°C, cSt	Viscosity Chg @ 40°C, %	Viscosity @ 100°C, cSt	Viscosity Chg @ 100°C, %
TEL-8040	0	287.9	-	12.79	-
	144	335.8	16.6	13.56	6.0
	240	363.0	26.1	13.95	9.1
	336	407.1	41.4	14.76	15.4
	408	433.0	50.4	15.19	18.8
TEL-8087	0	280.5	-	12.58	-
	120	324.3	15.6	13.36	6.2
	218	346.7	23.6	13.74	9.2
	288	365.0	30.1	14.08	11.9
	337	377.6	34.6	14.31	13.8

Corrosion Data, mg/cm²

Lubricant	Test Hours	Aluminum	Silver	Mild Steel	M-50 Steel	Waspaloy	Titanium
TEL-8040	408	-0.04	+0.02	+0.20	+0.08	0.00	0.00
TEL-8087	337	+0.18	+0.20	+0.38	+0.24	+0.16	+0.18

COMPARISON OF CORROSION AND OXIDATION TEST DATA FOR LUBRICANTS TEL-8039 AND TEL-8085 AT 330°C, D 4871 TUBES, INTERMEDIATE SAMPLING, 10 L/H AIRFLOW

	TEL-8039						TEL-8085					
	0 h	48 h	96 h	168 h	192 h	0 h	48 h	96 h	168 h	216 h	240 h	
Visc. @ 40°C	291.2	336.2	376.0	421.3	433.7	287.3	306.7	327.0	362.5	390.2	408.0	
Visc. Inc. @ 40°C	-	15.4	29.0	44.7	48.9	-	6.8	13.8	26.2	35.8	42.0	
Visc @ 100°C	12.77	13.53	14.25	14.94	15.05	12.76	13.03	13.39	14.02	14.50	14.76	
Visc. Inc. @ 100°C	-	6.0	11.6	17.0	17.8	-	2.1	4.9	9.9	13.6	15.7	

Corrosion of
Metal Specimens,
mg/cm

	192 h Test Time	240 h Test Time
A1	+0.02	A1 0.0
Ag	+0.10	Ag -0.04
MST	+0.16	MST +0.26
M50	+0.06	M50 +0.14
Wasp	+0.02	Wasp +0.04
Ti	+0.02	Ti +0.06

TABLE 4

CORROSION AND OXIDATION DATA
FOR LUBRICANTS TEL-8085, TEL-8087 AND TEL-8092
AT 340°C, @ 4871 TUBES, INTERMEDIATE SAMPLING,
10 L/H AIRFLOW

Lubricant	Test Hours	Viscosity @ 40°C, cSt	Viscosity Chg @ 40°C	Viscosity @ 100°C	Viscosity Chg @ 100°C
TEL-8085	0	287.3	-	12.76	-
	24	309.1	7.6	13.12	2.8
	48	331.2	15.2	13.50	5.8
	72	354.6	23.4	13.75	7.8
	96	377.6	31.4	14.27	11.8
TEL-8087	0	280.5	-	12.58	-
	24	314.6	12.1	13.19	4.8
	48	339.3	31.0	13.60	8.1
	72	366.9	30.7	14.13	12.3
	96	390.4	39.2	14.51	15.3
TEL-8092	0	280.3	-	12.55	-
	24	328.1	17.0	13.52	7.7
	48	375.2	33.9	14.45	15.1
	72	478.8	70.8	16.00	27.5

Corrosion Test Data, mg/cm²

Lubricant	Test Hours	Aluminum	Silver	Mild Steel	M-50 Steel	Waspalloy	Titanium
TEL-8085	192	0.00	-0.06	+0.20	+0.10	0.00	+0.02
TEL-8087	192	-0.02	-0.10	+0.22	+0.08	+0.02	-0.02
TEL-8092	144	0.00	-0.04	+0.10	+0.06	0.00	-0.02

TABLE 10

CORROSION AND OXIDATION TEST DATA FOR FLUID
TEL-8087, 320°C, 10 L/H AIRFLOW, INTERMEDIATE
SAMPLING AND USING MOIST (SATURATED) AIR

Test Hours	Viscosity at 40°C		Viscosity at 100°C	
	cSt	% Change	cSt	% Change
0	280.5	-	12.58	-
24	300.0	7.0	12.97	3.1
48	309.8	10.4	13.26	5.4
72	314.7	12.2	13.21	5.2

Corrosion of Metal Specimens, mg/cm²

Al	Ag	M. Steel	M-50	Waspaloy	Ti
+0.06	+0.30	+0.08	-0.02	-0.06	-0.04

The change in viscosity does not indicate that moist air increases the rate of degradation or the corrosion characteristics of fluid TEL-8087 as it did the O-67-1 fluid (Figure 11). Furthermore, varnish and coke formation were not observed on the blower tube and tube wall as compared with O-67-1.

(6) Summary

Corrosion and oxidation studies of various high temperature 5P4E lubricants have been completed. A wide variation in lubricant stability has been found along with the identification of fluid properties and test parameters which greatly affect lubricant stability. The Arrhenius plots presented showed lubricant life as a function of temperature using preestablished limiting life criteria for those lubricants showing good oxidative and storage stability.

A MIL-L-87100 type lubricant TEL-8092 showed very good oxidative stability and corrosion characteristics up to and above 325°C with the stability being close to MIL-L-87100 type lubricant coded O-67-1. Testing of

O-67-1 with and without condensate return showed that the loss of volatiles from the lubricant improves the oxidative stability as measured by viscosity increase. Stability testing of O-67-1 with moist air gave a large increase in the rate of degradation and significant silver corrosion which did not occur for lubricant TEL-8087.

Two experimental 5P4E inhibited lubricants TEL-8039 and TEL-8040 showed superior oxidative stability to O-67-1 or TEL-8092 when new, but had poor low temperature storage stability with the fluid oxidative stability decreasing with storage time.

b. Lubricant Analysis of Polyphenyl Ethers

(1) Introduction

Previously, the oxidation chemistry of polyphenyl ether had been investigated.² It had been shown that the oxidation products of O-67-1 (inhibited 5P4E) and O-77-6 (5P4E basestock) were higher molecular weight compounds consisting of a biphenylated dimer (HMW-1) and a complex mix of oxygenated higher molecular weight compounds (HMW-2). It was also shown that the tin containing antioxidant in O-67-1 quickly degraded during corrosion/oxidation testing to SnO_2 , which appeared to be the true antioxidant.

Reported here is further work on the characterization of the SnO_2 antioxidant by ^{119}Sn Mossbauer spectroscopy, investigation into the oxidation chemistry of a new PPE lube (TEL-8039) and correlation of oxidation product concentration in oxidized PPEs to viscosity increases in the lubricant.

(2) ^{119}Sn Mossbauer Analysis of Oxidized O-67-1

The ^{119}Sn Mossbauer spectroscopy analysis of a 24 hour C&O test sample at 320°C of O-67-1 revealed that the SnO_2 was the only tin containing

species in the lubricant.² It was also noted that throughout the 240 hour C&O test an acceleration in viscosity increase occurred and that this acceleration could be due to either a lessening efficiency of the antioxidant or to an instability of the oxidation products (HMW-2) that accumulate in the fluid. The ¹¹⁹Sn Mossbauer spectra of O-67-1 after 24, 120 and 240 hours of C&O testing at 320°C (Figure 13) reveals no detectable changes in the composition of the tin compounds in the lubricant. Because of the large penetrating depth of the gamma rays used in this technique, the Mossbauer signal will be a product of all the tin in the tin oxide particles and not just the surface. Therefore, it cannot be absolutely stated that no changes in the surface of the tin oxide, such as surface fouling by absorption of polar degradation products, are occurring. Nevertheless, there is no evidence to suggest that the antioxidant in O-67-1 is losing efficiency during C&O testing.

(3) GPC Analysis of TEL-8039 and TEL-8040

Two new PPE lubricants, TEL-8039 and TEL-8040, which have a similar 5P4E basestock as O-67-1 but possess a different antioxidant, displayed superior performance to O-67-1 in corrosion/oxidation testing.² GPC analysis of the 408 hour 320°C C&O test sample of TEL-8039 reveals that the antioxidant in this lubricant apparently inhibits the uptake of oxygen in the lubricant as evidenced by the lack of HMW-2 in the chromatogram (Figure 14). Since the dimer (HMW-1), which is the main oxidation product in TEL-8039, would be expected to be very stable, due to the bond strength of the biphenyl linkage, this would explain the linear increases in viscosity versus C&O stressing time for this lubricant.

(4) GPC Area Summation of Oxidized PPEs

The relationship between the high molecular weight oxidation

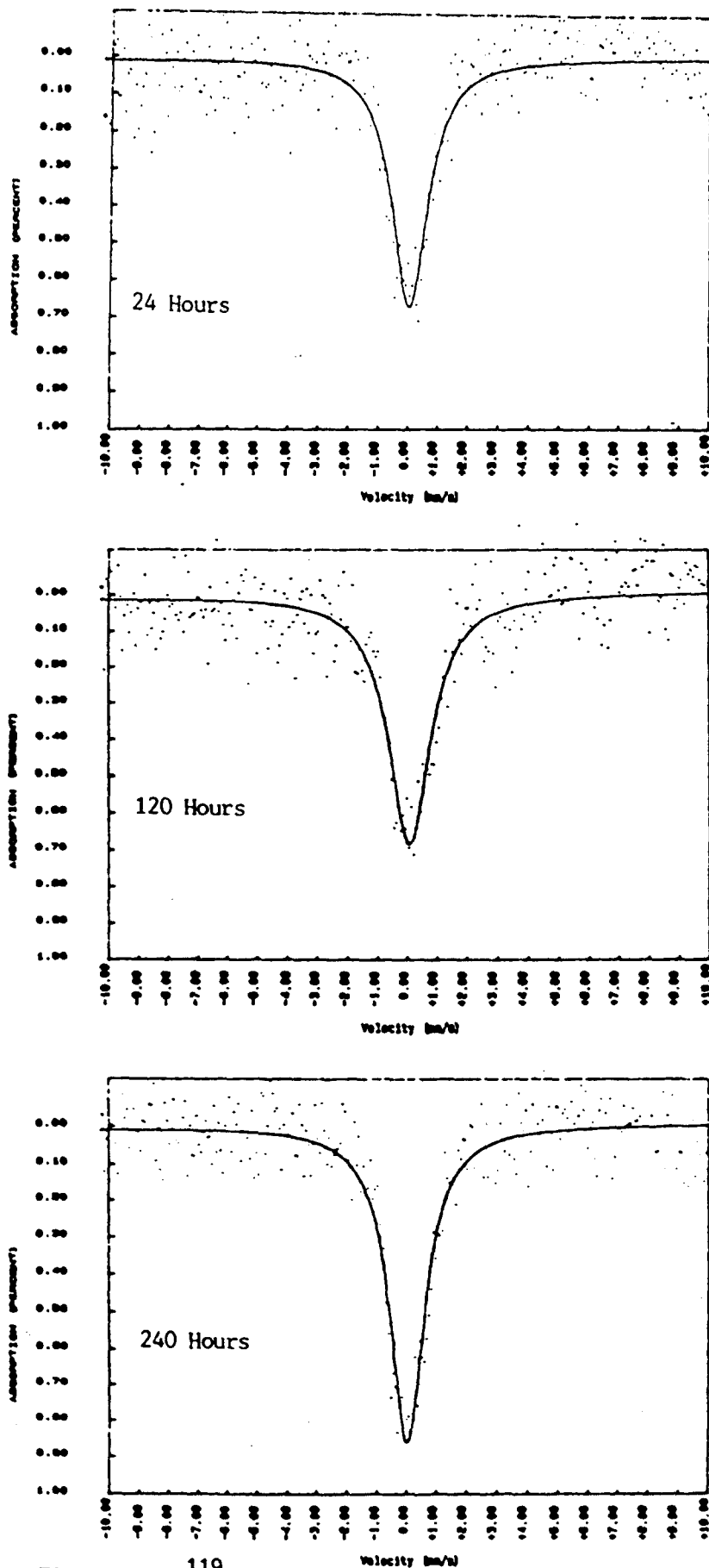


Figure 13. ^{119}Sn Mossbauer Spectra of the 24, 120 and 240 Hour Samples from the Corrosion and Oxidation Test of O-67-1 at 320°C

content and the viscosity increases of C&O tested O-67-1 and TEL-8039 was investigated by the area summation of HMW-1 and HMW-2 by GPC (See Figure 14). As anticipated, the GPC area summations versus time for both lubricants stressed at 320°C (Figure 15), show identical trends to their respective viscosity increases. The effect of these oxidation products on viscosity can be shown by a plot of GPC area summation versus the 40°C kinematic viscosity (Figure 16). It is observed that a linear relationship occurs for all but the highest viscosity sample. Furthermore, the nearly equivalent slopes for both lubricants indicate that the difference in the molecular weight distribution of the oxidation products of the two lubricants does not change their quantitative effect on viscosity increase. The difference in the y intercept is very likely due to differences in the extinction coefficients of the various compounds since UV detection was used. Similar behavior is observed with the 100°C viscosity (Figure 17) with the exception that the difference in y intercept between the two lubricants is noticeably larger. This may be due to a slight viscosity index effect at this temperature. These data explain why a linear relationship had been found between the fluorescence of oxidized PPEs (which should be proportional to oxidation product concentration) and the viscosity increases of the lubricants (see Task III). These data also indicate that viscosity measurements on these fluids are good indicators of lubricant degradation except possibly at very high viscosity increases.

c. Vapor Phase Corrosion of O-67-1

Vapor phase corrosion characteristics of MIL-L-87100 lubricant O-67-1 were investigated by using two sets of corrosion test metal specimens, one set being immersed in the stressed fluid and the second set supported by a 17 cm glass spacer positioned in the vapor phase directly below the tapered

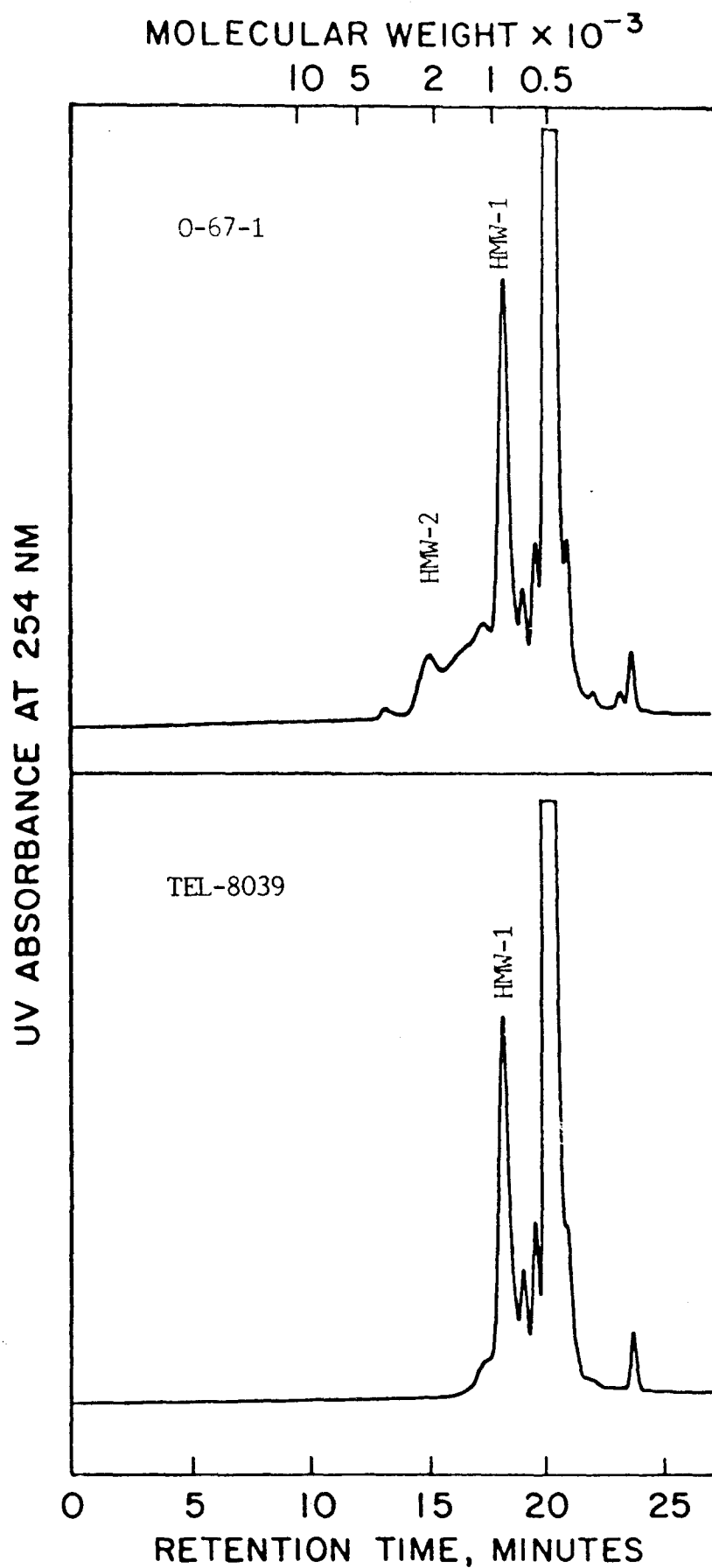


Figure 14. Gel Permeation Chromatograms of Corrosion and Oxidation Tested 0-67-1 and TEL-8039 at 320°C

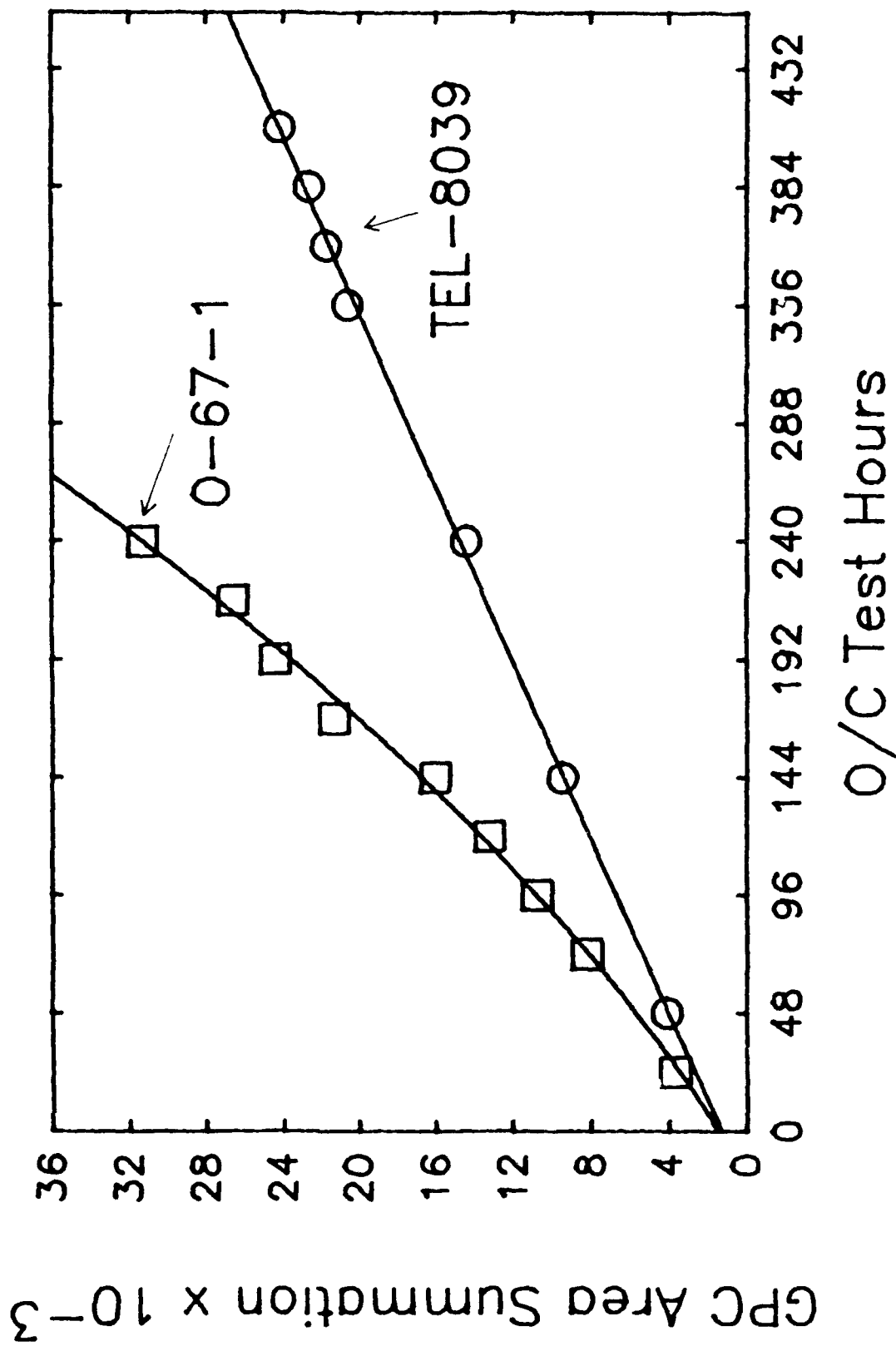


Figure 15. High Molecular Weight Oxidation Product Concentration, as Determined by GPC Area Summation, in O-67-1 and TEL-8039 During Corrosion and Oxidation Testing at 320°C

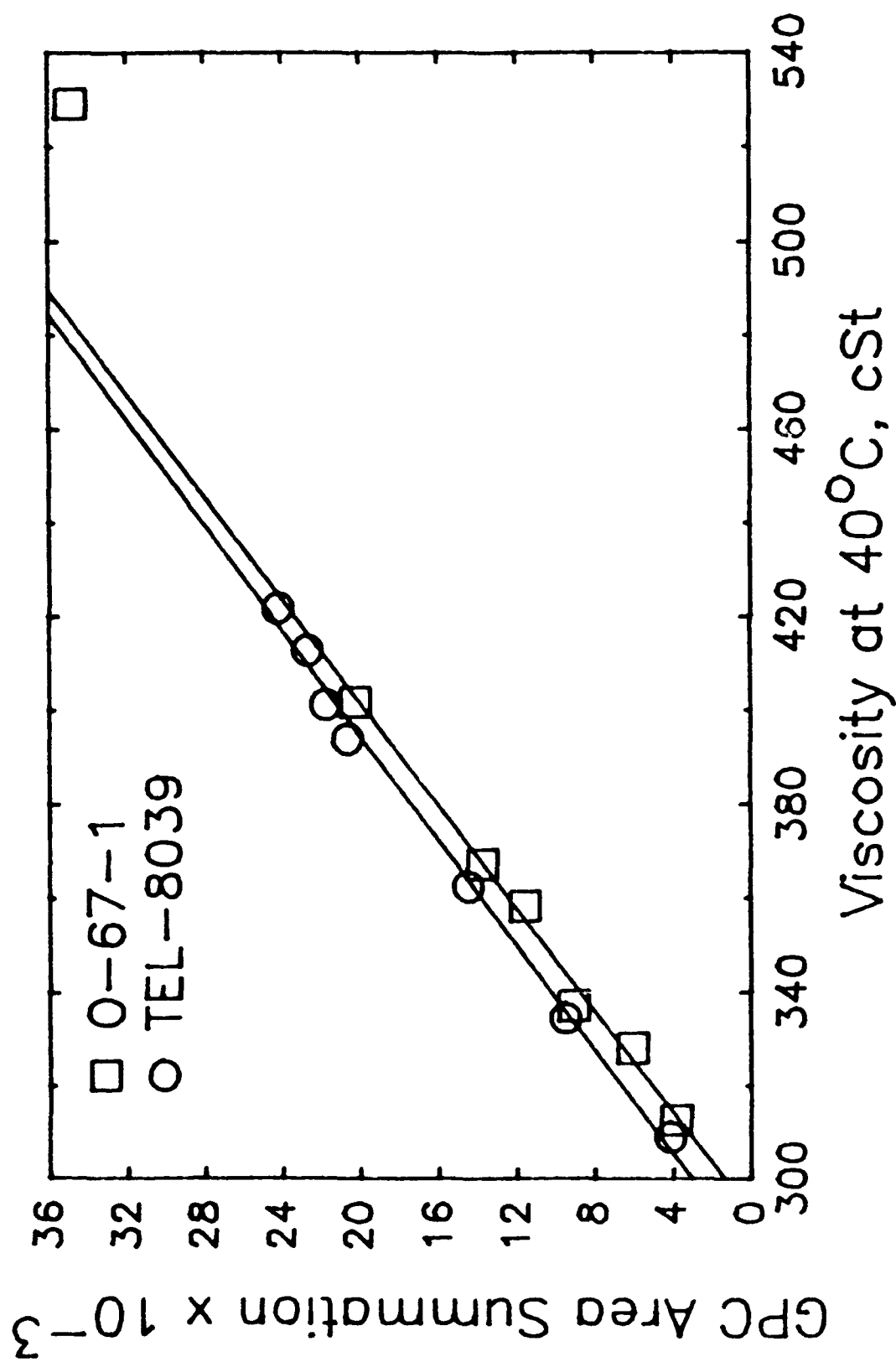


Figure 16. High Molecular Weight Oxidation Product Concentration Versus 40°C Kinematic Viscosity of O-67-1 and TEL-8039 from Corrosion and Oxidation Testing at 320°C

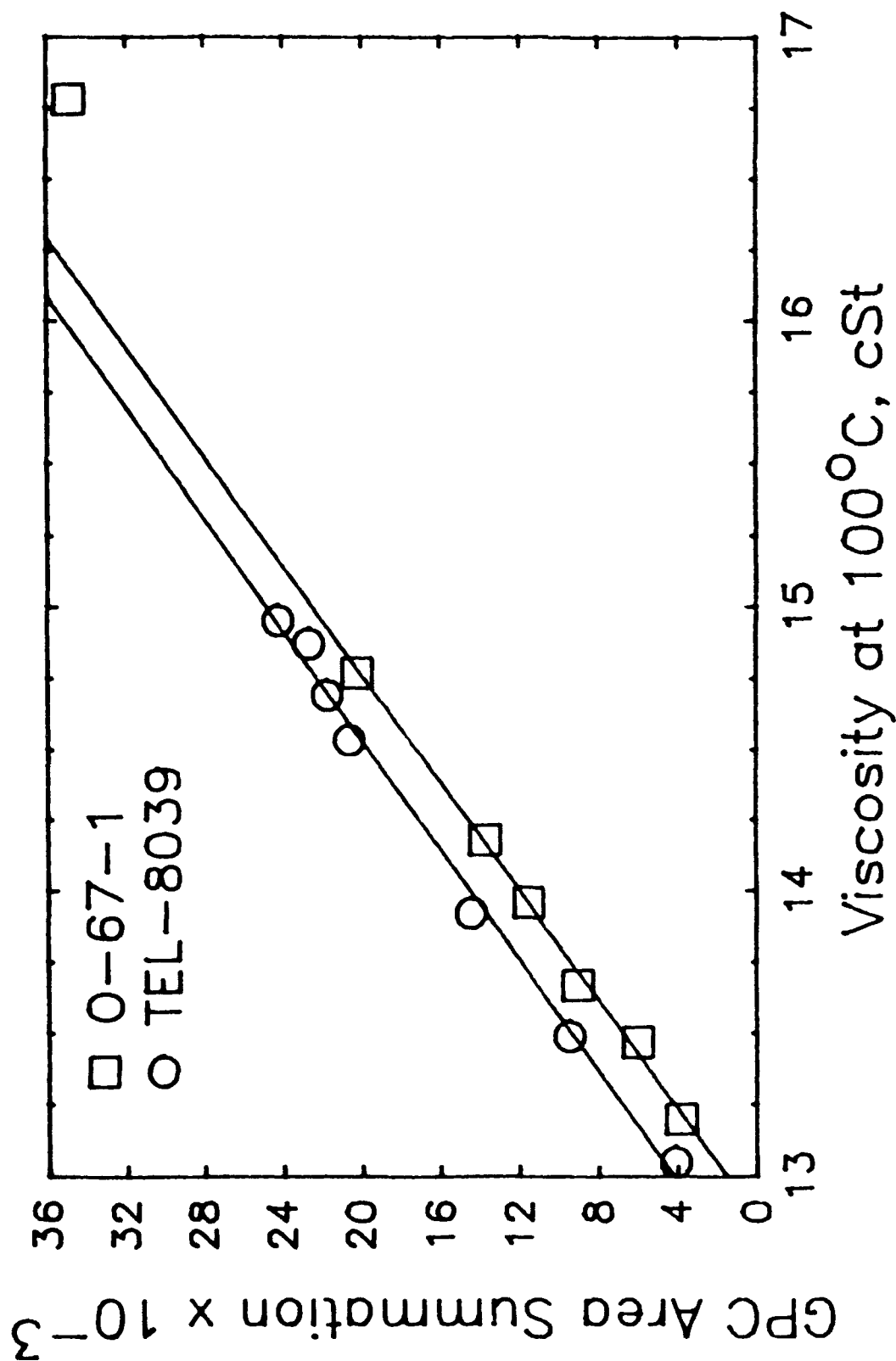


Figure 17. High Molecular Weight Oxidation Product Concentration Versus 100°C Kinematic Viscosity of O-67-1 and TEL-8039 from Corrosion and Oxidation Testing at 320°C

joint of the D 4871 tube. Testing was conducted at 320°C using an airflow of 10 L/h with the obtained data being given in Table 11.

TABLE 11

TEST DATA FOR O-67-1 LUBRICANT STRESSED 48 HOURS AT 320°C
WITH AND WITHOUT LIQUID AND VAPOR PHASE CORROSION SPECIMENS

	With Corr. Specimens	Without Corr. Specimens
Viscosity, cSt at 40°C	330.3	329.8
% Viscosity Increase	15.9	15.7
Metal Specimens Wt. Differences, mg/cm ²		
	Liquid Phase	Vapor Phase
Al	-0.14	-0.14
Ag	-0.30	-0.06
M-St	-0.25	-0.08
M-50	-0.22	-0.08
Wasp.	-0.16	-0.20
Ti	-0.20	-0.14

These data show that metal corrosion test specimens had very little effect on viscosity change of the 48 hour test. Although only minor corrosion of the test specimens occurred, the liquid phase corrosion specimens of silver and steel (both M-50 and M-St) had greater corrosion than the vapor phase test specimens. This shows that the volatiles produced during the degradation of polyphenyl ether (5P4E) are not corrosive.

d. Vapor Phase Corrosion of O-77-6 Fluid

(1) Introduction

Research was performed to determine the corrosiveness of the volatiles produced during the C&O testing of the 5P4E basestock O-77-6 fluid. To gain a better understanding of the oxidation mechanisms of the O-77-6 fluid, the C&O tests were performed at 300°C with and without metal specimens and the produced condensates were collected at 24 and 48 hour intervals.

The compounds present in the condensates were identified by gas chromatography/mass spectrometry (GC/MS) and the stain/deposits on the metal coupons were analyzed for elemental content by X-ray Photoelectron Spectroscopy (XPS). The C&O tests were performed using a 100 mL sample of O-77-6 fluid, a D 4871 tube, an air flow of 10 L/h and a test temperature of 300°C. For the C&O tests performed in the presence of metal coupons, two sets of test coupons were used; one set immersed in the stressed fluid and the second set supported by a 17 cm glass spacer positioned in the vapor phase directly below the tapered joint of the D 4871 tube. The test data for the stressed O-77-6 fluids and the weight changes of the liquid and vapor phase test coupons obtained at 48 hours are listed in Table 12.

(2) Test Data

The test data in Table 12 are in agreement with previous research and indicate that the corrosiveness of the stressed O-77-6 fluid and of the volatiles produced during stressing are similar causing minimal liquid and vapor phase specimen weight changes. However, the test data do indicate that the presence of metal specimens inhibits the thermal-oxidation of the basestock O-77-6 fluid.

(3) XPS Analyses of Stains/Deposits on Specimens

Since the presence of metal specimens inhibits the thermal-oxidation of O-77-6 fluid, the surfaces of the liquid phase mild steel (covered by blue colored stain) and silver (covered by tan colored stain) specimens were examined by the XPS analytical technique. The XPS elemental analyses of the liquid phase steel and silver specimens and of the fresh O-77-6 fluid (for reference) are listed in Table 13.

The elemental analyses in Table 13 show that the corrosion layers on the specimen surfaces are similar in composition and that the

TABLE 12

TEST DATA FOR O-77-6 FLUID STRESSED 48 HOURS AT 300°C
WITH AND WITHOUT METAL SPECIMENS

	With Specimens	Without Specimens
Viscosity (cSt at 40°C)	30.5	281.2
Metal Specimens Wt Differences, mg/cm ²		
	Liquid	Vapor
Al	+0.06	+0.06
Ag	+0.40	+0.38
Mild Steel	+0.30	+0.22
M-50	+0.38	+0.20
Waspalloy	+0.36	+0.18
Titanium	+0.34	+0.12

TABLE 13

XPS ELEMENTAL ANALYSES OF DEPOSITION ON MILD STEEL AND SILVER
SPECIMENS AND FRESH O-77-6

		% Atomic Weights		
Element		Mild Steel ^a	Silver ^a	O-77-6
C	CH	55.9	54.8 (57.6) ^b	62.9 (66.6)
	C-O	23.2	22.7 (23.8)	24.2 (19.0)
	C=O	3.3	2.3 (2.4)	B.D. ^c (2.0)
	Total	82.4	79.8 (83.8)	87.1
O	-O	14.3	13.0 (13.6)	13.0 (11.1)
	=O	3.3	2.4 (2.5)	B.D. (1.3)
	Total	17.5	15.4 (16.1)	13.0
Fe		B.D.	-	
Ag		-	4.8	

^a Metal Specimens from C&O testing of O-77-6 after 48 hours at 300°C

^b Percentage recalculated to determine elemental analysis of organic film only (Ag contribution negated)

corrosion layers contain more oxygen, and consequently, less carbon, than the fresh O-77-6 fluid. The extra oxygen content is both ether (C-O) and carbonyl (C=O) in nature and increases from silver to steel. The corrosion layer on the steel specimen was thicker than the layer on the silver specimen since iron was not detected by the XPS analysis (analysis depth 40 angstroms). These results are in agreement with previously reported IR and XPS data obtained for precipitates from wear tested and C&O stressed O-77-6 and O-67-1 fluids.

(4) O-77-6 Condensate

To gain further insight into the effects of metal surfaces on the thermal-oxidation of O-77-6 fluid, the condensates of the C&O tests were collected after 24 and 48 hours of stressing at 300°C. The GC/MS technique was used to identify the compounds present in the condensates and the GC technique was used to quantitate the identified compounds as listed in Table 14. A representative gas chromatogram is shown in Figure 18.

The compounds identified in Figure 18 and listed in Table 14 are in agreement with previously reported results except for unknowns 1 and 2. The compounds can be classified into two groups phenols (phenol and phenoxyphenol) and multiringed [dibenzofuran, 3P2E, 3P2E-C1, 4P3E and 5P4E (original fluid)]. The results in Table 14 show that the phenols increase with stressing time while the multiringed compounds decrease with stressing time. The results also indicate that the presence of metal specimens increases the concentration of multiringed compounds in the 24 and 48 hour condensates in comparison to the condensates produced in the absence of metal specimens. In the absence of specimens, the phenol concentration increases dramatically during the second 24 hours of stressing. In addition to compounds listed in Table 14, the unknown compounds 1 and 2 (Figure 18),

TABLE 14

COMPOSITIONAL DATA FOR O-77-6 CONDENSATES OBTAINED AT 24 AND 48
HOURS WITH AND WITHOUT METAL AND ALLOY SPECIMENS

Compound	Percent GC Area			
	With Specimens		Without Specimens	
	24 h	48 h	24 h	48 h
Phenol	4.1	4.5	6.5	36.5
Phenoxyphenol	1.2	3.6	2.1	7.6
Dibenzofuran	5.5	0.8	3.2	0.4
3P2E	11.4	3.9	6.1	2.8
3P2E-C1	4.8	2.0	2.3	1.2
4P3E	9.0	8.5	6.7	4.5
5P4E	63.8	76.7	73.0	46.7
Approx. Total Wt. (g)	1.1	1.3	2.1	2.6
Color	Red	Red	Light Orange	Very Dark

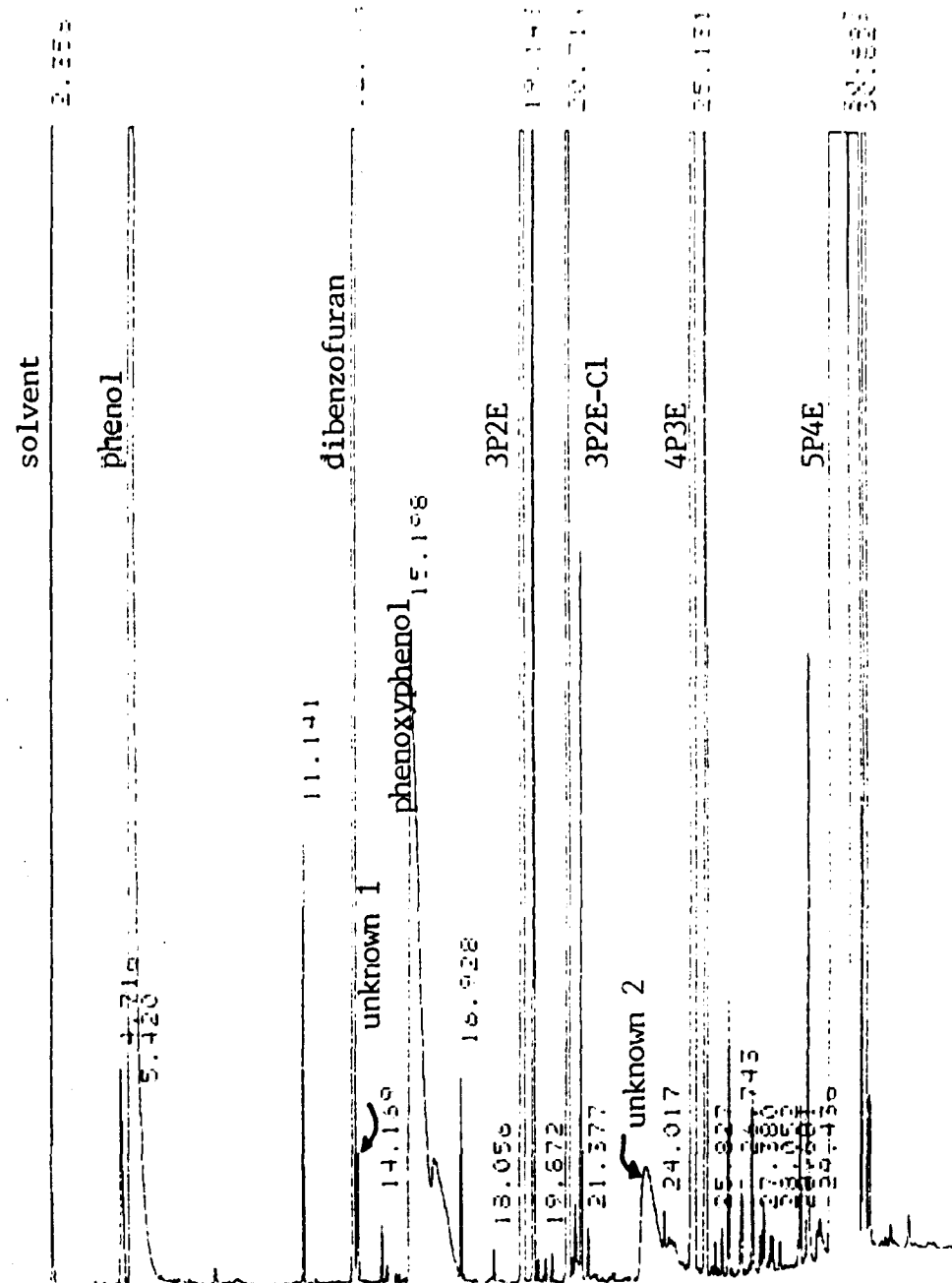


Figure 18. Gas Chromatogram of O-77-6 Condensate Collected After 24 Hours of Stressing at 300°C without Specimens Present

which were not detected in the metal condensate, increased with stressing time. However, the dramatic changes in the condensate composition did not affect the amount of condensate collected at each time interval as listed in Table 14.

(5) Summary

These results have shown that the degradation products of the O-77-6 fluid have low corrosiveness in the liquid and vapor phases and are greatly affected by the presence of metal surfaces. Although metal specimens are considered catalysts for C&O tests of most lubricants, the specimens inhibit the oxidation of the O-77-6 fluid. These results are in agreement with previously published research which showed metal oxides inhibit the thermal oxidation of polyphenyl ethers.² In the presence of metal specimens the major product was 3P2E which decreased with stressing time while in the absence of specimens the major degradation product was phenol which increased dramatically with stressing time.

e. Used Polyphenyl Ether Lubricants

(1) Corrosion and Oxidation of Used Polyphenyl Ether Lubricants

Corrosion and oxidation testing of six polyphenyl ether lubricant samples obtained from operating turbine engines was conducted at 320°C using D 4871 tubes, intermediate sampling, 10 L/h airflow and test times up to 120 hours depending on the fluid oxidative stability. The complete C&O test data for these samples (TEL-9028 thru TEL-9030 and TEL-9038 thru TEL-9040) are given in Appendix A. A summary of the 48 test hour intermediate sampling data is given in Table 15 since all samples were not tested for longer time periods. The data in Table 15 include C&O data for new O-67-1 fluid and tin and iron values of the used samples prior to C&O testing. These data show that significant differences exist in the oxidative

TABLE 15

SUMMARY OF CORROSION AND OXIDATION TEST DATA FOR NEW AND FIELD
STRESSED POLYPHENYL ETHER LUBRICANT SAMPLES (48 HOUR INTERMEDIATE
TEST SAMPLES, 320°C, 10 L/H AIRFLOW)

Sample	Eng. Hours	Initial Vis. at 40°C		320°C, 48 h C&O Test Data				
		Vis cSt	%Chg New Oil	Vis. cSt	% Chg Orig Oil	% Chg New Oil	Fe ppm	Sn ppm
New O-67-1	0	280.5	-	322.0	-	14.8	-	
TEL-9028 ¹	264	298.0	6.2	361.0	21.1	28.7	2 ³ (3) ⁴	116 ³ (96) ⁵
TEL-9029	417	284.9	1.6	382.7	34.3	36.4	2(3)	135(110)
TEL-9030	442	283.7	1.1	717.4	152.9	155.8	4(6)	50(40)
TEL-9038	594	288.4	2.8	403.8	40.0	44.0	3(5)	71(90)
TEL-9039 ²	570	298.1	6.3	337.3	13.1	20.1	3(4)	129(121)
TEL-9040	582	293.7	4.7	474.2	61.5	69.2	8(7)	75(87)

¹After removal of 15% tetrachloroethylene

²After removal of 1.9% trichloroethylene

³Atomic Emission

⁴ADM/Atomic Absorption

⁵Atomic Absorption

stability of the used fluids compared to the new lubricant and no clear correlation exists between engine hours, initial viscosity, percent viscosity change during C&O testing or initial Fe or Sn content of the samples. The wide variation in the oxidative stability of the "used" lubricants is shown in Figures 19 and 20, as measured by changes in viscosity. TEL-9028 had oxidative stability close to fresh lubricant while TEL-9030 showed a very large loss in stability. Only two of the six used lubricants still conformed to specification MIL-L-87100 requirements of a 25% maximum increase in the 40°C viscosity and then only after the removal of the solvent for sample TEL-9039. The largest effect of solvent being in lubricant samples prior to measuring the viscosity change due to corrosion and oxidation testing is the apparent high percent change after 24 to 48 hours because of solvent loss and the very low initial viscosity due to the solvent dilution from which the percent change in viscosity is calculated.

Two series of Spectrometric Oil Analysis Program (SOAP) size MIL-L-87100 lubricant samples were received with the series being coded TEL-9069 and TEL-9070. Viscosity and tin measurements were initially conducted on the TEL-9070 series for determining existing trending in these properties. The data presented graphically in Figure 21 show a fairly constant viscosity among the samples. The tin content shows a constant decrease until approximately 75 ppm at about 75 hours since oil change (HSOC). The addition of new make up oil at approximately 110 HSOC increased the tin content to about 100 ppm after which the tin decreased to about 75-80 ppm at about the same rate as the initial decrease. Initial studies have shown this to be normal for this specific lubricant and that the tin component can still have a significant effect on the oxidative stability of the lubricant even at these low levels. Samples from each series were

Engine Stressed Polyphenyl Ethers

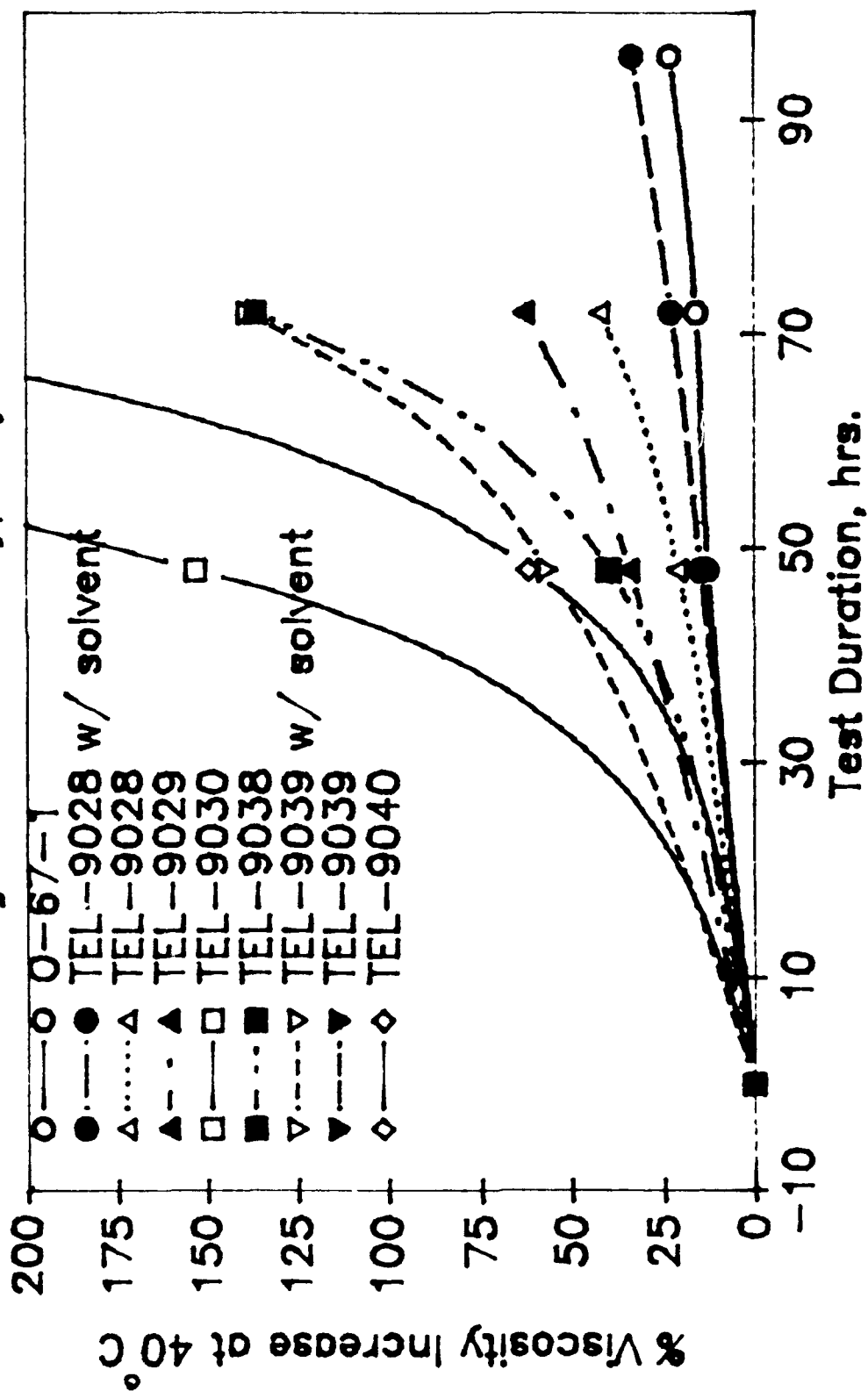


Figure 19. Changes in 40°C Viscosity of Engine Stressed Polyphenyl Ether (P4E) Lubricants During Corrosion and Oxidation Testing at 320°C

Engine Stressed Polyphenyl Ethers

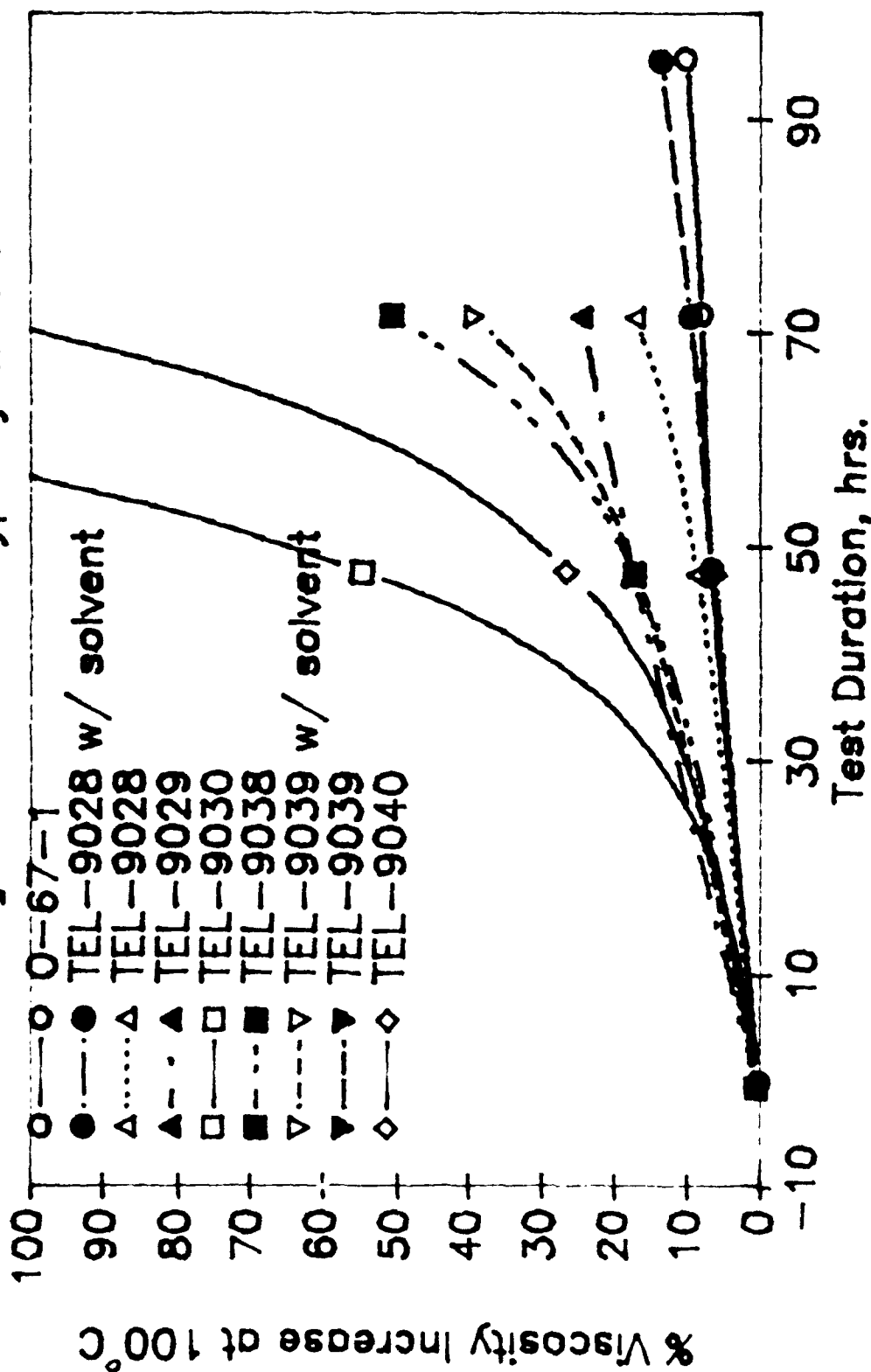


Figure 20. Changes in 100°C Viscosity of Engine Stressed Polyphenyl Ether 5P4E Lubricants During Corrosion and Oxidation Testing at 320°C

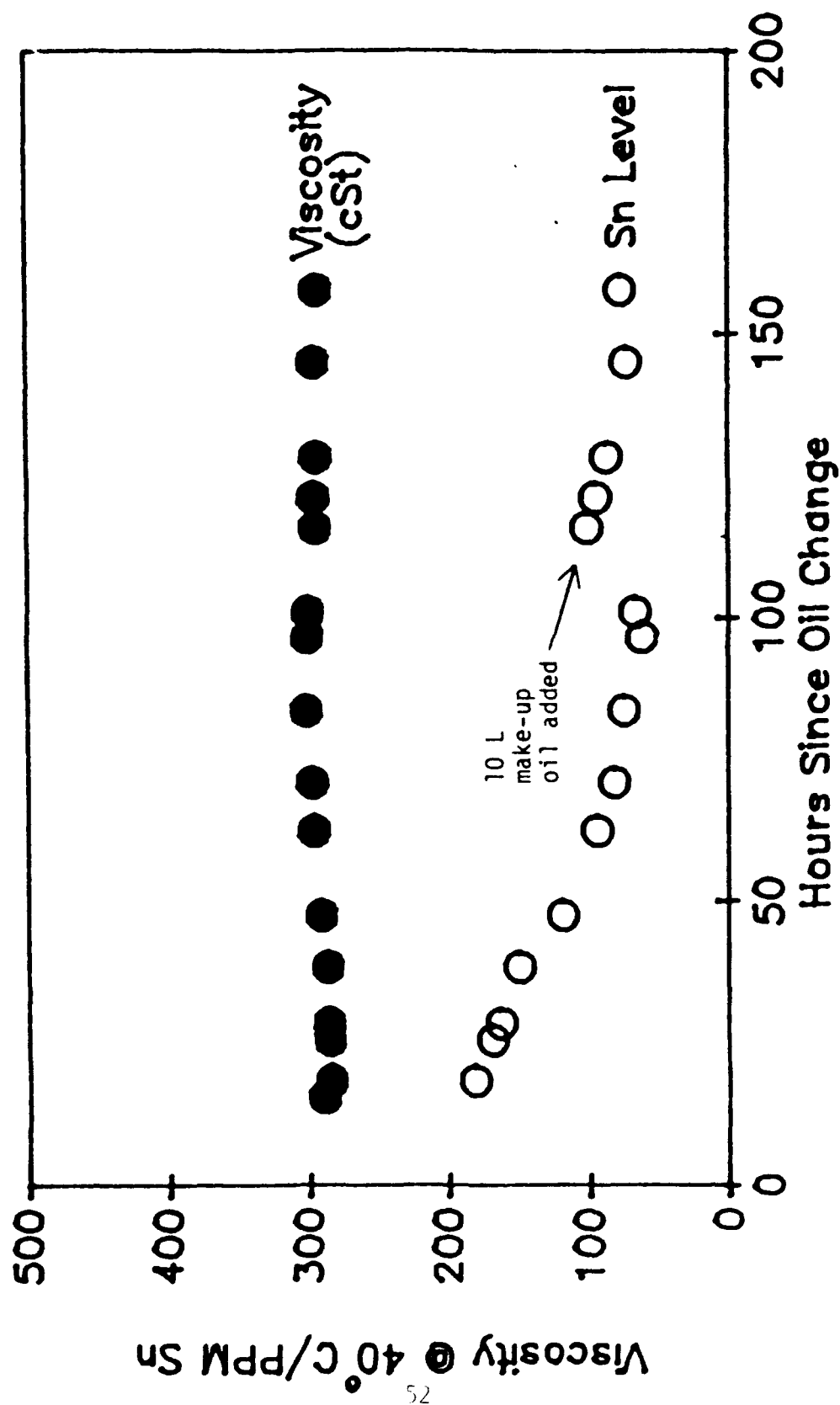


Figure 21. Variation of Viscosity and Sn with Time in TEL-9070 Series of Engine Test Samples

combined for corrosion and oxidation studies and will be discussed under Section (d) below, along with two additional engine stressed MIL-L-87100 lubricant samples coded TEL-90025 and TEL-90026.

(2) Effect of Filtration on Corrosion and Oxidation
Stability of Used Polyphenyl Ether Lubricants

The effect of 3 micron filterable solids on the oxidative stability of Four-ball wear test samples and used engine lubricant samples was investigated using a 48 hour, 320°C, 30 gram, "Squires" tube oxidation test. The samples were heated to 60°C, sonicated in an ultrasonic bath, to break down the agglomeration, and handshaken. A portion of each sample was filtered through a three micron silver membrane for providing samples prior to corrosion and oxidation testing.

A summary of this testing for samples CB-1, CB-2 and CB-3, TEL-9030 and TEL-9040 is given in Table 16 and depicted graphically in Figures 22 and 23. Complete data for each sample is given in Appendix A. The wear tested sample (CB-1) shows that removal of filterable solids greatly improves the oxidative stability of the fluid as measured by viscosity increase. The same trend is evident with engine test samples TEL-9030 and TEL-9040. Samples CB-2 and CB-3 showed about the same viscosity change before and after filtering with 40°C viscosity changes being between 15.6% and 19.5%. These values are only slightly higher than the 11.5% value for new MIL-L-87100 fluid. The tin content of CB-2 and CB-3 shown in Figure 24 indicates tin is still an effective inhibitor at greatly reduced levels. Also, 3 micron filtration did not reduce the tin levels of the CB-2 or CB-3 samples. The CB-1, TEL-9030 and TEL-9040 samples showed varying degrees of tin reduction (Figure 25) after wear or engine testing, but the tin reduction or tin content does not correlate with increased lubricant stability as shown

TABLE 16

EFFECT OF 3 MICRON FILTERABLE SOLIDS ON LUBRICANT
 STABILITY OF WEAR TESTED AND ENGINE TESTED
 MIL-L-87100 TYPE LUBRICANT

Lubricant Sample	% of Orig. Sn Content after Wear or Engine Testing	Viscosity at 40°C, cSt			
		After Engine or Wear Test	After Engine or Wear Test & 48 h O/C at 320°C	After Engine or Wear Test & 3 um Filtering	After Engine or Wear Test, 3 um Filtering & 48 h O/C at 320°C
CB-1	81	290.2	622.5	288.1	326.9
CB-2	89	285.8	335.6	284.4	340.0
CB-3	26	294.7	340.8	292.8	348.3
TEL-9030	13	286.2	717.4	288.4	381.1
TEL-9040	23	293.7	474.2	290.6	336.2

Note: O-67-1 (100% Original Sn Content) gives a 318.1 cSt 40°C
 viscosity value after 48 hours C&O at 320°C

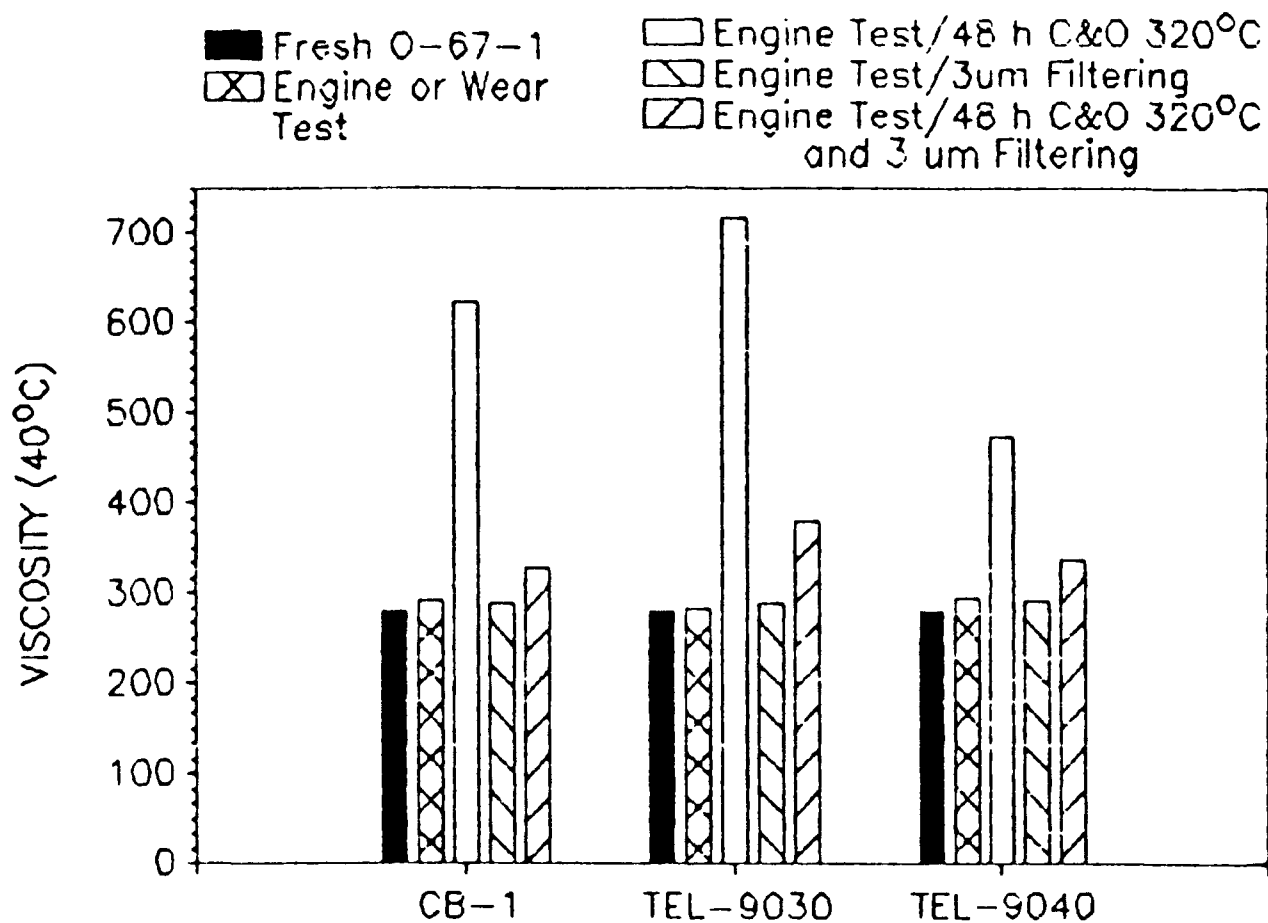


Figure 22. Viscosity @ 40°C for Fresh O-67-1 and Effect of Subsequent Wear or Engine Testing, 48 Hour C&O @ 320°C, and 3 Micron Filtering on CB-1, TEL-9030 and TEL-9040 Viscosity

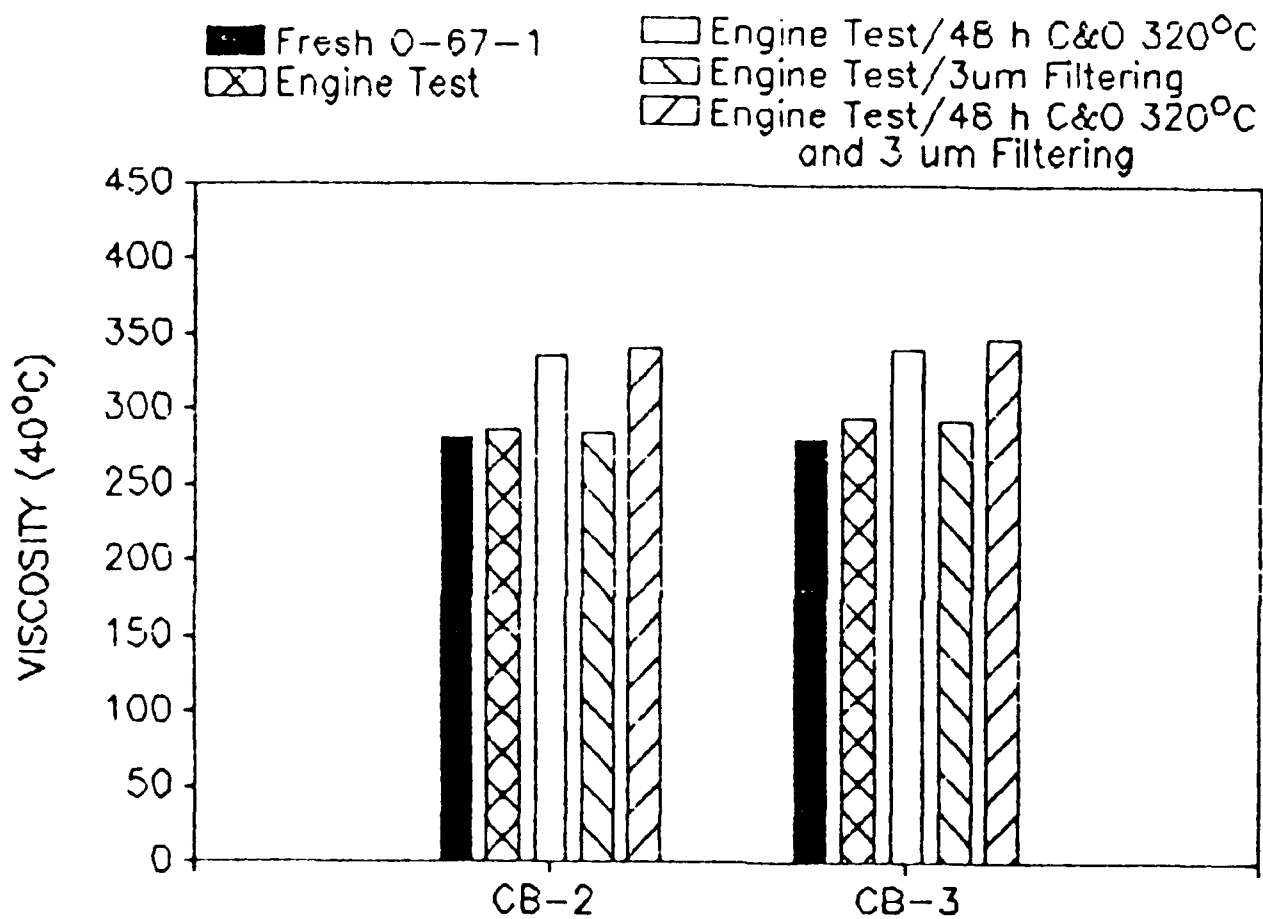


Figure 23. Viscosity @ 40°C for Fresh O-67-1 and Effect of Subsequent Engine Testing, 48 Hour C&O at 320°C, and 3 Micron Filtration on CB-2 and CB-3 Viscosity

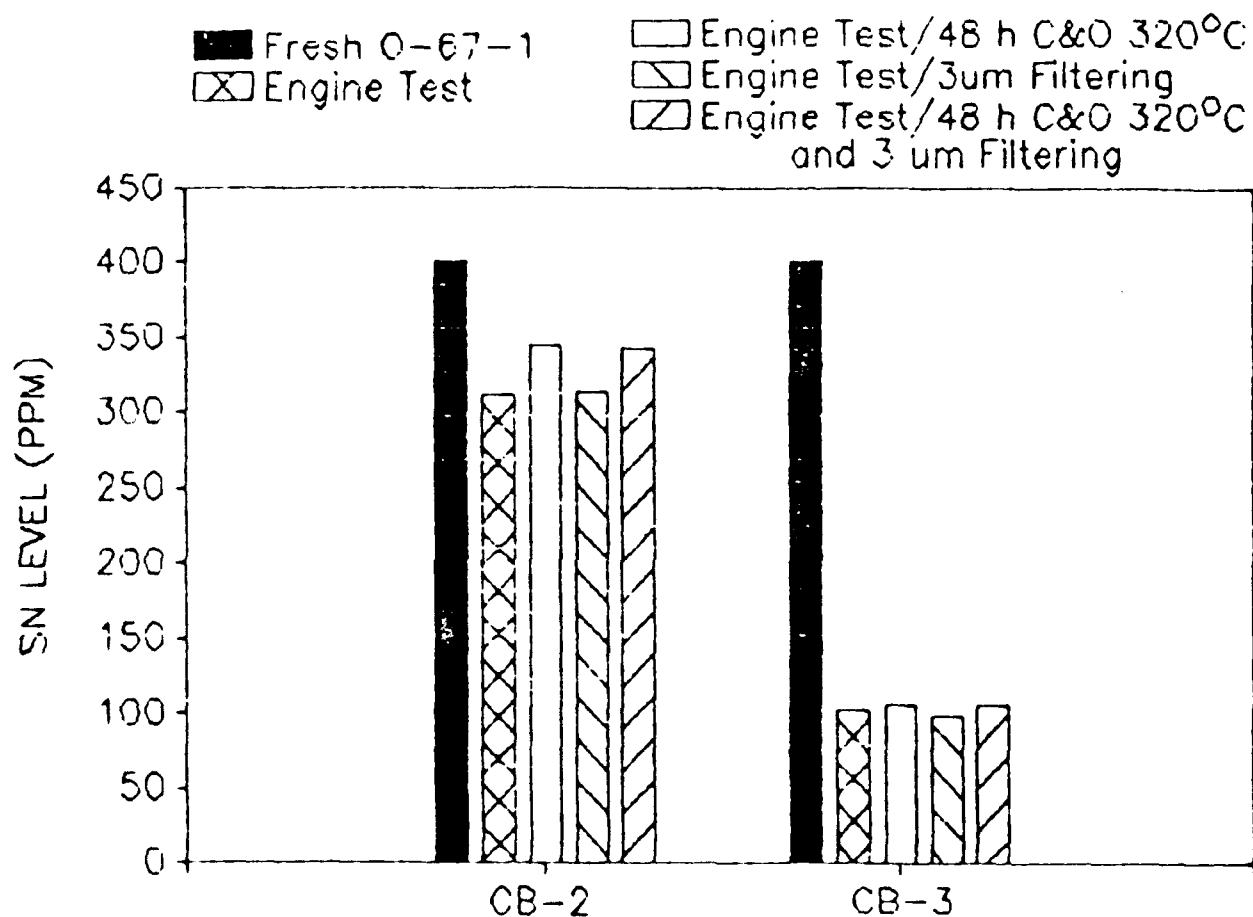


Figure 24. Sn Level of Fresh O-67-1 and Effect of Subsequent Engine Testing, 48 Hour C&O @ 320°C and 3-Micron Filtering on Sn Levels of CB-2 and CB-3

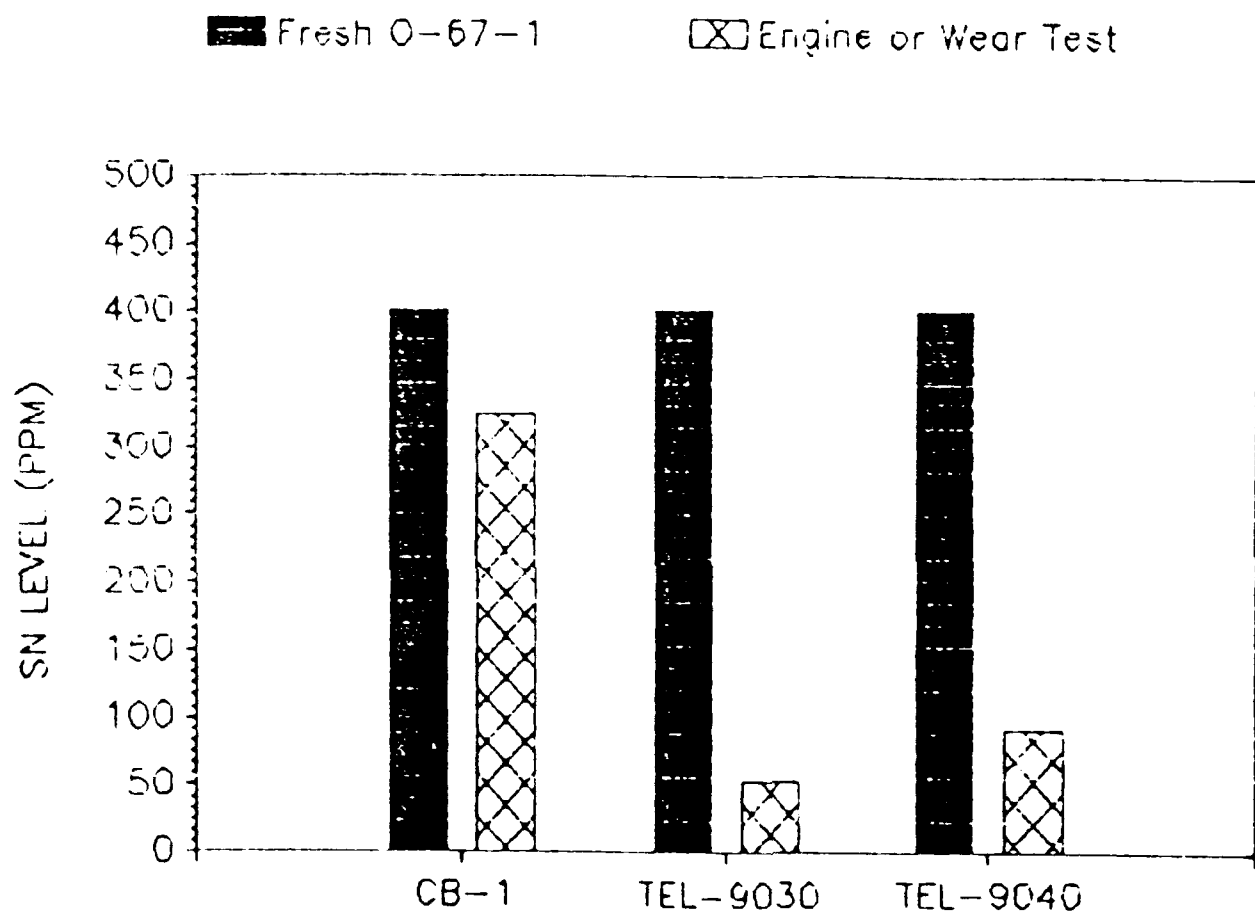


Figure 25. Sn Level of Fresh O-67-1 and Effect of Wear or Engine Testing on CB-1, TEL-9030 and TEL-9040

by the 48 hour C&O testing. These data show that the effectiveness of the tin inhibitor is greatly reduced when iron and polymeric wear material is present as was the case with sample CB-1. No significant change occurred in the corrosion characteristics of any of the five samples except for the silver test specimens of samples TEL-9030 and TEL-9040. The corrosion of the silver test specimens decreased from -0.14 mg/cm^2 to $+0.06 \text{ mg/cm}^2$ for TEL-9030 and from -0.22 mg/cm^2 (72 H) to -0.02 mg/cm^2 for TEL-9040 after filtering. Deposits formed in the sample tube and air tube during the CB-1, TEL-9030 and TEL-9040 C&O testing were greatly reduced by filtration.

The corrosion and oxidative stability of used "engine" MIL-L-87100 samples TEL-90025 and TEL-90026 was also determined before and after three micron filtration. Test conditions included a 320°C test temperature, 30 g sample, Squires tubes, 10 L/h airflow and 48 hour test duration. This test data, included in Appendix A, showed no significant change in viscosity, TAN, corrosion characteristics or sludge or coke formation after the 3 micron filtering. The initial viscosity and viscosity increase during the C&O testing were only slightly higher than values for fresh MIL-L-87100 fluid. The concentration of iron and tin was not significantly affected by filtration.

(3) Effect of Four-Ball Wear Test Parameters on the
Corrosion and Oxidation Stability of MIL-L-87100
Lubricant

(a) Corrosion and Oxidation Testing of Four-Ball
Test Fluids

Corrosion and Oxidation testing was conducted on several samples of lubricant O-67-1 after four-ball wear testing under various test parameters for determining effects on lubricant stability. Ferrography of the wear test samples showed a change in type of wear and an increase in the

formation of polymeric material with variations in loading and test temperature. Table 17 presents a summary of the test data with complete test data being given in Appendix A. The data in Table 17 give a summary of the test data and shows a small increase in the 40°C viscosity change as the wear test temperature is raised from 75°C to 315°C for the 33.5 N loading. This increase does not correlate with the iron content of the fluids prior to C&O testing. However, the viscosity change does appear to be related to loadings and test temperature when all tests are considered. None of the corrosion and oxidation tests displayed significant corrosion of any metal test specimen.

The effect of four-ball testing on O-67-1 stability was further defined by analysis of the four-ball tested lubricant as well as by determination of the thermal/oxidative stability of the organic wear debris (friction polymer) produced in these tests (also discussed in Section VI).

(b) Oxidation of O-67-1 during Four-Ball Testing

Based on previously developed Arrhenius equations for O-67-1, it would be expected that the degree of oxidation in a four-ball test at 150°C and 250°C for 20 hours would be minimal while mild oxidation, perhaps equivalent to a 5% 40°C viscosity increase, would be anticipated at 315°C . The degree of oxidation of O-67-1 after four-ball testing under various test conditions was examined by gel permeation chromatography (GPC). GPC is capable of determining molecular weight increases of the lubricant, which has been shown to be proportional to viscosity increases² and can yield results on milligram quantities without interference from solvent dilution or friction polymer (FP) formation. As expected, no particular oxidation was noted in the 150°C test samples with the 52100 test balls, even after 68 hours of testing with the production of 2.6% FP (which is not soluble in the

TABLE 17

CORROSION AND OXIDATION TEST DATA AT 320°C FOR
LUBRICANT O-67-1 AFTER FOUR-BALL WEAR TESTING
AT VARIOUS TEMPERATURES AND LOADINGS, 1200 RPM AND
3 HOUR TEST TIME (1 HOUR FOR TEST # 362)

Test Lubricant	Test Hours	Visc. 40°C, cSt	Visc. Chg 40°C, %	Visc. 100°C, cSt	Visc.Chg 100°C %	Fe (ADM) ppm	Wear Scar Dia., mm
New O-67-1	0	280.5	-	12.61	-		N/A
	48	318.1	13.4	13.47	6.8		N/A
Wear Test # 382 75°C, 33.5 N Load	48	323.8	15.4	13.33	5.7	13	0.632
Wear Test # 386 150°C, 33.5 N Load	48	325.3	16.0	13.47	6.8	40	0.949
Wear Test # 388 250°C, 33.5 N Load	48	330.9	18.0	13.57	7.6	23	1.112
Wear Test # 401 315°C, 33.5 N Load	0	301.6*	-	12.95*	-		
	48	343.7	14.0	13.79	6.5	29	1.099
Wear Test # 362 150°C, 145 N Load (1 h)	48	368.9	31.5	14.28	13.2	23	1.029
Wear Test CB-1 150°C, 145 N Load	48	622.5	121.9	19.81	57.1	63	1.238
Wear Test # 359 315°C 145 N Load	0	304.2**	-	13.07**	-		
	48	377.6	19.4	14.90	14.0	91	1.152

*Four-ball test # 414 (same test conditions as # 401)

**Four-ball test # 417 (same test conditions as # 359)

GPC solvent). However, the 20 hour 250°C test revealed considerably more oxidation than expected as did the 3 and 20 hour tests at 315°C (Table 18). Obviously, the oxidation rate of O-67-1 in a four-ball test is accelerated relative to a corrosion/oxidation test.

(c) Effect of Four-Ball Testing on Additive A in O-67-1

Since Additive A is the antioxidant used in O-67-1, its concentration was analyzed in various four-ball tests using a previously described gas chromatographic technique.² Previously, it had been shown that Additive A was a tin containing compound that was not very oxidatively stable and was rapidly converted into tin oxide, which is the active antioxidant. Thus, it was not surprising that Additive A was virtually depleted after 3 hours of four-ball testing at 250 and 315°C. However, the 150°C data (Figure 26) reveals an initial 8% drop in Additive A in the first hour of testing, a stable period of no change in concentration for about six hours, and then a more or less linear decrease in concentration until virtual depletion at 20 hours. These data are not suggestive of simple thermal oxidation, which would not experience an induction period before the onset of degradation. A more likely possibility would be that the Additive A is interacting with something being produced in the four-ball test.

In order to determine the latter point, a number of four-ball tested O-67-1 lubricants were placed in a 150°C circulating air oven for 18 hours and the change in their Additive A concentration determined. The results (Table 19) show that while the fresh (control) O-67-1 did not experience additive loss, the four-ball tested lubricants underwent various degrees of additive loss that was approximately proportional to their FP concentration. These results indicate that the loss of Additive A is due to some type of interaction with the friction polymer

TABLE 18

GPC ANALYSIS OF FOUR-BALL TESTED O-67-1 LUBRICANTS

Four-Ball ¹ Test No.	Test Temp., °C	Test Hours	GPC Data ²	
			Mn	Mw
370	150	68	451	455
381	250	20	460	470
417	315	3	461	470
365	315	20	481	528
O-67-1, fresh	-	-	451	456
24 h C&O at 320°C	-	-	452	468
120 h C&O at 320°C	-	-	483	531

¹ 52100 test balls, 145 N load² Mn = number average molecular weight, Mw = weight average molecular weight

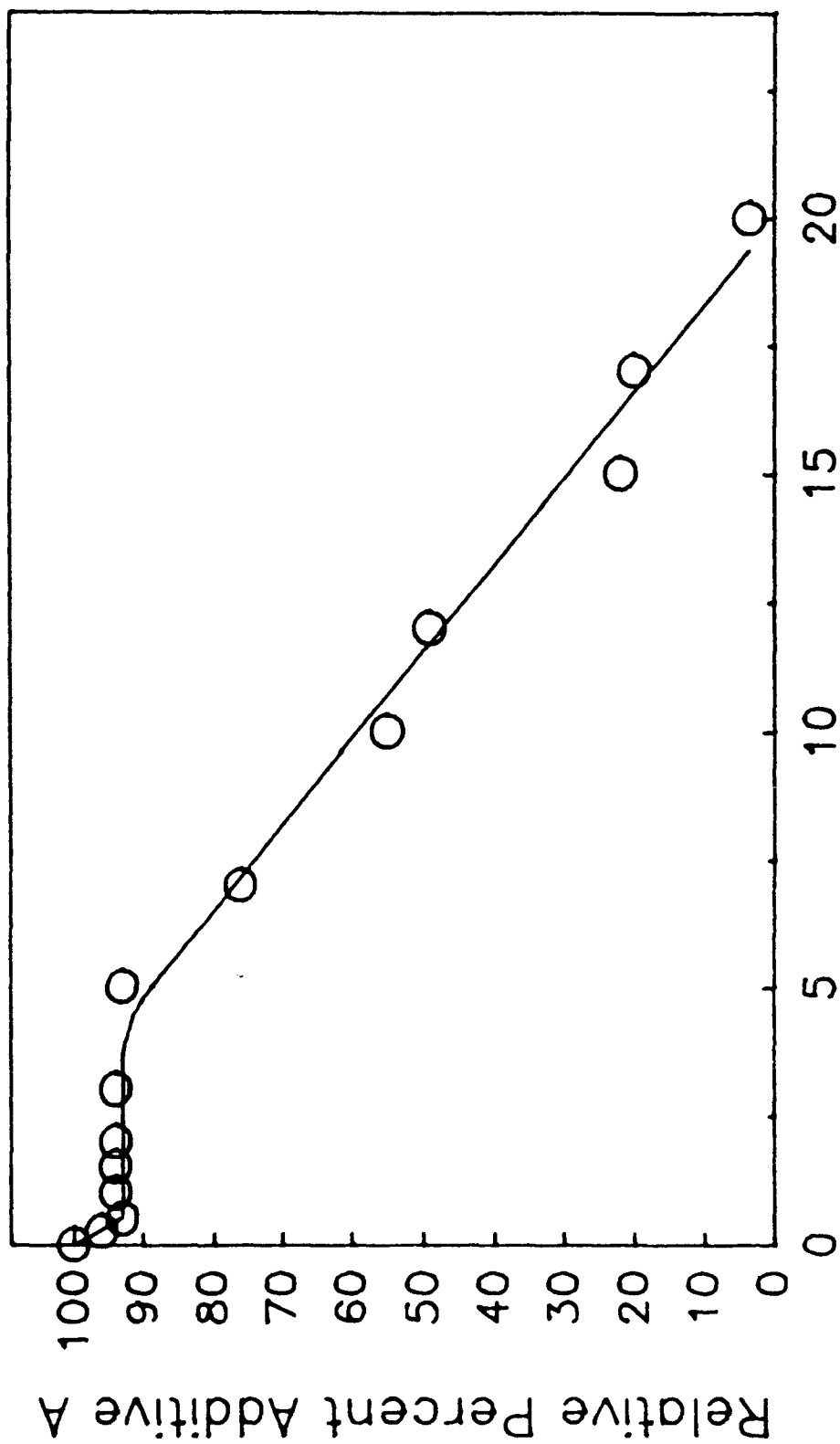


Figure 26. Change in Additive A Concentration During Four-Ball Testing of O-67-1 at 150°C, 145 N Load and 52100 Bearings

Four-Ball Wear Test Hours

TABLE 19

EFFECT OF 150°C OVEN STRESSING ON VARIOUS
FOUR-BALL TESTED O-67-1 LUBRICANTS

Test #	Four Ball Test Conditions				Relative % Additive A ²		
	Temp, °C	Load (N)	Time (h)	% Dep ¹	Pretest ³	Post-Test ⁴	% Chg
394	150	145	7	0.30	75	22	-53
393	150	145	5	0.20	89	48	-41
351	75	145	20	0.13	89	67	-22
369	150	145	3	0.069	86	75	-11
400	150	34	3	0.029	95	85	-10
364	75	145	3	0.020	92	92	0
O-67-1	-	-	-	0.010	100	99	-1

¹ Determined gravimetrically as trichloroethylene insoluble deposits

² Fresh O-67-1 lubricant is 100%, as determined by gas chromatography

³ Additive A content after four-ball wear test

⁴ Additive A content after four-ball wear test and stressing at 150°C for 18 hours

and not due to the wear process itself.

These data imply that oxidative destabilization of four-ball tested lubricants is due to interference with the functioning of the antioxidant. However, since SnO_2 is the true oxidation inhibitor in this lubricant, it is not clear what significance these results have with respect to the oxidative stability of four-ball tested lubricants.

(d) Oxidative Stability of FP

Since FP from four-ball testing of O-67-1 was shown to be responsible for the acceleration in the rate of oxidation of Additive A, an investigation was made into the oxidative stability of these friction polymers. The FP may be less stable than the O-67-1 basestock and consequently act as an initiator of oxidation. A similar effect has been previously proposed for the high molecular weight oxidation products that form during C&O testing of O-67-1.²

The thermal/oxidative behavior of the isolated FP was investigated by differential scanning calorimetry (DSC) and thermal gravimetric analysis (TGA). A typical DSC/TGA thermogram of an FP (Figure 27) reveals a fairly large DSC exotherm concurrent with a TGA weight loss. This behavior is not observed when the test is run in nitrogen. The DSC apex temperatures are directly proportional to the four-ball test temperatures and seem to be relatively independent of bearing material and percent iron (Table 20). This thermal behavior is not observed for FP from ceramic bearings or from high molecular weight oxidation products from C&O testing of O-67-1 (HMW-2), so it appears that iron, which was previously shown to be present in the FP in a reacted form, is crucial for this behavior. The post test TGA residue appears to be mostly a reddish magnetic iron oxide, although FTIR analysis indicates some carbonaceous residue. The percent residuals are

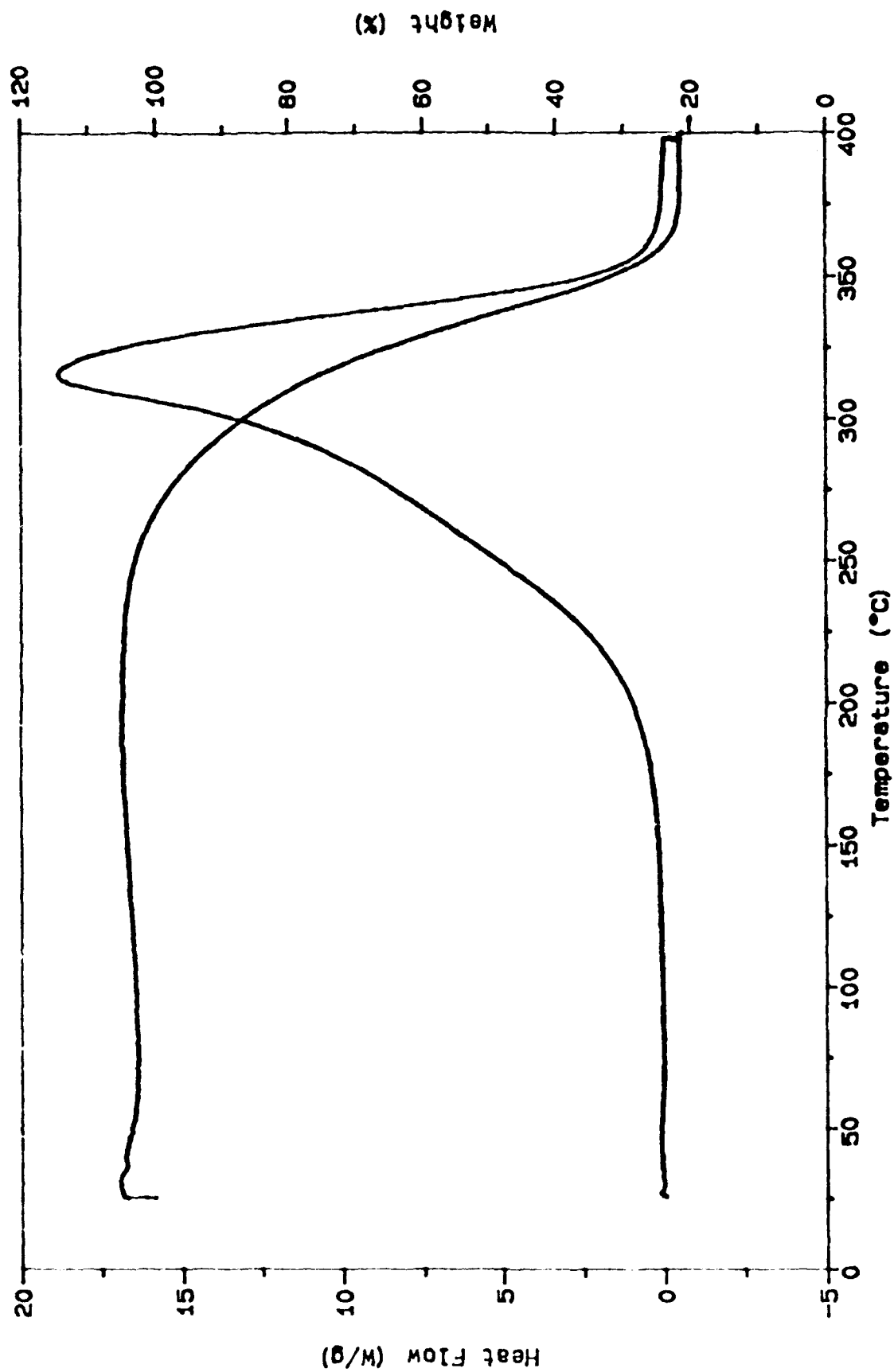


Figure 27. DSC and TGA Thermograms of Friction Polymer from Four-Ball Test # 426
(DSC and TGA Conditions: 5°C/Minute to 400°C, Air, 2.0 mg Sample)

TABLE 20

DSC AND TGA DATA FOR FRICTION POLYMER FROM FOUR-BALL TESTED O-67-1 LUBRICANT

Four-Ball Test Conditions				Friction Polymer Data		
Four-Ball Test No.	Test Temp., °C	Bearing	Load(N)	% Fe ¹	DSC Apex ² Temp., °C	TGA % Residuals
357	150	52100	145	6.8	316	16
381	250	52100	145	4.0	361	13
365	315	52100	145	2.6	375	4
468	150	M50	145	21.7	323	37
480	250	M50	145	12.9	348	40
470	315	M50	145	7.4	371	38

ND = Not Determined

¹Percent iron in friction polymer by AA-ADM²(TGA and DSC Conditions: 5°C/min to 400°C, 30 min. hold, in air,
2 mg samples)

approximately proportional to the percent iron in the FP from the 52100 test balls but not in the FP from the M50 test balls.

The DSC thermograms of FP from both M50 and 52100 bearings from different test temperatures (Figure 28) show that the 150°C FP displays considerable instability at 320°C (as indicated by the height of the exotherm) relative to those of the 250 and 315°C FPs. This behavior correlates well with the apparent effect of these deposits on the C&O stability of the fluids from which they were obtained. Note also that no real differences are observed between the thermograms of FPs as a function of bearing material.

These data indicate that the oxidative destabilization of four-ball tested O-67-1 is due to the lack of oxidative stability of the friction polymers produced during these wear tests. The oxidation of the FP would likely produce radicals or other unstable compounds that could act as initiators and accelerate the oxidation of PPE. This would explain the relatively lower oxidative stability of lubricants run at 150°C since this FP has proportionately lower oxidative stability as indicated by the DSC data. It would be expected that the relative rate of oxidative acceleration for a four-ball tested lube in a C&O test would be a function of both rate of decomposition of the FP as well as its concentration in the lubricant. However, insufficient data exist to prove such a relationship.

(4) Effect of Diluents on Polyphenyl Ether Fluid Stability

Corrosion and oxidation testing was conducted on fluids O-77-6 (with and without Additive A) and O-67-1 containing 25% (wt) of trichloroethylene or tetrachloroethylene diluent. Tests were conducted at 320°C using Squires tubes, 25 mL samples and 10 L/h airflow. The test duration was 48 hours except for fluid O-77-6 containing 25 relative percent

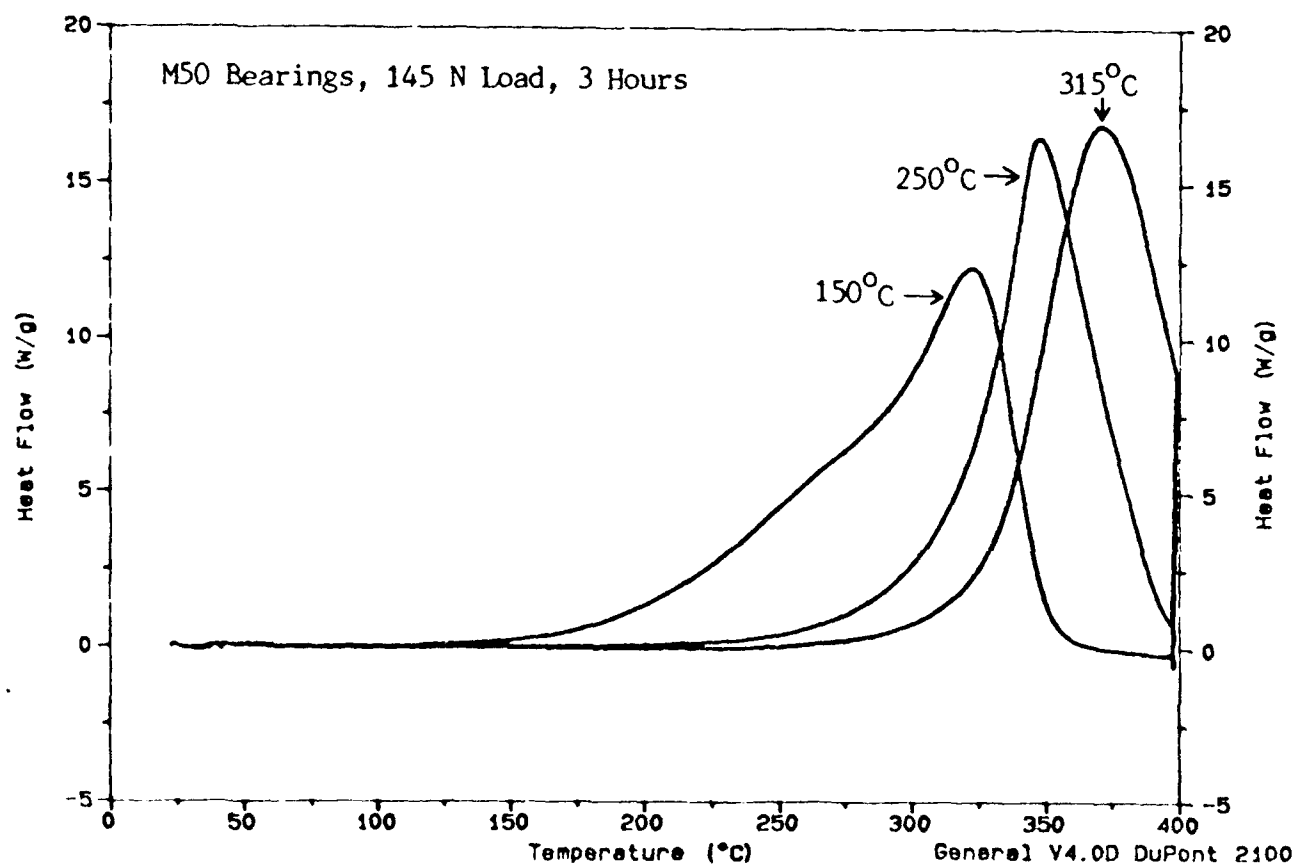
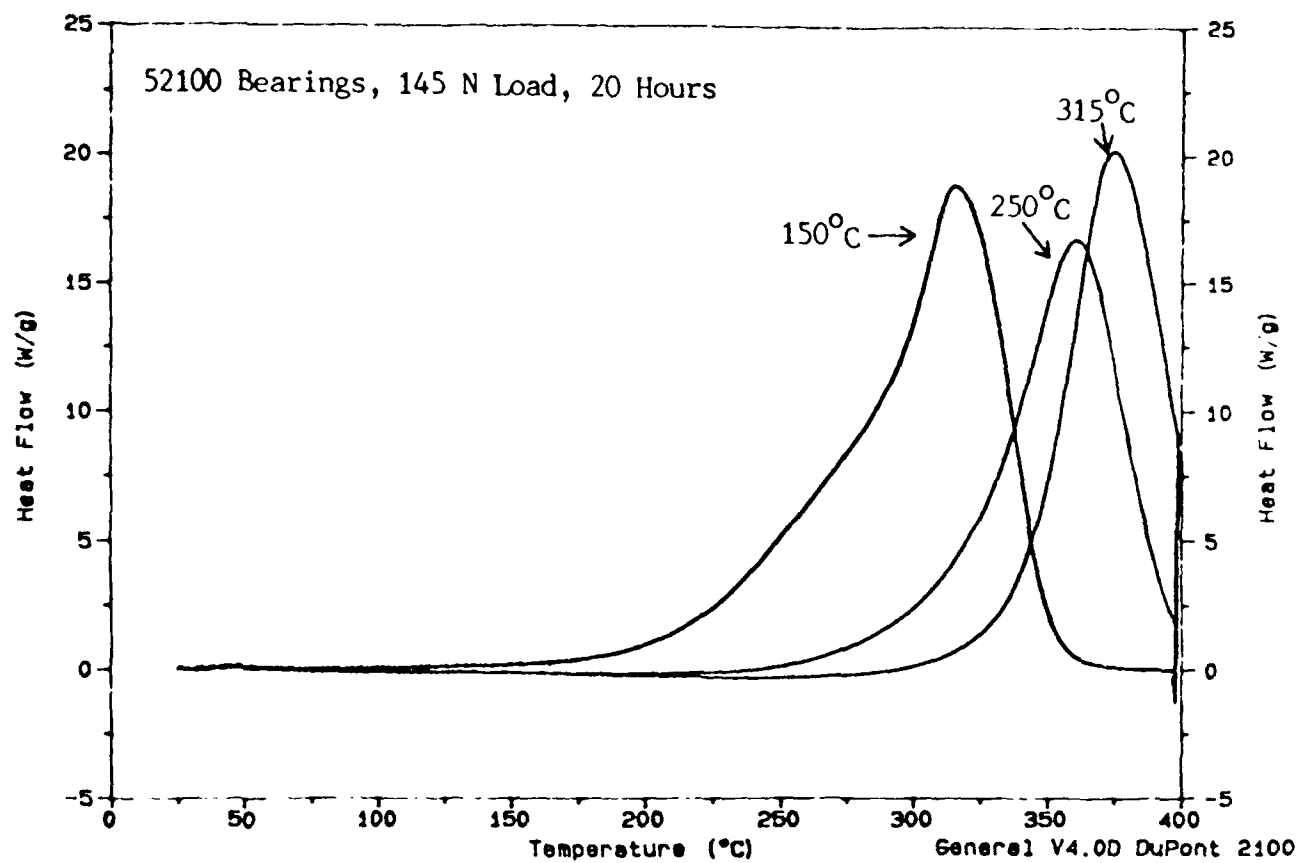


Figure 28. DSC Thermograms of Friction Polymer from Four-Ball Tests of O-67-1 at Various Temperatures

Additive A which was sampled after 24 hours. Standard metal corrosion test specimens were used except for the two O-77-6 plus Additive A and O-67-1 fluids where silver coupons were mistakenly replaced with aluminum coupons. A corrosion resistant thermocouple was inserted down through the air tube to the bottom of the Squires tubes for determining oil temperature as a function of test time.

Figure 29 shows the progress of the diluents trichloroethylene, (B.P. of 87°C) and tetrachloroethylene (B.P. of 121°C) evaporating from the lubricant. The initial lubricant stabilization temperature was approximately 150°C which appears to be the initial boiling point of the mixtures. The diluents are evaporated for as long as six hours before the oil temperature equilibrates with the test block temperature. Table 21 shows the changes in viscosity, lubricant loss and corrosion data for the various solvent diluted and undiluted fluids. The effect on viscosity increase during C&O testing of O-67-1 and O-77-6 plus Additive A fluids is very small (Figure 30) and is probably due to test reproducibility. The apparent improvement in the viscosity change (less increase) of the O-77-6 fluid containing either of the two diluents is probably due to the lower test temperature of the fluids at the start of the test and the very poor stability of O-77-6 at 320°C test conditions which has a "breakpoint" below 48 hours.² The effect of the diluents on the corrosion characteristics appear to be insignificant except for the O-77-6 fluid test with tetrachloroethylene which gave a silver test specimen change of $+0.32 \text{ mg/cm}^2$. Table 21 also shows that the dilution properties (lowering of viscosity) of trichloroethylene and tetrachloroethylene are nearly the same.

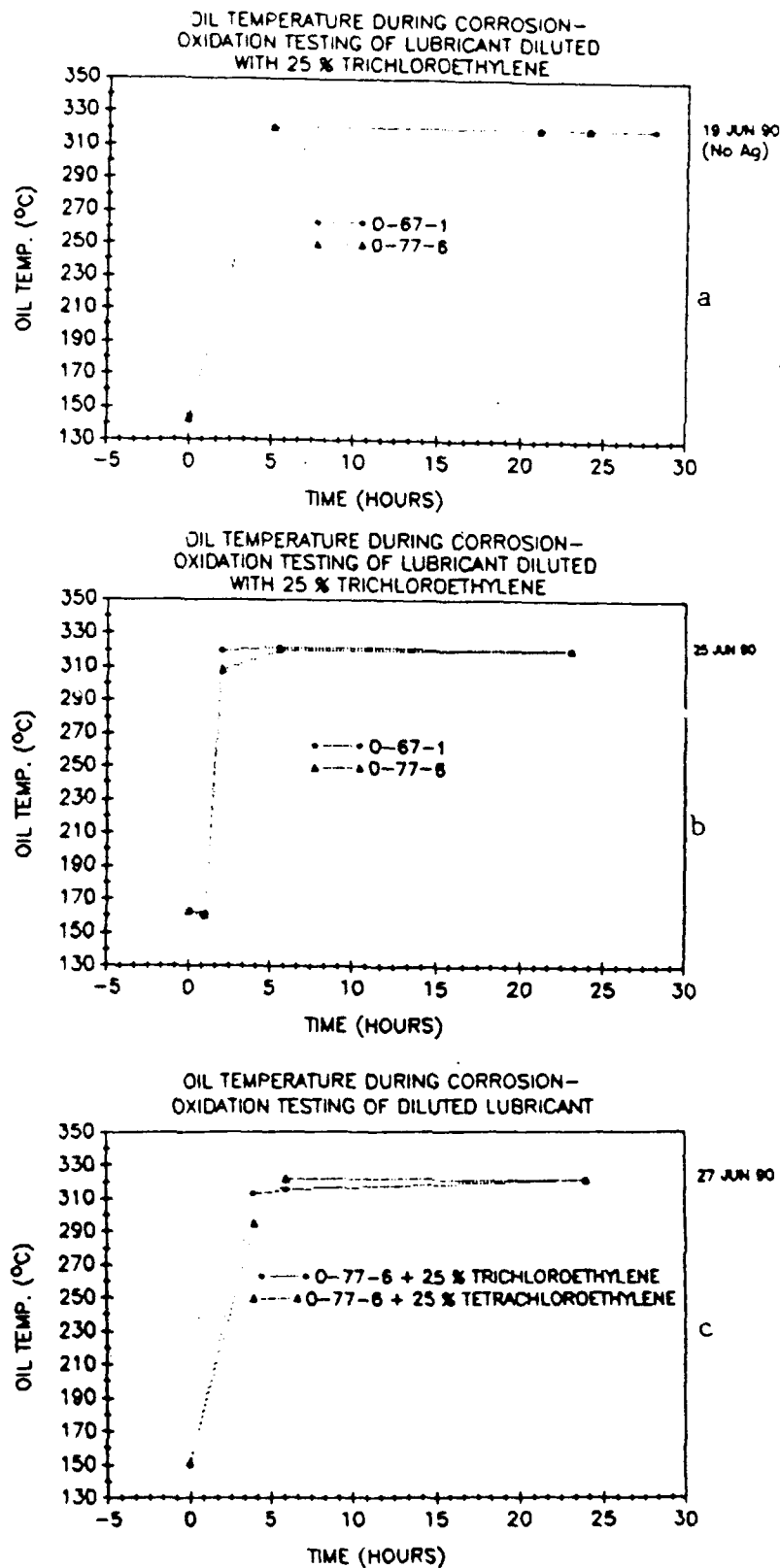


Figure 29. Plots of Oil Temperature vs. Time During Corrosion-Oxidation Testing Showing, a) the Difference Between O-67-1 and Additive A Contaminated O-77-6 without Silver Coupons, b) Same as a but with Silver Coupons Added to Test, and c) the Difference Between O-77-6 Diluted Fluids

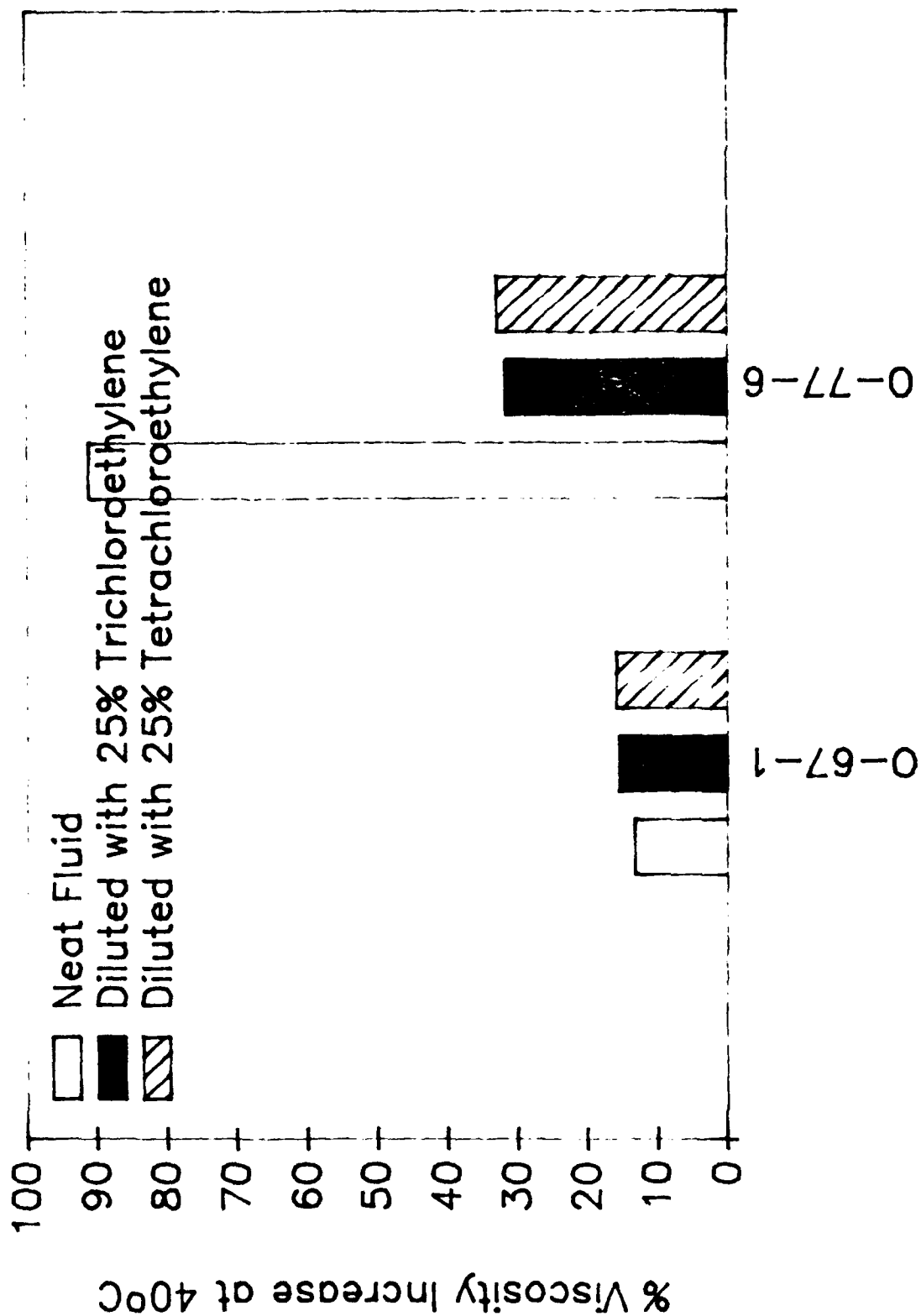


Figure 30. Effect of Solvent Dilution on 5P4E Fluids O-77-6 and O-67-1 Subjected to Corrosion and Oxidation Testing for 48 Hours at 320°C Using Squires Tubes and 10 L/h Airflow

TABLE 21

EFFECT OF DILUTION ON CORROSION-OXIDATION OF
O-67-1 AND O-77-6 AT 320°C USING SQUIRES
TUBES, 25 ML SAMPLES AND 10 L/H AIRFLOW (48 H)

Lubricant	Without Diluent		With 25% C ₂ HCl ₃			With 25% C ₂ Cl ₄	
	O-67-1 July 90	O-77-6 July 90	O-67-1 July 90	O-77-6 July 90	Nov 90	O-67-1 Nov 90	O-77-6 July 90
Init. Visc., at 40°C, cSt	280.8	279.5	280.8 15.67 ^a	279.5 14.65 ^a	279.5 13.59 ^a	280.8 21.95 ^a	279.5 22.15 ^a
Visc., cSt, at 40°C, after 48 h, 320°C C&O	318.1	534.5	324.3	368.4	365.8	325.6	371.4
% Visc. Inc. 40°C	13.3	91.2	15.5 ^b	31.8 ^b	30.9 ^b	15.9 ^b	32.9 ^b
Wt. Loss	4.4	7.5	4.3 ^c	5.8 ^c	7.4 ^c	6.9 ^c	6.1 ^c
Corrosion, mg/cm ²							
Al	0.00	-0.16	+0.02	+0.00	0.0	0.0	+0.02
Ag	0.00	-0.12	-0.02	+0.06	0.02	-0.1	+0.32
M-St	-0.04	+0.02	+0.04	+0.04	0.06	+0.06	-0.02
M-50	-0.08	-0.06	0.00	+0.04	0.06	+0.02	+0.02
Wasp	-0.12	-0.06	-0.04	0.0	0.0	+0.02	0.0
Ti	-0.08	-0.06	0.00	+0.02	0.02	+0.06	0.0

^aViscosity of lubricant + solvent

^bBased on % visc. change over fresh oil

^cLubricant loss after solvent loss

(5) Summary

The oxidative stability of several used (engine) samples of MIL-L-87100 lubricant showed various degrees in the loss of stability when compared to new fluid. The change in remaining oxidative stability did not correlate with any measured property such as initial viscosity, engine operating hours, iron content or tin content.

Three micron filtration of stressed MIL-L-87100 lubricants prior to C&O testing improved the oxidative stability of the samples, the amount of which depended upon the degree of "prestressing" and the amount of debris and polymeric material present in the fluid.

Corrosion and oxidation testing of four-ball wear samples of O-67-1 fluid obtained under various loadings and temperatures showed a small decrease in remaining oxidative stability as the test temperature was raised from 75°C to 315°C for 33 N loading. The oxidative stability of the fluid also appears to be related to combined changes in loadings and test temperatures.

The corrosion/oxidation test instability of some four-ball tested PPE lubricants is most likely due to the thermal/oxidative instability of the Friction Polymer (FP) that is produced. The relative stability of the FP, as determined by DSC and TGA, shows an approximate relationship to the acceleration in oxidation rates for the PPE lubricant from which they were isolated. It is theorized that the level of oxidative destabilization of any particular four-ball tested lubricant would be proportional to the concentration of the FP as well as its rate of decomposition.

Corrosion and oxidation studies of various 5P4E fluids containing diluents trichloroethylene and tetrachloroethylene showed these diluents to have minimal effect on the stability of these fluids.

TABLE 22

VISCOSITY INCREASE OF STRESSED TEL-9050

Test Hours	Test Temp., °C	40°C Vis., cSt	100°C Vis., cst	% Inc., 40°C Vis.	% Inc., 100°C Vis.
0	-	214.3	10.88	-	-
*24	280	230.7	11.58	7.7	6.4
*48	"	255.2	12.72	19.0	16.9
*72	"	295.6	15.02	37.9	38.1
72	"	261.8	13.25	22.2	21.8
96	"	292.5	14.46	36.5	32.9
*96	"	366.9	16.72	71.2	53.7
102	"	300.1	14.76	40.0	35.7
24	290	227.0	11.37	5.9	4.5
48	"	237.4	11.89	10.8	9.3
72	"	249.9	12.58	16.6	15.6
96	"	266.7	13.38	24.5	23.0
120	"	285.4	14.36	33.2	32.0
144	"	309.2	15.20	44.3	39.7
24	295	239.4	11.91	11.7	9.5
48	"	304.3	14.64	42.0	34.6
54	"	336.1	-	56.8	-
24	300	299.4	14.25	39.7	31.0
48	"	297.8	14.28	39.0	31.3
55.5	"	343.7	15.75	60.4	44.8

* 2nd Tube

TABLE 23

TOTAL ACID NUMBERS OF NEW AND STRESSED TEL-9050

Test Hours	Test Temp.	TAN, mg KOH/g
0	-	0.10
*24	280°C	0.22
*48	"	0.72
*72	"	1.12
72	"	0.53
96	"	0.98
*96	"	1.24
102	"	0.87
24	290°C	0.08
48	"	0.20
72	"	0.26
96	"	0.28
120	"	0.51
144	"	0.36
24	295°C	0.56
48	"	1.85
54	"	2.20
24	300°C	0.35
48	"	1.72
55.5	"	2.14

* 2nd Tube

f. Non-Polyphenyl Ether Based Experimental Fluids

(1) Corrosion and Oxidation Testing of TEL-9050 and TEL-9071

Corrosion and oxidation testing was conducted on experimental fluid TEL-9050 at temperatures of 280°C, 290°C, 295°C and 300°C using D 4871 tubes, with intermediate sampling and 10 L/h airflow. The initial (290°C) results showed this fluid to have equivalent stability but a higher corrosion tendency than the 5P4E O-77-6 fluid. The TEL-9050 fluid also showed measurable increases in total acid number and etching of the glassware used in the C&O test. Due to the instability of this fluid, testing at 280°C showed less oxidative stability than the 290°C test. The viscosity increase data given in Table 22 and total acid number increase data given in Table 23 both show erratic behavior for this fluid. For this reason its Arrhenius plots could not be developed. Except for the first test conducted at 290°C, the lubricant TEL-9050 becomes significantly corrosive to silver metal specimens used in the C&O test at the following temperatures and test times (Table 24).

TABLE 24

CORROSION MEASUREMENTS OF STRESSED TEL-9050

Test Time, h Temp., °C	Weight Change of Metal Specimens, mg/cm ²					
	Al	Ag	M-St	M-50	Wasp	Ti
102, 280	+0.04	-3.02	+0.06	+0.14	0.00	-0.02
144, 290	0.00	+0.06 ¹	+0.06	+0.02	+0.06	+0.04
54, 295	+0.10	-3.94	+0.12	+0.12	+0.10	+0.12
55.5, 300	+0.12	-3.78	+0.12	+0.12	+0.04	+0.10

¹ Heavy stain/deposit may have offset weight loss

The silver metal concentration was verified by AA-ADM analysis

(Table 25).

TABLE 25

SILVER METAL CONCENTRATION OF STRESSED TEL-9050

Test Time, h Temp., °C	AA-ADM, ppm	Calculated ppm Based on Wt. Change of Specimens
102, 280	109.6	106.9
144, 290	61.0	-
54, 295	149.5	138.6
55.5, 300	147.4	133.6

The test specimen after the 290°C test may have contained deposits which were not removed by the normal cleaning procedure. The high TAN values obtained during the C&O testing are the likely causes of the silver corrosion.

By-products generated during the C&O test of TEL-9050 have a detrimental effect on the glass condenser used in the test as vapors cause etching of the condenser end taper. This is also evidenced by the silicon analysis of the sample as shown in Table 26.

TABLE 26

SILICON CONTENT OF STRESSED TEL-9050

Test Time, h Temp., °C	AA-ADM Si (ppm)
102, 280	127
144, 290	227
54, 295	22.3
55.5, 300	5.3

The silicon concentration appears to become very high in tests having durations longer than 100 hours, even at lower temperatures.

TEL-9050 has a tendency to form heavy deposits during the C&O

test as shown in Table 27. The data show to some degree that the deposit formation is related to storage time of the fluid since the first test gave the least deposits.

TABLE 27

DEPOSIT FORMATION DURING C&O TESTING OF TEL-9050

Temp Time, h Temp., °C	Deposit Description
102 h, 280°C	Moderate varnish in test tube above oil level. Heavy coke in blower tube.
144 h, 290°C	Slight varnish in test tube above oil level. Moderate coke in blower tube.
54 h, 295°C	Heavy coke above in test tube oil level. Heavy coke in blower tube.
55.5 h, 300°C	Moderate varnish in test tube above oil level. Heavy coke in blower tube.

Fluids TEL-9050 and TEL-9071 (different sample of TEL-9050) were tested for moisture content along with selected C&O stressed samples of TEL-9050 due to suspected hydrolytic instability. The results shown in Table 28 do not represent a significant amount of water or a trend of increasing moisture content with exposure to the atmosphere.

TABLE 28

MOISTURE CONTENT OF TEL-9050

Sample	% H ₂ O
TEL-9050 (Lab sample, opened frequently)	0.01
TEL-9050 (Kept sealed in amber bottle)	0.01
TEL-9071 (Different bottle of TEL-9050 received at a later date)	0.02
TEL-9050, 102 h C&O at 280°C	0.04
TEL-9050, 144 h C&O at 290°C	0.08
TEL-9050, 54 h C&O at 295°C	0.02
TEL-9050, 55.5 h C&O at 300°C	0.02

The stressed samples do show an increase in water content with increased stressing time which is independent of temperature. This observation is consistent with the increase in silicon content due to acidic attack on the condenser.

(2) Corrosion and Oxidation Testing of TEL-90024

Corrosion and oxidation testing of TEL-90024 (TEL-9071 with inhibitor A) was conducted at 320°C with the test data being given in Table 29.

TABLE 29

CORROSION-OXIDATION TEST DATA FOR LUBRICANT
TEL-90024 AT 320°C USING 10 L/H AIRFLOW
100 ML SAMPLE AND D 4871 TUBES

Test Time, Hours	TAN mg KOH/g	Visc., 40°C (cSt)	η Visc., Chg 40°C	CORROSION DATA	
				Metal Type	Wt. Chg., mg/g
0	-	195.4	-	Al	+0.04
24	0.13	238.9	22.3	Ag	-0.10
48	0.19	266.8	36.5	M-Steel	0.00
72	0.37	313.7	60.5	M-50	+0.06
92	0.40	375.7	92.3	Wasp	-0.02

These data show that the inhibited fluid has improved oxidative stability and better corrosion characteristics than the base fluid TEL-9071. A vapor phase corrosion study of lubricant TEL-90024 was conducted at 300°C for 48 hours using 100 ml sample, D 4871 tube, airflow of 10 L/h and two sets of corrosion test specimens with one being in the liquid and one being suspended in the vapor phase area directly below the tapered joint of the D 4871 tube. The test data obtained from this testing are given in Table 30.

TABLE 30

TEST DATA FOR TEL-90024 LUBRICANT STRESSED 48 HOURS AT
300°C USING LIQUID AND VAPOR CORROSION TEST SPECIMENS

Viscosity (cSt at 40°C)	260.6
% Viscosity Increase	33
TAN (mg KOH/g of oil)	
Strong acid (Titrate to pH=7)	0.60
Weak acid (Titrate to pH=11)	0.02
Metal Specimens Wt differences, mg/cm ²	
	Liquid Vapor
Al	0.0 +0.1
Ag	-0.4 ¹ 0.0 ¹
Mild Steel	+0.1 ¹ +0.3 ¹
M-50 Steel	+0.2 ¹ +0.4 ¹
Waspaloy	+0.1 +0.1
Titanium	0.0 +0.1

¹Visible stain

The data in Table 30 show that the vapor phase corrosion of TEL-90024 using the above test conditions are about the same as the liquid corrosion except for silver corrosion which was much lower.

Corrosion and oxidation testing was conducted at 310°C and 320°C on fluid TEL-90059 which is a different batch of TEL-90024. Data obtained from this testing are given in Table 31. The data in Table 31 are inconsistent since the 310°C test gave a larger percent viscosity increase than that obtained at 320°C. The large amount of corrosion obtained in the 320°C test is due to the much higher test time causing severe degradation and high total acid number. A comparison of TEL-90024 and TEL-90059 is shown in Figure 31.

The viscosity increase is approximately the same at 24 hours for both fluids but TEL-90059 failed much more rapidly after 24 hours during the

TABLE 31

CORROSION AND OXIDATION OF TEL-90059 AT 310°C AND 320°C
USING D 4871 TUBES, INTERMEDIATE SAMPLING AND 10 L/H AIRFLOW

Test Hours	40°C Viscosity cSt	40°C Viscosity Change, %	TAN			
310°C Test Temperature						
0	195.4	-	0.01			
24	299.9	53.3	2.61			
320°C Test Temperature						
0	195.4	-	-			
24	241.9	23.8	0.15			
48	371.1	89.9	0.58			
70.5	397.3	103.3	1.44			
119	Oil Solidified	-	26.4			
330°C Test Temperature						
0	195.4	-	-			
24	320.2	63.9	-			
27	375.5	92.2	-			
Metal Corrosion, mg/cm ²						
	Al	Ag	M-St	M-50	Wasp	Ti
310°C Test	+0.08	-0.98	+0.04	+0.04	+0.04	+0.38
320°C Test	+2.70	+1.06	-43.86	-63.0	-0.30	-6.84
330°C Test	-0.04	+0.02	-0.04	+0.06	-0.02	+0.08

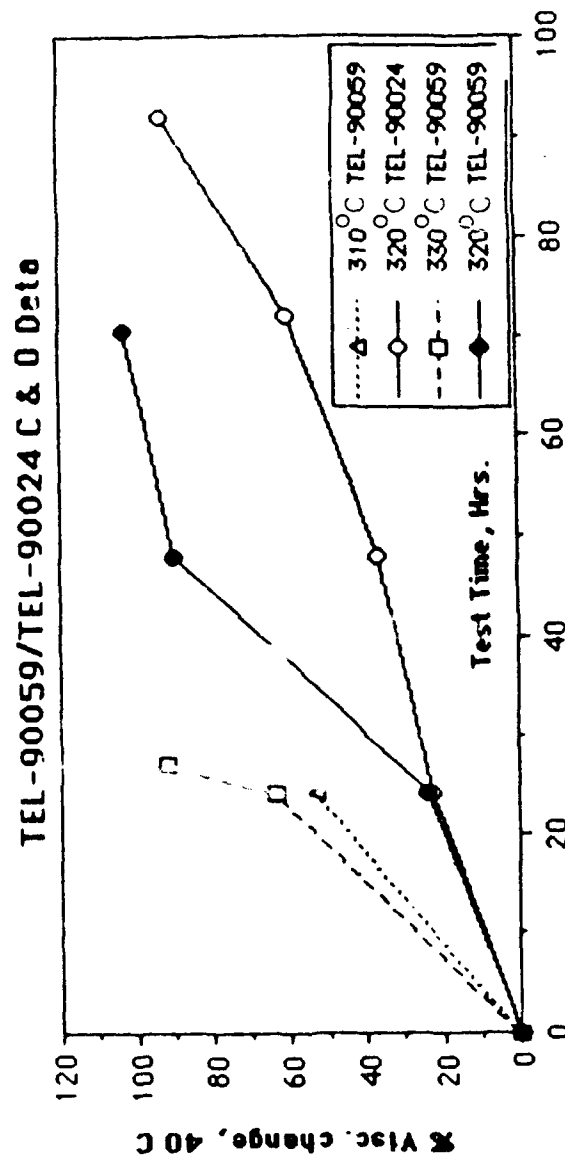


Figure 31. 40°C Viscosity Change During Corrosion and Oxidation Testing of TEL-90059 and TEL-90024 Using D4871 Tubes, Intermediate Sampling and 10 L/H Airflow. Filled Circle Represents New Data

320°C testing. At the termination of the TEL-90059 test at 119 hours, the lubricant had completely turned to a flaky charcoal like deposit which was insoluble in toluene. This deposit was heavily coated on the two steel specimens M-ST and M50 while leaving the Waspaloy specimen relatively clean. Even though M-ST and M50 steel specimens were the most heavily coated with deposits, they still showed a large weight loss. These events were not observed with the TEL-90024 C&O test at 320°C.

Corrosion and oxidation testing of experimental fluid TEL-90063 (TEL-9071 with different inhibitor B) was conducted at 310°C, 320°C and 330°C with the data being given in Table 32 and shown graphically in Figures 32 and 33. These figures show that the 310°C and 320°C tests give similar low levels of degradation up to 24 test hours after which both tests show a large change in the rate of degradation with the 320°C test rate being about double the 310°C degradation rate. Testing at 330°C for 24 hours shows a relatively high rate of degradation. All three tests showed significant post test corrosion for only the silver test specimen. Portable Wear Metal Analyzer (PWMA) analyses for trace metals in TEL-90063 at different corrosion and oxidation stressing times and temperatures are given in Table 33. Although very limited, these analyses agree with the metal corrosion test data given in Table 32 and show a correlation with TAN values as would be expected.

TABLE 32

CORROSION AND OXIDATION OF TEL-90063 AT THREE TEST TEMPERATURES
USING D 4871 TUBES, INTERMEDIATE SAMPLING AND 10 L/H AIRFLOW

Test Hours	40°C Viscosity cSt	40°C Viscosity Change %	TAN			
310°C Test Temperature						
-	215.4	-	-			
24	233.5	8.4	0.02			
48	326.2	51.4	2.87			
320°C Test Temperature						
24	237.8	10.4	0.14			
48	452.6	110.1	4.83			
330°C Test Temperature						
24	276.7	28.5	0.63			
Metal Corrosion, mg/cm ²						
	Al	Ag	M-St	M-50	Wasp.	Ti
310°C Test	+0.02	-7.56	+0.14	+0.14	+0.14	+0.16
320°C Test	+0.04	-4.52	+0.04	+0.02	+0.02	0.00
330°C Test	+0.02	-0.66	+0.02	+0.02	-0.02	+0.04

TEL-90063 C & O data

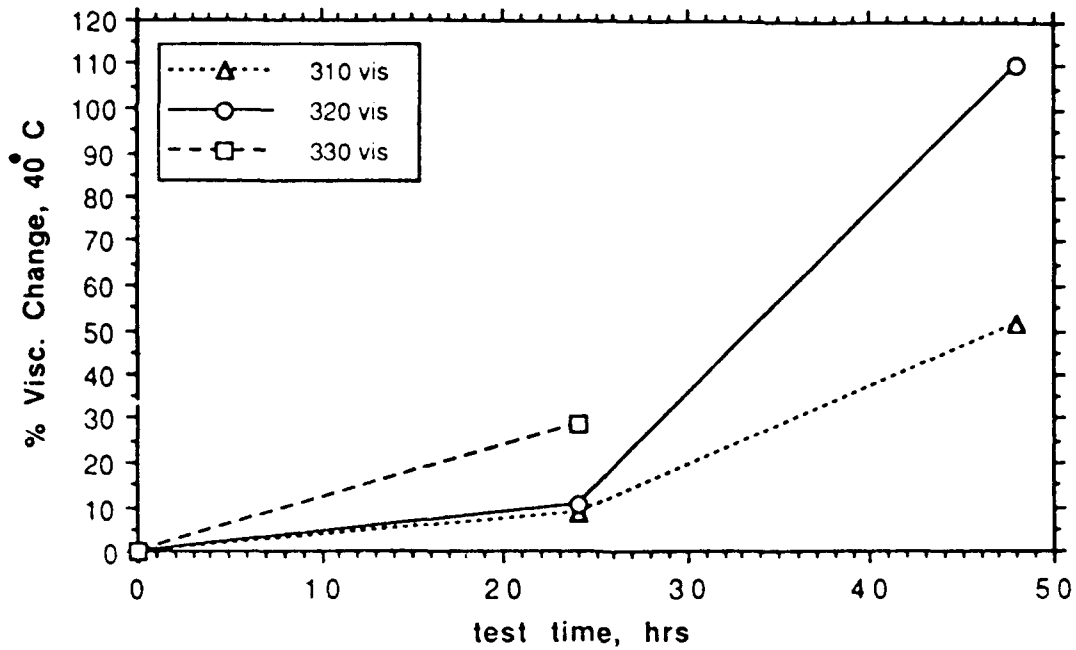


Figure 32. 40°C Viscosity Change During Corrosion and Oxidation Testing of TEL-90063 Fluid Using D4871 Tubes, Intermediate Sampling and 10 L/h Airflow

TEL-90063 C & O Data

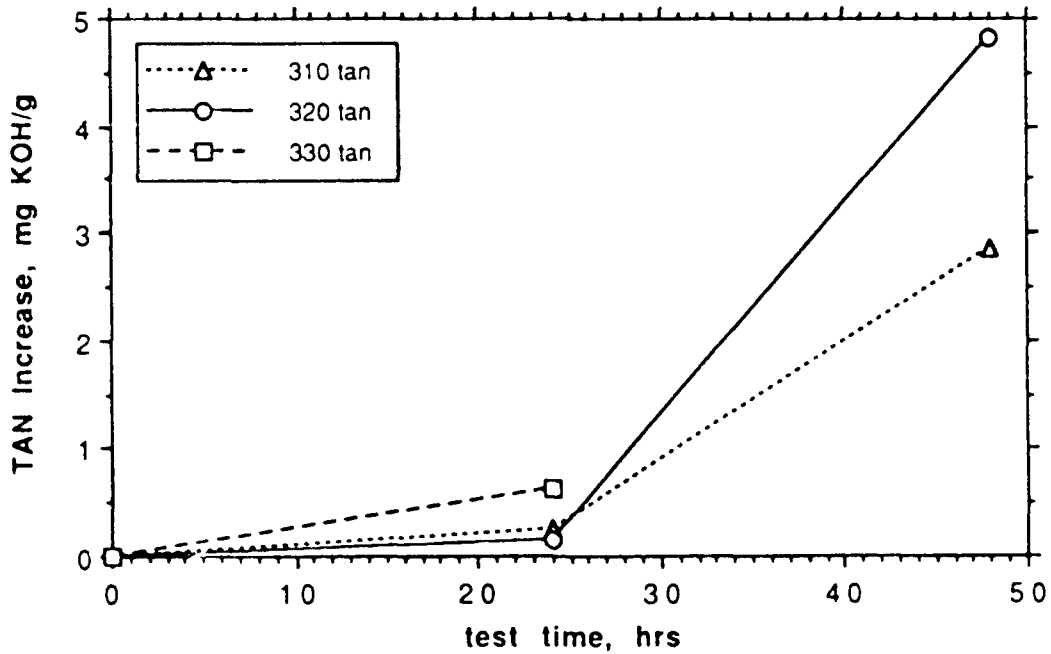


Figure 33. TAN Increase During Corrosion and Oxidation Testing of TEL-90063 Fluid Using D4871 Tubes, Intermediate Sampling and 10 L/h Airflow

TABLE 33

PWMA ANALYSIS OF TRACE METALS IN TEL-90063 AT DIFFERENT
CORROSION AND OXIDATION STRESSING TIMES AND TEMPERATURES

	Initial Conc., ppm	Conc. at 24 h & 330°C, ppm	Conc. at 24 h & 320°C, ppm	Conc. at 48 h & 320°C, ppm
Fe	0.1	3.0	1.2	2.4
Ag	0	19.0	9.2	122.1
Al	0	0	0	0
Cr	0	0	0	0
Cu	0	0	0	0
Mg	0	0	0	0
Ni	0	0.2	0.2	0.6
Si	0	0	0	0
Ti	0.1	0.4	0	0.6

Although fluid TEL-90063 has shown better storage stability (no increase in cloudiness upon standing) than fluids TEL-90024 or TEL-90059, the oxidative stability of TEL-90063 above 24 test hours appears to be no better than the fresh sample of TEL-90024.

A small sample (approximately 200 mL) of TEL-90001 was received and limited testing was initiated. A planned 48 hour 320°C C&O test was aborted after 24 hours due to a white vapor evolving from the test tube upward toward the condenser. The fluid was drained from the tube while warm and upon cooling the sample solidified, prohibiting viscosity measurements. The corrosion test data showed a weight loss of 0.28 mg/cm² for M-50 and a loss of 5.78 mg/cm² for silver. The total acid number increased dramatically to a value of 19.7 after 24 test hours.

(3) Vapor Phase Corrosion of TEL-9071

(a) Introduction

It has been shown that the vapors produced by the C&O testing of the TEL-9050 fluid etch the glass condenser of the test assembly causing the silicon concentrations of the stressed TEL-9050 fluids to

increase with time. Therefore, research was performed to determine if the vapors produced by the C&O testing of TEL-9050 were capable of corrosive attack on metal and alloy surfaces in the head space above the lubricant.

The 48 hour tests were performed using 100 mL samples of TEL-9071 (TEL-9050 received at a later date), the D 4871 tubes, intermediate sampling at 24 hours, air flows of 10 and 55 L/h, and test temperatures of 280 and 320°C. Two sets of test washers were used: one set immersed in the stressed fluid and the second set supported by a 17 cm glass spacer positioned in the vapor phase directly below the tapered joint of the D 4871 tube. The 55 L/h flow rate was used in an attempt to increase the amount of stressed TEL-9071 and degradation products in the vapor phase. The test data for the stressed TEL-9071 fluids obtained at 24 and 48 hours and the weight changes of the liquid and vapor phase test washers obtained at 48 hours are listed in Table 34.

(b) Viscosity Test Data

The test data listed in Table 34 for the 24 hour samples of the 280 and 320°C tests performed with 10 L/h airflow rates are as expected with the higher temperature producing a higher viscosity change. However, the 48 hour samples produced the opposite trend with the lower temperature producing the higher viscosity change. Since the 280°C results are in agreement with previous research and the 48 hour sample obtained from the 320°C test with the 55 L/h air flow rate produced the expected higher viscosity increase and underwent significant evaporation (20-30% weight loss), the viscosity decrease for the 320°C test (10 L/h) is attributed to the accumulation of volatile, low viscosity degradation products. The accumulation of the degradation products is most likely due to the vapor phase test washers which increase the condensate return of the C&O test

TABLE 34

TEST DATA FOR FRESH AND STRESSED TEL-9071 FLUIDS
USING LIQUID AND VAPOR CORROSION TEST SPECIMENS

Flow Rate (L/h)	10		10		55	
Temperature	280°C		320°C		320°C	
Viscosity (cSt at 40°C)						
24 h	229.5		275.5		230.3	
48 h	242.2		226.8		389.2	
					(evaporated)	
% Viscosity Increase						
24 h	8.0		28.9		7.7	
48 h	13.9		6.0		82.0	
TAN (mg KOH/g of oil)						
Strong Acid						
24 h	0.12		1.12		0.05	
48 h	0.22		2.10		0.76	
Weak Acid						
24 h	0.16		0.88		0.05	
48 h	0.19		1.48		0.46	
Color						
24 h	LIGHT		DARK		LIGHT	
48 h	LIGHT		DARK		DARK	
Fluoride (ppm)						
24 h	1		15		1	
48 h	1		300		5	
Metal Specimens Wt ₂ Differences, mg/cm ²	Liquid	Vapor	Liquid	Vapor ^a	Liquid	Vapor
Al	+0.48	0.0	-0.04	+2.14 ^b	-0.04	+0.02
Ag	-0.12	0.0	-0.62	+1.00 ^b	-0.48	+0.12
Mild Steel	+0.30	-0.06	-0.12	-2.10 ^b	+0.03	-0.12
M50 Steel	+0.24	-0.06	-0.18	-1.56	+0.10	+0.20
Waspaloy	+0.32	+0.16	-0.04	-0.06	+0.04	+0.22
Titanium	+0.38	+0.18	-0.10	-0.52	-0.18	-0.20

^a All Washers covered with thick coke deposit

^b Coating not removed by normal cleaning procedures

system.

(c) Thermal Gravimetric Analyses

To verify the presence of the volatile degradation products in the 48 hour stressed TEL-9071 fluid (10 L/h), thermal gravimetric analytical (TGA) weight percent loss versus temperature profiles were produced for the fresh and 48 hour stressed fluids and are shown in Figure 34. The TGA profiles in Figure 34 show that the initial weight loss of the 48 hour stressed TEL-9071 fluid occurs at a lower temperature than for the fresh TEL-9071 indicating the stressed fluid contains a volatile fraction not present in the fresh fluid. The TGA profiles in Figure 34 also show that the final weight loss of the 48 hour stressed TEL-9071 fluid is incomplete and occurs at a higher temperature than for the fresh TEL-9071 indicating that the stressed fluid contains a high boiling fraction not present in the fresh fluid.

The TGA profiles demonstrate that the stressed TEL-9071 fluids contain volatile degradation products as well as polymerized degradation products. Therefore, the viscosity measurements in Table 34 result from the combined effects of the volatile and polymerized degradation products, and consequently are strongly dependent on the condensate efficiency of the C&O test.

(d) Total Acid Number Test Data

In contrast to the viscosity measurements, the total acid number measurements in Table 34 are as expected for the 280 and 320^oC (10 L/h) tests with the acid levels increasing with time and temperature. The TAN measurements were separated into strong (titrate to pH=7) and weak (titrate pH=7 to pH=11) acids in order to better understand the corrosive nature of the stressed TEL-9071 fluids. The fact that the TAN measurements

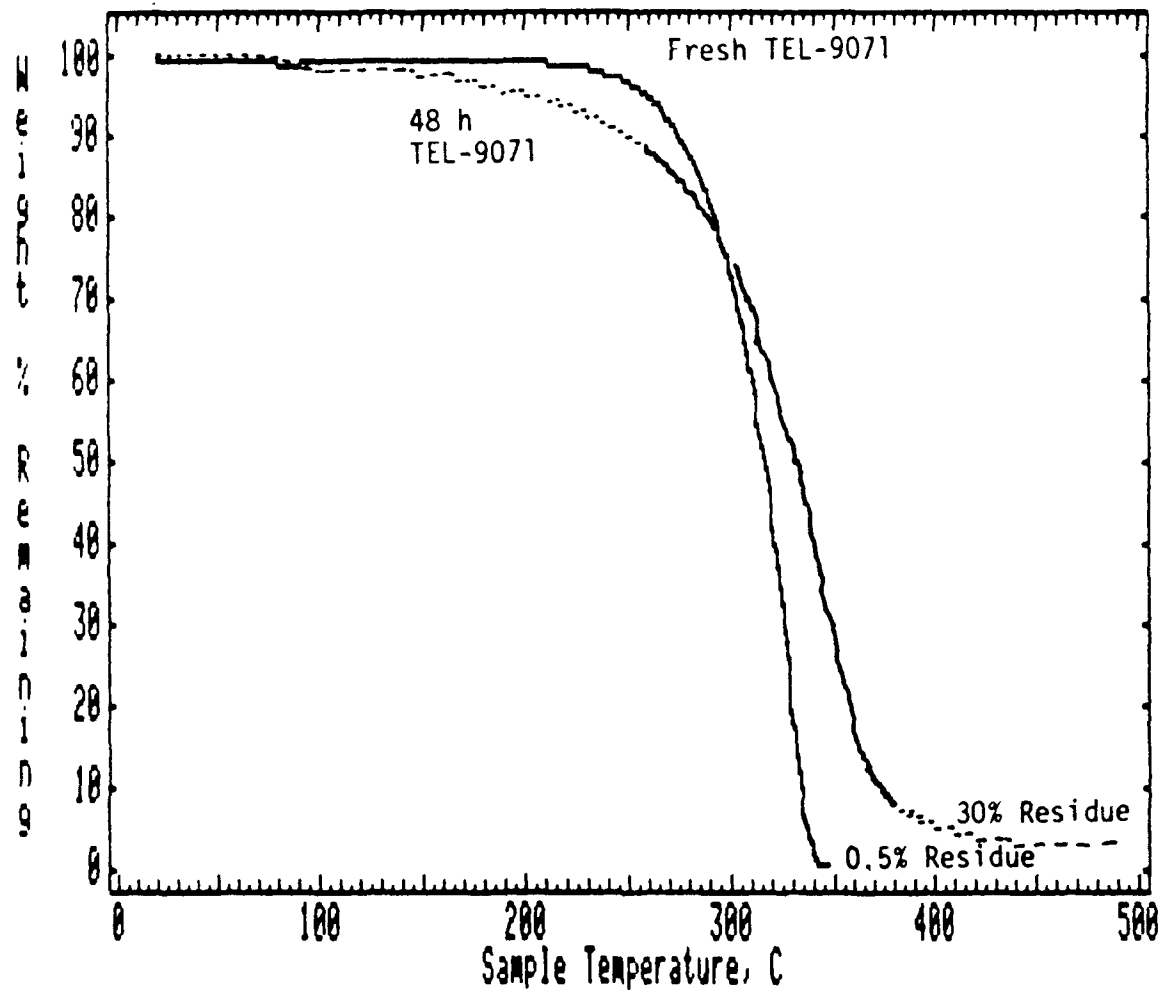


Figure 34. TGA Weight Percent Remaining Versus Temperature Profile (Nitrogen Atmosphere, 10 mg Samples) for Fresh and 48 Hour Stressed (320°C, 10 L/h) TEL-9071 Fluids (Sample Size = 10 mg; Heating Rate = 20°C/min)

increased from 24 to 48 hours for the 320°C (10 L/h airflow rate) test while the viscosity measurements decreased (Table 34) indicates that the volatile species produced by the TEL-9071 are highly acidic. Also, increasing the airflow rate from 10 to 55 L/h decreased the TAN measurements further indicating the volatile degradation products are highly acidic.

(e) Fluoride Test Data

Since earlier research had reported etching of the glassware, research was performed to quantitate the fluoride in the stressed TEL-9071 fluids. The fluoride content would then be related to the presence of hydrofluoric acid (etches glass). The fluoride analyses were performed using a solid-state fluoride specific electrode and the fluoride ions were extracted into an aqueous layer (buffered to pH=4) using heated ultrasonic agitation.

The test data in Table 34 indicate that the fluoride content of the stressed fluids is increased by increased temperature and by decreased air flow rate in agreement with the strong acid numbers. However, between 24 and 48 hours of stressing at 320°C (10 L/h) the strong acid number only doubles while the fluoride ion increases 20 fold. The 15 and 300 ppm fluoride concentrations in Table 34 would produce strong acid numbers of 0.04 and 0.88 (1.12 and 2.10 determined) if the fluoride ion was attributed completely to hydrofluoric acid. Thus, these results indicate that strong acids other than hydrofluoric acid are present and the percentage of strong acid which is hydrofluoric acid increases with time but decreases with air flow rate.

(f) Weight Changes of Test Washers

The corrosive nature of the stressed TEL-9071 fluids was tested in both the liquid and vapor phases. The weight losses of the test

washers in Table 34 show that the corrosive nature of the stressed TEL-9071 in the liquid phase increases with temperature and is decreased slightly by increased air flow rate in agreement with the TAN measurements. The weight losses of the test washers in Table 34 show that the corrosive nature of the stressed TEL-9071 in the vapor phase also increases with temperature but is decreased significantly by increased air flow rate.

In the case of the 320°C 10 L/h test, the vapor phase washers (except for the Waspaloy washer) underwent larger weight changes than the liquid phase washers. In the vapor phase the titanium and steel washers underwent significant weight loss, while in the liquid phase only the silver washer showed significant weight loss. The weight losses of the aluminum, silver, and mild steel washers could not be determined accurately since the washers were covered with a thick deposit after normal cleaning procedures.

In addition to the unremoved deposits, all of the vapor phase washers obtained from the 320°C, 10 L/h test were covered with large amounts of coke, e.g., 150 mg removed from M-50 steel washer. Heavy deposits also formed on the D 4871 tube above the liquid line of the stressed TEL-9071 fluid for the 320°C, 10 L/h test. The deposits and coke produced by the 320°C, 10 L/h test were time dependent and were not observed during the sampling of the 24 hour sample. In contrast to the 320°C, 10 L/h test, the tests performed at 280°C, 10 L/h and at 320°C, 55 L/h produced only slight stain/deposits on the test washers and glass surfaces.

(g) X-Ray Photoelectron Spectroscopic Analysis of Test Washers

In order to determine the effects of temperature, metal surface and fluid phase (liquid versus vapor) on the chemical compositions of stain/deposits produced by the stressed TEL-9071 fluid, X-ray photoelectron spectroscopic (XPS) analyses were performed on the the reacted specimens.

The mild steel specimens obtained from the liquid and vapor phases of the 280°C C&O test, the silver specimen obtained from the liquid phase of the 280°C C&O test, and the silver specimen obtained from the vapor phase of the 320°C C&O test were analyzed by XPS. The mild steel and silver (280°C) specimens were covered by thin (estimated to be less than 1 micron) stains while the surface of the silver specimen obtained from the 320°C C&O test was covered by a thick (determined to be 8.1 ± 0.3 microns), dark deposit. The XPS elemental analyses and the elemental ratios of the stains/deposits present on the surfaces of the silver and mild steel specimens are listed in Tables 35 and 36, respectively.

The results in Table 35 indicate that the elemental analyses of the stains/deposits are similar for the mild steel and silver specimens regardless of temperature, phase, or metal. All of the stains/deposits contained C, F, N, O and P. (H is not detected by XPS.) The F is present as an organic fluorine (ionic fluoride expected if metal fluorides present) and the P is present as a phosphate (PO_x).

To better determine the effects of temperature, phase and metal type on the compositions of the stains/deposits, various elemental ratios were determined and are listed in Table 36. The ratios listed in Table 36 demonstrate that the C and F contents (with respect to P) of the stains and deposits on the surfaces of the specimens are higher for the vapor phase than for the liquid phase. Although the C to F ratio is unaffected by the temperature, metal or phase, the C and F content is highest for the silver specimen obtained from the vapor phase of 320°C C&O test.

The elemental ratios listed in Table 36 also indicate that the N, F and C contents (with respect to P) are lower, while the oxygen content is higher, for the stain/deposit films on the mild steel specimens

TABLE 35

XPS ELEMENTAL ANALYSES OF STAINS/DEPOSITS PRESENT ON
MILD STEEL AND SILVER SPECIMENS

Atomic Percentage					
Element	Types	Mild Steel		Silver	
		Liquid ^a	Vapor ^a	Liquid ^a	Vapor ^b
C	C-F, C-O C=O, C-H	38.1	52.4	51.1	63.2
O	-O, =O	36.3	29.2	28.0	18.3
F	C-F	6.0	6.8	8.3	9.4
N	-	4.1	2.8	5.9	6.4
P	P-O	7.6	3.8	5.4	2.5
Fe	-	8.0	5.1	-	-
Ag	-	-	-	1.4	B.D.

^a280°C^b320°C

B.D. - Below Detection Limit of 0.1%

TABLE 36

XPS ELEMENTAL RATIOS OF STAINS/DEPOSITS PRESENT ON
MILD STEEL AND SILVER SPECIMENS

Ratio	Mild Steel		Silver	
	Liquid ^a	Vapor ^a	Liquid ^a	Vapor ^b
N/P	0.5	0.7	1.1	2.5
O/P ^c	3.5	4.8	2.9	1.1
F/P	0.8	1.8	1.5	3.8
C/P	5.0	13.8	9.5	25.3
C/F	6.3	7.7	6.2	6.7

^a280°C^b320°C^cOxygen = Oxygen (Total) - Oxygen (C=O) - Oxygen (C-O)

than for the silver specimen. These trends are not unexpected since the N and F would be expected to prefer the silver surface while the PO_x moiety would be expected to prefer the Fe in the mild steel surface.

(h) Scanning Electron Microscopic/Energy Dispersive Spectroscopic Analyses of Test Washers

Since the deposit on the silver specimen obtained from the vapor phase of the 320°C C&O test is much thicker than the stains on the mild steel and silver specimens obtained from the 280°C C&O test, an elemental depth profile was performed on the deposit. A ball bearing was used to produce a 10 micron depth crater in the deposit as shown by the Scanning Electron Microscopic (SEM) photograph in Figure 35. The white surface in the center of Figure 35 is the exposed Ag surface. The jagged outline of the inner Ag surface is a result of the machine markings on the surface of the specimen. The outer lighter ring is the wear debris produced by the cratering procedure. The SEM/EDS system was used for the elemental depth profile since the XPS system analyzes square centimeter areas and 1 square micron areas (SEM/EDS) were required for the depth profiles.

The Energy Dispersive Spectroscopic (EDS) spectra (N not detected) in Figure 36 were obtained for the inner (crater bottom) and outer (crater top) regions of the dark region in Figure 35. The EDS spectra in Figure 36 do not exhibit any peaks for Ag indicating the F is present as CF_x and not AgF in agreement with the XPS data in Table 35. The EDS spectra in Figure 36 demonstrate that the P and O contents increase with respect to the C and F contents as the EDS analyses progress from the top of the crater toward the bottom of the crater. The EDS results indicate that the high C and F contents and low O content detected by the XPS analyses of the thick deposit on the silver specimen (Table 36) are due to increased film thickness

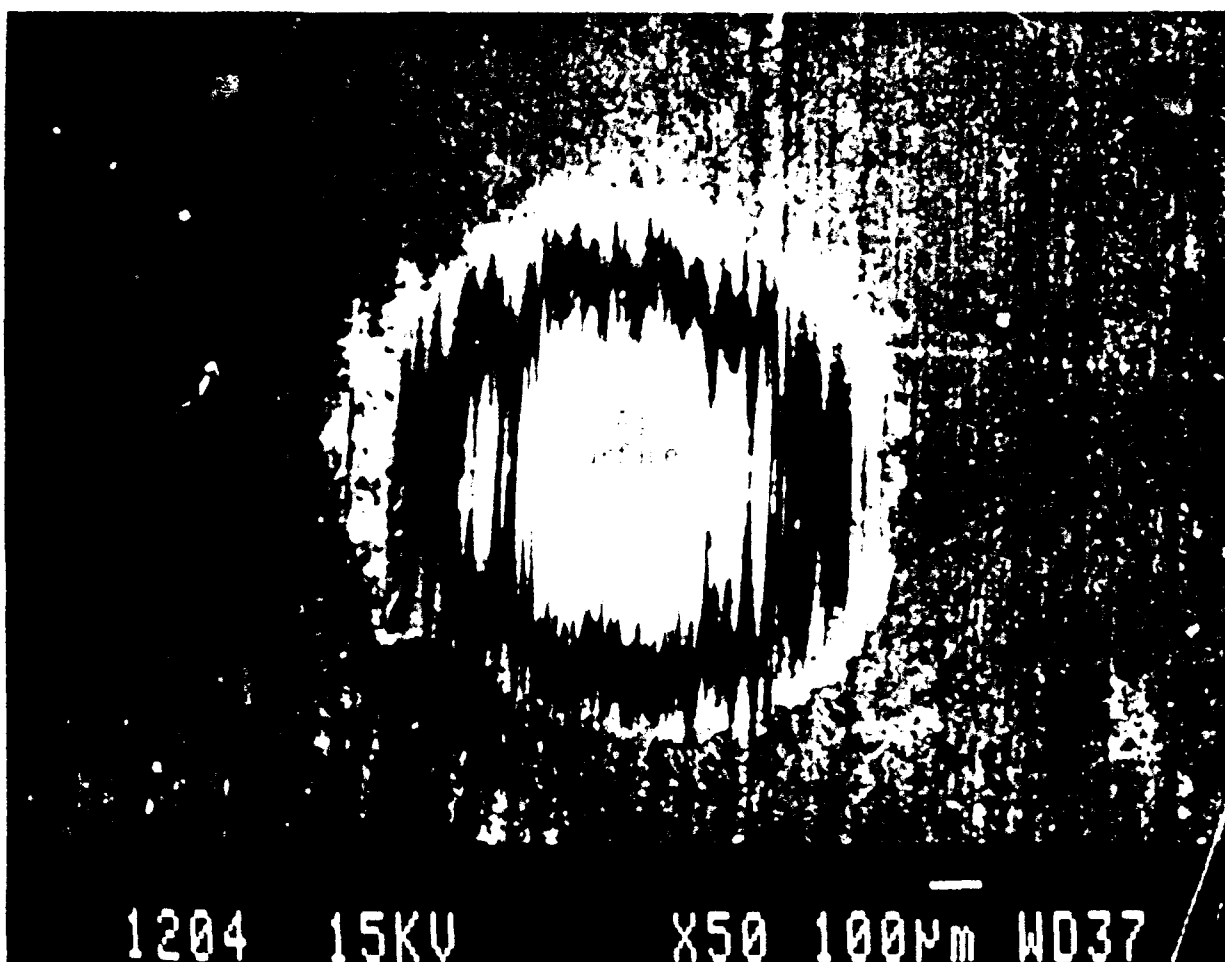


Figure 35. Crater Produced in the Deposit on the 320⁰C C&O Test, Vapor Phase Silver Specimen

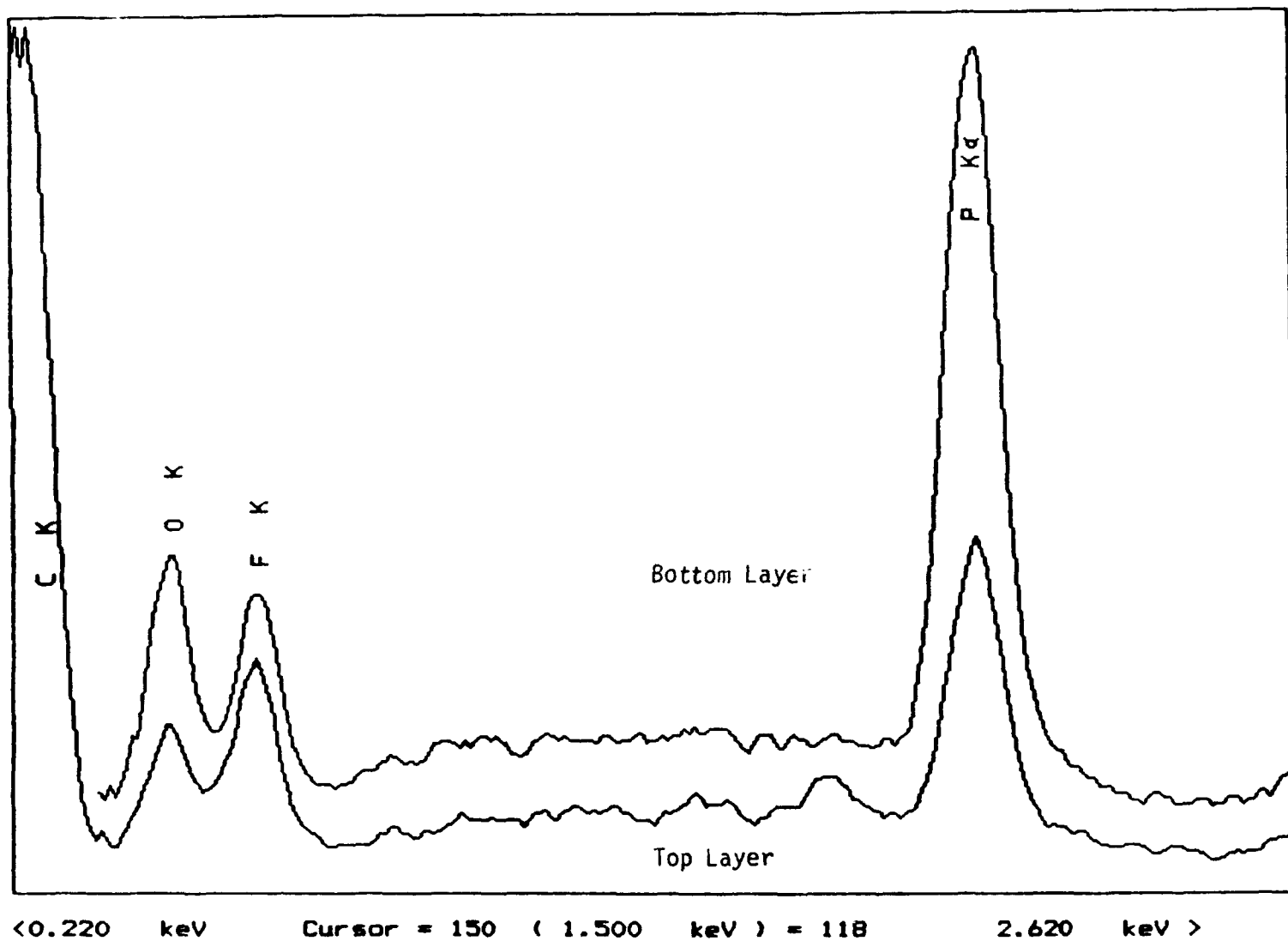


Figure 36. EDS Spectra of Top and Bottom Layers of Deposit on the 320°C C&O Test, Vapor Phase Silver Specimen

instead of temperature or metal effects.

(i) EDS Analyses of Glass Deposits

To confirm the white deposits present on the glass surfaces after the C&O testing of TEL-9071 fluid are a product of hydrofluoric acid attack, EDS analyses of the glass deposits were performed. The EDS analyses determined that the white deposits were silicon fluorides, the result of hydrofluoric acid attack on the glass surface.

(j) Analysis of Condensate

The condensates from the C&O tests of the TEL-9071 fluid were collected and analyzed by GC/MS. The major products were fluorinated phenolic species which are in agreement with the XPS analyses of the vapor phase deposits on the metal specimens.

(4) Summary

Corrosion and oxidation testing of several non-polyphenyl ether basestock fluids has shown much lower oxidative stability and increased corrosiveness when compared to either inhibited or uninhibited polyphenyl ether fluids. These fluids gave high TAN values during C&O testing which did not occur with 5P4E fluids. The high TAN values probably account for the high vapor phase corrosion of these fluids when uninhibited. The addition of additives to the base fluids did improve the corrosion characteristics but not the oxidative stability as measured by viscosity change during C&O testing. These fluids, in general, also had poor storage stability.

The test results obtained for the C&O testing of the TEL-9071 fluid indicate that both volatile and polymeric degradation products are present in the stressed fluid so that the viscosity measurements are strongly affected by the condensate return efficiency of the test setup. The results also indicate that the volatile degradation products are strong acids,

including hydrofluoric acid and fluorinated phenols. The percentage of strong acids present as hydrofluoric acid increased with time. Since the volatile degradation products are strong acids, the expected vapor corrosions of the test washers and glass surfaces were verified and were shown to be temperature dependent. In addition to the vapor phase corrosion, coking occurred on the vapor test washers which was time and temperature dependent. The fact that the concentration of hydrofluoric acid and the coking tendency of the TEL-9071 fluid increased dramatically between 24 and 48 hours of stressing at 320°C (10 L/h) implied that the two degradation products are related.

The results of the XPS and SEM/EDS analyses of the stains/deposits on the surfaces of the metal specimens and glassware demonstrate that the deposits produced by the stressed TEL-9071 fluid contain C, F, N, O and P (H not detected by XPS) and the elemental compositions are not significantly affected by temperature, metal surface or phase (liquid versus vapor). The XPS results indicate that the stains/deposits produced on the metal specimens in the vapor phase had higher C and F contents than those produced in the liquid phase and that the silver surface promoted the C, F and N contents of the stains/deposits while the mild steel surface promoted the O content. The depth profiling of the thick deposit on the silver specimen from the 320°C C&O test showed that the PO_x content of the film increased toward the metal surface.

3. LUBRICANT DEPOSITION STUDIES

a. AFAPL Static Coker

(1) Introduction

Satisfactory performance of a lubricant requires, among many properties, a low deposition tendency. As previously reported¹ many techniques have been investigated for measuring the deposit forming characteristics of a lubricant. One of these techniques involved the AFAPL Static Coker which has been investigated in depth and used for measuring the deposit forming characteristics of ester base MIL-L-7808 and MIL-L-23699 type lubricants.² The effort described here continues with the further development and use of the AFAPL Static Coker for investigating the deposition characteristics of high temperature lubricants and experimental fluids.

(2) Apparatus and Test Procedure

The AFAPL Static Coker and general test procedure have been previously described^{1,2} and will not be repeated. Changes made in the test equipment during this effort included the use of stainless steel sealing rings in place of the polytetrafluoroethylene seals and the subsequent use of stainless steel SS-302 metal test specimens in place of the normal shim stock (1010 steel) test specimens. A change in test procedure included the use of programmable temperature controllers which permitted temperature ramping during the test and reporting the weight of seal deposits along with test specimen deposit.

(3) Test Lubricants

Lubricants and fluids used and investigated during this study are presented in Table 37. Appendix A lists all the static coking data for all lubricants studied to date.

TABLE 37

DESCRIPTION OF TEST FLUIDS USED IN STATIC COKING STUDY

Test Fluid	Description	Visc. at 40°C, cSt
O-67-1	MIL-L-87100 Oil (5P4E)	280.3
O-77-6	Basestock for O-67-1	280.4
TEL-9028	Used MIL-L-87100	298.0 ¹
TEL-9029	Used MIL-L-87100	284.9
TEL-9030	Used MIL-L-87100	283.7
TEL-9038	Used MIL-L-87100	288.4
TEL-9039	Used MIL-L-87100	298.1 ²
TEL-9040	Used MIL-L-87100	293.7
TEL-9050	Experimental Fluid	214.3
TEL-90001	Experimental Fluid	235.4
TEL-90018	Polyphenyl Ether (6P5E)	-
TEL-90024	Inhibited TEL-9050	195.4
TEL-90025	Used MIL-L-87100 Fluid	288.3
TEL-90026	Used MIL-L-87100 Fluid	289.3
TEL-90028	Inhibited TEL-90018 Fluid	1468.4
TEL-90059	Different Lot of TEL-90028	195.4
TEL-90063	Experimental Fluid	215.4
CB-1	Blend of Four-Ball Wear Tests ³	290.2
W.T. 346	Wear Tested O-77-6 Fluid ⁴	-
W.T. 352	Wear Tested O-67-1 Fluid ⁴	-
W.T. 387	Wear Tested TEL-9030 Fluid ⁴	-

¹After removal of 15% tetrachloroethylene

²After removal of 1.9% trichloroethylene

³Residual sample of wear tests No. 369, 370 and 397 of O-67-1

⁴Reference Section V for details of wear tests

(4) Results and Discussion

(a) Initial Studies of Optimum Sample Size on Polyphenyl Ether Fluid O-77-6

Initial coking studies involved varying the sample size of basestock fluid O-77-6 using a 3 hour test period, shim stock test specimens and a 375°C test temperature. The data in Table 38 show the effect of sample size on the amount of deposits and test repeatability.

TABLE 38

AFAPL STATIC COKER DATA FOR FLUID O-77-6
AT 375°C, 3 HOURS TEST TIME USING
SHIM STOCK TEST SPECIMENS

Sample Size, mL	Deposits, mg/g	Std. Dev.
0.13 ± 0.01	34.3	3.5
0.17 ± 0.02	22.2	1.7
0.24 ± 0.02	16.4	0.2
0.35 ± 0.02	9.1	0.7
0.50 ± 0.02	6.5	0.4
0.74 ± 0.02	4.6	0.4

The data in Table 38 and displayed graphically in Figure 37 show that deposit levels are inversely proportional to sample size and that the standard deviation increases with decreasing sample size. No deposits were obtained on the stainless steel sealing rings for any of the twenty tests represented by the data in Table 38. All the tests gave hard dark brown deposits. During this testing no red iron oxide appeared on the shim stock test specimens as occurred with testing of the inhibited O-67-1 which will be discussed later. The data in Table 38 indicate an optimum sample size of 0.5 mL. Generally, the increase in deposits with decreasing sample

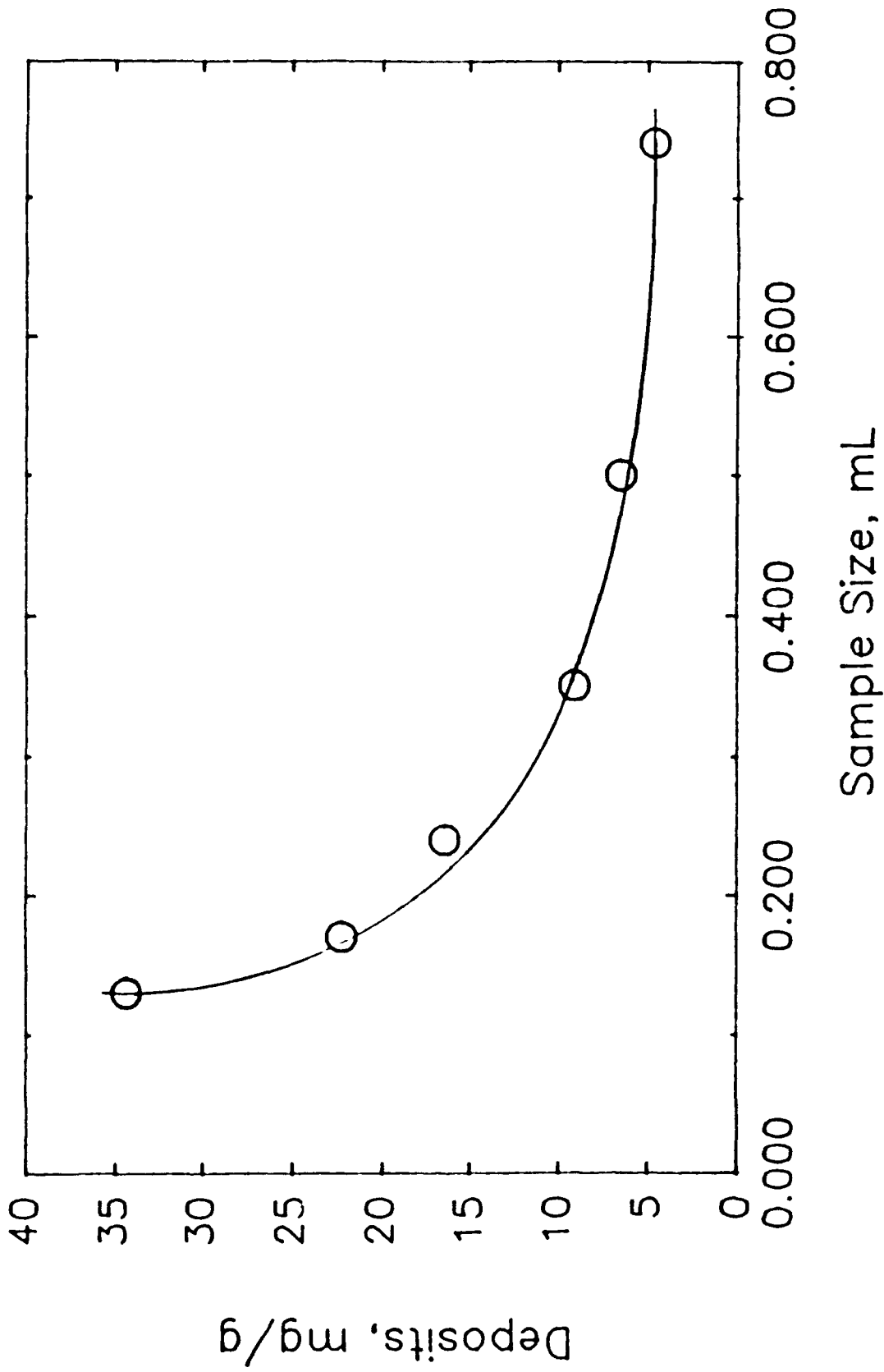


Figure 37. Effect of Sample Size on AFAPL Static Coker Deposits at 375°C, 3 Hour Test Time, Shim Stock Test Specimen and Lubricant 0-77-6

size of the high temperature fluids opposed to the ester based fluids is probably due to the increased oxygen availability of thinner films, less effects due to volatility before degradation and less cooling of the surface when adding the sample as the sample size is decreased. The larger standard deviation is partially due to the larger factor required for reporting the deposits in mg/g sample.

(b) Programmable Temperature Controller Studies

Subsequent to the initial O-77-6 fluid sample size studies, the four AFAPL Static cokers were modified by incorporating programmable temperature controllers. Since these new controllers could affect the variation between controller temperature and test specimen surface temperatures, a series of surface temperature measurements were made at different controller settings for determining temperature variations and any differences between the four coking units. Surface temperature measurements were made as described previously in Reference 1.

The correlation between AFAPL Static Coker controller temperature and measured coker surface temperature including the standard deviation of the four different cokers at each temperature is given in Table 39.

TABLE 39

CORRELATION BETWEEN AFAPL STATIC
COKER CONTROLLER TEMPERATURE AND
MEASURED COKER SURFACE TEMPERATURE

Controller Setting, °C	Surface Temp, °C	Std. Dev. of 4 Cokers
300	280	1.4
375	349	1.9
400	375	1.0
425	397	1.5
450	423	1.6
475	444	2.3

The standard deviation between the four cokers is good considering the problems of measuring the temperature of the coking surfaces. This correlation is presented graphically in Figure 38 and shows a linear relationship between the two parameters up to 450°C. Above 450°C, the difference between controller and surface temperature continues to increase with increasing controller temperatures.

(c) Initial Programmable Temperature Studies
of O-67-1 Using Shim Stock Test Specimens

AFAPL Static Coker testing of O-67-1 was conducted at 400°C and 425°C using temperature programming. The test apparatus including the test specimen was assembled and heated to 150°C (test specimen surface temperature) at a heating rate of 5°C per minute. The sample was then added to the test specimen at the start of a 30 minute soak period. The surface temperature was then increased to the desired test specimen surface temperature at a heating rate of 5°C per minute. The testing continued for 180 minutes at a constant test temperature. After the 180 minute test period, the controller turned off the coker heater and the test assembly was allowed to cool. The test specimen was removed after the controller indicator temperature was below 200°C.

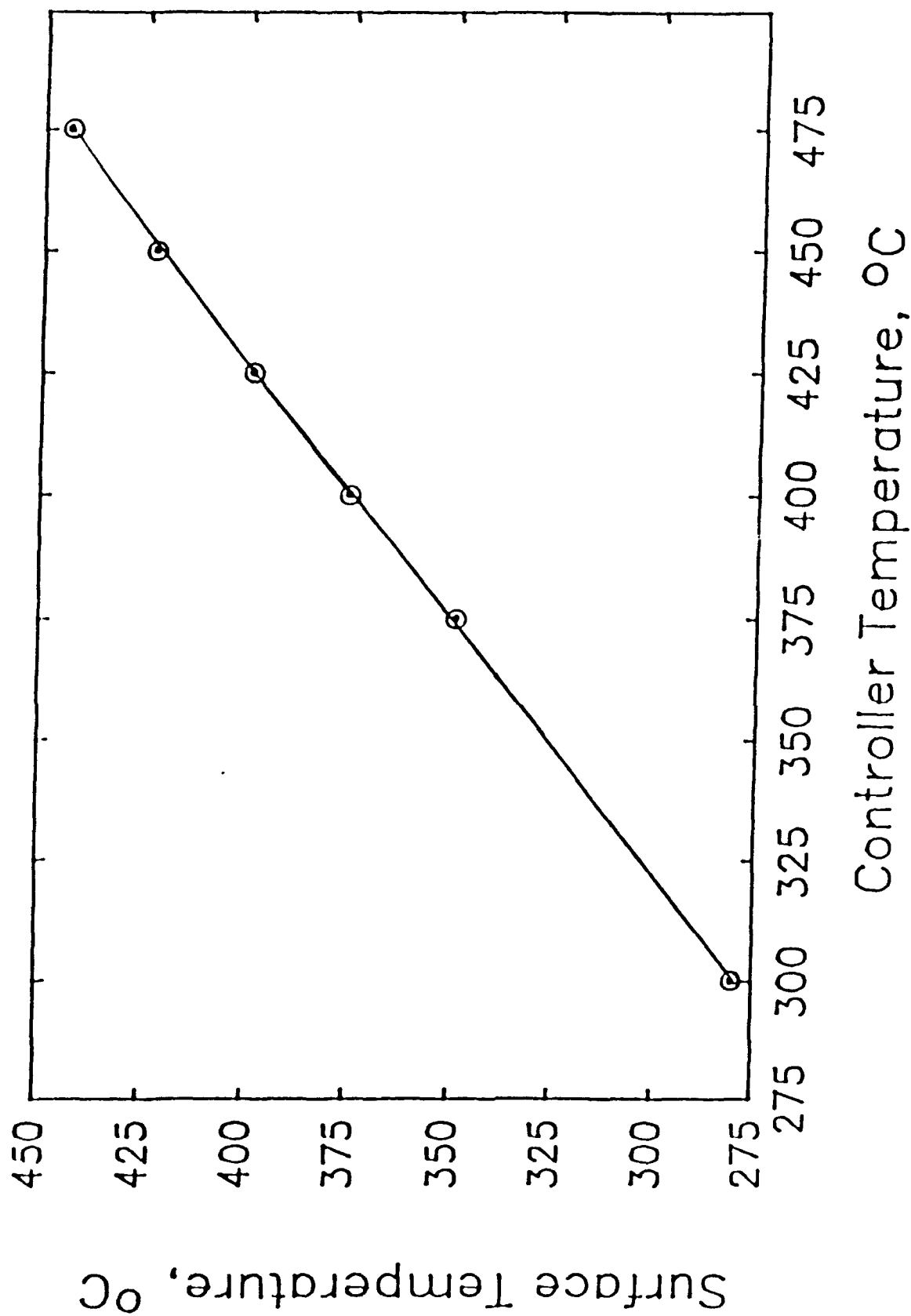


Figure 38. Correlation Between AFAPL Static Coker Controller Temperature and Test Surface Temperature

The first testing was conducted using shim stock test specimens and O-67-1 test lubricant. Although more deposits were obtained at 425°C than at 400°C, the deposits obtained were very similar consisting of a soft red "powder" deposit which suggested the formation of iron oxide. Testing was then conducted at 375°C, 400°C and 425°C using shim stock test specimens and the same temperature profile but without the addition of any sample. The deposits obtained (increased specimen weight) are given in Table 40 including the standard deviation for four tests. Table 40 also shows the deposit weight when testing O-67-1 at 400°C and 425°C using two sample sizes with and without considering the change in "blank" test specimen weight. These data show that most of the weighed deposits are due to the formation of iron oxide and not deposits formed from the lubricants.

Testing of O-67-1 was conducted using 0.019 inch thickness stainless steel test specimens with the test data being given in Table 40. The data show that new lubricant O-67-1 produces no deposits at 425°C with stainless steel test specimens or with shim stock after correcting for the formation of iron oxide. The use of 0.019 inch thickness steel test specimens presented sample sealing problems at high temperatures.

(d) Initial Programmable Temperature Studies of Optimum
Sample Size on New and Stressed O-67-1 Lubricant
Using 0.005 Inch T302 Stainless Steel Specimens

AFAPL Static Coker testing was conducted using 0.005 inch thick stainless steel (SS-302) test specimens. These coking tests were conducted since the normal air exposed shim stock (1010 steel) formed significant quantities of iron oxide at the high test temperatures (discussed above) and the thicker stainless steel specimens presented sealing problems. Testing of this material at 375°C surface temperature for 3 test hours using the standard ramping profile and without a test fluid showed no change in the

TABLE 40

EFFECT OF TEST TEMPERATURE ON SHIM STOCK
AND STAINLESS STEEL TEST SPECIMEN DEPOSITS AFTER THREE
TEST HOURS WITH AND WITHOUT TEST SAMPLE
AND USING TEMPERATURE PROGRAMMING

Test Temp °C	Test Spec. Material	Sample Size, mL	Weight Inc., mg	Std. Dev. (4 Tests)	Deposit, mg/g	
					No Blank Corr.	Blank Corr.
375	Shim Stock	None	2.5	0.2	-	-
400	Shim Stock	None	6.5	0.3	-	-
400	Shim Stock	0-67-1 1	3.5	0.1	3.6	0.0
425	Shim Stock	None	8.6	1.6	-	-
425	Shim Stock	0-67-1 0.20	7.7	0.7	28.1	0.0
425	Shim Stock	0-67-1 Wear Test 0.20	10.5	0.5	45.1	8.3
425	Stainless Steel	0-67-1 0.20	0.1	0.1	0.1	0.0
425	Stainless Steel	0-67-1 1	0.2	0.0	2.0	0.0
425	Stainless Steel	None	0.2	0.1	-	-

weight of the test specimens. AFAPL Static Coking test data obtained on fresh O-67-1 fluid and various sample sizes of "stressed" O-67-1 fluid are given in Table 41.

TABLE 41

EFFECT OF SAMPLE SIZE ON AFAPL COKING VALUES
(NEW O-67-1, 168, HOUR 320°C C&O SAMPLE,
COKING TEMPERATURE OF 375°C FOR THREE TEST
HOURS AND 0.005 INCH STAINLESS STEEL SPECIMENS)

Sample	Sample, Size, g	Deposit, mg/g		Total	Seal Deps. % of Total
		Specimen	Seal		
New O-67-1	1.18 \pm 0.01	0.0	0.0	0.0	0.0
168 h C&O Sample	0.25 \pm 0.01	4.2 \pm 0.73	1.3 \pm 0.88	5.5 \pm 0.48	24.0
168 h C&O Sample	0.54 \pm 0.01	9.0 \pm 0.25	2.2 \pm 0.40	11.2 \pm 0.24	19.4
168 h C&O Sample	1.12 \pm 0.02	9.9 \pm 0.94	6.3 \pm 0.86	16.2 \pm 0.53	39.0

The deposits formed on the test specimens and the stainless steel seals consisted of light to dark hard varnish. Although no seal leakage occurred with the thin test specimens, some deposits were on the test specimens outside of the seal. Visual examination of the seals showed that the test fluid had crept up and through the four vent holes in each of the seals and then down to the outside of test specimens. No coking occurred on the bottom of the test specimens or on the brass heating base. The data in Table 41 reaffirm that a sample size of 0.5 grams appears to be optimum for C&O stressed samples as well as fresh samples of PPE and that the repeatability is considered good for a high temperature coking test.

AFAPL Static Coker tests were conducted on new and C&O stressed O-67-1 fluid with and without temperature ramping for determining

the difference between the two test techniques. The non-ramping tests were conducted by heating the test specimens to the desired test temperature and then adding the sample to the test surface which is the starting test time. The temperature ramping tests were conducted by heating the test specimen at a rate of 5°C/minute to 150°C and then adding the test sample to test specimen. After a 30 minute dwell at 150°C, the test specimen surface temperature was raised at a heating rate of 5°C/minute to the desired test temperature. Test times using ramping are measured from the time the sample reaches the test temperature. Data obtained using the two test techniques for various sample sizes are given in Table 42.

TABLE 42

AFAPL STATIC COKER TEST DATA USING STAINLESS
STEEL TEST SPECIMENS, 375°C COKING TEMPERATURE
WITH AND WITHOUT TEMPERATURE RAMPING

Sample	Sample Size, g	Deposits, mg/g			
		Temp. Ramping		No Temp. Ramping	
		Specimen	Seal	Specimen	Seal
O-67-1	1	0.0	0.0	0.0	0.0
O-67-1 168 h C&O	0.25	4.2 \pm 0.7	1.3 \pm 0.9	2.7 \pm 0.5	13.0 \pm 1.0
	0.50	9.0 \pm 0.3	2.2 \pm 0.4	6.7 \pm 0.1	6.7 \pm 3.1
	1.00	9.9 \pm 9.4	6.3 \pm 0.9	-	-
O-67-1 240 h C&O	0.25	9.5 \pm 1.0	8.6 \pm 0.4	8.0 \pm 1.6	17.7 \pm 5.0
	0.50	18.0 \pm 2.3	10.4 \pm 1.4	15.3 \pm 1.6	7.4 \pm 2.7

The data in Table 42 show that temperature ramping gives slightly higher coking values than those obtained with no temperature ramping. These data also show that the 0.5 gram sample size is optimum for giving the lowest percent seal deposits. Seal deposits became much more significant for highly stressed O-67-1 fluids at the test temperature of 375°C as shown by the test data for the 240 hour C&O sample which has a 40°C

viscosity increase of 85% over new O-67-1 lubricant.

(e) Effects of Test Temperature, Test time and C&O Stressing on AFAPL Static Coker Deposits

A sample of O-77-6 was stressed using the C&O test at 290°C for 120 hours, to produce a highly stressed sample for the coking study (viscosity change 75.4% and 29.9% at 40°C and 100°C, respectively). The coking tendency at various test temperatures was expected to be quite higher than the new O-77-6 fluid, which showed no significant deposits at any of the conditions tested (Table 43). The stressed fluid was subjected to a 3 hour static coking test at 6 different temperatures (Table 44). All tests were performed with 0.5 gram samples, stainless steel specimens, and stainless steel seals.

TABLE 43

EFFECT OF TEST TIME AND TEMPERATURE ON DEPOSITS FOR NEW O-77-6

Test Temp., °C	Test Time, h	Deposits mg/g		Deposit Type
		Specimen	Total	
300	6	0.3 ± 0.1	2.2 ± 0.8	Slight Residue
325	6	0.2 ± 0.0	0.0 ± 0.0	None visible
325	9	0.3 ± 0.0	-*	None visible
350	6	0.6 ± 0.9	1.0 ± 0.7	None visible

*Seals not weighed, no visible deposits

TABLE 44

EFFECT OF TEST TEMPERATURE ON C&O 120 H, 290°C
STRESSED O-77-6 STATIC COKER
DEPOSITS USING 3 HOUR TEST TIME

Test Temp., °C	Deposits		Deposit Type
	Specimen	Total	
300	23.0 \pm 7.0	54.3 \pm 6.2	Hard dark brown non-uniform varnish
325	18.4 \pm 2.8	49.6 \pm 1.6	Hard dark brown varnish
350	26.1 \pm 4.5	42.7 \pm 2.9	Dark brown non- tacky varnish
375	17.4 \pm 0.7	32.1 \pm 2.4	Hard dark brown varnish, slightly flaky
400	10.8 \pm 1.9	14.2 \pm 2.5	Light brown to black very flaky varnish
425	4.7 \pm 1.9	8.1 \pm 2.9	Dark brown very flaky varnish

The results in Table 43 indicate that the new fluid mostly volatilizes leaving only slight amount of total deposits in the range of 1 to 2 mg/g. However, the highly stressed fluid gave total deposits of 54.3 mg/g at 300°C and the amount gradually decreased with temperature to 8.1 mg/g at 425°C.

Due to the low coking deposit value of the stressed O-77-6 at 425°C surface temperature and the extreme flaking which occurs at 400°C and 425°C, an experiment was performed to study the deposit formation over 1 hour intervals at 425°C with results being shown in Table 45 and Figure 39. The stressed O-77-6 was tested for 6 hours and observed to have practically no residue after this duration, compared to the 4.7 mg/g value after 3 hours. As expected, testing at 1 and 2 hour durations indicated a decreasing trend

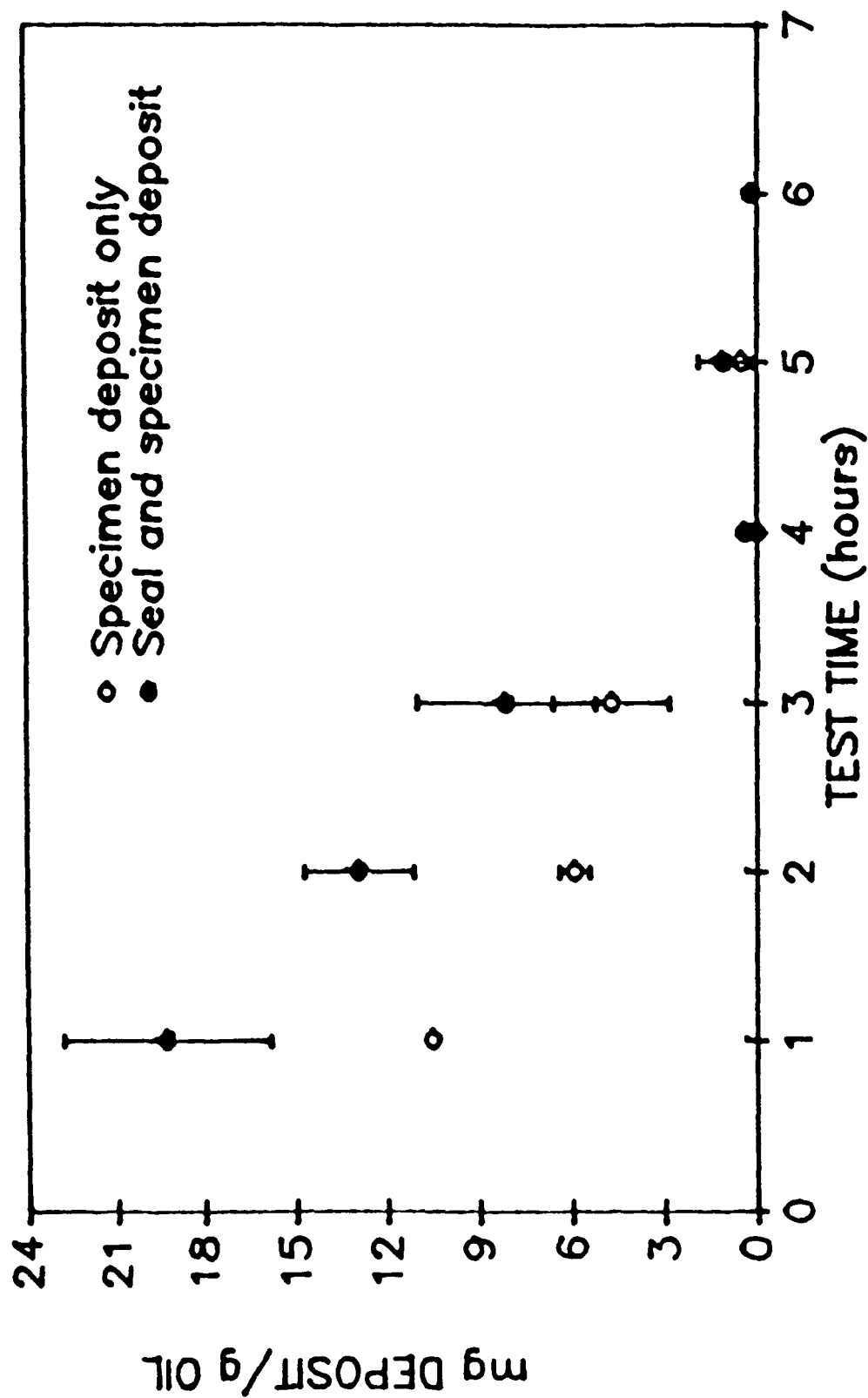


Figure 39. Effect of Test Time on Static Coker Deposits of 0-77-6 After 120 h C&O Stressing at 290°C Using 425°C Coking Test Temperature

in deposit formation. A procedure was developed to ensure that the decreasing values were not the result of deposit loss due to uptake of the flakes by the hood exhaust. The cokers were observed at 5 minute intervals initially. After ten minutes at 425°C the sample was observed to be liquid and vapor was still rising. After 20 minutes, no vapor was visible and a dark brown "dry" uniform deposit was formed. At this point, clean, pre-weighed, 40 mesh copper screens were placed on top of the coker chimneys. At 30 minutes, the uniform deposit showed a "cracked" appearance and at one hour was described as very flaky, but no flakes appeared on the screens. After 4 and 5 hours, the deposit had diminished and at the end of 6 hours of testing the specimens, seals and screens were weighed. Very few small dark flakes on the four hour specimens were not significant enough to produce a weight change. The five hour specimens showed a few dark flakes and very minimal weight gain. No deposits were visible on the screens and no weight change was observed for the screens. This study shows the deposits formed at short test times may be slowly volatilized and/or oxidized as test duration is increased and that flaky deposits are not lost through the coker chimneys.

TABLE 45

EFFECT OF TEST TIME ON STATIC COKER
DEPOSITS OF O-77-6 (120 HOUR C&O AT 290°C)
USING STAINLESS STEEL SPECIMENS, 0.5 ML SAMPLE
AND 425°C TEST SURFACE TEMPERATURE

Test Time, Hours	Deposits, mg/g		Deposit Type
	Specimen Only	Specimen and Seal	
1 ^a	10.5 ± 0.0	19.3 ± 3.5	Dark brown flaky varnish
2 ^a	5.9 ± 0.5	12.9 ± 1.8	Dark brown flaky varnish
3	4.7 ± 1.9	8.1 ± 2.9	Dark brown very flaky varnish
4 ^{a,b}	0.0 ± 0.0	0.4 ± 0.0	Small black coke particles
5 ^{a,b}	0.5 ± 0.4	1.1 ± 0.8	Small black coke particles
6	0.2 ± 0.0	0.2 ± 0.0	No visible deposits

^a two determinations

^b 40 mesh copper screen used

The effect of test time and temperature on new O-67-1 is given in Table 46 and shows that little deposit forms from new lubricant O-67-1 under any of the test times or temperatures investigated.

TABLE 46

EFFECT OF TEST TIME AND TEMPERATURE ON NEW O-67-1 STATIC COKER DEPOSITS

Test Temp., °C	Test Time, h	Deposit, mg/g		Deposit Type
		Specimen	Total	
325	6	0.2 ± 0.1	0.2 ± 0.1	Slight Residue
350	6	0.4 ± 0.3	0.5 ± 0.6	"
375	3	0.3 ± 0.2	0.6 ± 0.6	"

The effect of test temperature on C&O stressed O-67-1

lubricant is given in Table 47 and shows that the "stressed" lubricant produces much higher levels of deposits consisting of hard dark varnish for all temperatures from 300°C to 425°C. These data also show that below 375°C, seal deposits represent a large percentage of total deposits.

TABLE 47

EFFECT OF TEST TEMPERATURE ON O-67-1 (240 HOUR C&O AT 320°C
USING 3 HOUR TEST TIME AND 0.5 GRAM SAMPLE) STATIC COKER DEPOSITS

Test Temp., °C	Deposits, mg/g		Deposit Type
	Specimen	Total	
300	14.6 \pm 1.4	61.1 \pm 5.5	Hard dark varnish
325	14.9 \pm 1.0	49.7 \pm 3.7	"
350	16.5 \pm 1.0	38.3 \pm 4.2	"
375	18.0 \pm 2.3	28.4 \pm 1.4	"
400	8.2 \pm 1.7	12.4 \pm 2.0	"
425	2.1 \pm 0.6	5.6 \pm 0.4	"

AFAPL Static Coker testing of CB-1 fluid (combined four-ball wear test samples) was conducted on three micron filtered and unfiltered samples of new and C&O "stressed" CB-1 lubricant. These data given in Table 48 show that filtering of wear test samples improves the oxidative stability of the fluid and reduces the deposit forming characteristics after C&O stressing. The data also show that the wear debris in the wear test samples reduces the static coker deposits of the fluid compared to new O-67-1 lubricant.

(f) AFAPL Static Coker Deposits of Engine
Stressed MIL-L-87100 Lubricant

AFAPL static coker testing of engine stressed MIL-L-87100 fluids was conducted for determining coking differences between new and engine stressed lubricants. The results given in Table 49 indicate that the static coker deposits of engine stressed MIL-L-87100 lubricants are very

TABLE 48

AFAPL STATIC COKER TEST DATA FOR THREE MICRON FILTERED
AND UNFILTERED FOUR-BALL WEAR TEST O-67-1 FLUID BEFORE
AND AFTER C&O TESTING (0.5 GRAM SAMPLE, 3 HOUR TEST TIME,
TEMPERATURE PROGRAMMING AND STAINLESS STEEL TEST SPECIMENS)

Deposits, mg/g Oil and Std. Dev.

Sample	Test Specimen	Seal	Total	Type Deposit
CB-1 Unfiltered	0.6 ± 0.3	0.0 ± 0.0	0.6 ± 0.3	Orange Powdery Deposit
CB-1 Unfiltered after 48 h, 320°C C&O Test	22.0 ± 1.4	6.4 ± 2.3	28.4 ± 1.9	Brown/Black Coke
CB-1 Filtered & after 48 h, 320°C C&O Test	1.8 ± 0.2	1.3 ± 0.6	3.1 ± 0.5	Brown/Black Coke

TABLE 49

AFAPL STATIC COKER TEST DATA FOR ENGINE STRESSED
 MIL-L-87100 LUBRICANT USING A 375°C COKING
 TEMPERATURE, 0.5 GRAM SAMPLE, 3 HOUR TEST TIME,
 TEMPERATURE PROGRAMMING AND STAINLESS STEEL TEST SPECIMENS

Deposits, mg/g Oil and Std. Dev.

Sample	Test Specimen	Seal	Total	Type Deposits
TEL-9028	0.3 ± 0.1	1.5 ± 0.3	1.8 ± 0.2	Slight Brown Stain
TEL-9029	0.8 ± 0.2	0.3 ± 0.1	1.1 ± 0.2	No Visible Deposits
TEL-9030	0.2 ± 0.1	0.4 ± 0.2	0.6 ± 0.1	" " "
TEL-9038	0.2 ± 0.2	1.6 ± 0.1	1.8 ± 0.3	Very Slight Varnish
TEL-9039	0.2 ± 0.1	0.5 ± 0.1	0.7 ± 0.5	" " "
TEL-9040	0.5 ± 0.1	1.0 ± 0.2	1.5 ± 0.3	No Visible Deposits
TEL-90025	0.3 ± 0.09	-	-	Yellow Tarnish
TEL-90025 ¹	5.6 ± 0.4	-	-	Light Grey Tarnish
TEL-90026	0.1 ± 0.1	-	-	Light Brown Stain
TEL-90026 ¹	4.7 ± 0.03	-	-	Light Grey Tarnish

¹
 1010 Steel Shim Stock Test Specimens

close to that of new fluids. This is probably due to a low level of stressing and possibly the presence of some wear debris which has been shown to reduce coking deposits.

(g) Study of Test Specimen Material on Coking
Characteristics of Polyphenyl Ether Fluids

AFAPL Static Coker testing was conducted at 375°C and 3 hour test periods for stainless steel, brass, Pyrex and aluminum test specimens with the test data being given in Table 50. Shim stock (1010 steel) was not included in this experiment because experience with PPE on shim stock indicates that PPE volatilizes too quickly and promotes the formation of iron oxide.

These data show that for the new fluids, only brass showed an increase in deposit level over the other three materials. This could be partly due to oxidation of the brass specimens which appeared tarnished and gray in color. Brass test specimens gave the lowest levels of deposits for the stressed fluids which could be due to its catalytic effect on the fluids "breakdown" products formed during the C&O testing and which have been shown to produce deposits during static coker testing. The Pyrex specimens gave the highest deposits for the stressed fluids, followed by stainless steel and then aluminum. The effect of using brass test specimen material was found to be greater on polyphenyl ether fluids than on ester base lubricants.²

(h) Volatilization Study of Lubricant O-67-1

The volatilization characteristics of lubricant O-67-1 was investigated using the AFAPL Static Coker. Clean pre-weighed SS-302 specimens were heated to the desired test temperature and 0.5 g of O-67-1 was added by syringe. The oil was observed and time interval recorded at the point when vaporization of the oil could no longer be seen. This procedure

TABLE 50

EFFECT OF TEST SPECIMEN MATERIAL ON
 STATIC COKER DEPOSITS AT 375°C USING
 0.5 ML SAMPLES AND 3 HOUR TEST TIME

Lubricant	mg Deposit/g Oil			
	Stainless Steel	Brass	Pyrex	Aluminum
0-67-1, New	0.3 \pm 0.2 Tarnish (0.6 \pm 0.6 total)	2.6 \pm 0.5 Tarnish with gray darkening (4.5 \pm 0.6 total)	0.5 \pm 0.2 No visible deposits (1.9 \pm 0.0 total)	0.7 \pm 0.5 No visible deposits (2.0 \pm 0.6 total)
0-67-1, 240 h C&O at 320°C	18.0 \pm 2.3 Hard dark brown varnish (28.4 \pm 1.4 total)	3.1 \pm 0.5 Tarnish, gray to light brown stain (4.3 \pm 0.6 total)	18.3 \pm 0.4 Hard light to dk brown varnish (32.6 \pm 0.6 total)	14.8 \pm 2.0 Hard light to dk brown varnish (21.3 \pm 1.1 total)
0-77-6, New	0.3 \pm 0.1 Tarnish (0.3 \pm 0.1 total)	1.3 \pm 0.3 Tarnish and gray circle in middle (1.3 \pm 0.3 total)	0.0 \pm 0.0 No visible deposits (0.0 \pm 0.0 total)	0.2 \pm 0.1 No visible deposits 1.4 \pm 0.7 total)
0-77-6, 120 h C&O at 290°C	17.4 \pm 0.7 Hard dark brown varnish slightly flaky (32.1 \pm 2.4 total)	4.9 \pm 1.8 Slight rust colored to golden gray deposit (5.7 \pm 3.2 total)	21.9 \pm 1.4 Hard light brown to black vanish to coke (34.6 \pm 3.2 total)	16.4 \pm 3.4 Hard light brown to black varnish (26.8 \pm 7.1 total)

was repeated four times on the same specimen, and the time required for vaporization of each portion tabulated. The average weight of lubricant added was divided by the average minutes required for volatilization to provide grams of oil volatilized per minute. This procedure was performed at 3 test temperatures with the test data given in Table 51 and shown graphically in Figure 40.

TABLE 51

VOLATILIZATION RATE AND DEPOSIT AMOUNTS OF O-67-1
USING STATIC COKER AT VARIOUS TEMPERATURES

Test Temp., °C	Rate of Volatilization gram/min	Deposit mg/g	Residue Type
325	0.032	2.16 \pm 1.33	Stain, Tarnish, Oily
375	0.053	2.07 \pm 1.66	Stain Tarnish
425	0.125	1.44 \pm 0.68	Tarnish, Slight Varnish

This study can form the basis for a "constant addition" method to better characterize fresh lubricants. The rates obtained can be used to select addition rate at a particular test temperature. Lower temperature yields oily residue which can be retrieved for lube degradation analyses and higher temperatures provide the needed conditions for producing solid deposits and coke. A peristaltic pump could be used to deposit the lubricant on the specimen. These results are in agreement with previous test results that the amount of deposition is inversely proportional to the rate of volatilization and directly proportional to test temperature.

0-67-1

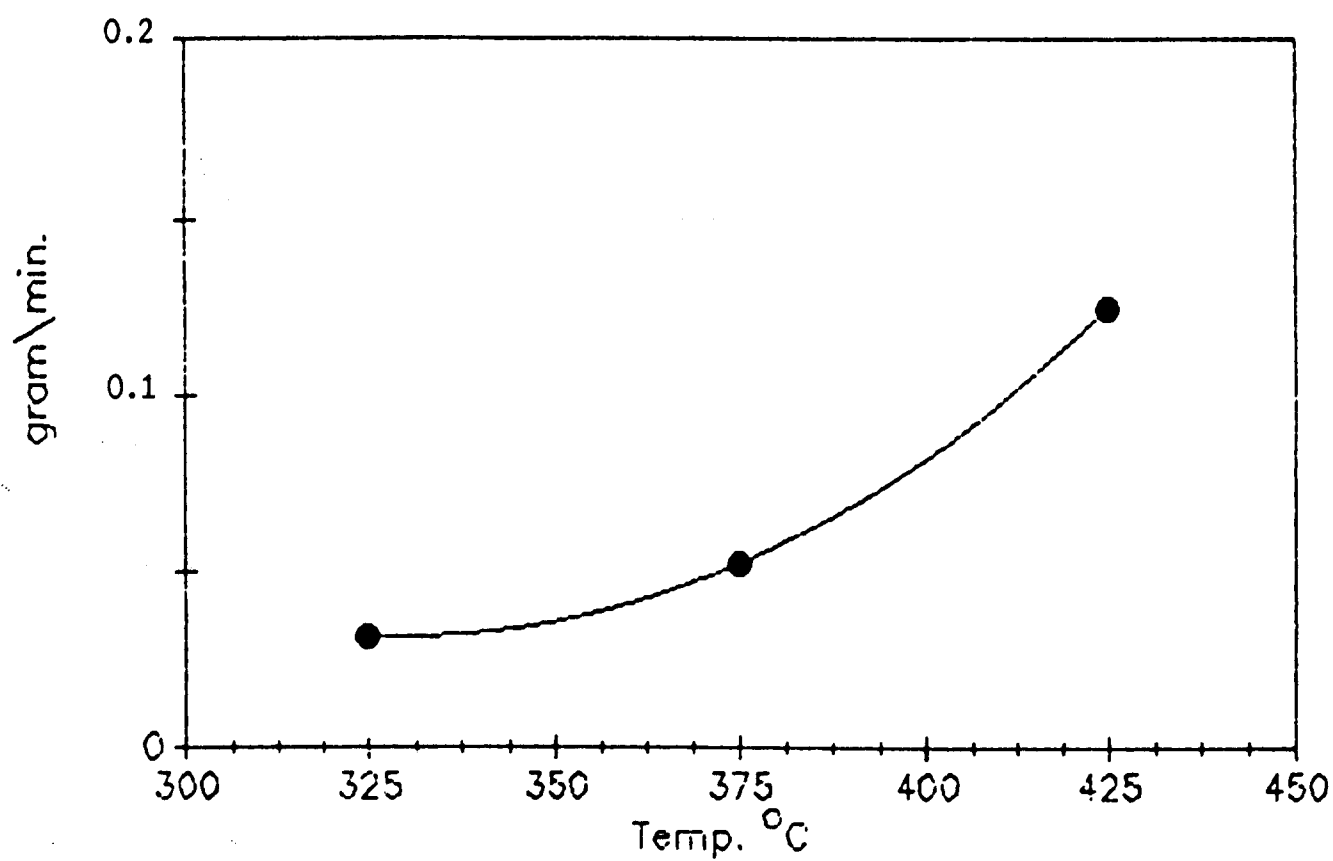


Figure 40. Volatilization Rate of 0-67-1 at Various Test Temperatures Using Static Coker with SS-302 Specimens

(i) Comparison of 5P4E and 6P5E Polyphenyl Ether Coking Characteristics Using the AFAPL Static Coker

AFAPL Static Coker testing was conducted on lubricant TEL-90028 which is an inhibited 6P5E formulated fluid. The data given in Table 52 show that the coking characteristics of 5P4E and 6P5E fluids are very similar with both having very low deposit levels.

TABLE 52

AFAPL STATIC COKER DEPOSITS FOR O-67-1 AND TEL-90028
(375°C, 3 TEST HOURS, SS-302 SPECIMENS AND TEMPERATURE PROGRAMMING)

Lubricant	Test Specimen Deposit, mg/g	Seal and Test Specimen Deposits mg/g	Deposit Type
O-67-1	0.3 \pm 0.2	0.6 \pm 0.6	Tarnish
TEL-90028	0.2 \pm 0.1	1.6 \pm 0.9	Lt. Stain

(j) AFAPL Static Coker Studies of Non-Polyphenyl Ether Base Fluids

AFAPL Static Coker Testing was conducted on five non-polyphenyl ether base fluids with the test data being given in Table 53. These data show that with the exception of fluid TEL-90001 these fluids have low static coker deposit values close to that of the polyphenyl ether fluids. A large difference in deposits did exist between fluids TEL-90024 and TEL-90059 which are supposed to be different lots of the same fluid. This may be due to batch differences or changes occurring with these fluids during storage. Additional studies are required on these types of fluids before understanding their deposition characteristics.

(k) Summary

Modifications of the AFAPL Static Coker and test procedure^{1,2} have resulted in the development of a lubricant coking test for

TABLE 53

AFAPL STATIC COKER DEPOSITION DATA ON NON-POLYPHENYL ETHER FLUIDS
USING 0.5 GRAM SAMPLES, SS-302 TEST SPECIMENS AND TEMPERATURE PROGRAMMING

Fluid	Test Time h	Test Temp °C	Specimen Residue mg/g	Seal Residue mg/g	Total Residue mg/g	Description of Deposits
TEL-9050	6	350	0.9 \pm 0.2	5.5 \pm 1.8	6.4 \pm 2.6	Slight Varnish on specimen, Oil on Seal
TEL-90001	3	375	13.5 \pm 2.5	15.5 \pm 2.9	29.0 \pm 3.2	Black Coke on Specimen White Deposit on Seals
TEL-90024	3	375	0.5 \pm 0.3	0.0 \pm 0.0	0.5 \pm 0.3	Very Light Deposit
TEL-90059	3	375	4.1 \pm 0.3	-	-	Light Yellow Dep on Specimens
TEL-90059 ¹	3	375	1.1 \pm 0.1	-	-	Light Brown Dep on Specimen
TEL-90063	6	350	0.1 \pm 0.0	0.4 \pm 0.2	0.5 \pm 0.2	Light Brown Film on Specimen

¹Shim Stock Test Specimen

high temperature lubricants with a coking temperature capability of at least 450°C. A sample size of 0.5 gram and test time of three hours have been determined to be the optimum conditions using stainless steel test specimens and temperature programming.

Coking values of new and engine stressed MIL-L-87100 lubricants are much lower than ester base lubricants. Oxidative stressing of the high temperature lubricants and experimental fluids increases deposit levels. Solid coke deposits continue to decrease with continued testing at the same temperature (375-400°C) and at a higher rate with increasing temperatures. As such, test temperatures and test times are very important in determining the deposition characteristics of high temperature lubricants.

The four-ball wear testing of the MIL-L-87100 type lubricant reduces the static coker deposit level of the lubricant which is probably due to the presence of wear debris. Static coker testing of engine stressed MIL-L-87100 lubricant showed very low levels of deposits. Three micron filtering of four-ball wear test samples or used MIL-L-87100 fluids increase the deposit forming characteristics of the samples.

Test specimen material has a great effect on Static Coker deposits for "stressed" fluid with brass giving the lowest deposits and pyrex the highest deposits. For new fluids, brass gave slightly higher deposits than stainless steel, aluminum or Pyrex.

No differences in the deposit levels were observed using the Static Coker for 5P4E fluid O-67-1 and 6P5E fluid TEL-90028 both of which contained the same type and quantity of inhibitor.

AFAPL Static Coker testing showed that the most stable non-polyphenyl ether experimental fluids had deposit levels slightly higher than MIL-L-87100 fluids.

b. Micro Carbon Residue Tester (MCRT)

(1) Introduction

Lubricant deposition studies have been conducted on high temperature lubricants and experimental fluids using the Micro Carbon Residue Tester (MCRT). This deposition test is somewhat similar to the AFAPL Static Coker such that both tests represent engine coking conditions of non-flowing lubricant. The MCRT simulates "pockets" or "pools" of oil subject to high temperatures where the static coker simulates conditions of thin film coking occurring upon engine shutdown.

(2) Apparatus and Procedure

The apparatus and test procedure have previously been described in detail.² Briefly, the MCRT test unit is essentially a temperature programmable sealed oven so that various heating cycles and test times can be conducted under varying and controlled atmospheric conditions. Test fluid samples are normally placed in glass vials circularly positioned in an aluminum basket.

The normal test procedure involves a one hour pre-soak at 150°C followed by a thirty hour coking period at 400°C using an air atmosphere (275°C coking temperature for ester base fluids) and then oven cool down to room temperature using normal static room air cooling. Some modifications to this procedure were used during this research and will be described under subsequent appropriate sections. At the end of all tests, the vials are reweighed and the percent weight of coke is determined for each vial. Normally, 12 vials are used for each test and the averages of all values are reported as the percent coking value for the test fluid.

(3) Test Lubricants

Lubricants and experimental fluids investigated during this

study are presented in Table 54. Appendix A lists the MCRT data for all lubricants studied to date.

(4) Results and Discussion

(a) Investigation of Temperature Uniformity of MCRT Ovens and the Reproducibility of Data from the Two Units

The temperature uniformity of each MCRT oven and the correlation of testing between two MCRT units were determined. Temperature uniformity within the MCRT coking chamber was determined using five thermocouples. Temperature measurements were made at the 3, 6, 9 and 12 o'clock positions with the thermocouples being placed 0.5 inch from the cell wall and at "top of test vial" height and with a fifth thermocouple being centered within the cell. The "Doric" temperature indicator used with the five "J" type thermocouples was checked for calibration. The thermocouples were also checked at 20°C and at 340°C and were within $\pm 1^\circ\text{C}$. Temperature data obtained for each of the two units are given in Table 55 and shown graphically in Figure 41. The data in Table 55 show that a temperature differential does exist in each unit with the average cell temperature ranging from 7 to 19°C above the MCRT displayed temperature depending upon the MCRT temperature setting (300 to 500°C). The two equations given in Figure 41 expressing MCRT displayed temperature as a function of the average cell temperature have very good degrees of correlation. The correlation between cell deposits and the measured cell position temperature for MCRT testing of lubricant O-86-2 at 275°C MCRT displayed temperature and 30 test hours is given in Figure 42 and shows that the cells having the highest residue values are in the area of highest temperature. A maximum difference in cell deposit weight was 1.43% with the maximum cell position temperature difference of 13°C.

TABLE 54

DESCRIPTION OF TEST FLUIDS USED IN MCRT COKING STUDY

Test Fluid	Description	Visc., at 40°C, cSt
O-67-1	MIL-L-87100 Oil (5P4E)	280.3
O-77-6	Basestock for O-67-1	280.4
O-86-2	Candidate Lubricant, Ester Base, 4 cSt	4.04
TEL-9028	Used MIL-L-87100	298.0 ¹
TEL-9029	" " "	284.9
TEL-9030	" " "	283.7
TEL-9038	" " "	284.4
TEL-9039	" " "	298.1 ²
TEL-9040	" " "	293.7
TEL-8085	Experimental Fluid	287.3
TEL-8087	" " "	280.5
TEL-9050	" " "	214.3
TEL-9071	Different Sample of TEL-9050	212.5
TEL-90001	Experimental Fluid	235.4
TEL-90018	Polyphenyl Ether (6P5E)	-
TEL-90024	Inhibited TEL-9050	194.4
TEL-90025	Used MIL-L-87100	288.3
TEL-90026	Used MIL-L-87100	289.3
TEL-90028	Inhibited TEL-90018	1468.4
TEL-90059	Different Lot of TEL-90024	195.4
TEL-90063	Experimental Fluid	215.4

Various Four-Ball Wear Test Samples³

¹After removal of 15% tetrachloroethylene

²After removal of 1.9% trichloroethylene

³Described under Section V

TABLE 55

UNIFORMITY OF TEMPERATURE WITHIN MICRO CARBON
RESIDUE TESTERS (MCRT)

MCRT NO. 1

MCRT Displayed Temp., °C	Thermocouple Position				Center	Range °C	Average °C	σ
	12 o'clock	3 o'clock	6 o'clock	9 o'clock				
300	303	304	316	312	305	13	308	5.7
400	410	412	423	418	413	13	415	5.3
500	515	518	526	522	516	11	519	4.6

MCRT NO. 2

	Thermocouple Position				Center	Range °C	Average °C	σ
	12 o'clock	3 o'clock	6 o'clock	9 o'clock				
300	304	307	311	307	304	7	307	2.9
400	409	412	417	411	409	8	412	3.3
500	512	516	521	514	511	10	515	4.0

Four outer thermocouples were placed 1/2 inch from side of cell and at top of test vial height

$$\Delta \quad Y = 1.04X - 1.60 \quad (r = 0.99997)$$

$$\bigcirc \quad Y = 1.03X - 1.08 \quad (r = 0.99999)$$

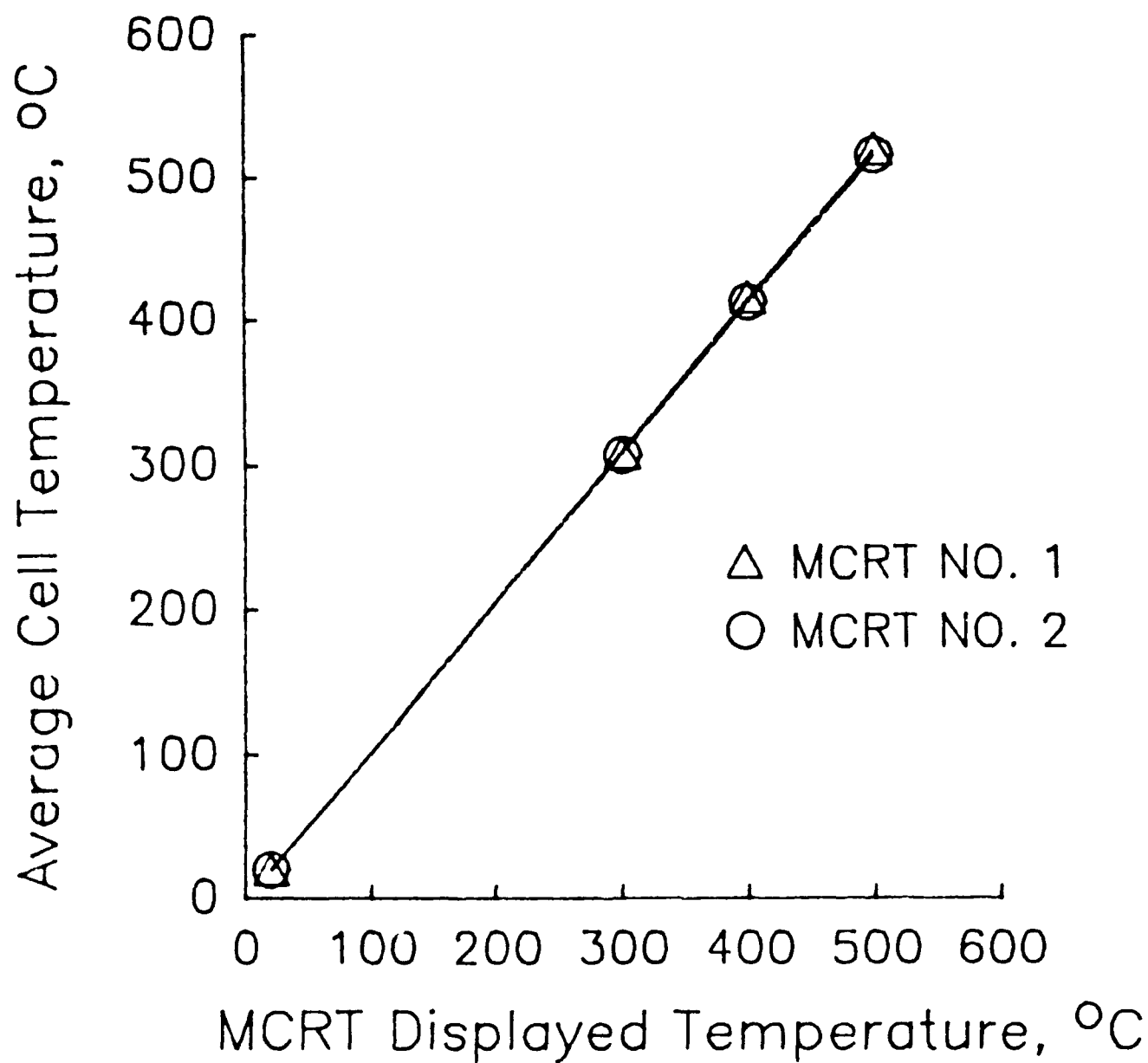
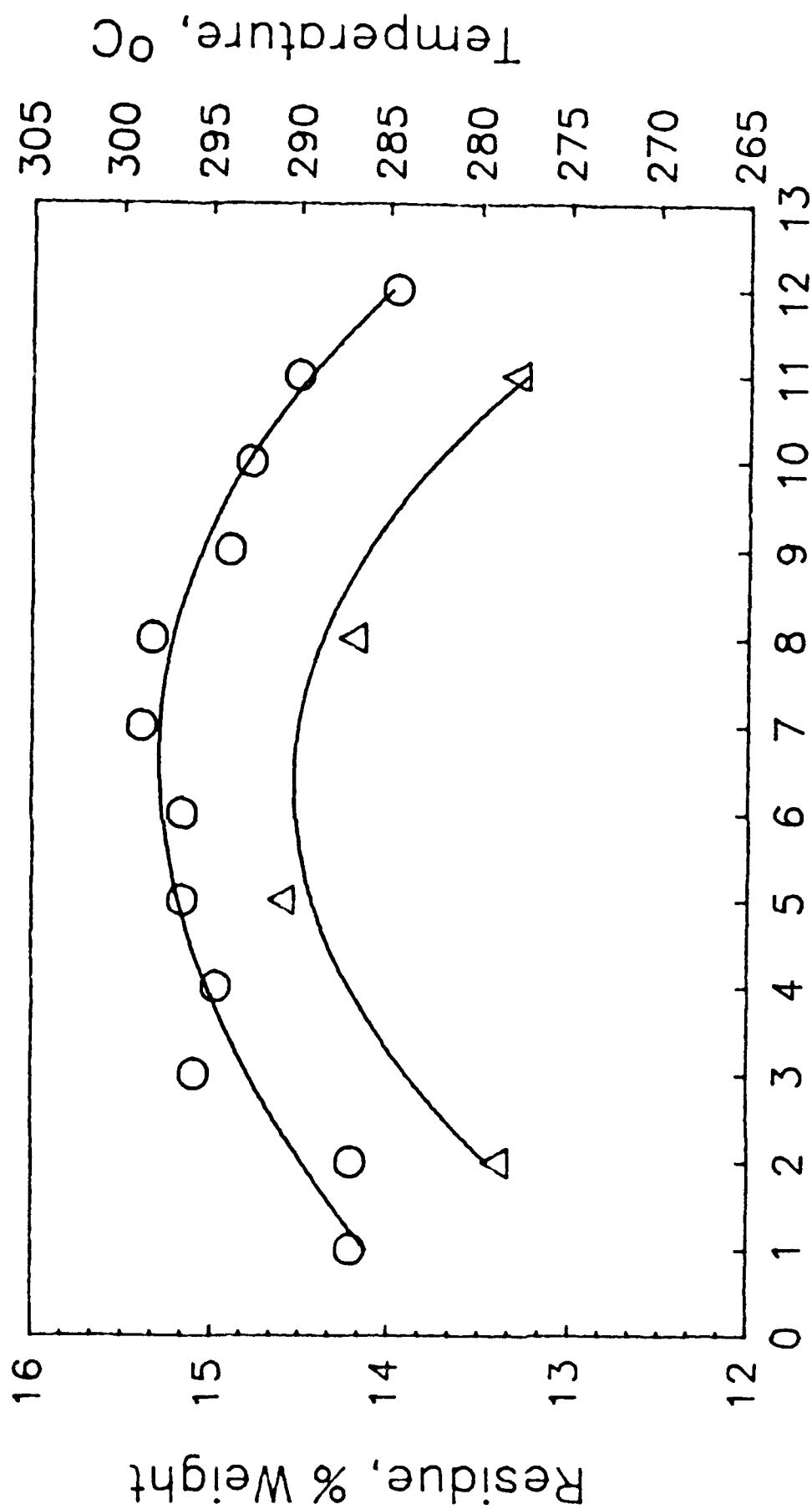


Figure 41. Correlation of MCRT Displayed Temperature and Average Cell Temperature



MCRT Test Cell Number

Figure 42. Correlation Between Cell Deposits (○) and Measured Cell Position Temperatures (Δ) for MCRT Testing of Lubricant O-86-2 at 275°C MCRT Displayed Temperature and 30 Hours Test Period

MCRT testing has been conducted at various temperatures using both MCRT units for establishing the correlation between the units at various temperatures using average cell temperatures for determining the effect of coking temperature on deposits. Test data obtained from this study are given in Table 56 and show two distinct trends. First, the two units show good correlation only between temperatures of approximately 280 to 300°C. Above and below these temperatures, MCRT Unit No. 2 gives higher deposit levels. Secondly, for both units the amount of deposits decreased with increasing temperatures up to approximately 285°C. Between 285 and 300°C, the deposits increase and then start to decrease at temperatures above 300°C.

(b) MCRT Testing of New and Stressed 5P4E Fluids Using Short and Tall Vials, Various Temperatures and Melting Point Determination of Deposits

MCRT evaluations of new and 320°C oxidatively stressed O-67-1 fluid were conducted using the short (35 mm height) and tall (76 mm height) vials. Residue values obtained at various test temperatures are given in Table 57 and show the following:

Deposit values decrease with increasing test temperature using both size vials.

Deposit values increase with degree of sample prestressing using both size vials.

The large vials gives 3 to 7 times more deposits than the small vials.

The percent increase in deposits due to stressing is greater using the small vials.

Melting point determinations were conducted on some of the deposits obtained using the tall vials at 400°C test temperature since a previous test showed a low melting point (54° to 58°C) on a hard glassy dark brown varnish. The melting point values are given in Table 58. The only

TABLE 56
CORRELATION OF MICRO CARBON RESIDUE TESTERS
NO. 1 AND NO. 2 AT VARIOUS TEMPERATURES AND
30 H TEST DURATION FOR LUBRICANT O-86-2

MCRT No.	Avg. Cell Temp., °C	Displayed Temp., °C	Deposits % Wt.	Std Dev.
1	265	256	40.77 ^a	1.94
2	265	258	44.08 ^a	1.34
1	275	266	17.21	0.41
1	275	266	17.14	0.50
2	275	268	19.32	0.69
2	275	268	19.87	0.80
1	284	275	15.25	0.50
2	282	275	15.42	0.49
1	290	280	16.64	0.39
2	290	283	16.29	0.66
1	300	290	17.97	0.30
2	300	292	17.54	0.56
1	310	300	15.30	0.37
1	310	302	15.59	0.36
2	310	300	16.56	0.75
2	310	302	16.33	0.27

^aLiquid residue. Coke near top of vial

TABLE 57

PERCENT WEIGHT MICRO CARBON RESIDUE TESTER (MCRT) VALUES
 USING 35 MM AND 76 MM HEIGHT SAMPLE VIALS
 FOR NEW AND STRESSED O-67-1 FLUID
 (30 HOUR TEST TIME)

Sample	Test Temperature, °C					
	350		400		425	
	35 mm Vial	76 mm Vial	35 mm Vial	76 mm Vial	35 mm Vial	76 mm Vial
New O-67-1	2.39 ¹ (0.52) ²	-	2.05 (0.49)	11.34 (1.69)	0.69 (0.27)	7.54 (1.86)
168 Hour O/C Test at 320°C	4.32 ¹ (0.29)	-	2.16 (0.26)	13.73 (1.35)	1.07 (0.17)	9.01 (1.15)
192 Hour O/C Test at 320°C	16.35 (2.14)	62.28 ³ (0.57)	2.58 (0.41)	14.68 (1.51)	Insufficient Sample	
240 Hour O/C Test at 320°C	8.69 ¹ (1.44)	47.23 ^{3,4} (1.33)	6.59 (0.16)	16.74 (1.01)	2.52 (0.60)	13.04 (1.15)

¹Displayed Temperature. Actual cell temperature of 362°C.

²Standard Deviation

³Liquid

⁴16.26% After 60 hours, 13.83% after 90 hours

deposit having an ascertainable melting point was not the residue from the test giving the highest deposit value; however, that test did have the lowest coking temperature and longer than normal coking time. This indicates that equivalent weight of deposits formed under different test times and temperatures may not have the same structure although all of the deposits in Table 58 were hard glassy dark brown deposits. Table 59 gives a description of the deposits referenced in Table 58. All deposits obtained at a test temperature of 400°C were dark brown glassy varnish while all the deposits obtained at 425°C were hard black coke.

Testing of the C&O stressed O-67-1 fluid (240 hours, 320°C) was conducted for 60 and 90 hour test times in addition to the normal 30 hour test time. Although these data are included in Tables 57 and 58, they are shown separately in Table 60 and graphically in Figure 43 to illustrate the great effect of test time on the amount and type of deposits.

The "deposits" after 30 test hours consisted primarily of viscous oil with some hard deposits on the inside and outside on top of the vials. The deposits after 60 hours were hard glassy dark brown deposits having conchoidal surfaces after being scraped from the test tube but had a fairly sharp melting point of 54 to 58°C as determined using the Mettler hot stage. The deposits after 90 test hours were also similar hard glassy dark brown deposits having conchoidal surfaces after being scraped from the test tube but did not melt or exhibit any observable phase changes up to 300°C which is the maximum temperature capability of the Mettler hot stage.

The effect of test temperature on the MCRT deposits of O-67-1 and O-77-6 using 30 h test time, air and 0.5 gram sample amount was investigated. This study required the use of both the tall (7.5 cm) and short (3.5 cm) vials in order to more fully explore the factors which

TABLE 58

MELTING POINT VALUES OF MCRT DEPOSITS

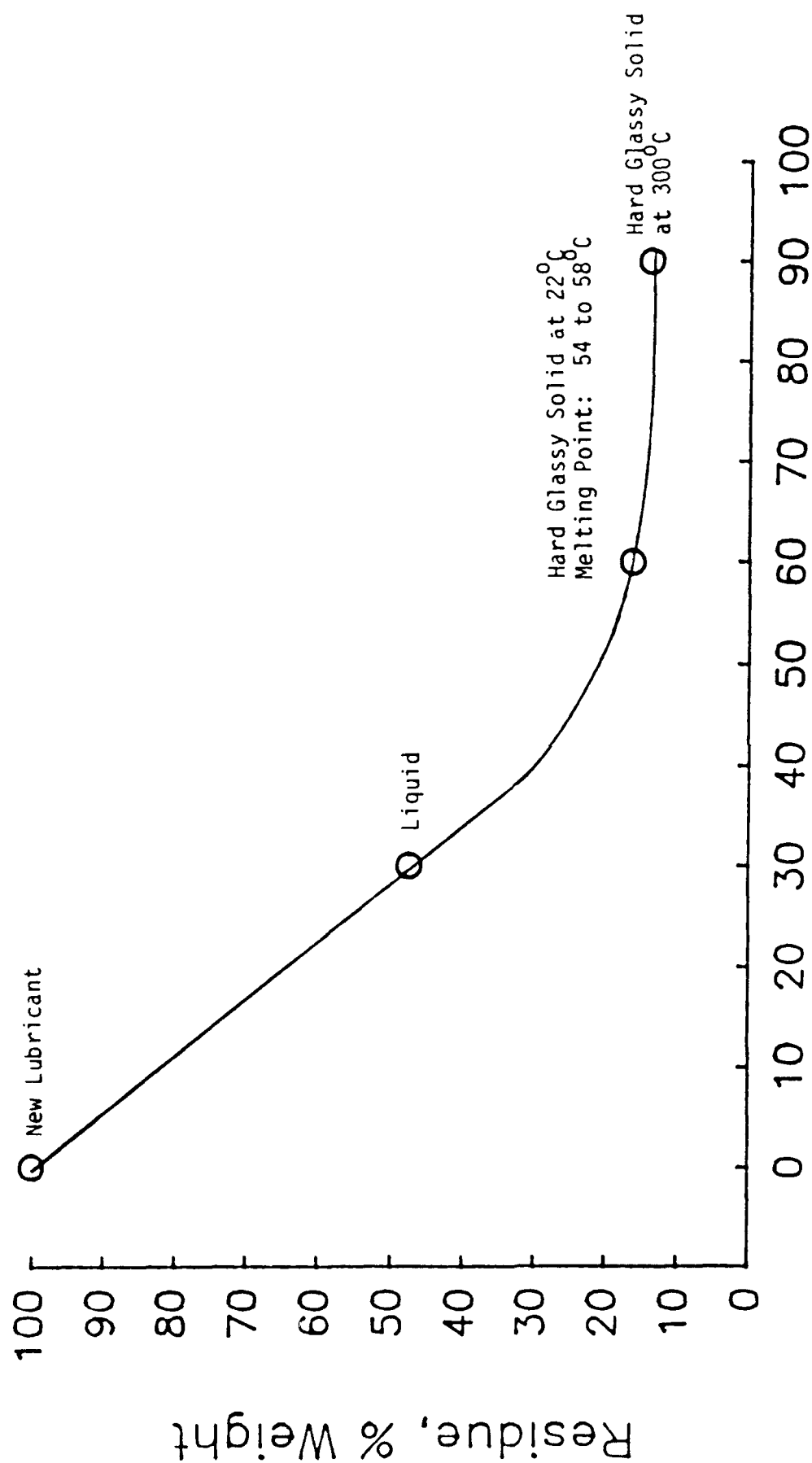
Sample	MCRT Test Temp., °C	Test Time, h	Deposit % Wt	Melting Point, °C
New O-67-1	400	30	11.34	>300
240 Hour O/C Test at 320°C	362	60	16.26	54 to 58
240 Hour O/C Test at 320°C	362	90	13.83	>300
240 Hour O/C Test at 320°C	400	30	16.74	>300

TABLE 59

DESCRIPTION OF MCRT DEPOSITS USING 35 MM AND 76 MM HEIGHT SAMPLE VIALS FOR NEW AND STRESSED O-67-1 FLUID (30 HOUR TEST TIME)

Sample	Test Temperature, °C					
	350		400		425	
	35 mm Vials	76mm Vials	35mm Vials	76mm Vials	35mm Vials	76 mm Vials
New O-67-1	D.B.V. ^{1,2}	-	D.B.V.	D.B.V.	H.B.C. ³	H.B.C.
168 Hour O/C Test at 320°C	D.B.V. ²	-	D.B.V.	D.B.V.	H.B.C.	H.B.C.
192 Hour O/C Test at 320°C	D.B.T.D. ⁴	Viscous Oil	D.B.V.	D.B.V.	No Sample	No Sample
240 Hour O/C Test at 320°C	D.B.V. ²	Viscous Oil	D.B.V.	D.B.V.	H.B.C.	H.B.C.

¹ D.B.V. - Dark brown varnish² Displayed Temperature. Actual cell temperature of 362°C³ H.B.C. - Hard black coke⁴ H.B.T.D. - Hard black tacky deposit



Test Time, Hours

FIGURE 43. MCRT Residue of the 240 h, 320°C C/O Test Sample of Lubricant 0-67-1 After Various Test Hours (350°C MCRT Displayed Temperature; 362°C Average Cell Temperature, Tall Vials)

TABLE 60

EFFECT OF TEST TIME ON THE MCRT RESIDUE VALUE OF THE 240 HOUR, 320°C
C&O STRESSED LUBRICANT AT 350°C MCRT DISPLAYED TEMPERATURE

Test Time Hours	Residue % Weight	Description of Deposits
30	47.23	oil
60	16.26	Hard glassy deposits, melting point range of 54 to 58°C
90	13.38	Hard glassy solid at temperatures up to 300°C

influence coking tendency. Using the short vials, the oil creeps over the top of the vials and forms deposits on the outside at 375°C. At 400°C and above, volatilization apparently occurs rapidly and no outer vial deposits are observed.

As shown by Table 61 and Figures 44 and 45, both O-67-1 and O-77-6 produce hard varnish to coke at 375 to 425°C using short vials. Reducing the temperature to 350°C yields dark viscous oil, resulting in much higher deposits. In contrast, the tall vials give hard deposits at 400 to 425°C, but when temperature is dropped to 375°C, dark viscous oil remains in the bottom of the tube with some hard varnish at the top. Several factors appear to influence the results, with the most important two being the rate of volatility and the rate of degradation with respect to deposition. Lubricant loss can occur during rapid volatilization resulting in lower deposit values. Volatility may be the predominant factor when using the short vial while thermal degradation of the lubricant may be the predominant deposition factor in the tall vial. Furthermore, air availability in the short vial could result in a more effective oxidation and subsequent degradation, leading to the formation of a hard varnish at 375°C relative to

TABLE 61

EFFECT OF TEMPERATURE ON MCRT DEPOSITS USING
30 HOUR TEST TIME AND 0.5 GRAM SAMPLE SIZE

Oil	Test Temp. °C	Deposit	
Regular Vials			
0-77-6	350	24.53 \pm 1.56	Dark viscous oil, varnish on top
	375	1.88 \pm 0.37	Hard dark brown varnish
	400	3.78 \pm 0.47	Hard brittle flaky coke
	425	1.00 \pm 0.25	Hard, black, loose coke
Tall Vials			
0-77-6	350	-	
	375	20.24 \pm 1.29	Viscous Oil, varnish up & over sides
	400	13.71 \pm 1.59	Hard dark varnish, up & over top
	425	9.03 \pm 1.77	Hard, black, brittle coke
Regular Short Vials			
0-67-1	350	19.88 \pm 1.96	Dark viscous oil, varnish on top
	375	1.72 \pm 0.20	Hard dark brown varnish
	400	2.65 \pm 0.13	Dark brown varnish
	425	0.69 \pm 0.27	Hard black coke
Tall Vials			
0-67-1	350	-	
	375	20.89 \pm 1.01	Viscous oil, hard varnish on top
	400	11.34 \pm 1.69	Dark brown varnish
	425	7.54 \pm 1.86	Hard black coke

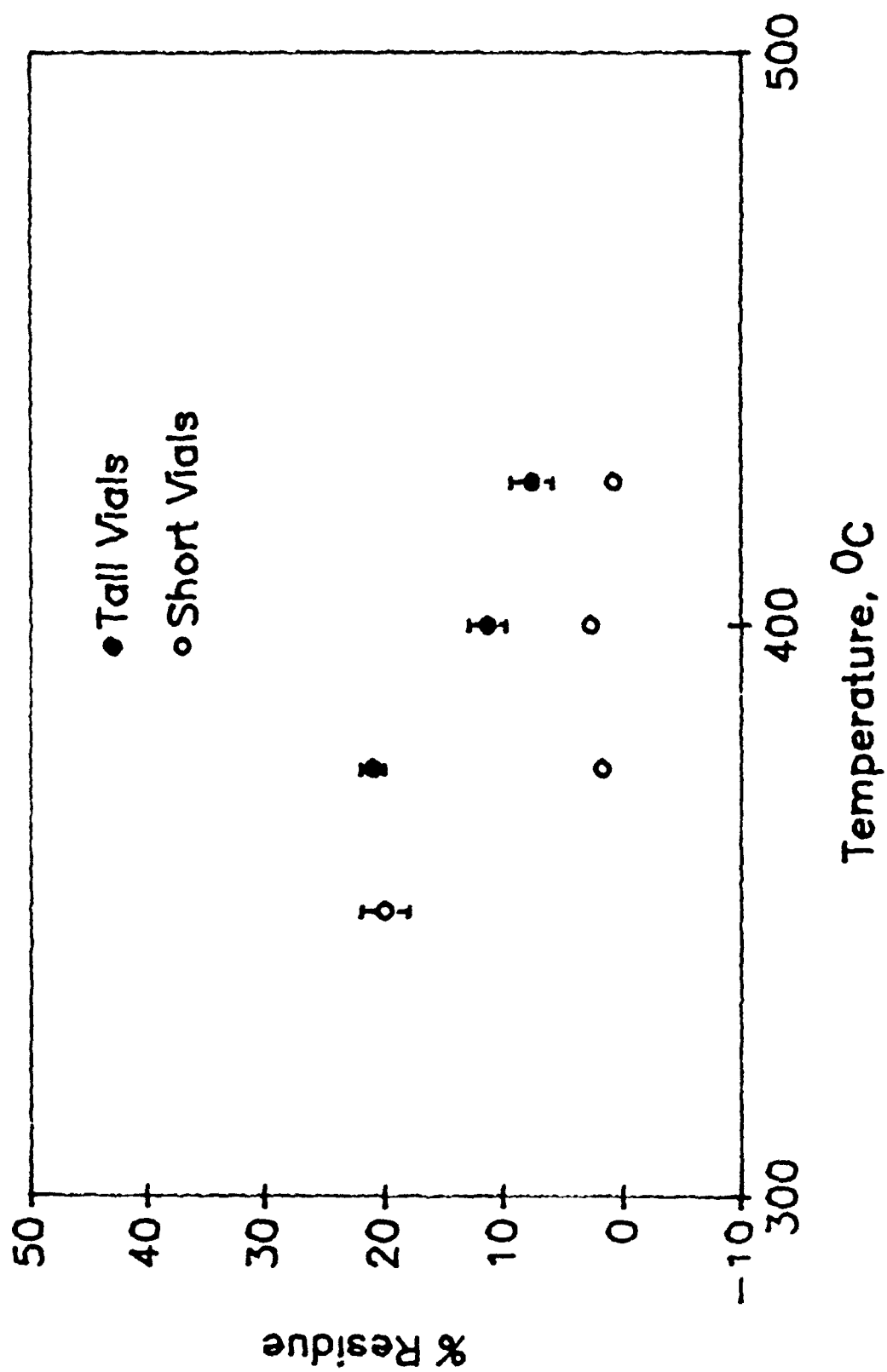


Figure 44. Effect of Temperature on MCRT Residue Using Tall vs. Short Vials for Lubricant 0-67-1

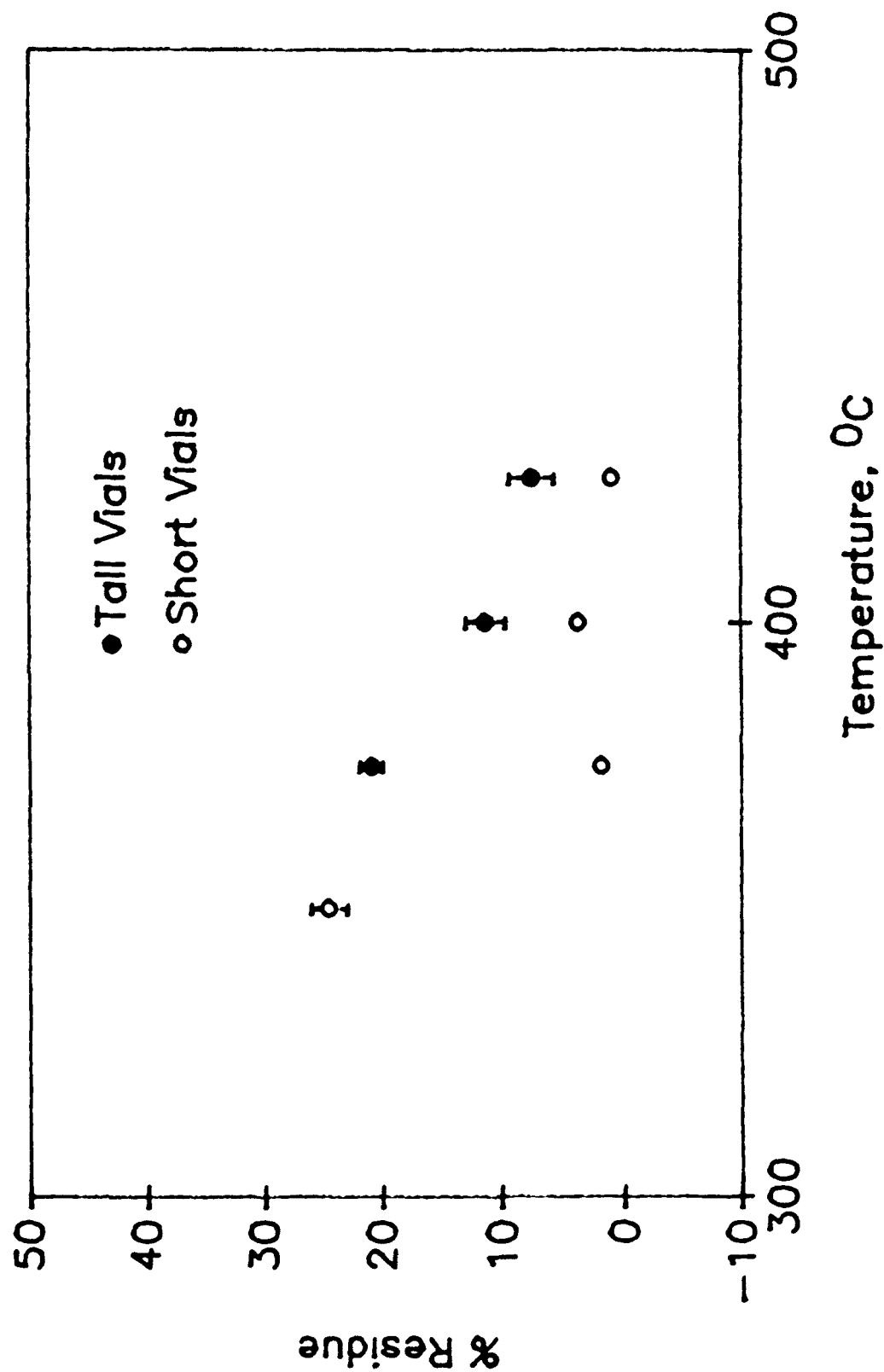


Figure 45. Effect of Temperature on MCRT Residue Using Tall vs. Short Vials for Lubricant 0-77-6

the viscous oil produced in the tall vial at the same temperature. The tall vial may act as a better "trap" for the lubricant as the vapors condense and return to the oil resulting in higher amounts of deposits. As expected the amounts of deposit produced in the tall vial decreased with an increase in temperature for O-77-6 and O-67-1. Except for the amount of deposit produced at 375°C, similar trending with temperature was observed for the short vials.

(c) Effect of Sample Size on MCRT Deposits

The effect of sample size on MCRT deposits of various high temperature fluids was investigated using short (3.5 cm) vials since limited previous testing had shown that sample volume is critical and its effect on deposit formation may depend upon the type of lubricant, test temperature, pre-stressing, and other factors. In this study, sample sizes of 0.25 g and 0.5 g of various lubricants were investigated using a 30 hour, 400°C MCRT test. The results of this study are given in Table 62 and shown graphically in Figure 46.

These data show that increasing the sample size of O-77-6 and O-67-1 from 0.25 to 0.5 gram increases by approximately seven times the amount of deposits which is probably due to reduced loss of fluid by volatilization. Lubricants in other classes show a different trend as seen with TEL-9050 which gives only about twice the amount of deposits when using the larger sample size. The effect of C&O pre-stressing continues to show an increase in MCRT deposits for both sample sizes and with differences in deposit values of the two different sample sizes being related to the degree of degradation occurring during C&O testing. The MCRT residue testing of the four-ball sample showed a reduced deposit value compared to new fluid for both sample size of O-77-6 and O-67-1 fluids. However, the differences in deposit values of the two sample sizes are not as apparent as with the other

TABLE 62

EFFECT OF SAMPLE SIZE ON MCRT RESIDUE
AT 400°C USING 3.5 CENTIMETER VIALS AND 30
HOUR TEST TIME

Lubricant	0.25 g Sample		0.5 g Sample	
	% Residue	Type Deposit	% Residue	Type Deposit
O-77-6	0.53 \pm 0.14	Hard dk varnish near top and on bottom	3.78 \pm 0.47	Hard brittle flaky black coke in bottom
O-67-1	0.41 \pm 0.13	Hard dk varnish in bottom, light brown varnish near top	2.65 \pm 0.13	Hard dark brown varnish, entire vial
TEL-9050	1.43 \pm 0.17	Hard dark brown coke and gray- black varnish, bottom only	2.39 \pm 0.68	Dark brown to black coke & varnish, bottom only
O-77-6, 120 h O/C at 290°C	1.67 \pm 0.50	Hard black loose coke bottom only	9.72 \pm 0.72	Hard brittle coke on bottom, slight varnish on top
O-67-1, 168 h O/C at 320°C	2.20 \pm 0.57	Hard dk varnish in bottom, slight loose coke on outside	4.05 \pm 0.15*	Hard dark brown varnish on top and bottom
Wear Test #411 (O-77-6, 32.5 lb, 1200 rpm 3 h, 250°C)	0.10 \pm 0.08	Red iron oxide on bottom, top clean	0.04 \pm 0.02	Red iron oxide in bottom, top clean
Wear Test #413 (O-67-1, 7.5 lb, 1200 rpm 3 h, 250°C)	0.07 \pm 0.03	Red iron oxide lighter pale yellow to light brown varnish on bottom	1.25 \pm 0.59	Flaky coke & varnish, hard coke in bottom top clean

*Repeat test on old sample, original value was 2.16 \pm 0.26 when freshly stressed

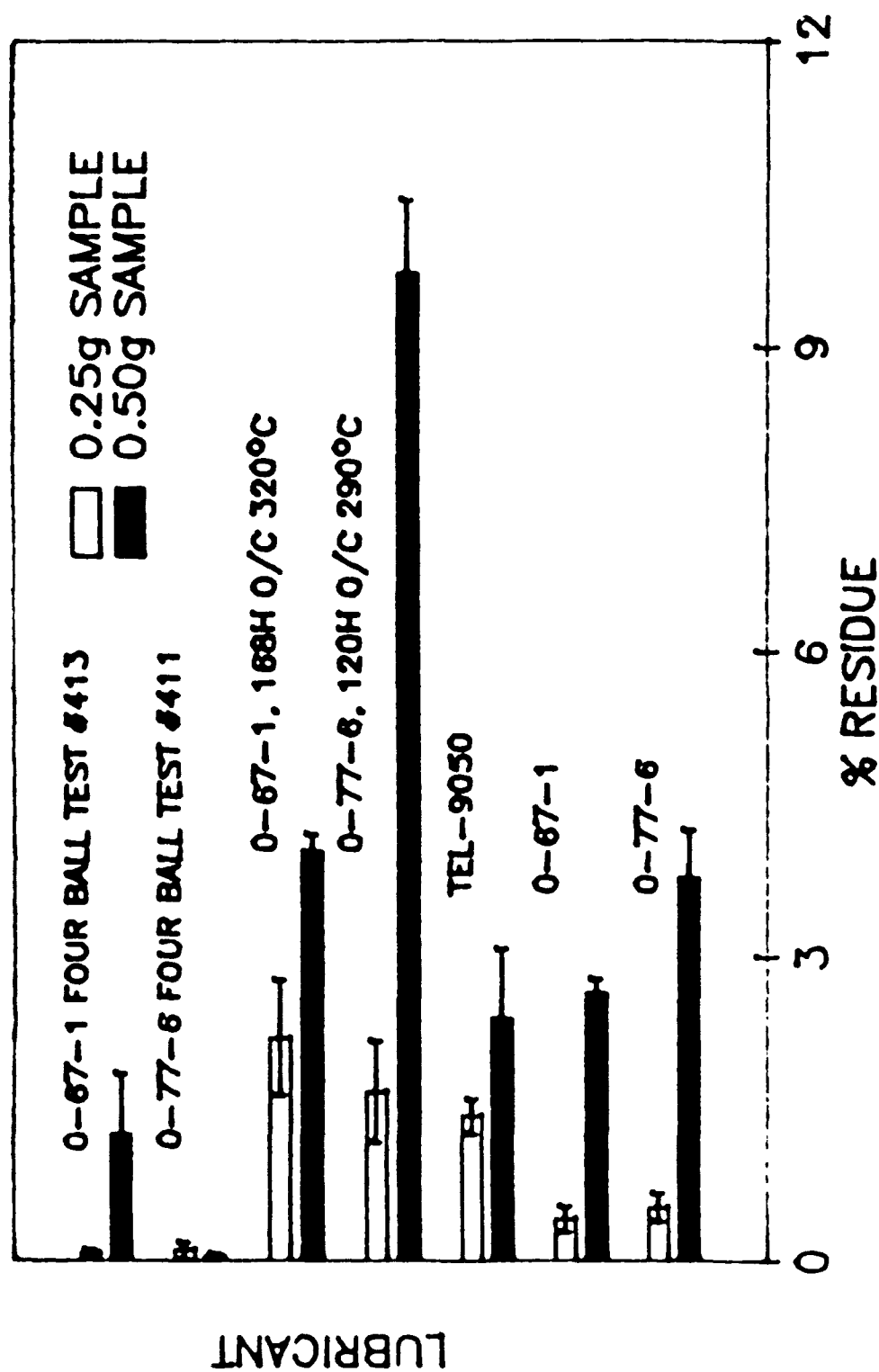


Figure 4b. Effect of Sample Size on MCRT Residue at 400°C Using 3.5 cm Vials and 30 Hour Test

test data. This difference may be related to the low levels of deposits and the difference in the amount of wear debris between the two wear test samples.

(d) Effect of Test Vial Material on MCRT Deposits

The MCRT vials used in this study were machined from T304 stainless steel and having the same dimensions as the regular 35 mm glass vials. Testing was conducted at temperatures of 350, 375, 400 and 425°C using the standard 30 hour coking period. The data are shown graphically in Figure 47 along with corresponding MCRT data using the standard glass vials. These data show that very little difference exists between the stainless steel vial and glass vial for inhibited fluid O-67-1 except a 0.9% increase in the glass vial deposits at 400°C compared to the 375°C value. At 425°C, both type vials gave about the same low level of deposits (approximately 0.6%). The effect of the stainless steel vial on MCRT deposits for the uninhibited fluid O-77-6 is much different than that for fluid O-67-1. The residue value decreases at a fairly constant decreasing rate of deposit formation when test temperature is increased from 350 to 425°C. Also, at 350°C the deposit level is approximately 10% lower using the stainless steel vials. The most probable cause for this effect is a catalytic degradation effect on the less stable uninhibited O-77-6 fluid.

(e) MCRT Coking Study of Unfiltered and Filtered Used MIL-L-87100 Lubricant

MCRT testing was conducted on 10 used MIL-L-87100 lubricant samples obtained from operational turbine engines. MCRT testing also included selected samples after being filtered (3 micron Ag membrane) for determining the effects of "fine" filtration on MCRT residue values for used MIL-L-87100 lubricant. MCRT test conditions were a 0.5 gram sample, 400°C

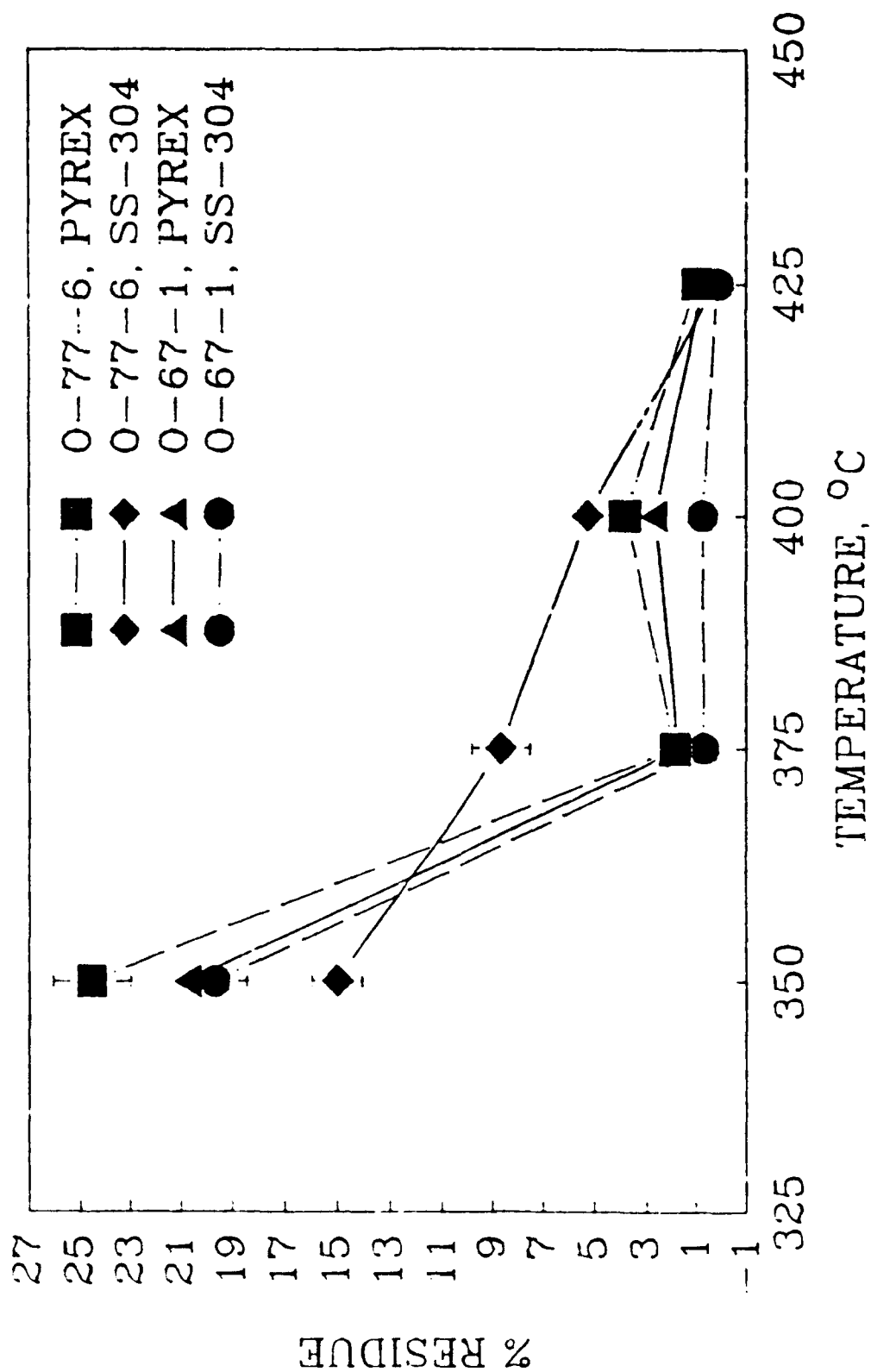


Figure 47. The Effect of Vial Material and Temperature on MCRT Percent Residue for 0-77-6 and 0-67-1

test temperature and 30 h test time. Test data obtained from this study are given in Table 63.

Sample CB-1 which is a blend of four-ball wear test samples of MIL-L-87100 lubricant O-67-1 has been included in Table 63 along with new O-67-1 lubricant for comparative purposes. The data in Table 63 show that MCRT deposit values for used MIL-L-87100 generally, but not always increase and show poor test repeatability. Samples TEL-9029 and TEL-9030 showed a slight decrease. Filtering of the used fluids ranged from having little effect (Sample CB-3) to greatly increasing the deposit level (TEL-90026). Generally, filtering tends to increase MCRT deposits values. One sample, TEL-9040, showed a slight decrease in deposit level due to filtering but this may be due to poor test repeatability of this sample. Four-ball wear test sample CB-1 shows a moderate increase in deposits (from 0.12 to 2.1%) after filtering. Overall, the effect of filtration on the MCRT residue values of used MIL-L-87100 depends upon the amount and type of wear debris which can reduce deposits and the degree of oxidative degradation which can increase deposits. The iron and tin analyses performed by atomic absorption (AA) are also included in Table 63. Filtering the oil through the 3 micron Ag filter reduces the Fe and Sn levels in the oil.

(f) Effect of Four-Ball Wear Testing and Four-Ball
Test Specimen Material on MCRT Deposits

Micro Carbon Residue Tester (MCRT) evaluations were conducted on 4 four-ball test samples obtained from wear testing using different test temperatures and test times. Test conditions, wear scar values and MCRT values are given in Table 64.

TABLE 63

MCRT DEPOSIT VALUES FOR MIL-L-87100 LUBRICANT FROM OPERATIONAL
ENGINES INCLUDING INITIAL IRON AND TIN CONTENT

Sample	Fe ppm	Sn ppm	Residue ¹ % Wt	Deposit Description
O-67-1	0	500	2.65 \pm 0.13	Brown Varnish
TEL-9028 ²	-	-	2.03 \pm 0.09	Brown Varnish
TEL-9028 ³	3	-	2.89 \pm 0.93	" " "
TEL-9029	3	-	1.24 \pm 0.43	" " "
TEL-9030	4	40	1.45 \pm 0.11	Hard Dark Varnish
TEL-9030 ⁴	1	42	3.88 \pm 0.77	Dark Flaky Varnish
TEL-9038	5	-	3.87 \pm 0.72	Black Coke
TEL-9039	4	-	2.70 \pm 1.35	" " "
TEL-9040	8	87	4.38 \pm 0.94	Dark Varnish
TEL-9040 ⁴	5	71	3.15 \pm 0.50	" " "
TEL-90025	3.7	130	6.86 \pm 0.43	Dark Flaky Varnish
TEL-90025 ⁴	2.4	116.7	5.03 \pm 0.71	Dark Varnish
TEL-90026	2.6	78.3	5.00 \pm 1.37	Dark Flaky Varnish
TEL-90026 ⁴	1.8	74.5	7.33 \pm 0.39	" " "
CB-2	2	330	1.56 \pm 0.26	Hard Varn. & White Dep
CB-2 ⁴	1	330	2.19 \pm 0.25	Hard Dark Varnish
CB-3	4	98	3.18 \pm 1.02	" " "
CB-3 ⁴	3	96	2.92 \pm 1.05	" " "
CB-1 ⁵	63	302	0.10 \pm 0.02	Light Orange Powder
CB-1 ⁴	0	309	2.11 \pm 0.31	Hard Orange Varnish

¹ MCRT Test Conditions: 400°C, 30 h, 0.5 g sample, 35 mm glass vials

² As received with 15% trichloroethylene

³ After removal of trichloroethylene

⁴ After 3 micron silver membrane filtering

⁵ Four-Ball wear test sample

TABLE 64

MCRT DEPOSIT VALUES FOR FOUR-BALL WEAR
TEST SAMPLES AT 400°C TEST TEMPERATURE AND
30 TEST HOURS

Test No.	Load N	Test Temp. °C	Test Time h	Wear Scar Dia., mm	MCRT Deposit % Wt
367	145	150	2.5	1.119	0.06 ± 0.04
369	145	150	3.0	1.232	0.05 ± 0.02
370	145	150	68.2	3.429	0.39 ± 0.09
382	33	75	3.0	0.632	2.17 ± 0.54
O-67-1	-	-	-	-	2.65 ± 0.13

(All test speeds were 1200 rpm and O-67-1 Lubricant)

Test data given in Table 64 show that MCRT deposits greatly decreased for the wear test samples conducted at 150°C and 145 N loading. The 75°C wear testing at 33 N did not significantly effect the MCRT value considering the standard deviation of the tests.

Four-ball wear tests on O-67-1 were conducted at various loads and temperatures at constant speed and test duration. MCRT test data for these samples are shown in Table 65. These data shown graphically in Figure 48 illustrate how the presence of nascent wear can greatly affect the MCRT results.

In general, the normal, rubbing, severe wear and cutting wear particles which occur in O-67-1 at 33, 78 and 145 N loadings do not appreciably change the coking values or affect the types of MCRT deposits when generated at 75°C. At 150°C, the resulting MCRT values are lower at all loads and red iron oxide plus varnish type deposits occur. This effect is attributed to the formation of very small iron particles along with polymeric material and/or iron-polymer complex, since 3 micron filtering yields higher

TABLE 65
EFFECT OF FOUR-BALL WEAR TESTING
ON MCRT RESIDUE USING 30 HOUR TEST
0.5 GRAM SAMPLE AND 3.5 CM VIALS

3 Hour Wear Test, 1200 rpm 145 N					
Lubricant	No Wear Test	75°C	150°C	250°C	315°C
O-77-6	3.78 \pm 0.47 Hard black coke	2.43 \pm 0.61 Hard black coke	0.04 \pm 0.02 Red iron oxide	0.04 \pm 0.02 Red iron oxide	0.64 \pm 0.36 Black loose coke
O-67-1	2.65 \pm 0.13 Hard dark varnish	1.78 \pm 0.44 Dark brown flaky coke	0.05 \pm 0.02 Light orange powder	0.11 \pm 0.04 Red iron oxide	0.09 \pm 0.04 Iron oxide/ sl. varnish
O-67-1 ^c	-	-	2.11 \pm 0.31 Hard dark varnish	-	-
O-67-1 ^d	-	-	1.22 \pm 0.37 Amber/black particles	-	-
O-67-1 ^e	-	-	1.04 \pm 0.20 Hard dark brown varnish	-	-
78 N					
O-67-1	-	3.65 \pm 0.68 ^b Hard black coke/slight varnish	1.64 \pm 1.29 Black loose coke/slight varnish	0.31 \pm 0.25 Black coke/ orange dust	0.11 \pm 0.02 Pale orange/ dark orange particles
33N					
O-67-1	-	2.17 \pm 0.54 Dark flaky varnish	0.34 \pm 0.31 ^b Dark brown flaky coke/ white dust	0.11 \pm 0.03 Dark flaky varnish/coke	0.11 \pm 0.03 Red iron oxide/slight varnish/coke

^a Average of two runs

^b Average of three runs

^c Filtered through 3 micron silver membrane after wear test

^d Subjected to 48 h C&O at 320°C after wear test

^e Same as "d" except filtered through 3 um filter prior to C&O

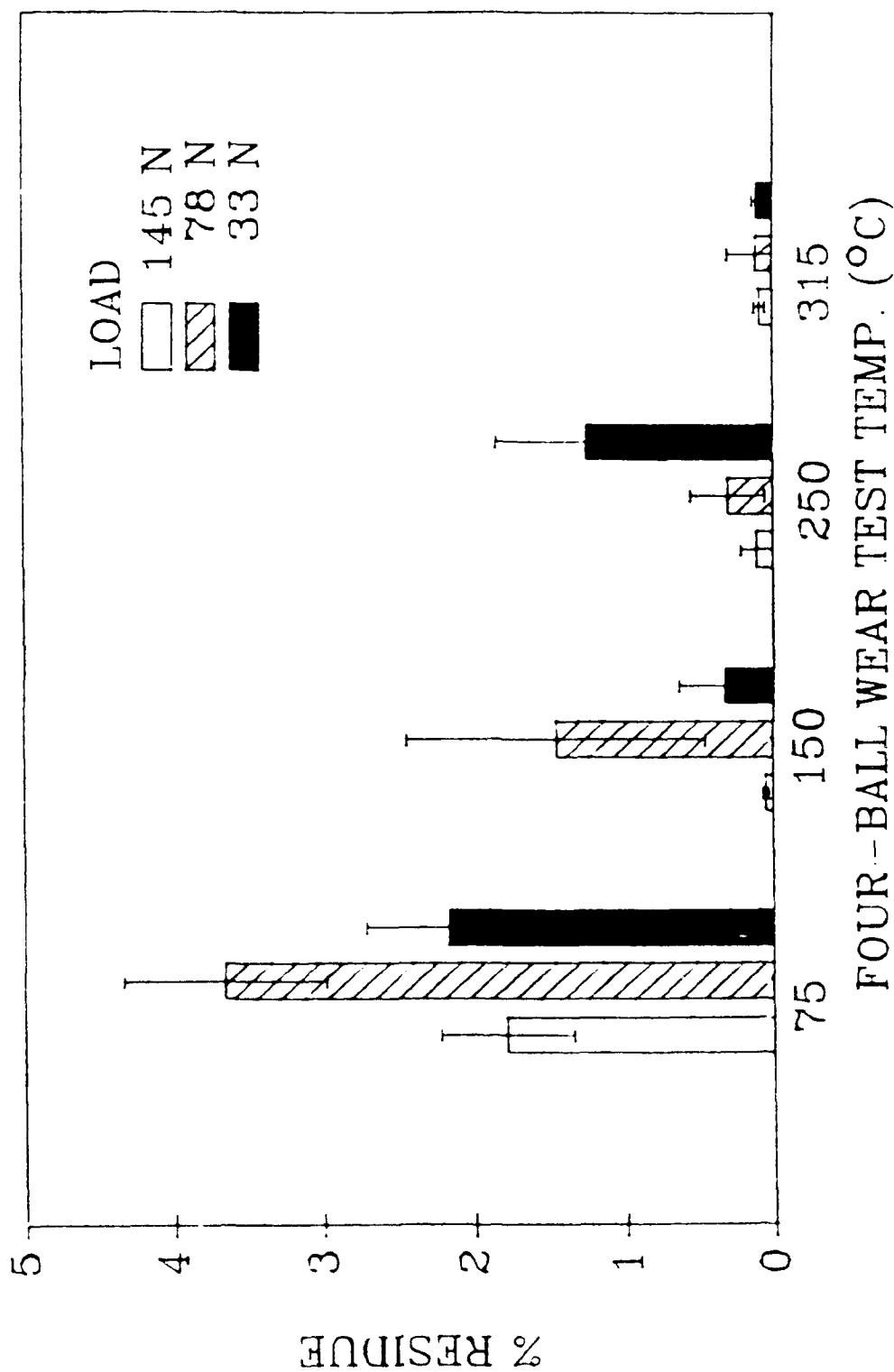


Figure 43. The Effect of Wear Metal Generated from Four-Ball Wear Tests Using Different Temperatures and Loads on MCRT Percent Residue for O-67-1

residue as shown in Table 63. C&O stressing after wear testing gives an increased residue (though not as great as wear testing alone), and is unaffected by filtering. At a wear test temperature of 250°C, the wear particles generated further decrease the residue values with the effect becoming greater as load is increased from 33 to 145 N. The deposits range from varnish and light orange residue at 33 N to red iron oxide at 145 N. At 315°C, all loadings produced iron oxide with coke except the 33 N which had slight varnish also. It appears from this data that higher temperatures and higher loads during wear testing may decrease the amount and affect the types of deposit formed. Although the 145 N load gives a decrease in residue at 150°C to 315°C, the effect is not pronounced at 75°C, in which case the residue is still near the level of the fresh lubricant at all three loadings. The data from these tests indicate that an important relationship exists between wear environments and the potential for deposit formation.

Two lubricants, O-67-1 and TEL-90024, were subjected to four-ball wear tests under identical conditions except for the top and bottom ball material. The wear test fluids were subjected to MCRT testing to evaluate changes in the coking characteristics of the used oils. The results of this study are presented in Table 66.

TABLE 66

FOUR-BALL WEAR TEST DATA AND MCRT RESULTS FOR
O-67-1 AND TEL-90024 LUBRICANTS USING Si_3N_4 , 52100
STEEL, M50 STEEL AND BRASS WEAR TEST BALLS

Wear Test ¹	Lubricant	Top Ball	Bottom Ball	MCRT % Residue	Total Wear Volume., mm ³
412	O-67-1	52100 Steel	52100 Steel	0.13 ± 0.03	4.67×10^{-1}
427	O-67-1	Si_3N_4	52100 Steel	3.30 ± 0.45	3.69×10^{-2}
428	O-67-1	52100 Steel	Si_3N_4	3.45 ± 0.78	5.83×10^{-2}
475	O-67-1	M50	M50	0.34 ± 0.06	6.57×10^0
476	O-67-1	Si_3N_4	Si_3N_4	3.97 ± 0.45	4.92×10^{-2}
477	O-67-1	Brass	Brass	0.13 ± 0.01	2.58×10^0
494	TEL-90024	52100 Steel	52100 Steel	2.59 ± 0.12	6.91×10^{-3}
-	TEL-90024	New Fluid		1.87 ± 0.06	-

¹Wear test conditions are: Load of 32.5 lbs., Chamber Temp. of 150°C, Speed of 1200 rpm, and Test duration of 3 hours.

²MCRT conditions are: Temp. of 400°C, Test duration of 30 hours, and chamber gas is air.

The amount of coke produced from the wear tests using Si_3N_4 balls is much greater than the tests using steel or brass, although the amount of wear on the balls is less. In fact, this is true for all the wear tests evaluated here by MCRT that coking tendency is inversely proportional to wear volume for O-67-1 fluids. For the O-67-1, the amount of coke produced from various types of material decreased in the order Si_3N_4 M50 52100 brass. The type of deposits change with ball material. A reddish-brown powder (probably iron oxide) was observed for wear tests 412 and 475 (steel balls). A slight gray powder (probably zinc oxide) was observed for wear test 477 (brass balls). A dark heavy varnish was observed for all the wear tests using Si_3N_4 balls. TEL-90024 cokes moderately when it

has been subjected to the four-ball wear test. Fresh TEL-90024 experimental fluid gave a coking value of $1.87 \pm 0.06\%$ which is a little lower than the value of $2.05 \pm 0.13\%$ for lubricant O-67-1. However, after wear testing using 52100 steel balls, lubricant TEL-90024 showed an increase in MCRT deposit over new TEL-90024 lubricant and approximately 20 times the deposit value of lubricant O-67-1 after wear testing using 52100 steel balls.

(g) Variable Temperature and Testing Time Study

The effect of shorter test time using the MCRT was examined to determine which temperatures would produce hard black coke at shorter (less than 30 hours) test times. Lubricant O-77-6 was subjected to coking temperatures from 400 to 550°C at increasingly shorter durations (Figure 49). All tests produced hard black coke, with values ranging from 13.71 to 0.26% except the 550°C test in which the lubricant left no residue in the vials. The objective of this study was to identify conditions under which even a very short residence time can produce coking and to demonstrate how lubricant performance can greatly be affected by the amount of time a lubricant resides in a high temperature environment.

When holding the temperature constant and varying time of test, the changes in the deposits produced can be observed. For example, if O-67-1 is tested for 30 hours at 375°C using 7.5 cm glass vials, 20.89% hard varnish is produced, and after 60 hours the value drops to 6.20%. Raising the test temperature to 400°C gives 11.76% black coke after 30 hours and at 60 hours gives 7.76%. An even lower residue value can be obtained if the test duration is increased to 90 hours, as a 350°C test at this duration yields only 4.33% deposit. However, the deposit is tacky to varnish rather than coke. Therefore, residue quantities produced at a specific temperature can be reduced by increased test time but will not necessarily produce types

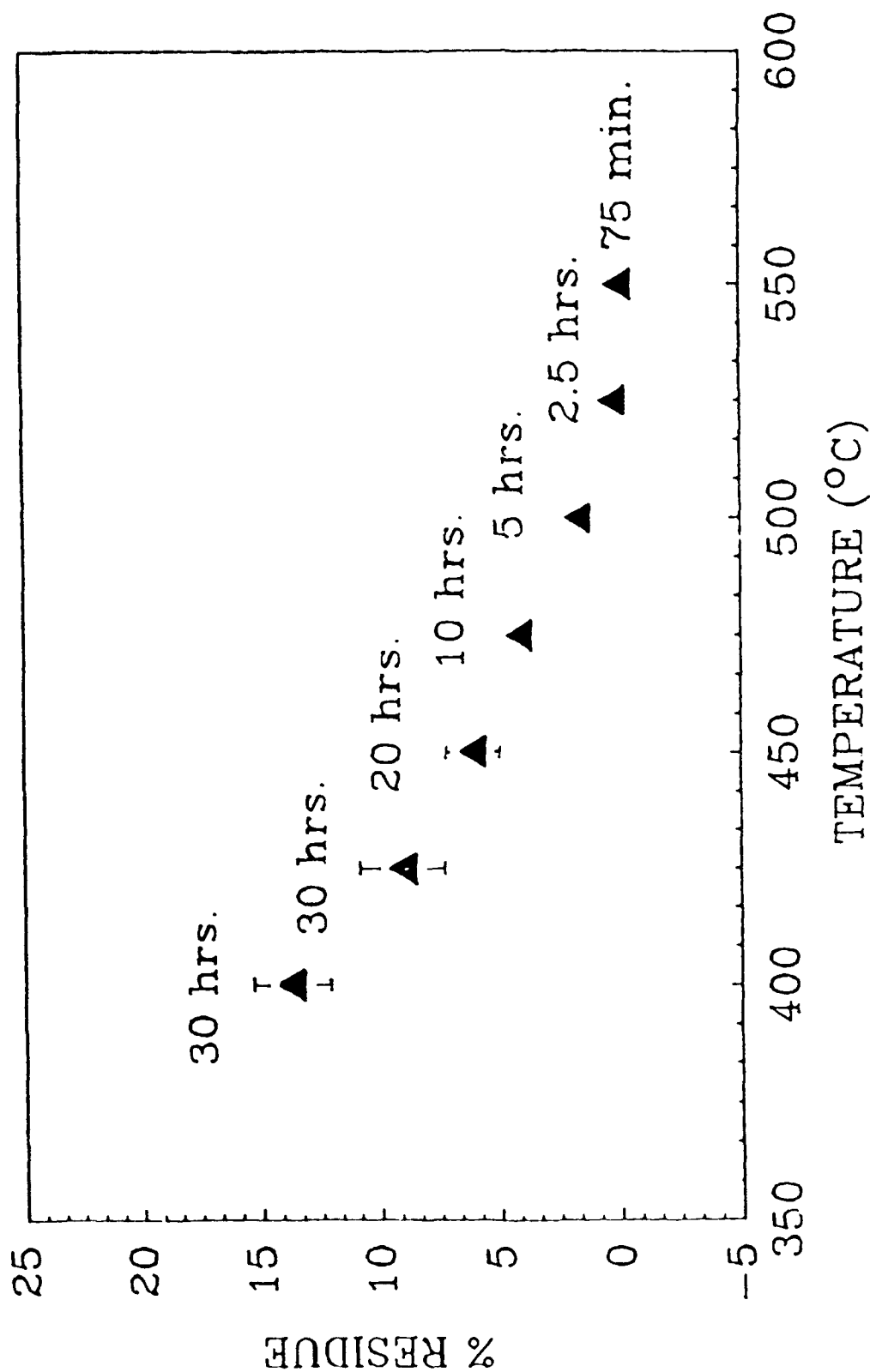


Figure 49. Effect of Test Time on Coking Tendency of 0-77-6 Using MCRT at Various Temperatures and 7.5 cm Pyrex Vials

of residue which are equivalent in nature. Consequently, the selection of test parameters in determining coking tendency is greatly influenced by the type of information desired, which is in turn affected by the engine conditions under which the lubricant is expected to perform.

(h) Argon Versus Air MCRT Deposit Study

MCRT testing was conducted on several new and stressed fluids using argon instead of air as the chamber gas. The test procedure remained the same as that for air which uses a gas pressure of 20 psi. This results in a gas flow of 150 cc/min for air and 127 cc/min for argon. This study was conducted to investigate the effects of pre-stressing and wear debris on the deposition characteristics of MIL-L-87100 fluids in an inert atmosphere.

The test data obtained from this study are given in Table 67. These data show that for the used engine samples of MIL-L-87100 lubricant (TEL samples) the percent deposits formed under argon are very low and much lower than corresponding deposits formed under air. This is due to low pre-stress levels of these fluids and the lack of oxidative degradation which produces breakdown materials which in turn forms the deposits obtained using air. The C&O test samples of MIL-L-87100 lubricant O-67-1 show that similar deposit levels are obtained using air and argon and that these deposits increase with C&O test time. This indicates that the degradation products causing the increased deposit levels are mostly in the fluids prior to MCRT testing and little oxidation occurs during MCRT testing using air. The effect of wear debris has very little effect on MCRT deposits when using argon but greatly reduces the deposits when using air.

TABLE 67

COMPARISON OF 30 HOUR, 400°C MCRT DATA USING
AIR AND ARGON FOR VARIOUS TEST FLUIDS

Air			Argon	
Sample	% Deposits	Description	% Deposits	Description
TEL-9028	2.89 \pm 0.93	Brown Varnish	0.50 \pm 0.10	Dark Varnish
TEL-9029	1.24 \pm 0.40	" " "	0.10 \pm 0.02	Brown Varnish
TEL-9030	1.45 \pm 0.11	Dark Varnish	0.21 \pm 0.11	" " "
TEL-9038	3.87 \pm 0.72	Black Coke	0.10 \pm 0.02	" " "
TEL-9039	2.70 \pm 1.35	" " "	0.30 \pm 0.04	" " "
TEL-9040	4.38 \pm 0.94	Dark Varnish	0.11 \pm 0.06	" " "
O-67-1	2.65 \pm 0.13	Brown Varnish	0.08 \pm 0.02	Brown Varnish
O-67-1 (168 h, 320°C C&O)	4.05 \pm 0.15	" " "	2.30 \pm 0.23	Dark Varnish
Wear Test 370	0.39 \pm 0.09	Red Iron Oxide	1.78 \pm 0.15	Flaky Coke & Gray Resid.
Wear Test 399 (168 h, 320°C C&O)	0.13 \pm 0.04	Orange Powder	2.89 \pm 0.19	Gray to Black Residue
O-67-1 (240 h, 320°C C&O)	6.59 \pm 0.16	Dark Varnish	4.21 \pm 0.47	Dark Varnish
Wear Test 405 (240 h, 320°C C&O)	2.14 \pm 0.45	Dark Varnish and Coke	5.26 \pm 0.35	" " "
O-67-1 plus 100 ppm Fe	2.41 \pm 0.27	Dark Varnish	-	
TEL-9050	2.83 \pm 0.07	Black Flaky Coke	-	

(i) MCRT Residue Studies of Various High Temperature Lubricants and Experimental Fluids

MCRT tests were conducted on various high temperature experimental fluids for determining the relative coking characteristics of these fluids. These test data are given in Table 68 and include data for some lubricants previously discussed for comparative purposes.

The data in Table 68 show several important factors. First, the type inhibitor has a great effect on MCRT deposits for 5P4E inhibited fluids as shown by the data for TEL-8085 and TEL-8087 versus O-67-1. The deposit level of TEL-8085 and TEL-8087 are very close to the deposit levels of four-ball wear tested O-67-1 lubricant. Second, the increase in the molecular weight of the polyphenyl ether basestock fluids greatly increases deposit levels probably due to decreased volatility. This is shown by the differences in deposits of O-67-1 (inhibited 5P4E) and TEL-90028 (same inhibited 6P5E). Third, the non-polyphenyl ether base fluids have a wide range of MCRT residue values (27.33% to 1.30%) with the most stable of these fluids having MCRT deposits equivalent to MIL-L-87100 lubricants.

(j) Correlation of MCRT and AFAPL Static Coker Test Data

The correlation between MCRT test deposits and the AFAPL Static Coker deposits is shown in Table 69 with the MCRT values being arranged from low to high.

In general there is little correlation between the two tests when considering all types of high temperature fluids. For new fluids, Static Coker deposits are much lower relative to the MCRT deposits except for the least oxidatively stable fluids. As fluids are stressed or degraded, both tests show increasing deposit values and the deposit values for both

TABLE 68

MCRT RESIDUE VALUES OF VARIOUS HIGH-TEMPERATURE
LUBRICANTS AND EXPERIMENTAL FLUIDS (400°C, 0.5 G
SAMPLE, 3.5 CM VIALS, 30 TEST HOURS)

Lubricant	% Viscosity Increase, 40°C	% Residue	Description of Deposit
O-67-1	-	2.65 \pm 0.13*	Hard dark brown varnish
O-67-1, 96 h at 320°C	25.6	2.68 \pm 0.25	Hard dark brown varnish
O-67-1, 168 h at 320°C	40.8	4.05 \pm 0.15	Hard dark brown varnish
O-67-1, 240 h at 320°C	85.4	6.59 \pm 0.16	Hard dark brown varnish
O-77-6	-	3.78 \pm 0.47	Hard brittle flaky black coke
O-77-6, 72 h at 290°C	26.9	6.09 \pm 0.36	Hard brittle flaky coke on bottom, slight varnish and flake on top
O-77-6, 120 h at 290°C	75.4	9.72 \pm 0.72	Hard brittle flaky coke on bottom, slight varnish on top
TEL-9050	-	2.39 \pm 0.68	Hard dark brown to black coke and varnish bottom only
TEL-9050, 24 h at 290°C	5.9	3.72 \pm 0.09	Hard dark flaky coke on bottom, light varnish above, hard dark varnish on top (3 phases)
TEL-9050, 120 h at 290°C	33.2	5.79 \pm 0.34	Hard dark flaky varnish on bottom
TEL-8085	-	0.12 \pm 0.02	Yellowish stain
TEL-8087	-	0.08 \pm 0.03	Yellowish stain
TEL-90018	-	27.55 \pm 1.69	Dark flaky coke
TEL-90028	-	24.50 \pm 2.51	Dark flaky coke
TEL-9071	-	1.6 \pm 0.11	Dark varnish
TEL-90001	-	27.33 \pm 3.39	Dark coke on bottom, varnish on top
TEL-90024	-	1.87 \pm 0.06	Black coke
TEL-90059	-	1.69 \pm 0.07	Dark flaky coke
TEL-90063	-	1.30 \pm 0.06	Dark flaky coke

* Repeat testing yielded 2.44 \pm 0.48 %

TABLE 69

CORRELATION OF MCRT AND AFAPL STATIC COKER DEPOSIT VALUES

Sample	MCRT ¹ Deposits, %	Static Coker ² Deposits, mg/g
CB-1 unfiltered	0.1 ± 0.02	0.6 ± 0.3
TEL-9028	1.24 ± 0.43	0.8 ± 0.2
TEL-9030	1.45 ± 0.11	0.2 ± 0.1
TEL-90059	1.69 ± 0.07	4.1 ± 0.3 ³
TEL-90024	1.87 ± 0.06	0.5 ± 0.3 ³
O-67-1	2.65 ± 0.13	0.0 ± 0.0
TEL-9039	2.70 ± 1.35	0.2 ± 0.1
TEL-9028 ⁴	2.89 ± 0.93	0.3 ± 0.1
O-77-6	3.78 ± 0.47	6.5 ± 0.4
TEL-9038	3.87 ± 0.72	0.2 ± 0.2
TEL-9040	4.38 ± 0.94	0.5 ± 0.1
TEL-90026	5.00 ± 1.37	0.1 ± 0.1
O-67-1 (240 h C&O)	6.59 ± 0.16	8.2 ± 1.7
TEL-90025	6.87 ± 0.43	0.3 ± 0.04
O-77-6 (120 h C&O)	9.27 ± 0.72	10.8 ± 1.9 ³
TEL-90028	25.43 ± 0.31	0.2 ± 0.1 ³
TEL-90001	27.33 ± 33	13.5 ± 2.5 ³

¹ 400°C Test, 30 Hour, 35 mm Vial, 0.5 Gram Sample

² 400°C Test, S. Steel Specimens, 0.5 Gram Sample 3 Hour Test

³ 375°C Test, S. Steel Specimens, 0.5 Gram Sample 3 Hour Test

⁴ Repeat

tests decrease after four-ball wear testing of the fluids. The Static Coker appears to have a higher volatility/degradation ratio than the MCRT as shown by samples O-67-1 inhibited 5P4E polyphenyl ether and TEL-90028 (same inhibited) 6P5E polyphenyl ether.

Since the test parameters and correlations are quite different between the two tests with each representing specific conditions occurring within turbine engines, both tests provide appropriate data for evaluating the deposition characteristics of turbine engine lubricants.

(k) Summary

The Micro Carbon Residue Tester (MCRT) has been shown to be a viable test for investigating and measuring the deposit forming characteristics of high temperature fluids. MCRT displayed test temperature is higher than the measured average cell temperature which means each MCRT should be calibrated using internal thermocouples for correlating test temperature with displayed temperature.

Deposit values decrease with increasing test temperatures for both the standard (3.5 cm) and tall (7.5 cm) vials and with the tall vials giving 3 to 7 times the amount of deposits depending upon the type sample. Some solid deposits at room temperature can have melting points slightly above room temperature which means these deposits would be soluble or suspended in hot lubricant. Solid deposit values continue to decrease upon continued testing up to at least 90 test hours or with increasing test temperatures. The use of T304 vial material had very little effect on all fluids except the uninhibited O-77-6 fluid.

Generally, four-ball wear testing using 52100 or M50 steel test balls greatly reduced MCRT deposits with the values decreasing with increasing temperature or loadings. MCRT deposit levels varied when using

various combinations of Si_3N_4 and steel or with brass balls under the same test conditions. MCRT coking tendency was inversely proportional to wear volume for the MIL-L-87100 (O-67-1) lubricant. For this fluid the amount of coke produced from the various materials decreased in the order of $\text{Si}_3\text{N}_4 > \text{M50} > \text{52100} > \text{brass}$.

The use of argon instead of air gives lower deposits for new or C&O stressed MIL-L-87100 fluids and higher residue values for four-ball wear test samples of the same fluids. The type of polyphenyl ether (5P4E versus 6P5E) has a great effect on MCRT deposits as opposed to no difference in the Static Coker Deposits of these two fluids.

Non-polyphenyl ether base experimental high temperature fluids have a wide range of MCRT residue values with the most oxidative stable fluids having residue values equivalent to MIL-L-87100 fluids.

4. LUBRICANT FOAMING STUDY

a. Introduction

The importance of the foaming characteristics of turbine engine lubricants has been previously discussed³ with excessive foaming and aeration causing increased gear and bearing temperatures, a decrease in lubrication, oil pump cavitation and, in some case, loss of oil "overboard" through oil system breathers. Previous efforts in the investigation and development of test methods for measuring lubricant foaming have been directed toward normal ester base lubricants with no investigation of lubricant foaming or aeration of high temperature lubricants at anticipated operating temperatures. The three test methods used for measuring the foam and aeration characteristics of lubricants include the dynamic foam test as described by Federal Test Method 791, Method 3214 which requires 1200 cc test sample and 8 hours test time using an oil circulation test rig, Federal Test Method 3213 requiring

200 mL of sample which is aerated in a 500 cc cylinder (modification of ASTM Method D 892) and a small volume (25 ml sample) test developed² for testing small volumes of experimental lubricants.

This study describes the development of test methods and the measurements of the foaming characteristics of high temperature lubricants under more normal operating temperatures

b. Test Apparatus and Procedure

Two test methods were modified and used during the course of this study. Federal Test Method 3213 was modified by raising the test temperature from the normal 80°C test temperature to various temperatures up to 200°C and the preheating of the air to the test temperature prior to entering the foam test cylinder. This was accomplished by using a high temperature viscosity oil bath modified to accept either the normal 500 cc foam test graduated cylinder or a 250 cc graduated cylinder. An air preheating coil was used in the bath which contained polyphenyl ether (5P4E) as the bath medium. The small volume test described previously² was modified by using the same test bath as the modified Method 3213 and by changing the aeration procedure to an initial testing with a low airflow rate (100 cc/min) and increasing the airflow after foam stabilization to various airflow levels until an airflow of 1000 cc/min is obtained. This testing used a 25 mL sample, 250 mL graduated cylinder and 5 micron pore size metal spargers having 13/16 inch diameter or an ASTM air diffuser stone.

c. Test Lubricants

Seventeen new and used high temperature lubricants and experimental fluids were investigated during this phase of study and are described in Table 70. Appendix A lists the foaming data for the lubricants investigated to date.

TABLE 70

LUBRICANTS AND FLUIDS USED FOR FOAMING STUDY

Lubricant or Fluid	Description	Viscosity at 40°C, cSt
O-67-1	MIL-L-87100 Oil (5P4E)	280.3
O-77-6	Basestock for O-67-1	-
TEL-9028	Used MIL-L-87100 Lubricant	298.0 ¹
TEL-9029	" " "	284.9
TEL-9030	" " "	283.7
TEL-9038	" " "	288.4
TEL-9039	" " "	298.1 ²
TEL-9040	" " "	293.7
TEL-9050	Experimental Fluid	214.7
TEL-9069 ³	Used MIL-L-87100 Lubricant	-
TEL-9070 ³	Used MIL-L-87100 Lubricant	-
TEL-90001	Experimental Fluid	235.4
TEL-90018	Polyphenyl Ether (6P5E)	-
TEL-90024	Inhibited TEL-9071 Fluid	195.4
TEL-90070	MIL-L-7808 Type Lubricant	-
TEL-90071	MIL-L-7808 Type Lubricant	-
TEL-90072	MIL-L-7808 Type Lubricant	-

¹After removal of 15% tetrachloroethylene; visc. as received = 50.55 cSt at 40°C

²After removal of 1.9% trichloroethylene; visc. as received = 217 cSt at 40°C

³Series of small SOAP samples taken from engine at different operating times.

d. Results and Discussion

(1) Low Temperature Testing of Polyphenyl Ether Fluids

Initial foaming studies were conducted on 5P4E fluid O-77-6 at 80°C and 100°C using the ASTM stone and a 13/16 inch diameter 5 micron metal sparger and aeration airflows ranging from 250 cc/min to 1600 cc/min. Data obtained from this study is given in Table 71. The "foam" consisted of severely aerated oil with no oil/foam interface for all tests regardless of the type diffuser or airflow rate. The increase in temperature from 80 to 100°C increased the amount of aeration (reported foam) except for the test using the ASTM stone at 250 cc/min airflow. The temperature increase had a greater effect when using the metal sparger than using the ASTM stone.

TABLE 71

FOAMING CHARACTERISTICS OF 5P4E
FLUID O-77-6 USING 200 ML SAMPLE

Airflow Rate cc/min	Foam Volume, mL Test Temperature			
	80°C		100°C	
	13/16" Sparger	ASTM Stone # 1	13/16" Sparger	ASTM Stone # 1
250	495 ^a	-	OF; 550 ^c (101) ^d	405
500	460 (137)	490 ^b (102)	OF; 550 ^c (81)	495 ^a
750	440	-	-	-
1000	455 (120)	470 (74)	OF; 550 ^c (129)	470 (47) ^e
1200	460	-	-	-
1400	450	-	-	-
1600	450	-	-	-

^a Oil/air mixture increased to 525 mL during first minute of test and then decreased to 495 mL volume and remained constant.

^b Oil/air mixture increased to approximately 525 mL during first minute of test and then decreased to 490 mL and remained constant.

^c OF = Over Foam, above 500 mL mark. Values after OF estimated foam volume.

^d Values in parenthesis are foam collapse time in seconds.

^e Oil/air mixture increased to approximately 525 mL during first minute of test and then decreased to 470 mL and remained constant.

Foam testing of the fluid O-77-6 5P4E using a 30 gram (25 mL) sample at 80°C and 100°C and using both the 13/16 inch diameter 5 micron pore size sparger and the ASTM diffuser stone was performed for comparison with the foam test data using 200 mL sample size (Table 71). This test data is given in Table 72 and shows the following:

TABLE 72

SMALL VOLUME FOAM TESTING OF FLUID
O-77-6 AT 80°C AND 100°C USING A
13/16" DIAMETER 5 MICRON PORE SPARGER
AND AN ASTM DIFFUSER STONE

80°C Test Temperature

Test No	Description of O-77-6 Fluid	Type Disperser	Airflow, cc/min.			
			1000	700	500	200
6	New	Sparger	122(65) ¹	104	75(55)	67(41)
12	New	"	145(197)	-	138	115(190)
15	Oil from Test # 14	"	86(53)	-	80(48)	74
16	New	"	140(194)	-	110(196)	94
16	After 200 cc/airflow	"	100	-	-	-
16	After 15 minute soak	"	74	-	76	-
17	Same Oil as 16, Clean Sparger	"	78	-	-	-
18	New Oil	"	154(>700)	-	153	143
19	New Oil	"	144(>300)	-	138(>300)	126(>310)
19	After 200 cc/airflow	"	134	-	136	-
7	New Oil	ASTM Stone	91(40)	82	82	75(37)
13	Oil From Test 12	"	100(198)	-	102	88
14	New Oil	"	102(216)	-	92	80(54)

100°C Test Temperature

8	New Oil	Sparger	128 (After 10 min)(38)			
		"	86 (After 30 min)(38)	60(27)	-	
9	New oil	"	120 (After 10 min)(54)			
			91 (After 30 min)(54)	56	16 ²	
10	Test 9 oil; Clean Sparger	"	68			
11	New Oil	ASTM Stone	120(140)	110(100)	104	86

¹Foam collapse time (sec) are in parentheses
²Oil/Foam interface

Fluid O-77-6 showed severe aeration at all airflow rates of 200 to 1000 cc/min.

The change in test temperature from 80°C to 100°C did not significantly change the aeration characteristics using either air diffuser.

The change of airflow from 200 to 1000 cc/min did not have a great effect on aeration characteristics.

Poor test repeatability was obtained using the metal sparger with some indication that the aeration value decreased with aeration time for some tests. This decrease could not be traced to cleaning of the test cylinder or air diffuser.

Only one test showed an oil/foam interface. This was obtained using a 200 cc/min. airflow and the 5 micron pore size metal sparger at 100°C test temperature. No oil/foam interface was obtained at these conditions using the ASTM stone.

The above testing was conducted using the standard airflow procedure of Federal Test Method 791, Method 3213. This method specifies an aeration of 1000 cc/min for 30 minutes and then determining the foam collapse time. After complete foam collapse has occurred foaming values are then sometimes obtained at reduced airflow rates such as 700, 500 and 200 cc/min by lowering the aeration rates. Testing of 5P4E fluid O-77-6 was conducted at 80°C starting with a low aeration rate and then increasing the aeration rate after foam aeration stabilization had occurred at the various aeration rates using an ASTM stone and 25 mL sample. Data obtained from this testing are given in Table 73.

TABLE 73

EFFECT OF INCREASING (LOW TO HIGH) AERATION RATE ON
FOAMING/AERATION CHARACTERISTICS OF 5P4E FLUID O-77-6
AT 80°C USING ASTM DIFFUSER STONE AND 25 ML SAMPLE

Aeration Rate cc/min	Foam Value ¹ mL
250	100
500	104
750	102
1000	99

¹No oil/foam interface

The data given in Table 73 do not show the decrease in foam value of 15 to 20 mL of foam as was shown by Table 71 when aeration was changed from high to lower values. This difference in testing may be due to test repeatability or changes in the lubricant sometimes occurring with aeration which has been previously shown to occur. All subsequent foam testing was conducted using the increasing airflow rate procedure.

(2) High Temperature Testing of O-67-1 and TEL-90018 Fluids

Foam testing of MIL-L-87100 lubricant O-67-1 was conducted at 200°C using both 200 mL and 25 mL sample sizes. The 200 mL testing was conducted using a 13/16 inch 5 micron metal sparger while the 25 mL testing was done using both a 11/16 inch and a 13/16 inch metal sparger (a fresh sample was used for each test). Data obtained from this testing are given in Tables 74 and 75. These data show that increasing lubricant temperature to 200°C greatly reduces the foam volume and foam collapse times. Aeration during all three tests produced large bubbles and a good clear oil/foam interface. The foam values of 32 mL and 34 mL compared favorably with the 20 mL of foam obtained using the standard 200 mL sample size and a 500 mL graduated cylinder.

TABLE 74

LUBRICANT O-67-1 FOAMING CHARACTERISTICS
AT 200°C (200 ML SAMPLE AND 13/16 INCH
DIAMETER 5 MICRON SPARGER)

Airflow cc/min	Oil Volume mL	Oil and Foam Volume mL	Foam Volume mL
100	240	245	5
250	240	250	10
500	247	260	13
750	255	270	15
1000	265	280	15
1100	265	285	20

Foam collapse time: 4 seconds

TABLE 75

LUBRICANT O-67-1 FOAMING CHARACTERISTICS
AT 200°C (25 ML SAMPLE AND 5 MICRON
METAL SPARGERS)

Airflow cc/min	11/16" Dia Sparger			13/16" Dia Sparger		
	Oil Vol, mL	Oil/Foam Vol. mL	Foam Vol mL	Oil Vol, mL	Oil/Foam Vol, mL	Foam Vol, mL
100	36	38	2	38	40	2
250	36	44	8	42	48	6
500	36	48	12	42	50	8
750	34	54	20	28	54	26
1000	24	56	32	24	58	34
Foam Collapse Time:			5 s			
						6 s

Foam test data obtained on 6P5E polyphenyl ether fluid TEL-90018 at 200°C using a 25 mL sample and a 13/16 inch diameter, 5 micron pore size sparger are shown in Table 76.

TABLE 76

FOAMING CHARACTERISTICS OF TEL-90018 AT 200°C
USING 25 mL SAMPLE AND 13/16" 5 MICRON SPARGER

Airflow cc/min	Oil Volume mL	Oil and Foam Vol. mL	Foam Volume mL
150	38	40	2
250	35	44	9
500	25	44	19
750	20	46	26
1000	16	52	36

Foam collapse time approximately 1 second

The foaming characteristics of TEL-90018 are very similar to those of the 5P4E polyphenyl ether fluids.

(3) High Temperature Testing of C&O and Engine Stressed
MIL-L-87100 Fluid

Foam testing was conducted on two corrosion and oxidation stressed O-67-1 fluids for determining the effects of lubricant degradation on foaming. The C&O testing was conducted for 24 hours and 96 hours providing a low stressed (10.7% 40°C viscosity increase) sample and a moderately stressed (22.7% 40°C viscosity increase) sample. Data obtained from this testing are given in Table 77 and show that oxidative degradation of the lubricant does not increase the foaming characteristics or foam collapse times of the MIL-L-87100 high temperature lubricant.

Foam testing of eight engine stressed samples was conducted at 200°C using a 30 gram (25 mL) sample and a 13/16 inch 5 micron pore size metal sparger. The results of this testing are summarized in Table 78.

TABLE 77

FOAMING CHARACTERISTICS OF CORROSION AND
 OXIDATION STRESSED O-67-1 LUBRICANT AT 200°C
 USING A 13/16 INCH 5 MICRON SPARGER AND 25 ML SAMPLE

Airflow cc/min	Oil Vol., mL	Oil Foam Vol., mL	Foam Vol., mL	Foam Collapse Time, Sec.
24 H C&O at 320°C				
150	37	41	4	
250	38	43	5	
500	39	47	8	
750	41	50	9	
1000	41	53	12	2
96 H C&O at 320°C				
150	39	42	3	
250	39	43	4	
500	40	46	6	
750	41	49	8	
1000	42	52	10	1

TABLE 78

FOAMING CHARACTERISTICS OF ENGINE STRESSED MIL-L-87100
 SAMPLES AT 200°C (25 ML SAMPLE AND 13/16" 5 MICRON SPARGER)

Airflow cc/min	Oil Vol., mL	Oil/Foam Vol., mL	Foam Vol., mL	Foam Collapse Time, Sec.
Sample TEL-9028				
150	38	42	4	
250	38	44	6	
500	40	48	8	
750	40	50	10	
1000	40	55	15	3
Sample TEL-9029				
150	40	48	8	
150	42	50	8	
500	44	54	10	
750	48	62	14	
1000	50	66	16	
Sample TEL-9030				
150	38	42	4	
250	38	44	6	
500	38	48	10	
750	40	53	13	
1000	40	60	20	8
Sample TEL-9038				
150	38	42	4	
250	38	44	6	
500	40	48	8	
750	42	52	10	
1000	44	54	10	7
Sample TEL-9039				
150	38	42	4	
250	38	42	4	
500	40	46	6	
750	42	48	6	
1000	44	52	8	3

Sample TEL-9040

150	36	42	6	
250	36	44	8	
500	38	47	9	
750	38	50	12	
1000	40	55	15	7

Sample TEL-9069-4

150	38	46	8	
250	39	49	10	
500	40	52	12	
750	41	59	18	
1000	40	69	29	16

Sample TEL-9069-8

150	38	44	6	
250	39	47	8	
500	40	52	12	
750	42	57	15	
1000	43	64	21	10

The aeration of all samples and air flowrates shown in Table 78 produced large bubbles and good clear oil/foam interfaces as was found with the C&O degraded samples. All the engine stressed samples showed very low foaming and low foam collapse times.

(4) Foaming Characteristics of Non-Polyphenyl Ether High Temperature Fluids

Foam testing was conducted on three non-polyphenyl ether type high temperature experimental fluids TEL-9050, TEL-90001 and TEL-90024. Tests were conducted at 200°C using 25 mL samples and a 13/16 inch diameter 5 micron pore size sparger. Due to a limited quantity of TEL-90001, foam testing of this fluid utilized a subsequent wear test sample. Results of this testing given in Table 79 show that all three experimental fluids have higher foaming characteristics than the MIL-L-87100 lubricants. Sample TEL-90024 was the highest foamer of the three fluids with overfoaming the test cylinder at a 750 cc/min airflow rate. Its basestock, TEL-9050, displayed much lower foaming values which indicate that the Additive(s) present in the TEL-90024 increases the foaming characteristics of the base fluid.

(5) Foaming Characteristics of Three MIL-L-7808 Type Lubricants

Foam testing was conducted on MIL-L-7808 lubricant samples TEL-90070, TEL-90071 and TEL-90072 using Federal Test Method Standard 791, Method 3213 and the small volume test utilizing a 25 mL sample instead of the 200 mL volume sample required by Method 3213. Testing was conducted at 80°C using an ASTM diffuser stone for the 200 mL testing and a 13/16 inch diameter 5 micron pore size sparger for the 25 mL volume testing. The method of aeration was conducted in accordance with Method 3213 for all testing of these three fluids. These data given in Table 80 show that all three fluids

TABLE 79

FOAMING CHARACTERISTICS OF TEL-9050, TEL-90001 AND TEL-90024
 EXPERIMENTAL FLUIDS AT 200°C USING A 25 ML SAMPLE AND A
 13/16 INCH DIAMETER 5 MICRON PORE SIZE SPARGER

Airflow cc/min	Oil Vol., mL	Oil/Foam Vol., mL	Foam Vol., mL	Foam Collapse Time, Sec.
Fluid TEL-9050				
150	15	72	57	
250	16	102	86	
500	5	160	155	
750	5	160	155	
1000	5	182	177	15
Fluid TEL-90001				
150	15	62	47	
250	12	99	87	
500	10	150	140	
750	10	128	118	
1000	11	110	99	15
Fluid TEL-90024				
150	17	80	63	
250	10	125	115	
500	< 5	210	> 205	20
750	Overfoam			

TABLE 80

STATIC FOAM TEST DATA FOR THREE MIL-L-7808 LUBRICANTS
USING FEDERAL TEST METHOD STANDARD 791, METHOD 3213
AND THE SMALL VOLUME (25 ML) FOAM TEST

1000 cc/min Airflow			
Lubricant	TEL-90070	TEL-90071	TEL-90072
Oil Volume, mL	216 (10) ¹	211 (10)	215 (10) ²
Oil & Foam Volume, mL	260 (112)	260 (118)	270 (115)
Foam Volume, mL	44 (102)	49 (108)	55 (105)
Foam Collapse Time, Sec.	5 (7)	5 (8)	6 (5)
500 cc/min Airflow			
Oil Volume, mL	215 (11)	211 (15)	215 (17) ²
Oil & Foam Volume, mL	240 (74)	245 (70)	250 (65)
Foam Volume, mL	25 (63)	34 (55)	35 (48)
Foam Collapse Time, Sec.	5 (9)	5 (8)	6 (3)

¹Data for small volume test

²Oil volume hard to read due to severe aeration

have approximately the same foaming value (about 49 mL) which is well below the 100 mL maximum specification MIL-L-7808J limit. The small volume test data also showed the three lubricants to have similar foaming characteristics. The 25 mL sample foaming values were higher than normally would be expected except for those lubricants having small bubble severe aeration.²

e. Summary

Foam testing of MIL-L-87000 lubricants and other experimental fluids has been investigated at temperatures up to 200°C using Federal Test Method Standard 791, Method 3213 and a small volume test method requiring a 25 mL sample. High temperature test capability was obtained using a high temperature viscosity bath modified to accept either a 500 mL or a 250 mL graduated test cylinder and preheating air coils.

This study has shown that MIL-L-87100 fluids have large foam values and foam collapse times up to 100°C. Between 100°C and 200°C the foaming characteristics and foam collapse times of these fluids decrease to very low values. No significant differences were observed between new, C&O stressed or engine stressed MIL-L-87100 lubricant foaming characteristics. Polyphenyl ether (6P5E) gave the same foaming value as the 5P4E fluids.

Foam testing of experimental non-polyphenyl ether type fluids gave much higher foam values than MIL-L-87100 fluids at 200°C with the inhibited fluids having larger foam values than the base fluid alone.

5. VISCOMETER EVALUATION

a. Introduction

Viscosity determinations of lubricants including high temperature fluids such as polyphenyl ethers are conducted in accordance with ASTM test method D-445. This method covers the use of various type viscometers but

most lubricant viscosity measurements are made using the Cannon-Fenske routine viscometer which requires approximately 7 to 10 mL of sample. For samples having limited volume, the semi-micro Cannon-Fenske type viscometer is used which requires approximately 1 to 2 mL of sample. A new extra low charge (ELC) viscometer (0.5 mL) similar to the semi-micro viscometer has been developed by Cannon Instrument Company. Viscosity measurements were made on new O-77-6 (5P4E basestock fluid) to determine the ELC capability of being used for measuring viscosities of polyphenyl ether fluids where very limited sample exists.

b. Results and Discussion

Viscosity measurements were made using the polyphenyl ether basestock fluid O-77-6 at 40°C and 100°C using the Cannon-Fenske Routine, Cannon-Fenske Semi-Micro and the new Cannon-Fenske Extra Low Charge (ELC) type viscometers. These data, given in Table 81, show that good reproducibility is obtained for each specific type viscometer. The correlation between the Semi-Micro and the Routine type viscometers is considered good since the differences are within reproducibility limits given by ASTM D-445. However, the Extra Low Charge (ELC) viscometer gave higher results. Viscosity measurement of a mineral oil standard (N350) showed the ELC viscometer to have a value 319.9 cSt at 40°C (23.83 cSt at 100°C) compared to the standard value of 310.9 cSt at 40°C (23.45 cSt at 100°C).

Since this difference could not be explained, a new size 400 ELC tube was provided by the manufacturer. A viscosity measurement of O-77-6 fluid was obtained using the new ELC tube at 40°C. A value of 280.3 cSt was obtained which compares very well with the Cannon-Fenske Routine Viscometer value of 280.4 cSt. This indicates that a calibration problem may have existed with the initial ELC viscometer.

TABLE 81

VISCOSITY OF O-77-6 USING ROUTINE
SEMI-MICRO, AND EXTRA LOW
CHARGE VISCOMETERS

Semi-Micro

Date	Operator	Viscosity 40°C, cSt	Viscosity 100°C, cSt
Jun 87	# 2	285.4 (Suspect)	12.52
Feb 88	# 1	276.2	12.45
Aug 89	# 3	277.2	12.54
Aug 89	# 4	276.7	12.56
AVE.		276.7	12.52
S.D.		0.5	0.05
%S.D.		0.2	0.4

Routine

Aug 89	# 3	280.6	12.52
Aug 89	# 4	280.1	12.51
AVE.		280.4	12.52
S.D.		0.4	0.01
%S.D.		0.1	0.1

Extra Low Charge

Aug 89	# 1	287.8	12.59
Aug 89	# 5	289.5	12.66
Sep 89	# 1	289.1	12.51
Sep 89	# 5	287.8	12.74
AVE.		288.6	12.63
S.D.		0.9	0.10
%S.D.		0.3	0.8

ELC tubes require skilled and experienced operators due to the difficulty in accurately determining the efflux time. This fact makes their use impractical for routine analyses. However, for samples of limited quantity, the tubes can be used provided the operator is aware of the extra care that must be taken to ensure precise measurements. These precautions include correct charging of the tube, careful attention to assure the absence of bubbles and most importantly, absolute cleanliness of the ELC tube. Normally the viscometers are cleaned using toluene, MIBK and isopropanol, with periodic chromic acid washes. With the ELC, the chromic acid wash is required after the normal cleaning following each run in order to achieve repeatable results.

c. Summary

The Extra Low Charge (ELC) viscometer can be satisfactorily used for measuring the viscosity of high temperature fluids such as MIL-L-87100 lubricants provided proper care is taken to ensure precise measurements. The importance of these precautions which apply to all glass viscometers should not be underestimated especially for experimental high temperature fluids having relatively large viscosities and limited solubilities. All viscometers should be periodically checked using appropriate ASTM viscosity standards to ensure proper viscometer calibration as well as proper test procedures. Participation in the annual ASTM viscosity correlation programs is recommended for ensuring accurate viscosity measurements.

SECTION III

DEVELOPMENT OF IMPROVED LUBRICATION SYSTEM HEALTH MONITORING TECHNIQUES

1. FERROSCAN AS AN IN-LINE MAGNETIC WEAR DEBRIS MONITOR FOR LUBRICATION SYSTEMS

a. Introduction

Diagnostic methods for determining the health of gas turbine engines include the use of oil contamination monitors as important indicators of the condition of lubricant-wetted components. The primary engine health monitoring technique used extensively by the United States Air Force is the Spectrometric Oil Analysis Program (SOAP). Health monitoring devices used by SOAP are specifically designed to monitor the change in specific wear metal concentration with time. Off-line methods, atomic emission (AE) and atomic absorption (AA) spectrometric analysis, involve measuring and trending of contamination levels while in-line magnetic plugs and chip detectors are used to detect a rapidly progressing component failure before it becomes catastrophic.

Emission and absorption spectrometers have been shown to be effective in detecting wear particles smaller than 3 to 10 microns.⁴ Chip detectors generally monitor particles larger than 100 microns. Wear particles with sizes above the SOAP spectrometer and below the chip detector detection limits can be determined using Ferrographic techniques.⁵

Analysis of wear metals has played a significant role in condition monitoring of lubrication systems by improving equipment reliability and reducing maintenance cost. However, current analytical techniques sometimes fail to provide timely data and accurate assessment of wear. Such limitations have encouraged consumers to provide support to develop supplementary diagnostic tools that can provide real time data and improve

cost effectiveness. One of the supplementary techniques recently developed is an in-line magnetic wear debris monitor called Ferroscan.⁶⁻⁸ These papers deal with evaluating the capability of the Ferroscan as a diagnostic tool for condition monitoring of lubrication systems. The Ferroscan sensor was installed on a lubricating oil test rig which simulated the oil circulation system in an engine. The sensor sensitivity was determined for various concentrations and sizes of magnetic particles. Sensor response was also determined as a function of bulk oil temperature and flow rate. Comparative results are presented that show the sensor capability in detecting the amounts of various types of magnetic wear debris in the main stream of lubricating oil.

Ferroscan is a sensing device that monitors in real time the concentration of magnetic wear particles generated in a lubrication system. This device was developed for the purpose of monitoring the health of the lubricated engine components in order to provide an early warning of impending failure before catastrophic failure occurs.

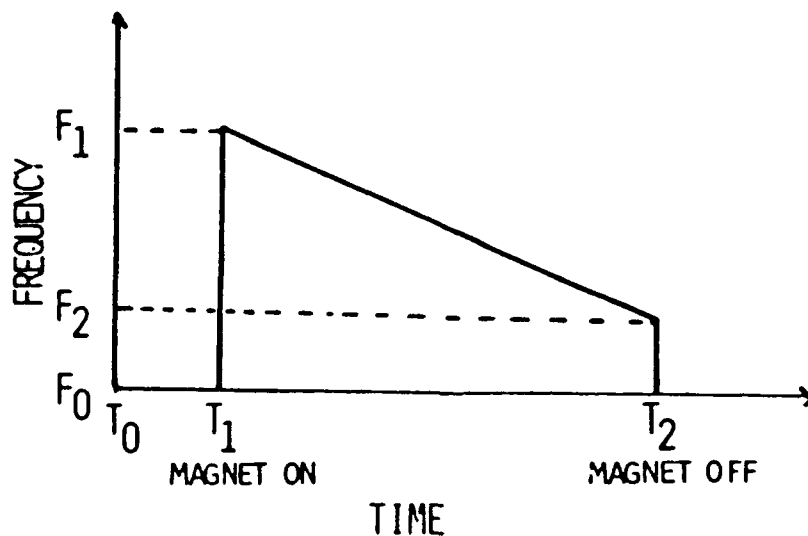


Figure 50. Sensor Frequency Versus Time

b. Theory

A power supply is connected to the controller which energizes the magnetic core to trap particles. When the magnetic core is energized, the frequency of the RF circuit increases from F_0 to F_1 (Figure 50). However, as the magnetic field traps particles, the frequency decreases linearly with time to F_2 . It was determined that the change of frequency rate is directly proportional to the concentration of the trapped wear debris. Changing the magnitude of the energizing current results in trapping different size particles. Therefore, the output frequencies for the different energizing currents are used to determine the relative particle size of the trapped material. The concentration of the trapped wear debris is the slope of the sensor frequency versus time (Figure 50). During the test, the microcontroller is capable of displaying the real time data of the trapped magnetic particle concentrations as FE1 and FE2. FE1 represents the concentration of the large particles while FE2 represents particles up to 1000 microns. FE1 and FE2 values are used to calculate the wear severity index (WSI) as follows:

$$WSI = \{1 - (FE2 - FE1) / (FE2 + FE1)\} \times 100$$

WSI is a dimensionless parameter that varies from 0 to 100 and is dependent on FE1 and FE2 values. If the concentration of the magnetic wear debris and particle size increases, the WSI would increase. Calibration conducted by Sensys using Fe particles having a size range of 6 to 9 microns yielded WSI values of 70 to 75. FE1 and FE2 are reported in terms of Hz per second, and in order to determine the concentration of the trapped magnetic wear debris in ppm, the sensor must be calibrated using various amounts and sizes of magnetic material. Sensys has provided calibration data for their sensor using various concentrations of 6 and 9 micron Fe particles. Under these

conditions the average responses for FE1 and FE2 for a 9.6 ppm particle concentration were 1146 and 1660 Hz per second, respectively. Increasing the Fe concentration to 21.5 ppm produced FE1 and FE2 values of 2571 and 3717 Hz per second, respectively. It can be seen from these results that for both concentrations the response in Hz per second divided by ppm yields the same values of 119.4 and 172.9 Hz per second per ppm for FE1 and FE2, respectively. Since the sensor produces a linear output proportional to concentration, Sensys recommends that a single point calibration would be sufficient with a different application.

c. Experimental

(1) Apparatus

The Ferroskan was installed on the microfiltration test rig (Figure 51) to evaluate its capability in monitoring the concentration of magnetic wear debris. The sensor consists of a 3/4 inch pipe surrounded by an annular electromagnetic assembly containing a magnetizing coil and an inner detector coil. A radio frequency (RF) oscillator circuit is connected between the electromagnetic assembly and the microcontroller. The microcontroller energizes the magnetic core and collects and stores the data. A Zenith 240 PC runs the menu driven software and interprets the results. The results are either printed as real time Hz/s values from two channels or plotted as Hz/s versus elapsed time.

(2) Procedure

A Ferroskan reading was taken for 10 to 15 minutes at 75°C oil temperature with oil flowing through a 0.75 inch i.d. line at 6.3 gpm (Velocity = 1.3 m/s). This reading was necessary to establish a baseline for subsequent Ferroskan readings. The oil tank was charged with approximately 5 gallons of MIL-L-7808 that was doped with Fe powder previously dry sieved.

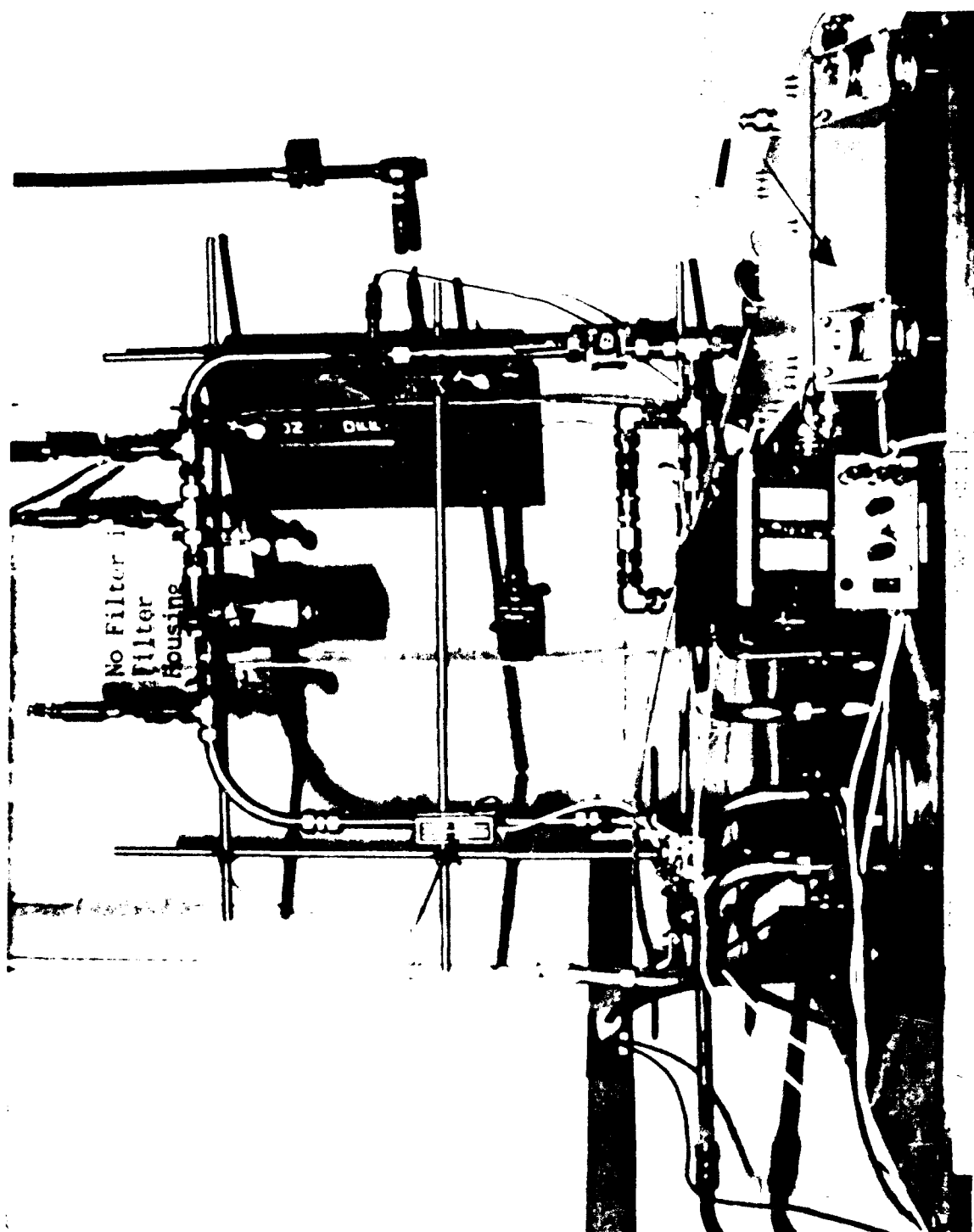


Figure 51. Microfiltration Test Rig Equipped with Ferrosan Sensor

The Fe particle sizes used are listed in Table 82.

TABLE 82

VARIOUS SIZES OF FE POWDER PRODUCED BY SIEVING A COMMERCIAL
FE POWDER HAVING AN AVERAGE PARTICLE SIZE OF 1-5 MICRONS

Fe Particle Size Range	Description
-5 micron	Passed through a 5 micron sieve
5-10 micron	Passed through 10 micron sieve but retained on 5 micron sieve
10-20 micron	Passed through 20 micron sieve but retained on a 10 micron sieve
20-30 micron	Passed through 30 micron sieve but retained on 20 micron sieve
30-45 micron	Passed through 45 micron sieve but retained on a 30 micron sieve
+ 45 micron	Retained on 45 micron sieve

The above Fe powder sizes will be referred to as -5, 5-10, 10-20, 20-30, 30-45 and +45 micron, respectively. In the first experiment, approximately 0.25 g of -5 micron Fe powder was added to the oil system. The Ferroskan was allowed to collect data for approximately 15 minutes at 6.3 gpm oil flow. The tank was sampled (50-100 mL) before and after the addition of Fe powder in order to determine the concentration of Fe in the oil system.

Another 0.25 g of -5 micron Fe powder was added and data collected for 10 to 15 minutes. The above procedure was repeated until 1 g of -5 micron Fe powder was added to the oil tank in order to study the effect of concentration of the -5 micron Fe powder on the Ferroskan response. At the end of the experiment, a 3-micron filter element was installed in the filter housing and the oil was allowed to pass through the filter to remove the Fe particles larger than 3 microns before the next larger size Fe powder could be added. The above procedure was repeated for every size of Fe powder

shown above (Table 82). The Ferroskan readings were documented and data stored for future manipulation. In a separate experiment, a 0.25 g of each size listed in Table 82 was added to the oil test rig sequentially in order to study the effect of particle size on the Ferroskan response. The Ferroskan large and small particle counts (FE1 and FE2) were manipulated to produce bar graphs showing not only the effect of particle size sequentially added to the rig but also the effect of particle size at different concentration levels.

d. Results and Discussion

(1) Effect of Particle Size on Ferroskan Response

Figure 52 shows the Ferroskan response Hz/s as a function of Fe concentration and particle size. The concentration of Fe was determined by the acid dissolution method (ADM). The highest Fe concentration determined ranged between 55 and 75 ppm. In all cases, the relationship between kHz/s and ppm was not linear. However, linearity was observed for concentrations between 0 and 25 ppm for FE2 and FE1. Another interesting trend was observed in the sensor response per ppm. For example, at 50 ppm, the sensor response increased with an increase in the particle size. Figure 53 shows graphically the definite increase in the Ferroskan readout as a function of particle size. However, this increase is not linear and seems to be hyperbolic in nature yielding greater slopes at increased concentrations and particle sizes.

(2) Effect of Particle Concentration on Ferroskan Sensitivity

Bar graphs (Figures 54 and 55) were developed to determine the sensitivity of the Ferroskan for all particle sizes and concentrations studied. Figure 54 was produced from Ferroskan responses of the data shown in Figure 52. However, Figure 55 was produced from a separate experiment

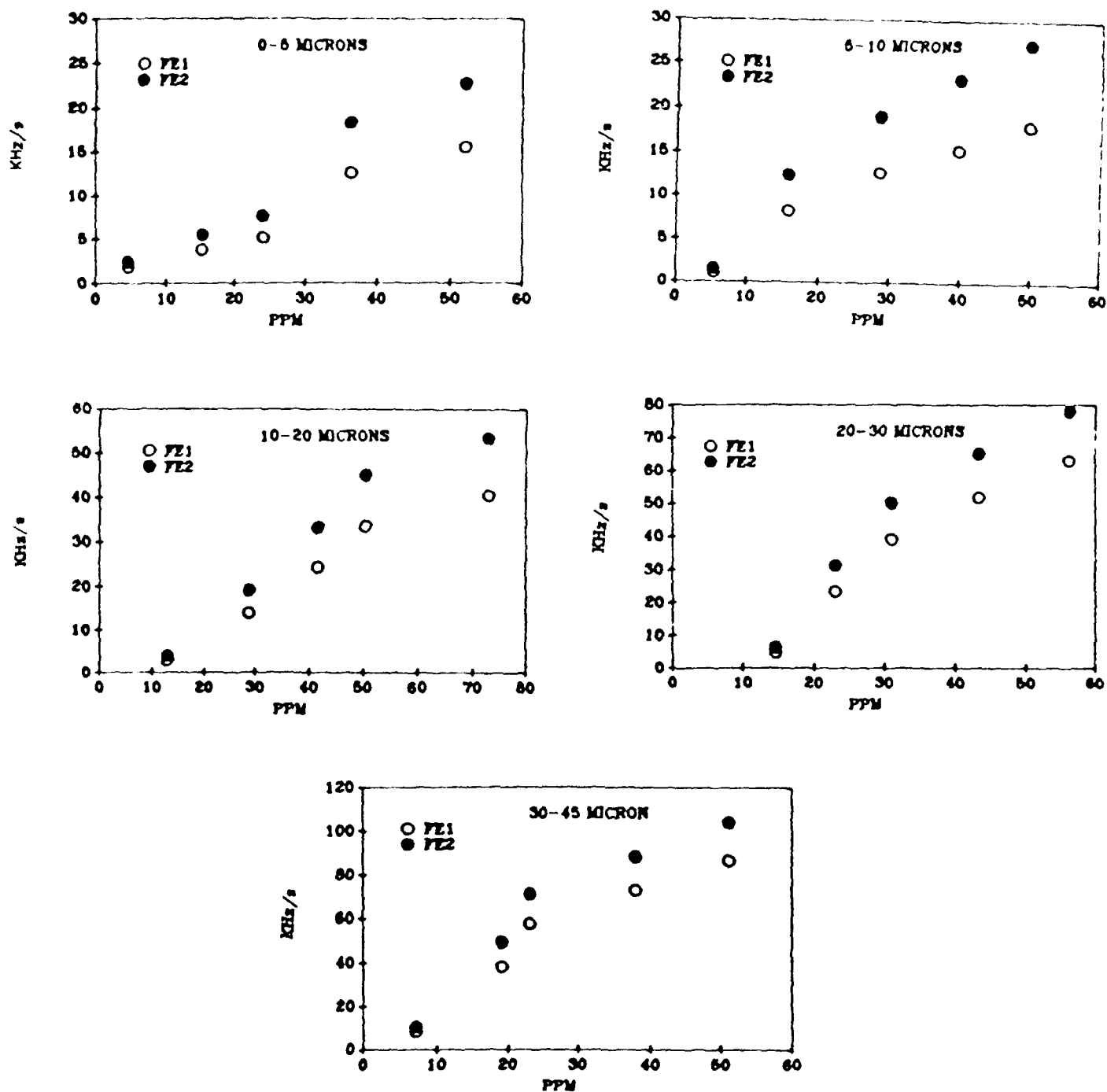


Figure 52. Ferroskan Sensor Readout of FE1 and FE2 Versus Concentration of Various Sizes of Fe Particles in MIL-L-7808. Conditions: 1.3 m/s Oil Velocity: 77°C Oil Temperature

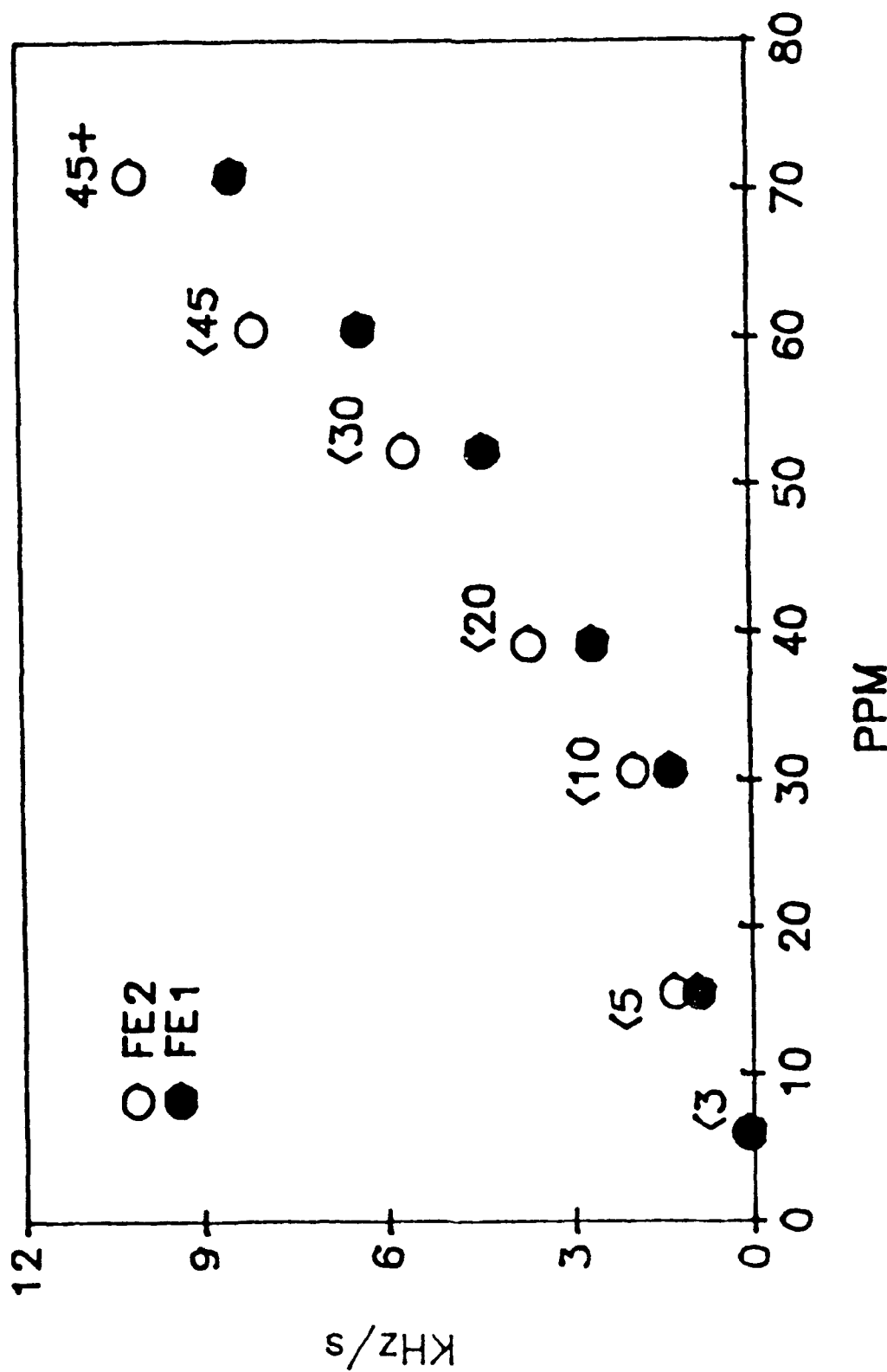


Figure 53. Ferroskan Readout of FE1 and FE2 Versus Concentration of Various Sizes of Fe Particles Added Sequentially. Conditions: 1.3 m/s Oil Velocity; 77°C Oil Temperature

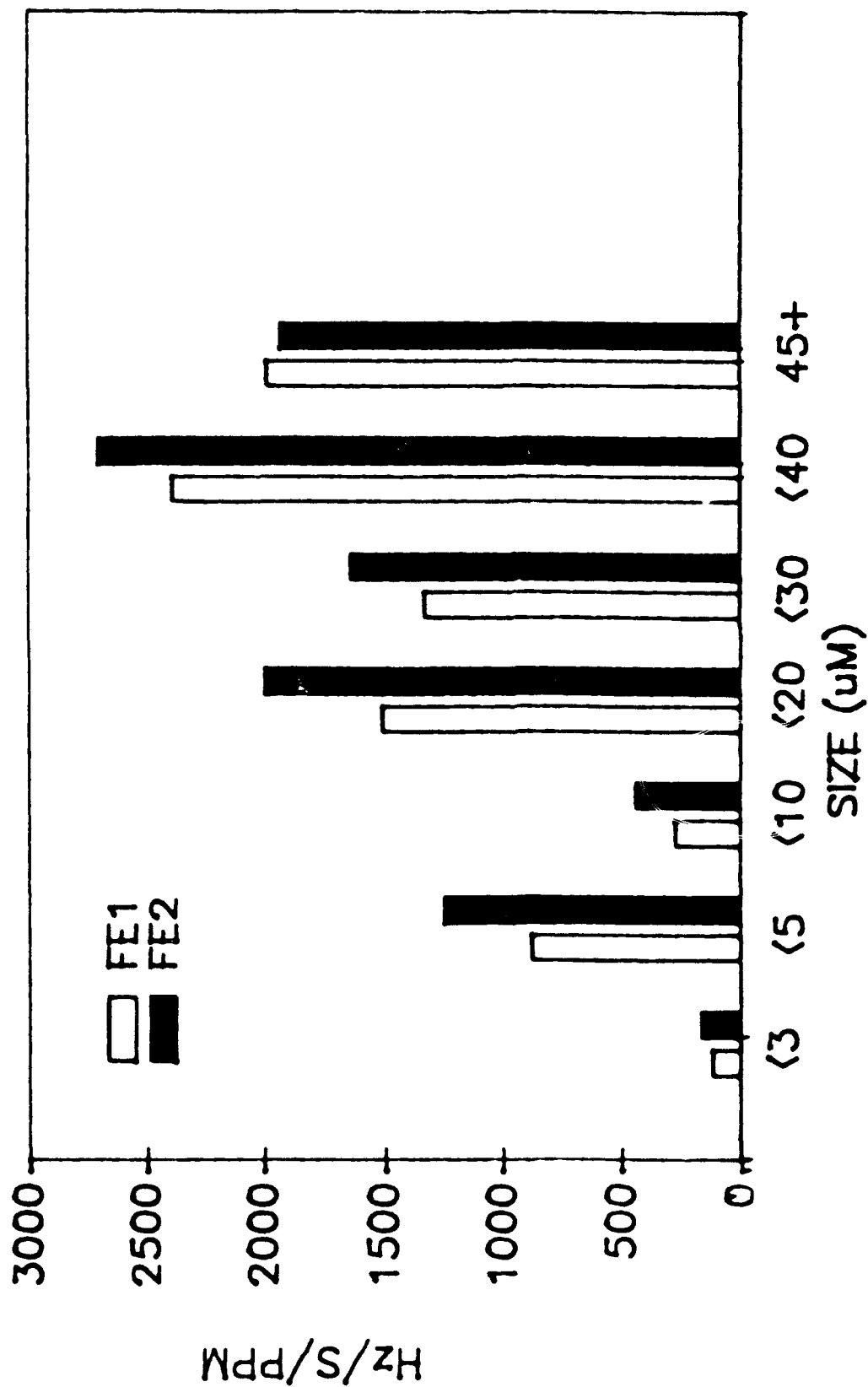


Figure 54. Sensitivities of Ferroskan Sensor in Hz/s/ppm Versus Fe Particle Size from Various Experiments

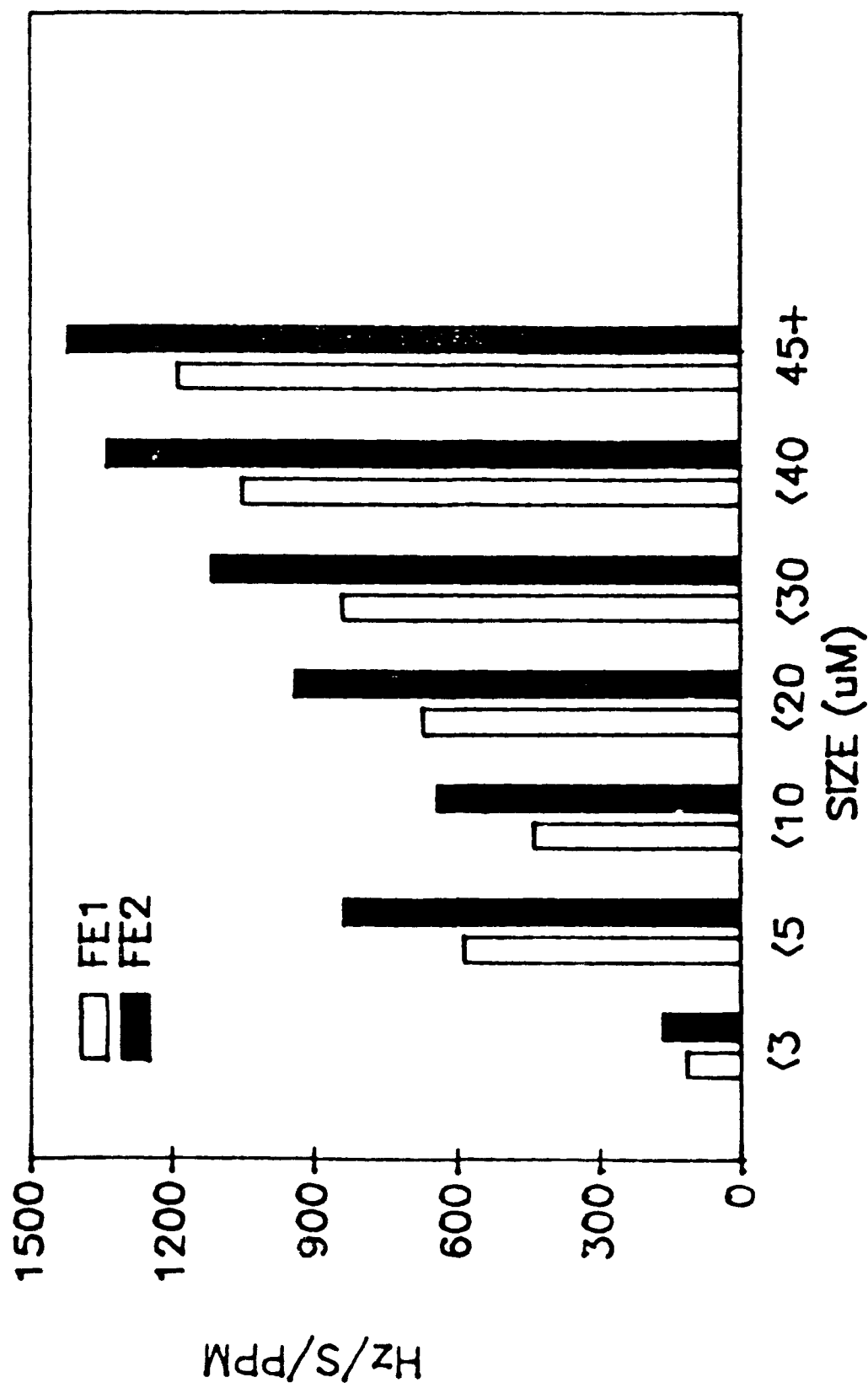


Figure 55. Sensitivities of Ferrosan Sensor in Hz/s/ppm Versus Fe Particle Size from Sequential Addition

where amounts of 0.25 g Fe of each particle size shown in Table 82 was added sequentially. Figure 56 illustrates the real time data of FE1 and FE2 for this experiment. The real purpose of Figures 54 and 55 is to show if the Ferroskan responses per ppm differ as a function of elapsed time. The data in Figure 54 were taken from several experiments performed at different times with the oil systems turned off and boled in between experiments. While in Figure 55, the oil system was not interrupted during the addition of the amounts of the various Fe particle sizes. Figure 54 shows erratic behavior of the Ferroskan response over long periods of testing. However, there is a definite overall increase in the response per ppm with an increase in particle size. Figure 55 shows a very good trend in the response of the sensor per ppm versus particle size except for the -5 micron particles. Similar behavior of the sensor was also observed for the -5 micron Fe in Figure 54. No explanation could be offered at this time for the -5 micron anomalous result of the sensor.

(3) Effect of Temperature on Ferroskan Response

In order to study the effect of temperature on the sensor response, the oil temperature was varied from 25°C to 77°C while the oil velocity was held at 1.3 m/s. Fe concentration in the oil system was approximately 10 ppm. Figure 57 shows that the sensor response increased 10 fold over a range of 50°C. The response then levelled off at approximately 2.8 kHz/s after the temperature of the oil was held at 77°C.

(4) Effect of Oil Velocity on the Ferroskan Response

The velocity of the oil was varied from low to high and from high to low so that the effect of oil flow on the magnetic sensor response could be determined. Figure 58 shows the real time plot for FE1 and FE2 (small and large particles) in kHz/s versus time during various oil flows.

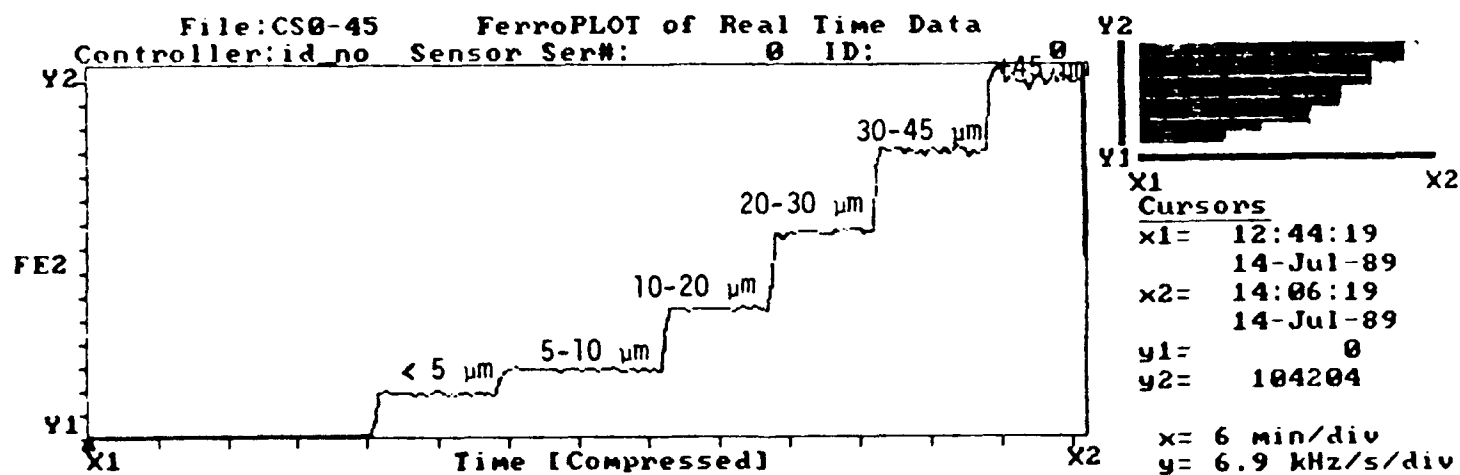
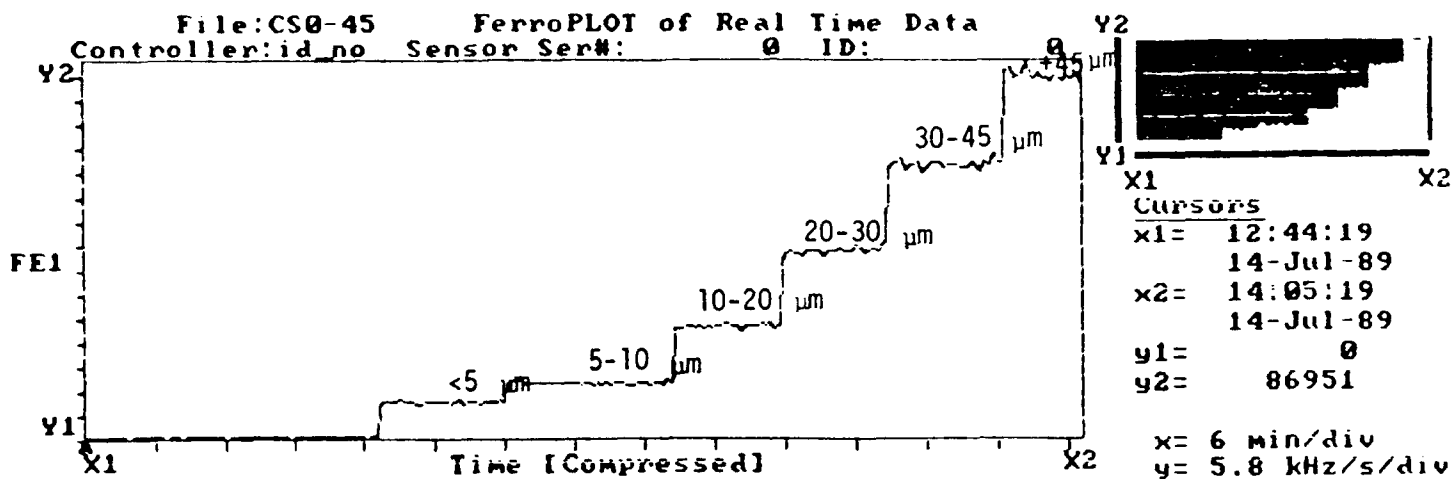


Figure 56. Real Time Data of FE1 and FE2 Versus Elapsed Time for Various Fe Particles Added Sequentially

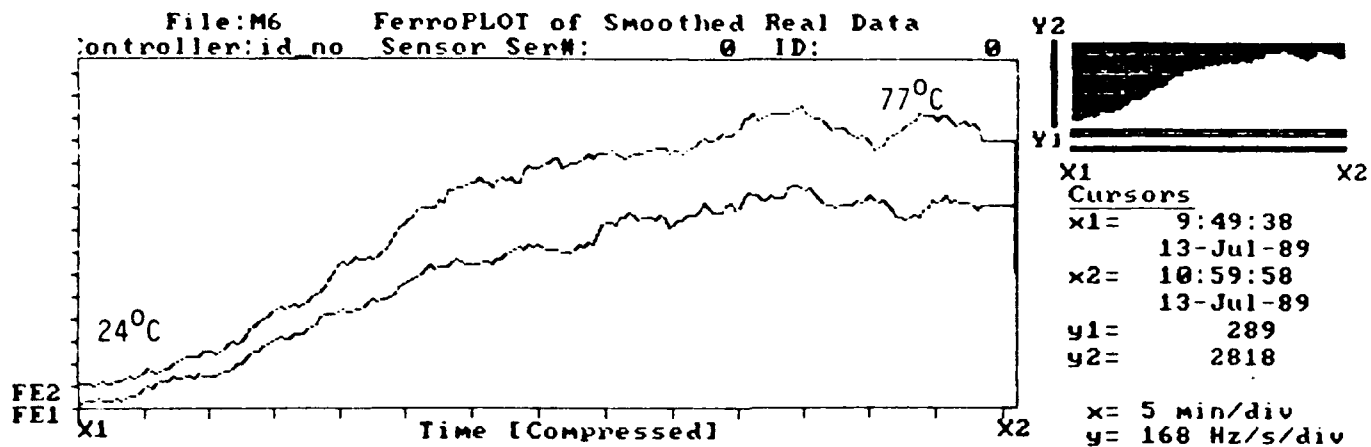


Figure 57. Effect of Temperature Rise on Ferroskan Output . Conditions:
 1.3 m/s Oil Velocity; 10 ppm Concentration of <3 Micron Fe
 Particles

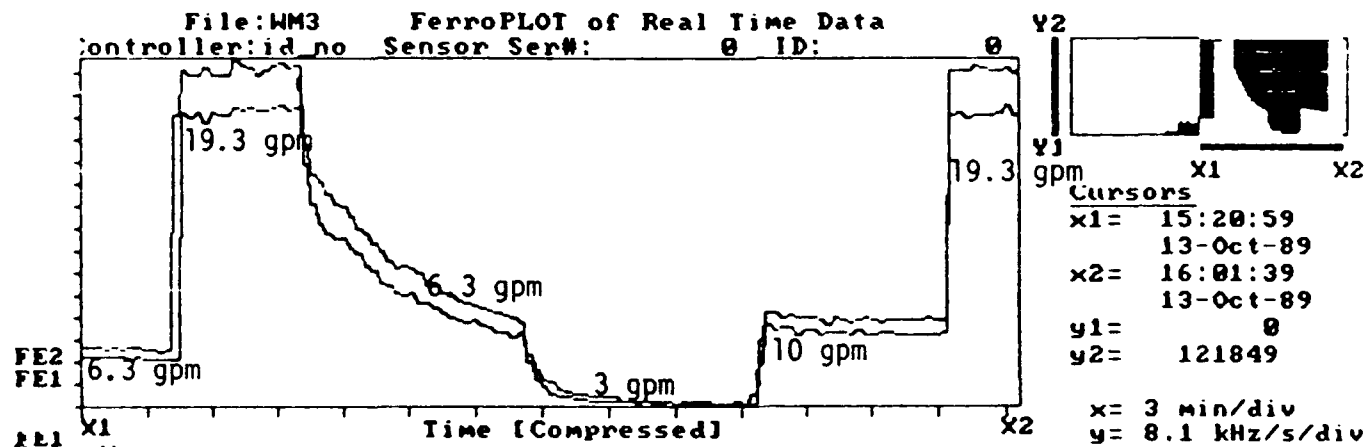


Figure 58. Effect of Oil Flow Rate on Ferroskan Output. Conditions:
 77°C Oil Temperature, 51.5 ppm Concentration of 0 to >45
 Micron Fe Particles

At the beginning of the test the oil temperature was stabilized at 77°C with the oil flowing through the sensor at 6.3 gpm (1.3 m/s). The concentration of Fe particles was also held constant at 51.5 ppm. The oil flow was suddenly changed to 19.3 gpm (3.7 m/s) by closing the bypass valve. The sensor response of FE2 changed almost immediately from 21.5 ± 0.6 kHz/s to 119.1 ± 1.9 kHz/s within 20 seconds. Both FE2 and FE1 changed but for brevity only FE2 will be considered. The flow was held at 19.3 gpm for approximately 5 minutes before the bypass valve was opened to change the flow rate back to 6.3 gpm. It is important to note that the sensor response due to the change of oil velocity from high to low was not sharp but showed a slow decaying response. It took approximately 10 minutes for the sensor to read 29.9 kHz/s which is not as low as it was (21.5 kHz/s) before the change in oil velocity. Decreasing the oil flow further to 3 gpm (velocity = 0.6 m/s) also yielded a slow response of the sensor. It took the sensor approximately 5 minutes before stabilizing the FE2 readout to 1.9 ± 0.3 kHz/s. The experiment was continued by changing the flow rate from 3 gpm to 10 gpm (velocity = 1.8 m/s). As a result, the sensor responded sharply from 1.9 kHz/s at 3 gpm to 30.9 ± 0.7 kHz/s within one minute. The flow was held at 10 gpm for 10 minutes before it was increased to 19.3 gpm. Again, the sensor responded almost immediately by changing the value of FE2 from 30.9 ± 0.7 kHz/s to 119.7 ± 0.7 kHz/s. This experiment reveals that the sensor response was immediate for velocity changes from low to high m/s but slow for changes from high to low m/s. It is also important to note that the sensor response does not change if conditions (flow, temperature ...etc) were held constant. At the beginning of the test, the FE2 readout at 19.3 gpm was 119.1 ± 1.9 kHz/s. This reading was achieved again by the sensor 119.2 ± 0.7 kHz/s after velocity changes were made from high to low to high.

(5) Effect of Concentration, Flow Rate and Noise
on a New Ferroskan Detector

The effect of concentration (0-10 micron Fe particles), flow rate and noise on Ferroskan readings were determined during a 50-minute experiment. These measurements were necessary to determine if the new chip installed in the microcontroller and the new sensing device improve the performance of the Ferroskan. Preliminary data show that the flow of 7 gpm was ineffective and no changes in the Ferroskan reading were observed for concentrations of 10 to 100 ppm. However, increasing the flow rate to 19 gpm increased the sensitivity of the Ferroskan. As a result this experiment was performed at 19.6 gpm. Bulk oil and line oil temperatures were 86°C.

The Ferroskan readings were monitored during the addition of several grams of 0-10 microns Fe powder. Figure 59 shows the real time data for the sequential addition of the Fe powder. The oil in the tank was sampled after each addition and the concentration of Fe was determined using the acid dissolution method and atomic absorption spectroscopy. Fe organometallic standard was used to calibrate the spectrometer. Table 83 shows the concentration of Fe after each addition along with the Ferroskan readings in Hz/s for FE1 and FE2.

TABLE 83

FERROSCAN READINGS FOR 0-10 MICRON FE POWDER

Sample Number	Fe, ppm	FE1, Hz/s	FE2, Hz/s
1	13.3	589	922
2	43.0	3742	5432
3	72.0	6293	9356
4	94.6	8063	11,983
5	129.3	10,578	15,546
6	158.3	12,705	18,039

After each addition, Ferroskan readings were taken for approximately 5 minutes and the maxima in kHz/s were plotted as a function of

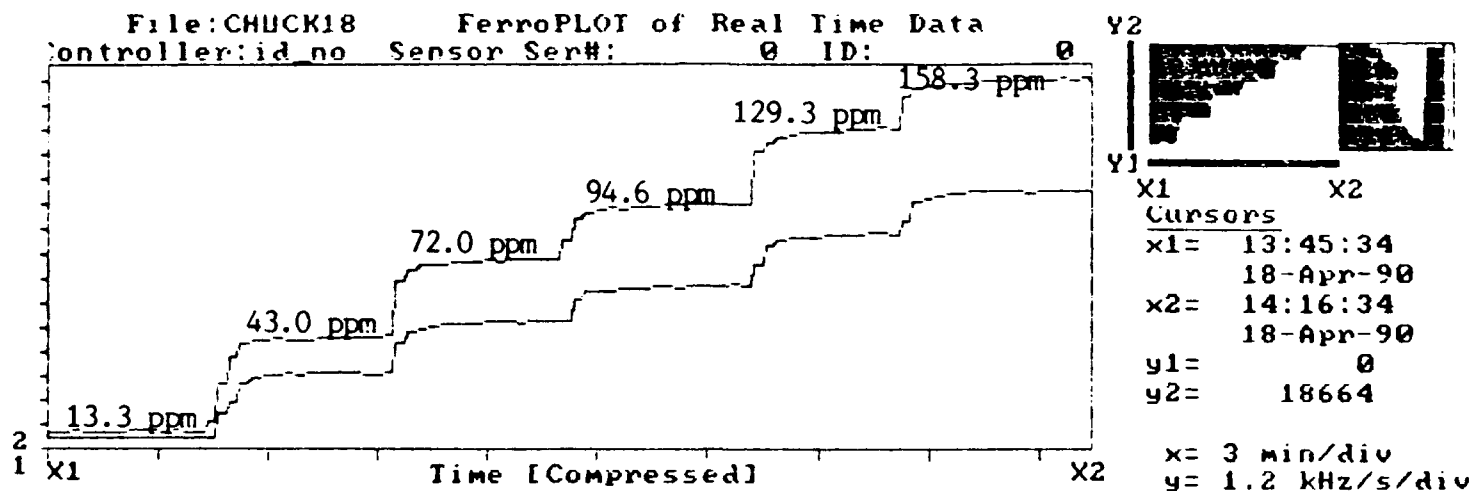


Figure 59. Ferrosan Real Time Data During the 0-10 Micron Fe Powder Addition

concentration (Figure 60). The data in Figure 60 show that both FE1 and FE2 readings are fairly linear with concentration in the range of 13 to 158 ppm. However, when plotting Hz/s/ppm versus the addition number (Figure 61), the Ferroskan response per ppm decays 9 to 12% of the maximum value. It seems that the Ferroskan reading per ppm might not be constant if readings were taken over a long period of time.

Vibrational noise from a vortex mixer was transmitted to the Ferroskan sensor after the final addition of the Fe powder (Fe concentration was 158.3 ppm). There were no appreciable differences in the sensor output even when gentle knocking was applied.

The effect of flow rate on the sensor readout was determined for flow rates of 7 to 19 gpm. When the flow rate was decreased from 19 to 7 gpm, FE1 and FE2 showed a decaying decrease (Figure 62). However, increasing the flow from 7 to 19 gpm shows a sharp increase in the data. These trends were similar to those obtained from the old sensor box.

(6) Repeatability

Two similar experiments were conducted seven weeks apart under identical experimental conditions to study the repeatability of the Ferroskan response with operational time. The effects of Fe concentration and flow rate on the Ferroskan response were determined. Ferroskan readings were continuously monitored during the addition of several grams of Fe powder. The data represent the results of the second experiment. The first experiment results were reported earlier (Figure 59). Figure 63 shows the Ferroskan real time data for the sequential addition of the 0-10 micron Fe powder. The oil in the tank was sampled after each addition to monitor the changes in Fe concentrations. Table 84 shows the concentrations of Fe, as determined by the acid dissolution method and atomic absorption spectroscopy,

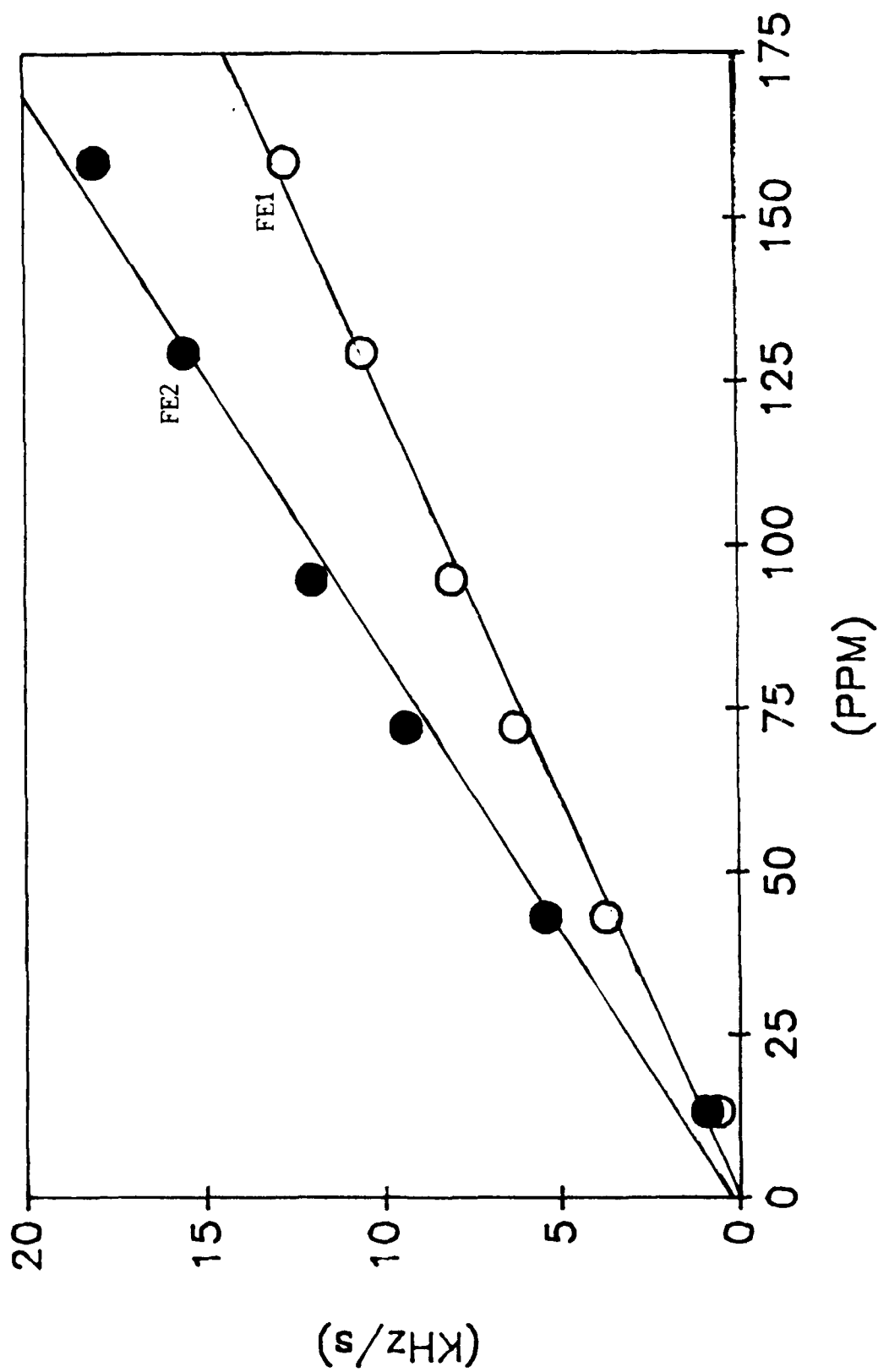


Figure 60. Effect of Concentration on Sensor Readout During the Sequential Addition of 0-10 Micron Fe Powder

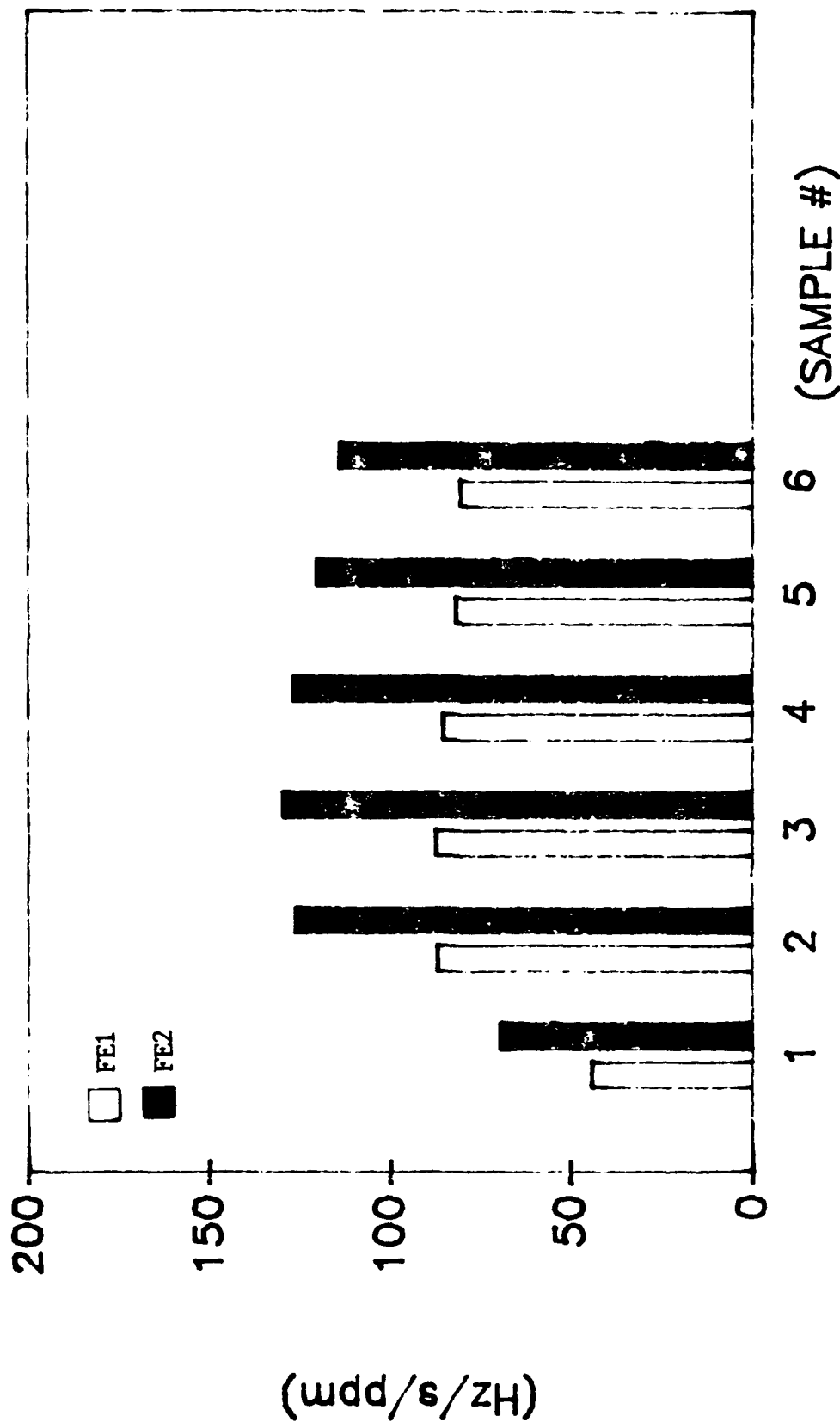


Figure 61. Ferroskan Readout per ppm as a Function of Concentration After Each Addition of 0-10 Micron Fe Powder

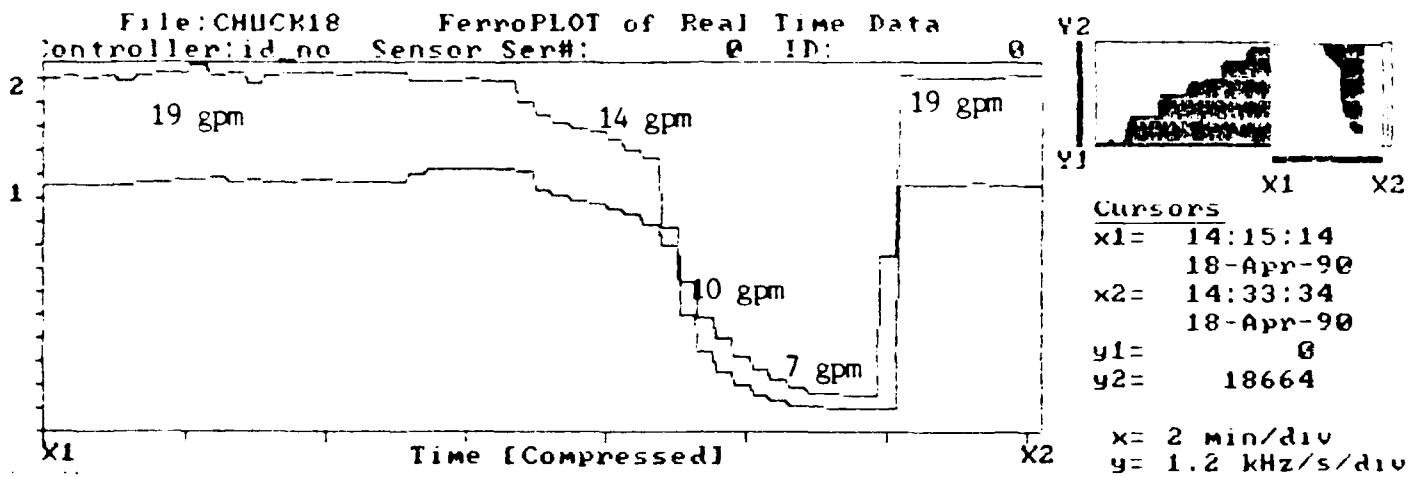


Figure 62. Effect of Flow Rate on Ferroskan Readings Using 0-10 Micron Fe Powder at 158.3 ppm

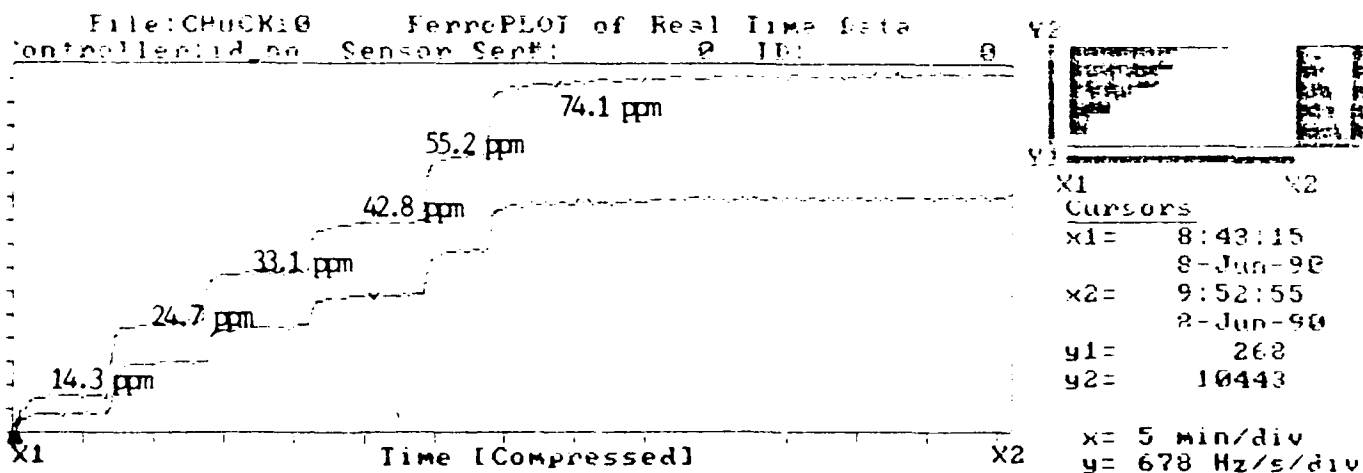


Figure 63. Ferrosan Real Time Data During the 0-10 Micron Fe Powder Addition

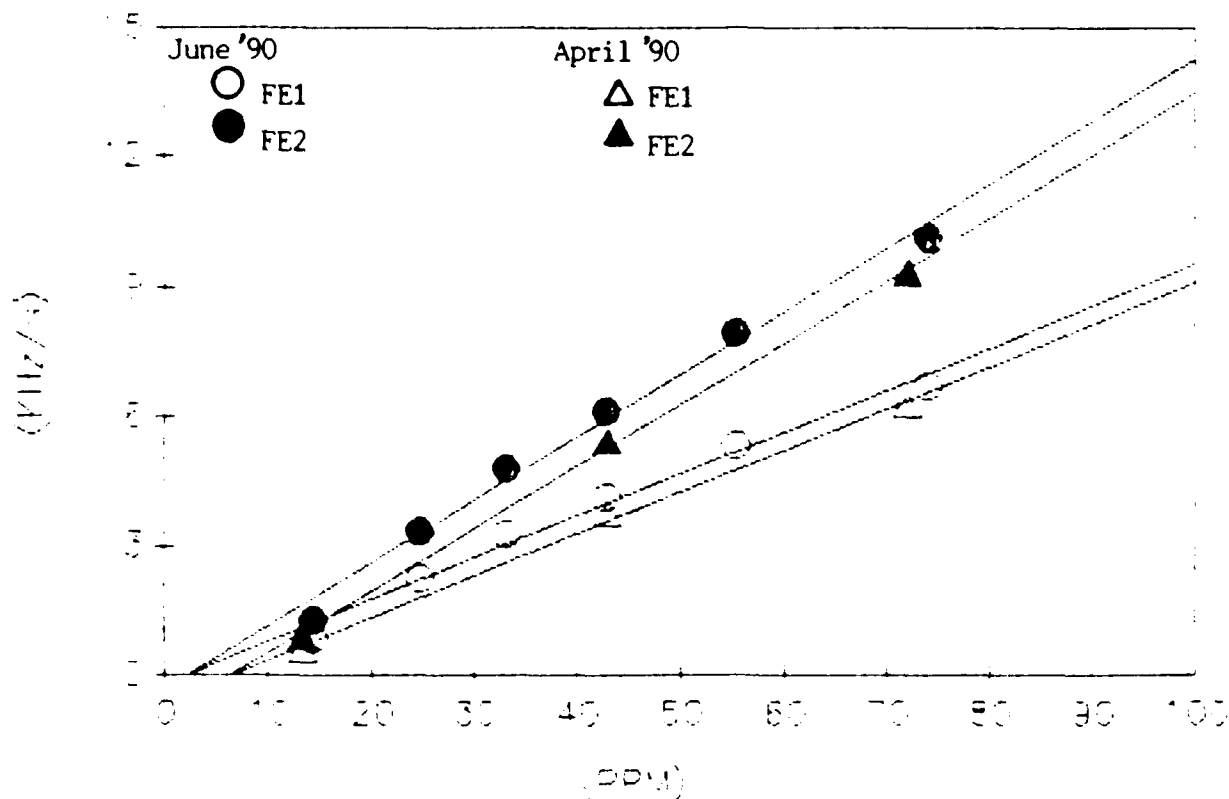


Figure 64. Comparative Curves Illustrating the Repeatability of Two Identical Experiments Showing the Ferrosan Response as a Function of Concentration for Fe Particles of Less than 10 Micron

along with the Ferroskan readings in Hz/s for FE1 and FE2.

TABLE 84

FERROSCAN READINGS FOR 0-10 MICRON FE POWDER
USING THE NEW DETECTOR

Sample Number	Fe, ppm	FE1, Hz/s	FE2, Hz/s
1	14.30	840	1314
2	24.67	2249	3363
3	33.06	3275	4778
4	42.78	4114	6137
5	55.24	5328	7936
6	74.05	6745	10138

After each addition, the Ferroskan readings were taken for a period of 5-10 minutes and the maxima in kHz/s were plotted as a function of concentration (Figure 64). Even though the data in Figure 64 are fairly linear, there is some decaying effect in the Ferroskan response with an increase in concentration. This effect was also observed in the first experiment (Figure 59). It is also shown when plotting the response in Hz/s/ppm against the addition number (Figure 65), the Ferroskan response decays by approximately 10% of the maximum value in the Fe concentration range of 14 to 74 ppm.

Slopes, intercepts and Ferroskan response per ppm (Hz/s/ppm) were calculated from two sets of data (Table 85) to determine the repeatability of the Ferroskan response of the two experiments performed seven weeks apart. The comparative results are shown in Figure 64 and Table 86. The slopes of the two sets of curves (FE1 and FE2) are almost identical for iron concentrations up to 75 ppm. However, the intercepts and Hz/s/ppm do differ. The intercepts of the second experiment were higher by approximately 600 and 400 Hz/s for FE1 and FE, respectively. The Hz/s/ppm were also higher by 12 to 14%.

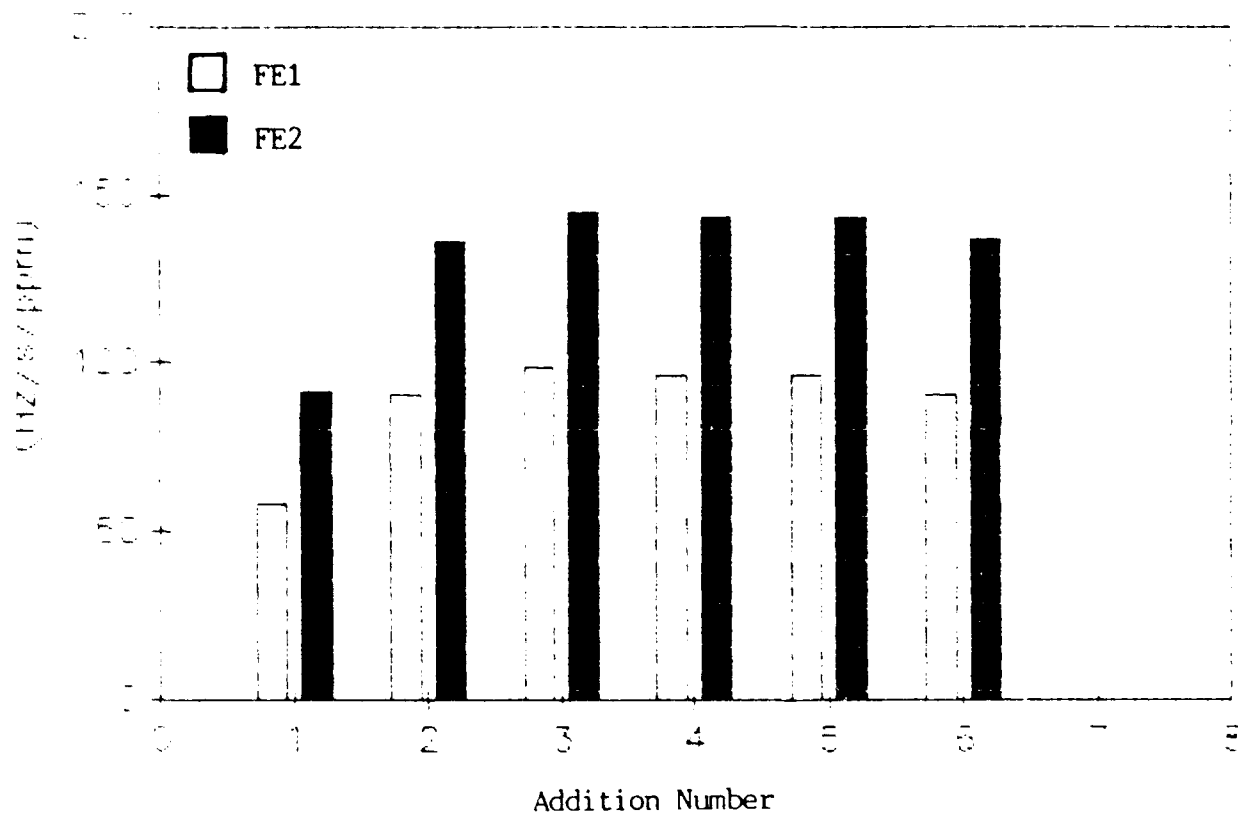


Figure 65. Ferroskan Readout per ppm as a Function of each Addition of 0-10 Micron Fe Powder

TABLE 85

FERROSCAN RESPONSE PER UNIT CONCENTRATION FOR
FE 0-10 MICRON AT CONCENTRATIONS BELOW 160 PPM
Performed 4-18-1990

Sample Number	Hz/s/ppm FE1	Hz/s/ppm FE2
1	44.2	69.2
2	87.0	126.2
3	87.4	129.9
4	85.2	126.7
5	81.8	120.2
6	80.3	114.0
Average	84.3 \pm 3.2	123.4 \pm 6.3

Performed 6-8-1990

	58.7	91.9
	91.0	136.1
	99.1	144.5
	96.2	143.5
	96.4	143.6
	91.1	136.9
Average	94.8 \pm 3.6	140.9 \pm 4.1

TABLE 86

COMPARATIVE DATA FROM TWO EXPERIMENTS USING SLOPES
AND FERROSCAN RESPONSE PER PPM FE FOR 0-10 MICRON

	Slope	Intercept	Hz/s/ppm [*]
Experiment 1			
	FE1 0.1460	-0.3308	94.8 \pm 3.6
	FE2 0.0975	-0.2078	140.9 \pm 4.0
Experiment 2			
	FE1 0.1438	-0.9140	84.3 \pm 3.2
	FE2 0.0973	-0.6190	123.4 \pm 6.3

* Fe concentration range is 14 to 75 ppm

(7) Detection of Steel Wear Debris from a Pin-on-Disk Wear Test

Ferroskan testing was conducted in order to evaluate the sensor sensitivity in detecting steel wear particles generated from a wear test device. Real time data were collected to show the sensor response as a function of concentration. The sensor response in Hz/s/ppm was also calculated and plotted versus sample addition number to show the stability of the signal as the concentration is increased.

Steel wear particles generated in MIL-L-7808 from a pin-on-disk wear test device were collected and added periodically to the microfiltration test rig (MFTR) equipped with the in-line magnetic wear debris sensor (Ferroskan). The 2 gallons of oil circulating at 19 gpm with bulk oil temperature of 90°C was sampled before and after each wear debris addition. The real time data collected during this experiment are shown in Figure 66. The Ferroskan data shows that the magnetic sensor did respond to the amount and concentration of steel particles added. The rise in the sensor response seems to be sharp and immediate. The counts in Hz/s before and after each addition were averaged and plotted as a function of concentration (Figure 67). The Fe concentration was determined by the acid dissolution method and atomic absorption spectroscopy. The 3-point curves for the small and large particles detected by the sensor as FE1 and FE2 were fairly linear. However, the response in Hz/s/ppm (Figure 68) was not constant and increased with concentration.

(8) Detection of Real Wear Debris

Used oil samples (MIL-L-7808) from various gas turbine engines were filtered through 3-micron pore size filters in order to isolate and collect the wear debris for the Ferroskan study. The wear debris retained on the filter elements were separated, weighed and examined for their magnetic

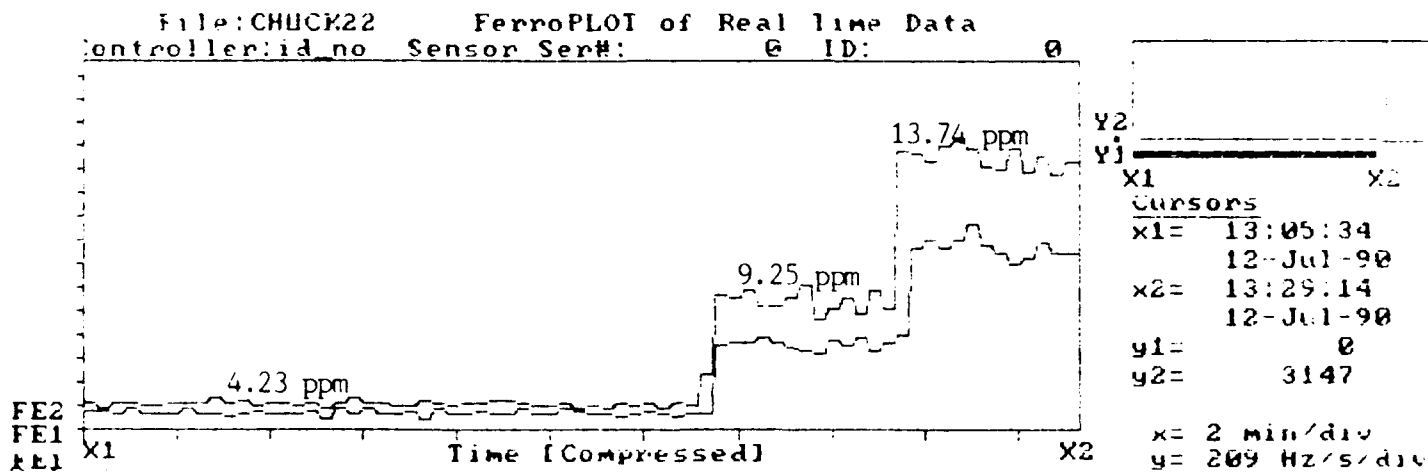


Figure 66. Ferrosan Real Time Data for Steel Wear Debris Generated from a Pin-On-Disk Wear Test Device

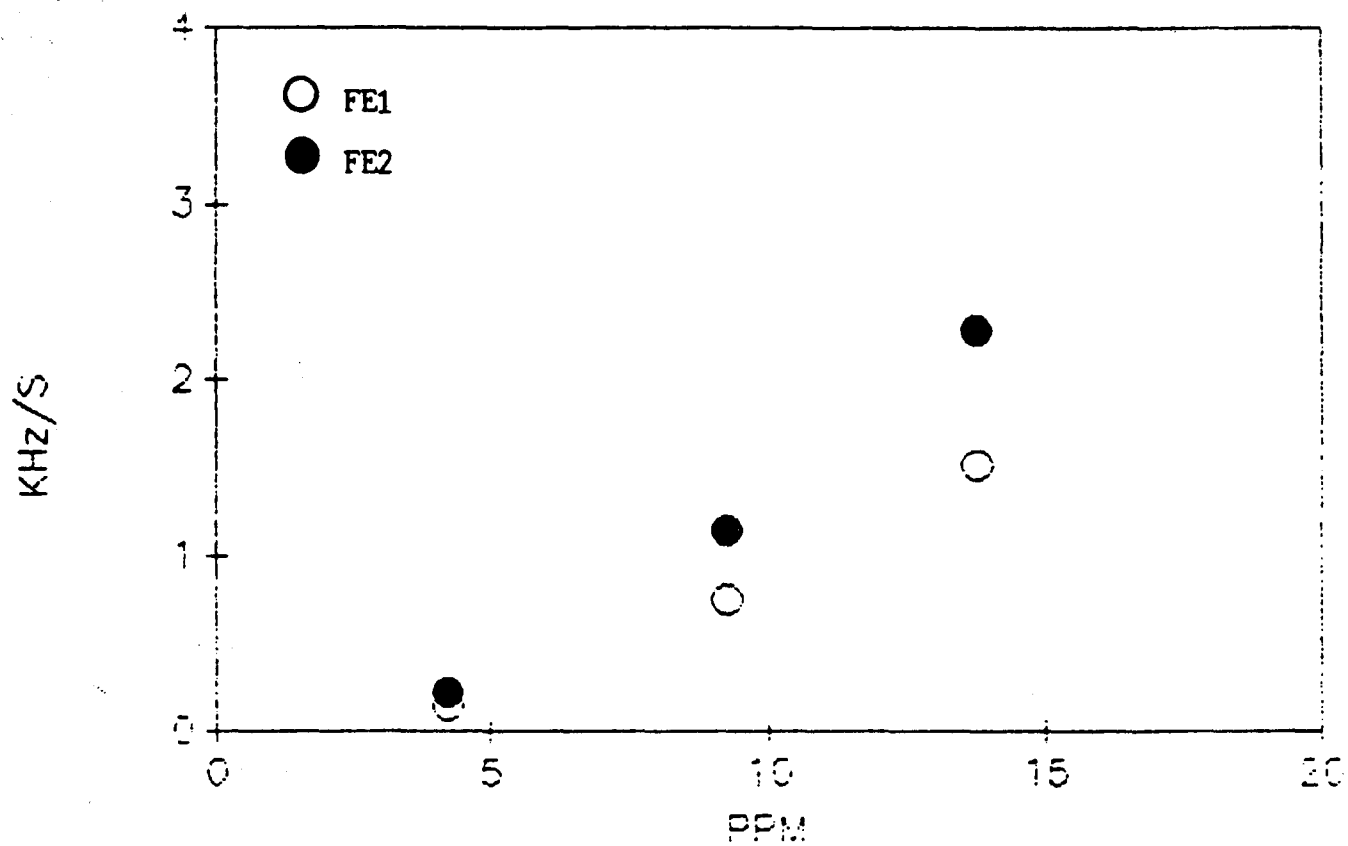


Figure 67. Ferroskan Response for Two Ranges of Particle Sizes, FE1 and FE2 as a Function of Concentration Using Steel Particles from a Wear Test

FERROSCAN OF STEEL PARTICLES GENERATED FROM A FIN-ON-DISK WEAR TEST

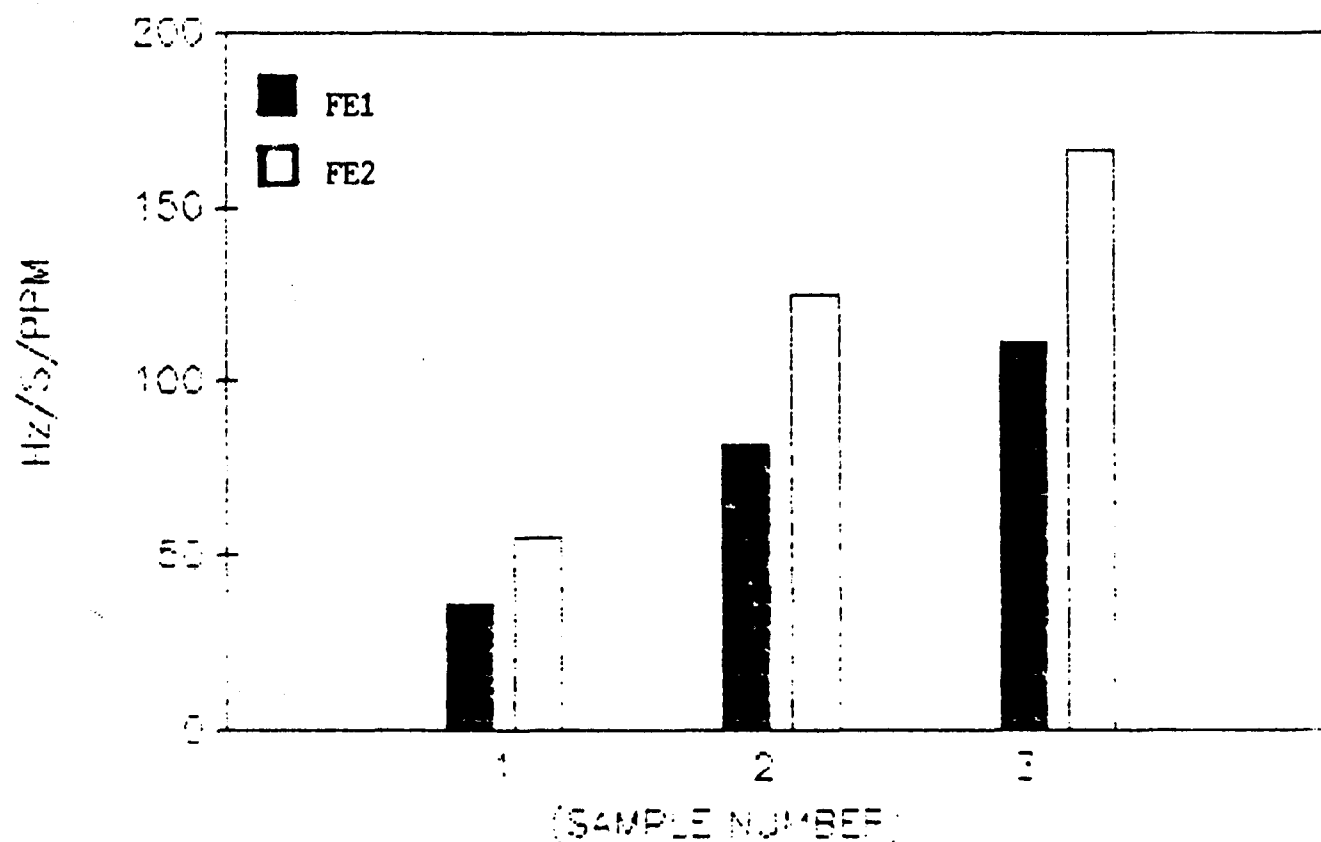


Figure 68. Ferroskan Response per ppm as a Function of Each Addition Using Steel Particles from a Wear Test

property. A bar magnet, held directly under a petri dish containing the debris, was able to magnetize the particles. The wear debris was then added to the circulating oil in the microfiltration test rig. The oil volume of 1.5 gallons, circulating in the rig at 19 gpm and heated to a temperature of 87°C, was sampled before and after the wear debris addition. The concentration of the wear debris was determined by the acid dissolution method and AA. The real time data collected before and after the single addition are shown in Figure 69. The data indicate that the Ferroskan sensor seems to respond to the addition of the magnetic wear debris. However, the response was sluggish and slow in contrast to the sharp and immediate response experienced during the addition of iron powder and steel wear particles generated from a wear test device. Several reasons might be responsible for this behavior. The wear particles might have been too large, millimeter in size, that their transport was slow due to their size and weight. The magnetic wear debris was also mixed with considerable amount of nonmetallic material which contributed to the particles' agglomeration and difficulty of transport to the in-line sensor. The sensor response in Hz/s before and after the wear metal addition was averaged and plotted as a function of concentration (Figure 70) and the response per ppm was calculated and shown to be 96 and 127 Hz/s/ppm for FE1 and FE2 (Figure 71), respectively. The response per ppm does not seem to be constant but increases with concentration.

e. Conclusions

Ferroskan sensitivities were determined for different concentrations and various sizes of Fe particle. Calibration curves were plotted for each particle size range versus the sensor response. The curves were not linear and it seems that the sensor sensitivity decreases at higher concentrations.

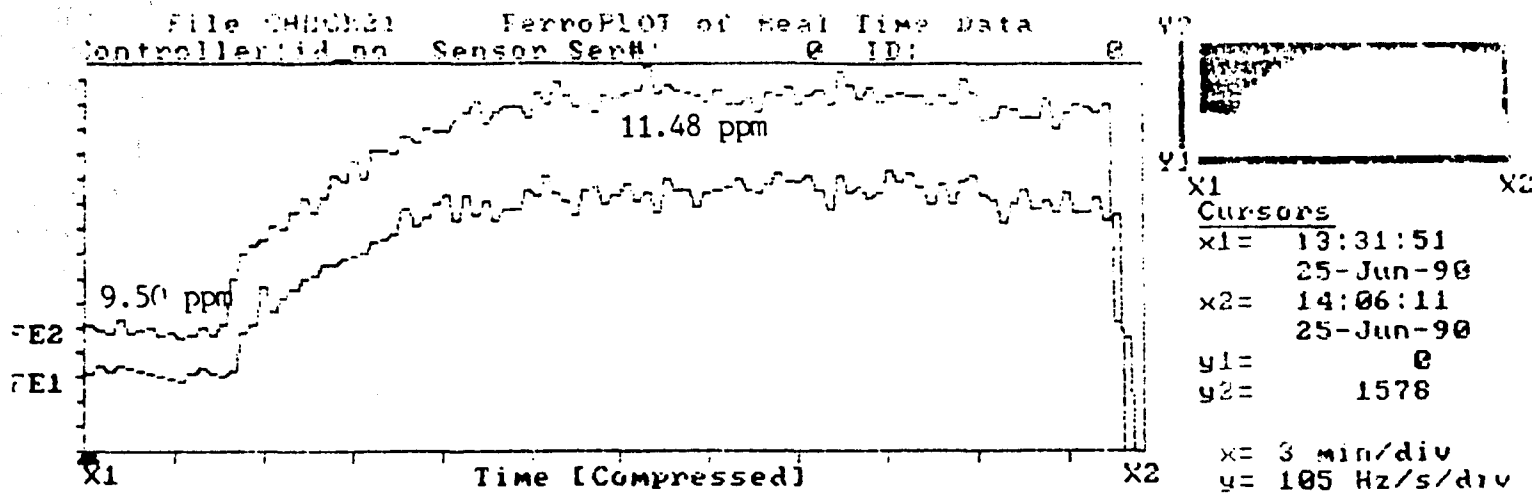


Figure 69. Ferrosan Real Time Data for Wear Debris Isolated from
 Gas Turbine Engine Used Oil Samples

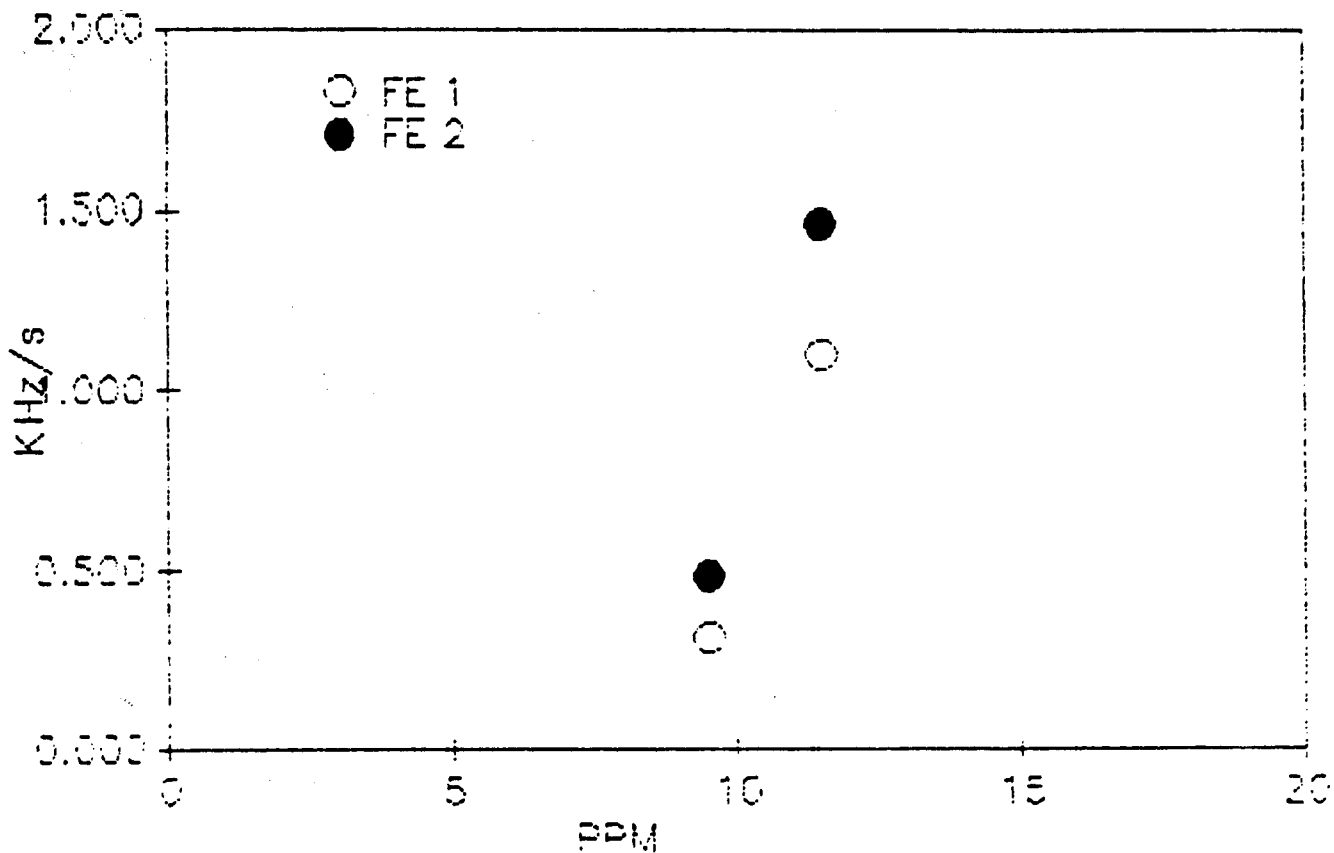


Figure 70. Ferroskan Response as a Function of Fe Concentration for Two Ranges of Particle Sizes Using Wear from Gas Turbine Engine Used Oils

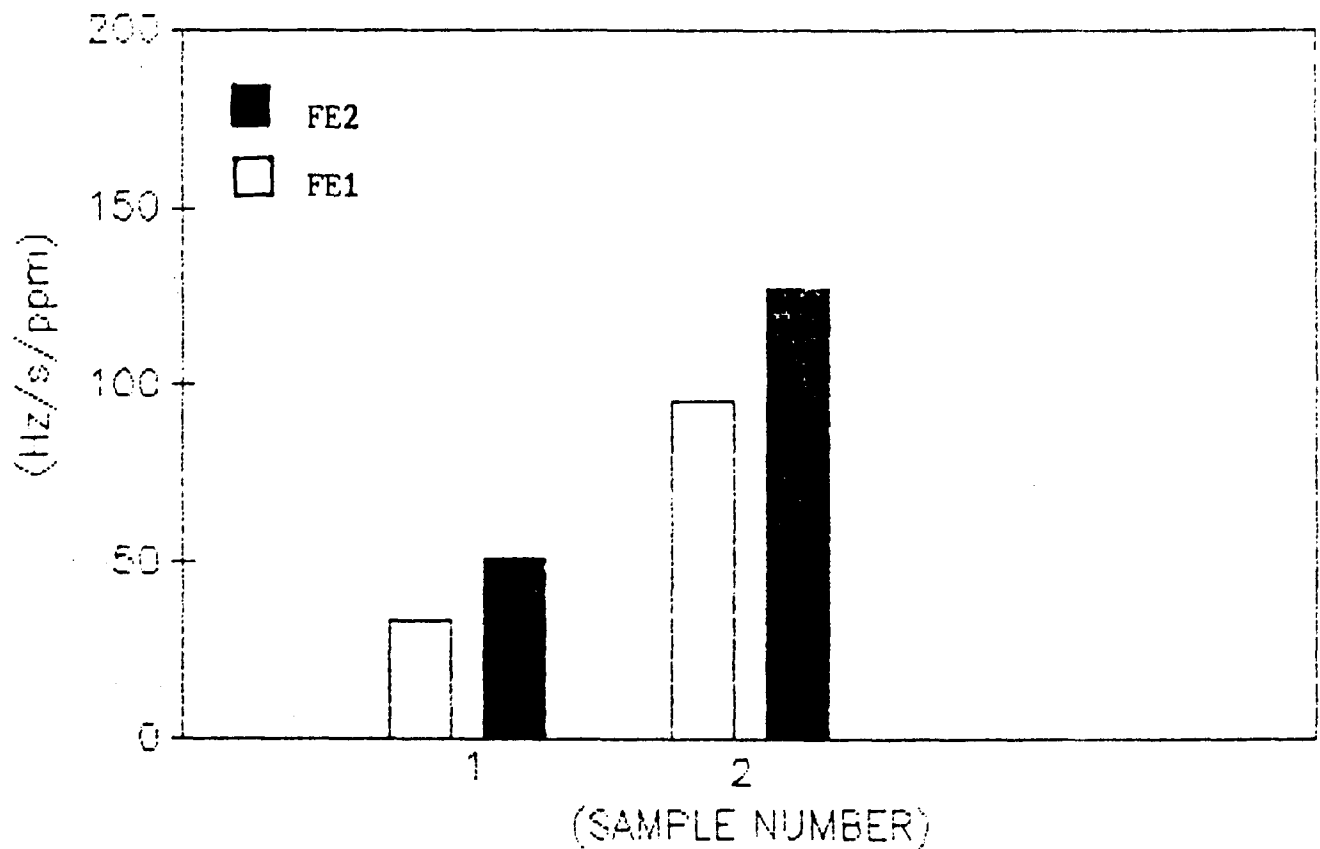


Figure 71. Ferroskan Response per ppm as a Function of Addition Number for Wear Debris from Gas Turbine Engines

Sensor sensitivities were found to be directly proportional to particle size. Sensitivity ranged from 1252 Hz/s for the less than 5 micron to 2705 Hz/s for the 30-45 micron Fe particles when each size was tested independently. Time between experiments, and not elapsed time during the experiment, has an effect on the sensor response. Sensitivities for the above particle size range were different when similar amounts of various size particles were added sequentially. In this case sensitivities were 835 and 1334 Hz/s for the -5 and 30-45 microns, respectively.

The effect of oil temperature and velocity on the sensor response was also determined. The response increased by one order of magnitude when the temperature increased by 50°C, and by 5.5 fold when the oil velocity increased by 2.4 m/s. Sharp and immediate changes in the sensor response were obtained when velocity changed from low to high. However, decaying response was obtained for velocity changes from high to low.

The new sensor introduced to the Ferroskan system had the following impact on Fe detection:

1. Relative to the old sensor the new sensor response was substantially reduced for similar size and concentration of Fe powder.
2. The flow rate of 7 gpm was ineffective and the flow of 19 gpm resulted in improved sensor sensitivity.
3. A 9 to 12% decrease in detection is expected in the sensor readout after an hour of testing.
4. Readings in kHz/s versus concentration were fairly linear up to 158 ppm for 0-10 micron Fe powder.

2. IMPROVING SAMPLE INTRODUCTION FOR TOTAL WEAR METAL DETERMINATION BY ATOMIC EMISSION SPECTROSCOPY

The sample introduction system of an AC spark atomic emission spectrometer was modified to allow greater detection of wear metal having particles greater than 1-3 microns. A 5-microliter sample was pipetted onto a paraffin coated stationary lower electrode. Ashing was performed to eliminate any matrix effect and preconcentrate the metal prior to exposing the electrode to a spark discharge for 20 seconds. Samples were obtained from operating aircraft engines and from four-ball wear tests. Particle size distribution was determined using previously developed filtration techniques. Emission spectrometer parameters studied were preburn time, exposure time, electrode gap setting, spark intensity, gas flow, and updraft pressure of exhaust. The use of a collimating lens proved to be very effective in improving signal repeatability. Bottom electrode geometry was optimized using several types of configurations. The use of a commercially available residue tester with operator selectable temperature ramping and gas flows was very beneficial in improving repeatability and accuracy of the ashing method. Comparative data demonstrate the improvement of the detection capability of this technique relative to the traditional rotating disc method. This work in its entirety is presented in Appendix B.

3. FERROGRAPHIC ANALYSIS OF HIGH TEMPERATURE FLUIDS

a. Introduction

Several diagnostic techniques have been investigated and used for determining the condition of gas turbine engines using either mineral oil or ester base lubricants. The primary two methods used by the United States Air Force utilize emission and absorption spectrometric techniques. Studies have shown these techniques to be effective in detecting wear particles smaller

than 3-10 microns.⁴ Wear particles having sizes above the SOAP (Spectrometric Oil Analysis Program) spectrometer detection capability and below chip detector capability (100 microns) can be determined using Ferrography.⁵ Various ferrograph techniques (analytical, direct reading and in-line) have been developed and utilized for mineral oil and ester base lubricants. However, the use of ferrography has not been applied to high viscosity high temperature lubricants. This study has been directed toward the use of analytical ferrography for the evaluation of wear debris in high temperature lubricants.

b. Test Apparatus and Procedure

The analytical ferrograph has been developed to magnetically precipitate wear particles according to their size onto a glass slide. A detailed description of the analytical ferrograph has been previously given and will not be repeated.⁹ Briefly, the ferrograph consists of a sample holder, sampling tube, peristaltic pump, glass slide having a fixed oil barrier, a magnet upon which the glass slide is placed and an oil collection system at the end of the magnet. The arrangement of the glass slide on the magnet is such that a magnetic gradient exists down the slide resulting in the separation and collection of particles according to their size and magnetic susceptibility as the oil flows down the slide.

Prior to ferrographic analysis the sample is heated, sonicated and then diluted (three parts oil/one part fixer) to reduce oil viscosity effects while the oil flows down the slide. The slide is then washed with additional "fixer" after the sample has flowed down the slide to remove residual oil and to fix the particles to the slide. The wear particles on the slide can then be determined quantitatively using percent area covered measurements (densitometer measurements) or evaluated with respect to wear particle

morphology using various types of microscopy.

c. Results and Discussion

(1) Initial Ferrograph study of O-77-6

The initial ferrograph study involved new O-77-6 (5P4E), 327°C oxidatively stressed O-77-6 having a 50% (40°C) viscosity increase and three samples of O-77-6 after four-ball wear testing. These ferrograms were made for determining the adaptability of the current ferrographic procedure and the identification of problems using high viscosity, low solubility, high temperature lubricants. Data obtained from these studies using sample sizes of 3 mL oil and 1 mL fixer are given in Table 87.

TABLE 87

INITIAL ANALYTICAL FERROGRAPH DATA FOR VARIOUS POLYPHENYL ETHER FLUIDS

Ferrogram No.	Fe (ADM) ppm	Entry	% Area Covered (Incident Light) Ferrograph Position					L/S ² Value	Wear Scar Dia., mm
			50 mm	40 mm	30 mm	20 mm	10 mm		
855	-	0.5	0.3	0.5	0.2	0.0	0.0	1.66	-
856	-	0.5	0.3	0.3	0.4	1.5	0.7	1.66	-
860	96	48.7 ¹	49.5	68.6	80.8	87.5	93.1	0.98	1.520
861	13	7.6	9.5	7.8	8.3	8.4	15.0	0.80	0.975
863	17	23.1	15.2	11.9	14.2	15.4	21.8	1.52	1.040

¹Few large (10 to 75 micron) blued severe wear particles

²L/S = Ratio of Entry/50 mm position values

Ferrogram Identification

Ferrogram # 855: New O-77-6 Fluid
 # 856: O-77-6 after 327°C C&O Test, 50% Vis. Chg.
 # 860: O-77-6, W.T. # 338; 250°C, 3.6 h, 1200 rpm, 145 N
 # 861: O-77-6, W.T. # 339; 75°C, 6.0 h, 1200 rpm, 145 N
 # 862: O-77-6, W.T. # 340; 75°C, 12 h, 1200 rpm, 145 N

The data in Table 87 show that very little wear debris existed

in the new and C&O stressed O-77-6 fluid. The four-ball wear test data show that four-ball testing of 5P4E produces mostly very small particles (<5 microns) as evident by the low L/S (ratio of large to small particles) values and the increasing percent area covered when going from the entry position to the exit position.

The standard dilution was not always satisfactory since occasionally a problem existed in getting the oil to flow down the ferrogram slide. MIBK (methyl isobutyl ketone) was tried as the "diluent and fixer" in preparing the ferrograms but was not satisfactory due to its dissolving of the oil boundary film on the ferrogram slide. At this time it appeared that decreasing the ratio of oil to fixer would provide the best ferrograms on polyphenyl ether fluids.

(2) Variable Oil/Fixer Ratio Study

Ferrographic analyses were conducted on two four-ball wear tested O-77-6 samples using various oil to fixer ratios. The identifications of the prepared ferrograms are given in Table 88 and with the analytical ferrograph data being given in Table 89. Ferrographic analyses of two samples of ester base transmission fluid DOD-L-85734(AS) are also included in these tables. Analyses of these samples were conducted for determining the differences in the amount and type of wear debris present in the samples but the data are included in Tables 88 and 89 for showing the differences in the type of ferrograph data obtained between the two types of fluids.

The data in Tables 88 and 89 show that most of the debris that gives the large percent area covered for the wear test samples of 5P4E fluid O-77-6 is an organic polymeric material being associated or mixed with small wear particles (less than 2 microns). The normal sample to fixer volume for ester base lubricants of 3 to 1 is not satisfactory for the high viscosity

TABLE 86

IDENTIFICATION OF SAMPLES USED
IN ANALYTICAL FERROGRAPHY STUDY
INCLUDING DESCRIPTION OF FERROGRAM DEBRIS

Ferrogram No.	Sample Identification	Description of Ferrogram Debris
876	O-77-6, Wear Test No. 338; 250°C, 3.6 h, 1200 RPM 145 Newtons	Heavy amount of organic debris, few to moderate amounts of normal and "blued" severe wear particles
874	Same as above sample	Same as for above sample
866	Same as above sample	Same as for above sample
882	Same as above sample	Heavy amount of organic debris, few normal and severe wear particles
863	O-77-6, Wear Test No. 340; 75°C, 12 h, 1200 RPM, 145 Newtons	Moderate amount of organic debris, few to moderate severe wear particles few normal rubbing wear particles, oxides and other non-wear debris
875	Same as above sample	Moderate amount of organic debris, moderate amounts of severe and cutting wear, few normal wear particles and non-wear debris
878	O-88-25 (DOD-L-85734) Wear Test No. 341; 75°C, 20 h, 1200 RPM, 145 Newtons	Few normal and severe wear particles. Very little debris
880	O-88-25 (DOD-L-85734) Wear Test No. 343; 75°C, 20 h, 1200 RPM, 145 Newtons	Same as above sample
871	TEL-8098 (DOD-L-85734) Wear Test No. 342; 75°C, 20 h, 1200 RPM, 145 Newtons	Few to moderate severe wear particles, few normal wear particles and non-wear debris
872	Same sample as above	Same as above

TABLE 89

ANALYTICAL FERROGRAPH DATA FOR DOD-L-85734 (AS)
FLUIDS AND O-77-6 FLUID AFTER FOUR BALL WEAR TESTING

Ferrogram No.	Sample Size	Type Fluid	Fe(ADM) ppm	Entry	% Area Covered (Incident Light) Ferrogram Position (mm)				L/S	Wear Scar Dia., mm.
					50	40	30	20		
876	3 mL ¹	Test No. 338	96	91.3	92.2	93.2	94.0	93.7	93.5	0.99
874	3 mL ²	"	96	75.3	83.7	91.5	93.3	92.8	93.8	0.90
860	1 mL ³	"	96	48.7	49.5	68.6	80.8	87.5	93.1	0.98
882	0.25 mL ¹	"	96	84.6	90.8	94.5	95.0	95.2	95.5	0.93
882	"	"	96	77.5 ⁴	57.3	96.4	96.1	96.9	96.9	1.35
863	1 mL ³	Test No. 340	17	23.1	15.2	11.9	14.2	15.4	21.8	1.52
872	3 mL ²	"	17	27.0	11.3	21.6	24.0	33.1	33.8	2.39
878	3 mL ³	Test No. 341	8	4.3	1.3	1.4	0.8	1.5	1.7	3.31
880	3 mL ³	Test No. 343	9	16.3	2.5	1.1	1.0	1.3	5.8	6.52
871	3 mL ³	Test No. 342	1	8.1	2.0	1.0	2.6	1.5	1.0	4.05
872	3 mL ³	Test No. 342	1	4.8	1.9	1.9	1.2	2.2	0.9	2.53
¹ 3 mL Fixer	² 2 mL Fixer	³ 1 mL Fixer	⁴ Transmitted Light							

5P4E fluids. Previous testing and test data given in Table 89 show that higher density readings are obtained when using a 1 to 3 ratio of sample to fixer which also reduces the viscosity of the mixture to prevent oil backup at the exit end of the ferrogram and oil overflowing the "barrier." The high percent area covered measurements of the O-77-6 wear test samples, due to the formation of gel or resin like particles, had a quantity of visibly severe wear debris no greater than the ester base oil wear test samples (Ferrograms 871, 878, 879 and 880) although the ADM iron content is 10 to 100 times greater for the O-77-6 wear test samples. This fact along with close optical examination of the ferrograms shows that the wear debris being developed with the wear tested O-77-6 fluids contain significant amounts of small (2 microns and below) normal rubbing wear particles although they are not readily observable. Some of the organic polymeric material was removed from one of the ferrograms obtained on wear test sample No. 338 and a melting point determination was made using the Mettler hot stage. The polymeric material did not melt or exhibit any observable phase changes up to 300°C.

(3) Effect of Varying Wear Test Parameters on Subsequent Ferrograph Analyses of O-67-1 Lubricant Wear Test Samples

Ferrographic analyses were conducted on lubricant O-67-1 after four-ball wear testing under various temperatures and loadings. The data obtained along with wear scar data and iron content (spectrometric analysis) are given in Table 90. Incident lighting was used for all ferrographic measurements. These data show the following:

Poor test repeatability was obtained for wear test No. 356 conducted at 75°C and wear test No. 352 conducted at 150°C with respect to percent area covered which is probably due to the polymeric material present.

All of the iron/polymeric material is not being collected on the

TABLE 90

ANALYTICAL FERROGRAPH DATA FOR O-67-1 FOUR-BALL
WEAR TEST SAMPLES USING VARIOUS TEST TEMPERATURES AND
LOADINGS. (1200 RPM AND THREE TEST HOURS UNLESS SHOWN)

Wear Test No.	Temp. °C	Load N	Scar Dia mm	% Area Covered ¹			Fe ² ppm	Comments
				Entry	50 mm	10 mm		
356	75	145	1.055	49.5	59.2	87.3	-	Moderate amount of polymer and severe wear
356	75	145	1.055	29.4	43.8	66.0	-	" " "
351	75	145	1.633 ³	13.1	29.5	80.7	83	Heavy amount of polymer
362	150	145	1.029 ³	57.8	31.5	65.2	-	Moderate amount of polymer
352	150	145	1.253	59.5	53.5	94.1	-	Heavy amount of polymer
352	150	145	1.253	51.3	75.3	94.5	-	" " "
353	150	145	2.388 ⁴	40.4	94.0	92.9	-	" " "
378	150	78	1.099	53.3	51.1	90.1	-	" " "
355	250	145	1.456	55.6	95.2	95.0	-	" " "
359	315	145	1.153	90.2	95.3	96.0	-	" " "
382	75	33	0.632	9.5	8.2	7.5	13	Small amount of polymer, moderate to heavy severe wear, few cutting wear
386	150	33	0.949	15.0	13.7	34.5	40	Moderate amount of polymer. Moderate amount of small rubbing wear, few to moderate severe & cutting wear particles

TABLE 90 (CONCLUDED)

388	150	33	1.112	80.5	80.5	94.4	23	Heavy amount of polymer. Moderate rubbing wear. Few severe wear particles
401	315	33	1.099	58.2	84.6	94.5	29	Heavy amount of polymer. Moderate amount of small rubbing wear and few severe wear particles
401 2nd Pass	315	33	1.099	17.0	31.8	93.6		Heavy amount of polymer. Smaller particle size than first pass
401 3rd Pass	315	33	1.099	39.2	46.4	89.3		Heavy amount of polymer. Very small particles

¹ 1 mL Sample and 3 mL Fixer

² Fe: Iron concentration in sample from wear test

³ 20 Test Hours

⁴ 1 Test Hour

ferrograms as shown by the high percent area covered measurements and the second and third pass testing for Test No. 401 when using a 1 mL sample diluted with 3 mL fixer.

In general, more severe wear particles were generated at 75°C testing and decreased as the wear test temperature increased. The amount of small iron or iron/polymeric particles greatly increased with increasing wear temperatures. Increasing the wear test loading also increased the amount of iron and polymeric material.

No correlation existed between wear scar diameter, iron content or the percent area covered at the various ferrogram positions.

(4) Analytical Ferrographic Analysis of a Rolling Four-Ball
Wear Test Sample of O-67-1 Lubricant

An analytical ferrogram was prepared from rolling Four-Ball Test No. 001 using 1 mL of sample and 3 mL of fixer. Test conditions were 145 N load, 75°C test temperature, 30 test hours and 2500 rpm. As expected very little wear debris was generated. The percent area covered ranged from 3.3% (Entry position) to 1.2% (10 mm or exit position). However, close examination of the ferrogram did show a slight amount of polymeric type particles similar to those formed in a much greater quantity during sliding four-ball wear testing.

(5) Effect of Oxidative Stressing of Four-Ball Wear Test
Samples of O-67-1 Lubricant on Analytical Ferrograph
Data

Corrosion and oxidation testing of four-ball wear test samples of O-67-1 was conducted prior to ferrographic analyses. The data obtained on these samples are given in Table 91 along with ferrograph data for the four-ball wear tested fluid prior to C&O testing and a repeat test for the 240 hour C&O stressed sample.

TABLE 91

EFFECT OF OXIDATIVE STRESSING OF FOUR-BALL WEAR TEST SAMPLES
OF O-67-1 LUBRICANT ON ANALYTICAL FERROGRAPH DATA

Sample	Entry	% Area Covered		Scar Dia. mm	Optical Evaluation of Deposits
		50 mm	10 mm		
Wear Test No. 352 (O-67-1, 150°C 145 N, 3 h)	59.3	53.3	94.1	1.253	Few to moderate normal and severe wear particles. Moderate to heavy amounts of polymeric material.
Wear Test No. 399 (168 h, 320°C O/C Sample, 150°C 145 N, 3 h)	14.8	21.1	92.7	1.276	Moderate amounts of normal and severe wear particles. Moderate to heavy amounts of polymeric material.
Wear Test No. 405 (240 h, 320°C O/C sample 150°C, 145 N, 3 h)	60.1	75.2	54.5	1.071	Few to moderate normal and severe wear particles. Moderate to heavy amounts of polymeric materials.
Wear Test No. 405 (Repeat)	55.8	42.3	36.6	1.071	Same as above test.

The percent area covered measurements were somewhat inconsistent. Measurements made on the ferrogram of wear test sample No. 399 (168 hours, 320°C O/C sample of O-67-1 prior to wear testing) gave very low values for the entry and 50 mm ferrogram position compared to the ferrogram of the wear test sample of unstressed O-67-1. The measurements made on the ferrogram of wear test sample No. 405 (240 hours, 320°C O/C sample of O-67-1 prior to wear testing) gave equivalent percent area covered measurements for the entry and 50 mm positions but a much lower reading at the 10 mm position when compared to the unstressed fluid. These data along with subsequent presented data indicate that larger wear debris is lost during C&O testing which must have formed part of the sludge and deposits remaining in the C&O tubes. The data also show that no additional polymeric material was formed during C&O testing.

(6) Effect of Filtration on Analytical Ferrograph Data

Ferrographic analyses were conducted on the previously described CB-1 (unfiltered) and CB-1 (filtered) samples before and after corrosion and oxidation testing with the test data being given in Table 92.

The data in Table 92 show that the unfiltered CB-1 sample had lost the larger debris during the corrosion and oxidation testing which must have formed part of the heavy amount of sludge and deposits remaining in the C&O tube. The loss of the large debris by filtering is as expected but the large loss of small particles (percent area covered at 10 mm position) was not expected since microscopic examination of the ferrograms showed most of these particles to be below three microns. It appears that removal of these particles was due to larger debris partially plugging the filter which reduced the effective filtration rating of the filter. The data do show that no polymeric particles or debris are formed during C&O testing which was also

TABLE 92

EFFECT OF 3 MICRON FILTRATION ON ANALYTICAL
FERROGRAPH DATA FOR C&O STRESSED AND
UNSTRESSED CB-1 SAMPLE (FOUR-BALL WEAR TEST
SAMPLE OF O-67-1)

Sample	% Area Covered			Elements
	Entry	50 mm	10 mm	
CB-1 Unfiltered	93.2	92.7	90.0	Heavy amount of rubbing wear & polymeric material. Few to moderate severe and cutting wear.
CB-1 Unfiltered After 48 h C&O at 320°C	20.8	17.1	91.4	Few rubbing wear. Heavy amount of polymeric material.
CB-1 Filtered (3 micron)	13.6	8.0	7.4	Few to moderate number of small polymeric particles. Some clear to white 15 to 30 micron particles (Possibly external contamination).
CB-1 Filtered After 48 h C&O 320°C	3.6	4.4	11.7	Few polymeric particles. Some clear to white 15 to 30 micron particles (Possible external contamination).

shown above in Section (5).

(7) Analytical Ferrographic Analysis of Engine Stressed
O-67-1 Lubricant

Analytical ferrographic analyses were conducted on six samples of engine stressed O-67-1 lubricant and after four-ball wear testing for one of these fluids. Ferrographic data obtained from this study are given in Table 93.

The above data show that little to moderate amounts of wear debris and moderate amounts of polymeric material were present in the engine stressed samples. The polymeric material appeared similar in microscopic appearance to the polymeric material generated in the four-ball wear tests. The amount of wear debris observed on the ferrograms is in agreement with the ADM/AA iron analyses which is 5 ± 2 ppm for all six samples. The amount of polymeric material that remains on a ferrogram is effected by particle size, amount of other debris, oil and fixer flow rate, and other factors. For these reasons, analytical ferrography is only semi-quantitative, at best, in measuring the amount of polymeric material in stressed 5P4E fluids. For fluids containing large amounts of polymeric material such as the higher loading four-ball wear tests, much of the polymeric material does not remain on the ferrogram slide.

(8) Summary

This study has shown that the normally used dilution of 3 parts oil to 1 part fixer in preparing analytical ferrograms of O-67-1 type lubricants is not satisfactory. This ratio should not be greater than 1 part sample to 3 parts fixer. Due to the formation of iron containing polymeric material in stressed O-67-1 type lubricants all wear debris may not be deposited on the ferrogram even after two or three passes.

TABLE 93

ANALYTICAL FERROGRAPH DATA FOR ENGINE
STRESSED O-67-1 SAMPLES

Fluid	Entry	% Area Covered		L/S ¹	Comments
		50 mm	10 mm		
TEL-9028	8.2	17.3	62.0	0.47	Few wear particles. Moderate amount of polymeric material
TEL-9029	2.0	3.6	27.3	0.55	Very few wear particles. Moderate amount of polymeric material.
TEL-9030	11.9	18.0	44.7	0.66	Moderate amount of normal wear and severe wear particles. Moderate amount of polymeric material.
TEL-9038	6.2	5.1	36.2	1.22	Moderate amount of normal wear particles and polymeric material
TEL-9039	2.0	3.4	23.8	0.59	Moderate amount of normal wear particles and polymeric material.
TEL-9040	8.2	6.9	32.2	1.59	Moderate amount of normal and severe wear particles. Moderate amount of polymeric material.
Wear Test No. 387 (TEL-9030, 150°C, 145 N, 3 h)	64.6	74.3	91.8	0.87	Few to moderate normal and severe wear particles. Moderate amount of polymeric material.

¹ Rate of Entry/50 mm position deposits

Ferrographic analysis of four-ball wear test samples of O-67-1 lubricant showed that more severe wear particles were generated at 75°C and decreased as the wear test temperature increased. The amount of small iron and iron containing polymeric particles greatly increased with increasing wear test temperatures. Increasing the wear test loading also increased the amount of iron and polymeric material. No correlation existed between wear scar diameter, iron content or the percent area covered at the various ferrogram positions.

A "rolling" four-ball test of O-67-1 lubricant produced a very low level of wear debris but did produce some polymeric material similar to that produced in larger quantities during sliding four-ball wear testing.

C&O testing of O-67-1 lubricant containing wear and polymeric material reduces the quantity of the larger debris which must form part of the sludge and deposits remaining in the C&O tube. The ferrograph data also show that polymeric debris is not formed during C&O testing.

Ferrographic analyses of field samples of "engine stressed" O-67-1 lubricant contain varying amounts of the polymeric material which is generated during four-ball wear testing.

The amount of debris and polymeric material formed in O-67-1 type lubricant and being collected on the ferrogram is affected by many factors and results in analytical ferrography being only semi-quantitative, at best, in measuring the amount of wear debris in this type fluid. However, the analytical ferrograph can be a very useful tool in determining the morphology of wear debris and polymeric material generated in MIL-L-87100 type lubricants.

SECTION IV

CANDIDATE HIGH TEMPERATURE LUBRICANT DIAGNOSTIC DEVICES

1. INTRODUCTION

The purpose of this task was to develop lubricant monitoring methods for high temperature lubricants. A method was developed to monitor polyphenyl ethers using fluorescence spectroscopy. Investigations were made into the use of a dielectric constant device with a heated cell for monitoring both polyphenyl ether (PPE) and MIL-L-7808 lubricants. High pressure differential scanning calorimetry data were correlated with physical property changes of C&O tested PPEs. A method was developed to accelerate oxidative stressing of PPEs by exposure to ultraviolet radiation. An investigation was made into the use of voltammetry for monitoring PPEs and voltammetric analysis procedures were optimized for on-line and off-line monitoring of a 4 cst ester lubricant (O-85-1).

2. FLUORESCENCE SPECTROSCOPIC CHARACTERISTICS OF STRESSED PPES

a. Introduction

Fluorescence spectroscopy was used to develop a lubricant monitoring method for oxidized polyphenyl ether (PPE) lubricants. Initially, excitation/emission characteristics and concentration/emission intensity properties of dilute solutions of the lubricants were defined. Based on that data, two excitation wavelengths were selected for the analysis of a series of oxidized PPEs and the results correlated with viscosity increases of the lubricants. In order to simplify the analysis, the weighing and solvent dilution steps were eliminated by directly analyzing the neat lubricant using the thin layer chromatography (TLC) accessory.

b. Description of Fluorescence Phenomenon and Instrumentation

Fluorescence in organic molecules is an absorption/emission phenomenon that occurs when the excited state produced by absorption of a quantum of radiation (UV-Vis range) undergoes a vibrational relaxation followed by a return to the molecule ground state by emission of radiation. The emitted radiation is lower in energy by an amount equal to the vibrational relaxation and typically occurs at 30 to 50 nm above the excitation spectrum but can be as large as several hundred nm. Fluorescence in organic compounds is generally found only in aromatic structures due to their structural rigidity which allows for relatively high quantum yields. This quantum yield, which is the ratio of molecular fluorescence emission to molecular absorption, is generally much less than one due to competing processes which result in excited state relaxation without emission of radiation such as quenching and various internal conversion mechanisms.

Fluorescence spectrometers consist of a radiation source with monochromator (wavelength selector) for irradiation of the sample solution and a detector/monochromator for detection of the fluorescence emission. Fluorescence is almost always measured in dilute solutions of the fluorophore in a non-absorbing solvent, typically in square quartz cuvettes. The majority of fluorescence instruments measure emission at right angles to the excitation source direction (emission occurs in all directions) which limits scatter of the excitation radiation into the detector. In general, fluorescence measurements are made on dilute solutions of the fluorophore because of severe distortion of the spectra that can occur with concentrated samples due to inner filter effects (i.e., absorption of part of the fluorescence emission by the sample itself). Measurements on such optically dense samples are made in either reduced volume cells or cells employing

off-center illumination, both of which reduce the optical path length, or by frontal face illumination. Such an arrangement was described for analysis of blood samples using a 0.1 mL cell at a 34 degree angle.^{10,11}

PPEs would seem to be a suitable material for fluorescence applications due to their previously shown formation of biphenylated compounds during oxidative stressing which should enhance fluorescence activity.²

c. Experimental

The instrument used in this work is a Perkin Elmer MPF-3 fluorescence spectrometer which is essentially as described above. 1,2-Trichloroethane was used as the diluting solvent due to its acceptable UV transparency and excellent PPE solvating properties. Oxidized PPEs from the corrosion and oxidation test at 320°C (O-67-1, TEL-8039 and TEL-8040) were analyzed at excitation wavelengths of 340 and 400 nm. The concentrations of the PPEs in the solvent (trichloroethane) were kept below the upper concentration limit that had been determined previously for the most heavily oxidized oils. Specifically, for an excitation wavelength of 340 nm the concentration was less than 0.1 mg PPE/mL solvent and less than 0.5 mg/mL for the excitation wavelength of 400 nm. The relative fluorescence intensity was determined by subtracting the emission intensity of the solvent from that of the sample solution and adjusting this value for concentration variations. The fresh (unstressed) PPE emission intensity was only very slightly higher than that of the solvent. The TLC accessory unit was designed to make fluorescent measurements of developed TLC plates but was used here to analyze neat lubricant films. Measurements of PPEs were made by placing the lubricant onto a thin microscope slide.

d. Fluorescence Excitation/Emission Characteristics of Stressed PPEs

In order to determine the fluorescent nature of oxidatively stressed PPEs, the emission spectra of a fresh PPE basestock (O-77-6) and TEL-8040 and O-67-1, stressed in the corrosion and oxidation test at 320°C for 408 hours and 240 hours respectively, were measured over excitation wavelengths of 280 to 480 nm. The results (Table 94) show that the emission maxima changes considerably with changes in the excitation wavelength. In general, it would not be expected that the fluorescence spectrum of an individual fluorophore would change with changes in the excitation frequency and so the emission maxima are the result of numerous fluorescing compounds produced by oxidation of the PPE. The data also show that the basestock (O-77-6) displays no measurable fluorescence at excitation wavelengths of 340 nm or greater and that the oxidized TEL-8039 and O-67-1 do not show identical emission spectra characteristics. Based on this data, fluorescence measurements of a series of oxidized PPEs were made at excitation/emission wavelengths of 340/365 nm and at 400/454 nm.

e. Concentration/Emission Intensity Relationships

In order to quantitatively analyze stressed PPE lubricants by fluorescence emission, it is necessary to determine the range over which concentration of the lubricant in the trichloroethane solvent is linear with the intensity of the fluorescence emission. The reason for this is that, typically, individual fluorophores above a particular concentration deviate from concentration/emission intensity linearity due to quenching and self-absorption (inner filter) effects. Quenching involves a relaxation of the excited state without emission of radiation (via molecular collisions) and results in a reduction in quantum efficiency while self-absorption involves absorption of the fluorescence emission by molecules present in

TABLE 94

FLUORESCENCE EMISSION MAXIMA OF OXIDIZED PPE LUBRICANTS

Excitation Wavelength (nm)	Emission Maxima, nm (Relative Intensity)		
	O-77-6 ¹	O-67-1 ²	TEL-8040 ³
280	308(650)	310(500)	308(570)
300	320(107)	346(300)	330(267)
320	346(21)	356(162)	352(90)
340	*	366(83)	372(47)
360	*	386(20)	396(18)
380	*	450(13)	430(10)
400	*	456(11)	452(7)
420	*	466(7)	456(4)
440	*	496(4)	476(1)
460	*	522(3)	528(1)
480	*	534(2)	*

* No Measurable Fluorescence

¹ Unstressed PPE Basestock

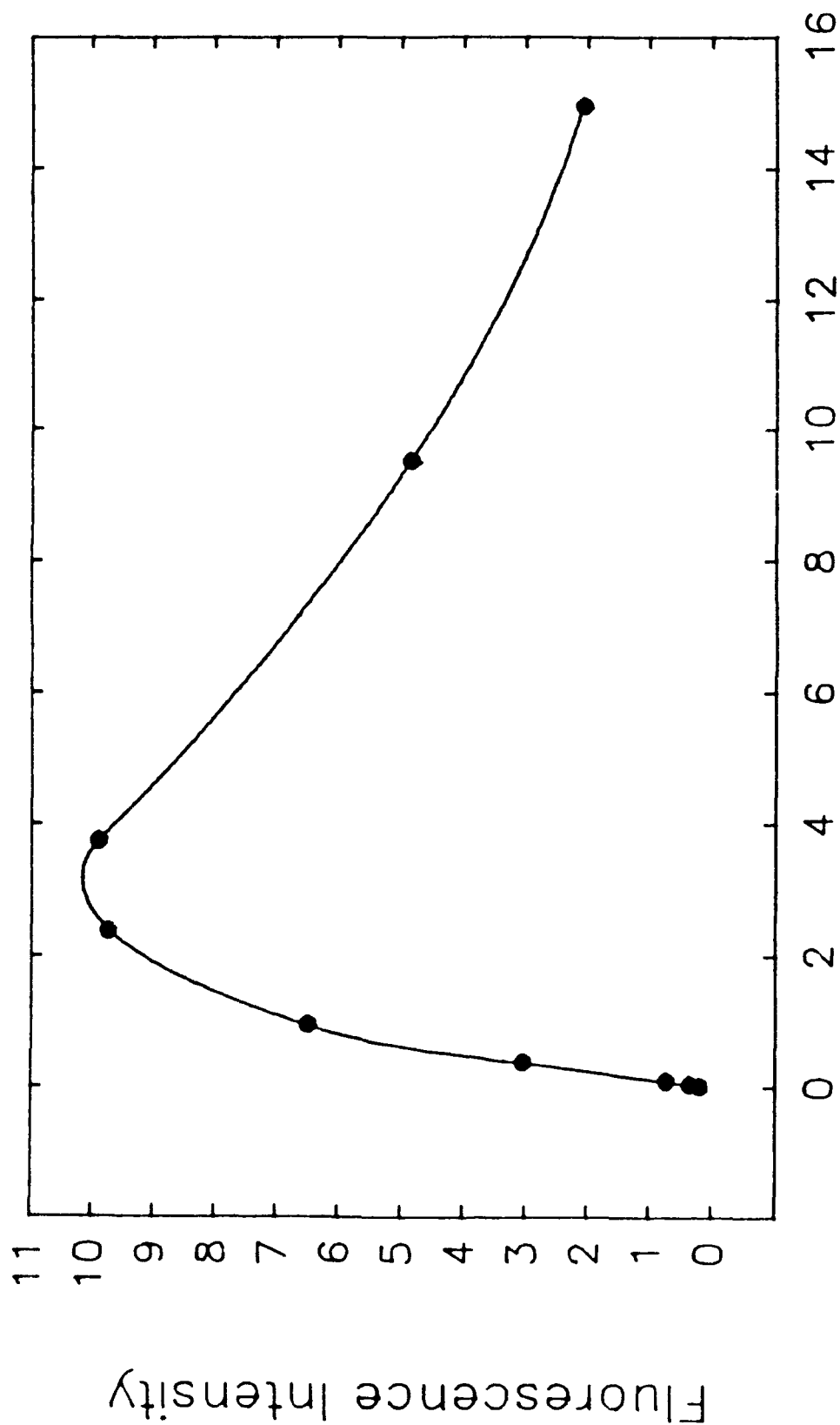
² After 240 Hour Corrosion and Oxidation Test
at 320°C, 81.9% Viscosity Increase

³ After 408 Hour Corrosion and Oxidation Test
at 320°C, 50.4% Viscosity Increase

solution and results in an apparent drop in quantum efficiency. Both effects result in a reduction in the measurable intensity of the fluorescing solutions versus that predicted by simple linear extrapolation.

Unfortunately, it is not possible to determine a true concentration/emission intensity relationship in stressed PPEs due to the unknown nature and concentration of the very complex series of fluorophores produced in the stressed lubricant. Instead, the most severely oxidized PPE lubricants will be used to establish an upper concentration limit at the aforementioned excitation wavelengths of 340 and 400 nm.

A typical concentration/emission intensity relationship is shown in Figure 72 for O-67-1 stressed 240 hours in the corrosion and oxidation test at 320°C at an excitation wavelength of 400 nm. It can be observed that the relationship is linear up to approximately 0.5 mg/mL before reaching a maximum at 2 to 4 mg/mL and then actually decreases in intensity with increasing concentration. This general relationship is also observed for this lubricant at 340 nm and is likewise observed for oxidized TEL-8040 at both excitation wavelengths. An approximate upper concentration limit was then determined for both oxidized TEL-8040 and O-67-1 and is shown in Table 95.



Concentration (mg PPE/mL Solvent)

Figure 72. Fluorescence Intensity as a Function of Concentration of (1,7-*i*-stressed at 320°C for 240 Hours, in the Oxidation and Oxidation Test. Excitation/ Emission Wavelengths of 400/454 nm)

TABLE 95

UPPER CONCENTRATION LIMITS FOR FLUORESCENCE OF OXIDIZED PPEs

	$\lambda_{\text{ex}} = 340 \text{ nm}$		$\lambda_{\text{ex}} = 400 \text{ nm}$	
	TEL-8040 ¹	O-67-1 ²	TEL-8040 ¹	O-67-1 ²
Upper Concentration Limit (mg/mL)	0.9	0.1	2.2	0.5

¹Corrosion and oxidation test at 320°C, 384 hours, 47.5% viscosity increase at 40°C

²Corrosion and oxidation test at 320°C, 240 hours, 81.9% viscosity increase at 40°C

Predictably, the stressed O-67-1 lubricant has a lower range than the stressed TEL-8040 due to the former being more heavily oxidized. All four data sets display good linearity over the indicated ranges (correlation coefficient >0.999) with nearly zero intercepts.

f. Emission Intensity of Oxidized PPEs

The relationship between fluorescence emission intensity increases and physical property changes that occur with oxidative stressing of PPEs is shown in Figure 73 for excitation wavelengths of 340 and 400 nm. The data show that the emission intensity/viscosity relationship is fairly linear for both TEL-8039 and TEL-8040 and the two data sets are virtually identical to one another, which is not surprising considering the similarity of these two formulations. The data also show that O-67-1 displays a consistently higher emission intensity for a given viscosity increase relative to TEL-8039 and TEL-8040 and also deviates somewhat from linearity. The differences between oxidation in O-67-1 versus that in TEL-8039 and TEL-8040 have been documented previously (see Section II this report) and were speculated to be due to differences in inhibition chemistry. Very likely, the high molecular weight

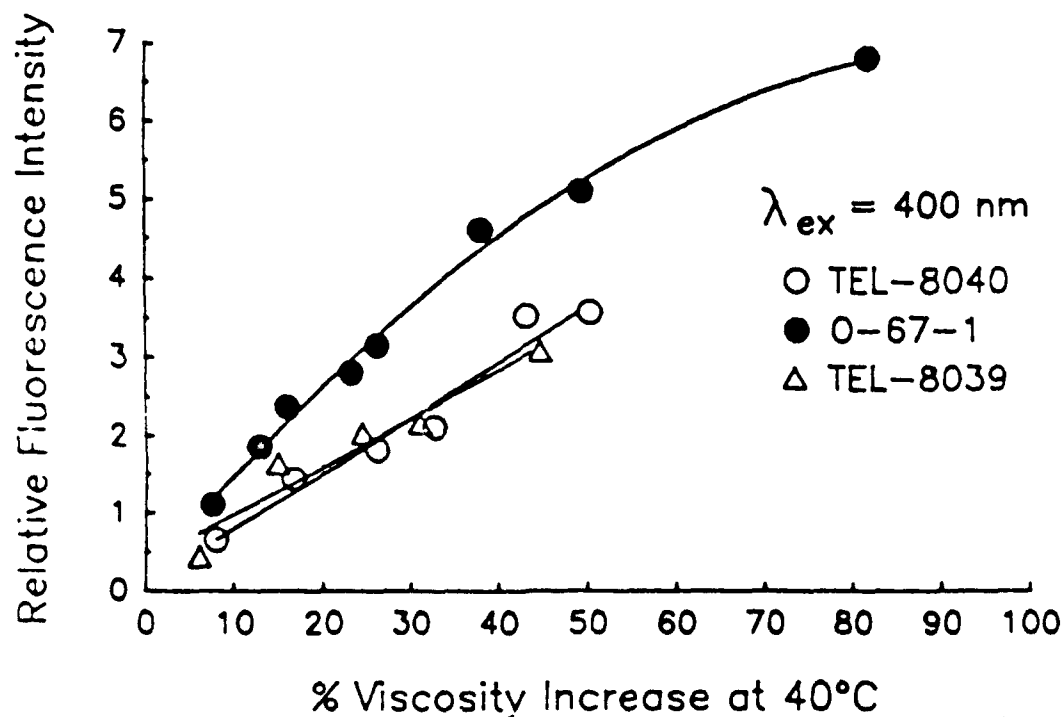
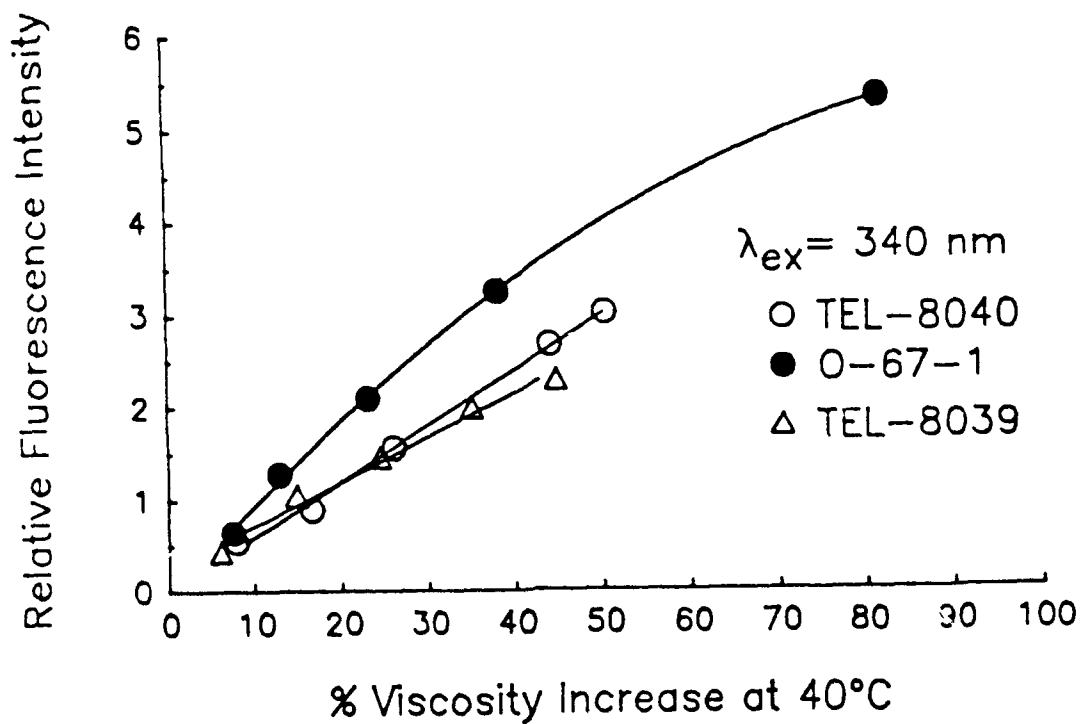


Figure 73. Relationship of Fluorescence Intensity to Viscosity Increase for PPFs from GVO Testing at 320°C (Excitation/Emission Wavelengths of 340/365 nm and 400/454 nm.)

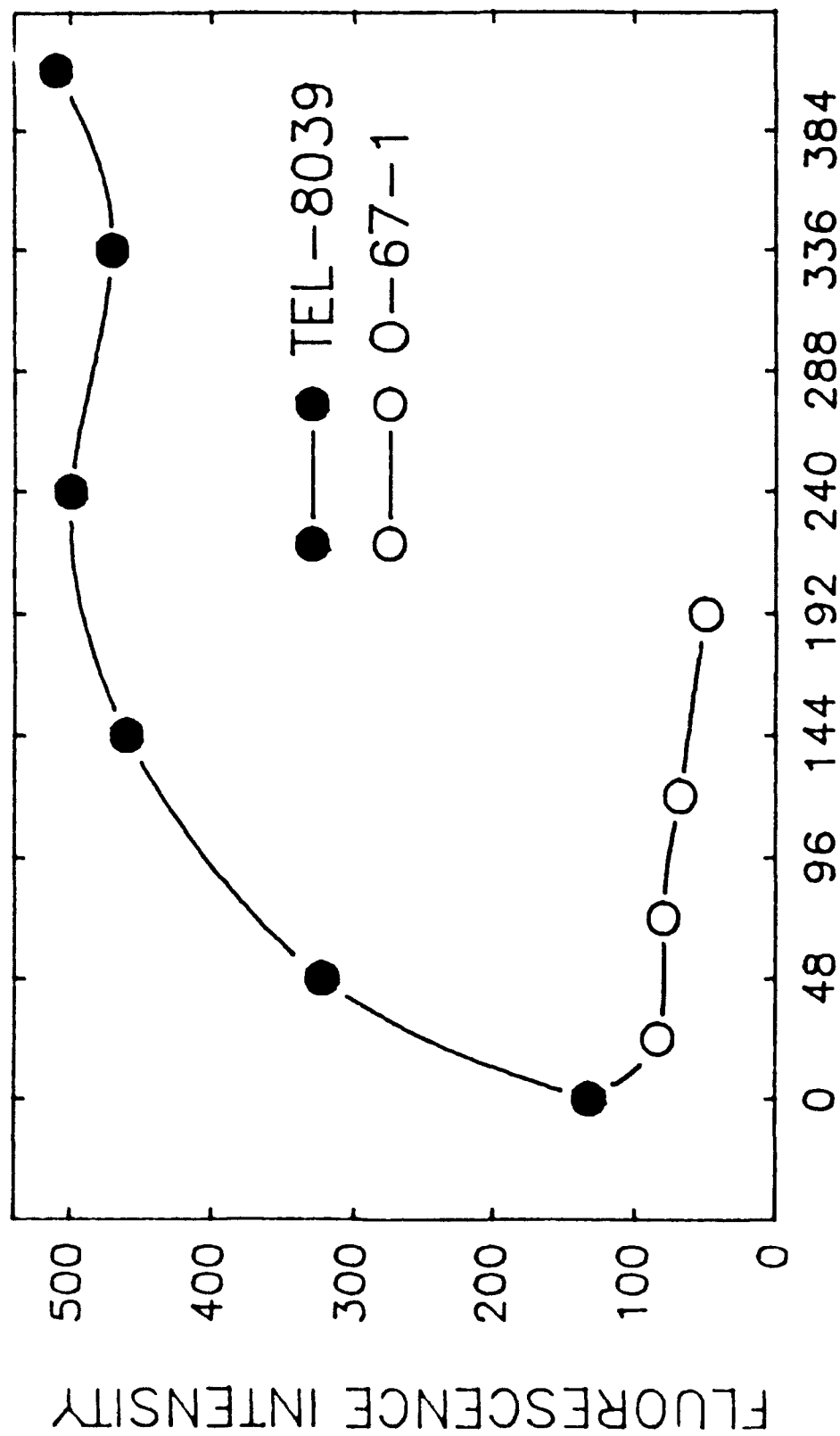
oxidation products present in O-67-1 that were shown to be absent in TEL-8039 and TEL-8040 result in an increase in fluorescence emission intensity disproportionate to viscosity increases. Nevertheless, the data show that a useful relationship exists between emission intensity and oxidation of PPEs.

g. Quantitative Fluorescence Measurements on Neat Polyphenyl Ethers

Since simplicity of use is a desirable property of any monitoring technique, it would be advantageous to eliminate the weighing and volumetric dilution steps necessary to measure fluorescence of dilute PPE solutions. Since the proper accessories for this type of analysis could not be found, fluorescence measurements were made on thick or thin films of the lubricants on glass slides using the TLC accessory.

(1) Fluorescence Measurements on Thick PPE Films

Initial measurements on PPE films using the TLC accessory were performed on films of unrestricted (fairly large) thicknesses on glass slides. In this manner a series of oxidation and corrosion tested O-67-1 and TEL-8039 PPE lubricants were measured by fluorescence using the previously described instrumental conditions, including an excitation/emission wavelength selection of 396/454 nm. The results of such analyses with dilute solutions had shown that O-67-1 displayed higher fluorescence with stressing time than TEL-8039 but that both lubricants gave similar results when weighed against physical property changes. The results on thick films (Figure 74) show that O-67-1 decreases in fluorescence intensity with time while TEL-8039 increases in intensity until leveling out at about 144 hours. The cause of this behavior is probably due to inner absorption effects (absorption of fluorescence emission by compounds present in the lubricant) that produced similar behavior in concentrated solutions. Since the fluorescence emission is in the visible range, the extreme darkening of O-67-1 causes much larger



TEST HOURS

Figure 74. Fluorescence Intensity of Thick Films of PPI's from the Corrosion and oxidation Test at 320°C. (Excitation/Emission wavelengths of 396/454 nm)

inner absorption effects than the lightly discolored TEL-8039 which accounts for the extreme differences between the fluorescence intensities.

(2) Fluorescence Measurements on Thin PPE Films

In order to reduce the inner absorption effects that were noted on thick films of PPE, an assembly was made that produced a film thickness of about 0.20 mm. This was made by epoxying two glass slides of about 0.15 mm thick onto a larger glass slide, placing the lubricant between the two slides and squeezing out the excess lubricant by firmly placing another glass slide on top. Using this assembly, oxidatively stressed PPEs were analyzed as previously and although the inner absorption effects were less troublesome, the TEL-8039 lubricants gave consistently higher readings than the O-67-1 lubricants.

To further reduce the inner absorption effects, the excitation/emission wavelengths were changed to 450/520 nm since this would reduce the total absorption and fluorescence emission in the lubricant sample. The results of these analyses (Figure 75) show that the oxidatively stressed O-67-1 displays higher fluorescence readings than TEL-8039 up to about 72 hours. Beyond this point, the O-67-1 lubricant levels off indicating that the inner absorption effects are still significant.

(3) Fluorescence Measurements on Very Thin PPE Films

Very thin films of the oxidatively stressed PPE lubricants were made by placing a small drop between two glass slides and applying force until a thin film formed. Although this technique would not be expected to produce a uniform and consistent film, fluorescence intensity measurements on the two PPE lubricants (Figure 76) show that the readings are much more consistent with their physical property changes, yielding results similar to those using dilute solutions.

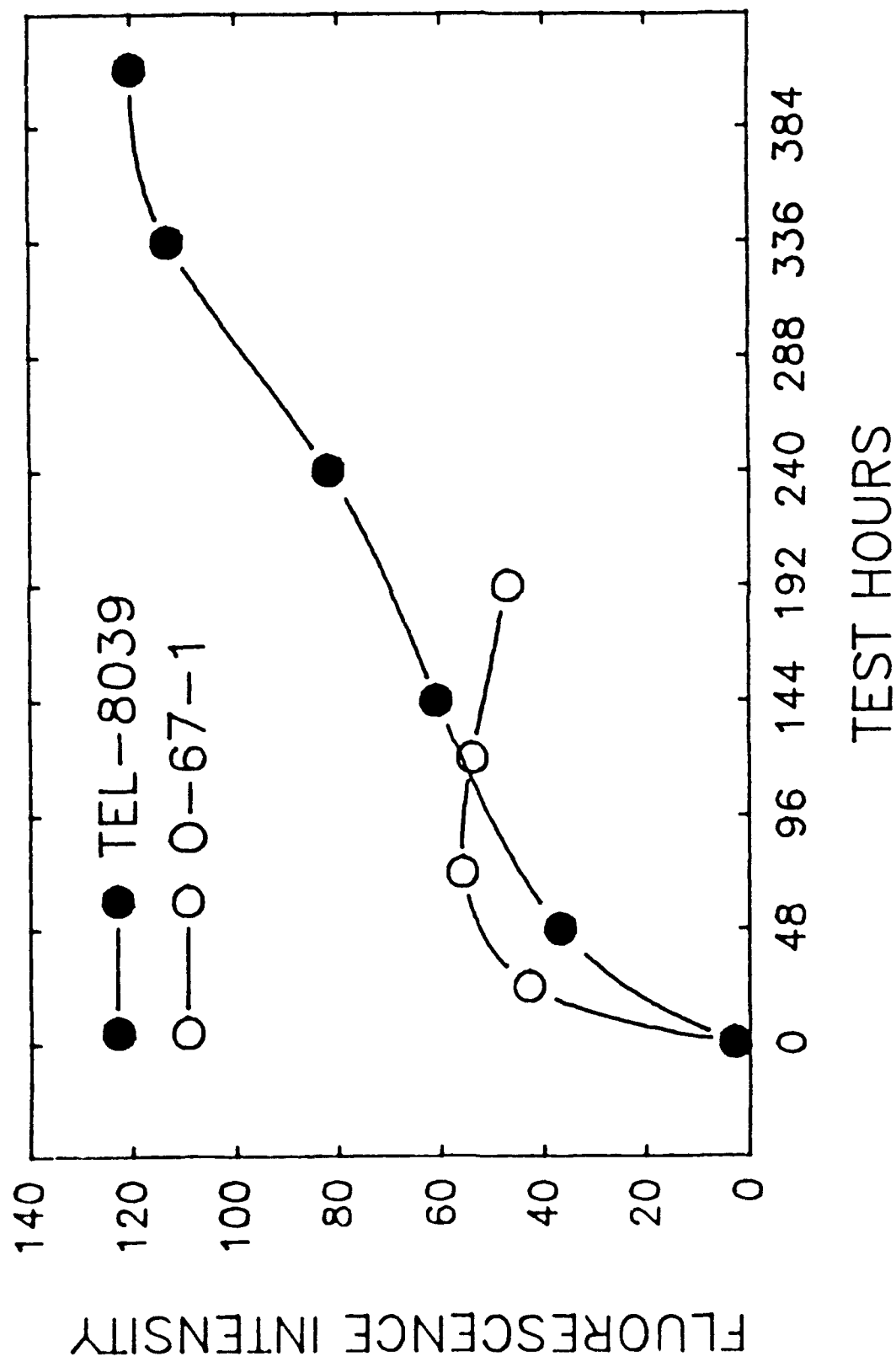


Figure 75. Fluorescence Intensity of Thin Films of PPEs from the Corrosion and Oxidation test at 320°C (Excitation/Emission Wavelengths of 450/520 nm)

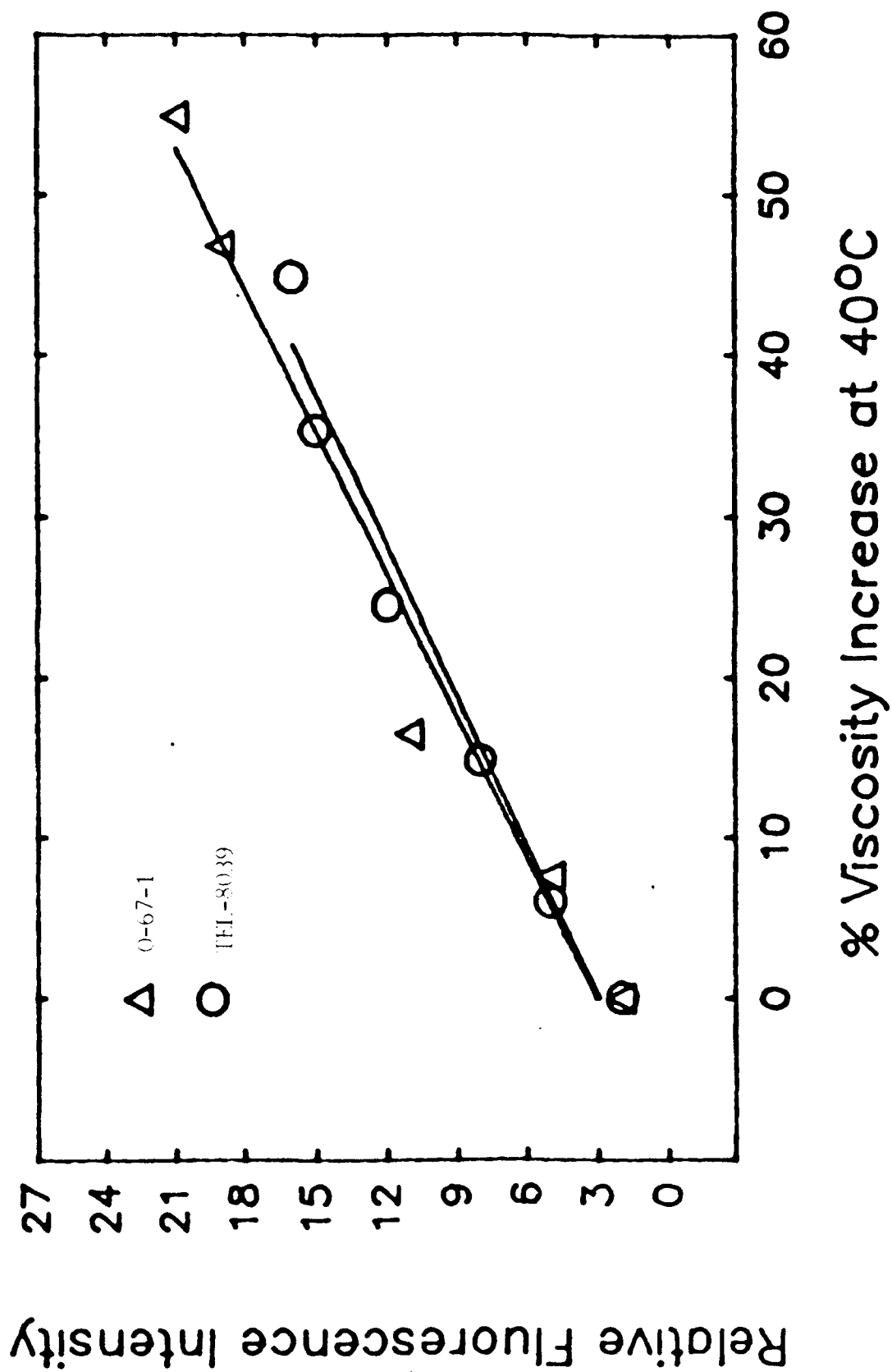


Figure 76. Fluorescence Intensity of Very Thin Films of PPFs from the Corrosion and Oxidation Test at 320°C (Excitation/Emission Wavelengths of 450/520 nm)

h. Conclusions

Fluorescence spectroscopy measurements of polyphenyl ether lubricants indicate that specific changes occur in its emission spectra during oxidative degradation of the fluid. Analysis of dilute solutions of a series of two different formulations of oxidatively stressed polyphenyl ethers at two separate excitation/emission wavelengths yields a mostly linear relationship between emission intensity and viscosity increases of the lubricant. In order to measure the fluorescence emission of neat polyphenyl ethers, severe spectral distortion, which is likely the result of inner absorption effects, was minimized by using very thin lubricant films. Under these conditions, a similar linear relationship between emission intensity and viscosity increase is observed and thus offers a simple technique for monitoring the condition of polyphenyl ether lubricants.

3. DIELECTRIC CONSTANT (DC) MEASUREMENTS AT EXTENDED CELL TEMPERATURES

a. Introduction

Previously, it was found that dielectric constant (DC) measurements of oxidatively stressed polyphenyl ethers (PPEs) decreased with time, a trend that was exactly opposite of oxidized ester lubricants.¹² A new DC instrument with a heated cell (Model NI-100) was received on loan from Northern Instruments Corporation (NIC) and used to measure oxidatively stressed PPEs. Conversations with NIC revealed this instrument to be very similar to the Lubri Sensor instrument used to make the previous DC measurements. That is, both instruments use a 5 MHz capacitance bridge and the same flat measuring cell. The NI-100 is not calibrated with a fresh oil like the Lubri Sensor but instead gives a reading in dimensionless units. The NI-100 appeared to be somewhat less sensitive and precise than the Lubri Sensor. Empirically it was determined that 50 μ A on the Lubri Sensor equaled

approximately 0.35 units on the NI-100 and that repeatability on the latter instrument was about 0.05 units.

b. DC Readings of Fresh PPEs at Various Temperatures

DC measurements on a fresh PPE (O-77-6) were made at cell temperatures from 30 to 80°C. The results (Figure 77) show that the DC reaches a maxima at about 40°C and then decreases with increasing temperature. This behavior is unusual in that, generally speaking, organic liquids will undergo a decrease in DC with increasing temperatures and the contrast can be seen with that of O-79-17 (MIL-L-7808), also in Figure 77, which shows only a decrease in DC with increasing temperature over the same temperature range. This behavior is due to the dipole moment contribution to the DC, and involves alignment of the permanent dipole with the electric field, which decreases with increasing temperature due to greater kinetic molecular motion. Also contributing to this effect are decreases in the density of the fluid. It can be speculated that the intermolecular forces in the PPE that make the fluid quite viscous at room temperature also inhibit dipole alignment and decrease the contribution of this effect to DC. As the lubricant is heated, increasing kinetic molecular motion decreases these intermolecular forces and facilitates dipole alignment and increases the DC of the fluid. It should be noted that the maxima in Figure 77 corresponds approximately to the point where the viscous PPE lubricant starts to become noticeably thinner. Further heating beyond this point only decreases the dipole alignment contribution and the DC decreases.

One compound reported to display similar temperature/DC maxima characteristics was glycerol.¹³ Furthermore, this phenomenon displayed a frequency dependence with a DC maxima at -40°C for a 1 kHz frequency increasing to +15°C for a 6000 kHz frequency. It would be expected that

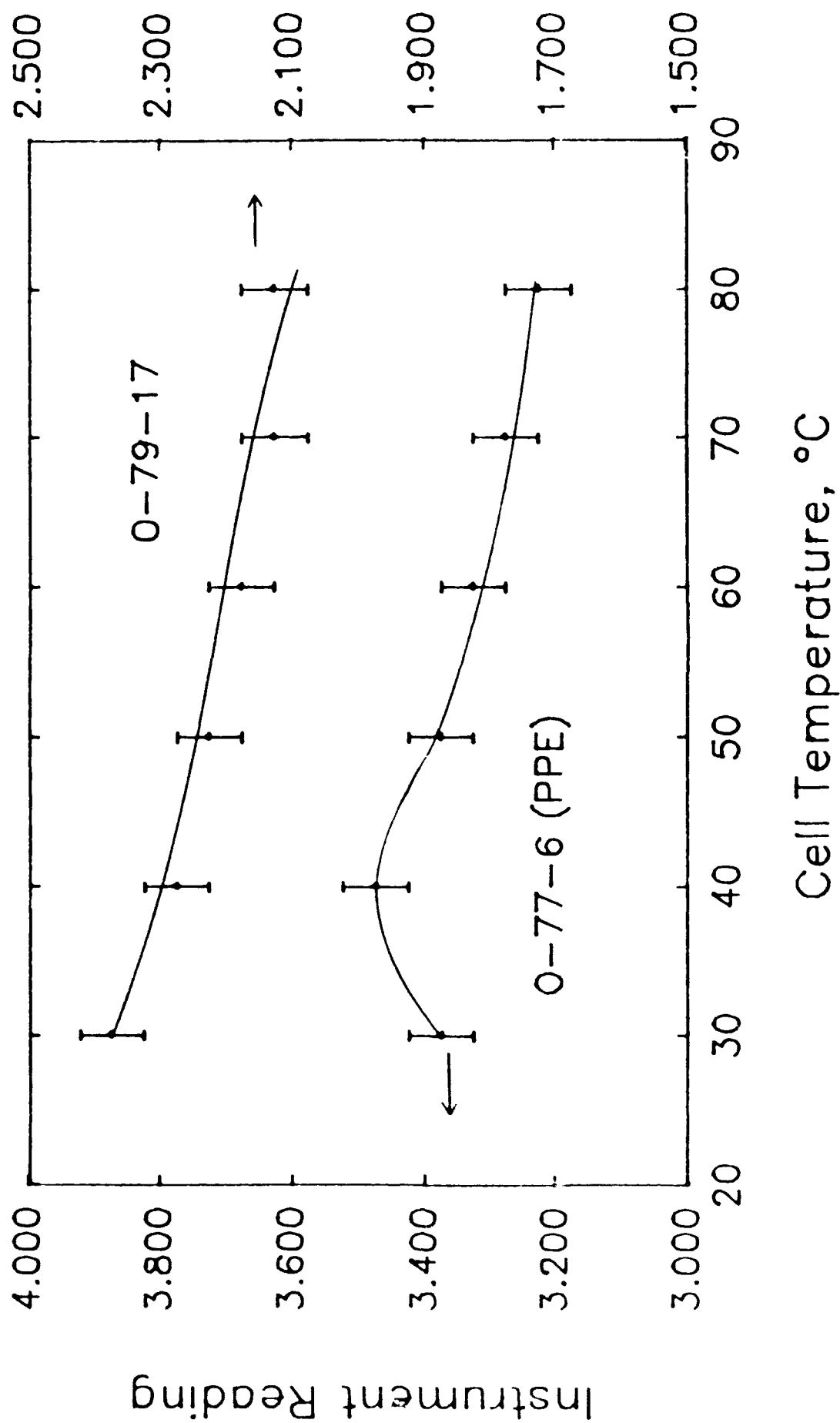


Figure 77. Relationship of Dielectric Constant to Temperature for a MIL-L-7503 (0-79-17) and a PFF (0-77-6) Lubricant

increasing the field frequency would make molecular dipole alignment more difficult, especially when strong intermolecular forces are present. PPE would likely show similar behavior but the NI-100 uses a fixed 5 MHz bridge and so it was not possible to do the necessary experiments.

c. DC Readings of Stressed PPEs at Different Cell Temperatures

The effect of cell temperature on DC readings of stressed PPEs was determined by measuring the DC of samples of O-67-1 from the corrosion and oxidation test at 320°C at cell temperatures of 30 and 50°C. The results (Figure 78) show the 30°C DC readings decrease steadily with stressing time, a phenomenon that had been observed with the Lubri Sensor. The 50°C readings, however, show very little change in DC readings with only 0.05 units difference between the fresh and 240 hour stressed lubricant. It had been assumed that the DC of the stressed PPEs dropped because of the presence of high molecular weight oxidation products which possessed a lower DC than the original 5P4E basestock. These results seem to indicate that the DC drop is due to an inhibition of the dipole alignment by increasing intermolecular forces brought on by the presence of high molecular weight oxidation products. At higher temperatures (e.g., 50°C) these forces are sufficiently disrupted such that little or no DC decrease is observed. Similar results were obtained for stressed TEL-8039.

d. DC Readings of MIL-L-7808 Oils at Different Cell Temperatures

It should be possible to observe similar types of effects in ester based lubricants that have been heavily oxidized and thus contain high molecular weight oxidation products. Thus DC measurements using NI-100 were made at 30°C and 50°C on five MIL-L-7808 oils stressed in the Squires oxidative test at 190°C. For comparison, similar measurements were made on the same five lubricants stressed in the Squires confined heat test at 190°C.

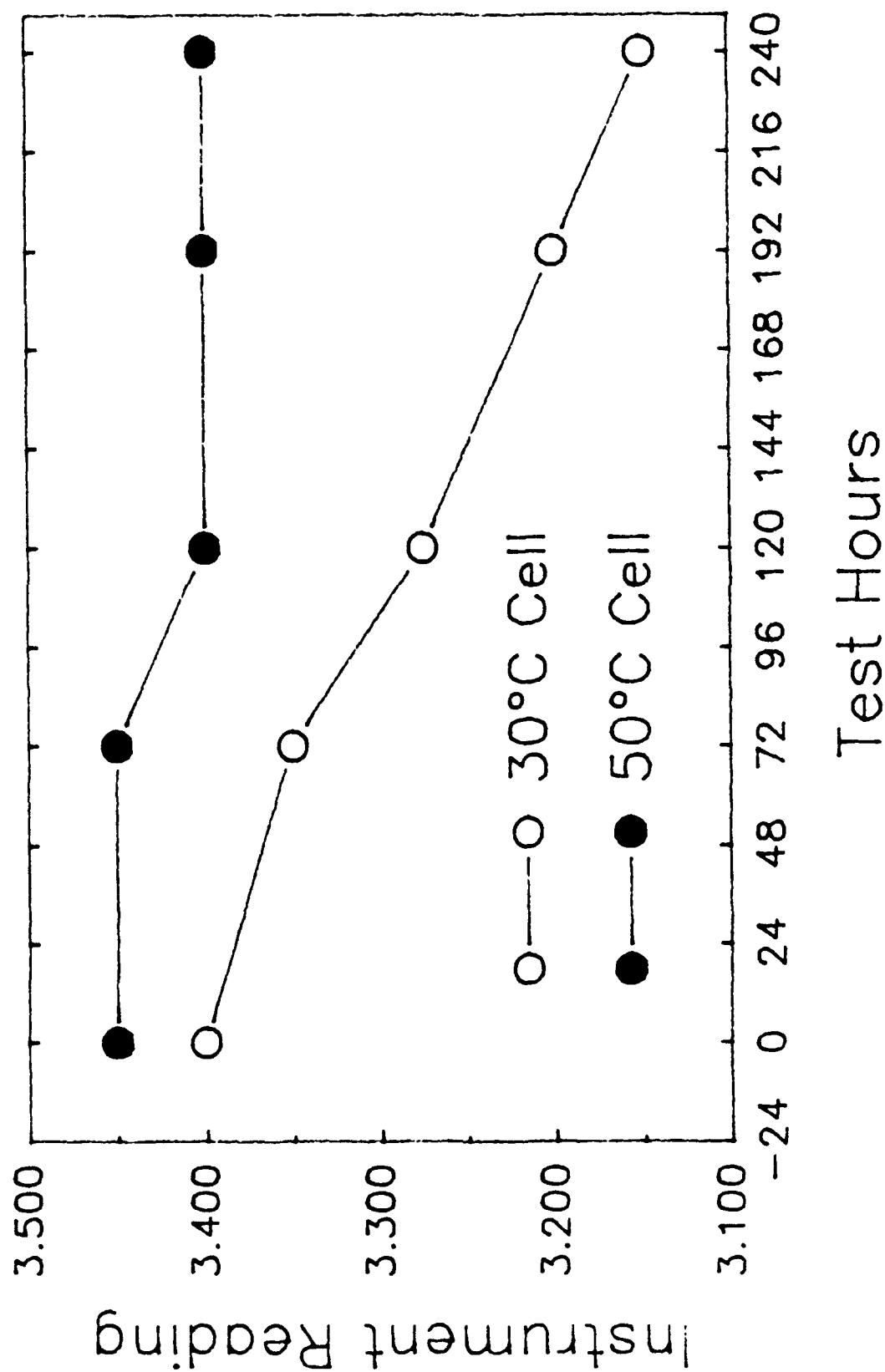


Figure 78. Dielectric Constant Readings at 30°C and 50°C of a PPE (O-67-1) from the Corrosion and Oxidation Test at 320°C

The results of these measurements for O-79-17, which are typical for all the data, are shown in Figure 79. The Confined Heat tested lubricant shows a 0.10 to 0.15 unit difference between the 30 and 50°C cell temperature measurements that remains fairly constant throughout the entire test. This would be expected since oxidative degradation and viscosity changes in the lubricant are generally small in this test. The oxidative test samples show similar results until oxidation and viscosity changes become rather large and the final sample (576 hours) actually shows a higher DC reading at 50°C than at 30°C. All five lubricants tested showed similar results although the magnitude varied somewhat.

It was also noted in the above data that all of the Squires oxidatively tested lubricants displayed positive changes in DC, as displayed in Figure 80 for 50°C cell temperature. This is quite different than the Lubri Sensor data for the six MIL-L-7808 lubricants tested which showed two oils increased, two oils decreased and two oils did not change DC readings.¹² Apparently some of the oils are more severely influenced by these dipole alignment inhibition effects but are largely eliminated by sufficient thermal energy.

e. Conclusions

Using a DC Tester with a heated cell eliminated the DC signal decay with stressed polyphenyl ethers. Measurement of oxidatively stressed polyphenyl ethers at 30 and 50°C cell temperatures indicates that the decrease in DC observed at room temperature for these fluids is due to an increasing high molecular weight oxidation product content. The resulting increase in viscosity inhibits the dipole alignment contribution to DC. At sufficiently high temperatures (50°C), the intermolecular forces responsible for the viscosity increase are disrupted enough such that the previously

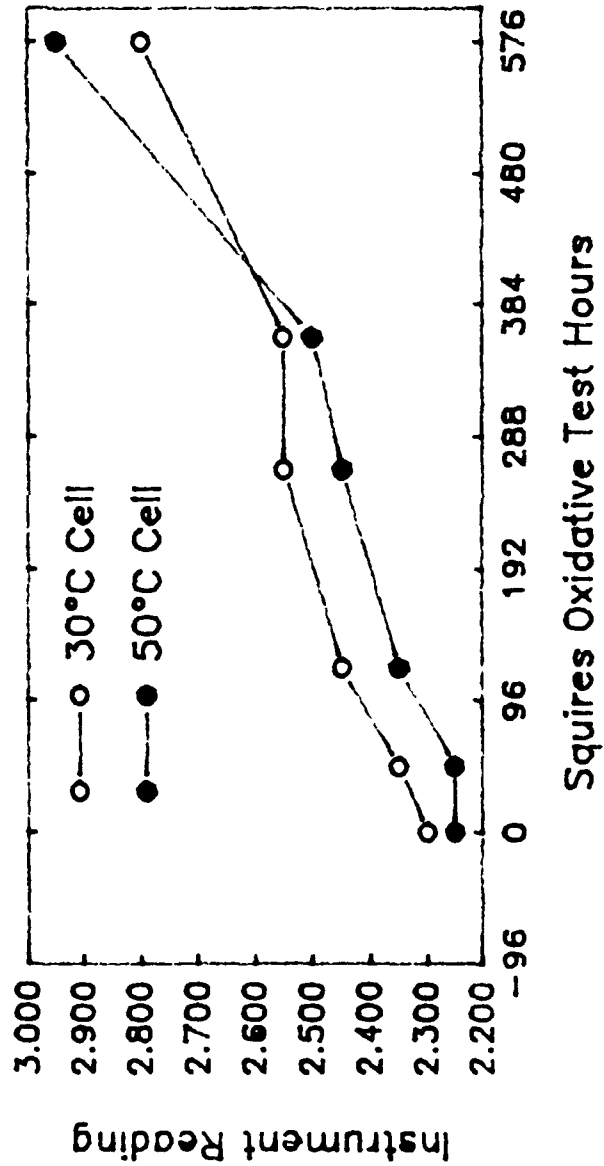
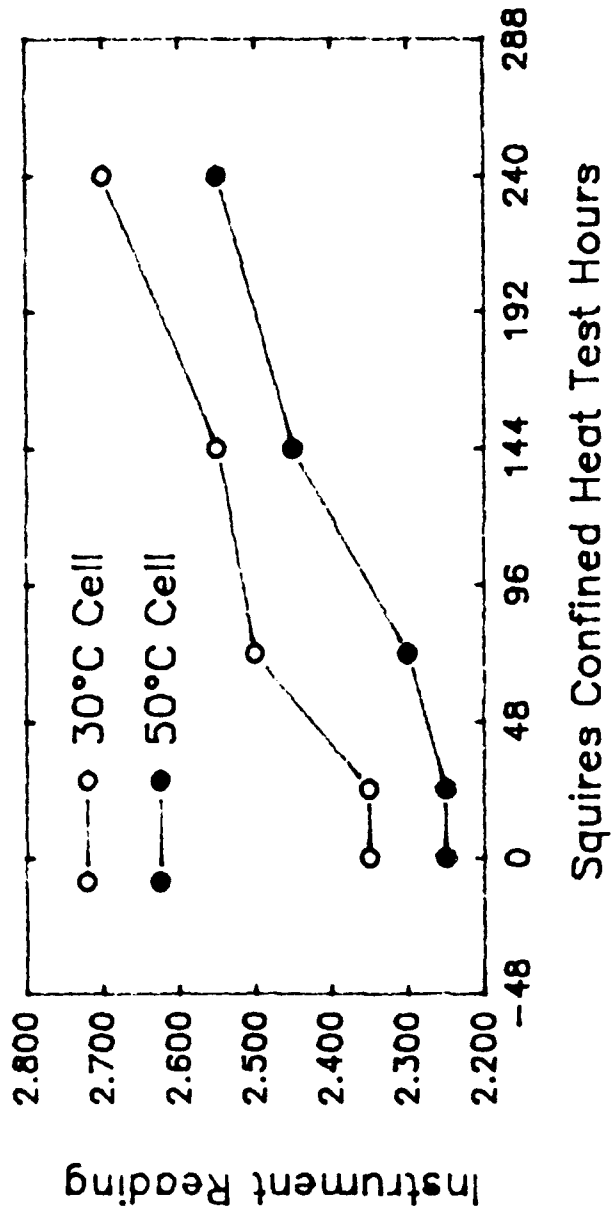


Figure 79. Dielectric Constant Readings at 30°C and 50°C for a MIL-L-7808 (0-79-17) Lubricant from the Squires Confined Heat Test and Squires Oxidative Test at 190°C

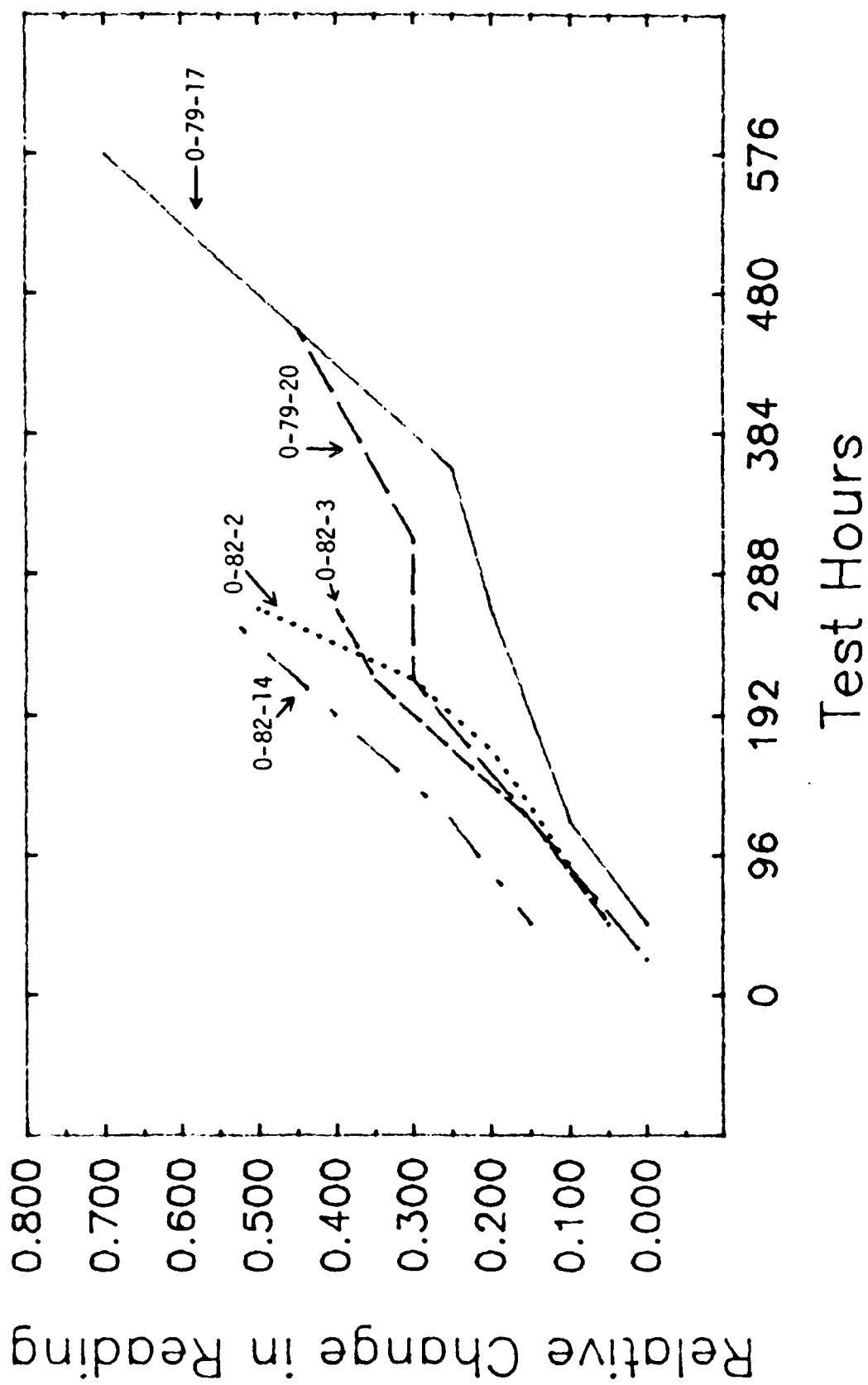


Figure 80. Dielectric Constant Readings at 50°C for MIL-L-7808 Lubricants from the Squires Oxidative Test at 190°C

observed DC decrease is eliminated. Similar effects were noted with heavily oxidized ester-based oils. Based on this data, it appears that a DC tester with a heated cell would be a superior instrument for monitoring both esters and polyphenyl ethers relative to the Lubri Sensor.

4. THERMAL ANALYSIS

a. Introduction

During this investigation, accelerated thermal analysis techniques were investigated for use with polyphenyl ether based lubricants. The investigated analytical techniques use thermal-oxidative stressing to rapidly deplete the antioxidants of the lubricant. Once the antioxidants become ineffective, the basestock of the lubricant rapidly degrades. The different thermal analytical techniques then use various methods to detect the onset time (isothermal conditions) or onset temperature (ramped temperature conditions) at which the rapid degradation of the basestock begins. The length of the onset time or the value of the onset temperature is then used to evaluate the oxidative stability of the lubricant.

The initial investigation concentrated on differential scanning calorimetric (DSC), high pressure (HP-DSC) and sealed pan (SP-DSC), techniques and on thermal gravimetric (TGA) analytical techniques since they are fully developed for lubricant analysis. The DSC and TGA techniques are well-suited for evaluating small quantities of candidate fluids since the techniques require less than 1 mL of lubricant and less than one hour to perform. The initial evaluations of the DSC and TGA techniques were performed using fresh O-77-6 polyphenyl ether (5P4E) basestock, fresh O-67-1 polyphenyl ether (5P4E) lubricant, and stressed (320°C) O-67-1 lubricants.

b. Sealed-Pan DSC

Previous research¹⁴ has shown that the oxidative stabilities of

laboratory stressed MIL-L-7808 type lubricating oils can be accurately evaluated using SP-DSC techniques. For this investigation, the SP-DSC technique used a sample size of 0.2 -2.0 μ L, a temperature range of 200-500 $^{\circ}$ C, a temperature ramp rate of 20 $^{\circ}$ C/minute, and an oxygen atmosphere (pan sealed inside a glove bag filled with oxygen).

As an initial evaluation of SP-DSC capability to measure oxidative stabilities of stressed polyphenyl ether oils, O-77-6 polyphenyl ether basestock and the fresh and 24 hour (320 $^{\circ}$ C) stressed O-67-1 polyphenyl ether oils were studied. The thermograms of the O-77-6 basestock and O-67-1 oils shown in Figure 81 contain exotherms at 340 $^{\circ}$ C which are related to the sealed sample pan (verified by performing SP-DSC analyses on empty pans).

The thermograms show that the O-77-6 basestock and the fresh O-67-1 oil undergo oxidation to produce exotherms of similar size in the temperature range of 375-450 $^{\circ}$ C. In contrast to the O-77-6 basestock and fresh O-67-1 oil, the 24 hour stressed O-67-1 oil does not produce an exotherm in the 375-450 $^{\circ}$ C temperature range. The exotherms (peak heights less than 0.5 mW) produced by the O-77-6 basestock and fresh O-67-1 oil are much smaller than the exotherms (peak heights greater than 6 mW) produced by the SP-DSC analyses of the MIL-L-7808 oils.¹⁴

The thermograms in Figure 81 indicate that the O-77-6 polyphenyl ether basestock undergoes a minimal amount of oxidation in the 375-450 $^{\circ}$ C temperature range which is not inhibited by the presence of an antioxidant (fresh O-67-1). However, once the antioxidant has changed form (24 hour stressed O-67-1 oil), the formulated 5P4E fluid does not oxidize (no exotherm) in the 375-450 $^{\circ}$ C temperature range.

The 24, 72, 120 and 192 hour 32 $^{\circ}$ C stressed O-67-1 oils were then evaluated for determining the effects of varying degrees of thermal-oxidation

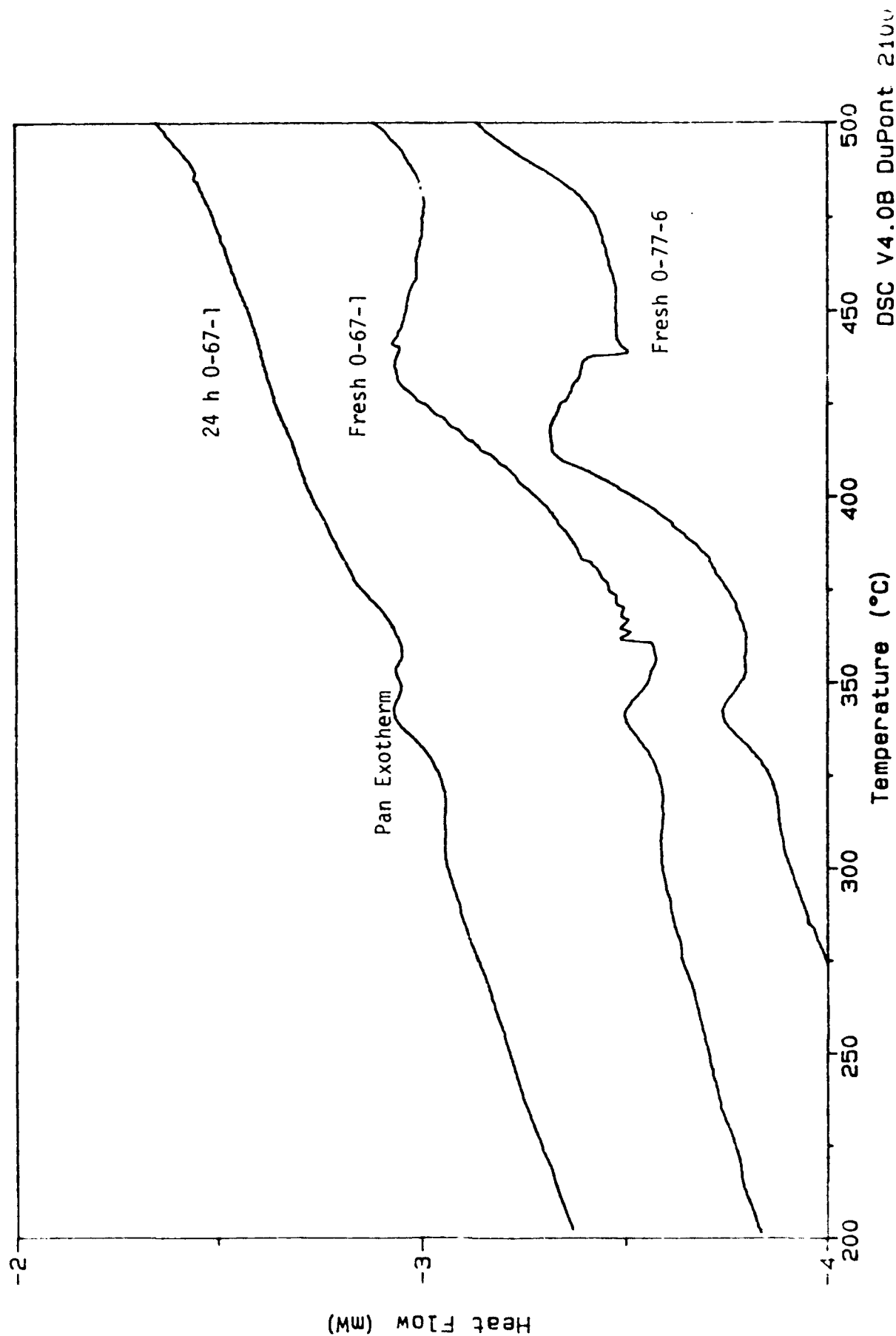


Figure 41. Sealed Pan-DSC Thermograms (200-500°C, 20°C/Minute Heating Rate) of the Fresh 0-77-6 Polyphenyl Ether Basestock and the Fresh and 24 Hour 320°C Stressed 0-67-1 Polyphenyl Ether Oils

on the SP-DSC analyses of polyphenyl ether oils. The thermograms of the 24-192 hour stressed O-67-1 oils shown in Figure 82 indicate that the polyphenyl ether basestock becomes more susceptible to oxidation (size of the exotherm increases) as the stressing time increases from 24-192 hours. Exotherms due to the basestock would be expected to remain constant in size as the stressing time increases.

In contrast to the MIL-L-7808 type oils,¹⁴ the temperature range in which the exotherms occur in Figure 82 is not affected by the stressing time of the oil sample, i.e., as the thermal-oxidation stability decreases, the onset temperature decreases. These results indicate that thermal-oxidation products of the polyphenyl ether basestock which increase with stressing time at 320°C are responsible for producing the exotherms in the 375-450°C temperature range.

Since the exotherms in Figures 81 and 82 are much smaller than expected, the effects of increasing the sample size on the produced thermograms were studied for the 192 hour stressed O-67-1 oil (largest exotherm in Figure 82). The sample sizes of 0.2 and 2.0 μ L were used for this study. The thermograms produced by the 0.2 and 2.0 μ L samples of the 192 hour stressed O-67-1 oil are shown in Figure 83.

Since the analyses are run in a sealed pan, the amount of oxygen available for reaction with the polyphenyl ether basestock is limited. Consequently, increasing the sample size above the 0.2 μ L optimal quantity was expected to have no effect or to decrease the size of the exotherm. As shown in Figure 83, the size of the exotherm produced by the 192 hour stressed oil is greatly increased by increasing the sample size from 0.2 to 2.0 μ L. These results again indicate that thermal-oxidation products (small concentration in stressed fluid does not deplete oxygen in sealed pan) of the

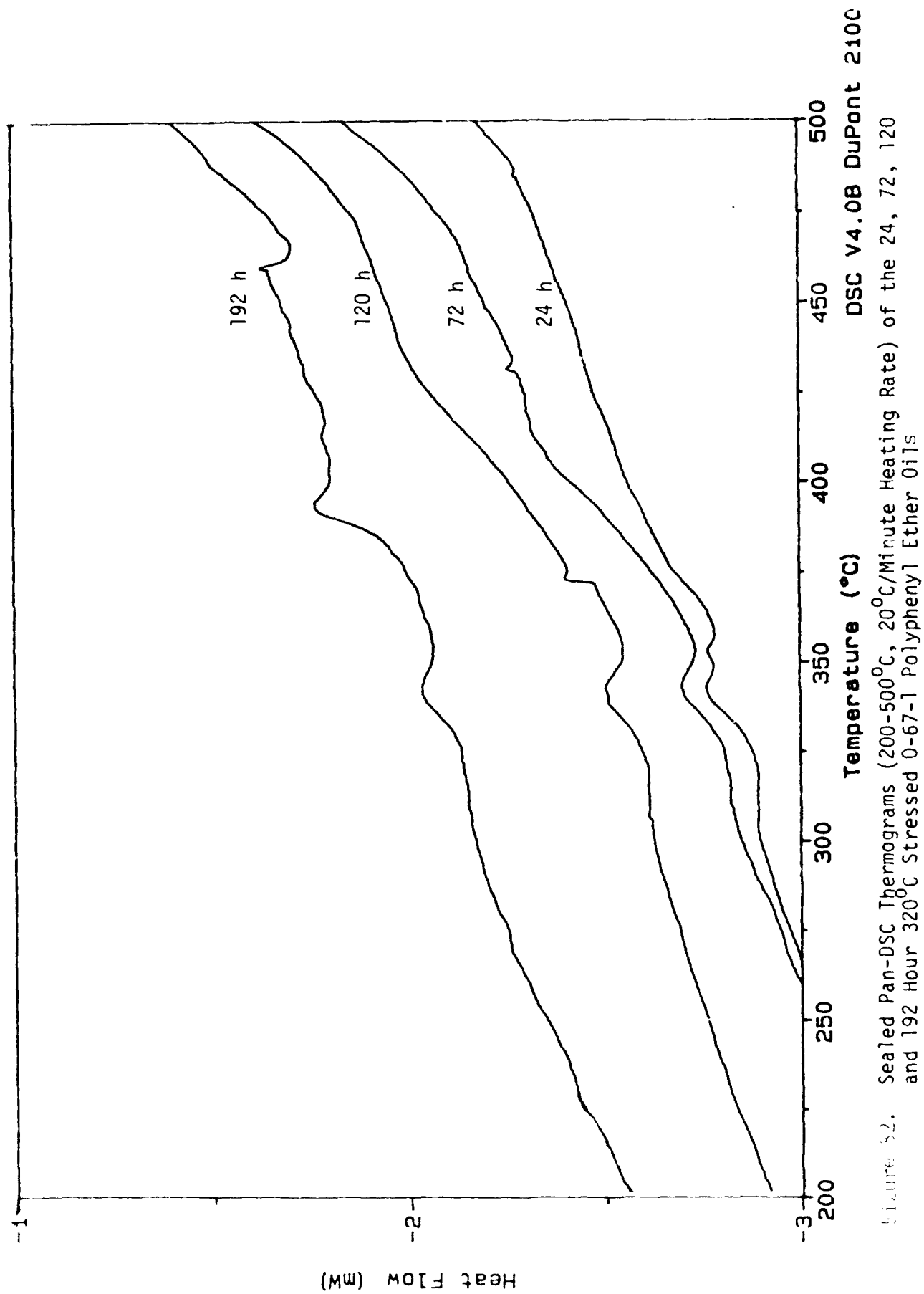
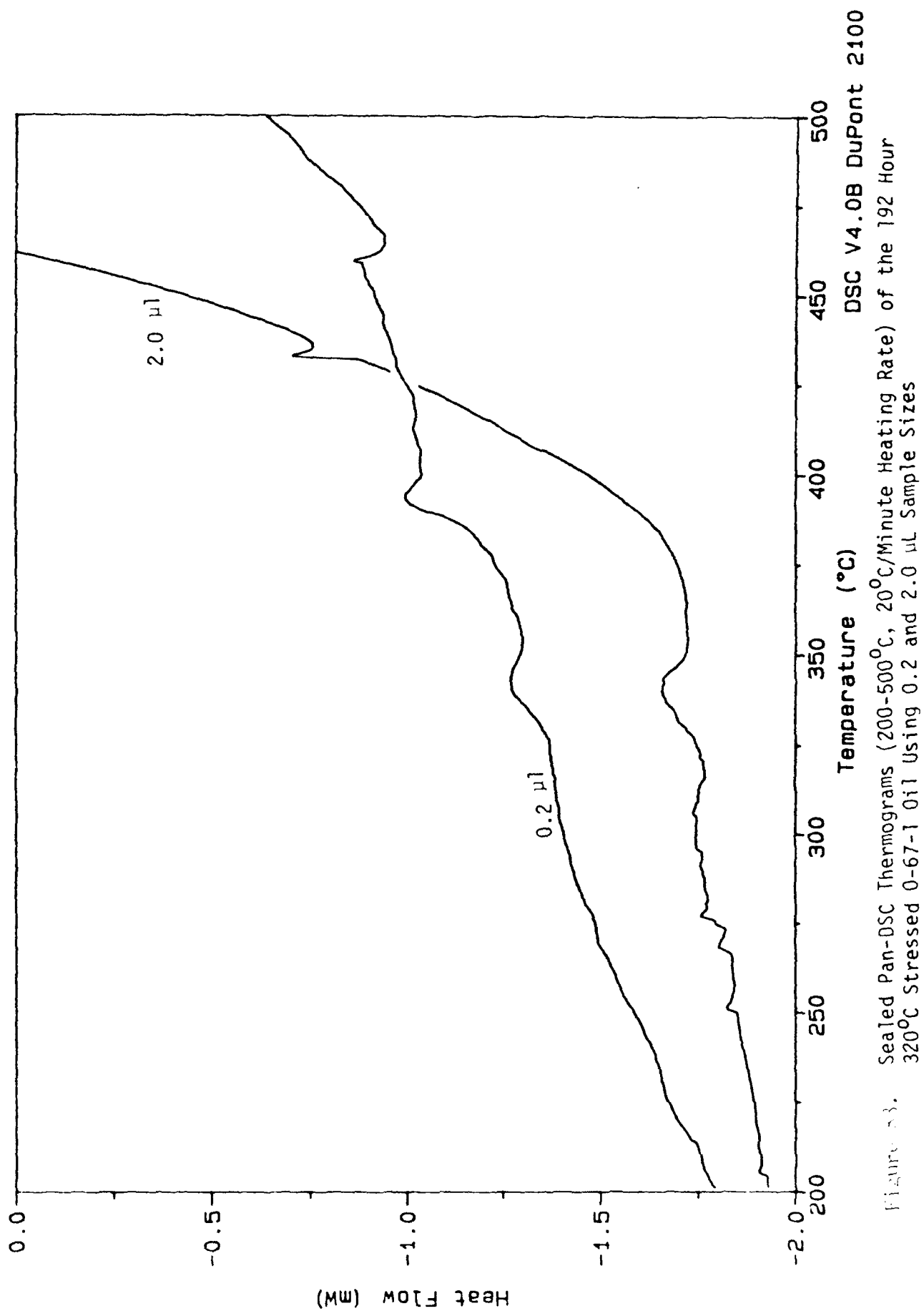


Figure 52. Sealed Pan-DSC Thermograms (200-500°C, 20°C/Minute Heating Rate) of the 24, 72, 120 and 192 Hour 320°C Stressed 0-67-1 Polyphenyl Ether Oils



polyphenyl ether basestock are responsible for the exotherms in the 375-450°C range shown in Figures 81-83. The results in Figure 83 also indicate that the optimal sample size used for the SP-DSC analyses of MIL-L-7808 type oils will need to be reoptimized for the SP-DSC analyses of polyphenyl ether based oils.

c. Thermogravimetric Analysis

Since the SP-DSC analyses were not able to detect the exotherms produced by the oxidation of the polyphenyl ether basestocks of the fresh or stressed O-67-1 oils, TGA was used to analyze the 24 and 192 hour stressed O-67-1 oils. In previous TGA work² it was shown that fresh O-67-1 oil became volatile (more than 5% weight loss) in a nitrogen atmosphere at 275°C. The thermograms of the 24 and 192 hour O-67-1 oils in Figure 84 were produced in an air atmosphere using a 25°C/minute heating rate and a 10 mg sample size.

The thermograms in Figure 84 demonstrate that the 24 and 192 hour samples are oxidatively stable (less than 5% weight loss) up to temperatures of 275°C. Thus the O-67-1 oils become volatile at temperatures below the temperature needed to oxidize the oils.

In addition to the vaporization of the polyphenyl ether basestocks, the thermograms in Figure 84 indicate that the 192 hour sample contains higher molecular weight species (weight loss in 320-450°C range) which are not present in the 24 hour sample. The higher molecular weight species are most likely the dimer and higher polymers of the polyphenyl ether basestock which were previously identified² in the 192 hour sample. The final weight loss in the TGA thermogram of the 192 hour sample in Figure 84 occurs in the same temperature range as the exotherm in the SP-DSC thermogram of the 192 hour sample in Figure 83.

Thus, the TGA results also indicate that the exotherms in the SP-DSC

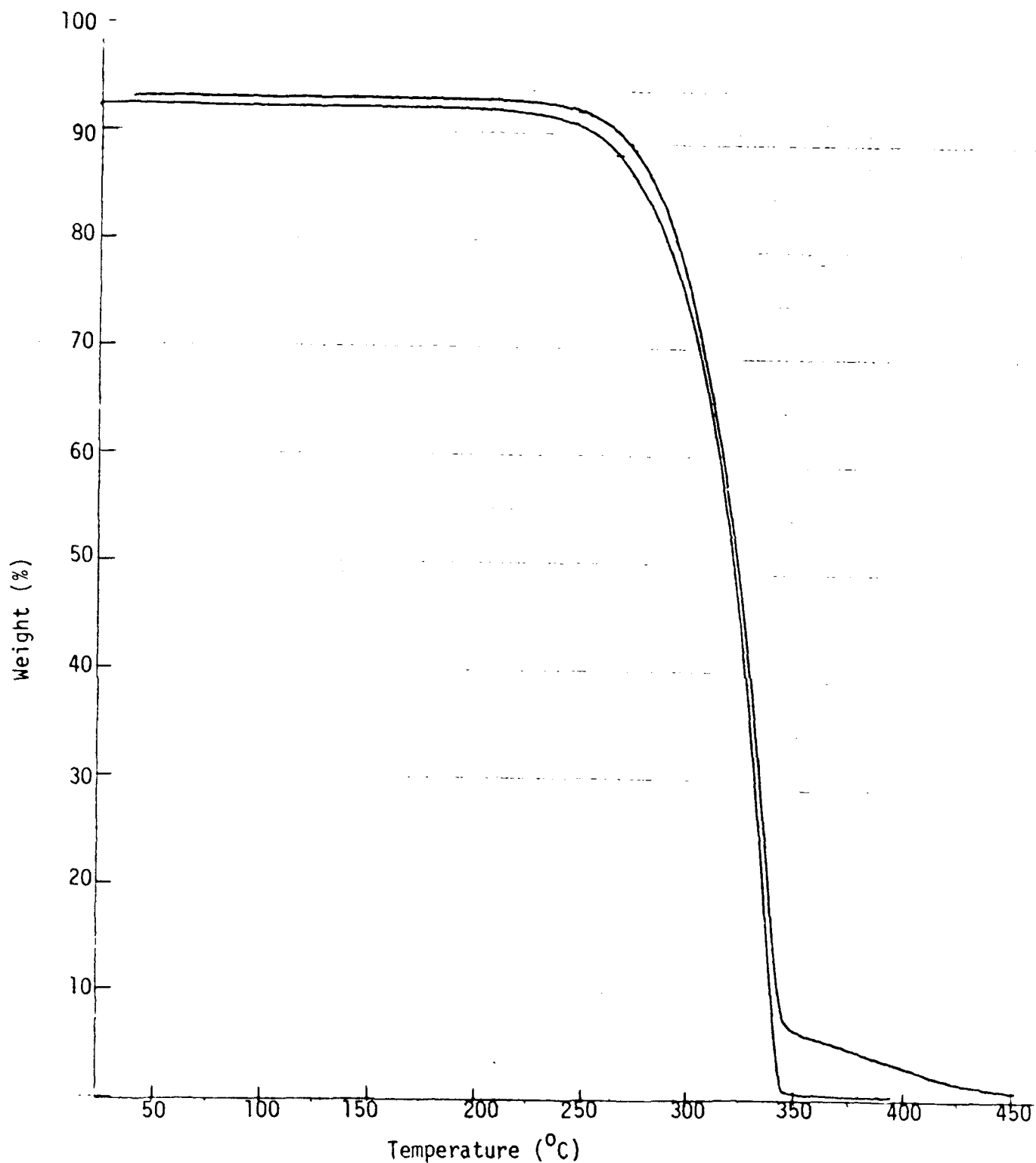


Figure 84. TGA Thermograms (25-400°C, 25°C/Minute Heating Rate) of the 24 and 192 Hour 320°C Stressed 0-67-1 Polyphenyl Ether Oils

thermograms of the 24-192 hour stressed O-67-1 oils (Figure 82) are produced by the oxidation products of the basestock which increase with stressing time.

d. High Pressure DSC

Since the TGA results indicated that the polyphenyl ether basestock of the O-67-1 oils was vaporizing prior to oxidation, HP-DSC analyses of the fresh and stressed O-67-1 oils were performed under high pressure (HP-DSC) to reduce the vaporization of the polyphenyl ether basestock prior to oxidation. The HP-DSC analyses were performed in an air atmosphere of 500 psig, using a sample size of approximately 30 mg and using a heating rate of 25°C/min from 25 to 475°C.

The HP-DSC analyses were performed on fresh and stressed (24, 120 and 240 hours at 320°C) O-67-1 polyphenyl ether based oils. The HP-DSC thermograms of the fresh and the 24 and 120 hour stressed O-67-1 oils are shown in Figure 85. As expected the rate of oxidation (initial slope of the exotherm) for the O-67-1 oils in Figure 85 increases with stressing time. However, the 240 hour stressed O-67-1 oil produces an exotherm (Figure 86) which is smaller than the exotherms produced by the 24 and 120 hour stressed oils (Figure 85).

The HP-DSC produced thermograms in Figures 85 and 86 are similar to the thermograms produced by SP-DSC in that the size of the exotherm, and not the time of the exotherm, is more related to stressing time. Thus, it appears that the HP-DSC is also monitoring the oxidation of the high molecular weight degradation products of the polyphenyl ether basestock. Whether the degradation products are produced by the thermal-oxidation stressing test at 320°C or during the HP-DSC test was not determined.

The effects of sample size on HP-DSC analyses of O-67-1 oils were

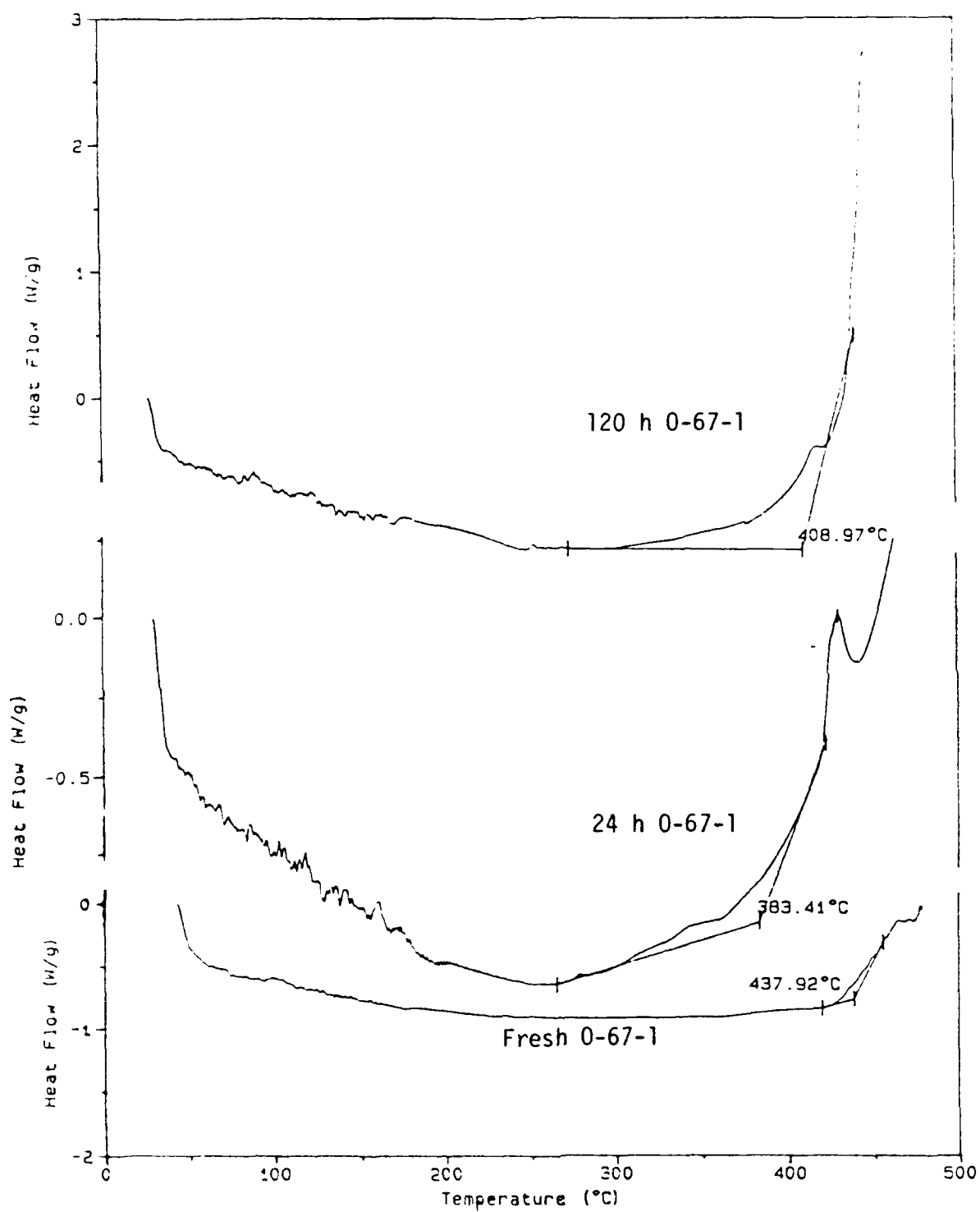


Figure 85. HP-DSC Thermograms Produced by the Fresh and Stressed (24 and 120 Hours at 320°C) 0-67-1 Polyphenyl Ether Oils

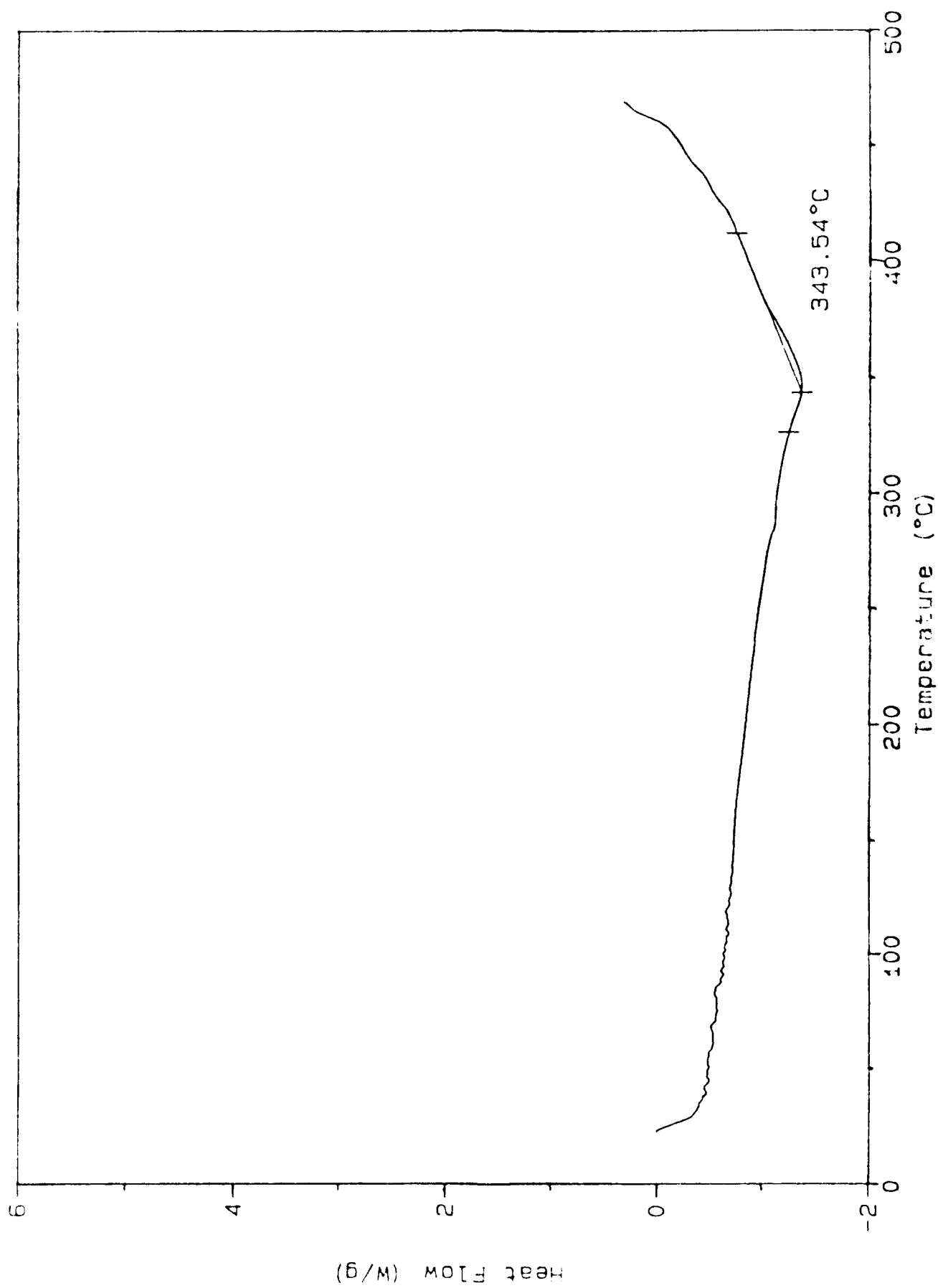


Figure 85. HP-DSC Thermogram Produced by the 240 Hour Stressed (320°C) 0-67-1 Polyphenyl Ether Oil

then studied by reducing the sample size from 25 ± 5 mg to 6.0 ± 0.5 mg. The HP-DSC thermograms produced by the fresh and stressed (24, 120 and 240 hours at 320°C) O-67-1 oils are shown in Figure 87. As expected the 240 hour stressed O-67-1 oil produced the largest exotherm. However, the 120 hour stressed O-67-1 oil produced the smallest exotherm. Consequently, the relationship between the size of the HP-DSC exotherm and the stressing time of the O-67-1 oil appears to be affected by experimental parameters.

e. Summary

The initial HP-DSC studies of the O-67-1 oils are indicating that there is a poor relationship between the HP-DSC results and the stressing time of O-67-1 oils. The initial research has also shown that the exotherms produced by SP-DSC and the residues produced by TGA increase with stressing time and are related to the high molecular weight degradation products of the polyphenyl ether oils.

5. SPECTROPHOTOMETRIC TECHNIQUES

a. Introduction

During this investigation various spectrophotometric techniques were also used to evaluate the chemical changes that occur in the O-67-1 oils during thermal-oxidation. The investigated techniques were based on Fourier transform infrared (FTIR) and ultraviolet-visible (UV-VIS) spectrophotometric methods. Fresh and stressed (24-240 hours at 320°C) O-67-1 polyphenyl ether oils were used for this study.

b. Fourier Transform Infrared Spectroscopy

As shown by the thermal analysis studies and previous research,² the polyphenyl ether basestock of the O-67-1 oil undergoes thermal-oxidation to produce higher molecular weight compounds (dimer, trimer, etc.). Therefore, a study was initiated to determine if FTIR could be used to detect the

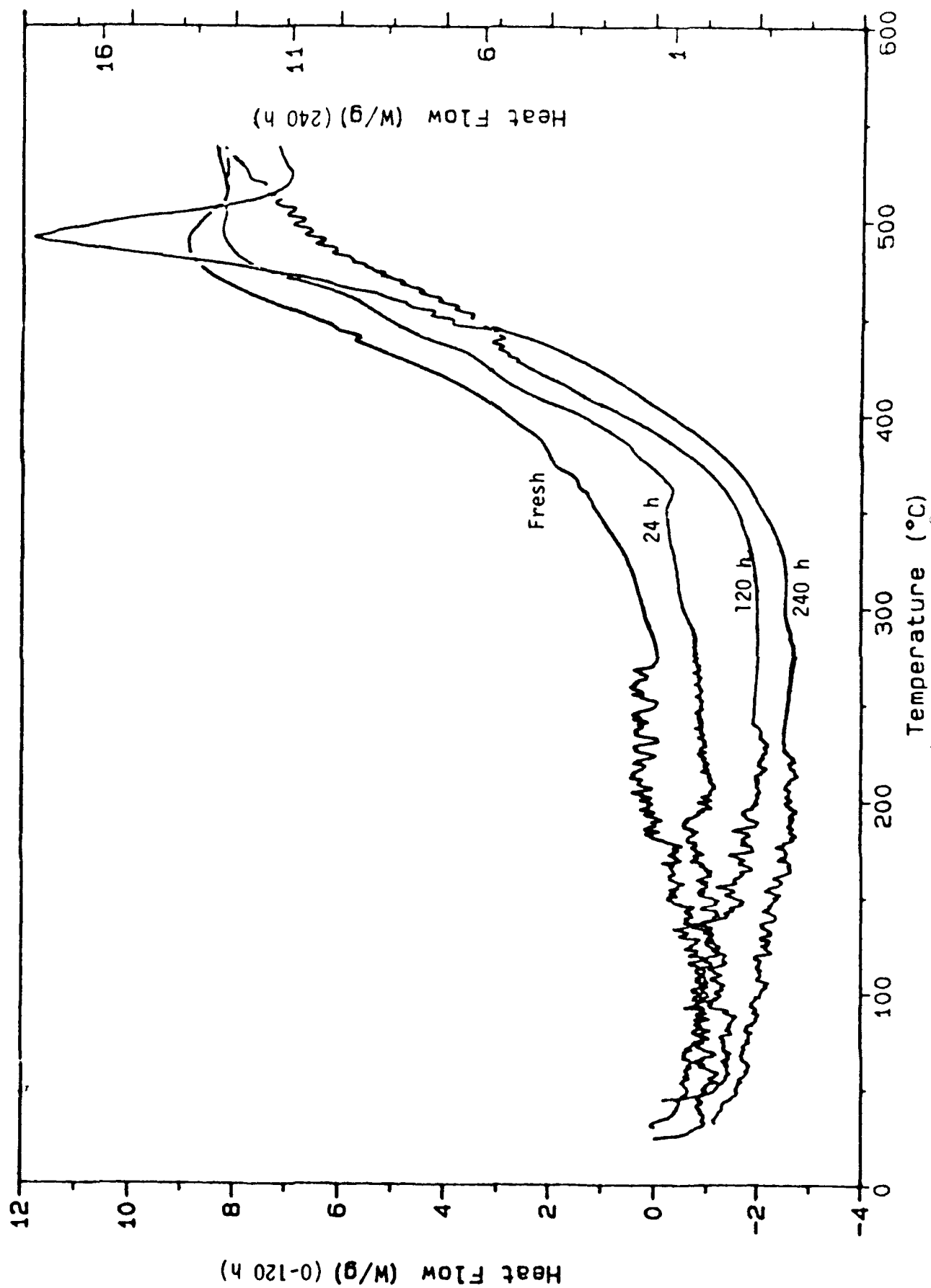


Figure 87. HP-DSC Thermogram (25-475°C, Ramp Rate of 25°C/min) of Fresh and Stressed (24, 120 and 240 h at 320°C) O-67-1 Lubricants (Sample Size 5 mg)

bridging bonds formed during the oxidative polymerization of the polyphenyl ether basestock. The 24 and 240 hour stressed O-67-1 samples were chosen for this study since they contain the lowest and highest amounts of the polyphenyl ether oxidation products, respectively. The spectra of the 24 and 240 hour O-67-1 oils shown in Figure 88 were obtained as thin oil films (neat) between KBr plates. The intensities of the spectra were matched using the band at 1500 cm^{-1} (* in Figure 88).

The spectra in Figure 88 for the 24 and 240 hour O-67-1 oils contain the same number of bands so that the bands, due to bridging bonds between polyphenyl ether molecules, are not detected. The main differences among the 24 and 240 hour spectra in Figure 88 are the sizes of the different bands in relation to the reference 1500 cm^{-1} band. The ratio between the sizes of the bands produced by the 24 hour oil and the sizes of the bands produced by the 240 hour oil varies throughout the FTIR spectra in Figure 88.

Thus, the initial results of the FTIR study indicate that the FTIR analyses are more suitable for qualitative comparisons than for quantitative determinations of oxidative degradation.

c. Ultraviolet-Visible Spectrophotometry with Solvent Dilution

Although FTIR spectrometry was unable to detect the new bonds formed during the oxidative polymerization of the O-67-1 oils, UV-VIS spectrophotometry was expected to be more suitable for monitoring the thermal-oxidation of the polyphenyl ether basestock. The higher sensitivity of the UV-VIS technique to polymerization is due to the fact that polymerization shifts the entire UV-VIS spectrum of the molecule toward a higher wavelength (toward visible) while for FTIR a single, weak band(s) must be resolved from a complicated IR spectrum. As an initial evaluation of the UV-VIS technique, the fresh and stressed (24-240 hours at 320°C) O-67-1 oils

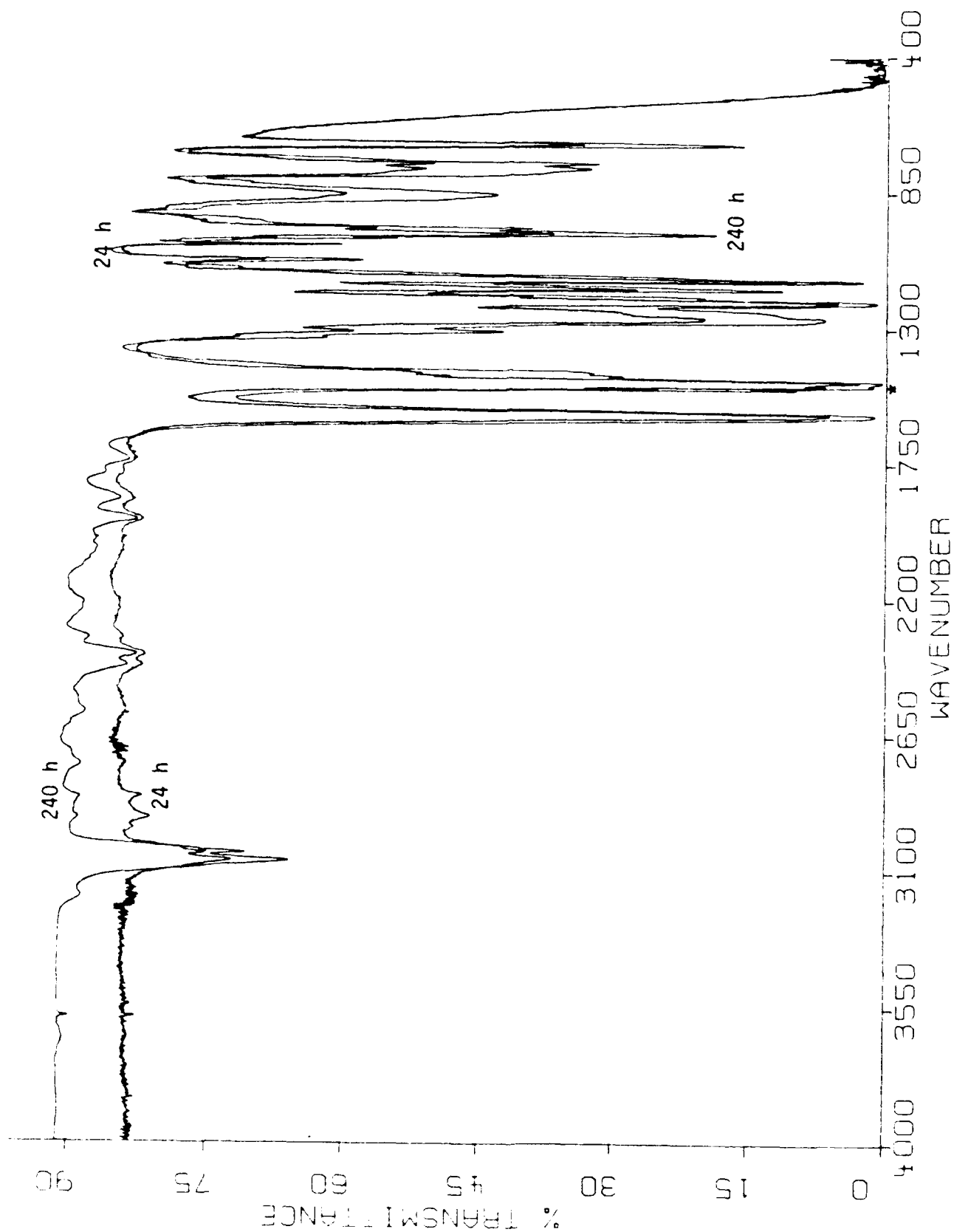


Figure 45. FTIR Spectra (4000-400 cm^{-1}) of the 24 and 240 Hour 320°C Stressed 0-67-1 Polyphenyl Ether Oils

were diluted 1:2000 with 1,2-dichloroethane (increase solubility of high molecular weight polymers) and pipetted into 10 mm width cells. A reference cell containing pure 1,2-dichloroethane was used to cancel out the absorptions of 1,2-dichloroethane in the 400-200 nm wavelength region. The produced UV-VIS spectra are shown in Figure 89 for the fresh and stressed O-67-1 oils.

The UV-VIS spectra show that a shoulder forms on the visible side (higher wavelength) of the UV band at 200 nm during the early stages of oxidation and the shoulder increases in size with increasing stressing time. The height of the UV band at 280 nm is unaffected by stressing time. The plots of the viscosity and UV absorbance at 320 nm versus the stressing time of each O-67-1 oil are shown in Figure 90. The plots in Figure 90 show that the absorbance at 320 nm and the viscosity of the O-67-1 oils increase at a similar rate with increasing stressing time.

A polyphenyl ether basestock (O-77-6) which had undergone extensive oxidative degradation (viscosity too high to measure) was then dissolved in the 1,2-dichloroethane and analyzed by UV-VIS spectrophotometry. Except for a slight precipitate, the degraded basestock was soluble in the 1,2-dichloroethane. The UV-VIS spectra of the badly degraded O-77-6 basestock and the 48 hour stressed O-67-1 oil are shown in Figure 91. As expected the badly degraded O-77-6 basestock produces a UV band in Figure 91 which is shifted strongly toward the visible (higher wavelength) and is very broad (due to numerous oxidation products) in comparison to the UV band produced by the 48 hour stressed sample.

To further evaluate the UV-VIS technique, the 24 and 192 hour (320°C) stressed samples of a polyphenyl ether lubricant with a different additive formulation, TEL-8039, were analyzed. The 48 hour stressed O-67-1 oil was

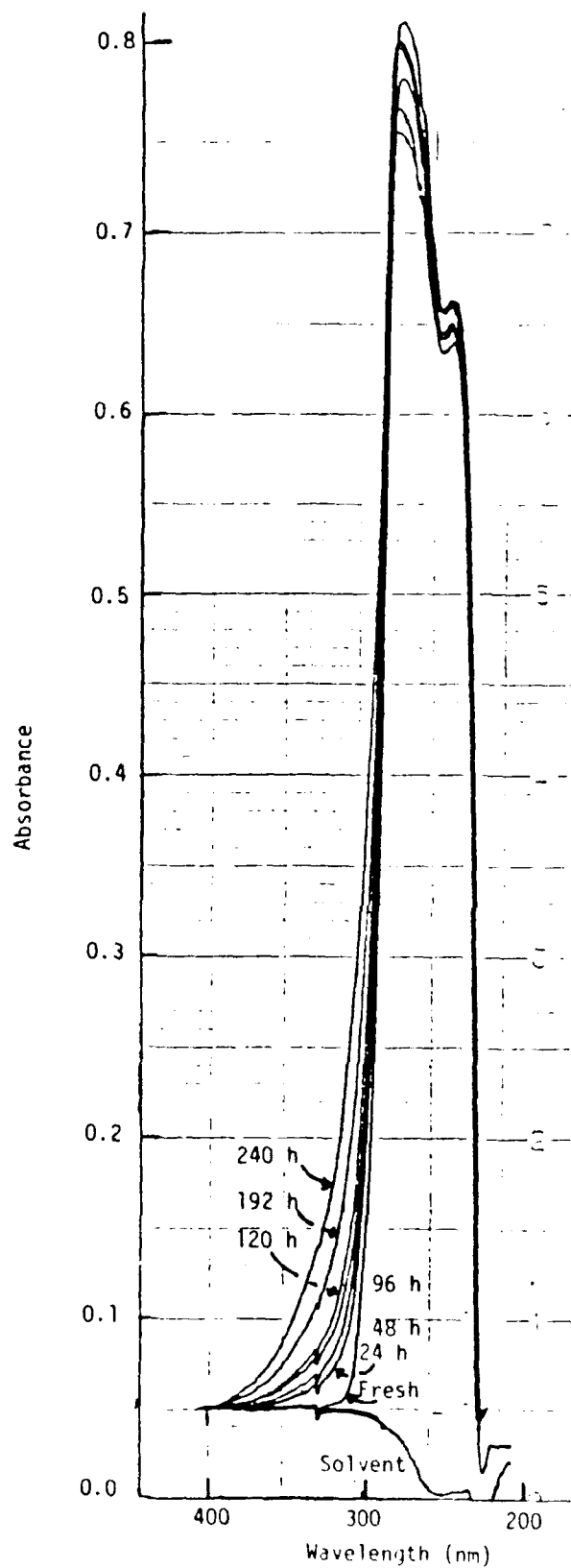


Figure 89. UV-VIS Spectra (400-200 nm) of the Fresh and 24-240 Hour 320°C Stressed 0-67-1 Oils in 1,2-Dichloroethane

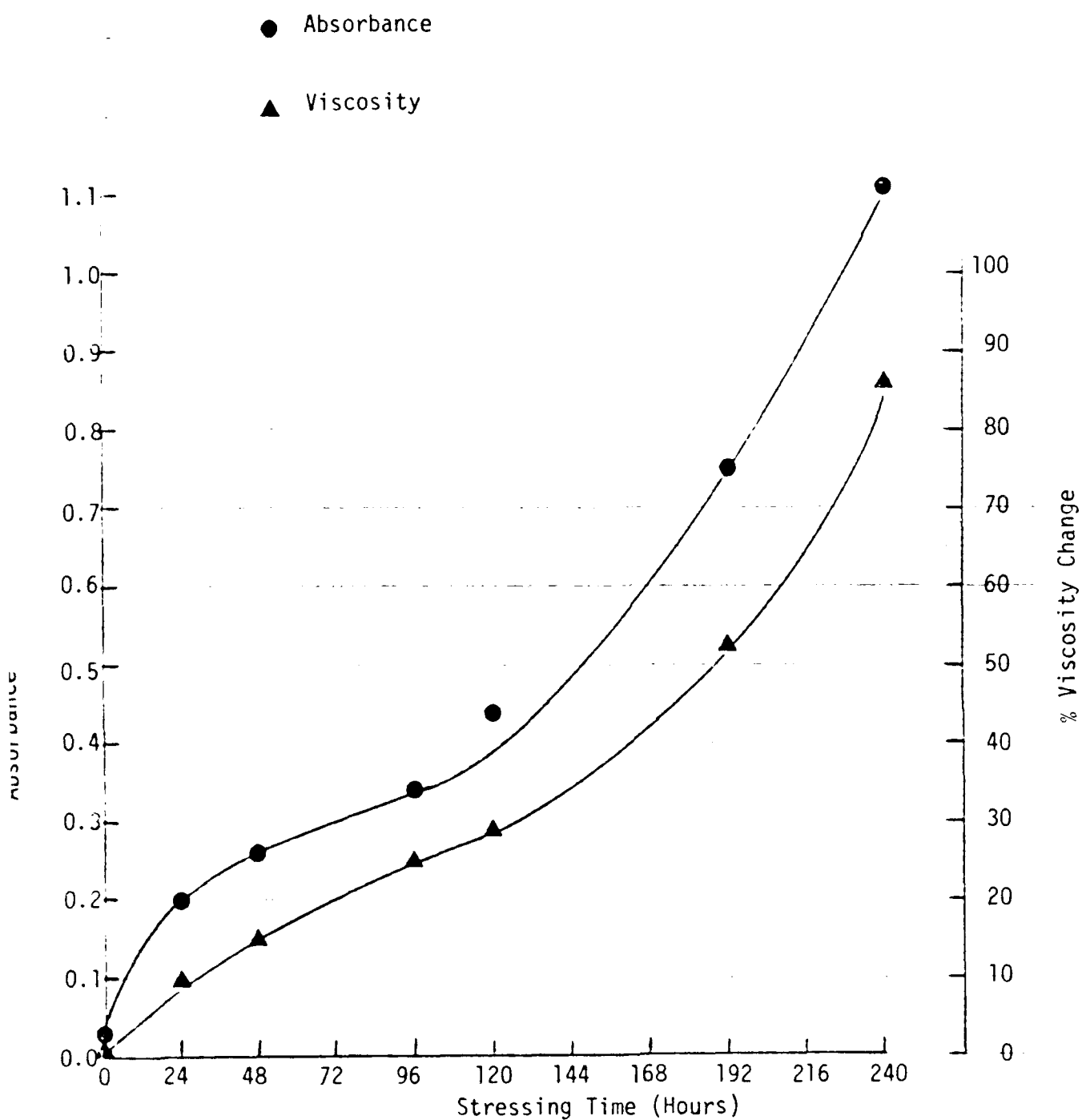


Figure 90. Absorbance at 320 nm and % Viscosity Change at 40°C Versus Stressing Time at 320°C for 0-67-1 Polyphenyl Ether Oil

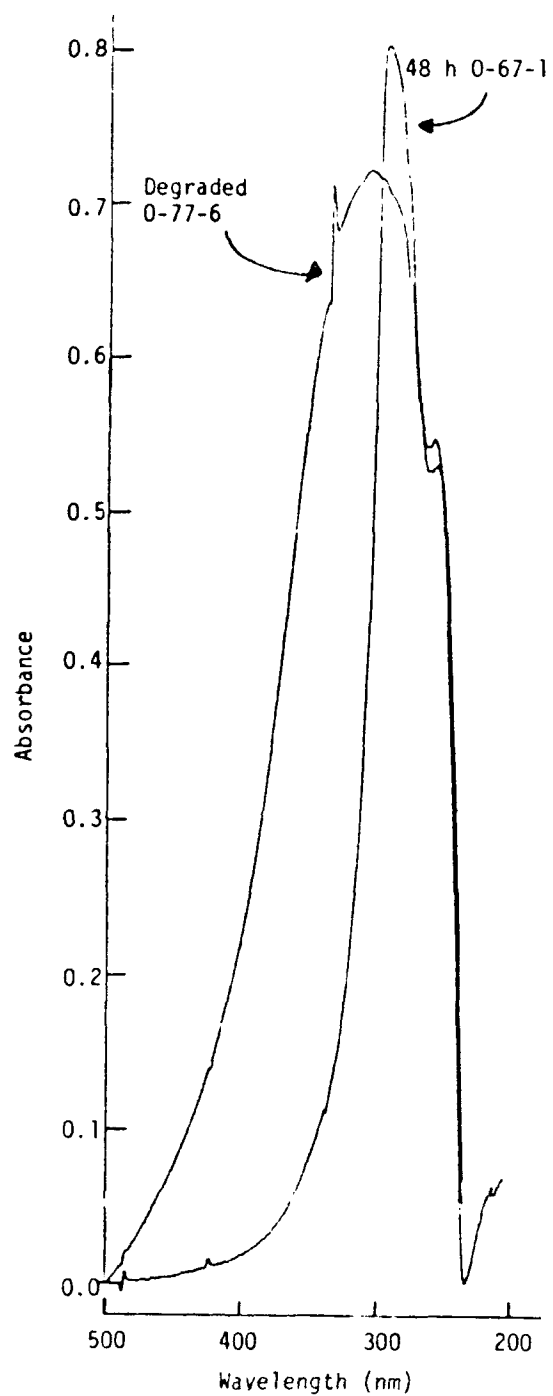


Figure 91. UV-VIS Spectra (500-200 nm) of the Badly Degraded 0-77-6 Oil and the 48 Hour 320°C Stressed 0-67-1 Polyphenyl Ether Oil

analyzed by UV-VIS spectrophotometry for comparison. The UV-VIS spectra (expanded vertical scale) of the stressed TEL-8039 and O-67-1 oils are given in Figure 92 and show an increase in the absorbance at 320 nm. The relative increases in Figure 92 are in good agreement with the viscosity increases exhibited by the stressed O-67-1 and TEL-8039 oils. Thus, these results indicate the UV-VIS technique monitors the degradation of the polyphenyl ether basestock and is independent of the additive(s) used in the lubricant formulation.

d. Ultraviolet-Visible Spectrophotometry Without Solvent Dilution

Since the 1:2000 dilution in 1,2-dichloroethane limits the suitability of UV-VIS techniques for routine or in-line use, research was conducted to develop solventless UV-VIS spectrophotometric techniques capable of monitoring the thermal-oxidation of polyphenyl ether based lubricating oils. The solventless UV-VIS spectrophotometric studies were performed using fresh and stressed (24 to 240 hours at 320°C) O-67-1 polyphenyl ether oils and three used polyphenyl ether lubricating oils obtained from gas turbine engines with operating times since oil change of 264, 417 and 442 hours.

To initially evaluate the potential of solventless UV-VIS spectrophotometric techniques for monitoring the thermal-oxidation of polyphenyl ether based lubricating oils, 10 microliter samples of fresh and stressed O-67-1 oils were pipetted onto separate 25 mm diameter and 2 mm thick quartz discs. A second quartz disc was placed on top of each deposited oil and pressed by hand until a thin film completely covered the inner surfaces of both discs. The sandwiched oil films were then placed into the sample cell of a scanning UV-VIS spectrophotometer. The absorbance spectra produced by the fresh and stressed O-67-1 oils in the UV region of 450-300 nm are shown in Figure 93.

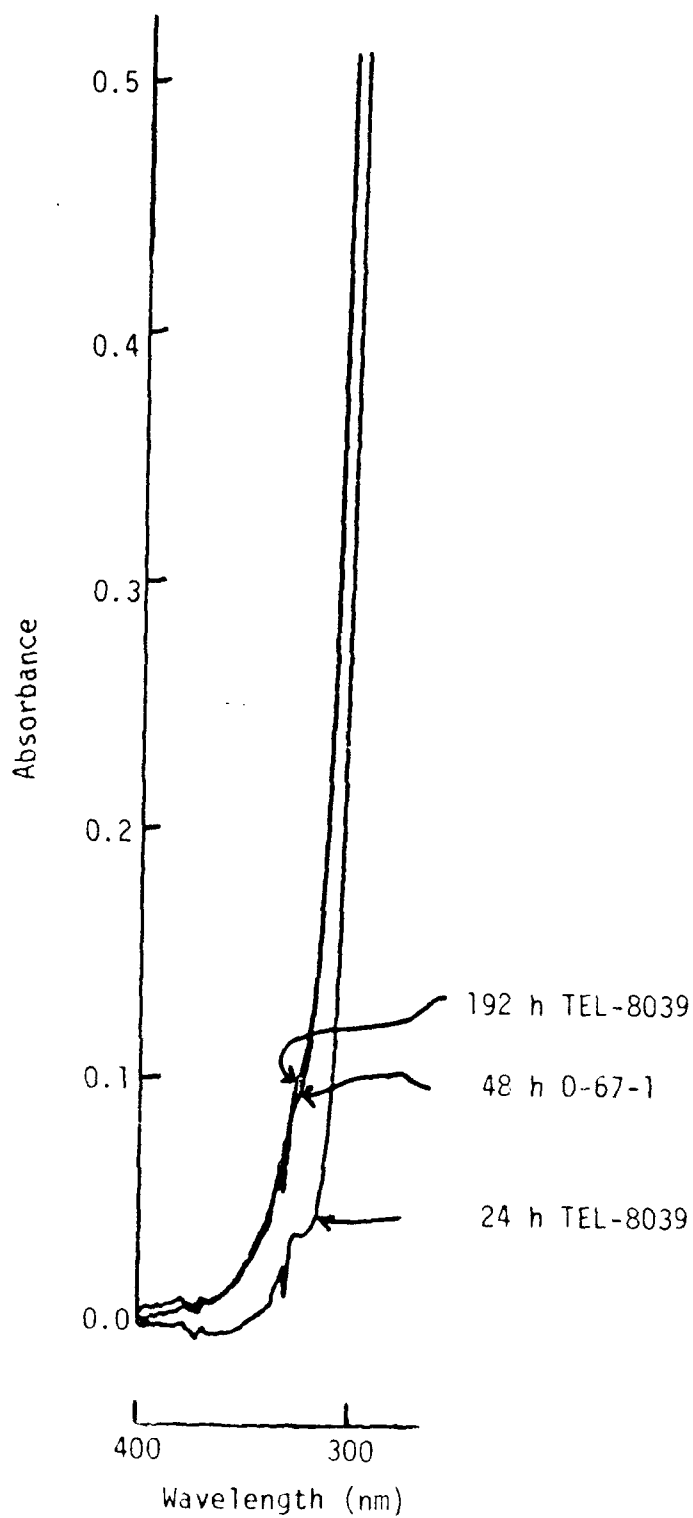


Figure 92. UV-VIS Spectra (400-300 nm) of the 24 and 192 Hour 330°C Stressed TEL-8039 and the 48 Hour 320°C Stressed O-67-1 Polyphenyl Ether Oils

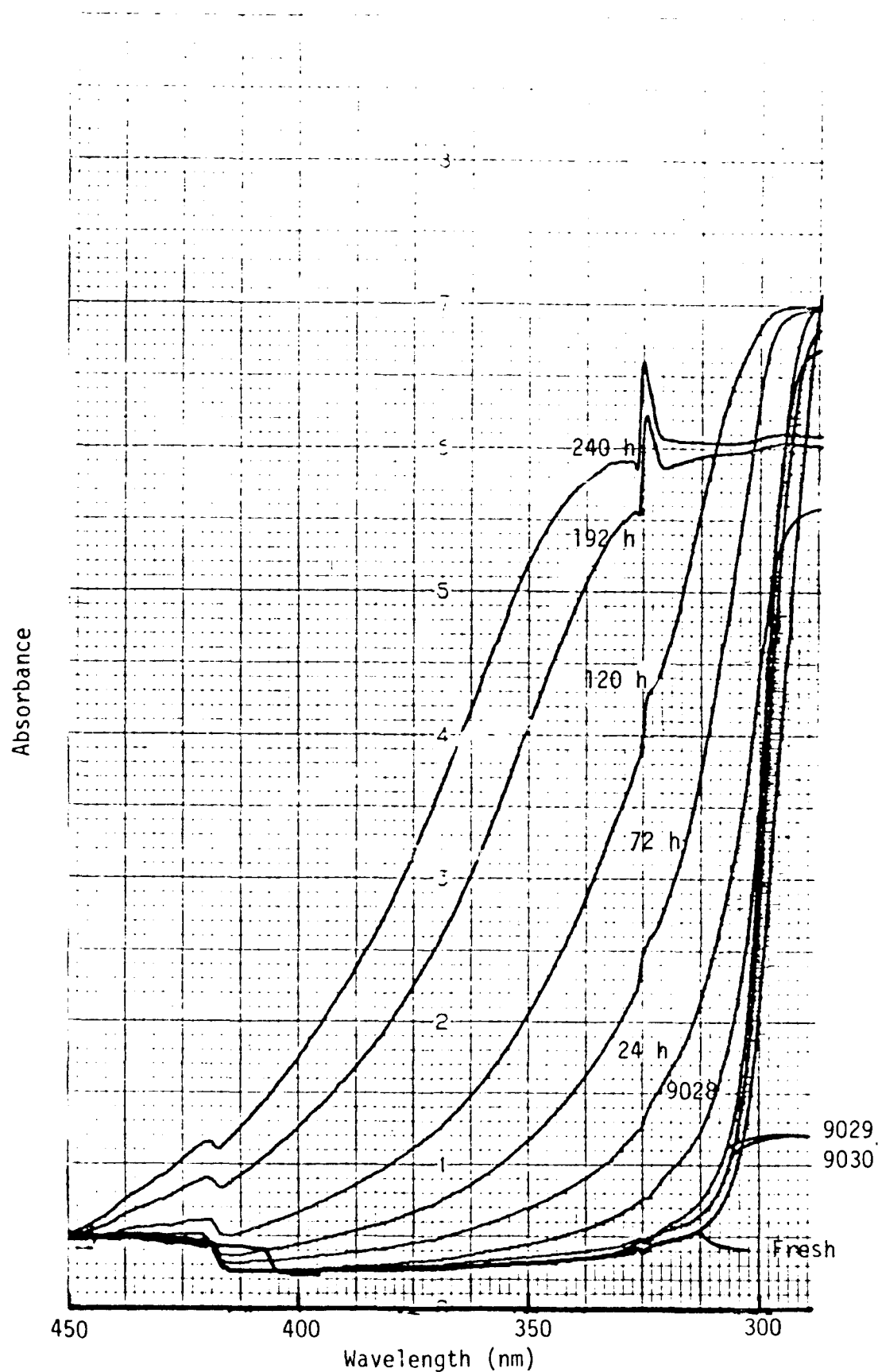


Figure 93. Absorbance Spectra of Fresh and Stressed (24-240 Hours at 320°C) 0-67-1 and Used (TEL-9028, TEL-9029 and TEL-9030) Polyphenyl Ether Oils

The absorbance spectra of the fresh and stressed O-67-1 oils in Figure 93 show that a shoulder forms on the visible side (higher wavelength) of the UV band at 310 nm during the early stages of oxidation and increases in size with stressing time. A second shoulder at 400 nm increases in size with stressing time for the O-67-1 oils with stressing times greater than 72 hours.

Thus, the absorbance spectra in Figure 93 indicate that solventless UV-VIS spectrophotometric techniques can be used to monitor the thermal-oxidation of O-67-1 oils. The 360 nm region is a practical region for thermal-oxidation determinations. Although the repeatability of the UV spectra is dependent on the thickness of the oil film, the variations in the oil film thickness did not limit the capability of the UV-VIS spectrophotometric technique to estimate the degree of thermal-oxidation of each O-67-1 oil.

To evaluate the capability of the solventless UV-VIS spectrophotometric technique to estimate the thermal-oxidative degradation of polyphenyl ether oils obtained from operating engines, three used polyphenyl ether based lubricating oils, TEL-9028, TEL-9029 and TEL-9030 with operating times of 264, 417 and 442 hours, respectively were analyzed. The absorbance spectra produced by the used oils in the UV region of 450-300 nm are also shown in Figure 93. The absorbance spectra of these used oils show that they have undergone slight thermal-oxidation when compared to the stressed O-67-1 oils in Figure 93. The absorbance (360 nm region) of the TEL-9028 oil is between the fresh and the 24 hour stressed O-67-1 oils while the absorbances of the TEL-9029 and TEL-9030 oils are similar in size to the fresh O-67-1 oil. These results indicate that the rate of thermal-oxidation was higher for the TEL-9028 oil than for the TEL-9029 and TEL-9030 oils since the

operating times for the TEL-9029 and TEL-9030 oils (417 and 442 hours) are higher than the operating time for the TEL-9028 oil (264 hours).

To initially evaluate the potential of the solventless UV-VIS spectrophotometric technique as an on-line technique or as a compact single UV wavelength instrument, an UV spectrophotometric system employing a long wave (360 nm maximum emission) UV light source and a light detector sensitive to the 360 nm region was constructed.

The sandwiched oil films were placed (laid flat) directly on top of the detector with the UV light source positioned one inch above the upper surface of the quartz discs. A voltmeter was connected to the UV detector to measure the output voltage of the detector (voltage decreases as transmission of oil film decreases) for the fresh and stressed O-67-1 oils. The results for the UV analyses of the fresh and stressed O-67-1 oils are listed in Table 96.

TABLE 96

UV ANALYSES OF FRESH AND STRESSED O-67-1 OILS

Stressing Time at 320°C	Output Voltage of Detector (V) ^a
Fresh	1.83 ± .01
24	1.63 ± .03
120	1.19 ± .02
192	0.74 ± .02
No Oil	1.89 ± .01

^a Triplicate, non-consecutive analyses

The results in Table 96 show that the output voltage of the detector decreases (absorbance increases) as the stressing times of the O-67-1 oils increase. These results indicate that a simple and inexpensive UV device could be designed for monitoring existing conditions of polyphenyl ether oils

in the field or directly in-line (use less sensitive wavelength).

e. UV Thermal Analytical Technique

The previously described research has shown that the high temperatures (450°C) used by thermal analytical techniques to accelerate the thermal-oxidative degradation of polyphenyl ether based lubricants cause vaporization of the lubricant prior to oxidation. High pressures of up to 500 psi did not inhibit the vaporization of the basestock. Therefore, other methods of accelerating the thermal-oxidative degradation of polyphenyl ether lubricants were investigated.

It has been reported¹⁵ that lubricant degradation can be accelerated by shortwave 254 nm ultraviolet light. It has also been reported that 254 nm UV light can be used to cause the rapid oxidation of the phenyl rings of butylstyrene molecules at room temperature.¹⁶ Therefore, 254 nm UV irradiation was investigated as a means to accelerate the thermal-oxidation of polyphenyl ethers while using temperatures below 300°C to limit vaporization of the lubricant. The long wave region (360 nm) of UV light was used to monitor the concentrations of high molecular weight polymers produced by the thermal-oxidation of the polyphenyl ether basestock.

The results reported here describe the initial research to optimize the wavelength of the UV light source and the atmosphere of the accelerated thermal-oxidation stressing test to obtain test times of less than 24 hours. Fresh O-77-6 polyphenyl ether fluid (no antioxidant) and fresh O-67-1 polyphenyl ether lubricant were used for this study.

To determine the effects of the UV light source on the rate of thermal oxidation of polyphenyl ether lubricants, a pen bulb (20 watt, 90% of output at 254 nm) UV light source was positioned above open vials containing 100 μL of fresh O-77-6 basestock. The long wave shield was placed on the UV

light source (UV light region: 320 to 400 nm) and the irradiated O-77-6 basestock was heated for five hours at 300°C. After 5 hours of stressing the O-77-6 basestock remained colorless and produced a UV spectrum (10 μ L between quartz plates scanned 450-300 nm on UV-VIS spectrophotometer) shown in Figure 94 which is identical to the fresh O-77-6 basestock. These results were expected since the fresh O-77-6 basestock does not absorb in the long wave UV region as demonstrated in Figure 94.

Therefore, the experiment was repeated with the long wave filter removed to produce UV light containing long (detection of degradation products) and short (acceleration of degradation) wavelength regions. After 5 hours of heating at 300°C, the irradiated O-77-6 basestock was dark in color and produced a UV spectrum in Figure 94 which has a large long wave shoulder in comparison to the spectra produced by the fresh and long wave UV stressed O-77-6 basestocks in Figure 94. The long wave shoulder has been shown to be directly related to the presence of thermal-oxidative degradation polymers (Figure 93).

To further study the effects of UV light on the thermal-oxidation of polyphenyl ether lubricants, two 100 μ L samples of O-77-6 basestock were placed in open vials and were heated at 300°C for 24 hours with and without UV irradiation. The O-77-6 basestock heated without irradiation remained colorless and underwent significant vaporization. Whereas, the O-77-6 heated with UV irradiation became a dark tar and also underwent significant vaporization.

To further accelerate the degradation of polyphenyl ether based oils, the effects of atmosphere on the rate of degradation were studied. Previous work² with thermal oxidative analytical techniques has shown that replacing an air atmosphere with an oxygen atmosphere accelerates the rate of basestock

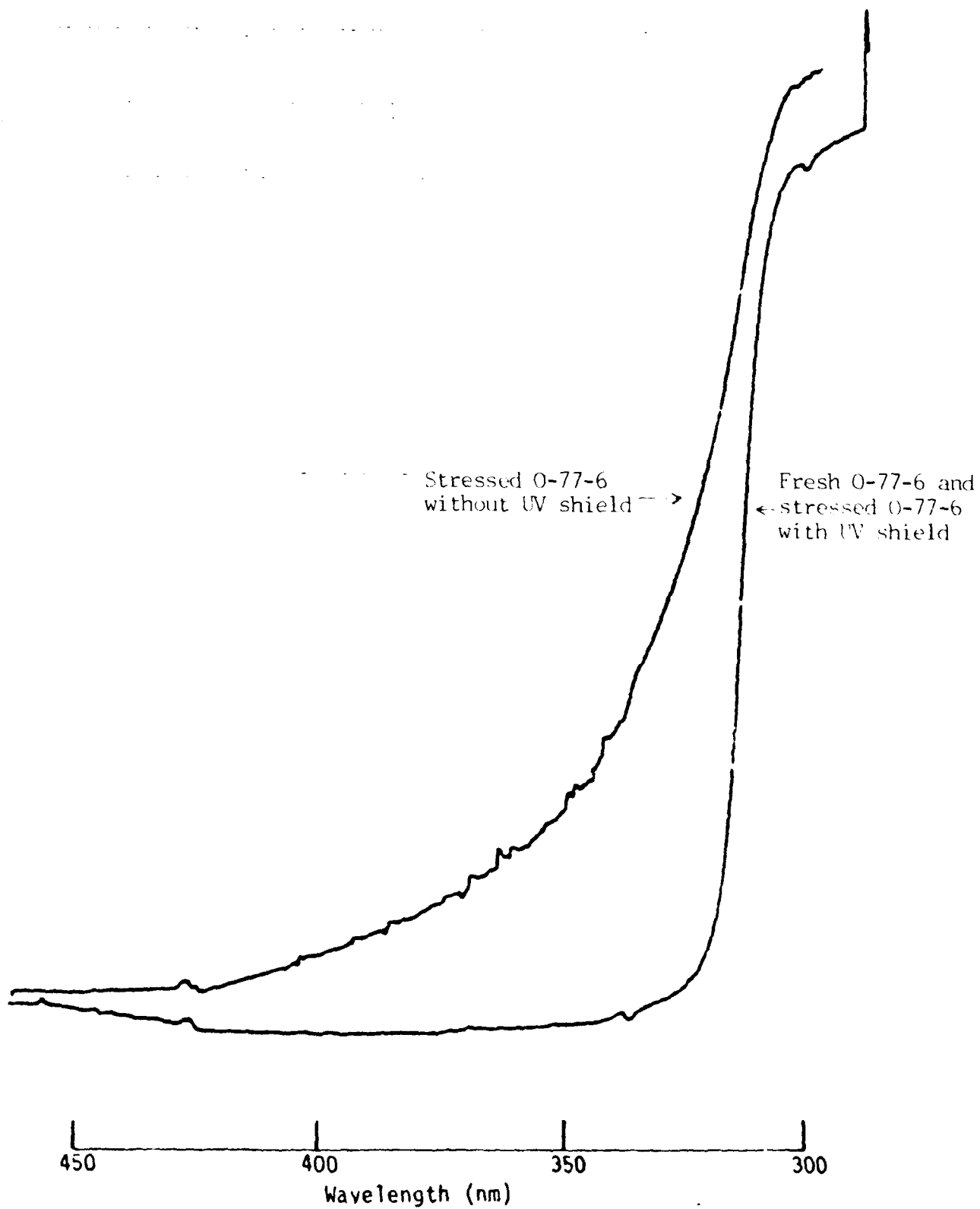


Figure 94. UV Spectra of Fresh and Stressed (300°C, 320-400 nm UV Light for 5 h) O-77-6 Polyphenyl Ether Fluids

degradation. To obtain an oxygen atmosphere, the open glass vial was replaced with a quartz vial constructed with a sidearm (oxygen inlet) and quartz lid on which the UV light source was positioned. A 100 μ L sample of the fresh O-77-6 fluid was placed on the bottom of the quartz vial which was flushed with oxygen prior to closing with the quartz lid. A slight (10 psig) oxygen pressure was maintained inside the vial during the 2-hour test at 300°C.

At the end of the 2-hour test, the O-77-6 fluid was colorless and produced a UV-VIS spectrum similar to the spectrum produced by the fresh O-77-6 fluid in Figure 94. The absence of O-77-6 fluid degradation in the enclosed oxygen atmosphere appears to be caused by a thin layer of polyphenyl ether which deposited on the quartz lid during the test. The thin layer of polyphenyl ether quickly degraded to produce an opaque, brown film. Therefore, future development of the UV-thermal analysis technique will be performed with the quartz vial placed on the UV light source to negate the effects of deposited polyphenyl ether films. Placing the vial on the UV light source will increase the amount of short range (below 200 nm) UV light reaching the test sample since air and oxygen atmospheres absorb short wave UV light.

f. Summary

These initial results have shown that UV light can be used to both determine (long wave) and accelerate (short wave) the thermal-oxidative degradation of polyphenyl ether fluids. The effects of atmosphere and temperature on the UV thermal analytical technique need to be optimized to obtain short analysis times (less than 24 hours) without causing vaporization of the polyphenyl ether basestock. Once the experimental parameters have been optimized, a series of fresh and stressed polyphenyl ethers will be

studied to determine if UV accelerated degradation can be used as a small sample volume test to determine the remaining thermal-oxidation stabilities of polyphenyl ether lubricants.

6. ELECTROCHEMICAL TECHNIQUES

a. Introduction

Previous research^{2,17} has shown that cyclic voltammetric techniques have great potential as lubricant monitoring techniques for MIL-L-7808 and MIL-L-23699 type lubricating oils. The cyclic voltammetric techniques require that a sample (100 μ L) be withdrawn from the operating engines and then diluted with an electrolyte containing polar solvent prior to analysis. However, initial research² on polyphenyl ether based lubricants indicated that the electrolyte interfered with the cyclic voltammetric analyses.

Therefore, research was initiated to develop a technique based on cyclic voltammetry capable of performing lubricant analyses of polyphenyl ether based lubricants. The research reported here was performed in two steps. The first step of the research was to conduct a literature search to identify cyclic voltammetric techniques capable of performing electrolyte-free analyses. The second step was to optimize the identified techniques for off-line analyses of polyphenyl ether lubricants.

Research was also performed to optimize the identified techniques for the off-line and on-line analyses of an advanced 4 cSt ester based lubricant (O-85-1).

b. Literature Search

The literature search identified cyclic voltammetric analyses that can be performed in electrolyte-free solvents. The electrodes used in the absence of electrolytes utilized a membrane coating on the electrode surface^{18,19} or were made from metal wires with 10 micrometer or less

diameters.²⁰ Since the membrane coatings tend to separate upon long term exposure to organic solvents and require an electrolyte dissolved in the coating, the research to develop off-line and on-line voltammetric systems concentrated on electrodes made from metal wires with diameters less than 25 micrometers.

c. Cyclic Voltammograph Optimization

To evaluate the identified cyclic voltammetric techniques for 4 cSt and polyphenyl ether based lubricant analyses, a 10 micrometer diameter platinum wire (Pt-10: working electrode) was combined with a 0.25 mm platinum wire (combined auxiliary - reference electrode). Since the Pt-10 electrode has a surface area of 75 square micrometers and the glassy carbon electrode used by the previous cyclic voltammetric technique² has a surface area of 7×10^6 square micrometers, the gain of a commercially available cyclic voltammograph was increased from microamp/volt to nanoamp/volt for this study.

Initial tests showed that the scanning voltage range of 6V (+3 to -3V) produced by the commercially available voltammograph did not produce peaks for new O-85-1 (4 cSt) oil dissolved in isobutyl acetate in the absence of an electrolyte. Therefore, the voltage scan range of the commercial voltammograph was expanded from 6 V(+3 to -3V) to 120 V (60 to -60V). The modified voltammograph has a voltage scan range that can be varied from 0 to 120 V and a scan rate that can be varied from 0.01 to 100 V/sec. The ability to vary the voltage scan parameters has been shown by previous research² to be essential in optimizing cyclic voltammetric techniques for oil analysis.

d. Effects of Sample Preparation

Initially the Pt-10 electrode was used to analyze isobutyl acetate (electrolyte free) diluted fresh and stressed oils. The cyclic voltammograms

of the diluted fresh and stressed (360 hours at 175°C) O-85-1 oils and of the diluted fresh and stressed (120 and 240 hours at 320°C) O-67-1 polyphenyl ether oils are shown in Figures 95 and 96, respectively.

The cyclic voltammograms of the fresh and stressed O-85-1 oils in Figure 95 show that two different species are detected in the O-85-1 oils. The oxidation waves (A in Figure 95) are produced by the oxidation of the antioxidants in the oils. As expected, the oxidation waves decrease (antioxidants decrease) with the stressing time of the oils. The reduction waves (B in Figure 95) are produced by the reduction of the hydroperoxides in the oils which increase with the stressing time of the oils.

In contrast to the cyclic voltammograms of the O-85-1 oils, the cyclic voltammograms of the O-67-1 polyphenyl ether oils in Figure 96 did not produce a response in the positive scan direction; i.e., no oxidation waves were produced (insensitive to Additive A). Although the O-67-1 oils produce reduction waves (B in Figure 96), the sizes of the reduction waves produced by the first scans are not affected by the stressing time of the O-67-1 oils. However, the reduction waves produced by the second scans increase with the stressing time of the O-67-1 oils. Therefore, it appears that the reduction waves in Figure 96 are due to the reductions of the thermal-oxidation products of the O-67-1 oils (increase with stressing time) and are unrelated to the Additive A concentration. The factors causing the reduction waves to increase with successive voltammetric scans were not studied during this project.

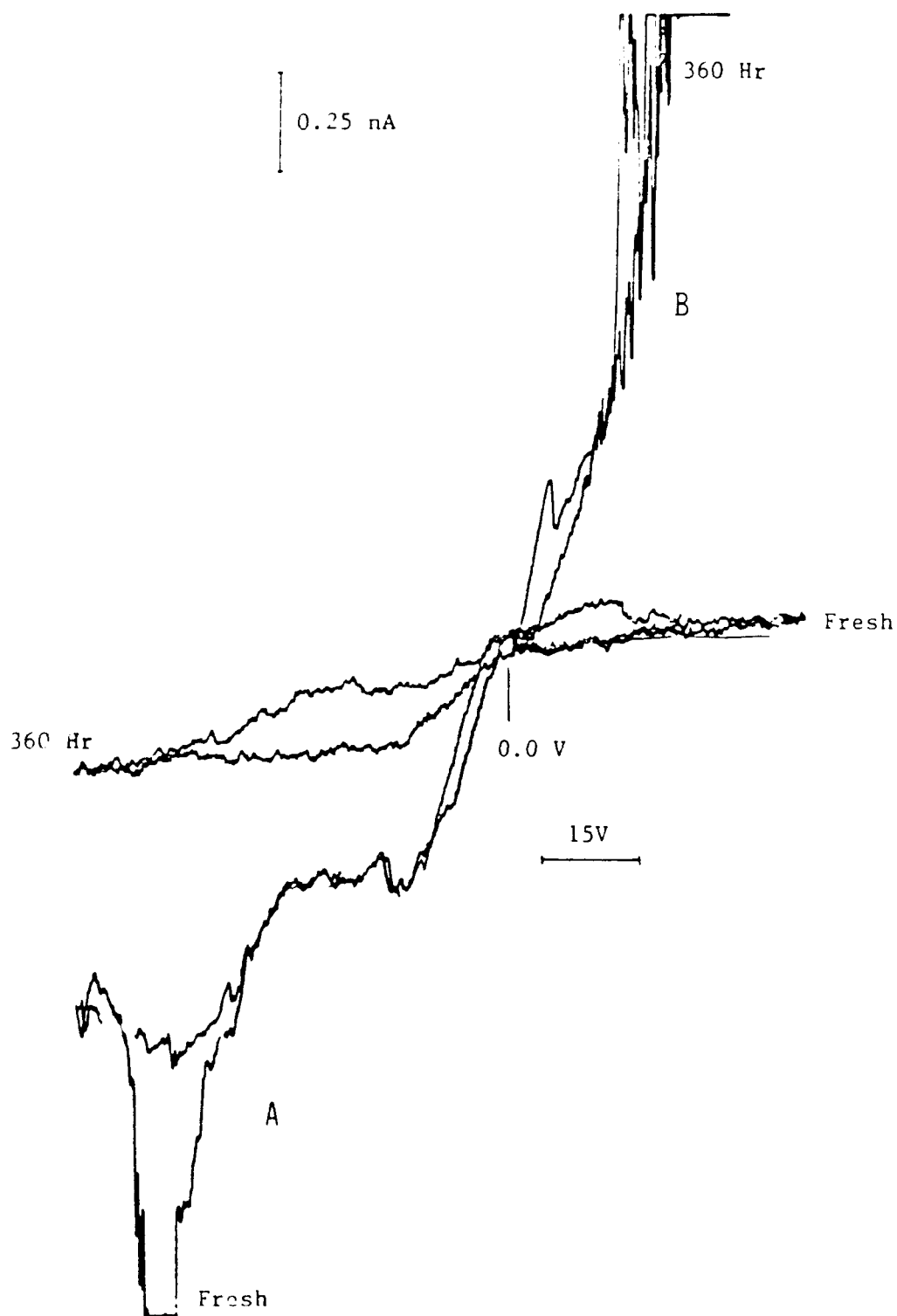


Figure 95. Cyclic Voltammograms of Fresh and Stressed (360 h at 175°C) 0-85-1 4 cSt Oils Diluted in Isobutyl Acetate (without Electrolyte) Using the Pt-10 Electrode and a +60 to -60 V Scan Range

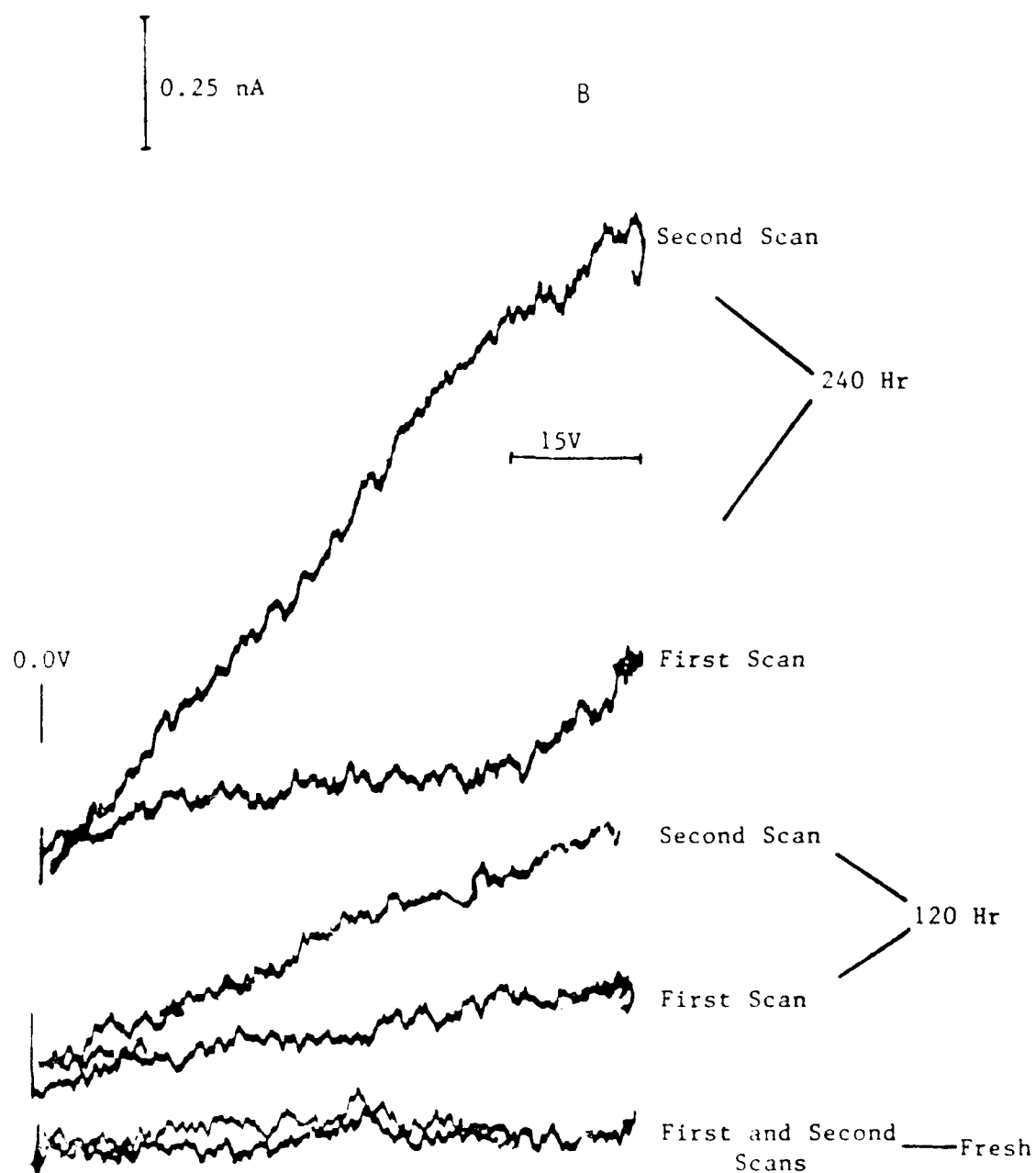


Figure 9b. First and Second Reduction Scan Voltammograms of Fresh and Stressed (120 and 240 h at 305°C) 0-67-1 Polyphenyl Ether Oils Diluted in Isobutyl Acetate (without Electrolyte) Using the Pt-10 Electrode and a +60 to -60 V Scan Range

e. Effects of Electrode Design

To determine the effects of electrode design on the capability of the cyclic voltammetric technique to perform on-line lubricant analyses, the effects of the working electrode diameter and composition on the voltammetric results of fresh and stressed O-85-1 and O-67-1 oils were studied.

The effect of the working electrode diameter was studied since it has a strong effect on the voltage at which the species in the lubricants become electroactive. The voltage drop (V) that occurs between the working and auxiliary electrodes is dependent on the product of the current flow (I) and resistance (R) between the electrodes ($V = IR$) and is known as the IR effect. Since the resistance cannot be reduced by the use of electrolytes or polar solvents for on-line analyses, the IR effect must be reduced by decreasing the current flow. By decreasing the electrode diameter from 3 mm to 10 micrometer, the current decreases from microamps to nanoamps making the IR effect smaller in relationship to the oxidation potential of the electroactive species. The resistance is decreased by decreasing the distance between the working and auxiliary electrodes surfaces to less than 0.1 mm.

As an initial evaluation of the working electrode diameter, the Pt-10 (10 micrometer) and a UDRI manufactured 25 micrometer diameter platinum electrode (Pt-25) (sealed 25 micrometer wire inside a 3 mm pyrex glass tube 4 inches long; electrical connection made with silver epoxy) were used to analyze fresh and 360 hour stressed O-85-1 oils heated to 175°C as shown in Figure 97.

In contrast to Figure 95, the cyclic voltammograms in Figure 97 show that, regardless of the stressing time of the oil or the working electrode diameter, the antioxidants (oxidation waves) in the O-85-1 oil were not

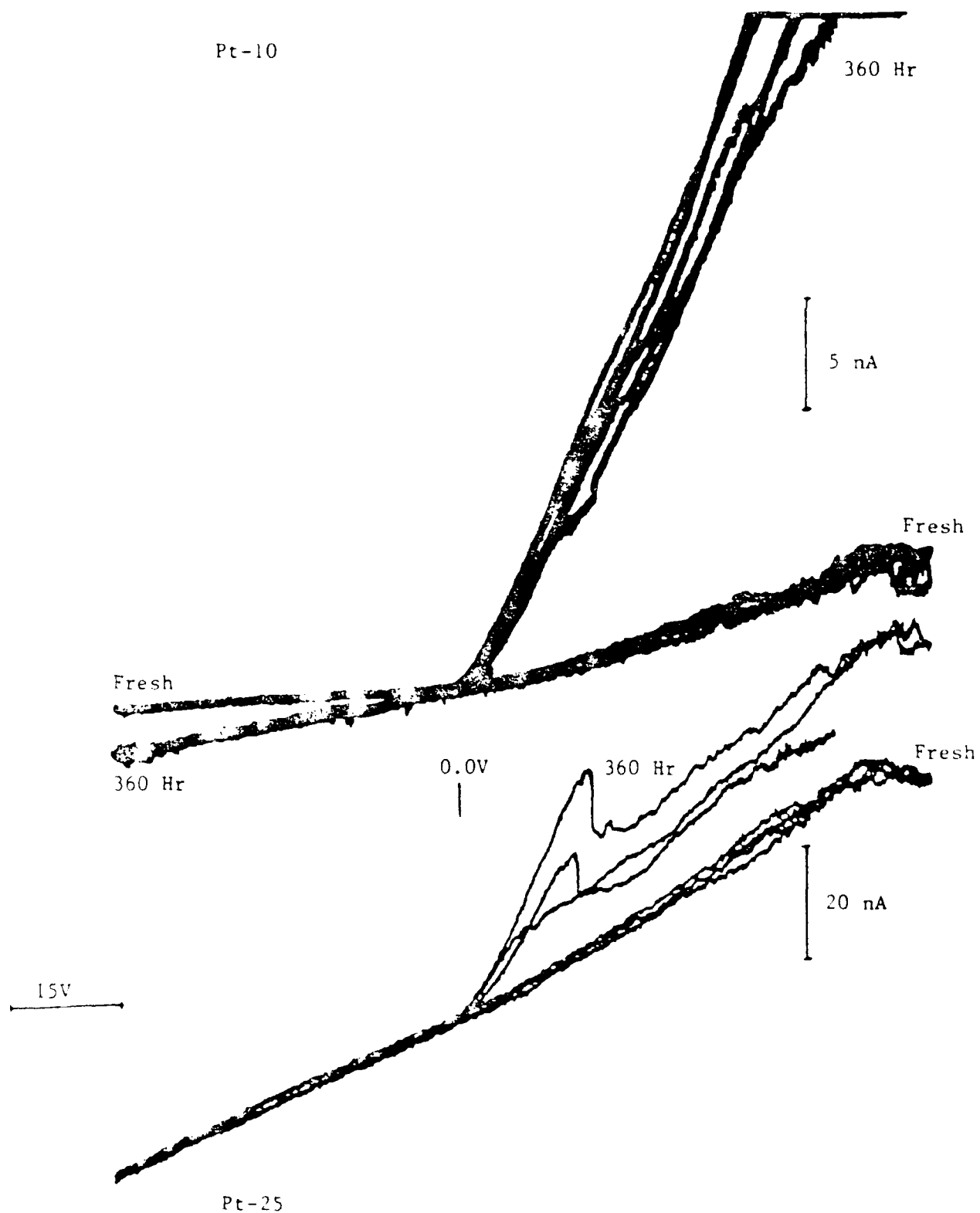


Figure 17. Cyclic Voltammograms of Solventless Fresh and Stressed (360 h at 175°C) 0-85-1 Oils Using the Pt-10 and Pt-25 Electrodes, a Voltage Scanning Range of +60 to -60 V, and an Analysis Temperature of 175°C

detected by the oxidation scans out to 60V. The slopes of the voltammograms in the oxidation scans are mainly due to increasing current flow as the voltage is increased from 0 to 60V, and thus, could be used for monitoring lubricant conductivity.

In contrast to the oxidation scans in Figure 97, the reduction scans of the fresh and stressed O-85-1 oils in Figure 97 show that the Pt-10 and Pt-25 electrodes are able to detect electroactive species (peroxides) in the oils. The difference among the reduction voltammograms produced for the fresh and stressed oils by the Pt-10 electrode are much greater than for the Pt-25 electrode. The increased sensitivity of the Pt-10 electrode is due to the lower current flow that occurs as the voltage is increased. The Pt-25 electrode reduction voltammograms in Figure 97 contain a small current flow due to the reduction of the peroxides and a large current flow due to the increasing voltage. The Pt-10 electrode reductive voltammograms in Figure 97 are dependent primarily on the current flow produced by the reduction of the peroxides.

Thus, these initial results indicate that the Pt-10 electrode is much better suited for on-line analyses of lubricants than the Pt-25 electrode.

Since the electrochemical reactions that occur at the surface of the working electrode are affected by the composition of the electrode, working electrodes were manufactured by sealing 12.5 micrometer gold (Au-12.5) and 10 micrometer tungsten (W-10) wires in 3 mm pyrex glass tubing. The gold surface was expected to be less reactive than the platinum surface while the tungsten surface was expected to be more reactive than the platinum surface. The cyclic voltammograms produced by the Pt-10, Au-12.5 and W-10 electrodes for fresh and 360 hour stressed O-85-1 oils were performed at 175°C and are shown in Figure 98. The electrodes were run under identical gains, voltage

scan rates, and voltage scan ranges in order to better compare their capabilities.

The cyclic voltammograms in Figure 98 again demonstrate that the oxidation scan regardless of the electrode composition is unable to detect the antioxidant species in the O-85-1 oils. For each electrode the slope of the oxidation scan is greater for the stressed O-85-1 oil than for the fresh oil (Figure 98). The small oxidative wave (A in Figure 98) produced by the Pt-10 electrode for the stressed O-85-1 oil is thought to be caused by the oxidation of the platinum surface in the presence of the oxidized oil.

The cyclic voltammograms in Figure 98 also demonstrate that all three electrodes are capable of detecting hydroperoxides in the stressed O-85-1 oil. The sensitivities of the Pt-10 and Au-12.5 electrodes for detecting the peroxides are much greater than the sensitivity of the W-10 electrode.

To further evaluate the reactions of the lubricant with the surface of the electrode, the Pt-10, Au-12.5, and W-10 electrodes were used to analyze fresh and 168 hour stressed O-67-1 oils heated to 250°C. The cyclic voltammogram of the Au-12.5 and W-10 electrodes for the fresh and stressed O-67-1 oils are shown in Figure 99. The Pt-10 electrode produced cyclic voltammograms similar to the voltammograms produced by the Au-12.5 electrode. The Pt-10 electrode results were not included because the Pt-10 electrode degraded during use (epoxy electrical connection near surface) so that the results could not be duplicated.

The cyclic voltammograms produced by the Au-12.5 and W-10 electrodes in Figure 99 are mainly current flows due to the voltage scan from 60 to -60 V. No peroxides were detected in the stressed O-67-1 oils. In addition to the current flows produced by the voltage scan, the W-10 electrode voltammogram contains peaks A and B (Figure 99) which are thought to be

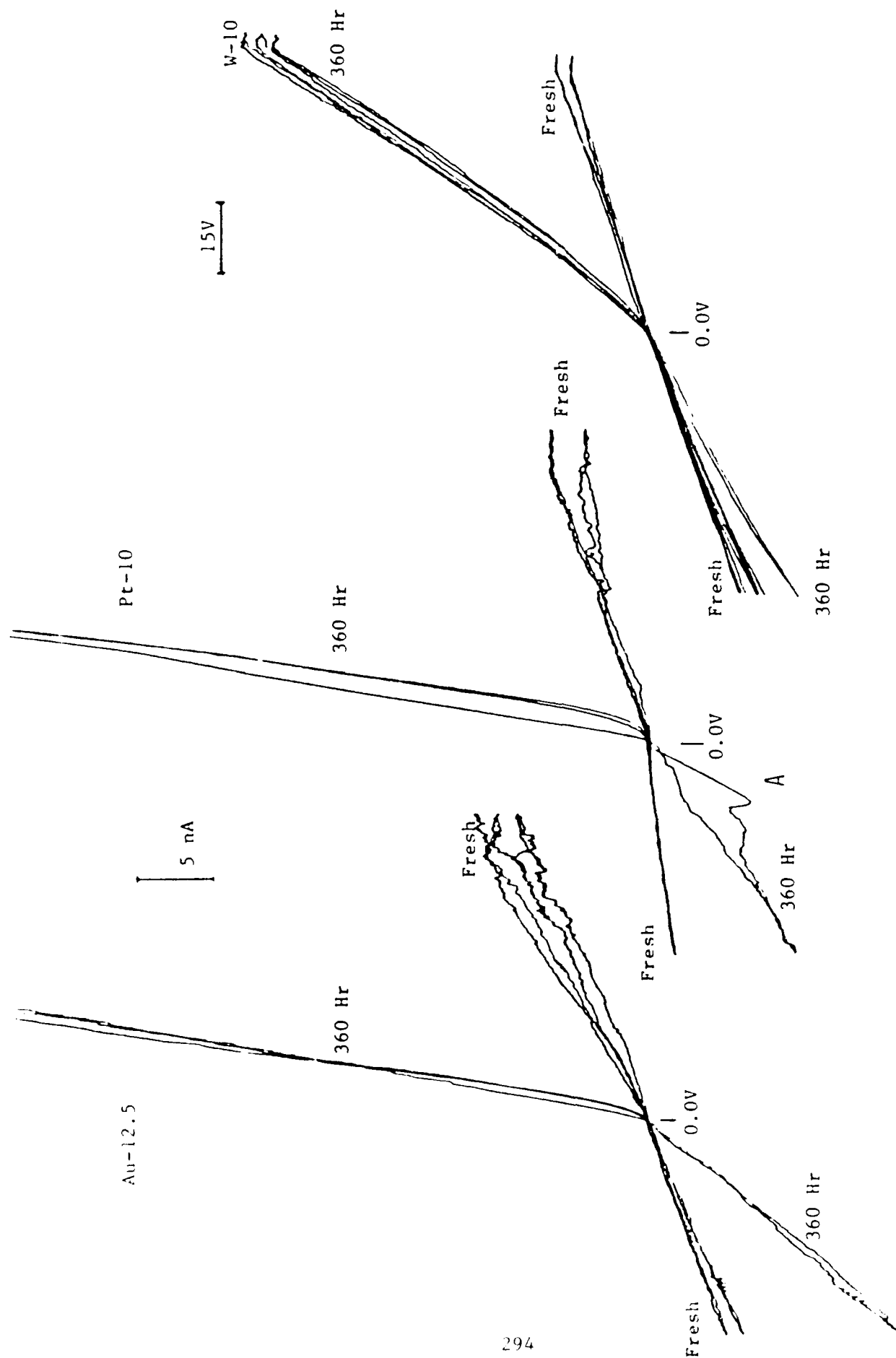


Figure 98. Cyclic Voltammograms of Solventless Fresh and Stressed (360 h at 175°C) 0-85-1 Oils Using the Au-12.5, Pt-10, and W-10 Electrodes, a Voltage Scanning Range of +60 to -60 V, and an Analysis Temperature of 175°C

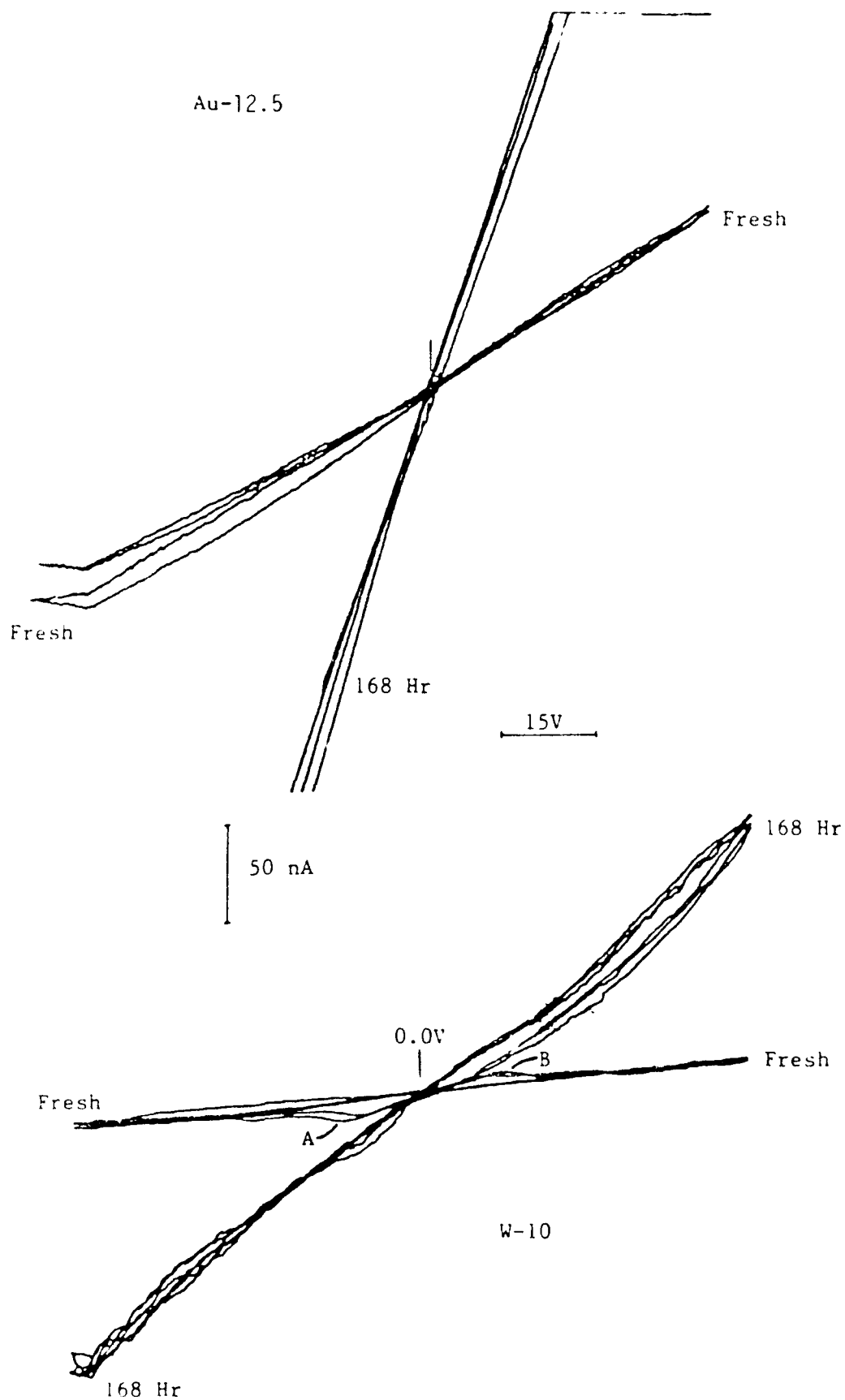


Figure 99. Cyclic Voltammograms of Solventless Fresh and Stressed (168 h at 305°C) 0-67-1 Polyphenyl Ether Oils Using the Au-12.5 and W-10 Electrodes, a Voltage Scanning Range of +60 to -60 V, and an Analysis Temperature of 275°C

caused by oxidation and reduction of the tungsten surface. In comparing the cyclic voltammograms produced by the Au-12.5 and W-10 electrodes in Figure 99, it can be seen that the Au-12.5 (and Pt-10) electrode is more sensitive to the conductivity increase produced by increased stressing time than the W-10 electrode. Whether the oxidation and reduction peaks produced by the W-10 electrode are beneficial or detrimental to on-line lubricant analysis will require further study.

f. Summary

The initial results of the optimization study have shown that microelectrodes have potential for performing off-line and on-line analyses of 4 cSt and polyphenyl ether based lubricants. The results have shown that the electrode diameter should be 10 micrometers or less and may be gold, platinum, tungsten, or some other composition.

SECTION V

LUBRICANT LOAD CARRYING CAPABILITY TEST ASSESSMENT

The Falex Gear Test has been evaluated as a possible LCC bench test for evaluating high temperature candidate lubricants. The test consists of two rollers (pinions) driven by a rotating upper surface (driver) and supported by a stationary lower surface (gear specimen) as shown in Figure 100. The driver contacts the pinions at the center of the pinion length and drives the pinions with a "rolling contact" while the pinions slide against the gear surfaces. Falex claims that this setup matches the slip/roll ratio found on a gear tooth and is proposed as a replacement for gear test rigs. A more detailed description of this test setup has been described by Voitik and Heerdt.²¹

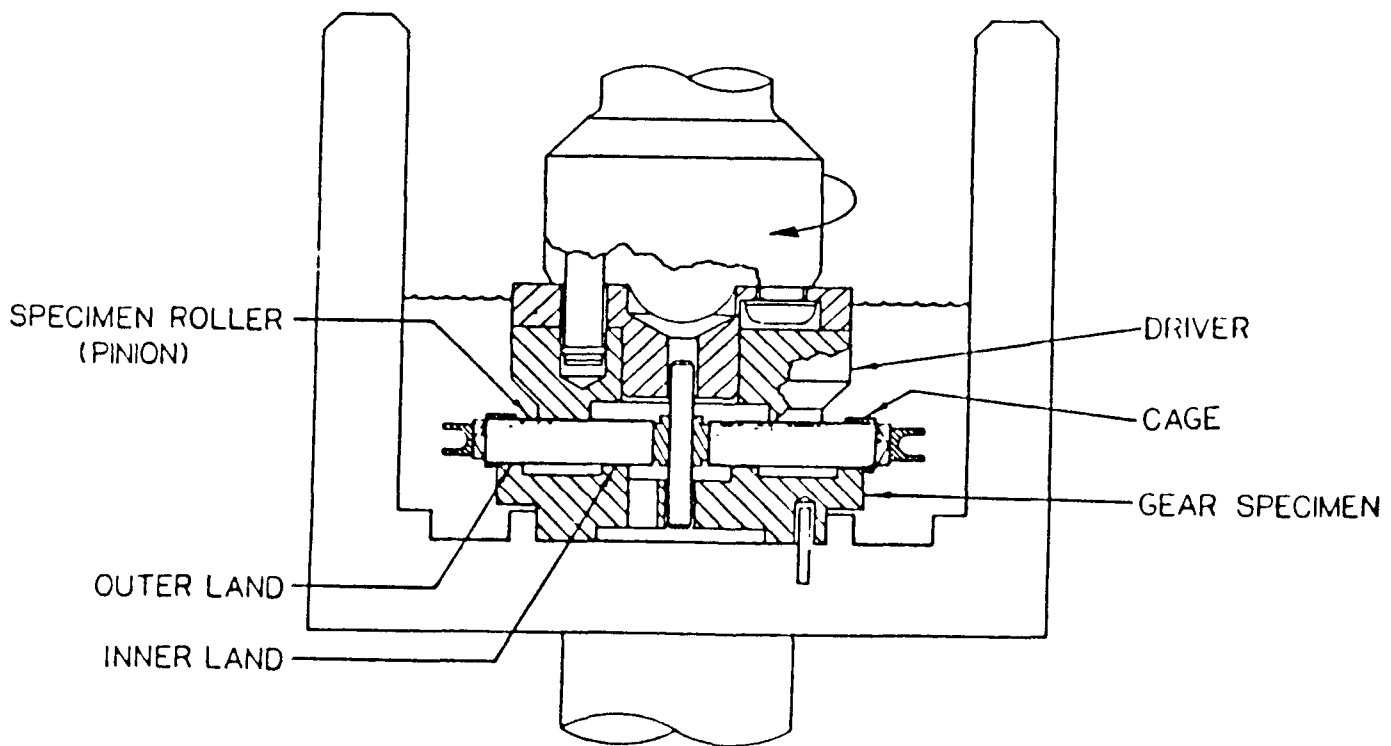


Figure 100. Gear Test Configuration Using the Falex Multispecimen Wear Test Machine

Unfortunately, the theoretical evaluation of this test rig does not correlate to the actual operation. With pure rolling between the driver and pinions there should be no wear at the center of the pinions, especially for the short duration test (one hour). However, wear at the pinion centers was observed for all ten ester lubricants tested. In addition, some tests displayed severe wear at the pinion centers. The wear over the entire length of the pinion is not completely unexpected. The length of contact between the driver and pinion is 0.340 inch and this is 42.5% of the total pinion length. With this geometry there is no certainty of the point of rolling contact, or if there is any rolling contact, between the driver and pinions. In fact, there is no certainty in the point of rolling contact or sliding speed anywhere along the pinion. As wear particles and/or other debris enter any of the contact zones, the rolling contact position may change. Also, the rotation speeds of the two pinions cannot be assumed to be identical. Finally, unusual wear scars appeared on the end of some pinion specimens which cannot be explained. The test configuration is being studied to determine the nature of its mechanics and how it can be modified to produce a slip/roll effect. Some modifications being considered are crowning of the driver or pinions and knurling of the driver and/or pinions.

Future work on modification of the Falex Gear Simulation test is being considered. Currently, a single-piece test specimen with bevelled surfaces at the driver is being studied as a possible alternative to the two flat rollers. The bevelled surface can be designed to assure pure rolling at the driver provided the friction forces at the sliding contacts are not too large.

SECTION VI

TRIBOLOGICAL EVALUATION OF CANDIDATE FLUIDS

1. INTRODUCTION

The tribological properties of all lubricant samples in this research have been investigated using the sliding four-ball wear test. This bench test consists of a set of four 0.5-inch diameter bearing balls, three of which are secured in a triangular configuration while the fourth one rests in the cavity made by the other three and is rotated under a set load (Figure 101). The ASTM standard for this test (D4172-82) limits the duration of the test run to one hour and wear is described by the average of all the measurements of length and width on the resulting wear scars formed on the three lower balls.

Some shortcomings of this standardized test method include the loss of any quantification of the scar shape and surface roughness. In addition, this test assumes that the wear on the upper ball is negligible and can be ignored. As will be shown, upper ball wear is significant in tests of high temperature candidate fluids. In fact, the degree of upper ball wear directly determines the shape of the lower ball wear scars.

Tests were done using the usual ASTM standards of load ($147 \text{ N} \pm 2 \text{ N}$) and speed ($1200 \text{ rpm} \pm 60 \text{ rpm}$). A test temperature of 315°C could be attained after modifications were made to protect the machine and test durations as long as 68 hours were reached (although testing at 315°C was limited to 20-hour tests).

In our earlier work,²² the formulas of Bos²³ and Feng²⁴ were shown to be valid for small, circular scars. The Bos equation relates the vertical

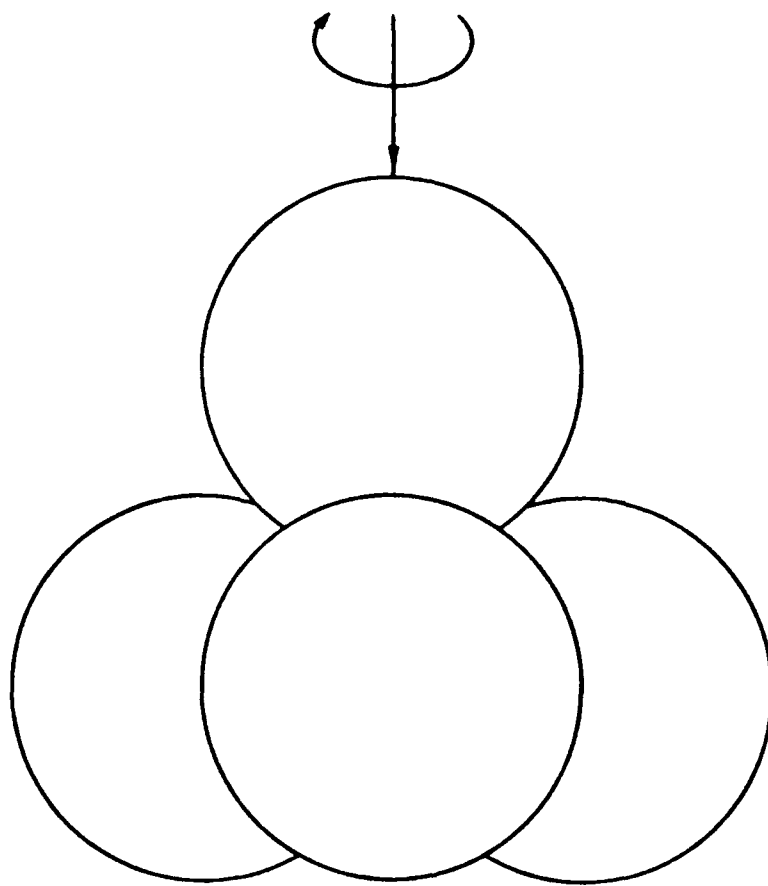


Figure 101. Four-Ball Configuration

displacement of the upper ball to the lower ball wear scar diameter. Feng's calculation generated a wear volume given the lower ball scar diameter. In conjunction, these two relations allow a history of the vertical position of the upper ball to be converted into volume of material removed.

Unfortunately, both of these relations assume smooth, circular scars are formed and the upper ball has no wear. Willermet and Kandah²⁵ found the wear of the rotating ball can be greater than that of the stationary balls. In preliminary tests of polyphenyl ethers (PPE), scars were occasionally seen to be neither smooth nor circular depending on test conditions (Figure 102). The wear of the top ball is obviously significant and any assumption of negligible top ball wear is not practical. A method was derived to relate the final scar shape to a wear volume by taking into consideration top ball wear. Based on the geometry of the four-ball configuration, a parameter, alpha, defines the degree of top ball wear and is computed using only the length and width of the lower ball scars.

With this method for relating vertical displacement to wear volume, continuous monitoring of the upper ball position during a long duration test can translate into the amount of wear at every data point during the test. All statistics used to report the wear of four-ball tests are based on the geometric analysis previously mentioned. Furthermore, a technique for optically measuring non-circular wear scars was developed in conjunction with the geometric analysis and was used to evaluate all test scars.

With a more rigorous means for analyzing four-ball test data, many tests were done to evaluate different lubricants under varying conditions. Concentration on high temperature tribological characteristics of oils led to a change from the 52100 steel balls prescribed by the ASTM standard to more appropriate high temperature specimens. The peculiarities of the

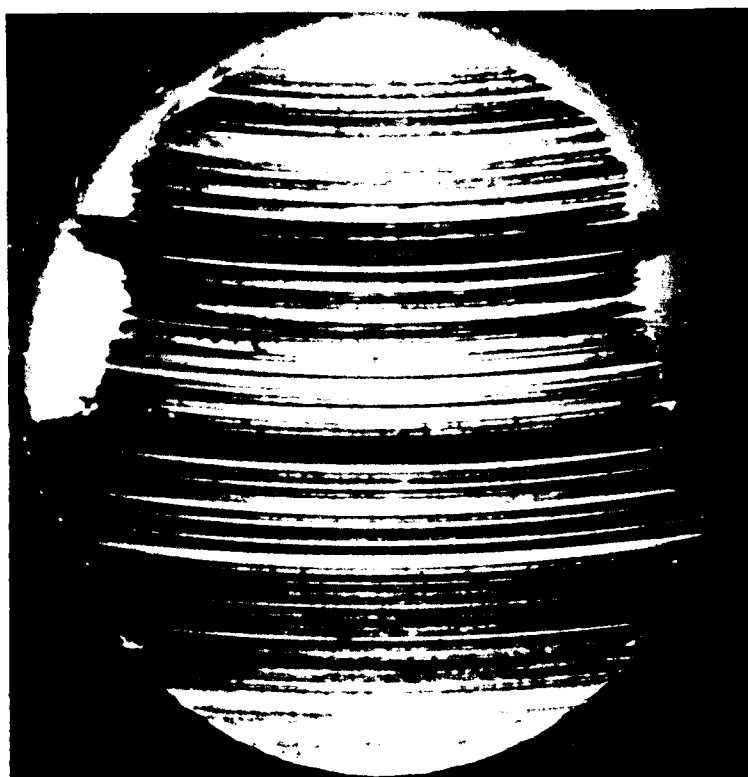


Figure 102. Non-Circular Lower Ball Wear Scars Formed on 52100 Steel Specimens by Lubrication with Polyphenyl Ether (48X Actual Size)

high-temperature candidate fluids to different specimen materials are also examined.

2. APPARATUS

The Falex Multi-Specimen Wear Machine used for this research is shown in Figure 103. In its four-ball configuration, the test rig allows continuous monitoring of torque, temperature, rotational speed, and upper ball position. Modifications made to the machine in the course of this research include a heat exchanger to allow cooling of the oil in the rig drive spindle during high temperature runs and a system for delivering a gas flow into the test cup (providing data to be taken for various atmospheres). The 100-lb. capacity load cell of the test machine was replaced with a 5-lb. capacity instrument to measure torque more precisely. The data acquisition system was also modified in order to allow collection of more data points and reduce sampling time between data points. The current program has a limit of 500 data points in contrast to the former limit of 100.

As mentioned in the Introduction, a history of the upper ball position is useful if displacements can be related to scar size and wear volume. A linear variable displacement transducer (LVDT) is secured to the loading arm of the four-ball machine to provide such information. As the upper ball bores into the lower balls, the loading arm pivots, deflecting the spring loaded LVDT five times the displacement of the upper ball. After calibrating the output signal of the instrument to millimeters, the data can be manipulated to give a curve of the upper ball position versus time during a test.

Preliminary tests of high-temperature candidate fluids were performed using 52100 steel ball specimens (grade 25, HRC 62). Due to material softening at high temperatures, 52100 was deemed inappropriate due to loss of

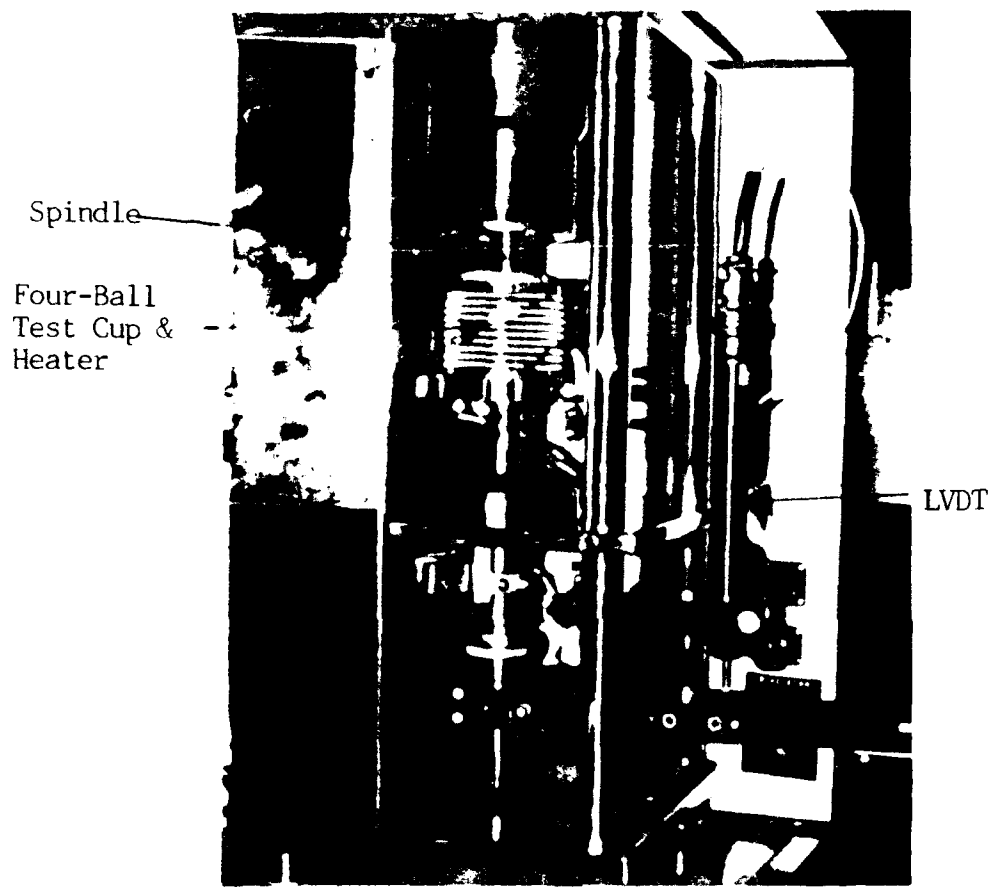


Figure 103. Falex Four-Ball Wear Test Machine Showing Spindle, Test Cup, Heater and LVDT

hardness. M-50 steel specimens were obtained (grade 10, HRC 61) and the evaluation of tribological properties was based on tests using M-50 specimens.

A select number of Si_3N_4 balls (grade 5, HRC 78) were purchased in order to run four-ball tests of candidate fluids on ceramic specimens. The thermal stability and high strength to weight ratio of ceramics are some of the characteristics that make these materials particularly attractive for turbine engine components.

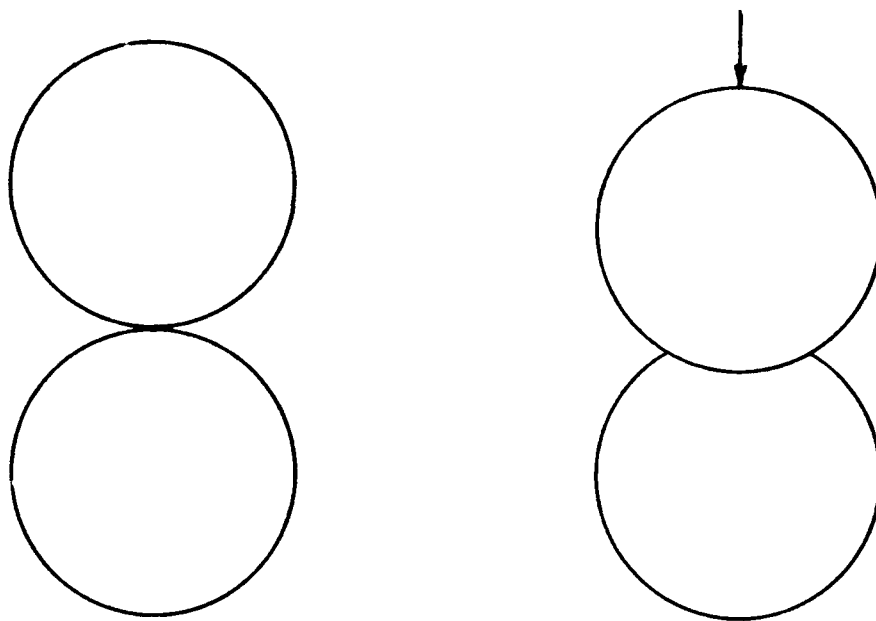
3. FOUR-BALL WEAR MODEL

a. Background

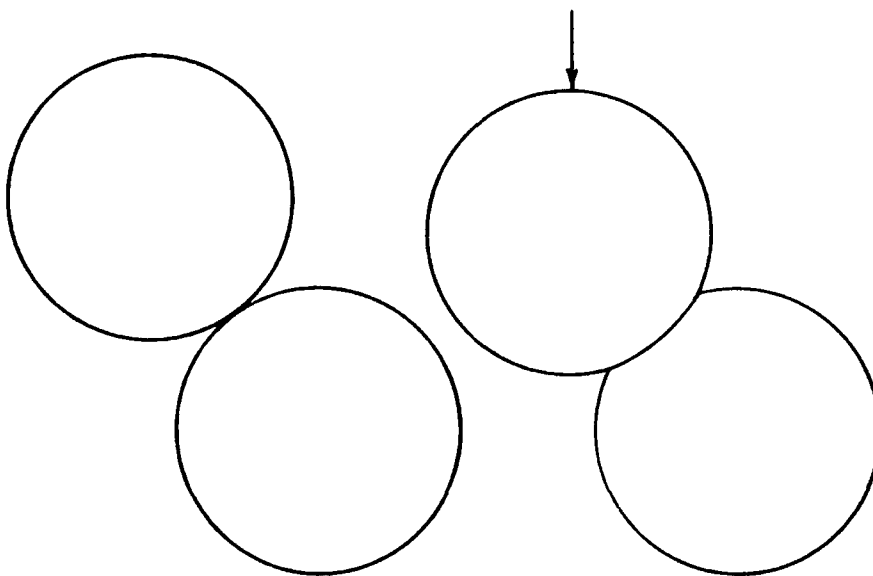
As stated earlier, Bos derived a relation between upper ball displacement and scar size. In his model, the contact between the upper ball and one of the lower balls is isolated. He modeled this contact by letting the line between the centers of both balls coincide with the axis of rotation (Figure 104). In actuality, the line between the centers of the upper ball and a lower ball is originally at an angle of 35.26° from the axis of rotation (Figure 104). This second model which correctly interprets the dynamics of wear in the four-ball system will be used to derive the relation between the vertical displacement of the upper ball to the resulting scar length on the lower ball(s).

b. Four-Ball Geometry

Figure 105 illustrates the geometry of the upper ball and one lower ball, before and after wear, in the x-y plane. During wear, the vertical distance between the upper and lower ball centers changes from k_0 to k . Due to the axisymmetry of the lower balls, the upper ball remains centered on the y' axis, and the horizontal distance between the ball centers, h , is constant.



a



b

Figure 104. Upper Ball and One Lower Ball, Before and After Wear, Corresponding to the (a) Bos Model and (b) Actual Geometry

The region bounded by the curves s_1 and s_2 between the points p_1 and p_2 represents the cross-section of the material that must be removed or deformed in order to allow the center of the upper ball to move from k_o to k . If the upper ball does not wear or deform, the profile of the scar on the lower ball would be exactly represented by s_1 . This ideal case will be referred to as the "geometric intersection". Unfortunately, the upper ball does wear, and the balls will undergo some elastic deformation due to the load and frictional heating. To represent the cross-section in either case, the points p_1 and p_2 must be located, and the profile connecting these points must be accurately modeled.

c. Scar Chord

There are two factors that influence the location of p_1 and p_2 , wear and elastic deformation. If it is assumed that the balls wear without deformation, the end points of the scar will be the same as points p_1 and p_2 in Figure 105. This "geometric assumption" would hold true regardless of the relative amount of lower and upper ball wear.

If a chord is drawn to connect the centers of the two balls in Figure 105, its length can be found to be $\sqrt{h^2 + k^2}$. If a second chord is drawn to connect p_1 to p_2 , the two chords will bisect each other. Defining the chord connecting p_1 and p_2 as c , we can relate c to the vertical position, k , by solving the right triangle containing the side $c/2$. The scar chord length, c , is given by the following relation:

$$c = \sqrt{4R^2 - k^2 - h^2} \quad 1$$

Equation 1 allows the scar chord length to be predicted at any point during a test by using an LVDT. This equation, however, has been derived by neglecting the contribution of elastic deformation to the scar size. Since

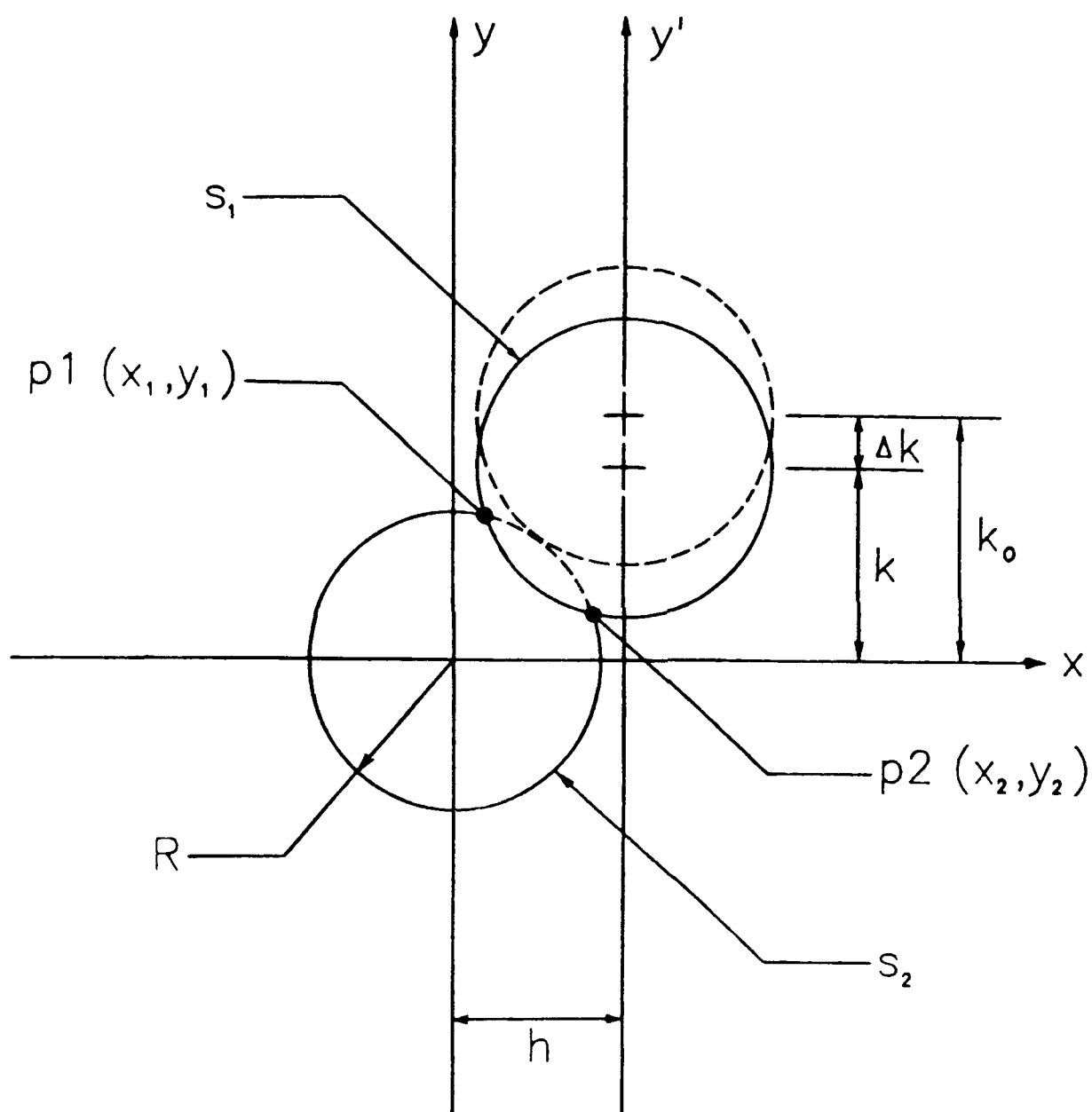


Figure 105. Four-Ball Configuration and Nomenclature for the Upper Ball and One Lower Ball, Before and After Wear

deformation does take place, the resulting contact area causes the centers of the upper and lower balls to approach one another. Figure 106 shows the elastic deformations, δ_1 and δ_2 , of the balls due to the normal component of loading and how these deformations result in a vertical displacement, δ_y . For a load, P , of 147 N, a vertical displacement of approximately 0.0028 mm results, and the corresponding Hertz diameter is 0.1893 mm (calculated using the appropriate equations and graphs from Reference 26). If this displacement from deformation is inserted into Equation 1, the resulting chord length is calculated to be 0.2427 mm. Any calculation for the wear scar volume which relies on Equation 1 will be in error to some degree since the deformed volume of the balls is included. In a later section, a lower limit for scar chords will be defined beyond which the error due to deformation is negligible.

It is worth noting, however, that although the two factors (wear without deformation and deformation without wear) contribute similar chord lengths for the displacement due to deformation, the contribution from the deformation is negligible after a sufficiently large scar has been produced. From the LVDT data for a 20-hour test at 150°C, the initial rate of upper ball vertical displacement is nearly 0.0020 mm per minute for 0-67-1. Since the value of the vertical displacement from elastic deformation is less than the vertical displacement rate from wear, the Hertzian contribution to scar size diminishes with continuing wear, and any associated errors with LVDT measurements can be neglected.

A curve generated from Equation 1 is shown in Figure 107 (where upper ball vertical displacement is found by subtracting k from k_0). The upper ball displacements of discrete tests (derived from LVDT data) and their measured chord lengths are also included in Figure 107. In spite of

$$\delta_y = (\delta_1 + \delta_2) \cos \psi$$

$$(\psi = 35.26^\circ)$$

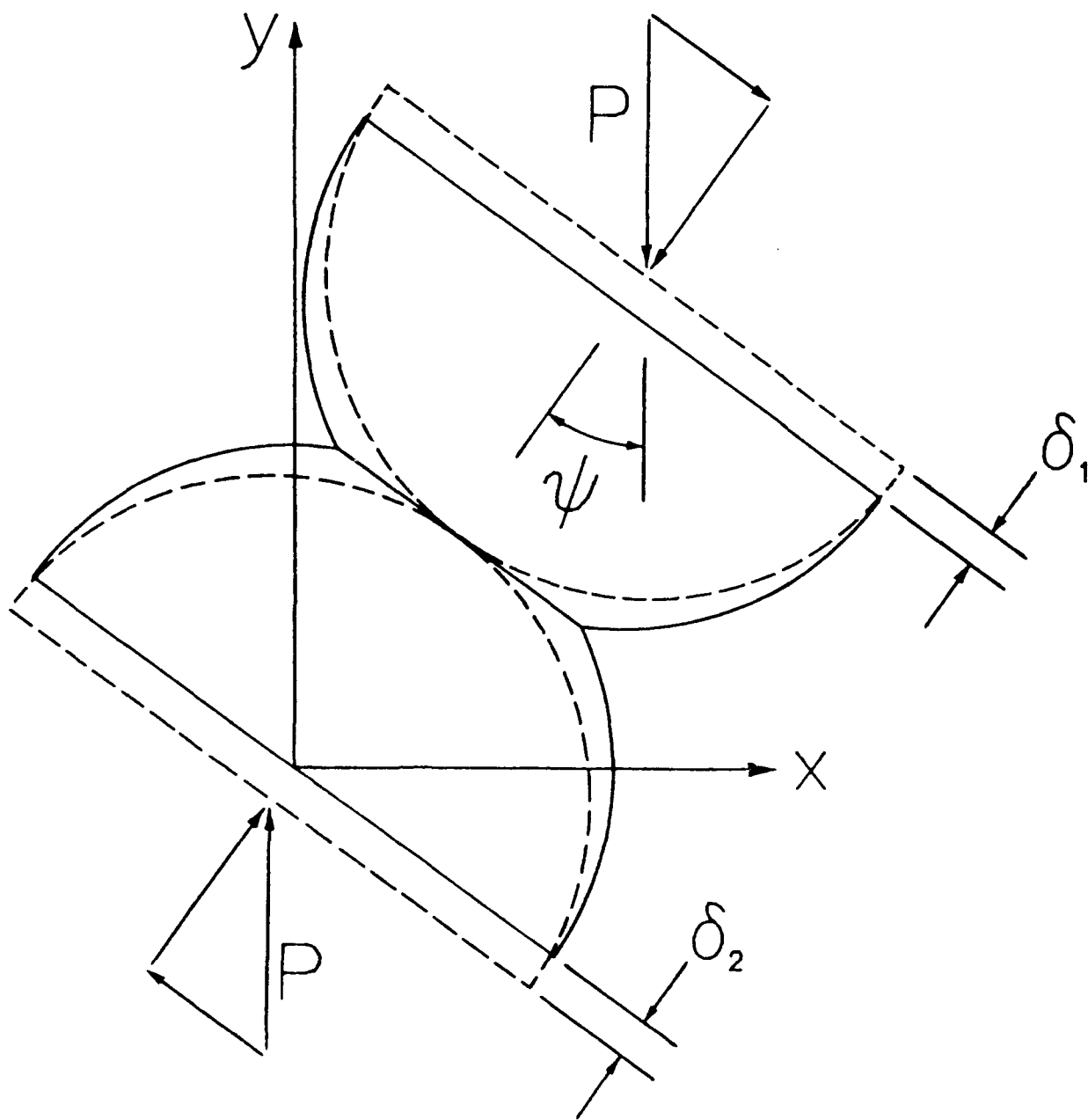


Figure 106. Ball Displacement Caused by Elastic Deformation

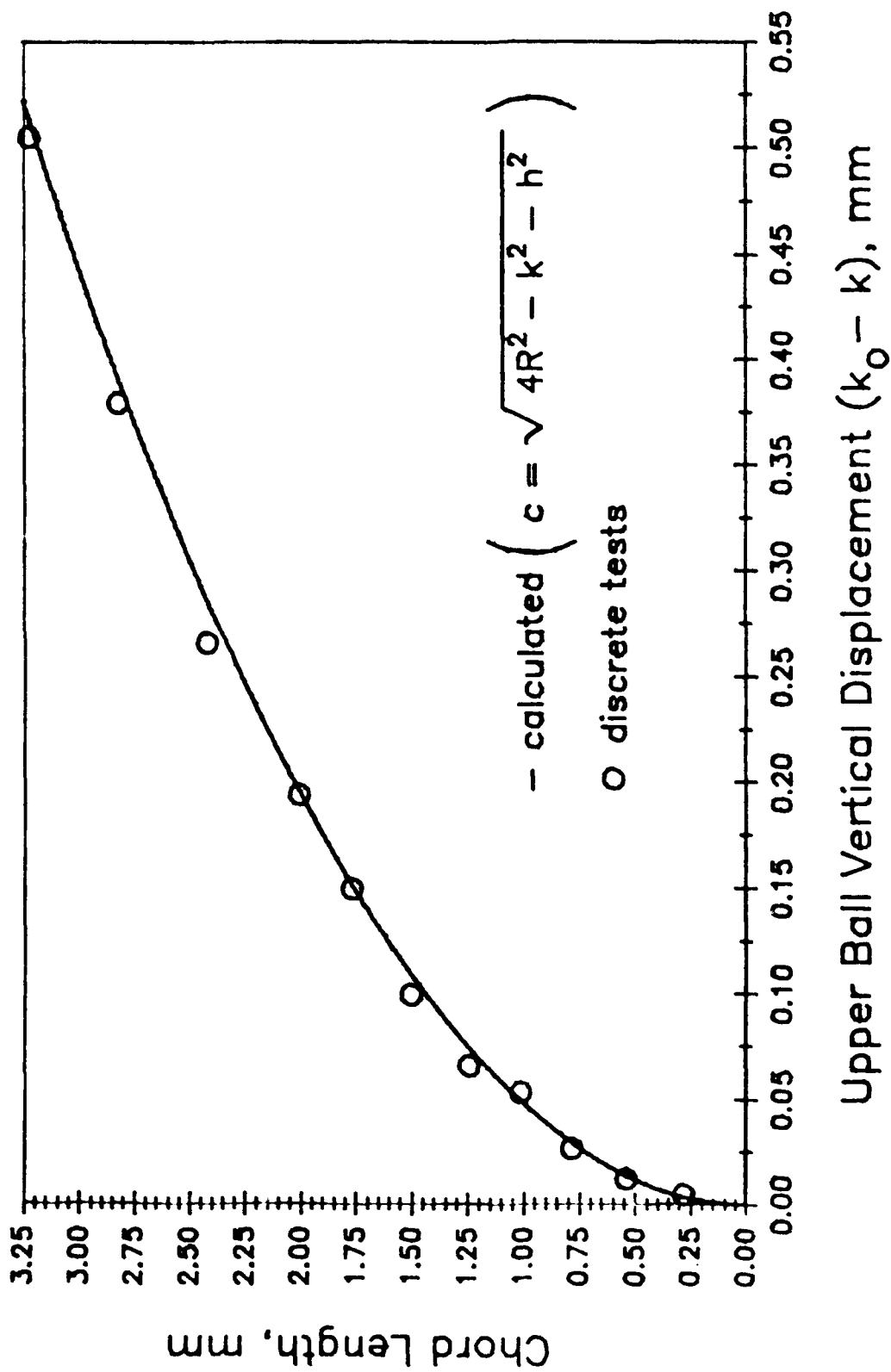


Figure 107. Relationship Between Upper Ball Displacement and Chord Length
(Theoretical and Experimental)

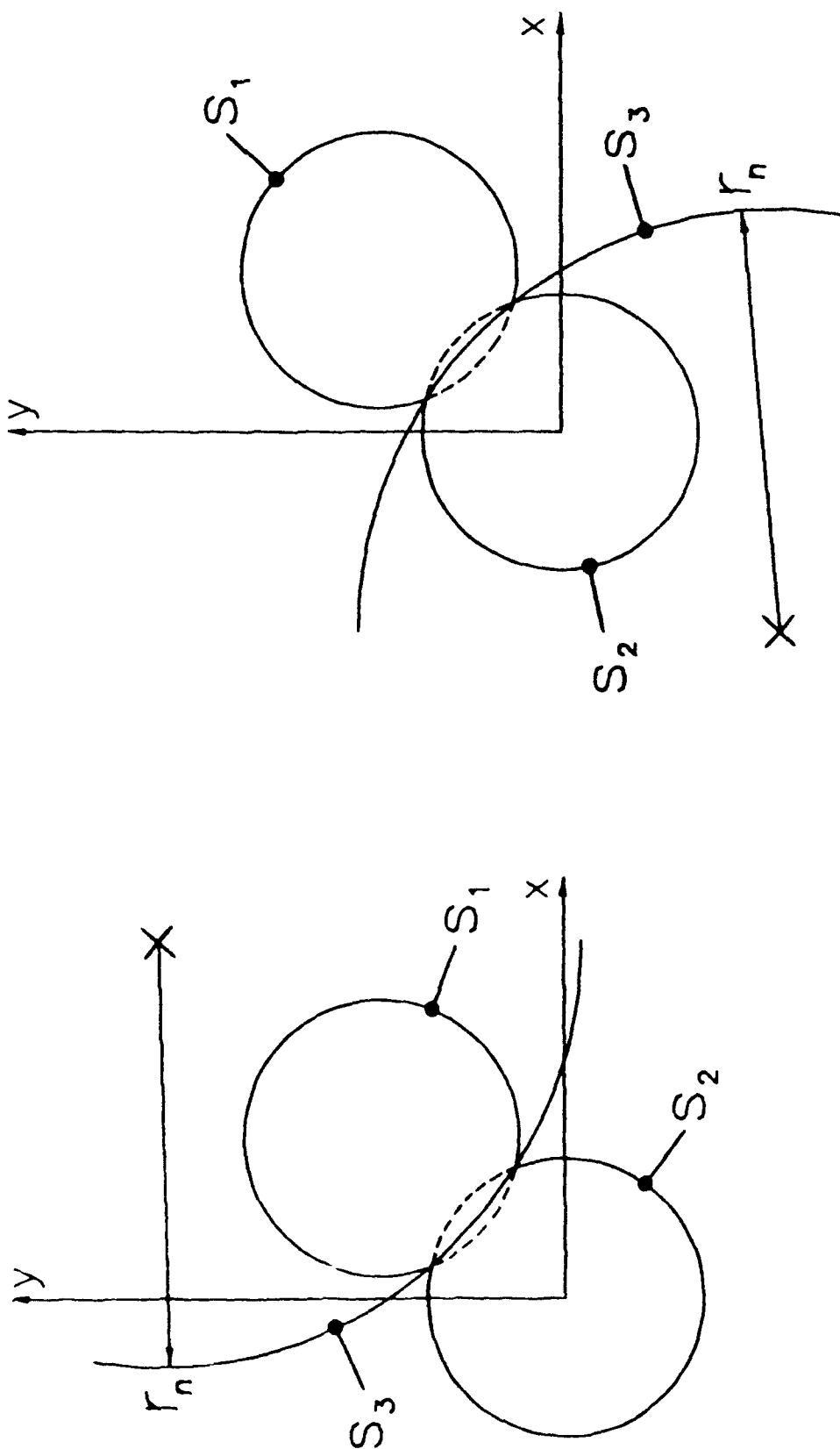
measuring uncertainty, correlation between test results and theory is excellent, thus validating the geometric assumption. Moreover, this correlation exists independent of test duration, lubricant, specimen material, or temperature since discrete data points came from tests done with a variety of oils, ball materials, and operating conditions.

d. Derivation of Scar Equation

With the end points of the scar located, the only region left to model is the actual path connecting p_1 and p_2 . From Figure 105, it is apparent that the scar surface must lie somewhere between s_1 and s_2 . If the assumption is made that the scar cross section normal to sliding is circular, the scar profile may be represented by either of the surfaces, s_3 , shown in Figure 108. The regions between the upper ball and the large circular arcs would represent upper ball wear, and the regions between the lower ball and these arcs would represent lower ball wear.

Choosing a circular arc to approximate the scar surface is valid despite the roughness of the scars. Figure 109 illustrates that a single circular arc would apply to both upper and lower ball surfaces since their surface profiles are nearly a perfect match. Despite the roughness for the given scale (these scars were from a test which produced large amounts of wear), an equivalent profile can be chosen to average the depths and heights of all the valleys and peaks to represent the surfaces as circular arcs (Figure 109 includes the scar profile parallel to the sliding direction to demonstrate how an equivalent profile might look.)

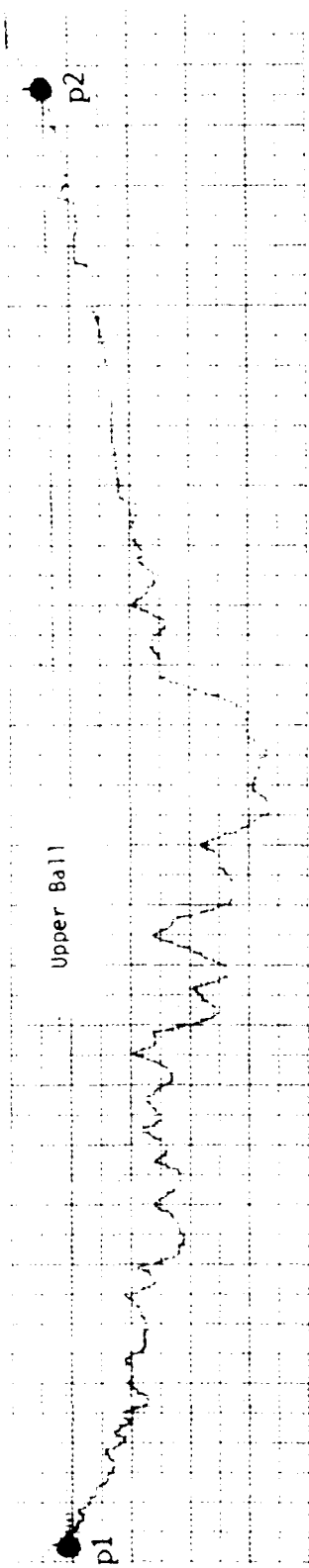
Instead of working from actual surface traces to arrive at an equivalent profile circle, the equation for the circle may be found by forming a linear combination of s_1 and s_2 between p_1 and p_2 . The surface, s_1 , is described by the equation for the upper ball in the x-y plane:



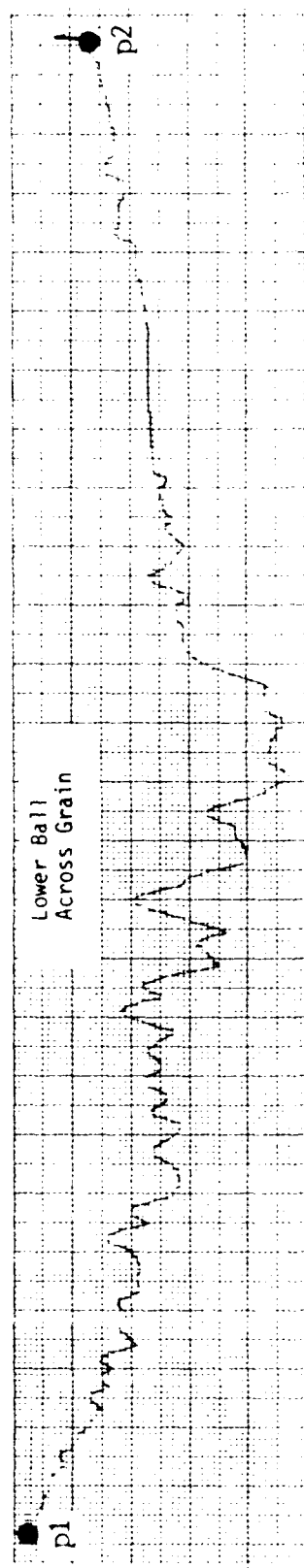
a

b

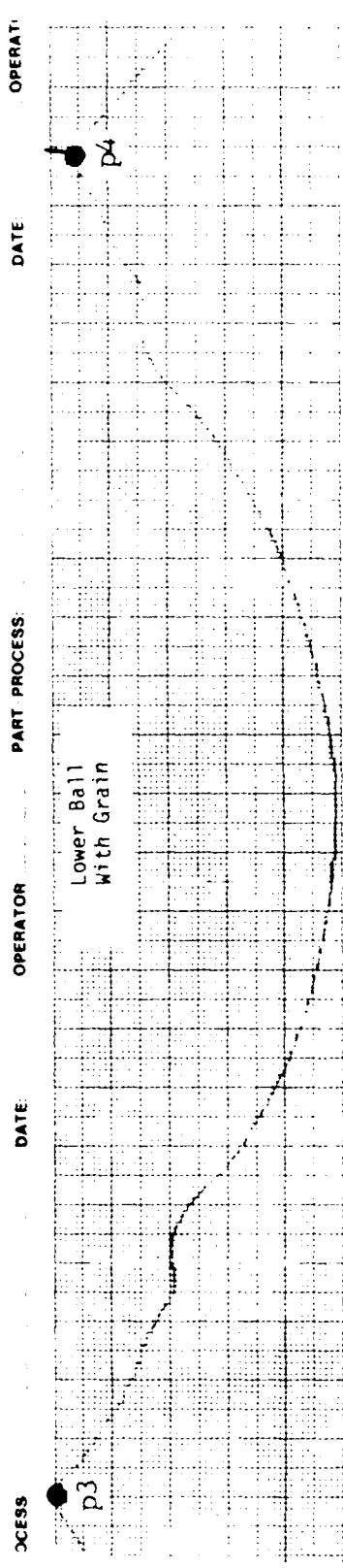
Figure 108. Two Possible Scar Surfaces, s_3 . Assuming the Scar Profile can be Approximated with a Circular Arc; (a) s_3 Centered on the Same Side of Contact as the Upper Ball and (b) s_3 Centered on the Same Side of Contact as the Lower Ball



DATE OPERATOR PART PROCESS DATE OPERATOR PART PRC



O OCH-01013 FEDERAL PRODUCTS CORP., PROVIDENCE, RHODE ISLAND, U.S.A. CHART NO OCH-01013 FEDERAL PRODUCTS CORP., PROVIDENCE, RHODE ISLAND



ND, U.S.A. CHART NO OCH-01013 FEDERAL PRODUCTS CORP., PROVIDENCE, RHODE ISLAND, U.S.A. CHART NO OCH-01013 FEDERAL PRODUCTS CORP., I

Figure 109. Scarf Profiles from a 20-hour Test of 0-67-1 at 150°C (1200 RPM, 145-N Load, 52100 Balls). Upper Ball Profile is Inverted to Illustrate the Similarity of Mating Surfaces. Profile Made with the Grain of the Lower Ball is Included as an Example of how a Circular Arc May Average the Roughness

$$(x - h)^2 + (y - k)^2 = R^2 \quad 2$$

Similarly, s_2 is given by the equation of the lower ball in the x-y plane:

$$x^2 + y^2 = R^2 \quad 3$$

The linear combination of s_1 and s_2 can be formed as:

$$\alpha_1[(x - h)^2 + (y - k)^2 - R^2] - \alpha_2[x^2 + y^2 - R^2] = 0 \quad 4$$

where α_1 and α_2 are weighting functions such that:

$$\alpha_1 + \alpha_2 = 1 \quad 5$$

and

$$\alpha = \alpha_1 = 1 - \alpha_2 \quad (0 \leq \alpha \leq 1) \quad 6$$

Using Equation 6 to substitute for α_1 and α_2 of Equation 4 gives:

$$x^2 - \left(\frac{2ah}{2a-1}\right)x + y^2 - \left(\frac{2ak}{2a-1}\right)y + \frac{ah^2}{2a-1} + \frac{ak^2}{2a-1} - R^2 = 0 \quad 7$$

Equation 7 can be rearranged into the general form of a circle:

$$\left(x - \frac{ah}{2a-1}\right)^2 + \left(y - \frac{ak}{2a-1}\right)^2 = R^2 - \left(1 - \frac{a}{2a-1}\right)\left(\frac{ah^2}{2a-1} + \frac{ak^2}{2a-1}\right) \quad 8$$

Equation 8 will be referred to as the "scar equation" and generates the imaginary circles illustrated in Figure 108. These circles are centered at $\left(\frac{ah}{2a-1}, \frac{ak}{2a-1}\right)$ and have a radius, r_n , of $\sqrt{R^2 - \left(1 - \frac{a}{2a-1}\right)\left(\frac{ah^2}{2a-1} + \frac{ak^2}{2a-1}\right)}$.

The value of the alpha parameter influences the scar equation in the following manner. When alpha is equal to 1, Equation 8 reduces to the equation of the upper ball. This situation corresponds to the geometric intersection shown in Figure 105 and represents no upper ball wear.

Conversely, when alpha is 0, Equation 8 reduces to the equation of the lower ball, and no lower ball wear occurs. For alpha values between 0.5 and 1, the upper ball wears, but the scars on the lower balls remain concave both normal and tangent to the sliding direction (see Figure 108 for when s_3 is centered on the same side of contact as the upper ball). When alpha is between 0 and 0.5, the wear scar on the lower ball remains concave tangent to sliding, but becomes convex normal to the sliding direction, and the resulting contours of the lower balls scars are "saddle-shaped" (see Figure 108 for when s_3 is centered on the same side of contact as the lower ball).

e. Relationship Between Alpha and the Scar Dimensions

Figure 110 shows the radius, r_t , in an x-z plane within the worn region of the upper ball. The cross-section taken in Figure 110 is at the y value corresponding to the mid-point of the chord. The distance from the point p3 to the point p4, therefore, is the scar width at the middle of the chord. By calculating the value of r_t , the coordinates of the point, q, along the scar profile can be found. The scar equation can then be used to solve for the alpha parameter. As is shown in Appendix C, any scar shape may be represented by an equivalent ellipse whose elliptical width corresponds to the width of the scar at the mid-point of the chord (the distance from p3 to p4). Appendix C also details the procedure for calculating alpha from the chord length, c, and the elliptical width, w.

Figure 111 shows the variation of scar width to chord length for selected values of alpha ranging from 0 to 1. Figure 111 gives physical meaning to the alpha parameter and suggests that alpha is a function of the ratio of width to length since all of the lines are essentially linear.

f. Alpha as a Function of k

Because alpha locates the interface between the upper and lower ball,

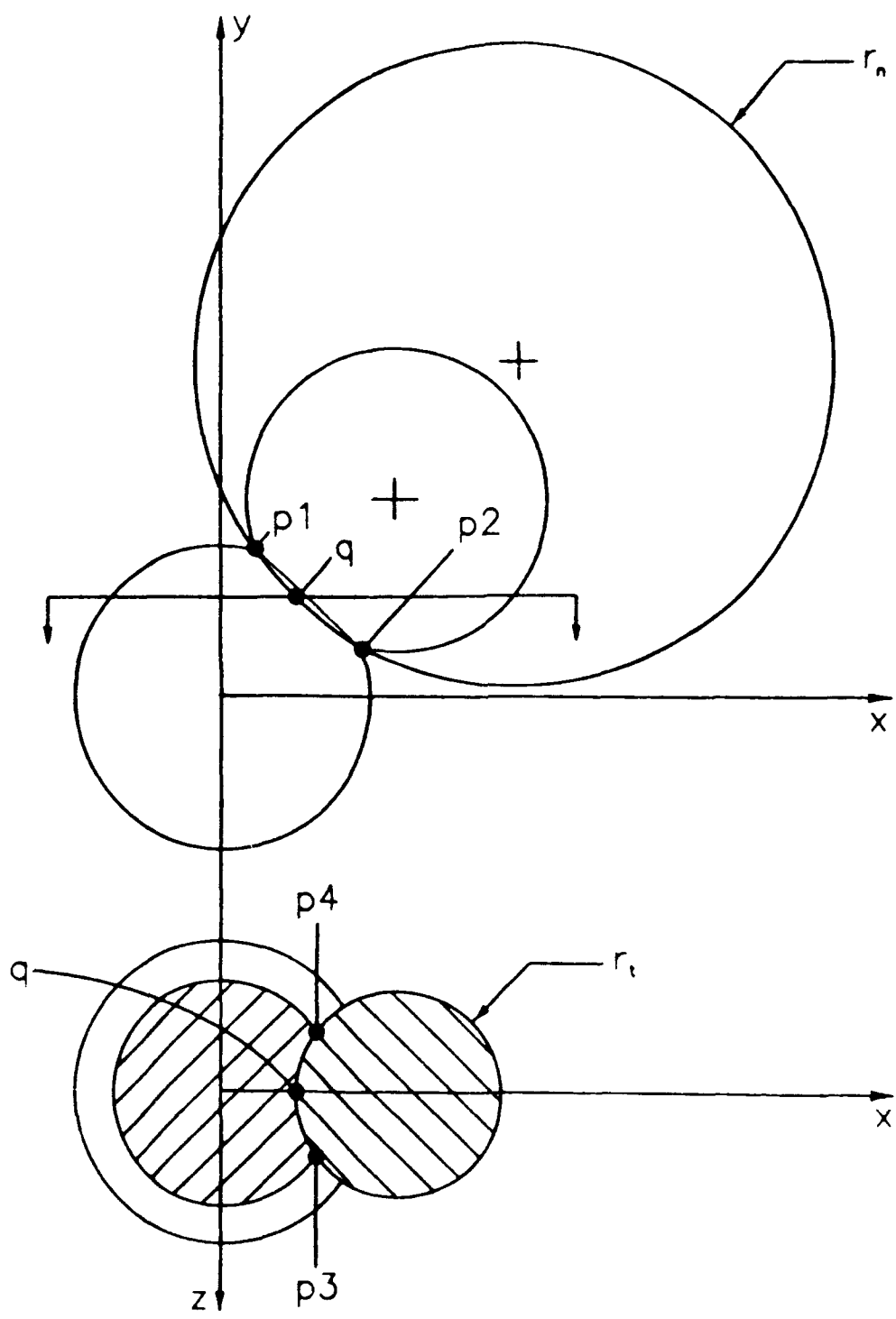


Figure 110. Cross-Sectional Areas of the Upper and Lower Balls at the Mid-Point of the Chord Length

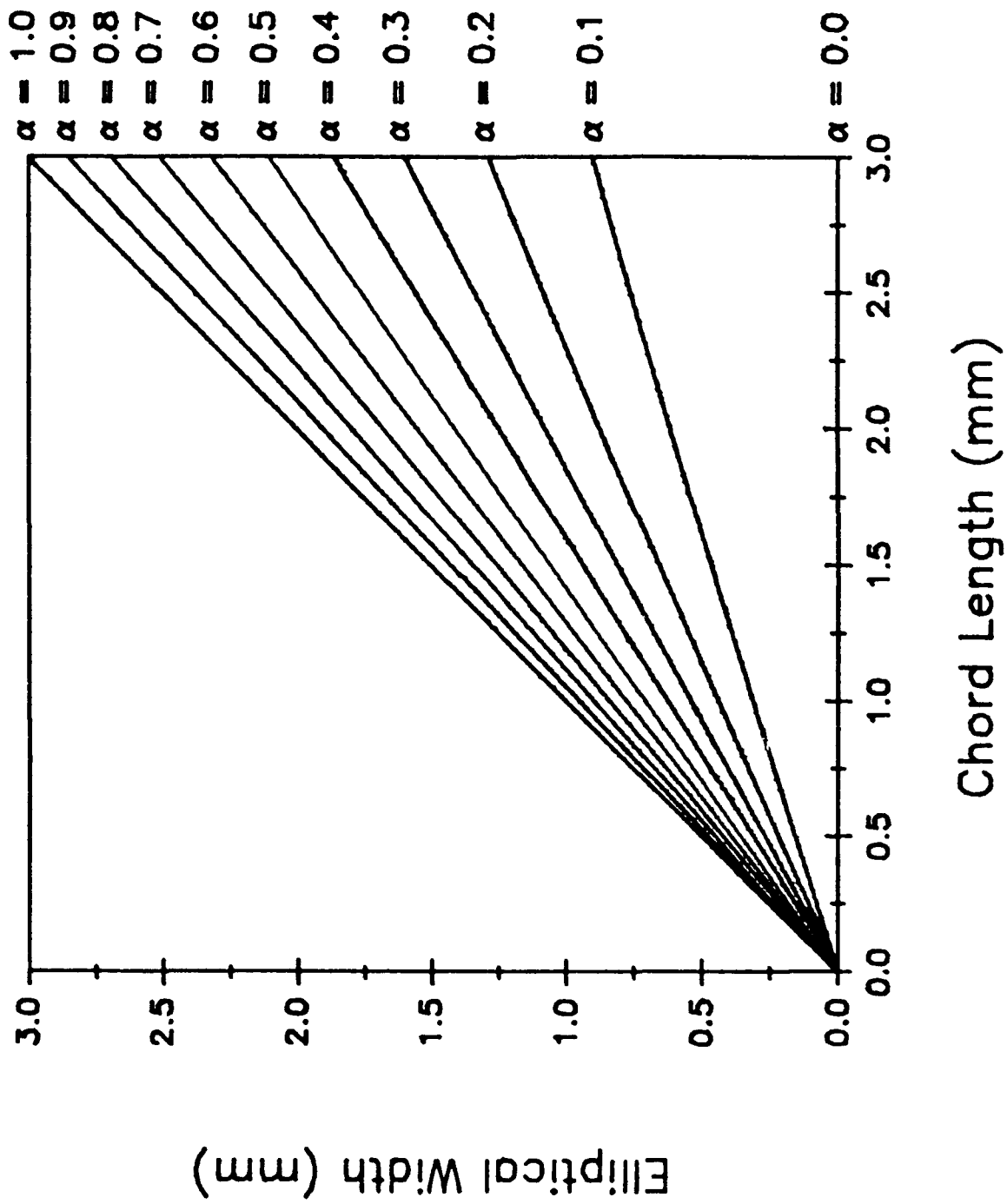


Figure 111. Relationship Between Scar Length, Width, and Alpha

it is informative to know how alpha varies throughout a test as the upper ball moves down. In Appendix C, the scar lengths and scar widths measured on the lower balls after a test are shown to define the alpha parameter. It may also be possible to determine a relationship between alpha and the upper ball displacement empirically by plotting the data of several tests. Figure 112 shows data points from a series of tests at the same conditions run at various lengths of time. Despite the scatter, a linear regression is made through the points in order to approximate the variation of alpha as wear continues.

Figure 112 also includes the dividing line where the upper ball and total lower ball wear volumes are equal. For 0-67-1, the top ball wear volume is greater than the total bottom ball wear volume for each test. To illustrate the proportion of upper ball wear to lower ball wear, wear volumes at each data point throughout a 20-hour test are plotted versus time in Figure 113 (the balls from this test were used for the profiles in Figure 109). Volumes were calculated for every LVDT data point using the regression line for alpha versus upper ball displacement given in Figure 112. The precise procedure used for calculating wear volumes is detailed in the next section.

g. Upper and Lower Ball Wear Volumes

The wear volume on the lower balls was found by rotating s_3 , between points p_1 and p_2 , about the y' axis and intersecting this solid of revolution with a sphere (lower ball) at the origin. This volume could be calculated exactly by solving the triple integral over the region. Such a calculation may not be easily solved due to the unusual geometries involved. Instead, the volume was calculated by dividing the region into n horizontal slices of equal thicknesses. Slices of the upper and lower balls taken mid-way along

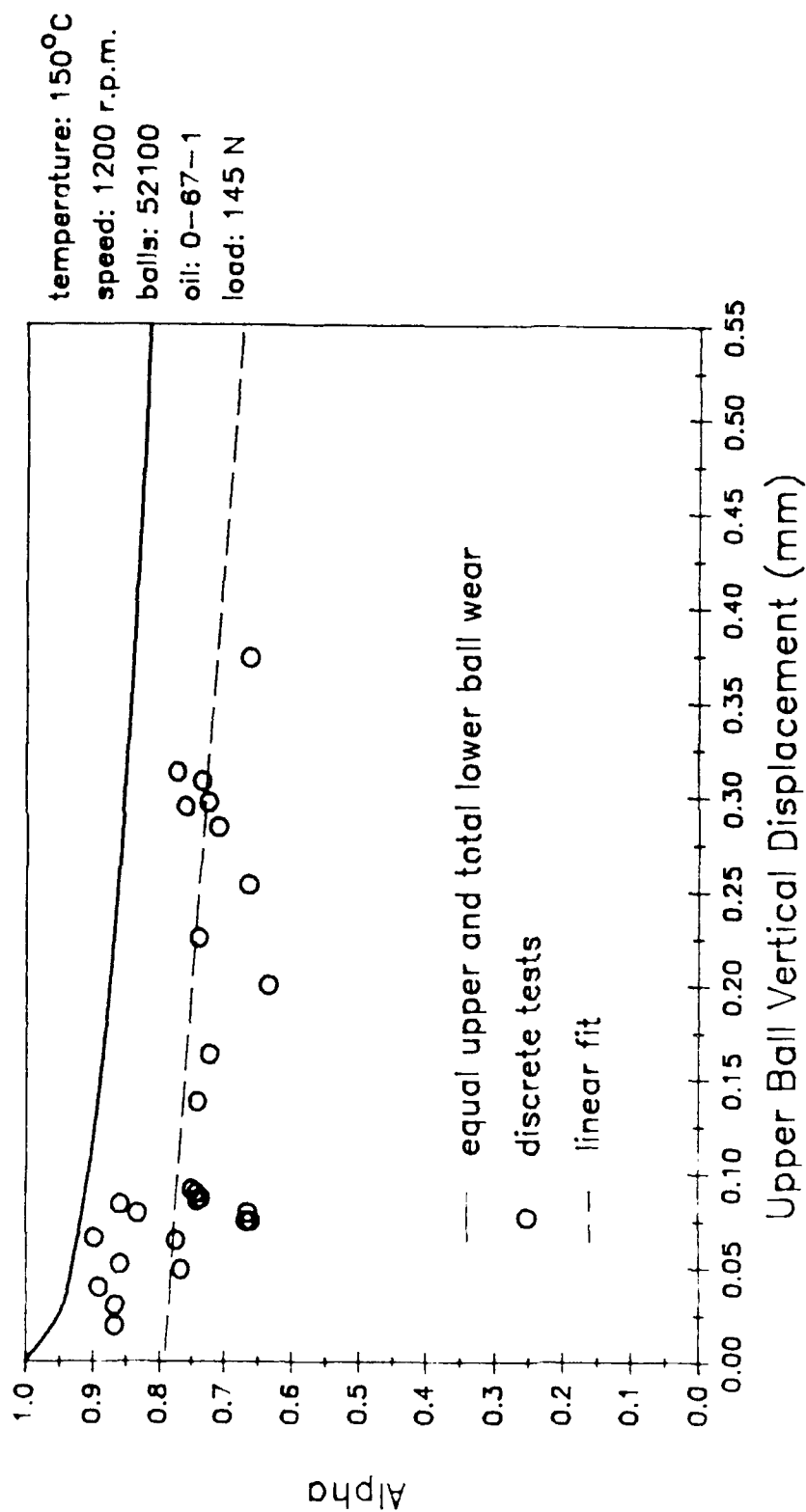


Figure 112. Relationship Between Upper Ball Displacement and Alpha for Giver Lubricant and Test Conditions Compared to the Curve Representing Equal Upper Ball and Total Lower Ball Wear Volumes

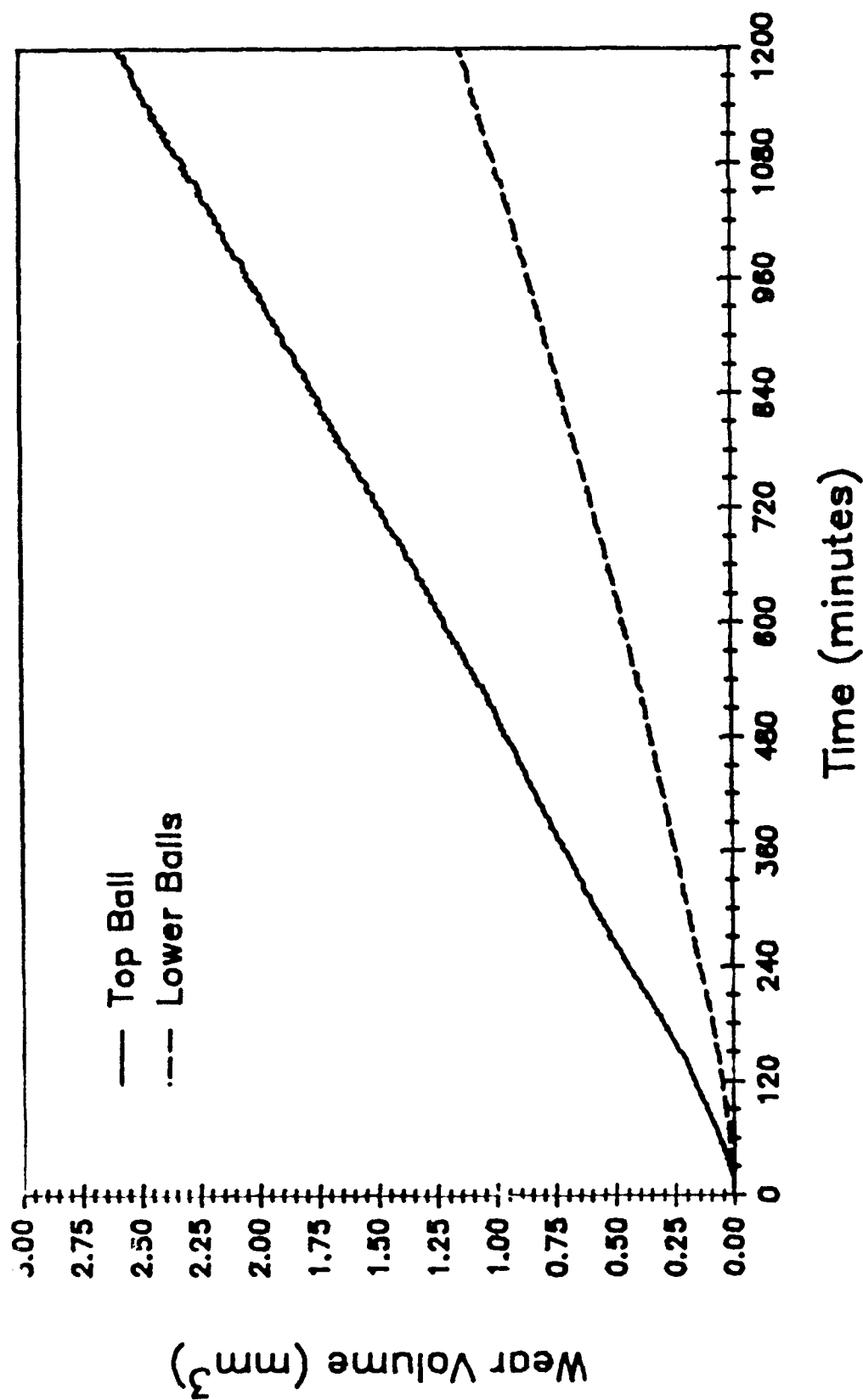


Figure i13. Wear Volume History of a 20-Hour Test of 0-67-1 at 150°C (1200 RPM, 145-N Load, 52100 Balls) Generated from the LVT Data and the Linear Variation on Alpha Shown in Figure i12

the chord are shown in Figure 114. The worn away areas of the upper ball and the lower ball are calculated at each slice. Consecutive areas are averaged and then multiplied by the slice thickness to generate a volume increment. The n volume increments are summed to calculate the wear volumes for the upper and one lower ball. A total of 50 slices are sufficient to accurately determine wear volumes. This value was chosen by assuming an alpha of 1 (no upper ball wear) and comparing the resulting lower ball wear volume to the volume of two spherical caps calculated from a standard geometrical formula.

The sensitivity of volume calculations on the correct value of alpha is illustrated in Figure 115. The volumes were calculated at various upper ball displacements by assuming different values for alpha. Notice that using the correct value of alpha becomes increasingly more important in tests involving large upper ball displacements. For upper ball displacements less than 0.0100 mm (chord lengths less than 0.4562 mm), the value of alpha is not critical, and the Feng equation is valid. Assuming a circular scar on the lower ball as Feng does is equivalent to choosing a constant alpha of 1.

It was stated before that these analyses are appropriate only for scars with chord lengths greater than a critical value governed by the calculations for elastic deformation. This small scar limit can be imposed by comparing volume calculations for different scar chords. Since Figure 115 indicates that an alpha of 1 may be assumed for chords less than 0.4562 mm, the volumes associated with a chord of 0.4562 mm and a chord of 0.2427 mm can be compared by assuming all the wear occurs on the lower balls. The 0.2427-mm chord, recall, is the chord predicted by Equation 1 for the vertical displacement caused by contact stresses. The total volume of deformation for a chord of 0.2427 mm is $1.6096(10)^{-4} \text{ mm}^3$ while the total volume from wear for a chord of 0.4562 mm is $2.0101(10)^{-3} \text{ mm}^3$. The true wear

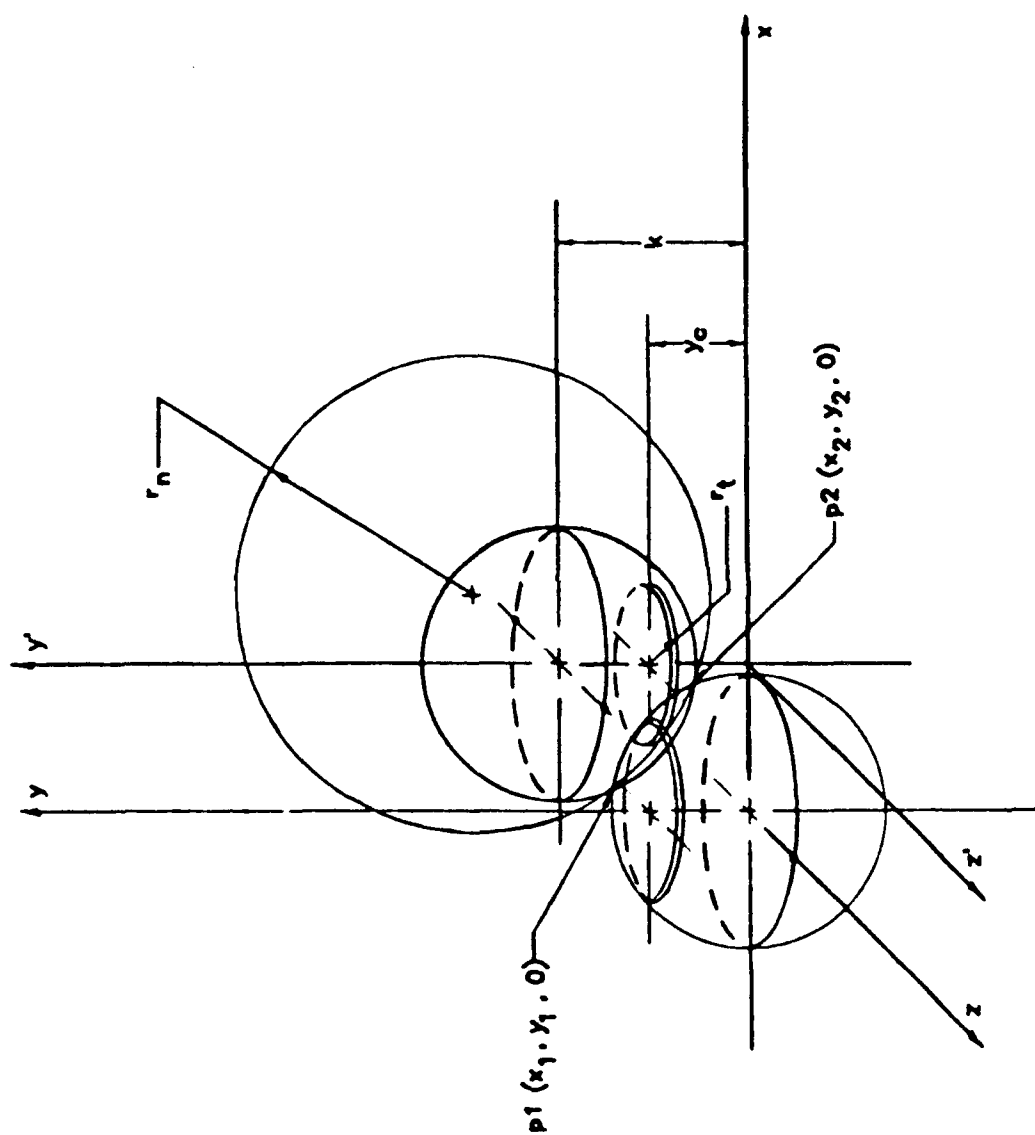
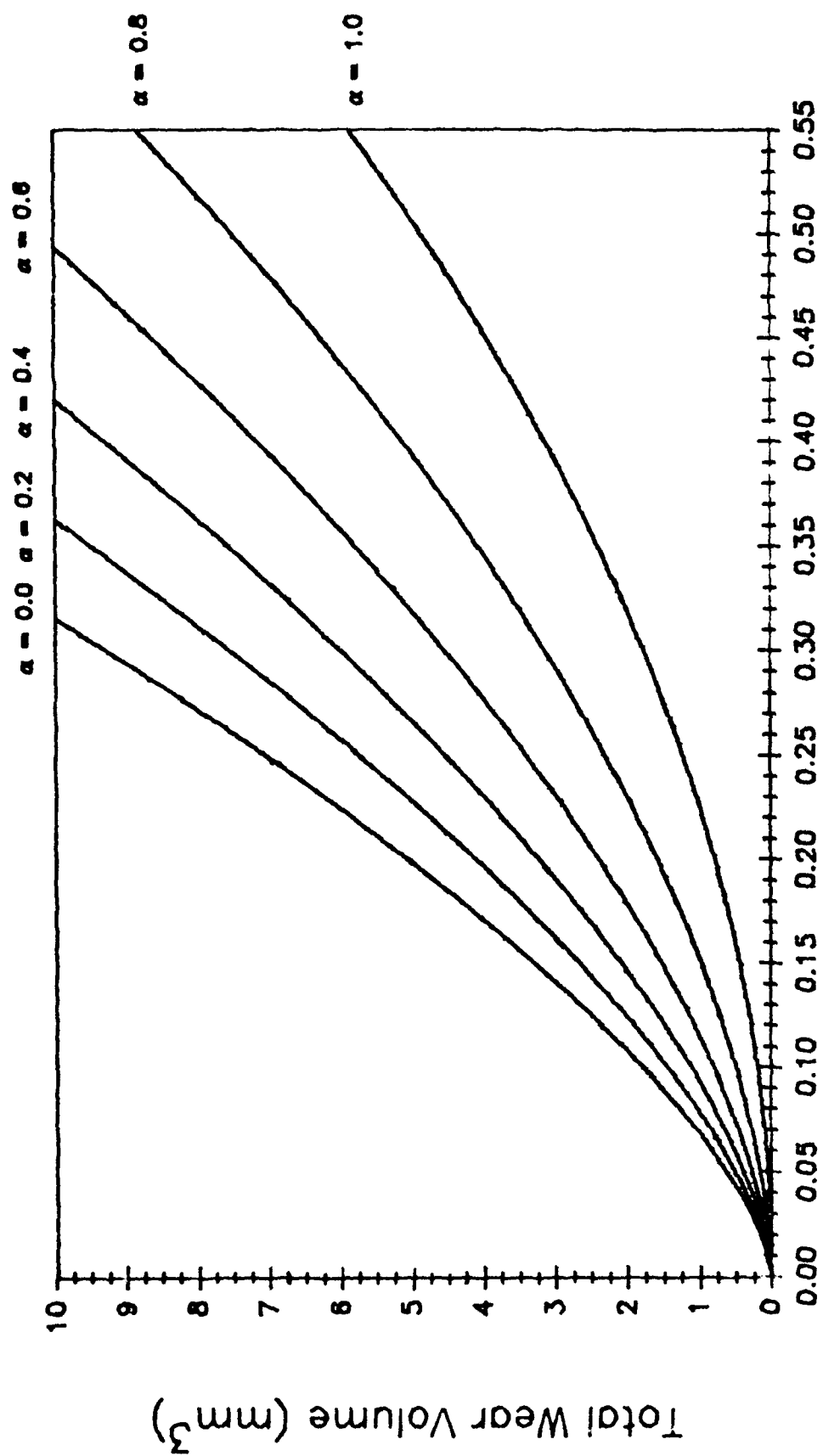


Figure 114. Slices of Upper and Lower Ball Wear Volumes



Upper Ball Vertical Displacement (mm)

Figure 115. Sensitivity of Volume Calculations to the Alpha Parameter

scar volume for the 0.4562-mm chord can be found by subtracting off the volume contribution from deformation. The error introduced by including the volume of deformation with the true wear volume is 8.7%. As previously stated, the error will diminish as scars grow, and the value of 0.4562 mm can be arbitrarily chosen as the small scar limit for this study.

h. Lower Ball Scar Shape

It can be seen from the x-z plane of Figure 110 that at a given y coordinate, the lower ball scar is defined by the radius, r_t , of the worn portion of the upper ball. At every y value between p1 and p2, a different value of r_t passes through the lower ball. As the r_t 's sweep out tracks in the lower ball, two factors combine to dictate the scar shape. As seen in the x-y plane of Figure 110, r_t would be longest at p1 and shortest at p2. The radius of curvature of the scar parallel to sliding, therefore, is greatest at p1 and shortest at p2. In addition, because the surface of the lower ball is closer to the y' axis at p2 than at p1, the shorter values of r_t near p2 still remove wide sections of the lower ball.

These two mechanisms combine to give the following results. When there is no upper ball wear, the scars on the lower balls are circular. With increasing upper ball wear, the width becomes increasingly smaller than the chord length. An example of a scar with a chord length of 2.000 mm and a scar width of 1.625 mm (which gives an alpha of 0.662) is shown in Figure 116. The points shown lie along paths swept out by various r_t 's from y_1 to y_2 . When these paths are projected onto the plane containing points p1, p2, p3, and p4, they appear to be curved. The paths are curved more sharply near p2 because r_t is shorter at p2, giving the scar a greater depth for a given width near p2 than it does at p1. Figure 117 shows the variation of the lower ball scar shape as alpha varies for a constant chord length. As alpha

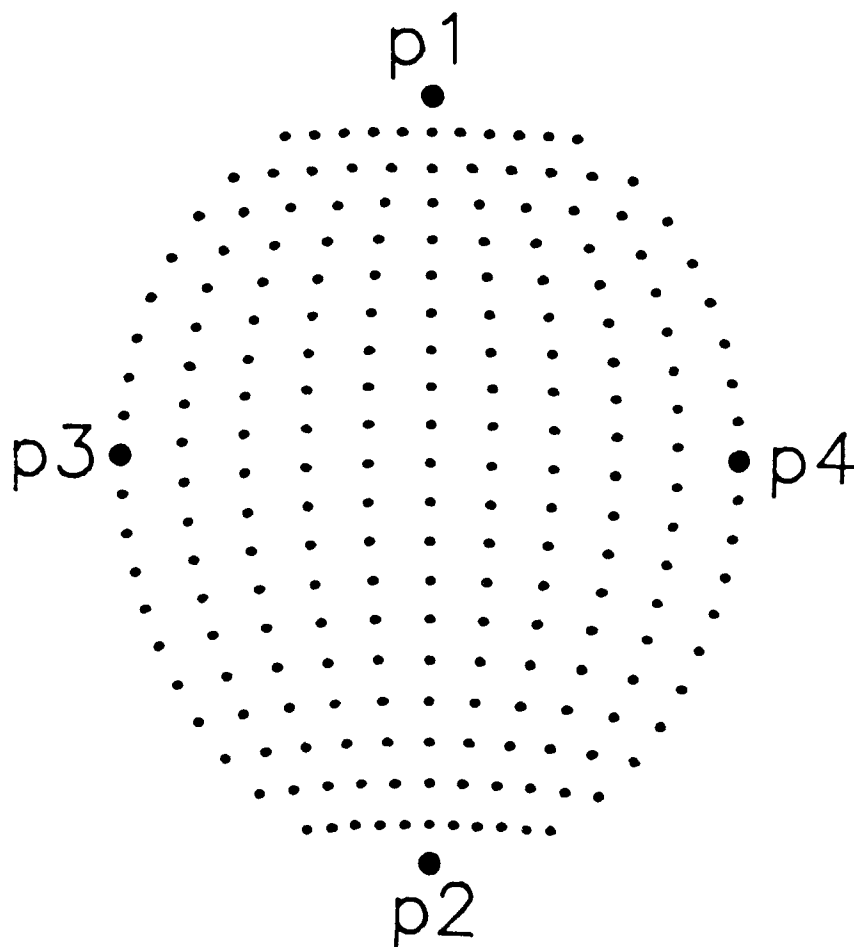


Figure 116. Scar Shape Predicted by the Geometric Analysis of the Four-Ball Configuration for a 2.000-mm Chord Length and a 1.625-mm Elliptical Width (giving an alpha of 0.662)

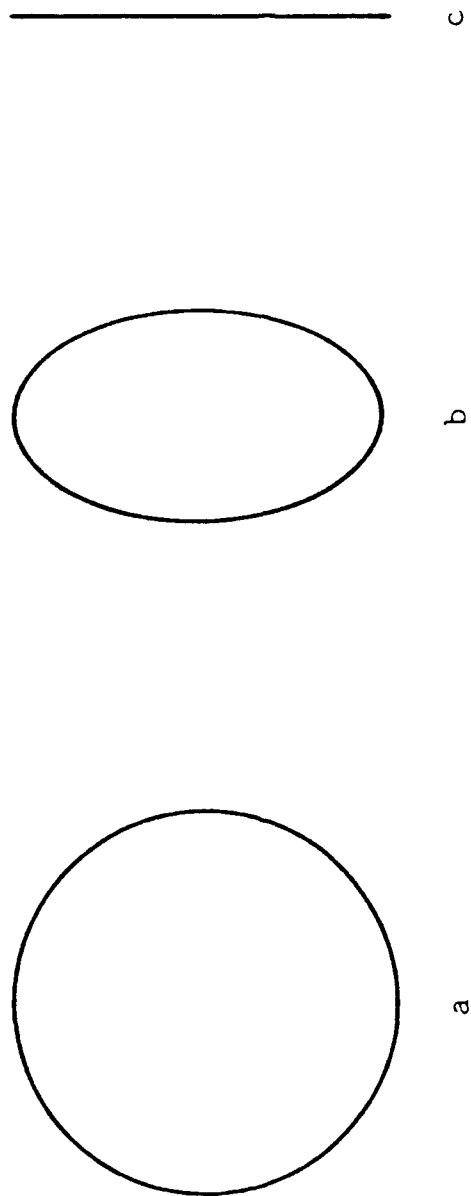


Figure 117. Lower Ball Scar Shapes for Alpha Values of (a) 1 (circular scar), (b) 0.33 (elliptical scar), and (c) 0 (no scar)

decreases from 1 to 0, the scar width also decreases, and the scar shape changes from a circle to an ellipse and then eventually becomes a line. Appendix C details the procedure for determining the equivalent elliptical width of the lower ball wear scars and for calculating alpha from this width and the chord length. Appendix C also addresses the problem in measuring unusual scar geometries generated by four-ball testing.

4. EFFECT OF OILS, SPECIMENS, AND EXPERIMENTAL CONDITIONS ON WEAR SCAR

a. Length-Width Relationship

Equation 1 provides an accurate means of predicting the chord length from an LVDT-measured displacement (see Figure 107). In order to convert the continuous ball travel data recorded by the LVDT into an instantaneous wear volume, an accurate history of the elliptical width is also needed to establish an alpha parameter at every data point. As seen in Table 97, the alpha parameter cannot be assumed to remain constant throughout an entire test. Indeed, alpha is rarely constant even in tests run for the same duration. Furthermore, an attempt to relate the alpha parameters from several tests of various durations to the upper ball displacement showed so much scatter (Figure 112) that any predicted alpha value will have a high degree of uncertainty. Based on these observations, a method of evaluating the elliptical width at any moment during a test seems unattainable.

Before making an effort to predict scar width at any point during a test, a typical characteristic of the four-ball test should be addressed. Figure 118 is a log-log plot of the LVDT position versus test time for a 20-hour test of an ester-based lubricant. There are three regions of interest on the LVDT trace. The first region is at the beginning of the test and represents "run-in" wear. The data in this transient region cannot be interpreted. The second region has a constant slope which indicates the

TABLE 97
VARIATION IN THE ALPHA PARAMETER FOR VARIOUS TEST TIMES

Oil: 0-67-1
Speed: 1200 rpm
Balls: 52100
Load: 145 N

Test No.	Time (minutes)	Temperature °C	Alpha
356	180	75	0.887
364	180	75	0.889
193	1200	75	0.975
351	1200	75	0.937
372	15	150	0.866
368	30	150	0.866
373	45	150	0.890
362	60	150	0.858
374	75	150	0.765
366	90	150	0.773
376	105	150	0.897
363	120	150	0.830
377	135	150	0.658
367	150	150	0.664
352	180	150	0.732
369	180	150	0.857
371	180	150	0.662
397	180	150	0.740
398	180	150	0.747
412	180	150	0.739
393	300	150	0.739
394	420	150	0.720
389	600	150	0.632
395	720	150	0.736
392	900	150	0.661
396	1020	150	0.708
353	1200	150	0.731
357	1200	150	0.771
421	1200	150	0.758
426	1220	150	0.721
391	1800	150	0.660
370	4095	150	0.749
200	180	250	0.636
472	180	250	0.649
381	1200	250	0.871
466	1200	250	0.875

temperature: 75°C
 speed: 1200 r.p.m.
 balls: 52100
 load: 245 N

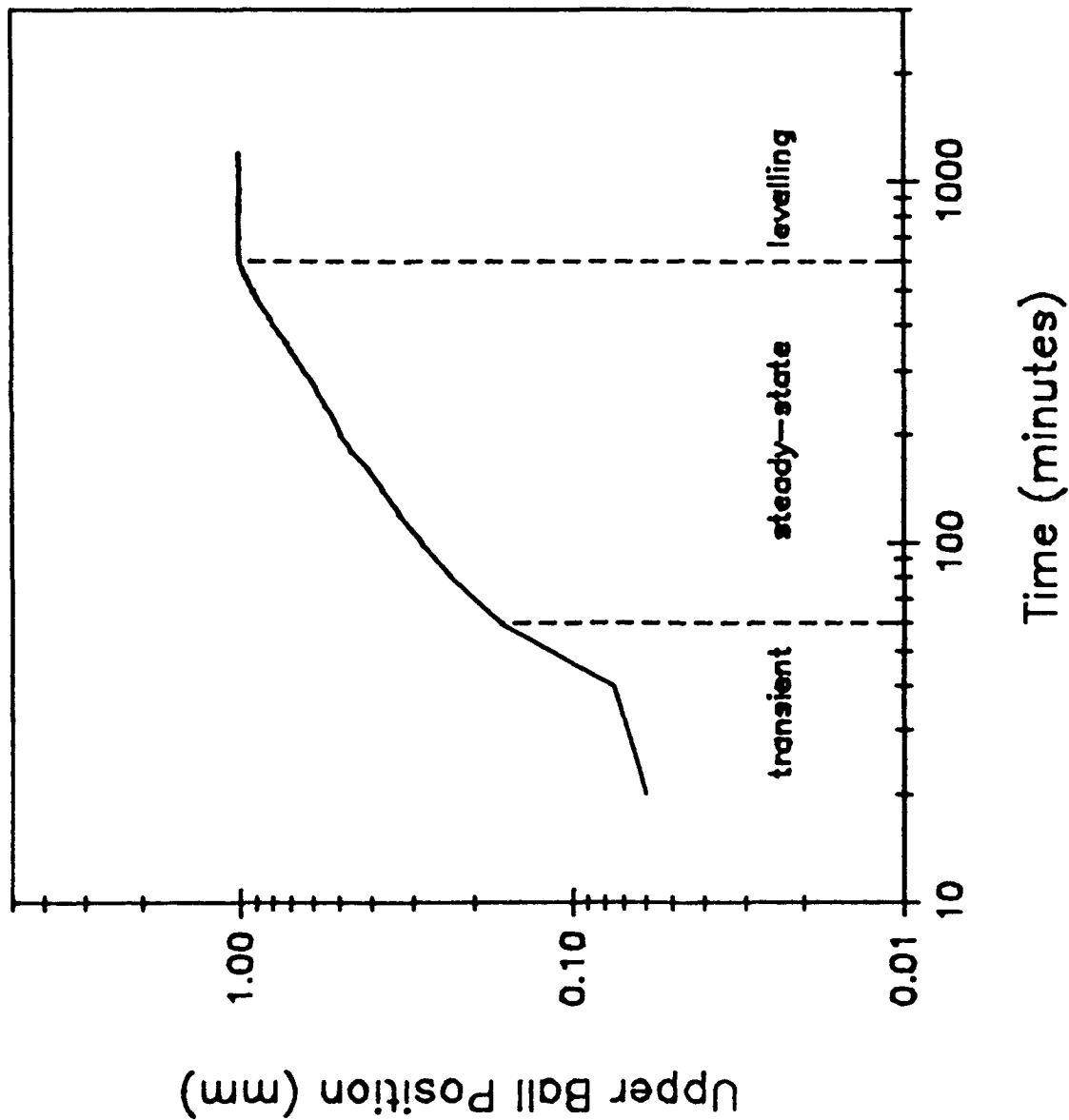


Figure 118. Three Wear Regions of the Sliding Four-Ball Test Represented by the Upper Ball Position Versus Time for an Ester-Based Lubricant

relative ball displacement is changing at a fixed, logarithmic rate. The second region indicates "steady-state" wear. The last region shows no change in the relative ball displacement with time, indicating that wear has stopped or been significantly reduced. These three areas of the LVDT versus time curve are general trends of the sliding four-ball test.²⁴

Figure 119 is a plot of the chord length versus test time for the PPE-based lubricant O-67-1 for two identical tests. The chord lengths at each data point during these tests were calculated from the LVDT data using Equation 5. Note that in Figure 119, after a suitable run-in period (approximately 30 minutes), the two curves reach the same chord length. After this point is reached, the slopes of both curves are parallel for the remainder of the test and indicate equivalent wear rates. During the run-in period, the relationship between chord length and time cannot be ascertained. Furthermore, when conditions are not at equilibrium which occur when the balls are brought together to start a test, frictional heating causes thermal expansion of the balls, and a negative LVDT displacement results. An example of this phenomenon is shown by the solid line of Figure 119 (Test 357). Neglecting run-in wear, the two tests shown exhibit excellent repeatability.

Figure 120 illustrates the two chord traces again but includes chord lengths from discrete tests run at various durations. The chord traces of tests 357 and 421 converge on the discrete tests after approximately 5 hours. Figure 120 shows that there is accurate modeling of wear rates for long test times, but the transient run-in period significantly affects the wear geometry model when LVDT data are measured relative to time. To eliminate the error caused by this transient period, another basis of analysis is needed which is independent of time.

During a sliding four-ball test, the only continuously monitored

temperature: 150°C
speed: 1200 r.p.m.
oil: 0-67-1
balls: 52100
load: 145 N

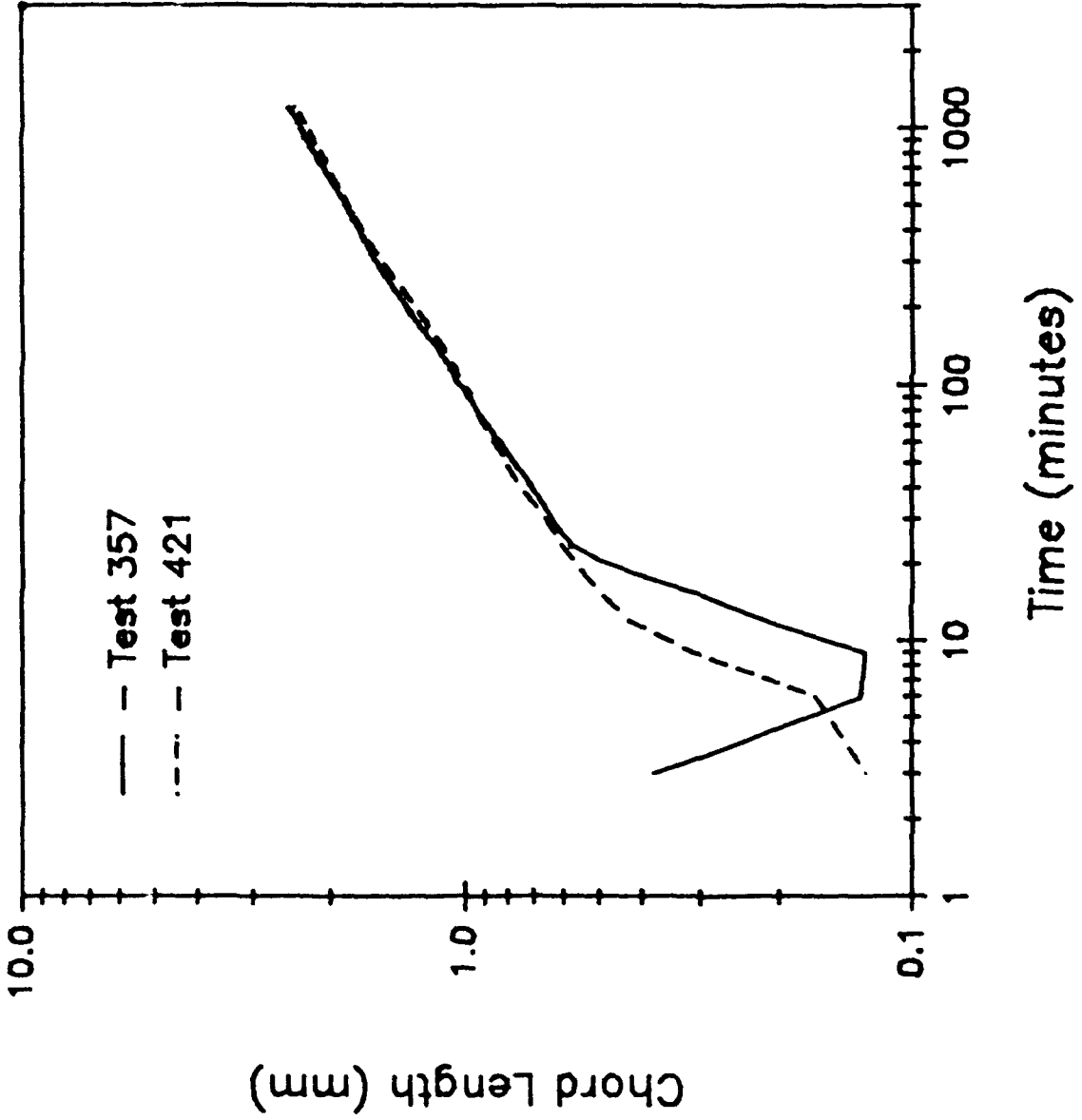


Figure 119. Chord Length Calculated from LVDT Data Versus Time for Two 20-Hour Tests Run Under Identical Conditions

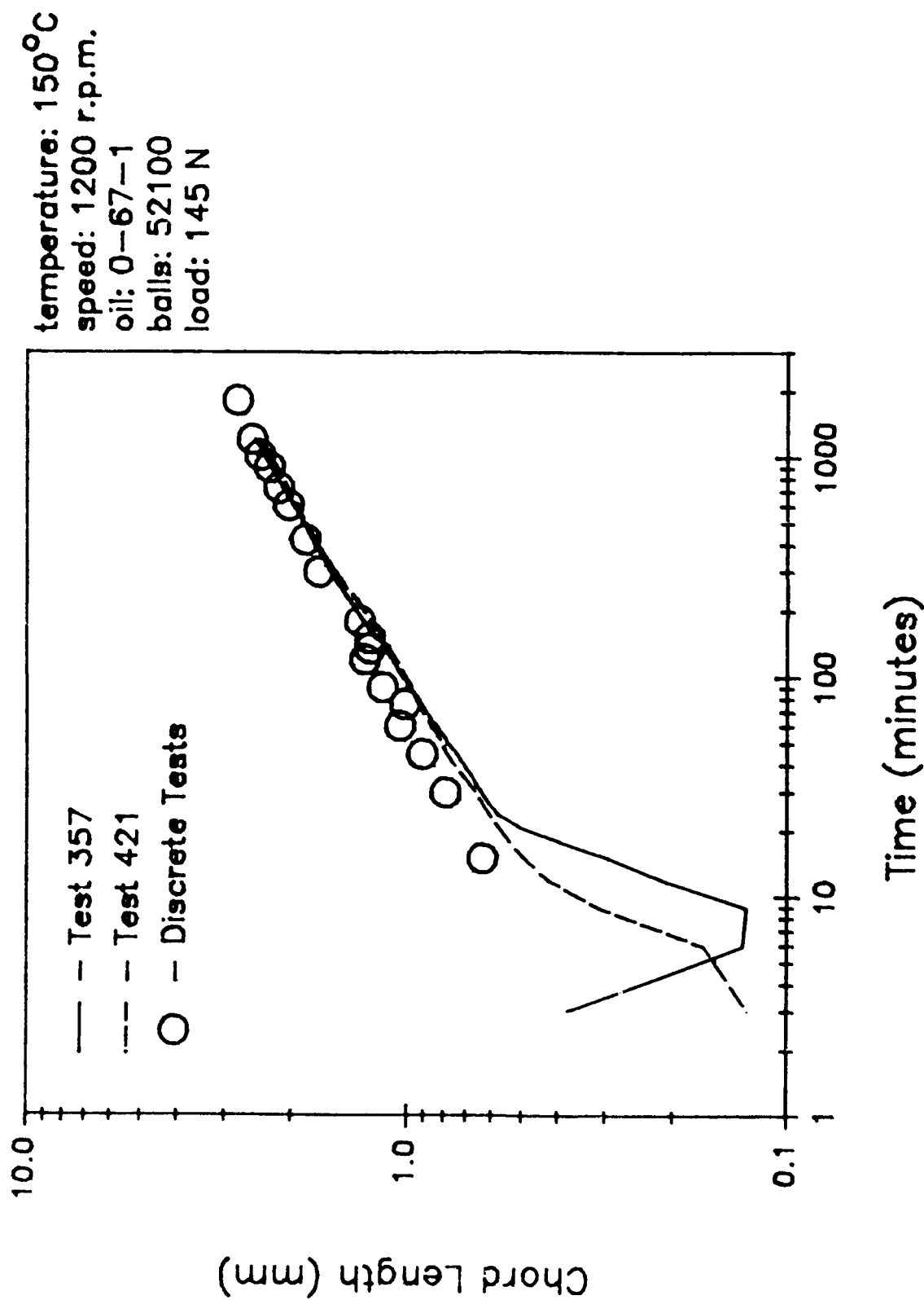


Figure 120. Chord Length Versus Time for a Series of Discrete Tests. (Data Shown in Figure 119 is Included for Comparison)

conditions that can be related to the scar shape (i.e., the alpha parameter) are test time and ball displacement. Because of the inherent error associated with run-in time, the LVDT position (i.e., the chord length) will be used. Figure 121 illustrates the elliptical width of the lower balls scars versus chord length for the ester-based lubricant of Figure 118. A linear relationship between elliptical width and chord length is apparent. Moreover, the linear relation extends into the regions of run-in wear (left end of the line) and no wear (right end of the line).

Figure 122 shows a similar linear relationship between elliptical width and chord length for O-67-1. The difference between Figures 121 and 122 is the equation for the linear regression through the data points. For the ester, the slope is 0.922 and indicates a high value for the alpha parameter. The slope corresponding to O-67-1 is 0.792, suggesting a lower value for alpha than the ester. The intercept values in the width-length equations offer a measure of the change in alpha as scars grow. For instance, in the case of the ester, the value of the intercept (0.041) is small compared to the slope (4.5% of the slope), and a constant ratio of width to length can be assumed for all sizes of scars. The intercept corresponding to O-67-1 (0.102), however, is significant (12.9% of the slope), and the ratio of width to length changes for different size scars.

A scar width to length ratio is a barometer of the alpha parameter. Two curves relating width over length to the alpha parameter are given in Figure 123. The alpha values of the solid curve were calculated using a chord length of 0.5 mm while the values of the dashed curve were based on a 4-mm chord length. For large values of alpha (greater than about 0.8), the relationship of width over length to alpha is independent of scar size.

Because of the drastic differences between the two lubricants used to

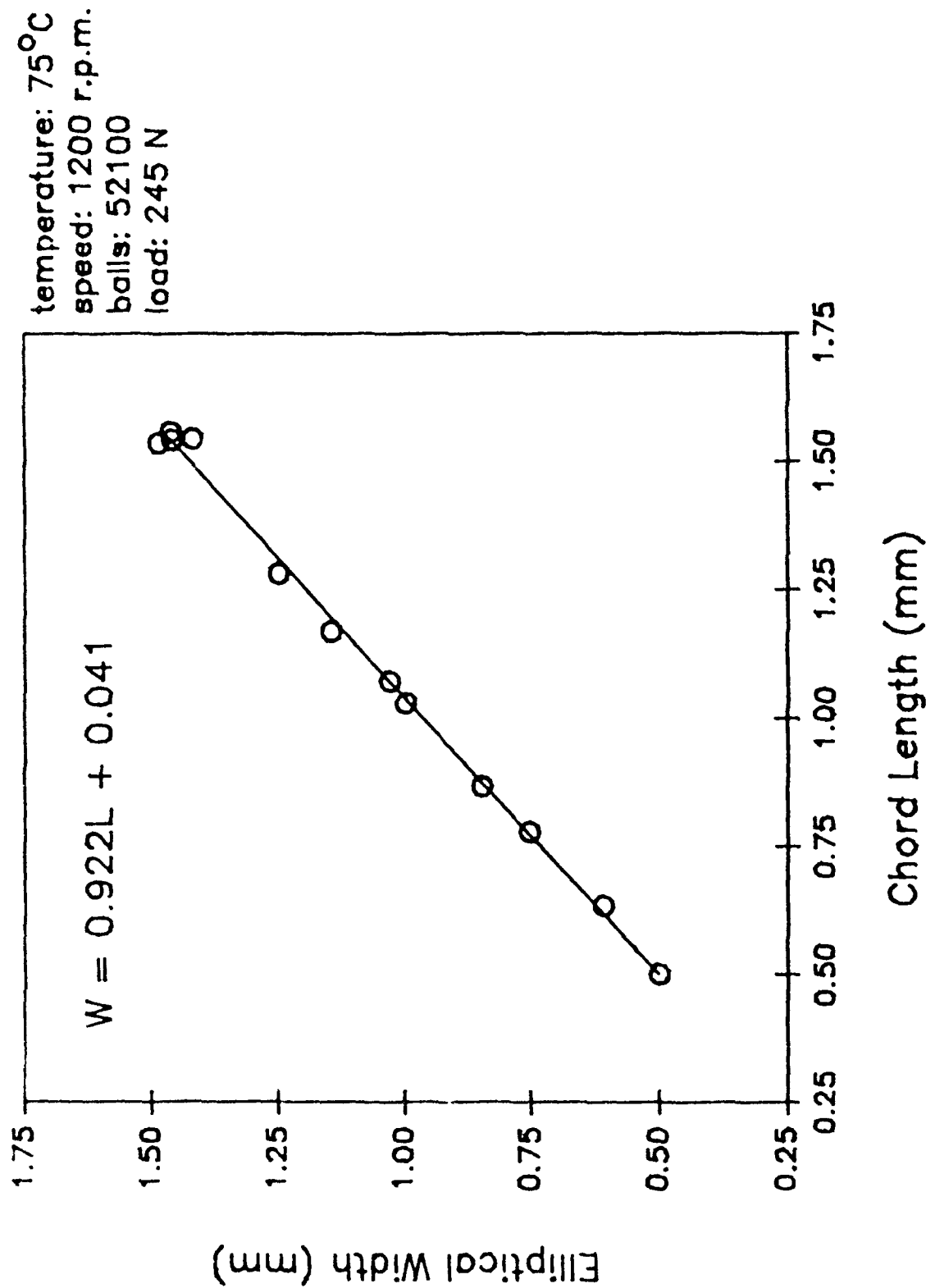


Figure 121. Elliptical Width Versus Chord Length for an Ester-Based Lubricant. Discrete Tests Ranged from 10 Minutes to 30 Hours in Duration

temperature: 150°C
 speed: 1200 r.p.m.
 oil: 0-67-1
 balls: 52100
 load: 145 N

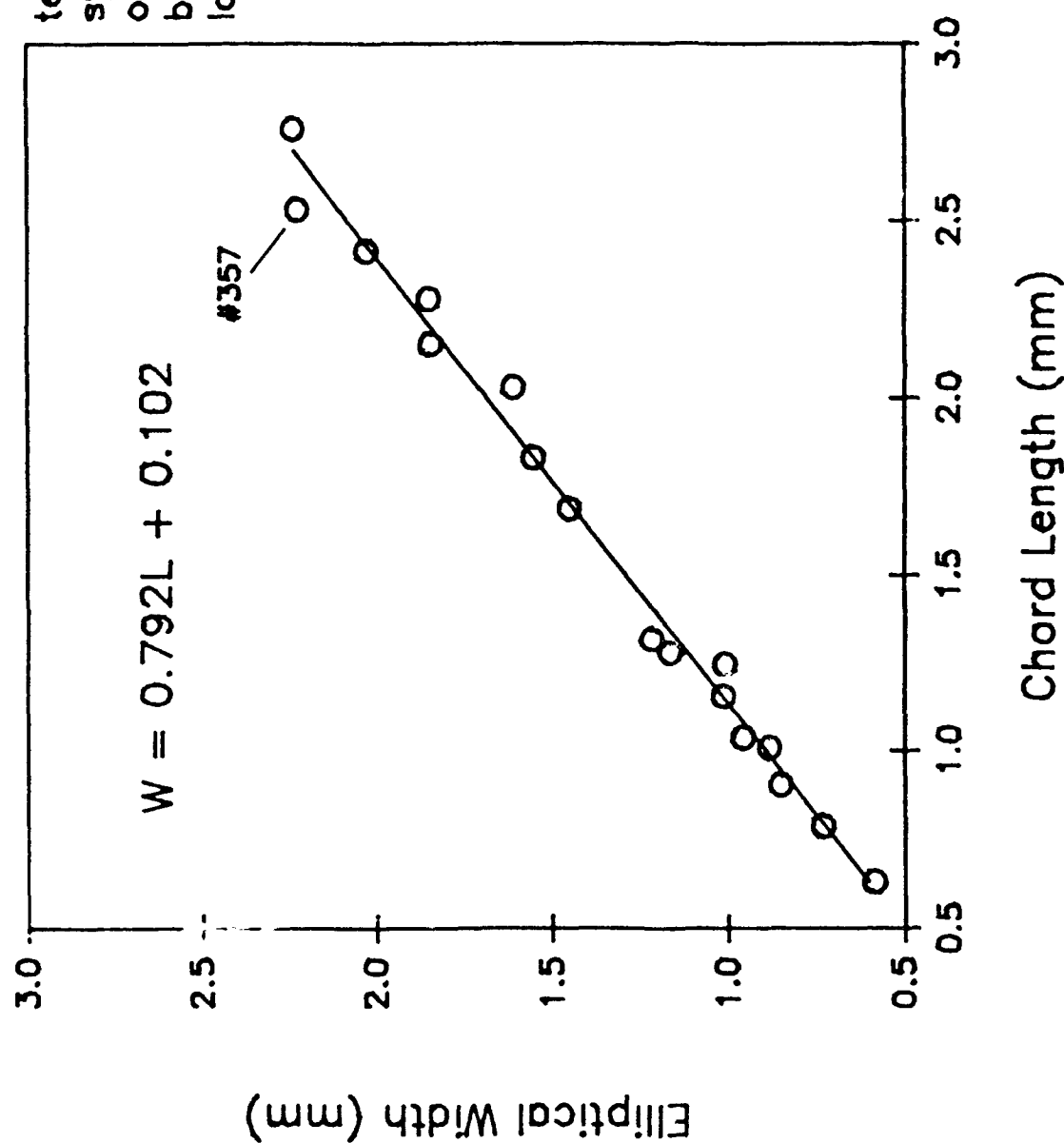


Figure 122. Elliptical Width Versus Chord Length for PPF-Based Lubricant. Discrete Tests Ranged from 15 Minutes to 30 Hours in Duration

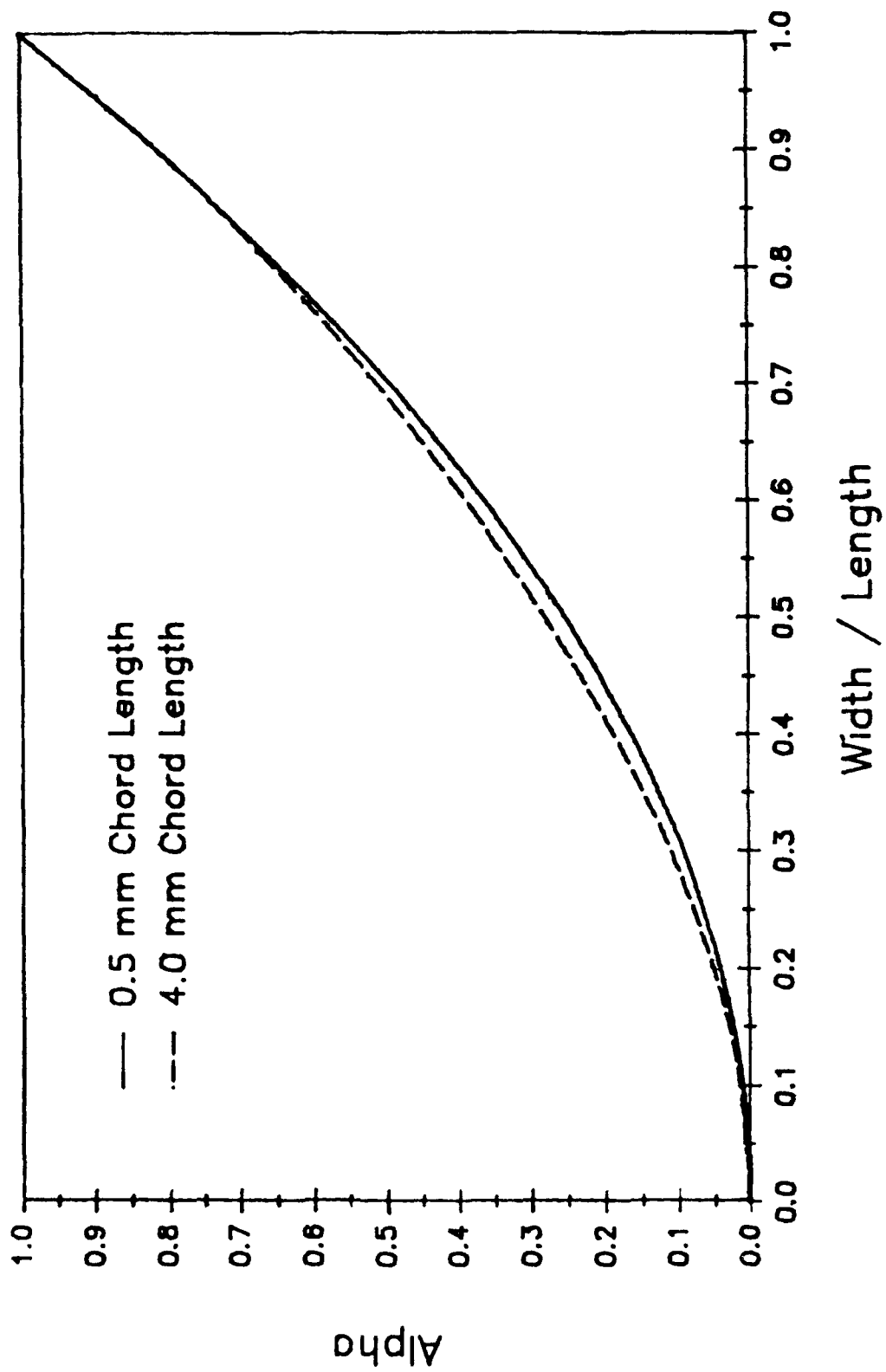


Figure 123. Variation of the Alpha Parameter as a Function of the Width to Length Ratio

construct the width to length relations of Figures 121 and 122, these linear equations may be viewed as characteristic of the sliding four-ball test. Not only were the lubricants physically different (viscosity, thermal stability, chemical composition, etc.) these tests were run under different loads at different temperatures (245 N and 75°C for the ester, 145 N and 150°C for O-67-1). Assuming there is linearity between elliptical width and chord length for any oil run under any condition in the four-ball machine allows the data from only two tests to generate the equation relating elliptical width to chord length. In order to reduce the effects of measurement error on the regression line, test durations should be relatively distant from one another to provide large and small values for the scar width and length. For O-67-1, the data from 3-hour and 20-hour tests are suitable for constructing the linear width to length relations.

Figure 124 illustrates the construction of one such linear relationship using four tests at 250°C. The data are from pairs of identical 3-hour tests (200 and 472) and 20-hour tests (381 and 466). The two 3-hour tests hardly differ in either chord length or elliptical width. The 20-hour tests, however, have noticeably different lengths and widths. Because of this difference, plotting chord length against time would suggest difficulty in generating repeatable results in the four-ball apparatus. However, plotting width against length eliminates the dependency of the data on time and shows that the linear relationship is maintained in spite of the variation in wear seen in these two 20-hour tests.

Figure 125 is a further illustration of the consistency of a linear relation when results from identical tests lack repeatability. At 75°C, the linear relationship is again constructed using two 3-hour tests (356 and 364) and two 20-hour tests (193 and 351). For the 3-hour tests, there is only a

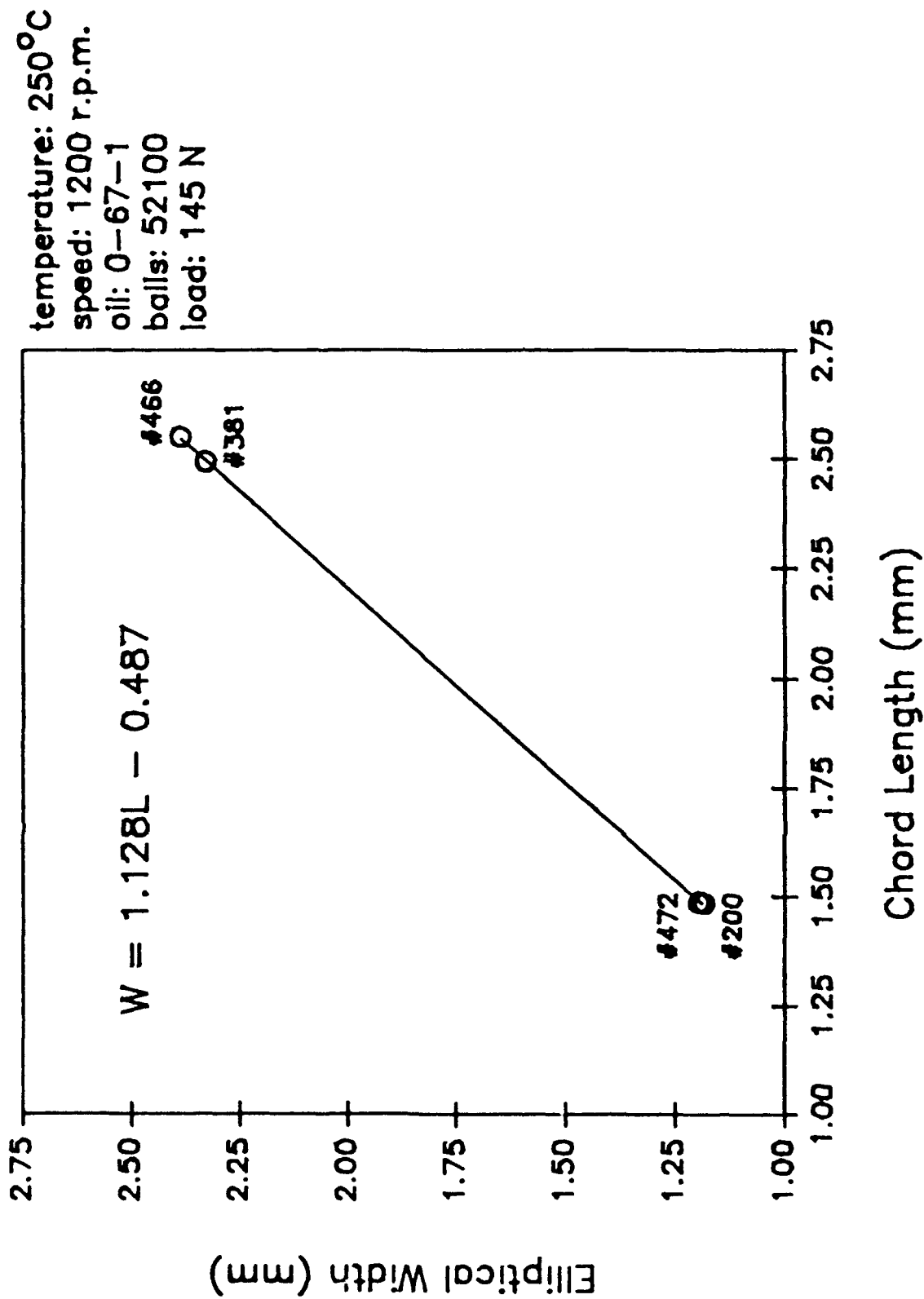


Figure 124. Elliptical Width Versus Chord Length for PPE-Based Lubricant at 250°C (Width-Length Relationship Constructed Using Two 3-Hour Tests and Two 20-Hour Tests)

temperature: 75°C
 speed: 1200 r.p.m.
 oil: 0-67-1
 balls: 52100
 load: 145 N

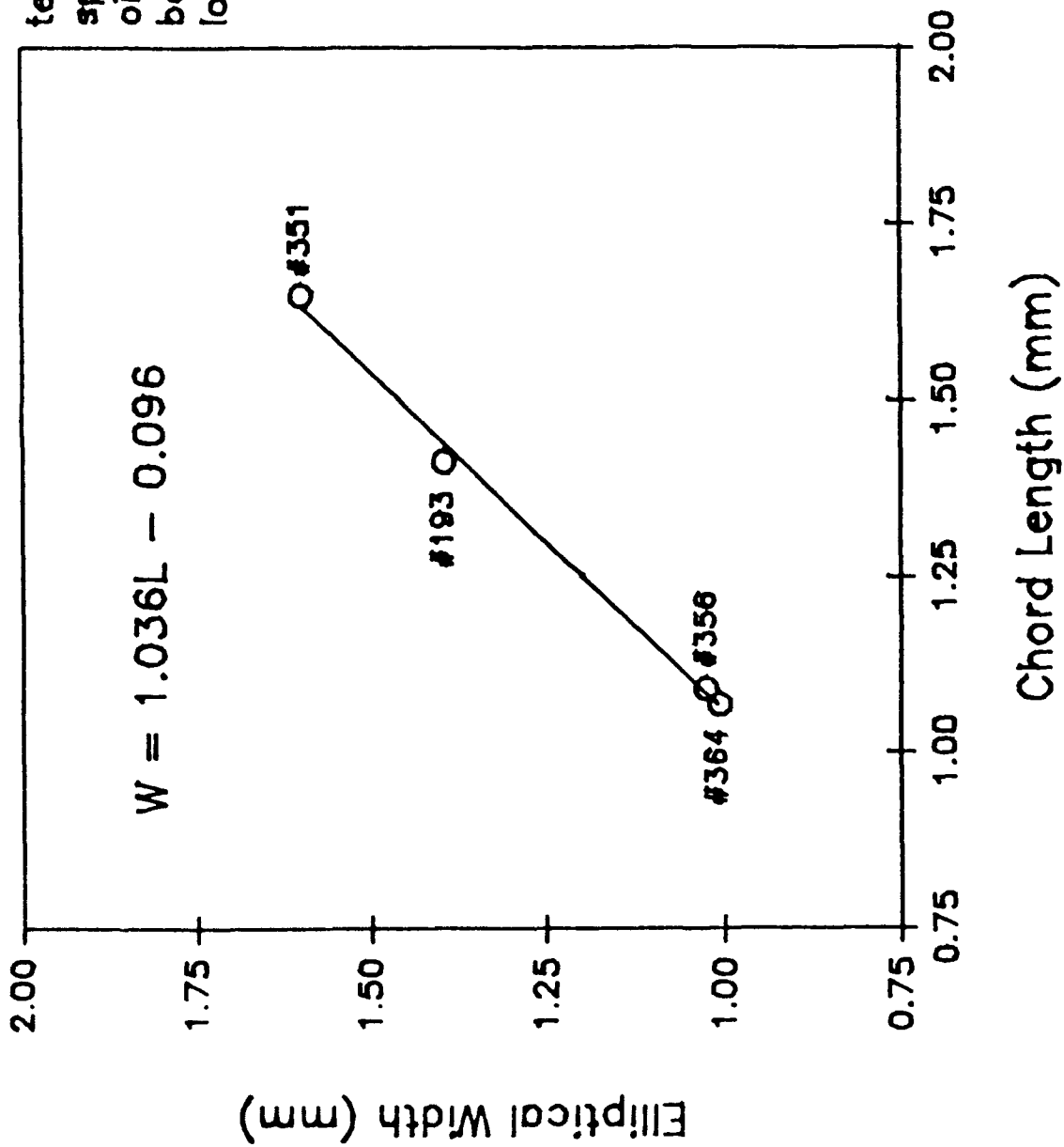


Figure 125. Elliptical Width Versus Chord Length for PPE-Based Lubricant at 75°C (Width-Length Relationship Constructed Using Two 3-Hour Tests and Two 20-Hour Tests)

slight deviation in the chord lengths, but a tremendous difference exists between the values of the 20-hour tests. Despite the substantial deviation associated with the long duration tests, a linear relationship between elliptical width and chord length is still evident.

Figures 121, 122, 124 and 125 suggest that the sliding four-ball test is "path" dependent and not time dependent. In other words, wear occurs along a specific path for a given set of test conditions, specimen material, and lubricant although the rate at which the scars grow may vary from test to test. Dimensionally, the scars grow the same between identical tests; there is a unique elliptical width for each chord length even if the rates of chord growth vary between tests.

Using the linear relationships between elliptical width and chord length along with the wear geometry model, the wear volumes of the rotating ball and stationary balls can be calculated at each interval of the LVDT data. Since the width-length plots tend to mask experimental and measurement errors, the wear volumes will be examined on both a parameter and rate basis. Figure 126 is a log-log plot of the volumes of wear occurring on the upper ball and the three lower balls for a series of discrete tests run on O-67-1 for various test times under identical conditions. The data points were obtained by individual measurements on the final scar size for each test. The linearity of the discrete measurements indicates that the volumetric wear rates for both the upper and lower balls are constants.

In Figure 127, the scar volumes from a 20-hour test (357) are calculated at each time interval using the LVDT data and width-length equation of Figure 122. The LVDT-generated volumes are plotted as dashed lines, and the regression lines of Figure 126 are included for comparison (shown as solid lines). The LVDT volumes show considerable error to the

temperature: 150°C
 speed: 1200 r.p.m.
 oil: 0-67-1
 balls: 52100
 load: 145 N

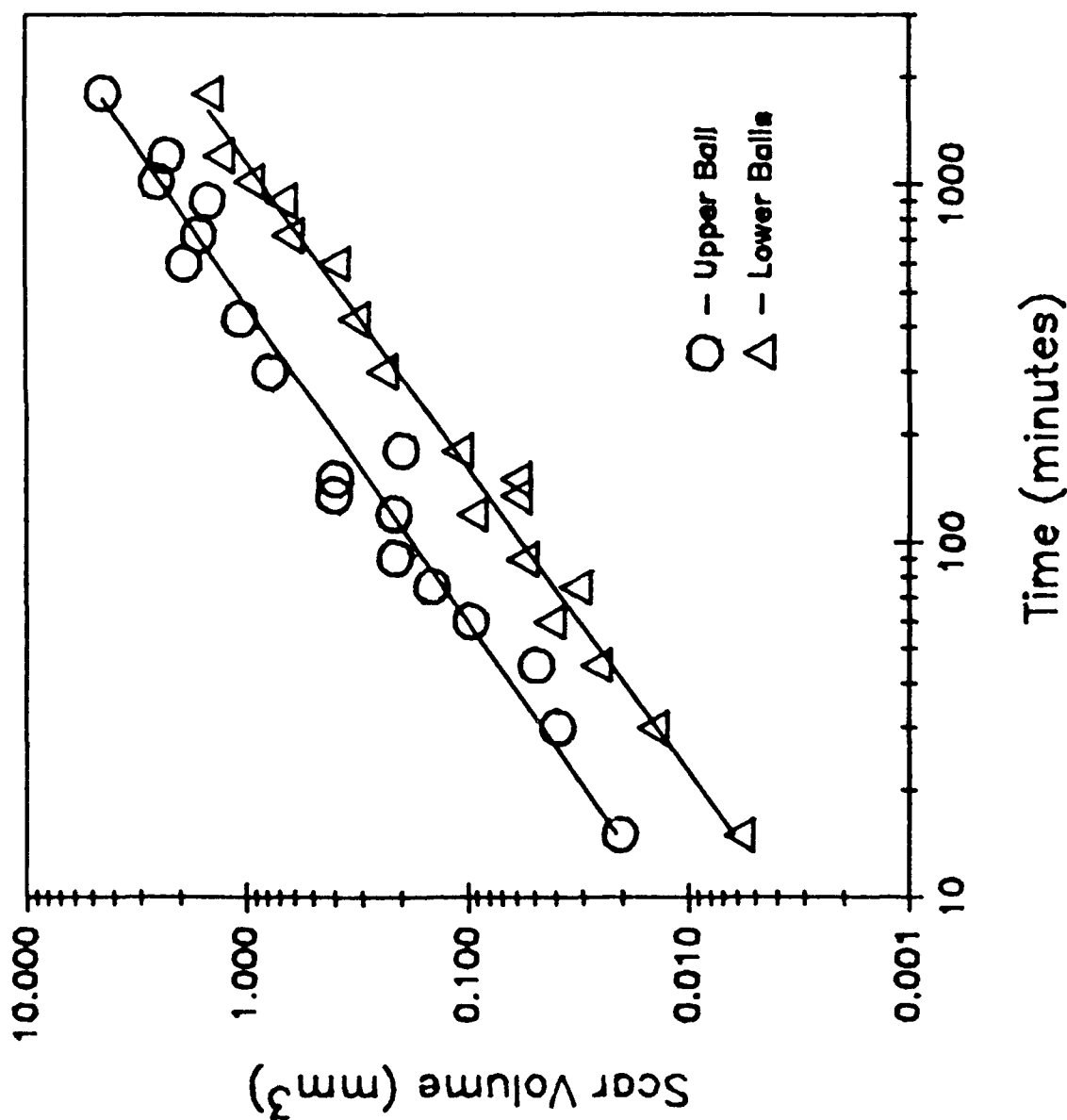


Figure 126. Time Basis Illustration of Wear Volume for PPE-Based Lubricant with Linear Regressions of Discrete Tests

temperature: 150°C
 speed: 1200 r.p.m.
 oil: 0-67-1
 balls: 52100
 load: 145 N

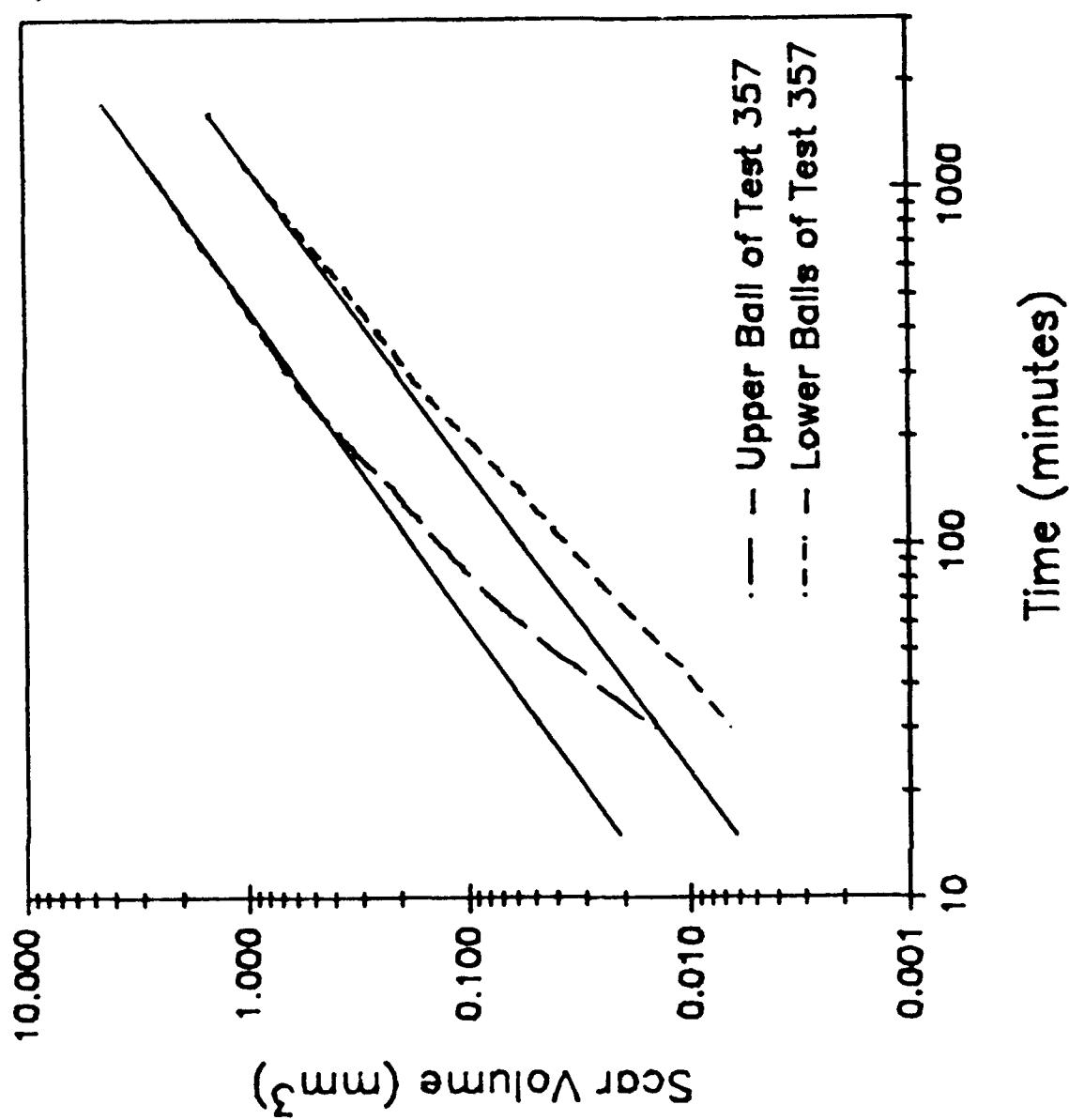


Figure 127. Time Basis Illustration of Wear Volume for PPE-Based Lubricant Calculated from LVDI Data. Linear Regressions from Measurements of Discrete Tests (Figure 126) are Shown by the Solid Lines

lines of the discrete tests until approximately five hours into the test. Beyond this point, however, both curves compare quite well to the discrete measurements.

Figures 128 and 129 examine scar volumes on a parameter basis (chord length) rather than a rate basis (time). In Figure 128, the discrete tests again show linear behavior over a large variation of the basis. Figure 129 illustrates the variation in the LVDT volumes compared to the discrete test volumes and the correlation is excellent.

Figures 126 through 129 provide more evidence that the sliding four-ball wear test is path dependent. Figure 119 demonstrated that the LVDT versus time data was repeatable after run-in wear. Unpredictable run-in wear results in the transient error associated with the graphs plotted on a rate basis (Figures 120 and 127). Analysis of wear data using time as a basis of comparison is valid only for a specific wear path and not an explicit characteristic of LVDT position.

The question remains as to the extent of error masking due to logarithmic plotting and the width-length graphs. Figure 130 compares the variation of total lower ball wear volume versus chord length of discrete tests to the LVDT data using a linear scale. This figure shows that the path predicted by the LVDT data is accurate although the final wear volume predicted by the LVDT data of test 357 (the end of the curve) is less than the measured wear volume from this test (shown by arrow). Similarly, Figure 131 compares the upper ball wear volumes, but now the final value predicted by the LVDT data of test 357 exceeds the final measured value of test 357.

The final values of the wear volumes predicted by LVDT data are incorrect because the end of a test is defined by time (20 hours for test 357). The wear volume prediction by LVDT data is accurate when the

temperature: 150°C
 speed: 1200 r.p.m.
 oil: 0-67-1
 balls: 52100
 load: 145 N

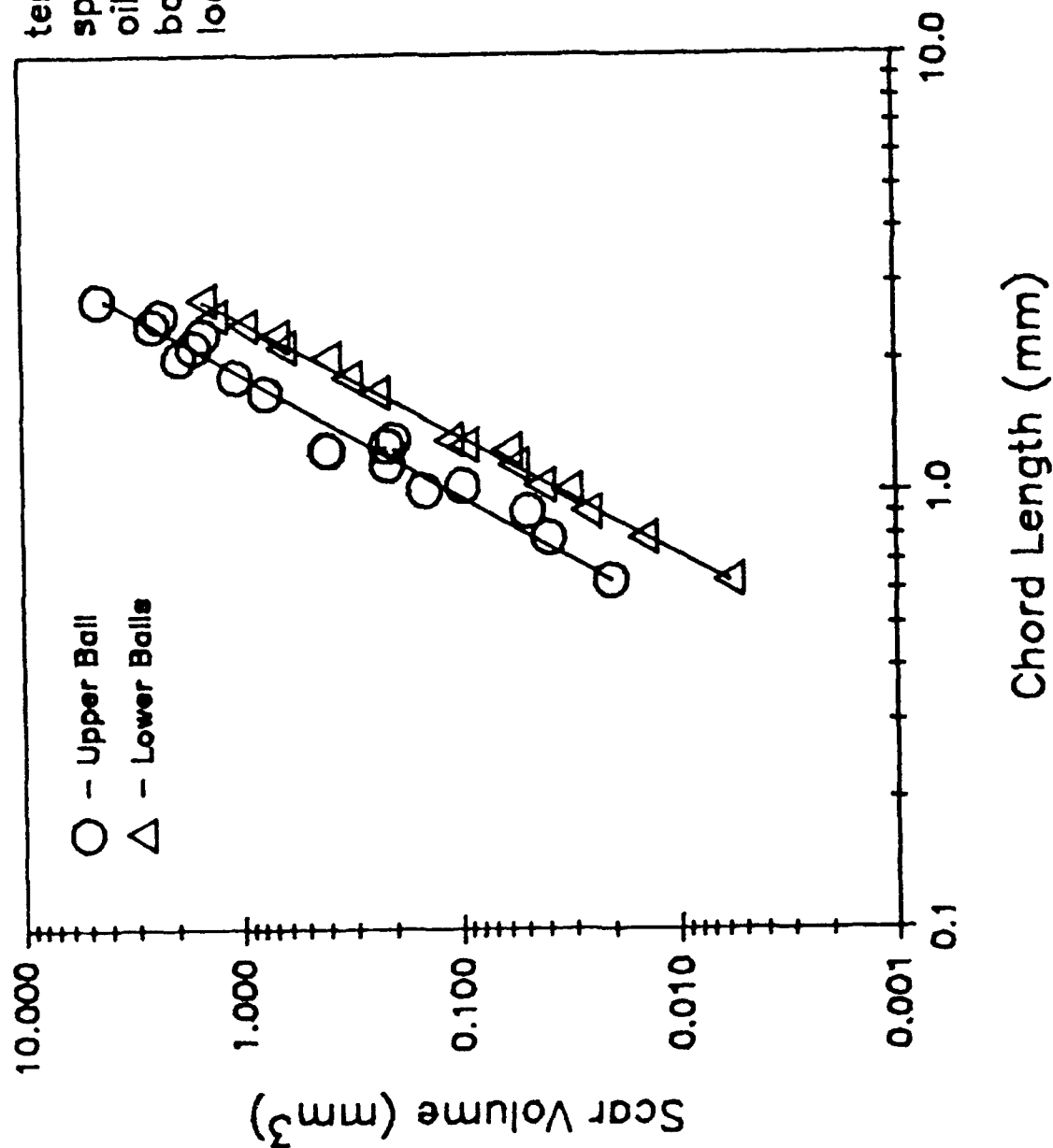


Figure 128. Parameter Basis Illustration of Wear Volume for
 PPF-Based Lubricant with Linear Regressions of
 Discrete Tests

temperature: 150°C
 speed: 1200 r.p.m.
 oil: 0-67-1
 balls: 52100
 load: 145 N

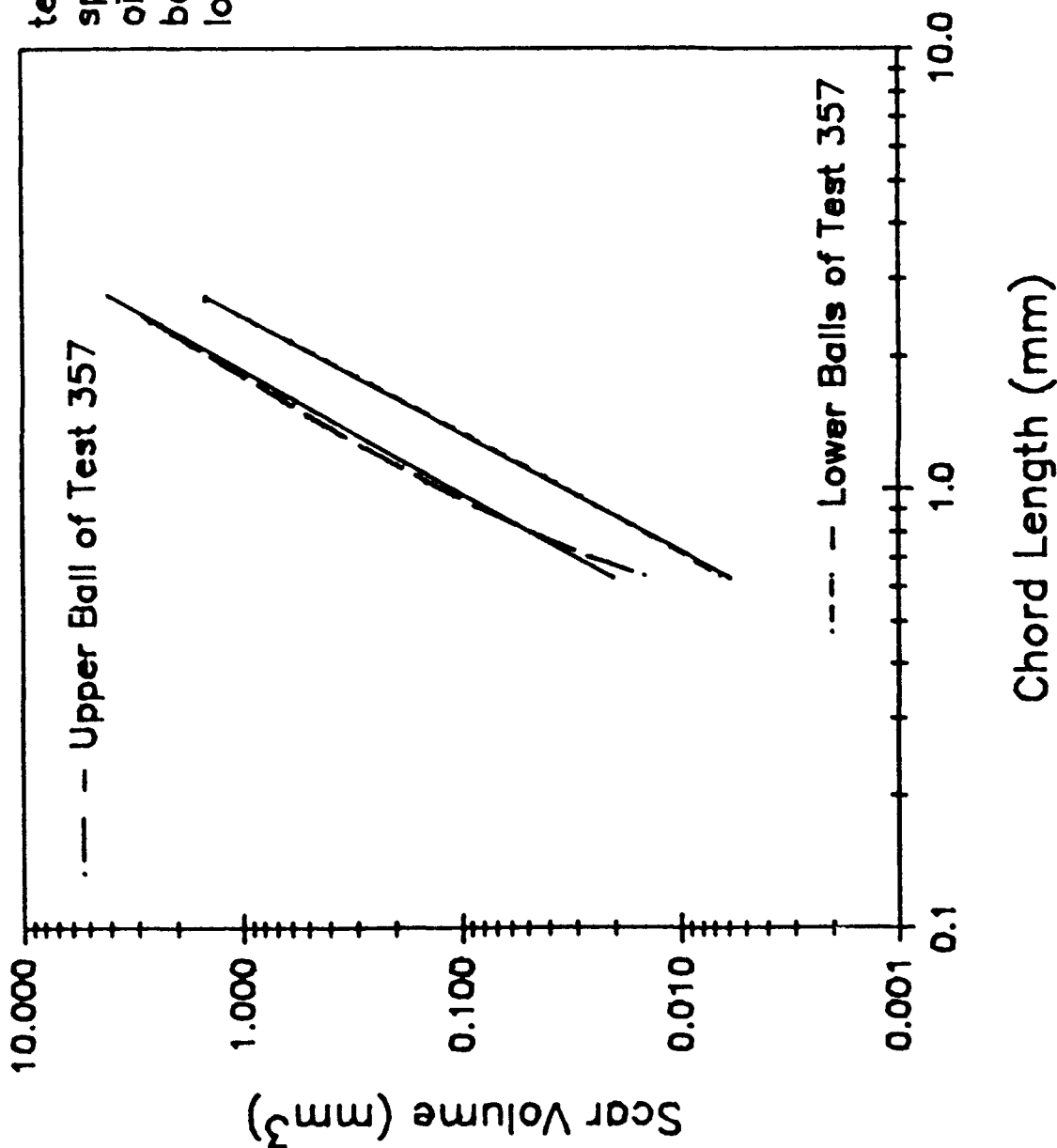


Figure 129. Parameter Basis Illustration of Wear Volume for PPE-Based Lubricant Calculated from LVDT Data. Linear Regressions from Measurements of Discrete Tests (Figure 128) are Shown by the Solid Lines

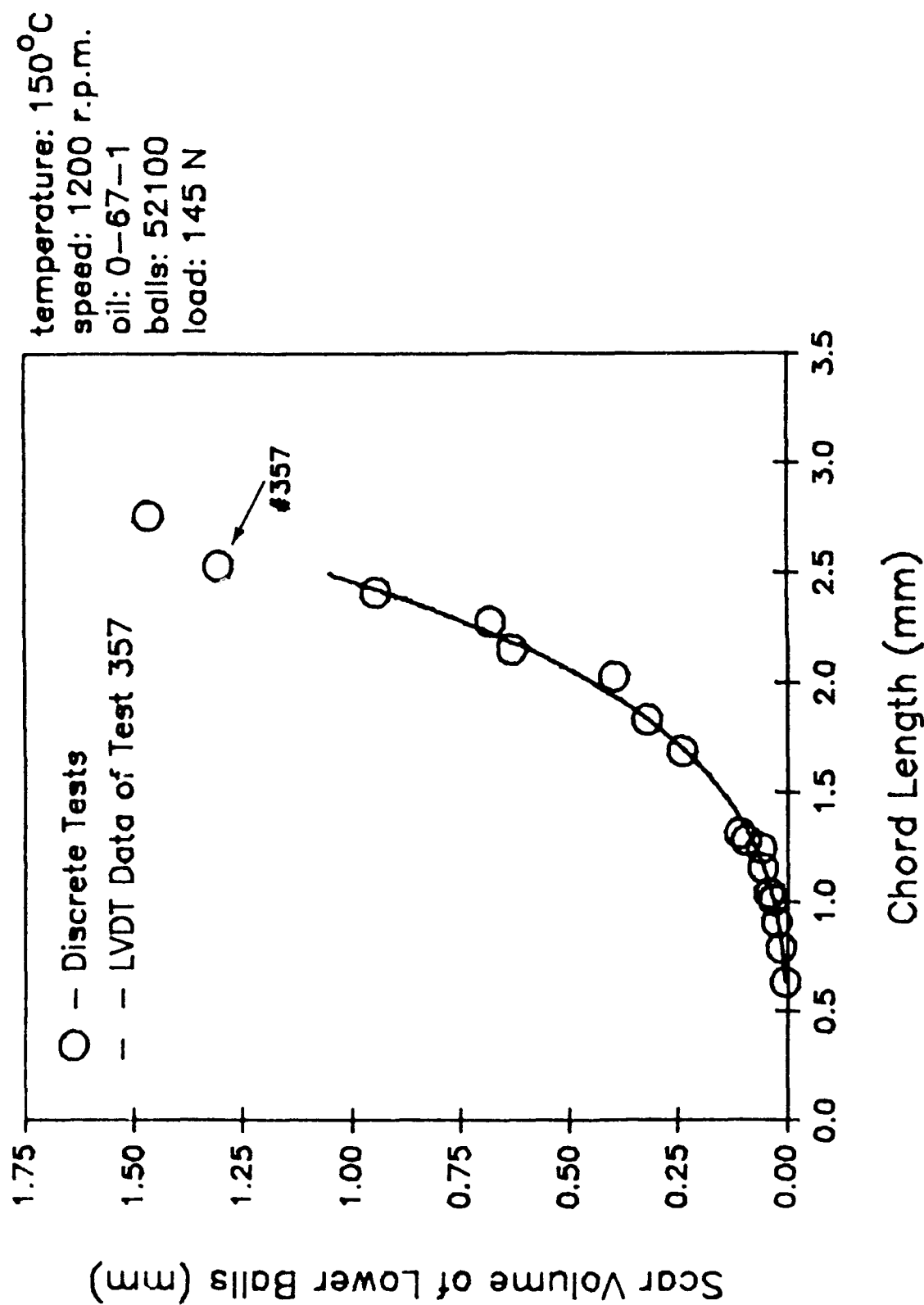


Figure 130. Parameter Basis Illustration of Total Lower Ball Wear Volume for PPE-Based Lubricant Calculated from LVDT Data and from Discrete Tests

temperature: 150°C
 speed: 1200 r.p.m.
 oil: 0-67-1
 balls: 52100
 load: 145 N

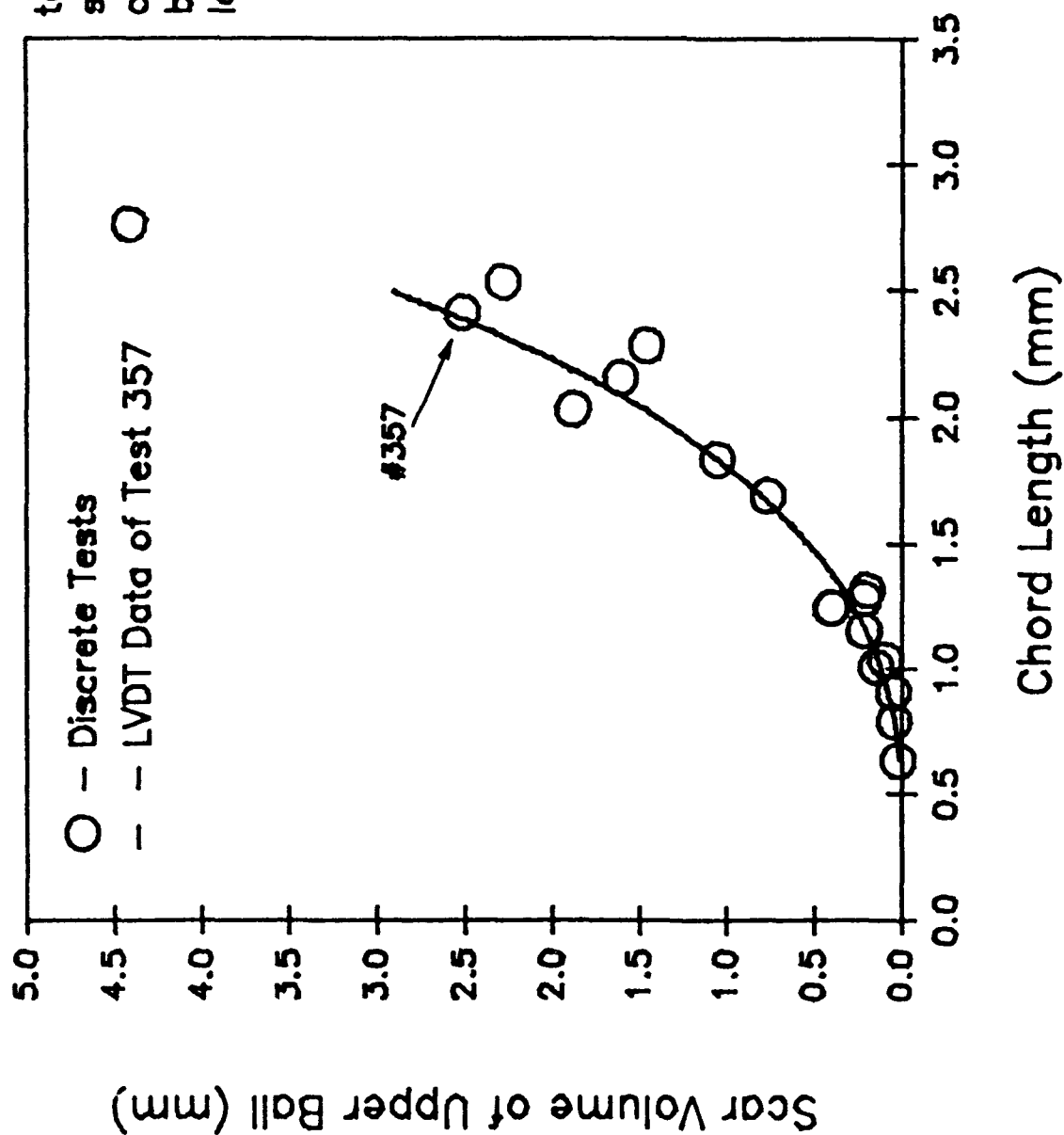


Figure 131. Parameter Basis Illustration of Upper Ball Wear
 Volume for PPE-Based Lubricant Calculated from
 LVDT Data and from Discrete Tests

comparison basis is chord length. For a specific chord length, the linear empirical relations and the LVDT data can be used to find wear volumes on any of the balls. Based on these results, the linear width-length relationship appears to be an effective empirical comparison despite its natural error masking. These errors are largely the result of associating chord lengths with specific test times. This association is strongly dependent upon the transient conditions at the beginning of the test and although this transient period does not prevent repeatable test results, wear rates are not accurate until a sufficient time into the test (seen in Figure 120).

b. Comparison of Oils and Specimen Materials

Testing of a variety of candidate fluids was initially performed using 52100 steel balls, as prescribed by the ASTM Standard for the four-ball test. Testing oils at 315°C with this material produced scars which showed as much smearing of metal as wear (Figure 132). As seen in Figure 133, the hardness of 52100 steel decreases substantially at temperatures above 300°F (150°C). Since a hardness of HRC 55 is generally considered the minimum for most bearing applications, 52100 steel specimens are unacceptable above 450°F.²⁷ A material with high hot hardness is needed to effectively evaluate wear up to 315°C. According to Figure 133, M-50 steel has high hardness up to 800°F (425°C). M-50 steel was chosen to be the material to evaluate not only the high temperature tribological properties of candidate fluids, but the low temperature properties as well.

Before M-50 was chosen to be exclusively used for evaluating candidate fluids in the four-ball machine, a substantial amount of testing had been conducted using 52100 specimens at temperature intervals of 75, 150, 250 and 315 °C. Rather than completely disregard a great deal of data, the results of tests conducted at 75, 150 and 250°C will be discussed while most

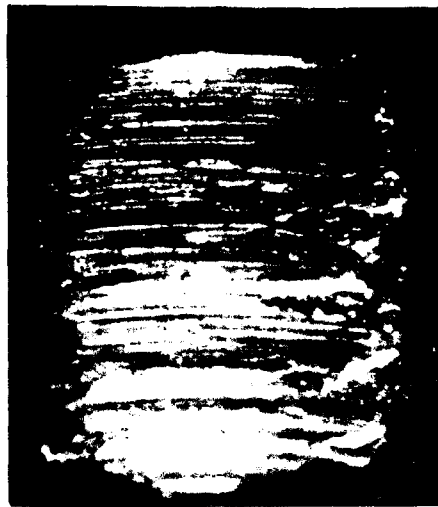


Figure 132. Lower Ball Scar Formed on 52100 Steel Specimen at 315°C (47X Actual Size)

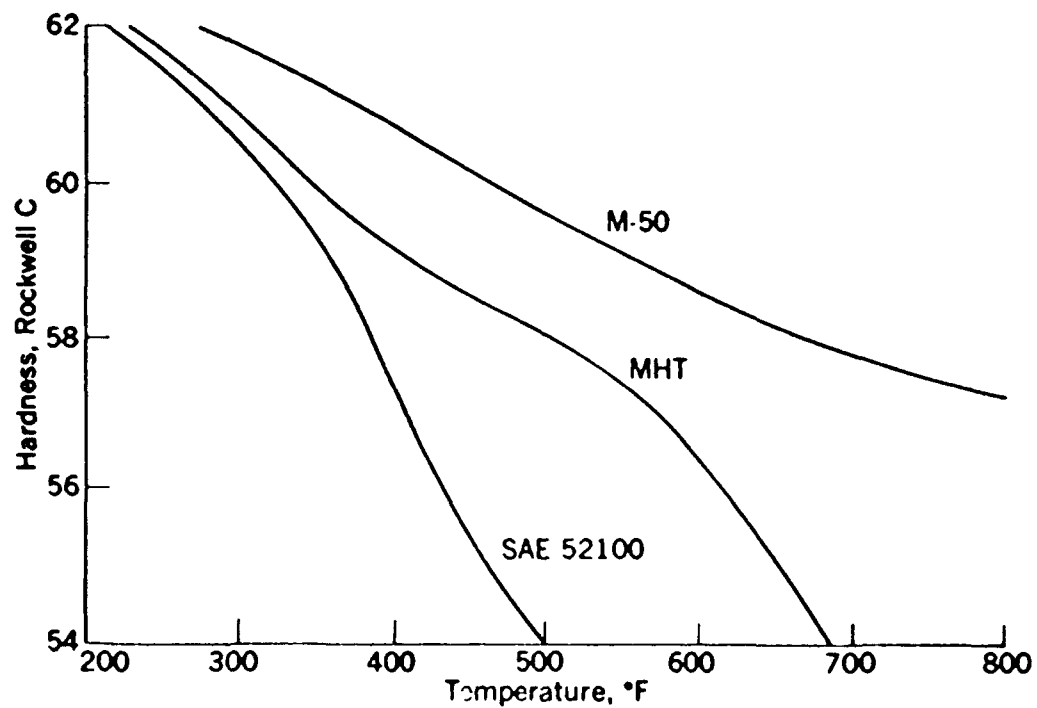


Figure 133. Hardness as a Function of Temperature for Three Bearing Steels (from Ref. 27)

data at 315°C will be ignored because of softening of 52100.

A comparison of wear scars from four-ball tests of high temperature oils is shown in Figures 134 and 135. Figure 134 ranks the scar dimensions of 52100 balls for seven lubricants at 150°C while Figure 135 is a similar ranking at 250°C. In general, PPE had larger wear scars than the experimental fluids and had greater variation between lengths and widths for each test (reflected by the alpha parameters given in Table 98). Except for the oil TEL-90001, the alpha parameters of the experimental fluids are very close to unity.

Using the wear geometry model, scar volumes were calculated for the tests of the various oils. Figure 136 shows the scar volumes generated by the oils of Figure 134. By referring to the alpha parameters in Table 98, it is seen that the oils having lower values for alpha caused wear in the top ball greater than the combined wear of the three lower balls (O-77-6, O-67-1, TEL-90028 and TEL-90001). The oils TEL-9071 and TEL-90063 had alpha values of 1.000 and 0.998, respectively. For these oils, no wear was incurred on the upper balls. The alpha parameter for oil TEL-90024 is 0.964, and without the aid of an optical microscope, lower ball scars from this oil appear perfectly circular. Figure 136, however, indicates that wear volumes of the lower balls and the upper ball are about equal. The validity of using scar volumes of the upper and lower balls is apparent; small deviations between chord lengths and elliptical widths of lower ball scars indicate an increase in the contribution of wear by the upper ball. Furthermore, upper ball wear quickly exceeds the total wear of the lower balls as scars become even slightly elliptical.

Figure 137 is another ranking of wear volumes corresponding to the oils tested at 250°C. Comparing respective oils to results at 150°C shows no

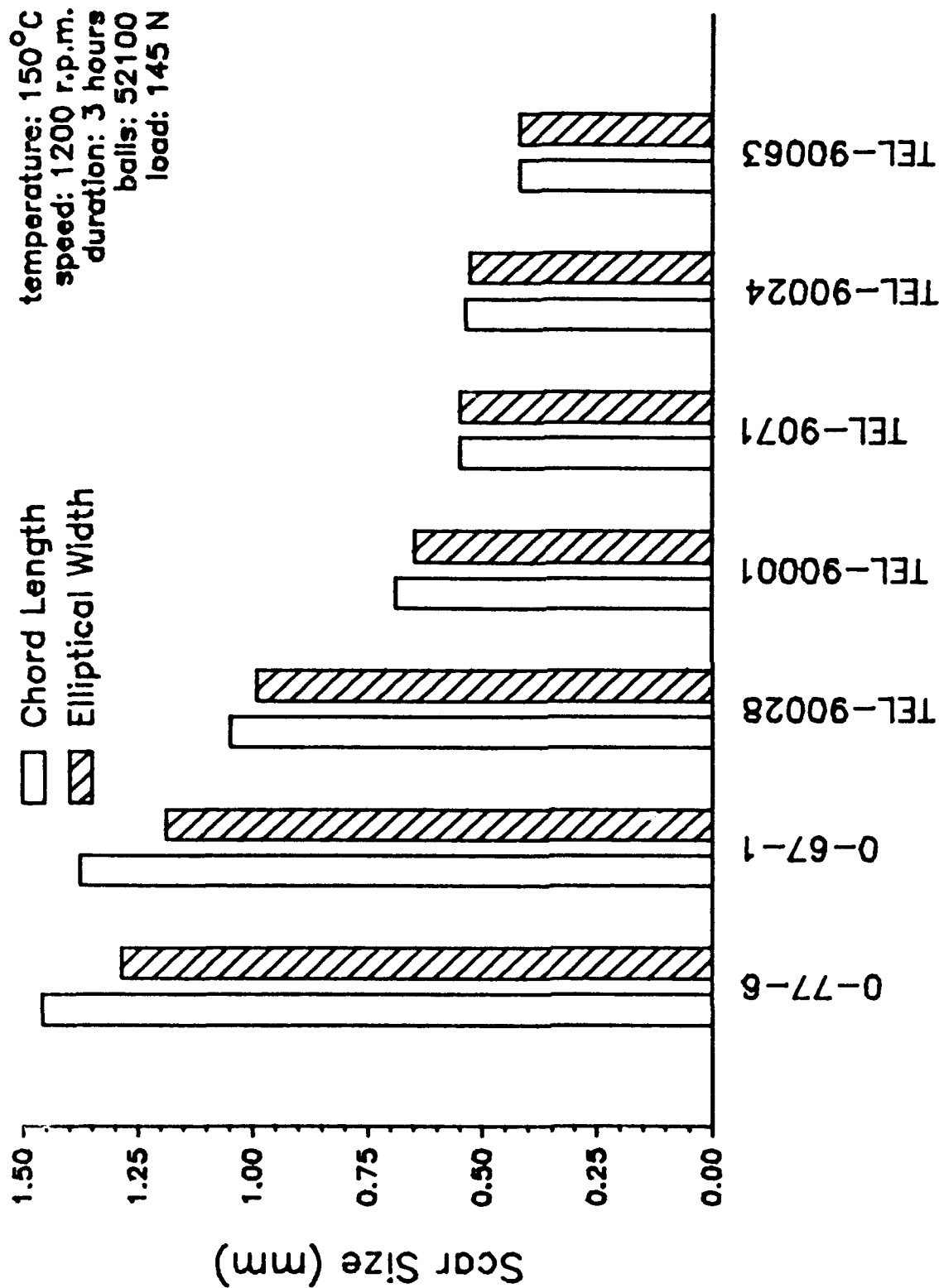


Figure 134. Wear Comparison of Various High-Temperature Fluids Based on the Scar Sizes of 52100 Steel Balls Run at 150°C

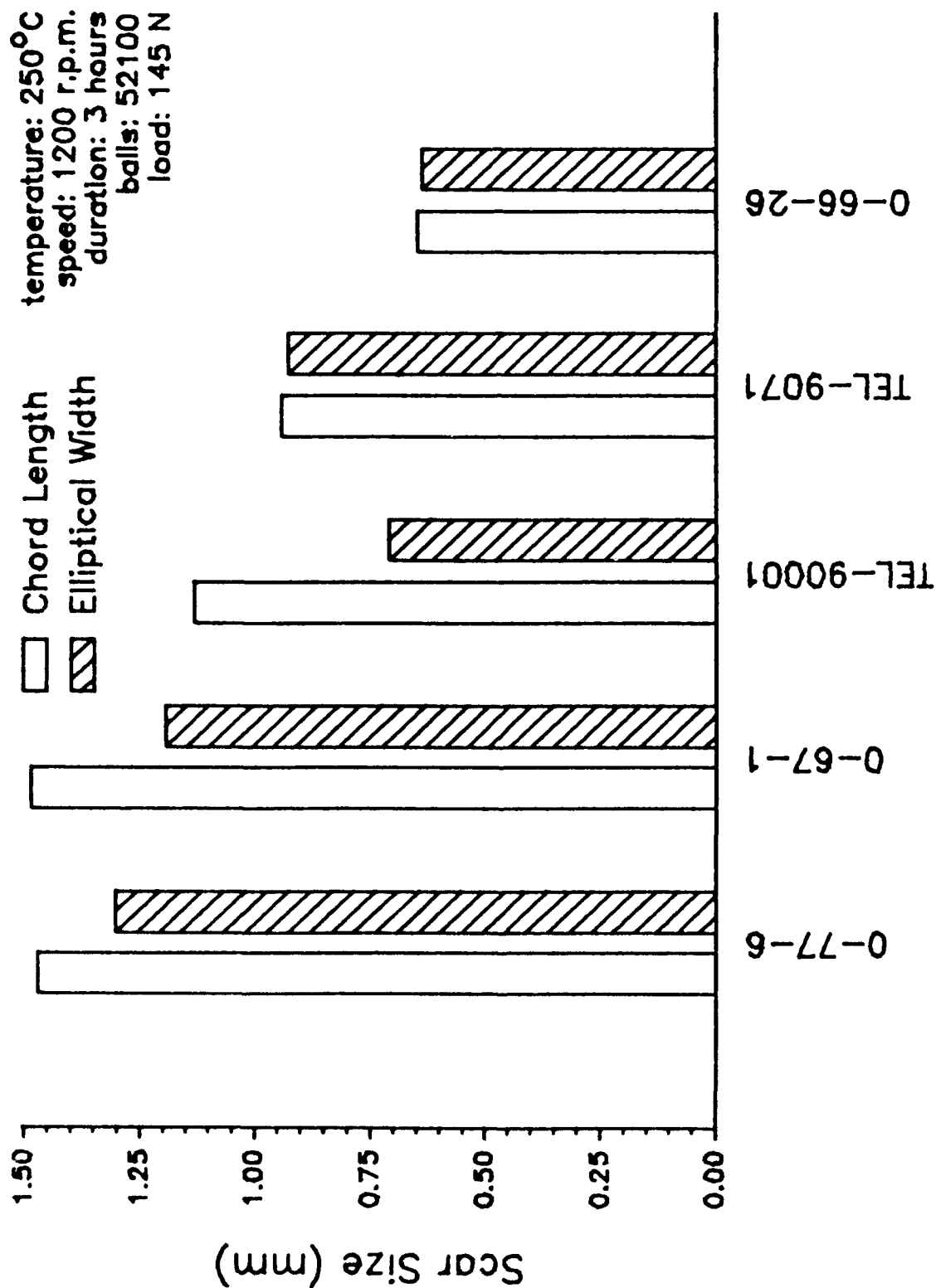


Figure 135. Wear Comparison of Various High-Temperature Fluids Based on the Scar Sizes of 52100 Steel Balls at 250°C

TABLE 98

VARIATION IN THE ALPHA PARAMETERS AND TOTAL
WEAR VOLUME FOR VARIOUS OILS

Duration: 3 hours

Speed: 1200 rpm

Load: 145 N

Test No.	Lubricant	Specimen Material	Temperature °C	Alpha	Total Wear ₃ Volume, mm
346	O-77-6	52100	150	0.778	0.5634
398	O-67-1	52100	150	0.747	0.5085
497	TEL-90028	52100	150	0.892	0.1228
444	TEL-90001	52100	150	0.881	0.0323
429	TEL-9071	52100	150	1.000	0.0042
508	TEL-90063	52100	150	0.998	0.0015
345	O-77-6	52100	250	0.783	0.5734
472	O-67-1	52100	250	0.649	0.8196
529	TEL-90001	52100	250	0.387	0.5528
430	TEL-9071	52100	250	0.969	0.0507
198	O-66-26	52100	250	0.967	0.0133
468	O-67-1	M50	150	0.416	6.9885
500	TEL-90028	M50	150	0.448	2.7077
523	TEL-90001	M50	150	0.934	0.0346
525	TEL-9050	M50	150	0.932	0.0040
522	TEL-90059	M50	150	0.933	0.0033
524	TEL-90063	M50	150	0.977	0.0007
487	O-67-1	M50	250	0.220	3.9017
528	TEL-90001	M50	250	0.905	0.4830
530	TEL-9050	M50	250	0.717	0.5366
531	TEL-90059	M50	250	0.994	0.0125

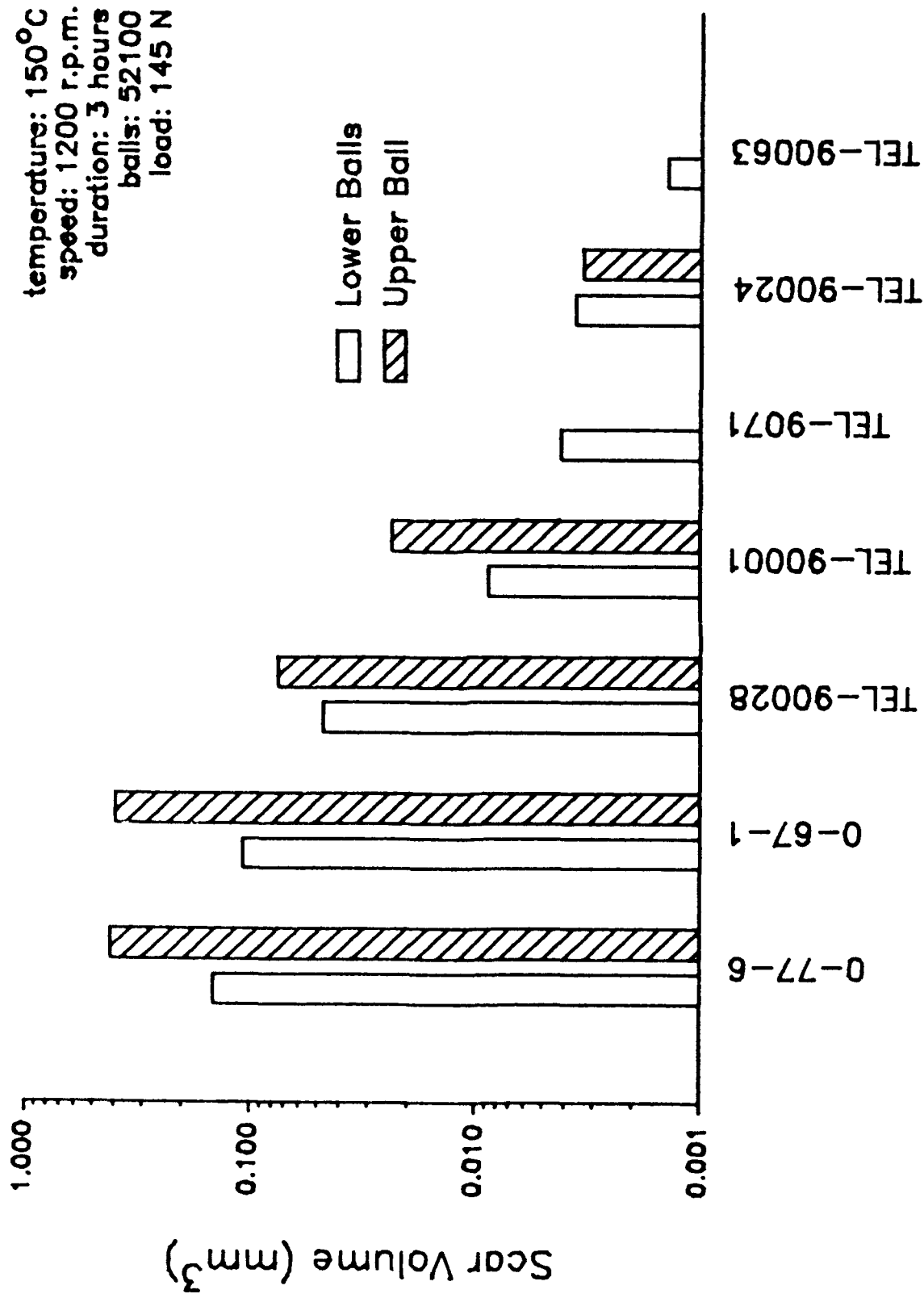


Figure 136. Wear Comparison of Various High-Temperature Fluids Based on the Scar Volumes of 52100 Steel Balls at 150°C

temperature: 250°C
 speed: 1200 r.p.m.
 duration: 3 hours
 balls: 52100
 load: 145 N

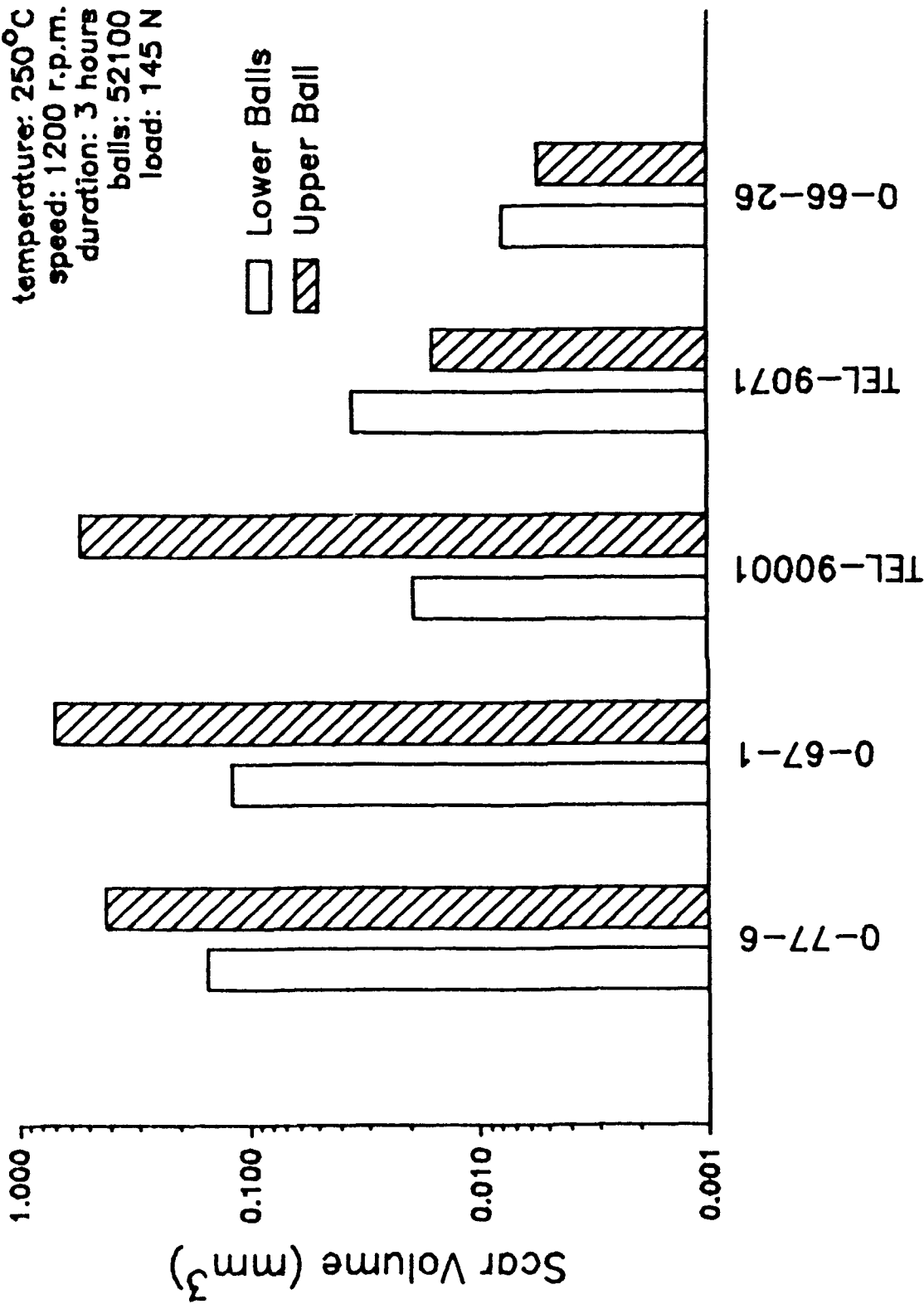


Figure 1.37. Wear Comparison of Various High-Temperature Fluids Based on the Scar Volumes of 52100 Steel Balls at 250°C

significant deviation in the amounts of wear for O-77-6 and O-67-1. Upper ball wear is again seen to exceed total lower ball wear for these oils. At 250°C, wear increased substantially for TEL-90001 and the proportion of upper ball wear to bottom ball wear increased due to a reduction in the alpha parameter from 0.881 at 150°C to 0.397 at 250°C. The upper ball from a test of TEL-9071 has measurable wear although its wear volume is not in excess of the three lower balls. Finally, the lubricant O-66-26 (Krytox) is seen to cause the least wear at 250°C. This lubricant was included for comparison.

A similar ranking of high-temperature fluids at 150 and 250°C was constructed for tests of M-50 specimens. Six oils are compared in Figure 138. The PPEs yield the largest scars, and the large length to width ratios correspond to values of the alpha parameter which are below 0.500 (see Table 98). Scars from the experimental fluids TEL-9050, TEL-90059 and TEL-90063 have scars of similar size and shape, but the experimental fluid TEL-90001 produced larger wear scars. Four of the six oils tested at 150°C were again tested on M-50 specimens at 250°C. The scar sizes from these tests are compared in Figure 139. Except for O-67-1, scars from the 250°C tests are larger than those formed at 150°C for respective oils. Table 98, however, shows the alpha parameter for O-67-1 at 250°C to be only 0.220. Alpha for the experimental fluid varied from 0.717 for TEL-9050 to 0.994 for TEL-90059.

The wear volumes calculated for the M-50 balls at 150 and 250°C are given in Figures 140 and 141. At 150°C (Figure 140), the upper ball scar volumes for the two PPE's are an order of magnitude greater than the total lower ball wear scar volumes. Even with the experimental fluids, the amount of wear on the upper ball exceeds the amount of wear on the lower balls, although not to as great an extent. At 250°C (Figure 141), O-67-1 produces an upper ball scar volume which is two orders of magnitude greater than the

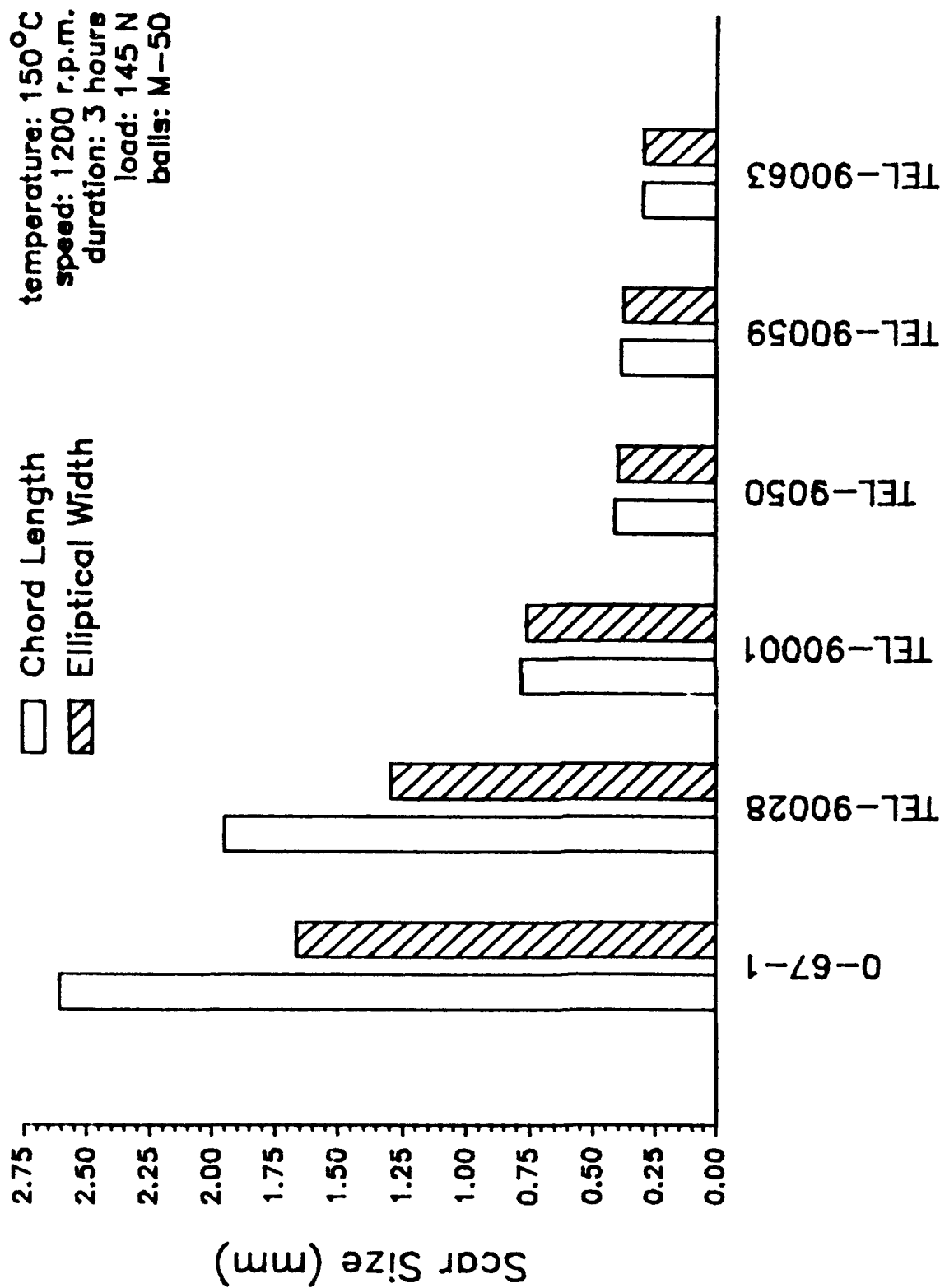


Figure 138. Wear Comparison of Various High-Temperature Fluids Based on the Scar Sizes of M-50 Steel Balls at 150°C

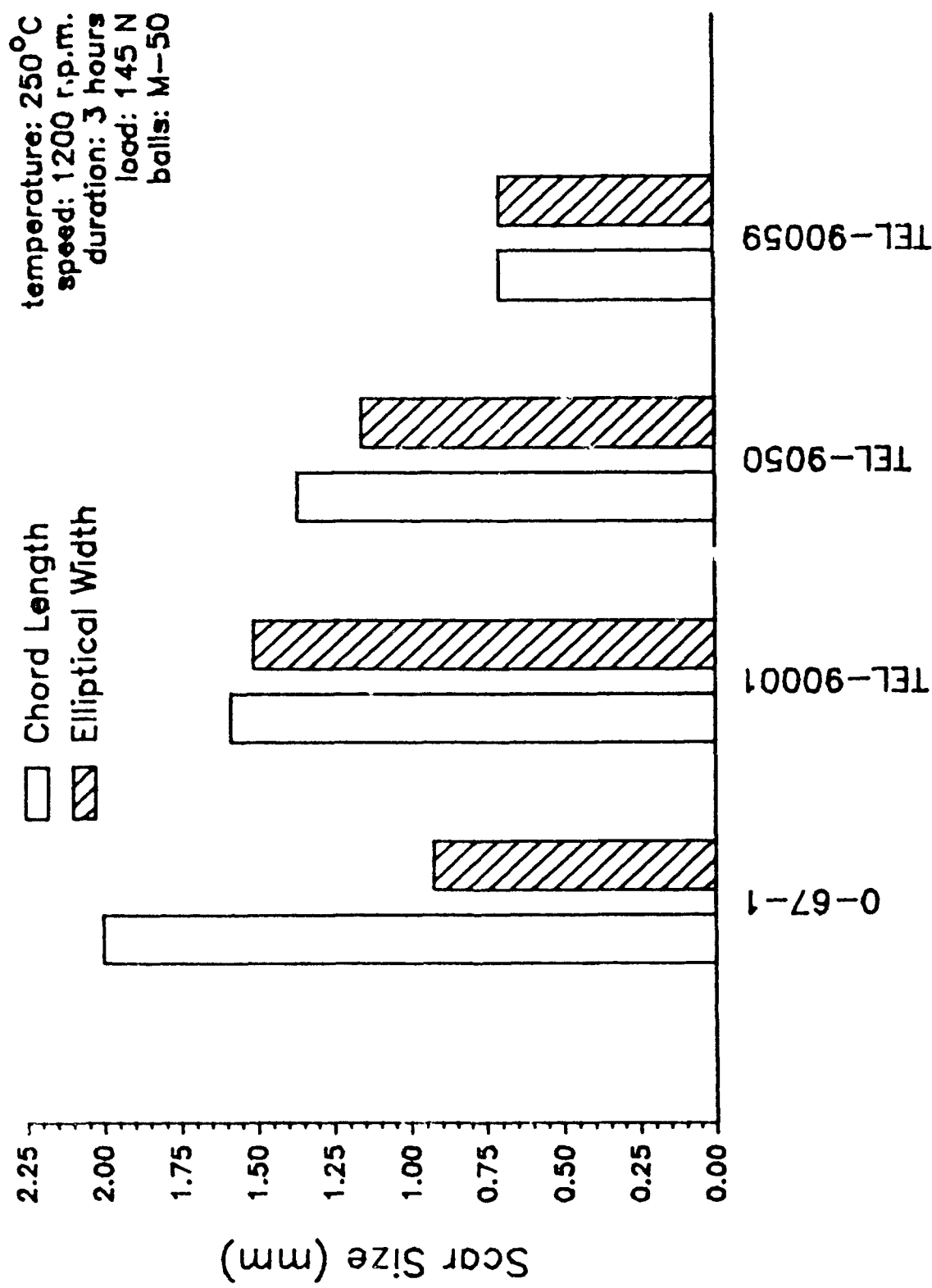


Figure 139. Wear Comparison of Various High-Temperature Fluids Based on the Scar Sizes of M-50 Steel Balls at 250°C

temperature: 150°C
 speed: 1200 r.p.m.
 duration: 3 hours
 load: 145 N
 balls: M-50

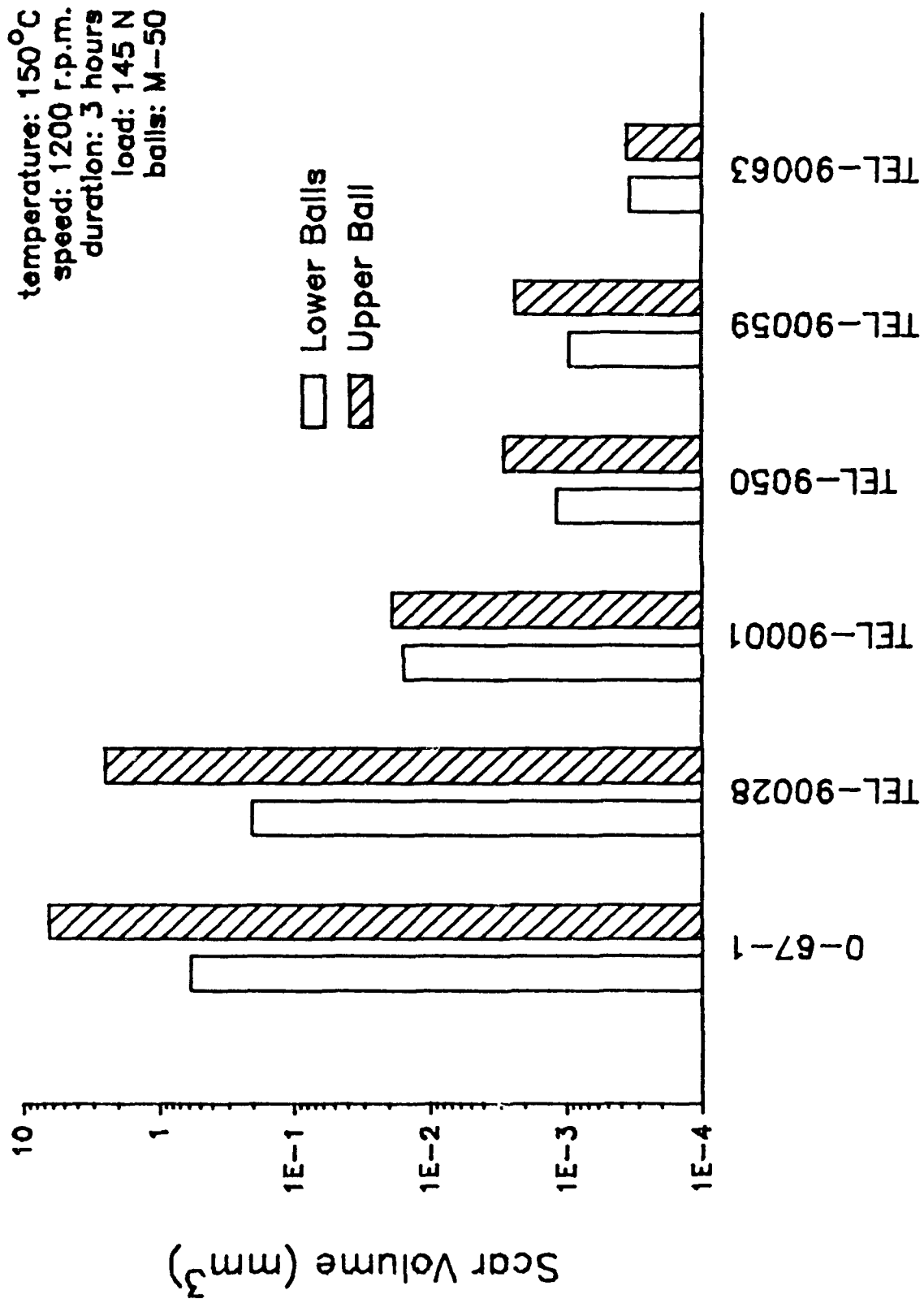


Figure 140. Wear Comparison of Various High-Temperature Fluids Based on the Scar Volumes of M-50 Steel Balls at 150°C

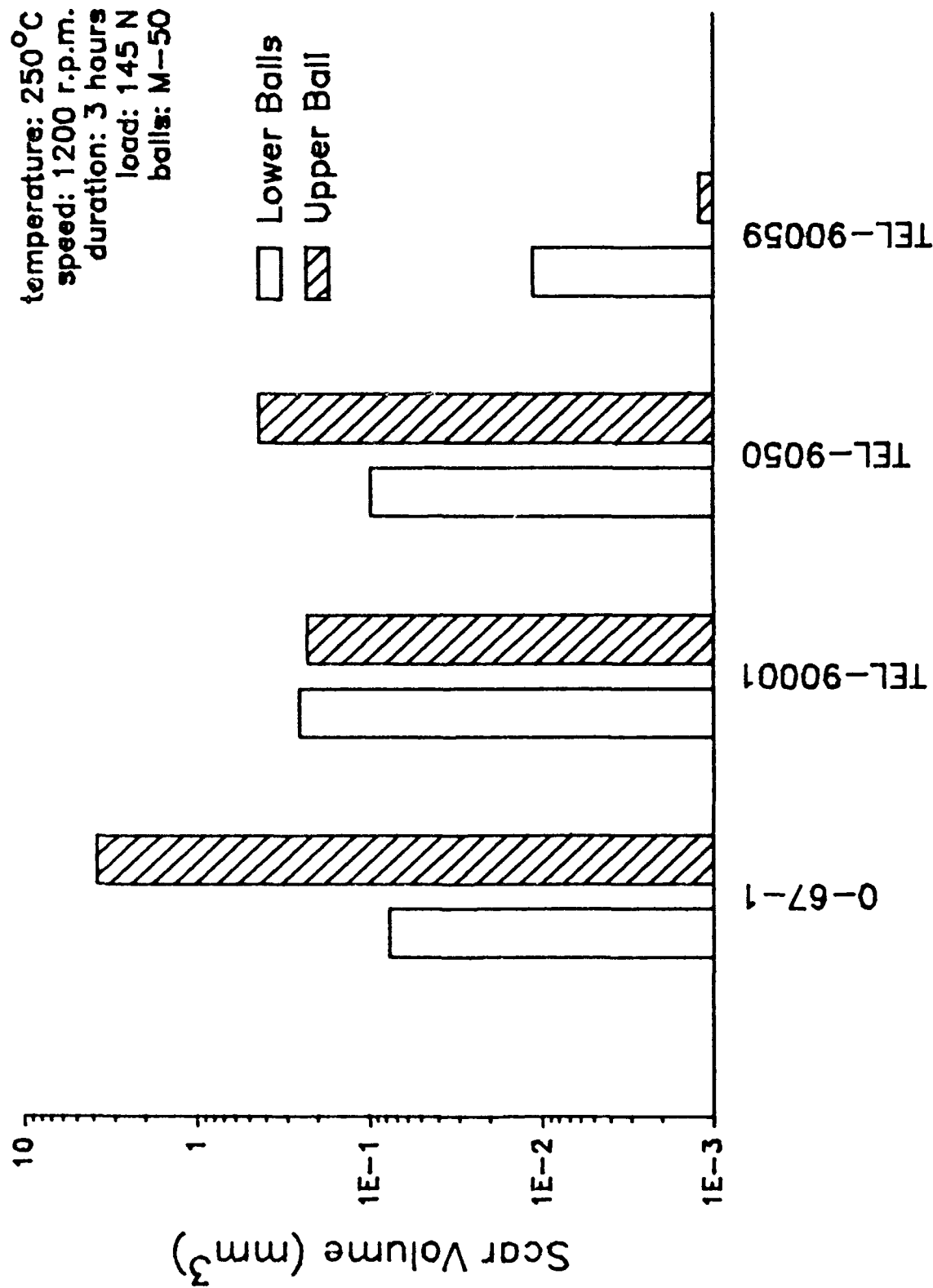


Figure 141. Wear Comparison of Various High-Temperature Fluids Based on the Scar Volumes of M-50 Steel Balls at 250°C

combined volumes of the lower ball scars, and the amount of wear at 250°C is less than that at 150°C. Conversely, the wear volumes for the experimental fluids are greater at 250°C than at 150°C. Although TEL-9050 was consistent in having greater wear on the upper ball for these two temperatures, TEL-90001 and TEL-90059 had greater lower ball wear at 250°C. The change in the wear regime is most dramatic for TEL-90059; the volume of the lower ball scars is an order of magnitude greater than the volume of the upper ball scar.

Some interesting observations can be made by comparing the scar sizes and volumes of like tests of 52100 and M-50 specimens. Figure 134 shows the scar length and width from a test of O-67-1 on 52100 to be about 1.30 and 1.15 mm, respectively. In comparison, Figure 138 gives values of about 2.60 and 1.65 mm for scar length and width for a test of O-67-1 on M-50. Consequently, the amount of wear on M-50 balls using O-67-1 is an order of magnitude higher than when 52100 balls are used (Figures 136 and 140). At 250°C, O-67-1 on 52100 yields scars about 1.50 mm long and 1.25 mm wide (Figure 135). At the same conditions, M-50 scars are about 2 mm long and 0.95 mm wide (Figure 139). Although the width of M-50 scars is less than 52100 scars, the resulting low value of alpha for M-50 scars translates into an enormous amount of top ball wear, and comparing Figure 137 to Figure 141 shows the wear on M-50 balls to be an order of magnitude greater than the wear on 52100 balls for O-67-1 at 250°C.

Although the behavior of the PPE TEL-90028 is consistent with that of the PPE O-67-1, there were only two instances when an experimental fluid exhibited greater wear with M-50 balls than with 52100 balls. By comparing the scar volumes at 150°C (Figures 136 and 140) and the scar volumes at 250°C (Figures 137 and 141) it is not easily seen which tests have greater total

wear (combined wear volumes of upper and lower balls) due to the log scale. As listed in Table 98, the total wear from TEL-90001 at 150°C and from TEL-9071 (a.k.a. TEL-9050) at 250°C was higher for M-50 specimens. The values of the total wear volume from TEL-90001 for the two materials are close enough to each other, however, that they can be considered equal within the accuracy of the measuring procedure (Appendix C). Thus, M-50 balls had less wear than 52100 for the experimental fluids except for one test at 250°C.

It is again worthwhile to point out that if only an average of the lower balls wear scars is used to quantify wear, it would appear that the oil TEL-90001 causes more wear on M-50 balls than with 52100 balls (0.767 mm at 150°C and 1.547 mm at 250°C for M-50; 0.668 mm at 150°C and 0.923 mm at 250°C for 52100). Averaging scar lengths and widths, as directed by ASTM procedure allows much valuable information to be lost. By considering the width and length separately, the degree of upper ball wear can be calculated, and as seen with these high temperature fluids, the upper ball wear scar can be the primary contributor to the total wear volume generated in a four-ball test. Furthermore, the extent of upper ball wear can vary due to temperature, lubricant, or ball material.

c. Surface Analysis of Wear Scar

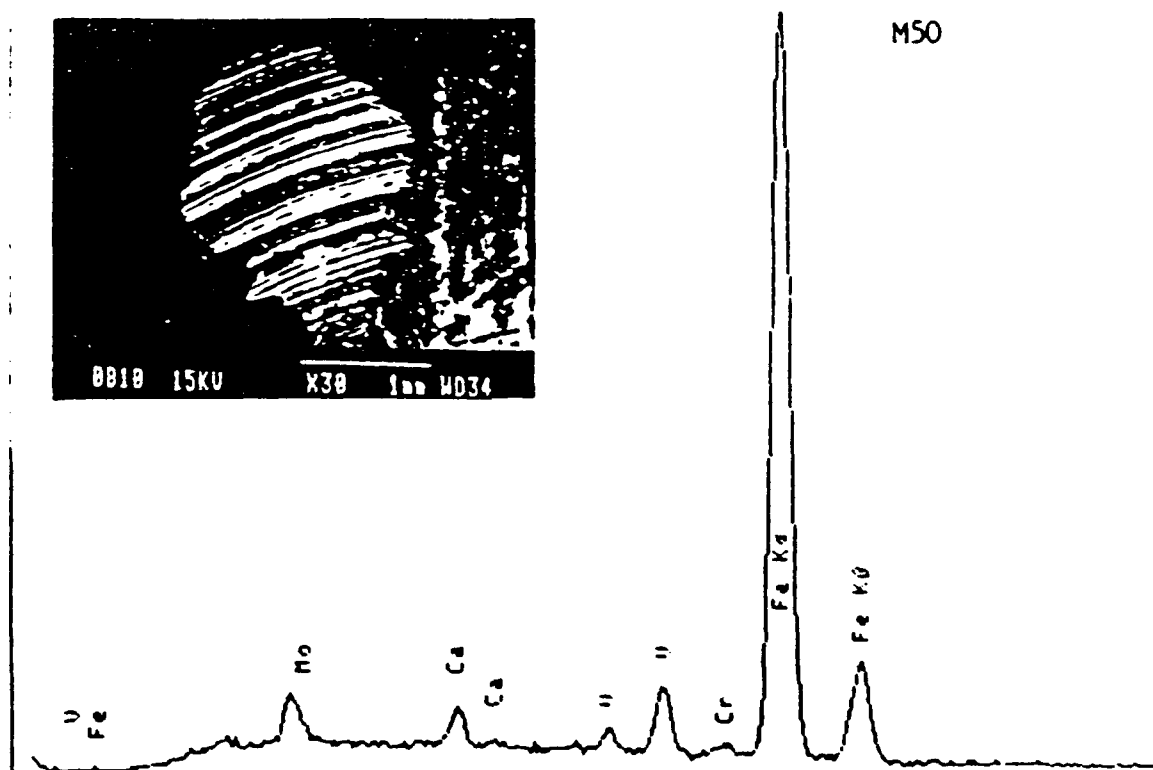
The question remains, however, as to why PPEs always produce more severe wear on M-50, a material with superior material properties than 52100. Surface analyses were performed on the wear scars of M-50 and 52100 balls by both SEM/EDS and Auger emission spectrometric (AES) techniques to determine whether surface chemistry is responsible for the unusual wear behavior of these two metals.

Typical EDS elemental analyses of the lower ball wear scars on M-50

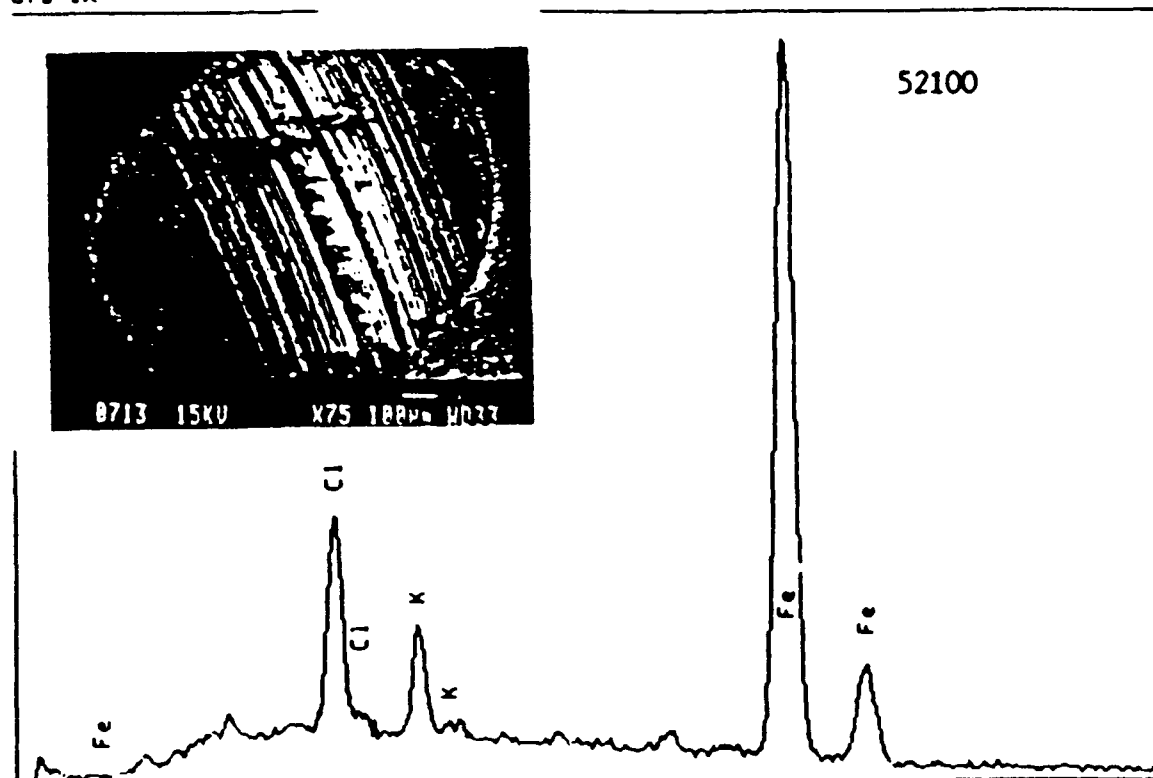
and 52100 specimens are shown in Figure 142. Photomicrographs within Figure 142 show the representative shapes of the lower ball wear scars for the PPE O-67-1 at 150°C for 3 hours (1200 rpm, 145 N). Except for the differing metallurgies of the steel surfaces, the presence of chlorine on the 52100 scar is the only significant difference between the surface compositions on the M-50 and 52100 wear scars. The presence of potassium on the 52100 ball and calcium on the M-50 ball was not studied during this research. The concentration of chlorine was higher on the upper ball than on the lower balls for 52100 and varied along the surface of the scar.

The AES elemental depth profiles of the wear scars on the upper ball and one of the lower balls for each material are shown in Figures 143 and 144, respectively. The elemental depth profiles are based on atomic percentages (not weight percentages) and were produced using a sputtering rate of 5 nm per minute. In agreement with the SEM/EDS analyses, the AES analyses in Figure 143 indicate that the surface of the 52100 ball upper wear scar contains a higher level of chlorine than the wear scar of the lower ball. Also in agreement with the SEM/EDS results, Figure 144 shows no detectable chlorine on either the upper or lower M-50 balls.

The depth profiles in Figures 143 and 144 also indicate that the polymeric films on the surfaces of the wear scars are much thicker for M-50 specimens than for 52100 specimens. The films on the upper balls of either specimen material are always thicker than those on the lower balls. The approximate thicknesses (intersection of carbon and iron plots) of the films are 0.03 and 0.005 microns for the upper and lower 52100 balls, respectively, and 0.14 and 0.04 microns for the upper and lower M-50 balls, respectively. The polymer film on the M-50 ball appears to be two-layered with the interface at 0.07 microns (14 minutes).



Cfs 1K



1 <0.000 keV Cursor = 744 (7.440 keV) = 27 9.600 keV >

Figure 142. SEM Microphotographs and EDS Elemental Analyses of Wear Scars Produced on Bottom Balls During O-67-1 Four-Ball Tests with M50 and 52100 Steel at 150°C

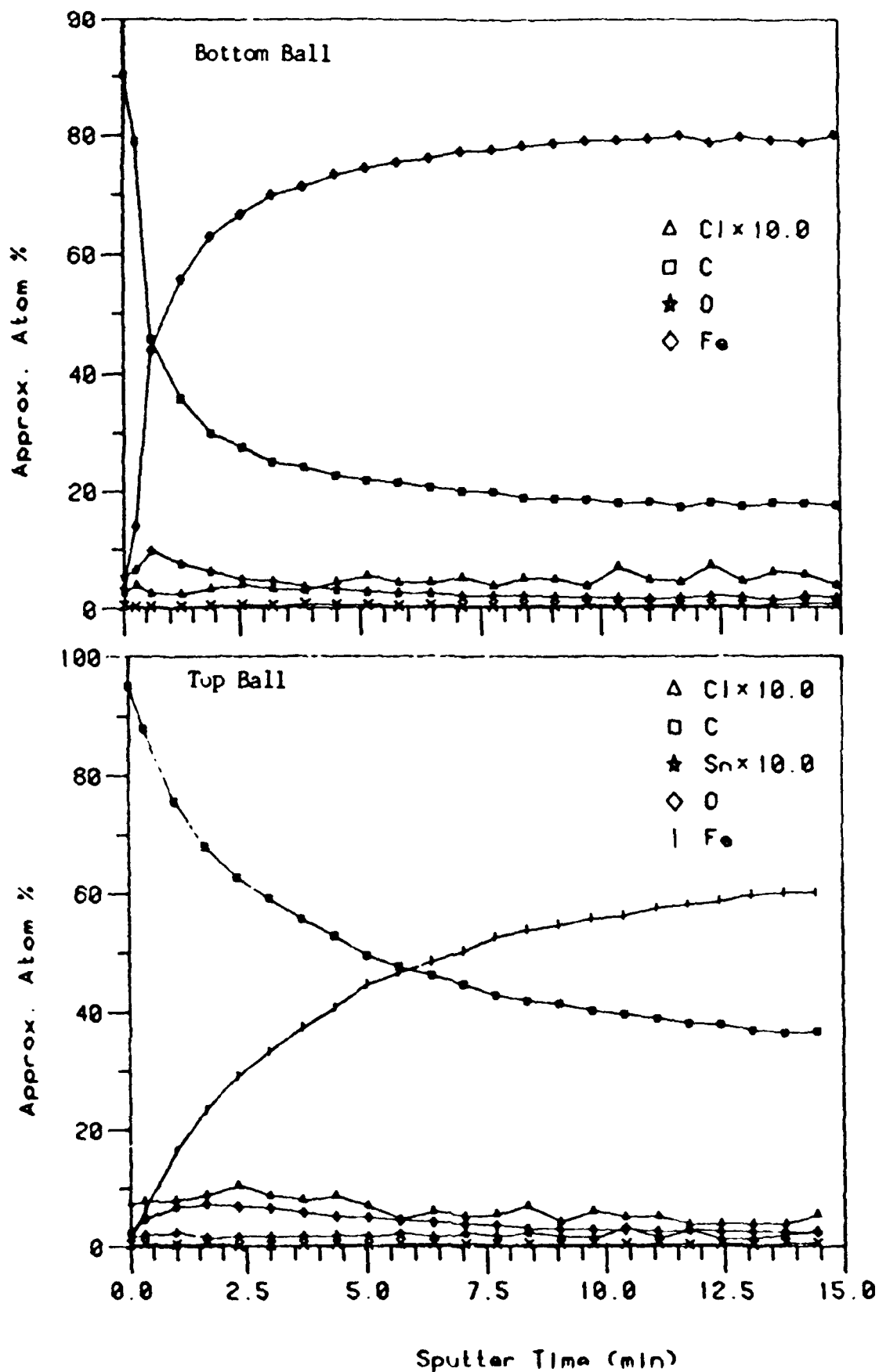


Figure 143. AES Depth Profiles (5 nm/minute) of Wear Scars Produced on Bottom and Top Balls During O-67-1 Four-Ball Test with 52100 Steel at 150°C

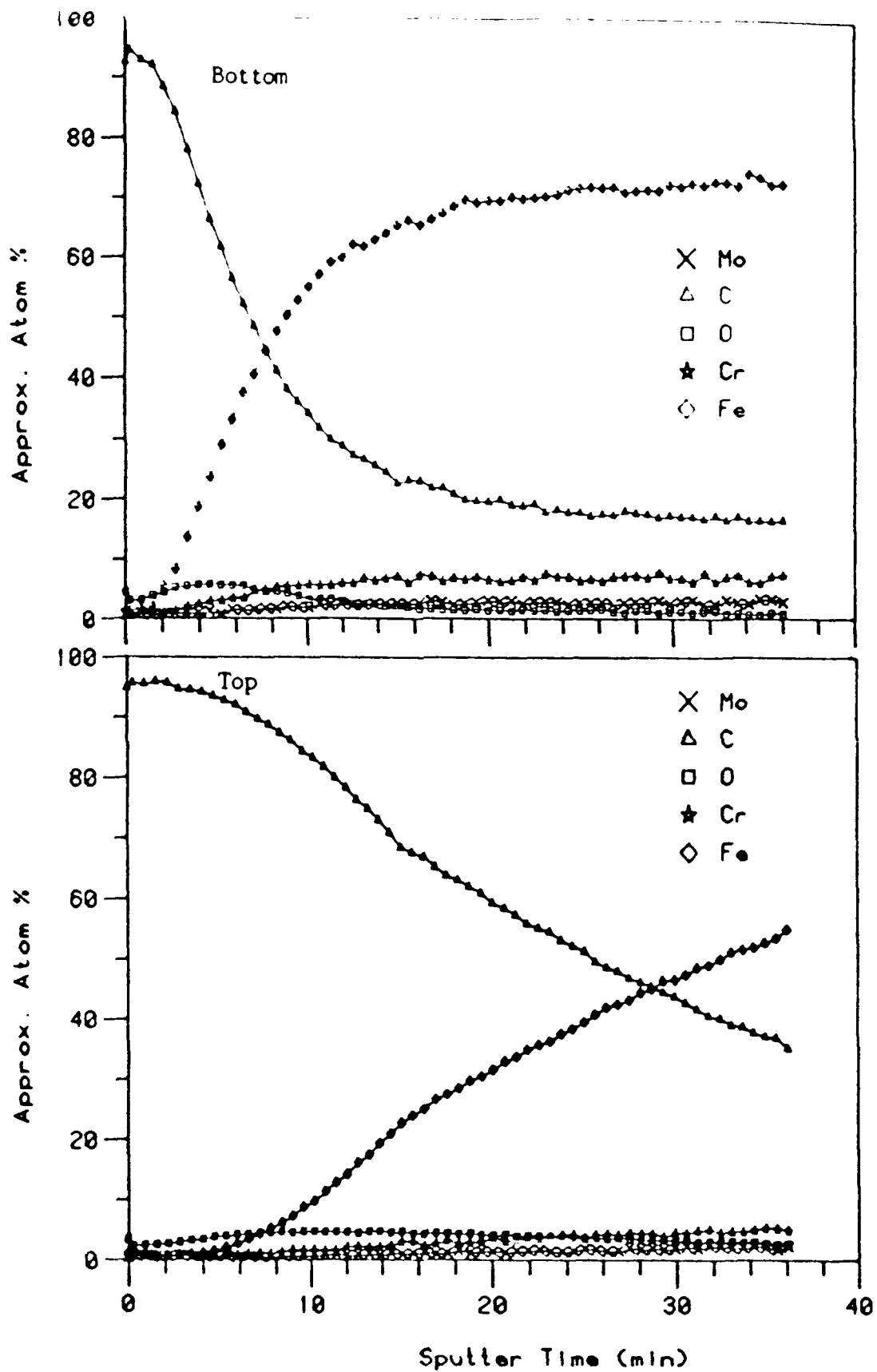


Figure 144. AFS Depth Profiles (5nm/minute) of Wear Scars Produced on Bottom and Top Balls During 0-67-1 Four-Ball Test with M-50 Steel at 150°C

In addition to their thicknesses and presence or absence of chlorine, polymeric films on the M-50 and 52100 also differ in oxygen content. The wear surfaces of the 52100 balls contain a maximum of about 10% oxygen (Figure 143) while the M-50 balls' wear surfaces contain about 5% oxygen (Figure 144). The oxygen concentration appears to be related to the iron oxide content of the polymer film. Whether the iron oxide detected by AES is present in the polymeric film or as steel surfaces (due to thin spots in the polymeric coating) cannot be determined from the data in Figures 143 and 144.

AES analyses of 52100 four-ball specimens tested at 315°C no longer show detectable levels of chlorine (0.1%). From Figure 145, the film thicknesses of the upper and lower 52100 balls are 0.015 and 0.005 microns (compared to 0.03 and 0.005 micron films at 150°C) and the oxygen content increased from 10% to 16%. Since the increase in temperature had little effect upon the film thickness, the wear at each temperature would likely be similar. Although material softening of 52100 occurs at 315°C, a comparison of the wear rates at 150 and 315°C is made by plotting the vertical position of the upper ball against test time for the two temperatures (Figure 146). The similarity in the slopes of the two curves echoes the similarity between the thicknesses of the polymer films formed at these two different temperatures.

The effect of temperature on the film thickness of M-50 balls is more dramatic than with 52100. From Figure 147, the film thickness on the upper M-50 ball at 315°C is 0.03 microns. The thickness of the film on the lower ball wear scar is less than 0.005 microns. Although the presence of chlorine is still undetectable at the surface of the M-50 balls, the reduction in the polymeric film thickness results in a significant reduction of the wear rate (indicated by the slopes of the upper ball position curves of Figure 148).

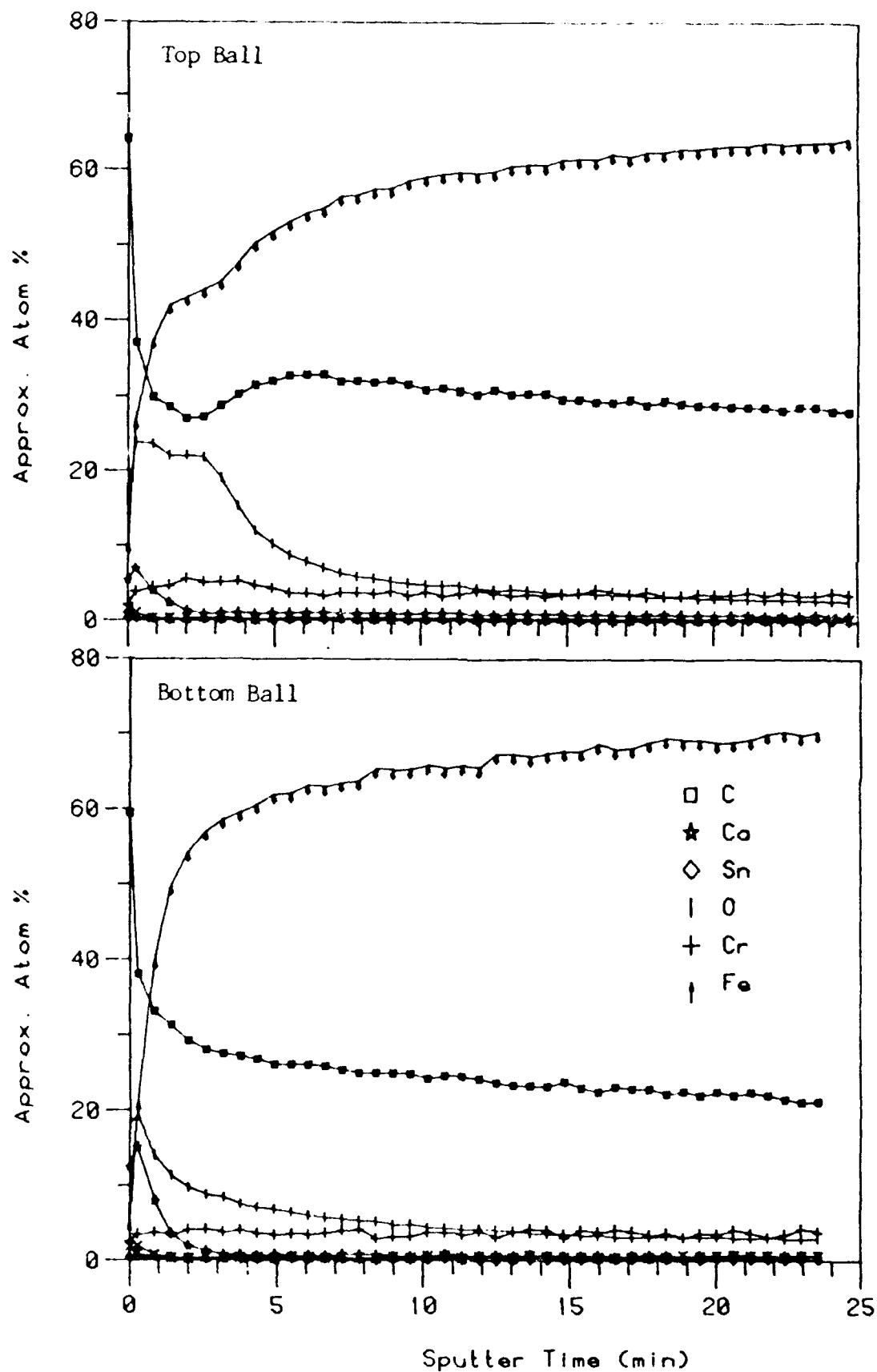


Figure 145. AES Depth Profiles (5 nm/minute) of Wear Scars Produced on the Top and Bottom Balls During 0-67-1 Four-Ball Wear Test with 52100 Steel at 315°C

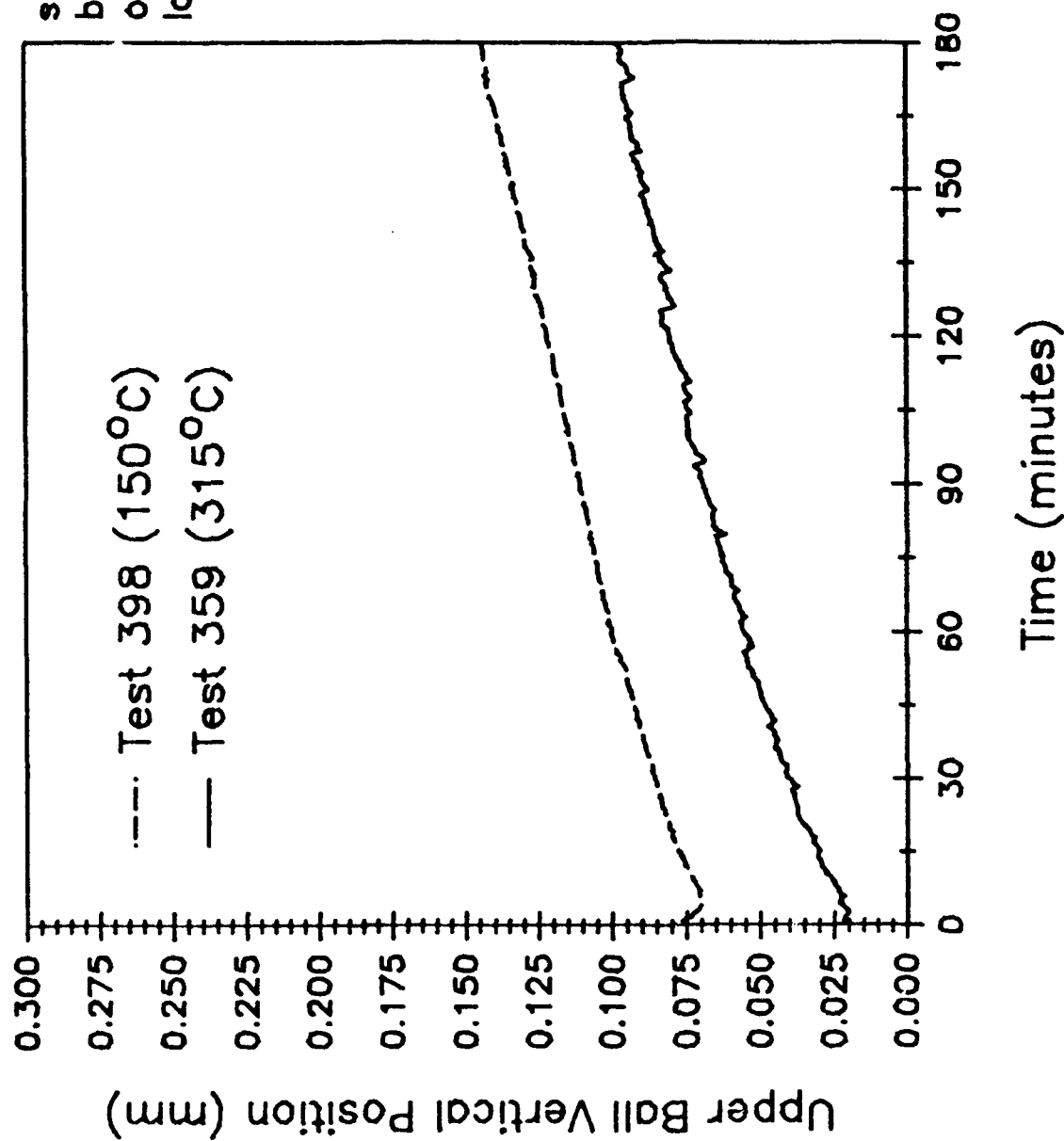


Figure 146. Wear Rate Comparison Between Tests of 52100 Balls Lubricated with PPE at 150°C and 315°C Represented by the Upper Ball Travel (LVDT Data)

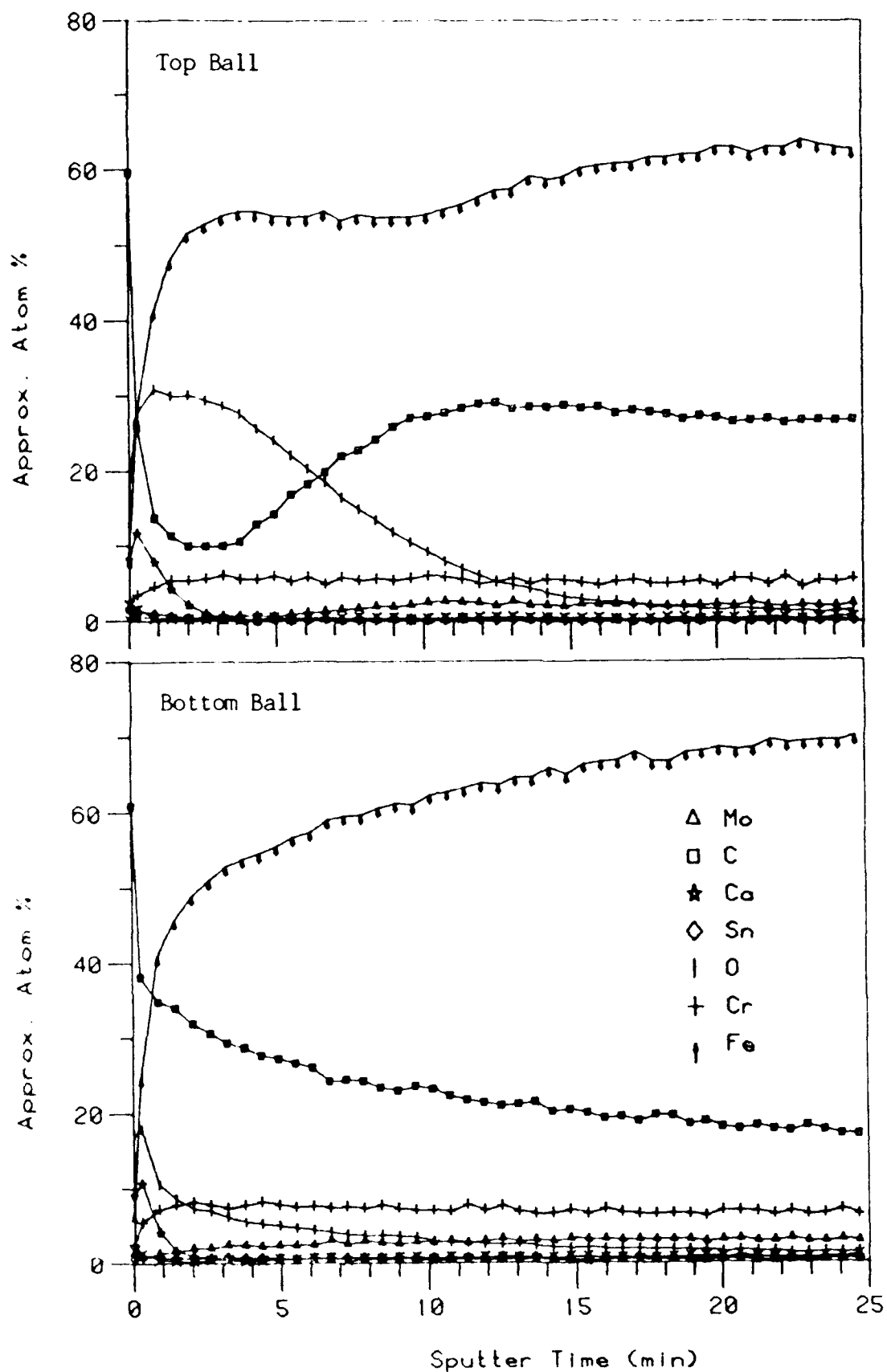
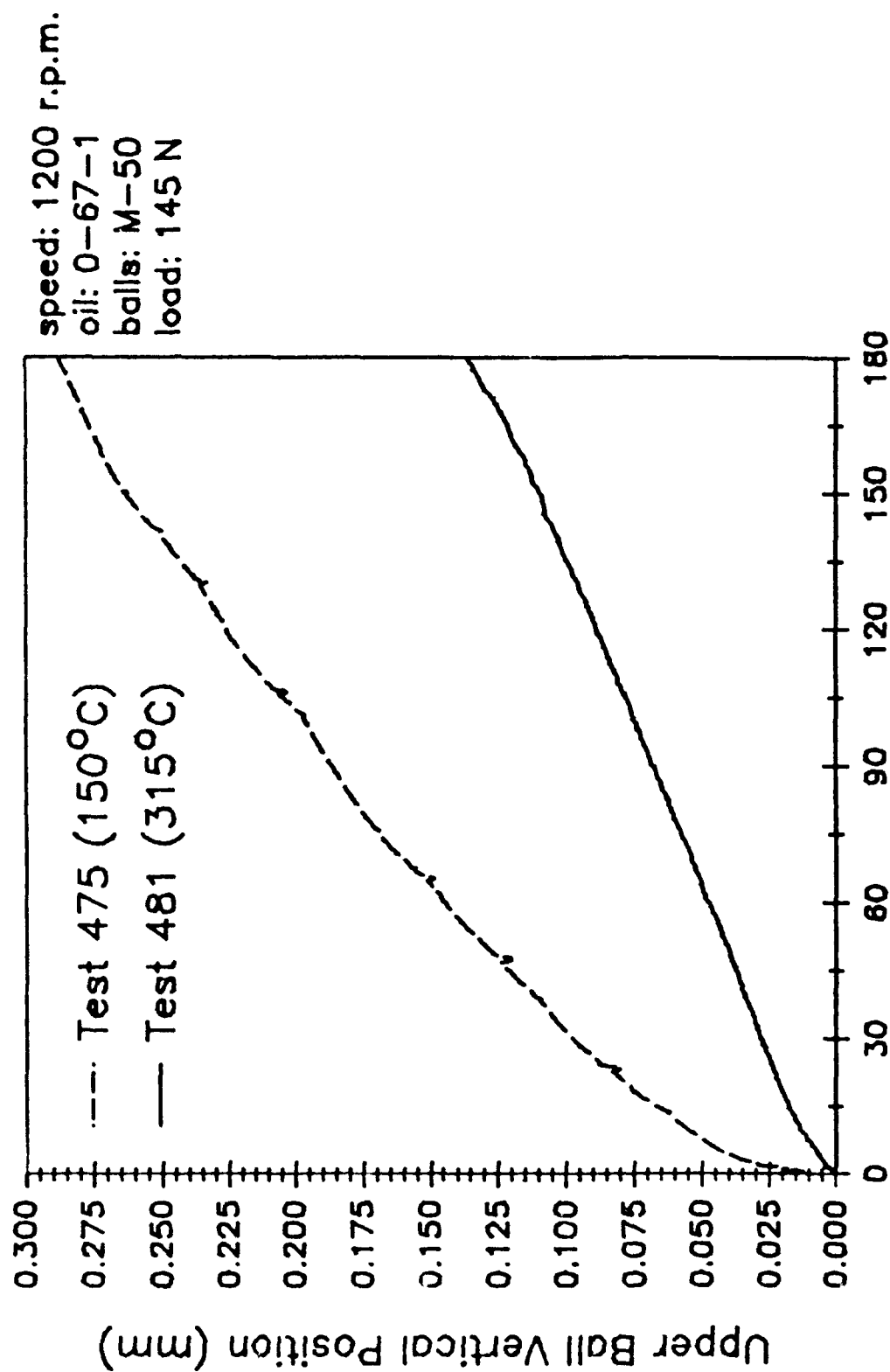


Figure 147. AES Depth Profiles (5 nm/minute) of Wear Scars Produced on the Top and Bottom Balls During 0-67-1 Four-Ball Wear Test with M-50 Steel at 315°C



Time (minutes)

Figure 148. Wear Rate Comparison Between Tests of M-50 Balls Lubricated with PPE at 150°C and 315°C Represented by the Upper Ball Travel (LVDT Data)

The unusual wear encountered with the PPE O-67-1 on these two steels led to an investigation of other materials with drastically different properties. Brass was chosen as a soft material (low hardness) and silicon nitride (Si_3N_4) was chosen as a very hard material. Figure 149 shows the variation of scar length and width on brass, 52100 steel, M-50 steel, and Si_3N_4 balls lubricated by O-67-1 at 150°C for 3 hours. Two additional runs of M-50 on 52100 and Si_3N_4 on 52100 are included to illustrate the effects of using materials of different hardness and composition on one another in the four-ball test. In terms of the scar size, tests of M-50 and brass yielded the largest scars while tests of 52100 and Si_3N_4 had the smallest scars. For the two hybrid tests, the chord length and equivalent width did not change drastically from tests corresponding to the upper ball material; the scars from a test of four M-50 balls have similar dimensions to the scars on three 52100 balls worn by an M-50 ball, and the scars from a test of four Si_3N_4 balls have similar dimensions to the scars on three 52100 balls worn by an Si_3N_4 ball.

The volumes of the upper and lower ball wear scars for these tests are shown in Figure 150. Referring to Figure 149, the disproportion between length and width of scars from the two tests using M-50 as a material results in extremely high values of upper ball wear. Despite M-50's vastly superior hardness to brass', the total wear on four M-50 balls is more than twice the wear on four brass balls (6.99 mm^3 for M-50 while only 3.13 mm^3 for brass).

The tribochemical reaction between PPE and the sliding surfaces is the primary factor governing the wear mechanism. Although the mechanical properties of M-50 make this material an excellent choice for bearing conditions, under sliding, some of its constituent elements may react with PPE to create abrasive particles which actually promote wear. In practice,

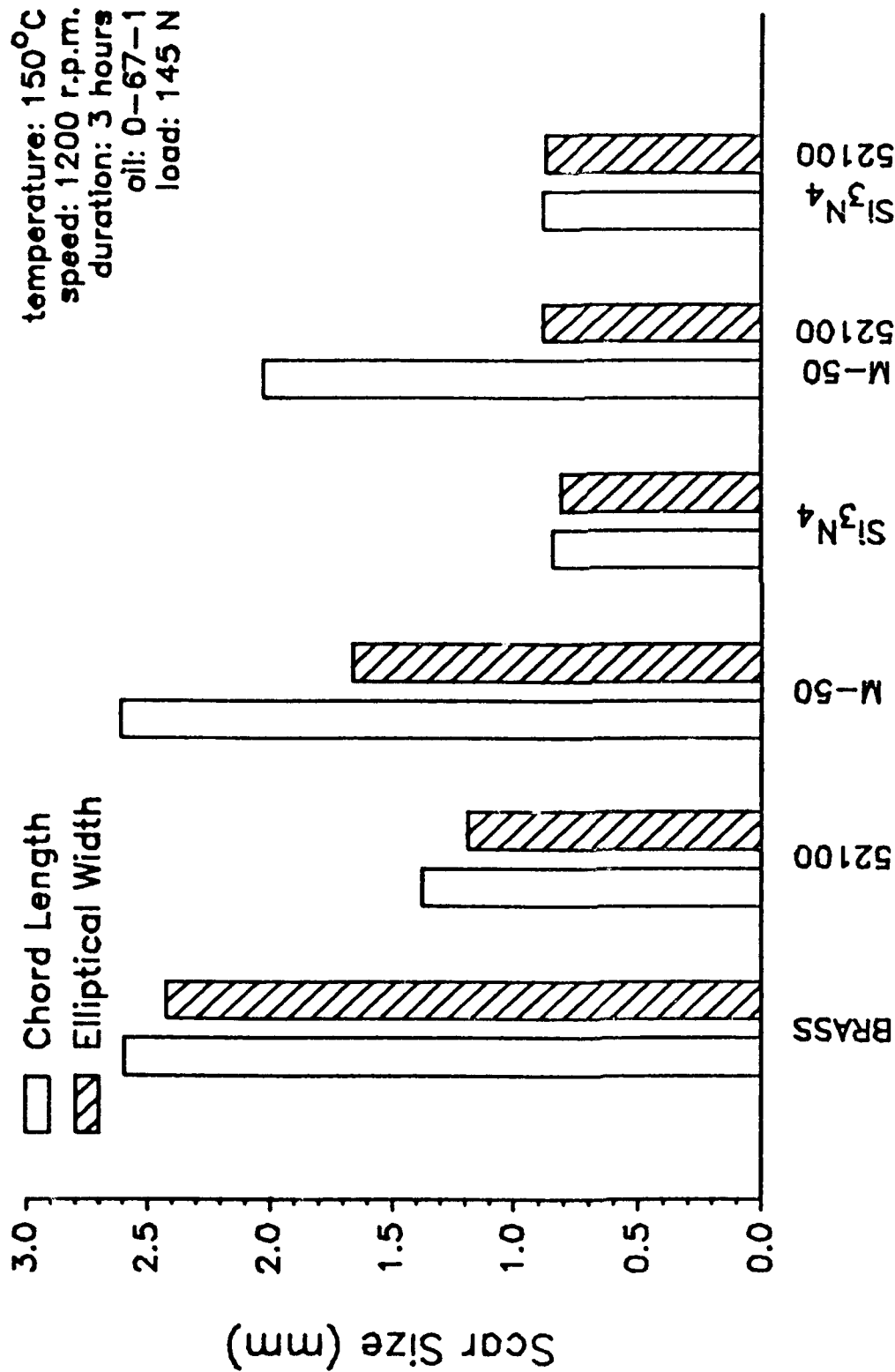


Figure 149. Material Comparison Based on the Scar Sizes of Balls Lubricated with PPE at 150°C

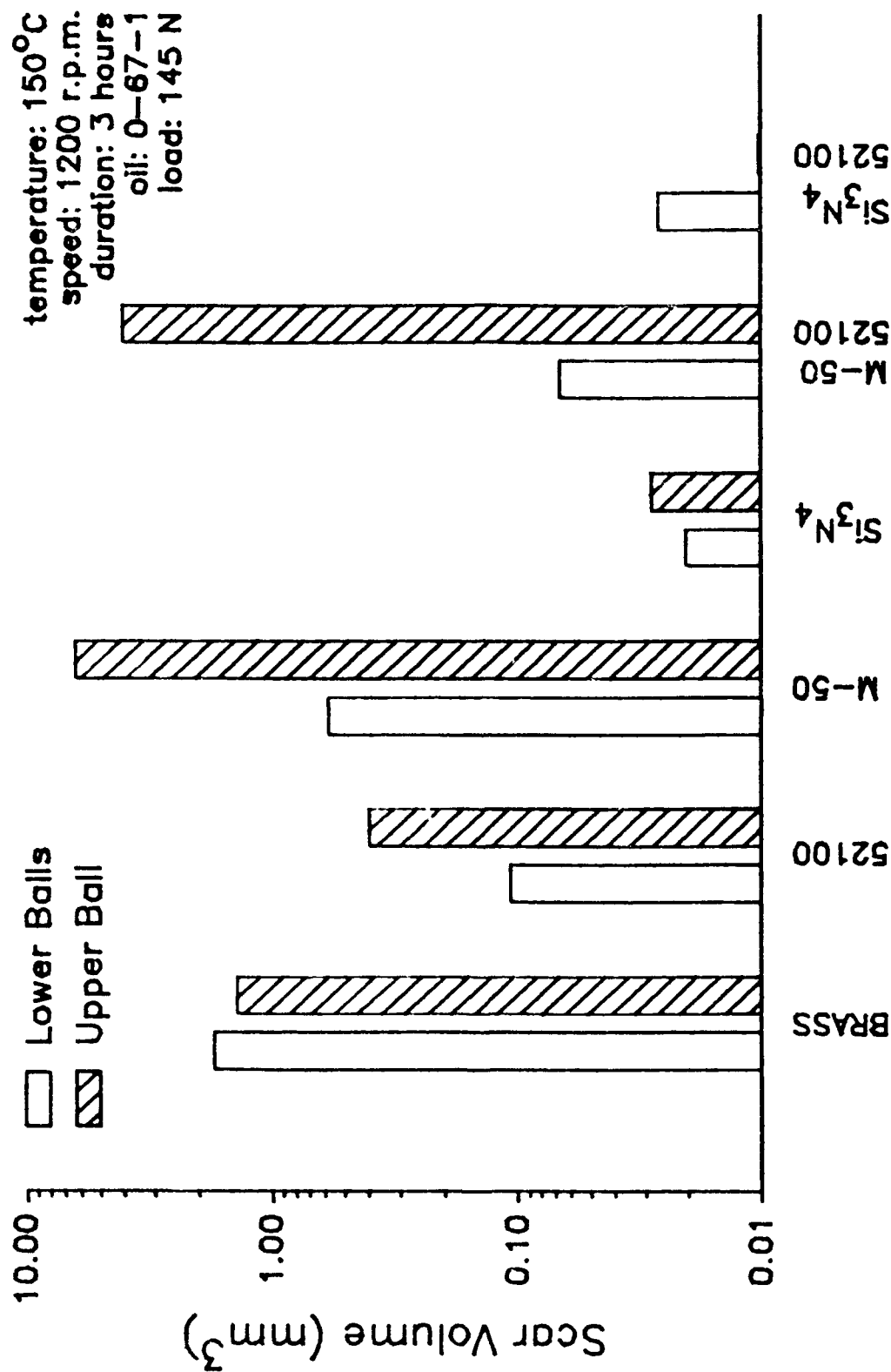
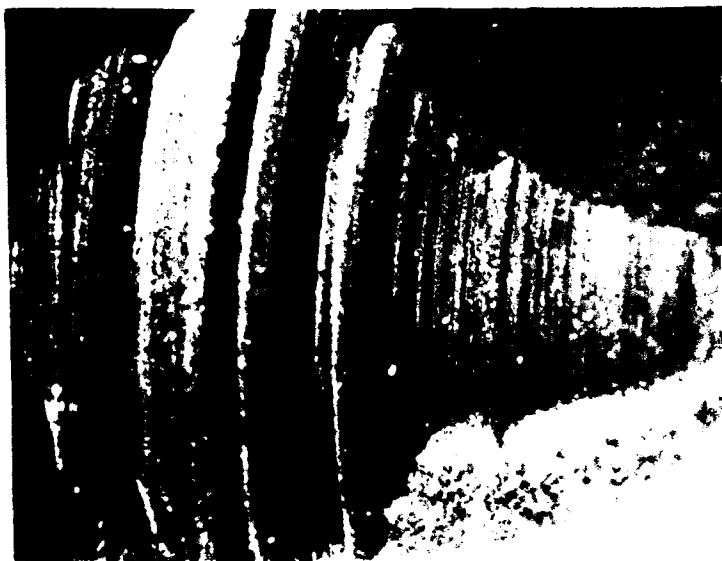


Figure 150. Material Comparison Based on the Scar Volumes of Balls Lubricated with PPE at 150°C

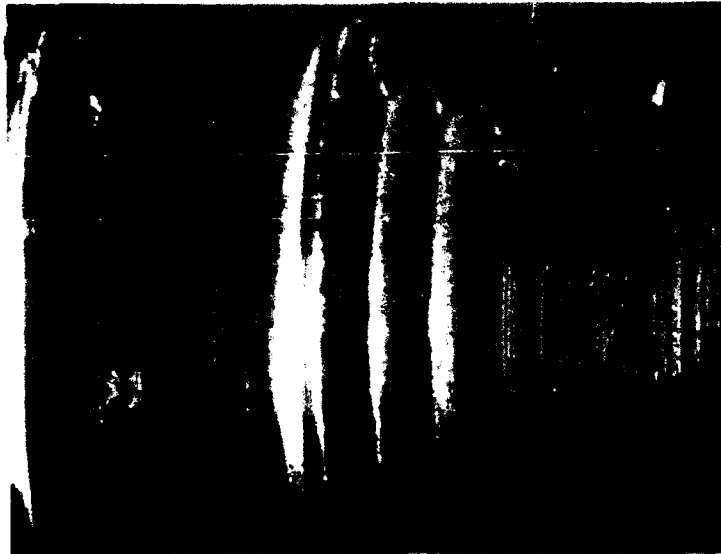
tests of O-67-1 on M-50 balls left large sludge deposits along the leading edge of the lower ball wear scars at every test temperature from 75 to 315°C. These build-ups, which were either absent or present to a lesser extent for all other ball materials, can keep wear particles localized around the sliding contacts. If a tribochemical reaction between the ball material and the lubricant creates abrasive wear debris, build-ups at the perimeter of the sliding contacts can severely affect the scar formation.

The lower ball scars formed on brass and Si_3N_4 specimens lubricated with PPE are typically circular. The inherent inertness of ceramics prevents Si_3N_4 from having any tribochemistry with PPE, and the superior wear resistance of Si_3N_4 prevents significant amounts of wear debris to accumulate near the wear scars. Although brass specimens exhibit severe wear, sludge accumulation is not observed in the few tests of brass balls. For these two materials, sludge build-ups did not influence the scar shape. Wear scars formed on the two steel ball materials (52100 and M-50), however, were influenced by the sludge accumulation. Although scar shapes on 52100 balls occasionally differ drastically from simple circles, scars on M-50 specimens are typically far removed from any simple geometric shape (see Figure 151).

Unusual scarring on the two steel materials takes place at temperatures of 150°C or greater, and the scars formed on M-50 balls are unique for every test. Although the scar measuring procedure detailed in Appendix C allows unusual scars to be measured more accurately than by merely averaging the longest and widest points on the scar, the consistent deviations in the lower ball scars of M-50 specimens prevent an accurate assessment of the wear to be made since repeatability of identical tests cannot be obtained. In order to yield consistent results for PPE at high temperature, the contribution of sludge buildup to the wear on the high



a. 3 Hours at 150°C, 1200 RPM,
145 N Load



b. 3 Hours at 250°C, 1200 RPM,
145 N Load

Figure 151. Lower Ball Scars Formed on M-50 Steel Specimens Lubricated with Polyphenyl Ether (38X Actual Size)

temperature ball material (M-50) must be minimized.

d. Introduction of Gas into the Four-Ball Test Cup

Although testing of PPE on M-50 specimen balls revealed unusual scar shapes which were not consistent between tests at identical conditions, individual tests at 250 and 315°C had simple, elliptical scars which contrasted dramatically with the shapes seen in other tests. In tests where unusual scars were formed, sudden surges in the wear rates could be seen by examining a plot of the upper ball position versus test time as recorded by the LVDT instrument. In the two tests where smooth, elliptical scars formed, the upper ball position versus time curves had smooth, even slopes (wear after the run-in period). A comparison of these two different situations is shown in Figure 152. The solid plot exhibits periods of accelerated wear after 2 hours into the test while the dashed plot shows an even wear rate for the entire test duration.

It is believed that sludge formation around the wear scars caused the sudden surges in the wear rates of most of the high temperature tests. The absence of any instances of accelerated wear as in the dashed plot of Figure 152 indicates that sludge accumulation is not yet significant enough to alter the wear regime. Since the wear rates between identical tests were seen to be repeatable before the periods of accelerated wear (i.e., the slopes of the two plots of Figure 152 are approximately equal for the first 2 hours of the tests), shorter duration tests of PPE on M-50 balls would allow wear to remain within the steady-state region. Although sludge accumulation would still occur, the point at which it alters the wear mechanism would be avoided, and repeatability of wear scars should follow.

A preliminary test of PPE at 315°C for only 1 hour exhibited the same periods of accelerated wear as were present in 3-hour tests but the onset of

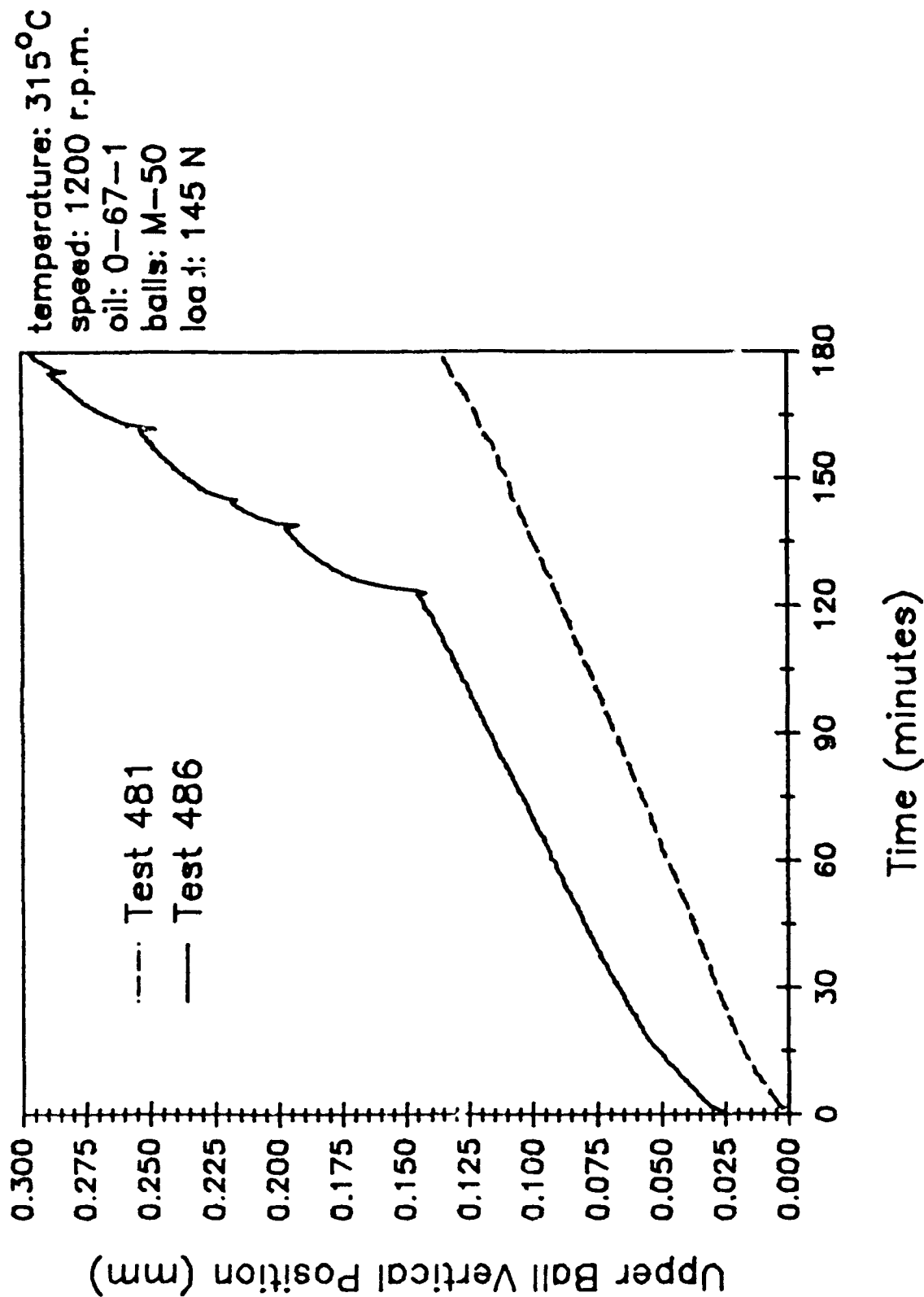


Figure 152. Wear Rate Comparison Between Tests of M-50 Balls Lubricated with PPE Under Identical Conditions Represented by the Upper Ball Travel (LVDT Data)

these sudden surges occurred after 30 minutes. However, another test for 1 hour at 315°C was successful in avoiding wear surges. Because the critical point of sludge accumulation is unpredictable, a method of preventing sludge or at least minimizing it is needed.

It is reasoned that sludge accumulation can be avoided by providing a thorough mixing of the oil in the test cup. Increased agitation of the oil is achieved with the introduction of an airflow into the test cup. To provide an entrance for the gas, a small hole (1/16 inch) was drilled into the bottom-center of the test cup which coincides with an existing drain hole in the base plate of the four-ball machine. By securing an air line to the outlet of the oil drain reservoir, the bubbling of oil which results when air is introduced is sufficient to prevent sludge accumulation at 250 and 315°C.

After preliminary tests to decide upon a suitable flow rate, a rate of 1.31 L/min was satisfactory in preventing sludge accumulation without causing such an excess of agitation as to deplete the oil in the test cup. Of particular concern was the amount of smoking which results during 315°C tests. Although loss of lubricant is unavoidable at this temperature, by placing an excess amount of oil in the test cup and restricting test time to 1 hour, depletion of lubricant is not a problem.

In addition to the benefit of preventing sludge accumulation, the introduction of an agitating gas allows testing to be done in inert atmospheres such as nitrogen. Initial tests at 315°C are sufficient to compare results for systems with an oxidizing gas (air), an inert gas (nitrogen) and no gas. The following data show the scar sizes from 1-hour tests of O-67-1 at 1200 rpm under 145-N load:

Test	Agitating Gas	Scar Length (mm)	Scar Width (mm)
538A	none	1.512	1.396
538B	none	1.128	0.831
546	nitrogen	2.086	1.896
547	air	0.906	0.728

The data include two tests without gas agitation to illustrate the variation in scar size which results from sludge accumulation (Test 538A had periods of accelerated wear while test 538B did not). The introduction of air into the ball cup reduces the scar size slightly from the results of Test 538B. The slight improvement can be attributed to the removal of sludge deposits because although Test 538B had no wear surges, sludge had still accumulated near the wear scars. The most severe wear which was incurred for the three operating conditions was caused by the nitrogen. Although no sludge buildup was formed, scar dimensions from Test 546 (nitrogen) are more than 100% greater than Test 547 (air) and more than 33% greater than Test 538A (no gas but periods of accelerated wear). The effect of an inert environment upon the tribological properties of PPE has been well documented. In a paper by Jones,²⁸ pin-on-disk studies of 5P4E had least wear in moist atmospheres (either inert or oxidizing). When dry atmospheres were used, oxidizing atmospheres gave less wear than inert atmospheres.

It is worthwhile to note that at 315°C, the polymeric surface films change considerably when excess oxygen is introduced by an air flow. Figure 153 shows the AES depth profiles on the top and bottom ball wear scars of a 1-hour test at 315°C. Although the previous profiles of M-50 balls in Figure 147 were from a 3-hour test at 315°C, a comparison to Figure 153 is still valid. The composition of the film on the upper ball of Figure 147 is

approximately 60% carbon, 20% oxygen, and 10% iron with the balance being mainly chromium and calcium. The composition of the upper ball given by Figure 153 is approximately 50% carbon, 20% oxygen, 10% iron, and a balance again of mainly chromium and calcium. Although the relative amounts of the component elements have not been significantly altered and the thickness is relatively unchanged (0.03 micron for the 3-hour test and 0.04 micron for the 1-hour test) the addition of excess oxygen generated a significant amount of chlorine on the top ball scar surface (1 to 2%). The chlorine seen in Figure 153 is the first instance of M-50 scars having detectable amounts of this element although it was readily seen on scars of 52100 balls.

e. Testing of Diluted Polyphenyl Ether

The presence of chlorine on the surface of M-50 scars has been shown to coincide with a decrease in wear. It has also been reported that the addition of chlorinated compounds to lubricants has increased the lubricant load carrying capacity²⁹. One chlorinated compound, trichloroethylene, (TCE), is a solvent used to dilute PPE for low temperature start-up of gas turbine engines. To study the effects of excess chlorine on the tribological characteristics of PPE, a dilution of the PPE basestock O-77-6 with 25% TCE was used in the four-ball test at various temperatures. The 3:1 dilution has a viscosity of 14.6 cSt, only 5% of the original viscosity of O-77-6.

Tests were run at 75, 150, 250 and 315°C for 3 hours at 1200 rpm and 145 N load. The 52100 steel balls were chosen as the specimen material in order to make one-to-one comparisons to previous tests of undiluted O-77-6. Figures 154 and 155 show the scar sizes and wear volumes for the undiluted and diluted four-ball test pairs. Beyond 75°C, no significant variation is seen between O-77-6 and the dilution. At 75°C, a reduction of more than 25% in the scar length and width from the dilution by TCE results in total wear

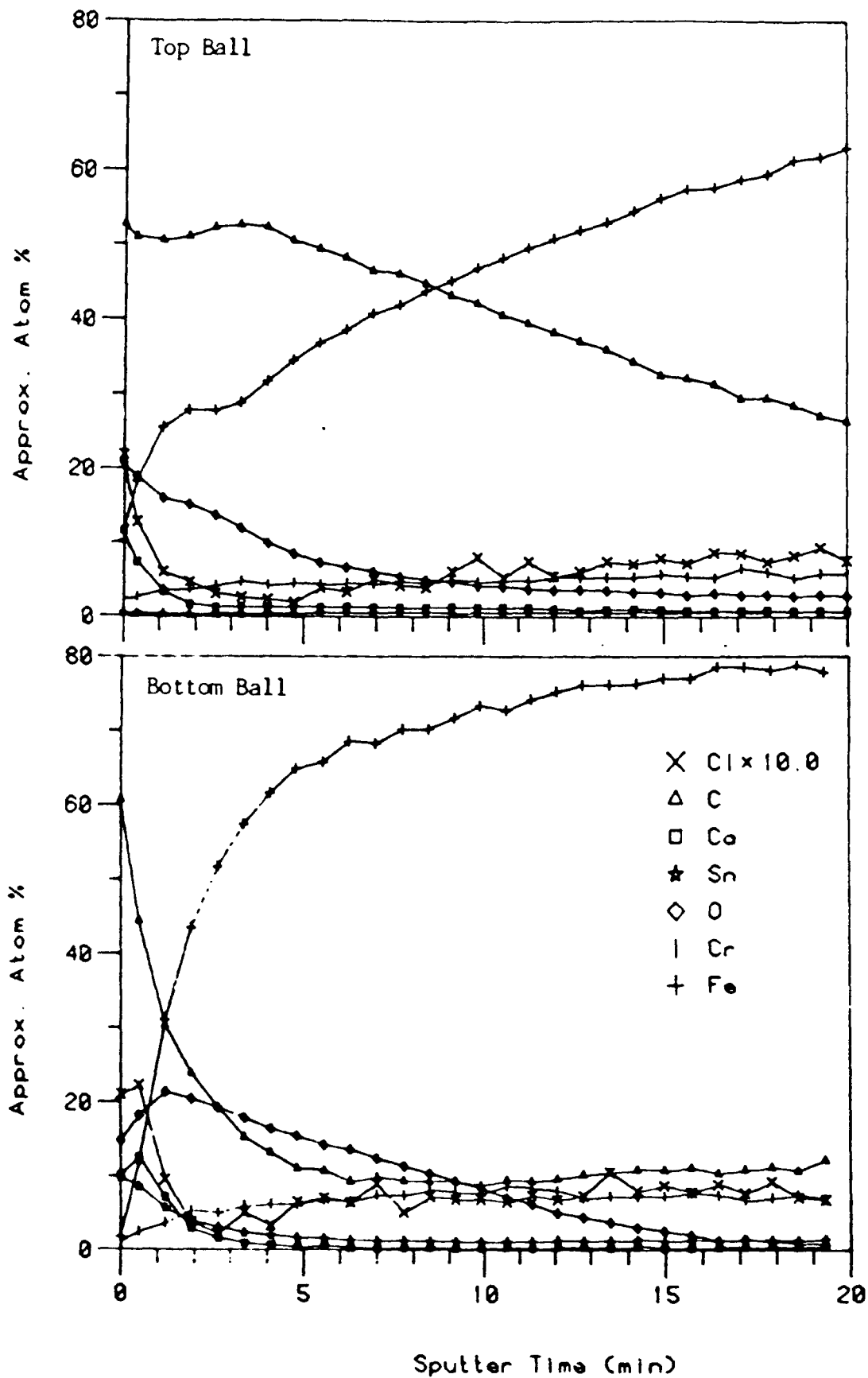


Figure 153. AFS Depth Profiles (5nm/min) of Wear Scars Produced on the Top and Bottom Balls During 0-67-1 Four-Ball Wear Test with M-50 Steel at 315°C and Excess Air

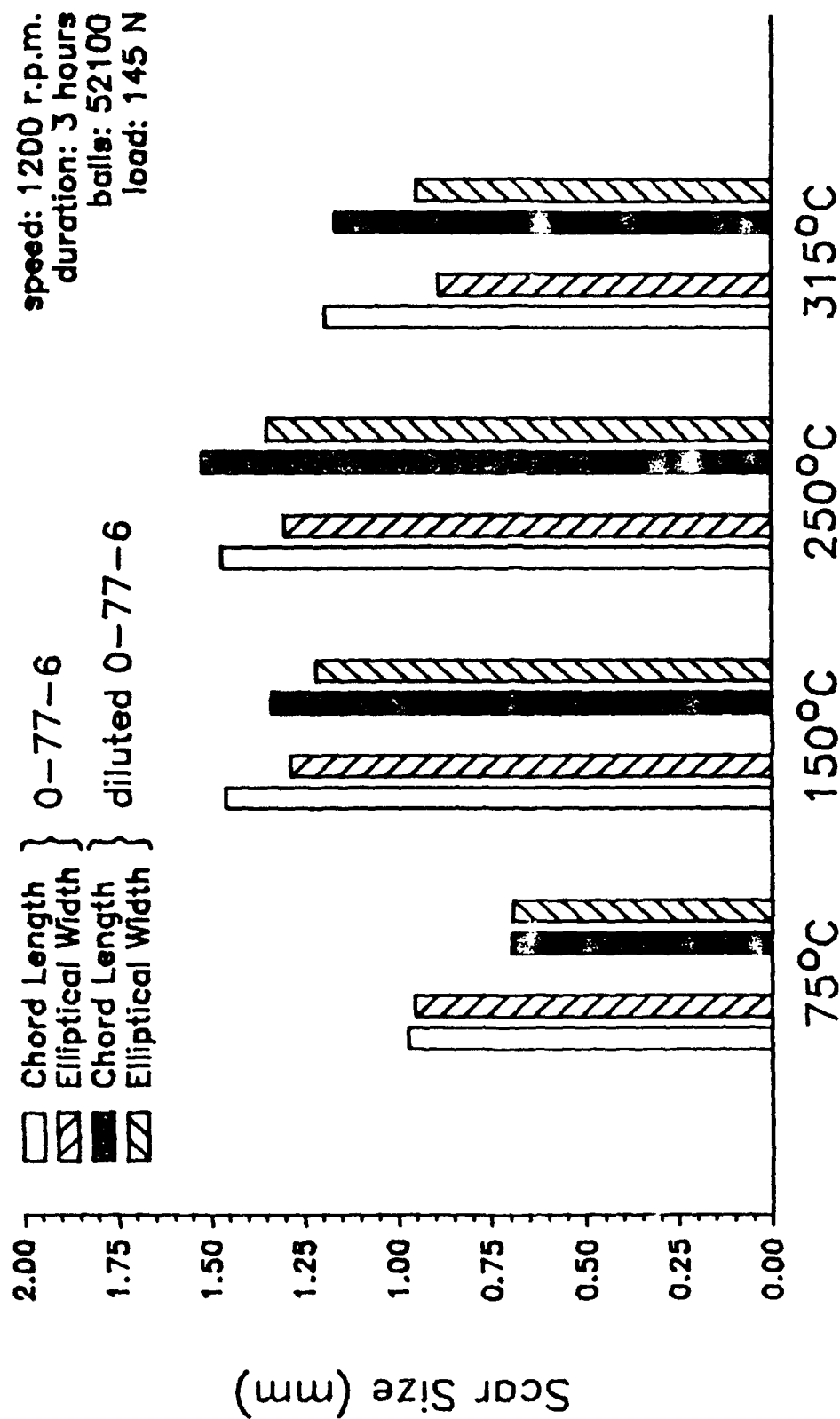


Figure 154. Comparison of PPE to PPE Diluted with 25% TCF at Various Temperatures Based on the Scar Sizes of 52100 Steel Balls

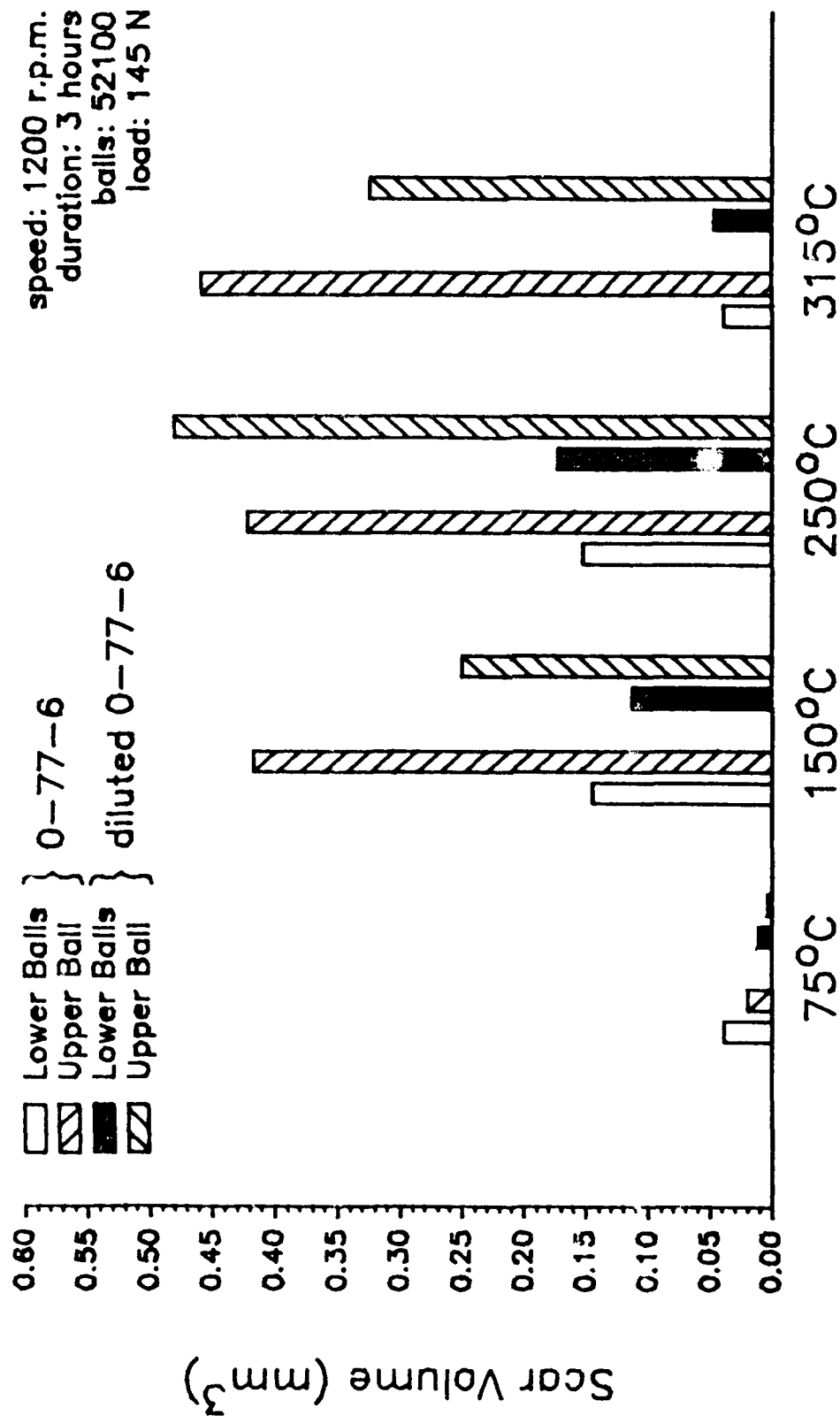


Figure 155. Comparison of PPE to PPE Diluted with 25% TCF at Various Temperatures
Based on the Scar Volumes of 52100 Steel Balls

reduction by a factor of four. The effect of the TCE diminishes at higher temperatures due to loss of the solvent from boiling.

AES profiles of upper and lower balls from tests of undiluted and diluted O-77-6 at 150°C are shown in Figures 156 and 157. The approximate thicknesses of the top and bottom balls scar films are 0.02 and 0.005 micron for O-77-6 and 0.005 and 0.003 micron for TCE-diluted O-77-6. Apart from the decrease in polymeric film thickness, the TCE-diluted O-77-6 increases the oxygen content of the film but only slightly increases its chlorine content.

f. Testing of Stressed Polyphenyl Ether

Another area of interest is the change in the wear properties of PPE after the fluid has been stressed. Several samples of stressed PPE were obtained and used in the four-ball test to compare tribological properties to unstressed PPE. Figure 158 shows the scar sizes produced by several samples of stressed O-67-1. The oils shown in Figure 158 are as follows: O-67-1 (Test #398: a typical test of unstressed O-67-1 shown for comparison), TEL-9030 (Test #387: O-67-1 which was first used in an engine test stand), O-67-1* (Test #399: O-67-1 which was first used in an oxidation-corrosion test for 168 hours at 320°C), O-67-1** (Test #406: O-67-1 which was first used in an oxidation-corrosion test for 240 hours at 320°C), TEL-90026, and TEL-90025 (Test #533 and Test #534: oil drained from separate operational engines).

Figure 159 compares the upper and lower scar volumes for the tests of stressed O-67-1. Although the variation in the chord lengths and elliptical widths seen in Figure 158 is not seemingly significant, analyzing the volume data of Figure 159 indicates little variation between unstressed O-67-1 and oils drained from turbine engines (TEL-9030, TEL-90025 and TEL-90026). The most noticeable change in wear volumes is associated with the two O-67-1

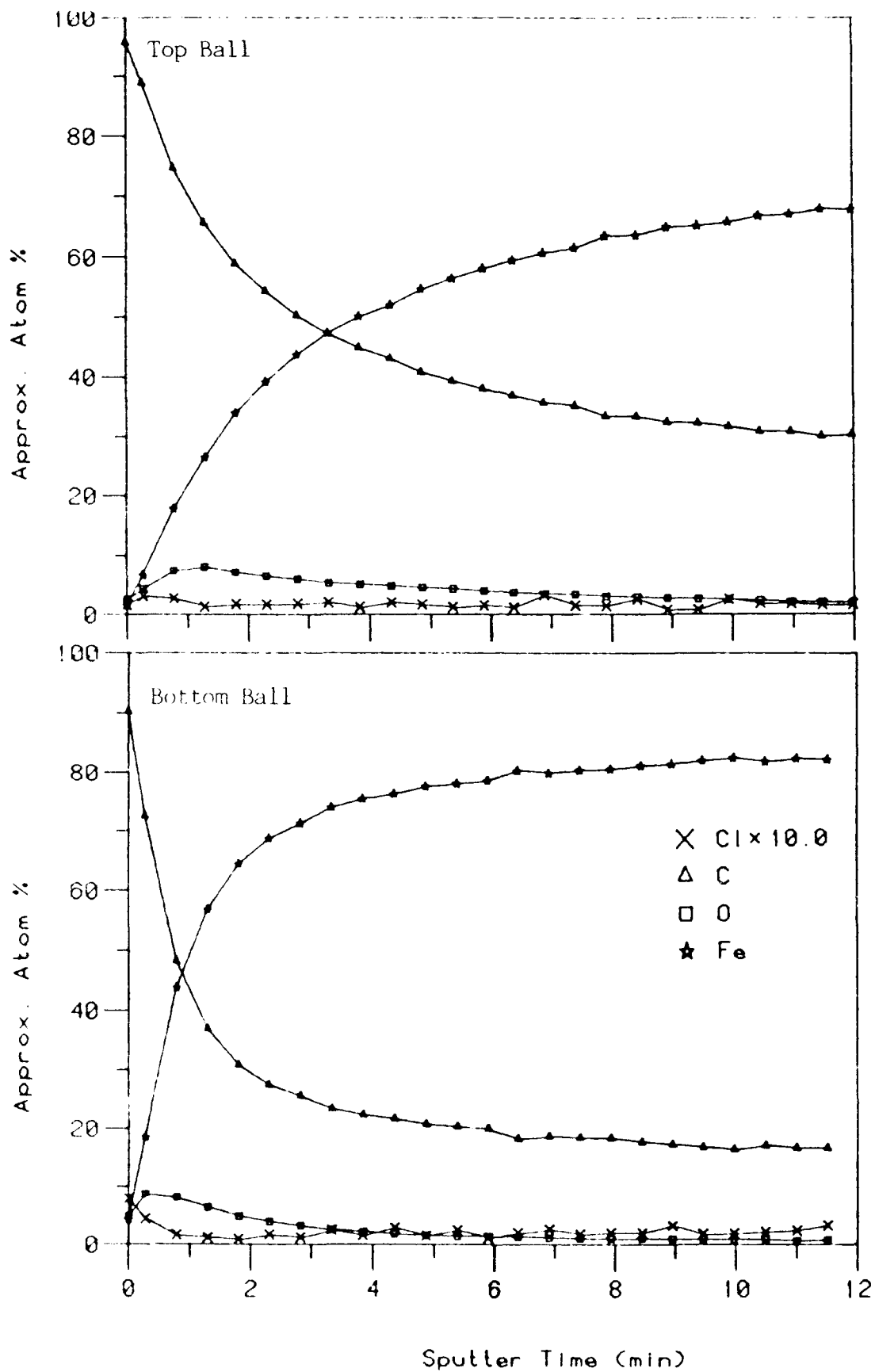


Figure 15b. A1S Depth Profiles (5 nm/minute) of Wear Scars Produced on the Top and Bottom Balls During 0-77-6 Four-Ball Wear Test with 52100 Steel at 170°C

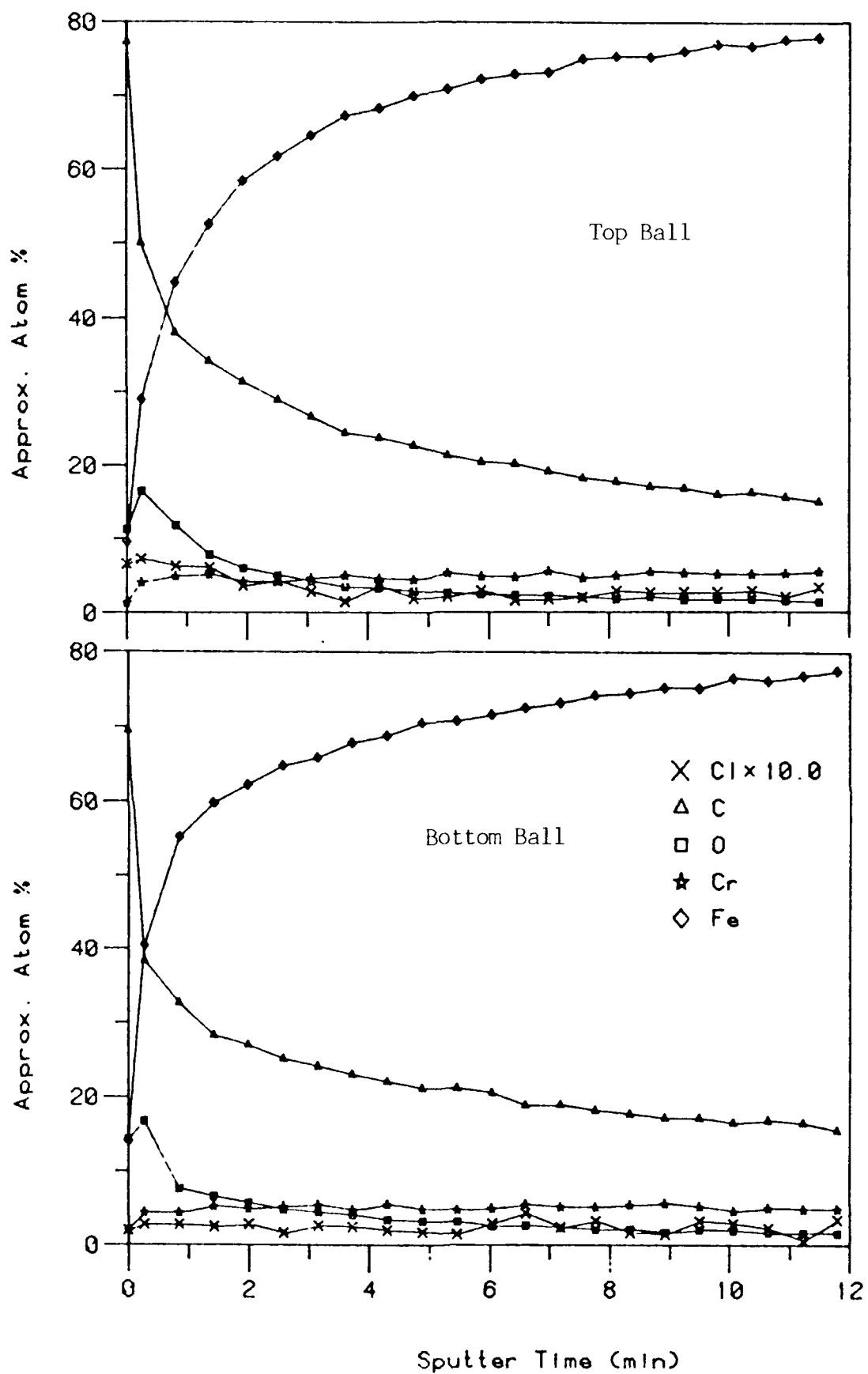


Figure 157. AES Depth Profiles (5 nm/minute) of Wear Scars Produced on the Top and Bottom Balls During TCE-Diluted O-77-6 Four-Ball Wear Test with 52100 Steel at 150°C

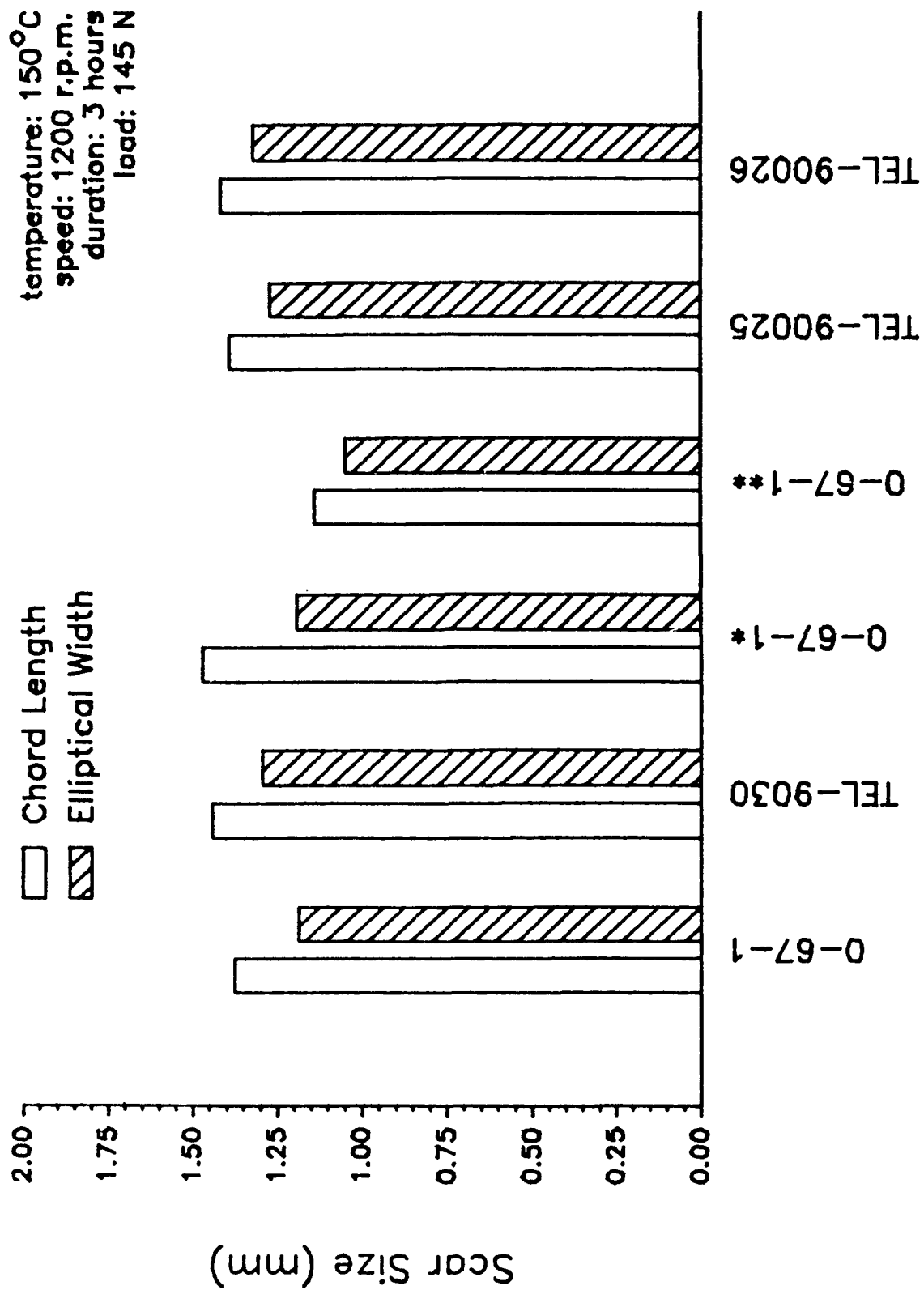


Figure 158. Comparison of Various Stressed Samples of PPE Based on the Scar Size of 52100 Steel Balls at 150°C

temperature: 150°C
 speed: 1200 r.p.m.
 duration: 3 hours
 load: 145 N

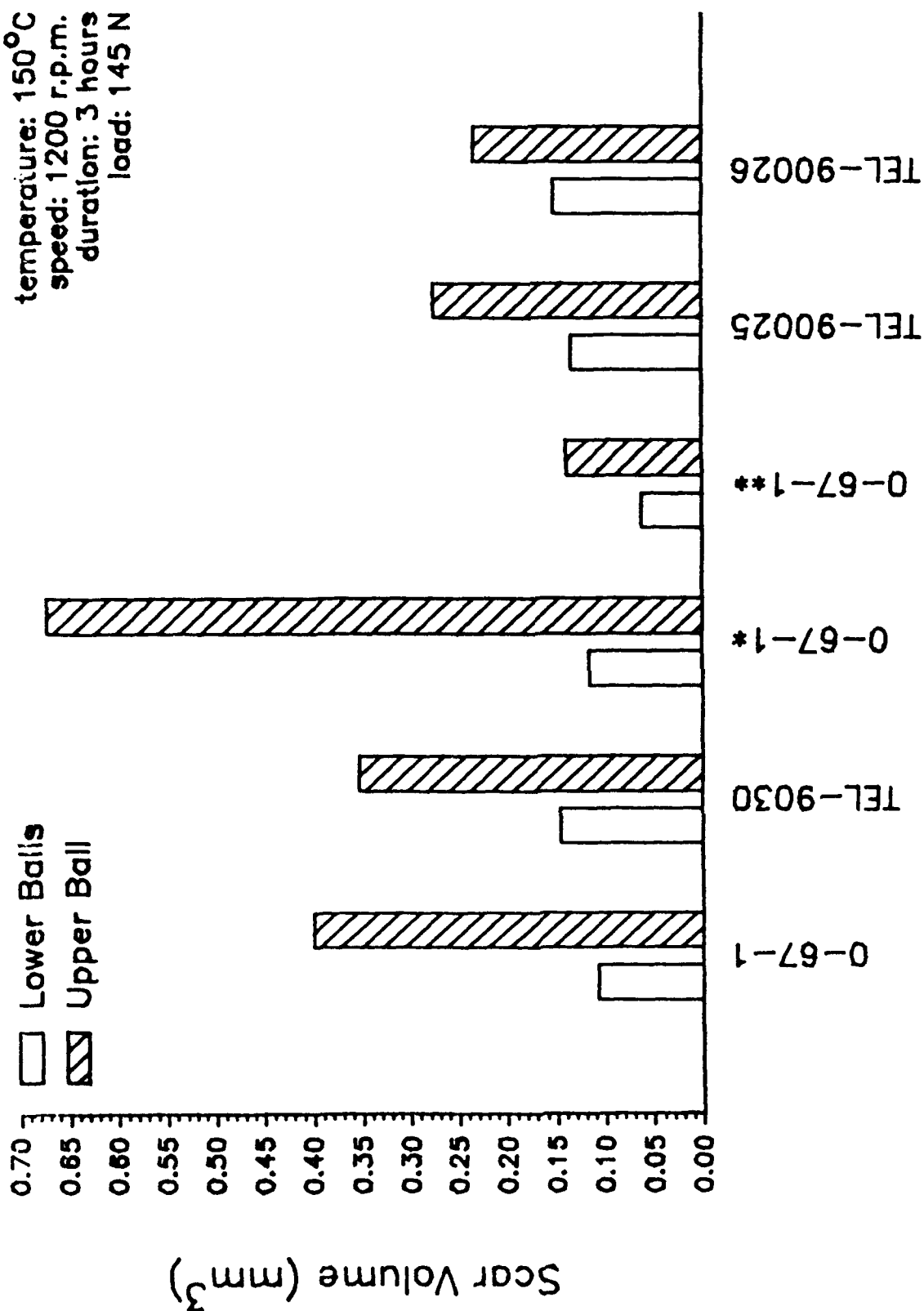


Figure 159. Comparison of Various Stressed Samples of PPF Based on the Scar Volumes of 52100 Steel Balls at 150°C

samples which were stressed in oxidation-corrosion tests (O-67-1* and O-67-1**). The results from these two samples are not consistent although the conditions at which they were stressed are similar: O-67-1** (which had the least wear) was kept at 320°C 72 hours longer than O-67-1* (which had the most wear). If the test of O-67-1* is discounted, the tribological properties of PPE show improvement when the lubricant is stressed.

It is most likely, however, that stressing of PPE by the methods used in this study has neither a detrimental nor beneficial effect on its wear characteristics. Figure 160 shows a ranking similar to Figure 158. In Figure 160, the scar sizes from six identical tests of unstressed PPE are compared at the same conditions used in the study of the stressed fluids. Just as in Figure 158, variation between tests is not seen to be significant. A check of the rankings of the scar volumes (Figure 161), however, shows Test 369 to have a noticeable reduction in upper ball wear. Referring to the scar volume rankings for the stressed fluids (Figure 159), it is seen that upper ball wear is the parameter which varies the greatest between tests. Therefore, since only discrete tests were made in the evaluation of the stressed fluids and variation of wear is within an order of magnitude, changes in the tribological properties of stressed PPE are not observed at 150°C.

g. Temperature Study at the Ball Contact Zone

Reports have suggested that shearing of asperities within points of contact can reach extremely high temperatures during sliding conditions³⁰. Since the four-ball test machine used in this research monitors the bulk temperature of the oil using a thermocouple located within the wall of the test cup, the temperature at the sliding contacts is actually higher than the

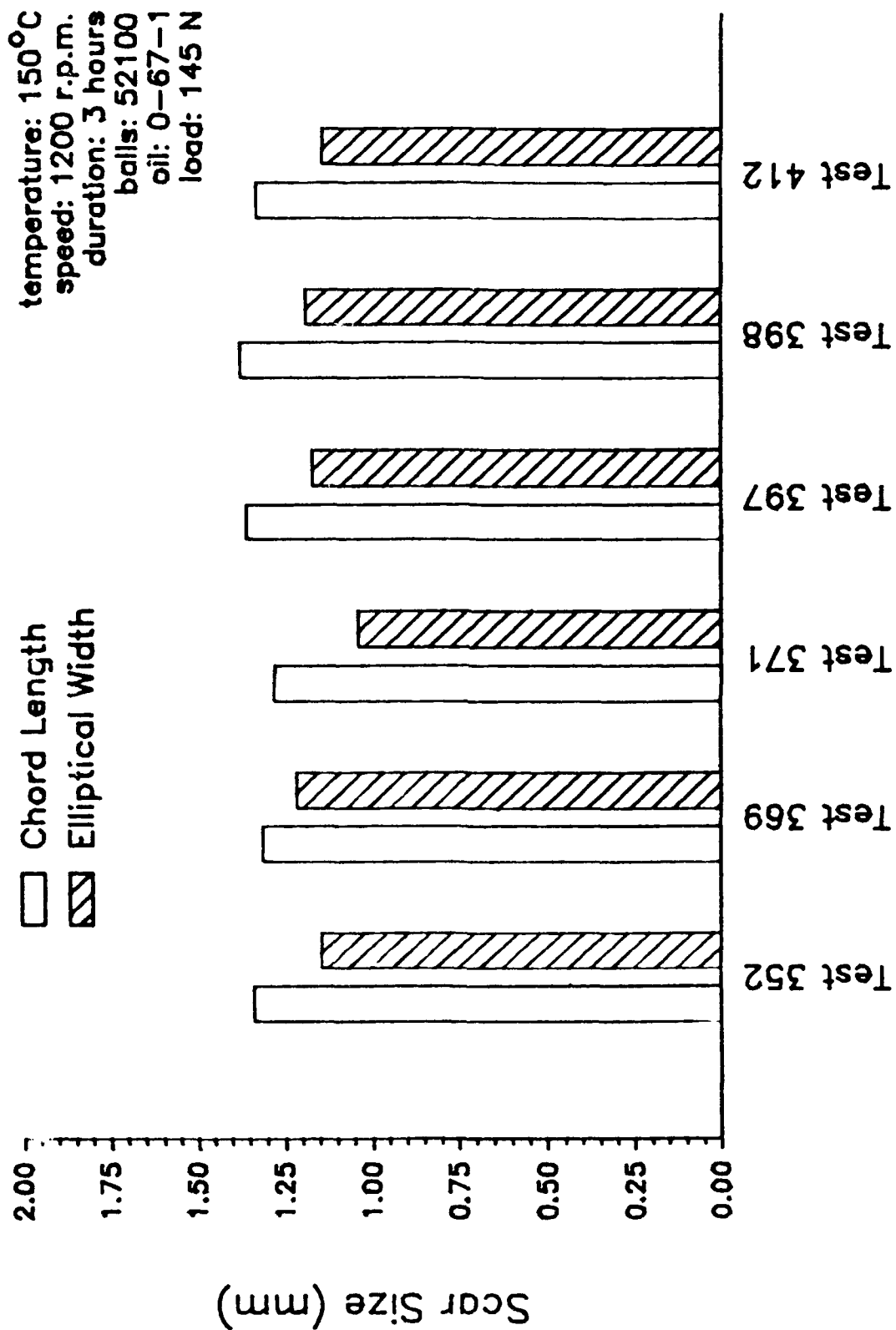


Figure 160. Variation of Scar Sizes from Identical Tests of O-67-1 on 52100 Steel Balls at 150°C

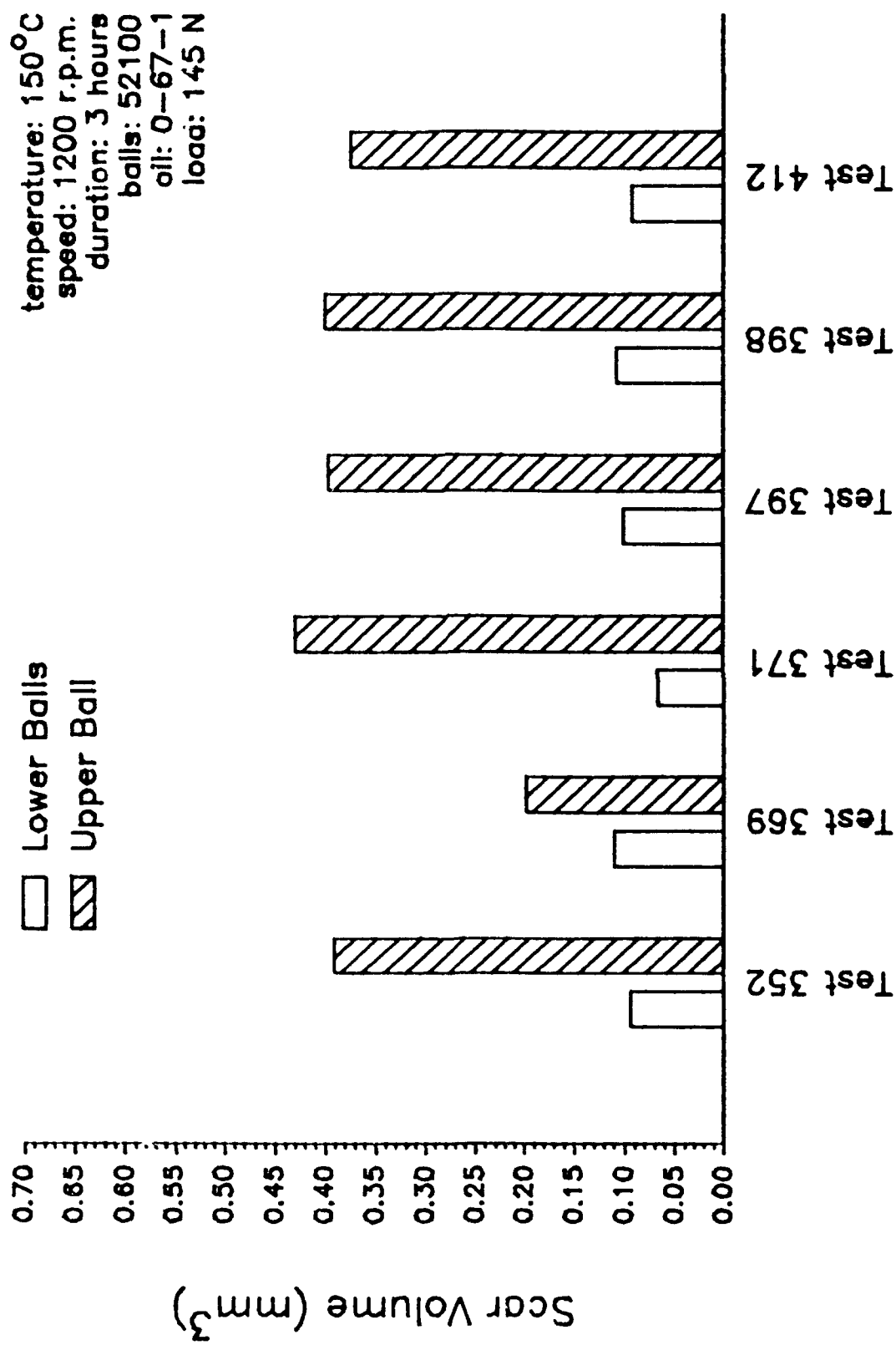


Figure 161. Variation of Scar Volumes from Identical Tests of 0-67-1 on 52100 Steel Balls at 150°C

recorded temperature. To more accurately predict the conditions within the sliding junctions, a test was performed with a specimen ball containing a hole to allow a 0.01-in (outer diameter) thermocouple to be inserted. With the tip of the thermocouple located just below a contact point, the temperature at the contact zone can be more accurately monitored.

A test of the O-67-1 lubricant at room temperature was made to monitor the heating provided by only the friction at the sliding junctions. Figure 162 compares the bulk temperature to the specimen temperature over a period of 20 hours. Although there is a slight variation in the specimen temperature throughout the entire test, the difference between bulk and specimen temperatures stays consistent for the whole test, including the run-in period. The temperature gradient, calculated by subtracting the average bulk temperature from the average specimen temperature, is 18°C.

Although the difficulty in alignment and delicacy of the thermocouple prohibits mass testing with the specimen temperature measured, the temperature gradient observed in Figure 162 indicates that bulk temperature is a conservative estimate of the conditions at the surface contacts, and although this preliminary test was performed without outside heating, the value of the temperature gradient should be at least as large at higher bulk temperatures.

h. Summary

The tribological behavior of the high temperature candidate fluids is quite unlike that of more conventional lubricants. For an ester-based lubricant, the three characteristic wear regions of four-ball testing were observed for the 20-hour test of Figure 118. Twenty-hour tests of candidate fluids were primarily under 145-N loads, but in contrast to the wear curve of an ester under a much greater load (Figure 118), the log-log plots of upper

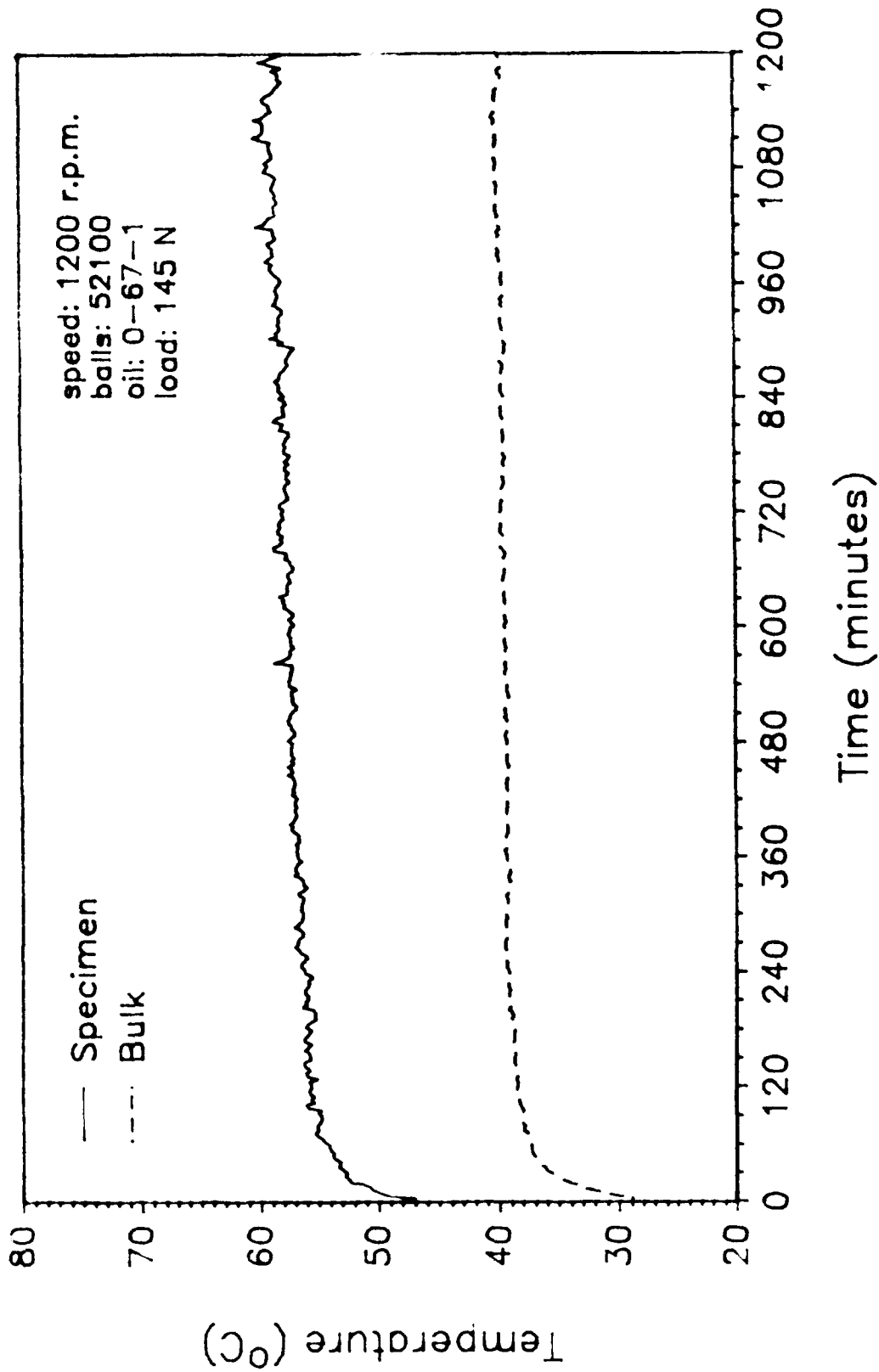


Figure 162. Temperature Variation Within the Four-Ball Test Cup

ball position versus test time for the candidate fluids did not have a leveling region where wear had ceased. The absence of a leveling region of was typical for wear curves of 20-hour tests of the PPE 0-67-1 even with loads as low as 33 N at temperatures of 75, 150, and 250°C. Of the experimental fluids, only TEL-9071 and TEL-90001 were tested as long as 20 hours. As with 0-67-1, neither test of the two oils showed a leveling of wear. A single test of TEL-9071, however, was repeated with only a 75-N load, and its wear curve did exhibit all three of the characteristic wear regions.

5. ANALYSIS OF FRICTION POLYMER FROM FOUR-BALL TESTING OF POLYPHENYL ETHER

a. Background

The production of polymeric material at metal interfaces in the presence of organic compounds (often called friction polymer) is a frequently observed phenomenon first reported in 1958 by Hermance and Egan³¹ on precious metal contacts in the presence of contaminant organic vapors. Since then, friction polymer has been observed to form with a variety of lubricants³²⁻³⁸ which has led to the formulation of liquid lubricants^{39,40} as well as the design of lubrication systems^{41,42} that facilitate the formation of such materials in metal contact zone in order to reduce friction and wear.

The formation of a friction polymer in polyphenyl ethers during wear testing has been previously noted. Spar and Damasco⁴³ reported its formation during pump testing as well as four-ball testing, which consisted of 2 to 5 microns, irregularly shaped black debris that was a mixture of metal and carbonaceous compounds. Loomis⁴⁴ reported the formation of wear debris that was judged to be half carbonaceous and half iron oxide from a rider on rotating disk friction and wear device. Jones²⁸ also reported the formation

of friction polymer during ball on disk testing of 5P4E.

Reported here is the characterization of friction polymer (FP) from four-ball testing of O-67-1 (5P4E with antioxidant) produced under a variety of test conditions and materials. This characterization consists of qualitative and quantitative analysis of the organic and metallic content of the friction polymer and comparison to debris isolated from engine tested PPEs.

b. Quantitation of FP in Four-Ball Testing of O-67-1

A gravimetric method for determining the amount of FP in four-ball tested O-67-1 was developed which takes advantage of the apparent insolubility of FP in any organic solvent. One gram of the tested lubricant is dissolved in 10 mL of trichloroethylene and is filtered through a previously weighed 0.22 micron filter (13 mm, Durapore). Although O-67-1 and its oxidation products are readily soluble in this solvent, it should be noted that extensive oxidation of the lubricant, as can happen at high test temperatures, will yield some insolubles that are not FP, as was shown previously.² This method was used to quantitate FP from four-ball tests of O-67-1 under various conditions. The data (Table 99) show that the highest loads (145 N) at 150 and 250°C produce the most FP. Also, despite the greater hardness of M50 bearings, considerably more FP (and wear) was observed for these bearings relative to 52100 or ceramic bearings. Analysis of a series of test lubricants run at 150°C and 145N load with 52100 bearings indicated that the rate of FP is approximately linear up to 30 hours of testing (Figure 163). This mirrors the more or less linear increase in wear volume that is observed.

c. Iron Content in FP from O-67-1

Ferrographic analysis of four-ball tested O-67-1 revealed, in

TABLE 99

FRICTION POLYMER CONTENT IN VARIOUS FOUR-BALL
TESTED O-67-1 LUBRICANTS

Four-Ball Test No.	Bearing	Test Temp, °C	Load (N)	Time, hrs	% FP in Lubricant
402	52100	75	7.50	20	0.010
400	52100	150	7.50	3	0.029
403	52100	150	7.50	20	0.048
419	52100	150	7.50	20	0.034
388	52100	250	7.50	3	0.069
401	52100	315	7.50	3	0.100
379	52100	75	17.50	3	0.010
378	52100	150	17.50	3	0.039
364	52100	75	32.50	3	0.020
351	52100	75	32.50	20	0.126
372	52100	150	32.50	0.25	0.020
373	52100	150	32.50	0.75	0.038
362	52100	150	32.50	1	0.031
366	52100	150	32.50	1.50	0.069
363	52100	150	32.50	2	0.078
367	52100	150	32.50	2.50	0.107
352	52100	150	32.50	3	0.118
369	52100	150	32.50	3	0.069
371	52100	150	32.50	3	0.115
393	52100	150	32.50	5	0.198
394	52100	150	32.50	7	0.304
389	52100	150	32.50	10	0.470
395	52100	150	32.50	12	0.540
392	52100	150	32.50	15	0.783
396	52100	150	32.50	17	0.733
353	52100	150	32.50	20	0.880
391	52100	150	32.50	30	1.260
370	52100	150	32.50	68.25	2.630
355	52100	250	32.50	3	0.127
381	52100	250	32.50	20	0.850
359	52100	315	32.50	3	0.130
365	52100	315	32.50	20	0.522
471	M50	75	32.50	3	0.059
468	M50	150	32.50	3	0.492
475	M50	150	32.50	3	0.436
467	M50	250	32.50	3	0.534
470	M50	315	32.50	3	0.447
410	Si ₃ N ₄	150	32.50	3	0.068
476	Si ₃ N ₄	150	32.50	3	0.079
477	Brass	150	32.50	3	0.067
479	Brass	150	32.50	3	0.069

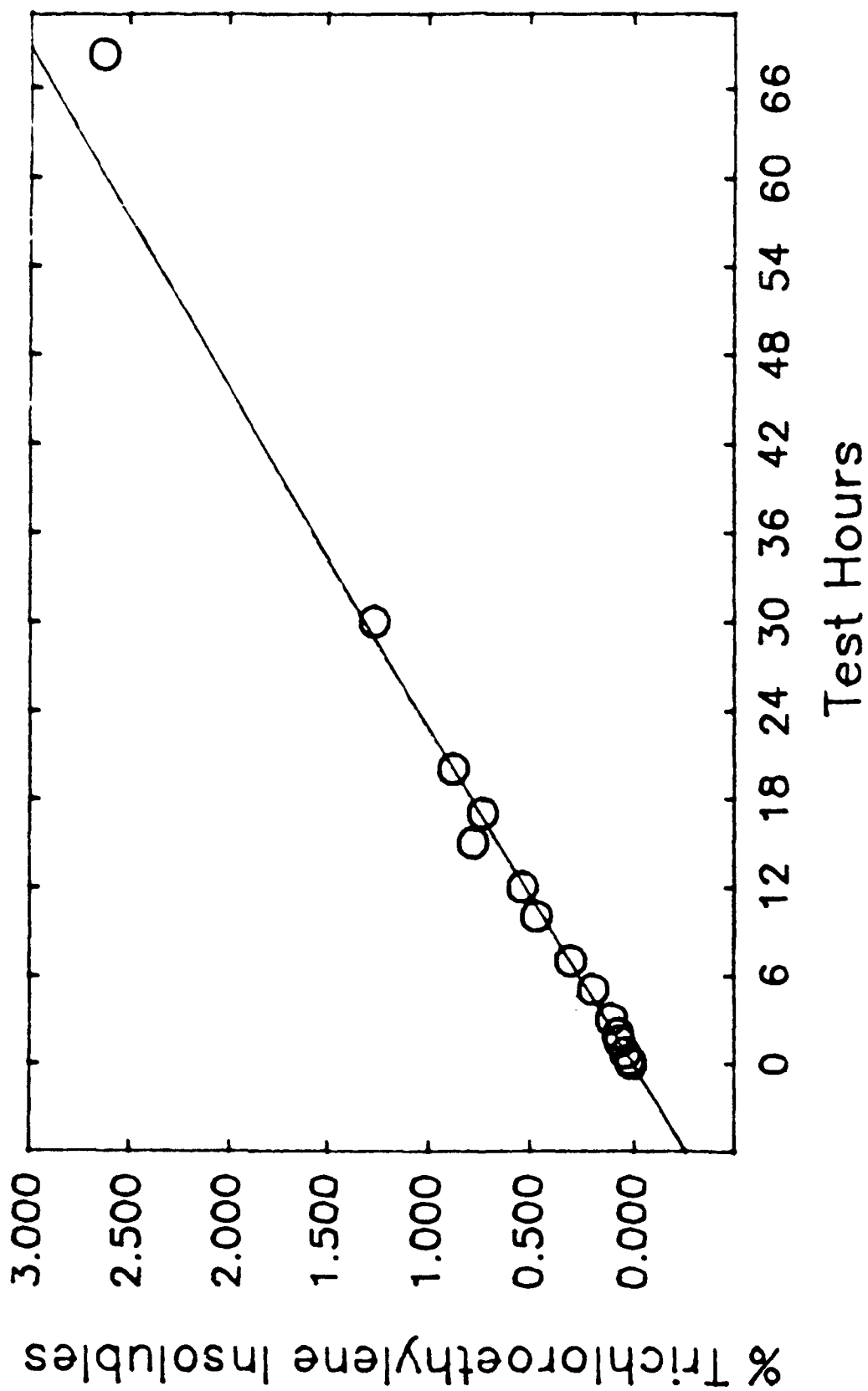


Figure 163. Percent Friction Polymer, as Trichloroethylene Insolubles, from Four-Ball Testing of O-67-1 at 150°C, 145 N Load, 52100 Bearings

general, a lack of normal wear particles. Since the FP from PPEs were reported to contain iron, the following quantitative and qualitative analyses for iron were made on various FP samples

(1) Quantitative Analysis of Iron in FP

The total iron in FP from four-ball tested O-67-1, isolated by filtration from trichloroethylene solutions of the lubricant, was determined on various test lubricants by acid dissolution method - atomic spectroscopy (ADM-AA).⁴⁵ The results (Table 100) show a fairly constant level of iron in FP produced from a wide variety of test conditions with the 52100 bearings ($6.0 \pm 1\%$). In general, the percent iron decreases with increasing test temperature while the M50 bearing tests produce 3 to 4 times as much FP (and wear) as the equivalent 52100 bearing test. In general, the metal content is considerably less than that reported previously by other researchers (50%).^{43,44}

Because the ADM-AA procedure was developed for normal wear debris and not for metal or metallic species encased in an organic matrix, this procedure may not be accurate for total iron analysis in FP. In order to check the accuracy of the ADM-AA procedure, the total iron in three FP samples was analyzed by ashing the sample (thus removing the organic matrix) in a 550°C furnace, solubilizing the residue in 1.0 M sulfuric acid and then analyzing by AA. The results (Table 101) show that both techniques yielded comparable numbers, indicating that ADM-AA can give accurate total iron on FP from O-67-1.

(2) Qualitative Analysis of Iron in FP

Based on the ferrographic analysis of FP produced during wear testing of PPE in various atmospheres, Jones²⁸ concluded that a corrosive wear mechanism, as described by Goldblatt for wear testing using

TABLE 100

TOTAL IRON IN FRICTION POLYMER FROM VARIOUS FOUR-BALL TESTED
O-67-1 LUBRICANTS

Four-Ball Test No.	Test Temp., °C	Load(N)	Time (H)	Bearing	% Iron ¹
364	75	145	3	52100	6.5
400	150	33.5	3	52100	6.3
378	150	78	3	52100	6.2
352	150	145	3	52100	5.9
357	150	145	20	52100	6.8
391	150	145	30	52100	6.6
355	250	145	3	52100	5.9
381	250	145	20	52100	4.0
365	315	145	20	52100	2.6
468	150	145	3	M50	21.7
467	250	145	3	M50	12.9
470	315	145	3	M50	7.4

¹Determined on isolated friction polymer by ADM-AA

TABLE 101

TOTAL IRON IN FP BY ADM-AA AND ASHING-AA

Four-Ball Test No.	% Iron ¹	
	ADM-AA	Ashing-AA
468	21.7	19.4
467	12.9	12.3
470	7.4	7.5

¹As determined on isolated friction polymer from the indicated four-ball test

TABLE 102

QUALITATIVE IRON ANALYSIS OF FP USING EXTRACTION TECHNIQUES

Four-Ball Test No.	Test Temp., °C	Bearing	Relative % Iron		
			Metal	Oxide	Organo-Iron
357	150	52100	56	10	33
381	250	52100	0	80	20
365	315	52100	0	91	9
468	150	M50	0	99.5	0.5
467	250	M50	20	80	0
470	315	M50	55	45	0

methylnaphthylene,³⁵ was operative. In this mechanism, wear produces fresh metal surfaces that result in the discharge of exo-electrons which cause the formation of molecular anionic species in the lubricating film. These species go on to react with the metal as well as the lubricant to form polymers. If such a mechanism was occurring with the polyphenyl ethers, then organo-iron species should exist in the FP. Extraction methods have been developed for differentiating between iron metal, iron oxide and organo-iron in wear debris.⁴⁶ These techniques, which involve extraction of the wear debris with various solvents and analysis of the extract by AA, were used to analyze various FP from four-ball testing of O-67-1. The results of these analyses (Table 102) show tremendous variations in the proportion of various iron species in the FP as temperature or bearing material is varied. Organo-iron content is indicated in the 52100 FP but is virtually absent from the M50 FP. The oxide content increases with increasing temperature for 52100 FP while the reverse is true for the M50 FP. It is conceivable that the organo-iron could decompose at the higher test temperatures to iron oxide, but the presence of iron metal in some of the FP samples, which would be the result of normal wear, is not supported by Ferrographic analysis. An SEM iron X-ray map of all the FP in Table 102 indicated a very fine dispersion of iron in the carbonaceous matrix, as was found by Jones.²⁸ X-ray diffraction of some of the FP revealed no crystalline components greater than 1000 Å, which is the resolution limit of the instrument. These data indicate that the iron in the FP is well dispersed and either amorphous or micro crystalline.

It is rather difficult to determine the nature of the wear process that occurs for O-67-1 during four-ball testing based on the extraction/AA data. The possibility exists that the extraction techniques

used to characterize the iron, which were developed for wear debris from esters, are not accurate for FP analysis. Therefore, analyses were made on the FP samples using ^{57}Fe Mossbauer spectroscopy.

^{57}Fe Mossbauer (nuclear gamma ray resonance) spectroscopy is capable of determining valence states, electronic configuration and, often, the chemical composition of the iron compound. This analysis technique is especially useful for amorphous samples. The room temperature spectra from analysis of five FP samples (Figures 164 and 165) reveal that all of the samples are very similar, consisting of high spin iron (III), which is indicated by similar isomer shifts (0.36 ± 0.2 mm/sec). The spectra of three of the samples could be deconvoluted into three separate doublets with similar isomer shifts but slightly different quadrupole splitting. The Mossbauer data from the five samples are displayed in Table 103. These data indicate that, unlike the extraction data, virtually all of the iron in the FP under all test conditions exists as a reaction product (Fe III). Since there is no evidence of iron oxide in the spectra, this must be the result of chemical corrosion of the type indicated by Goldblatt³⁵ and Jores.²⁸

d. Analysis of the Organic Fraction of FP

Very little has been reported on the carbonaceous portion of FP from wear testing of PPEs. It was assumed that it was polymeric^{28,43} and that it formed catalytically and/or thermally in the metal-metal contact zones. The FP from various four-ball wear tests of O-67-1 were analyzed by elemental analysis and FTIR and compared to previously analyzed polymeric compounds from oxidation/corrosion tests of O-67-1.

(1) Elemental Analysis

Carbon and hydrogen analyses were made on FP isolated from various four-ball tests of O-67-1 using M50 or 52100 bearings. The results

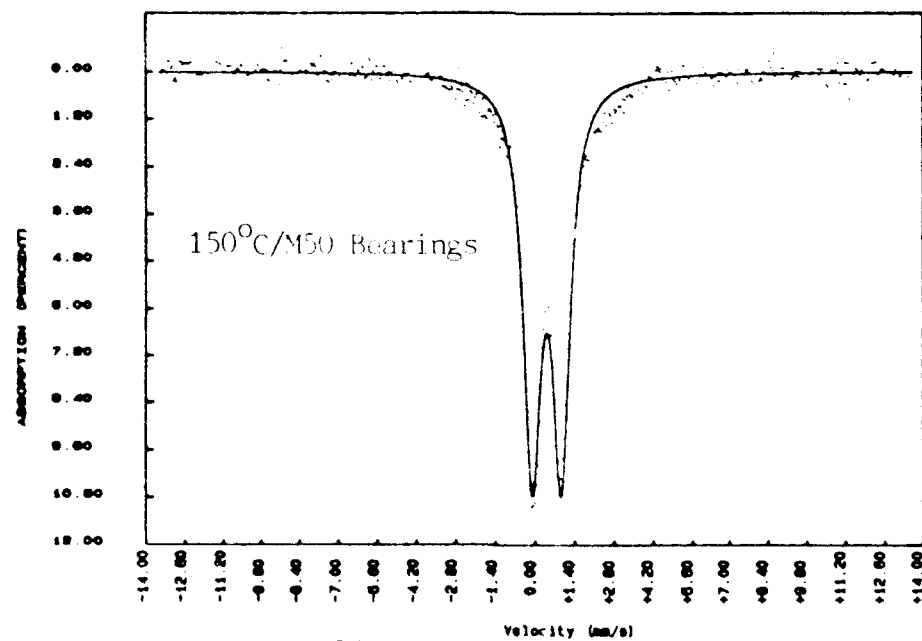
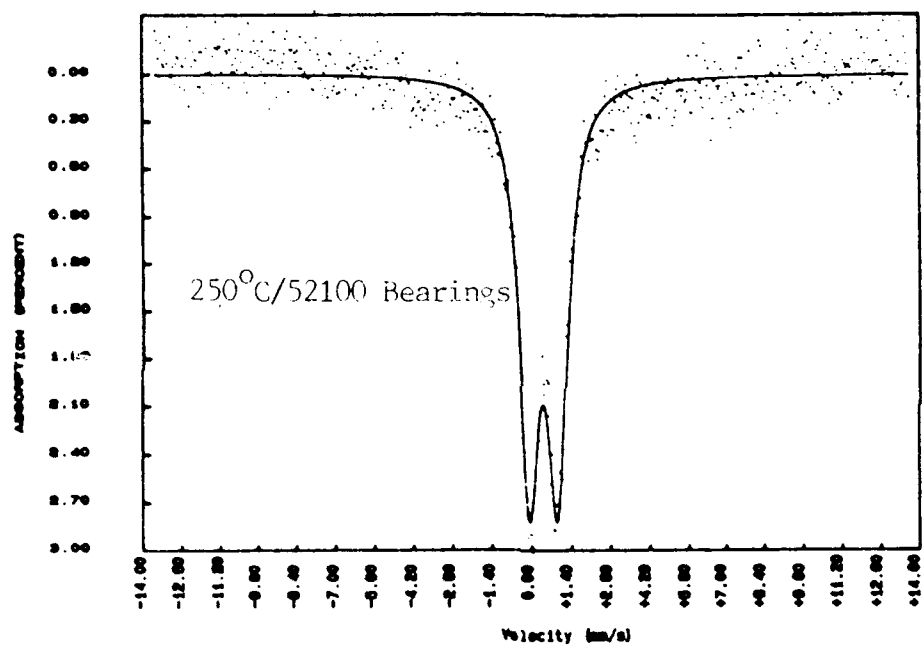
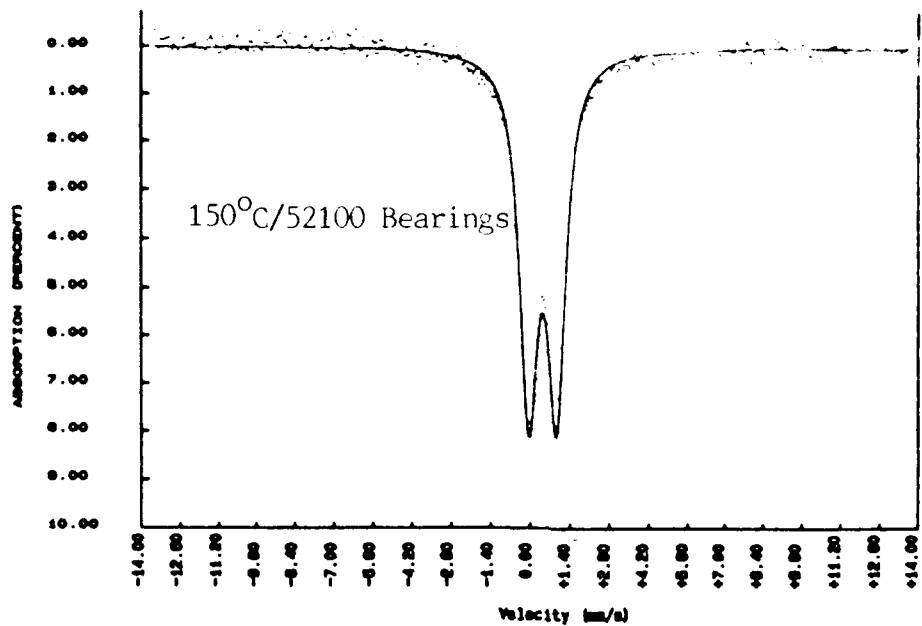


Figure 164. ⁵⁷Mo Mössbauer spectra of Friction Polymer from Four-Ball Testing of 0-67-1 at 145 N Load

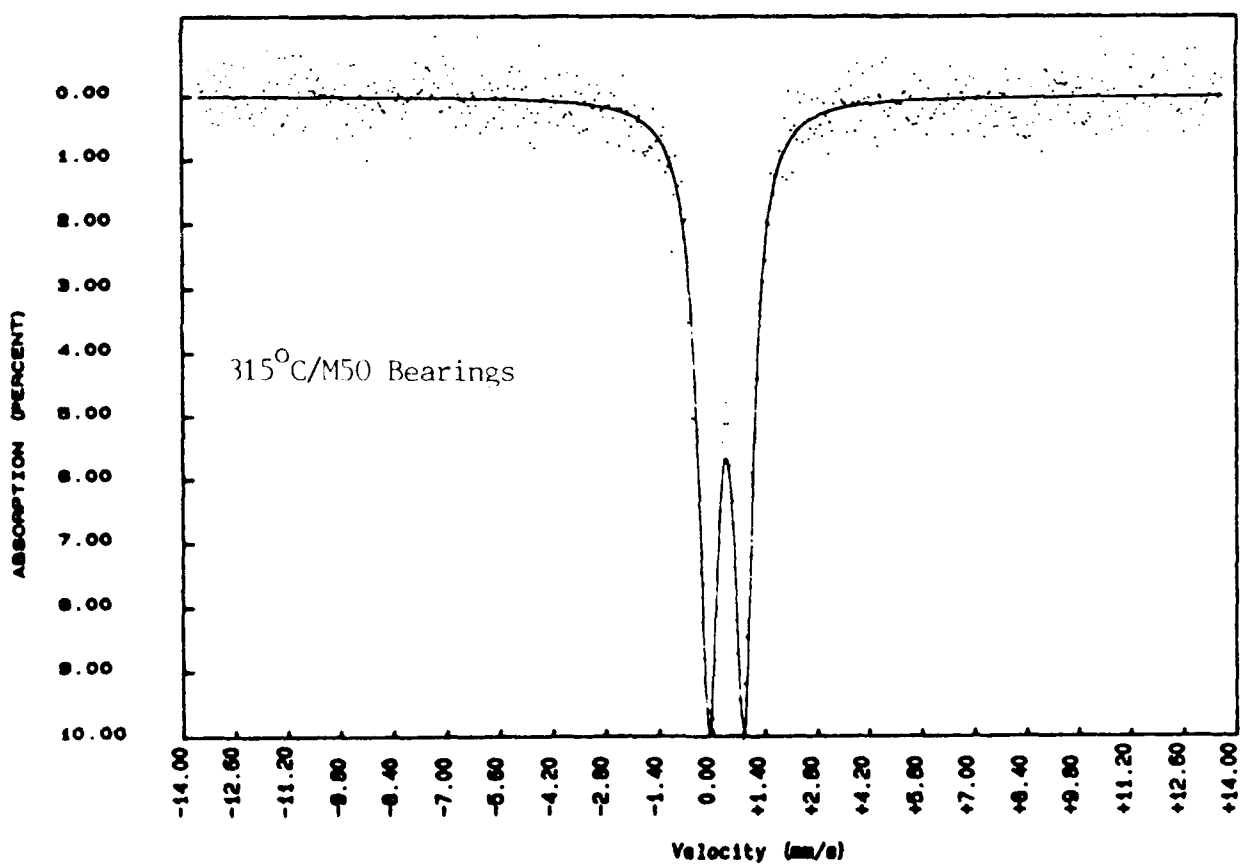
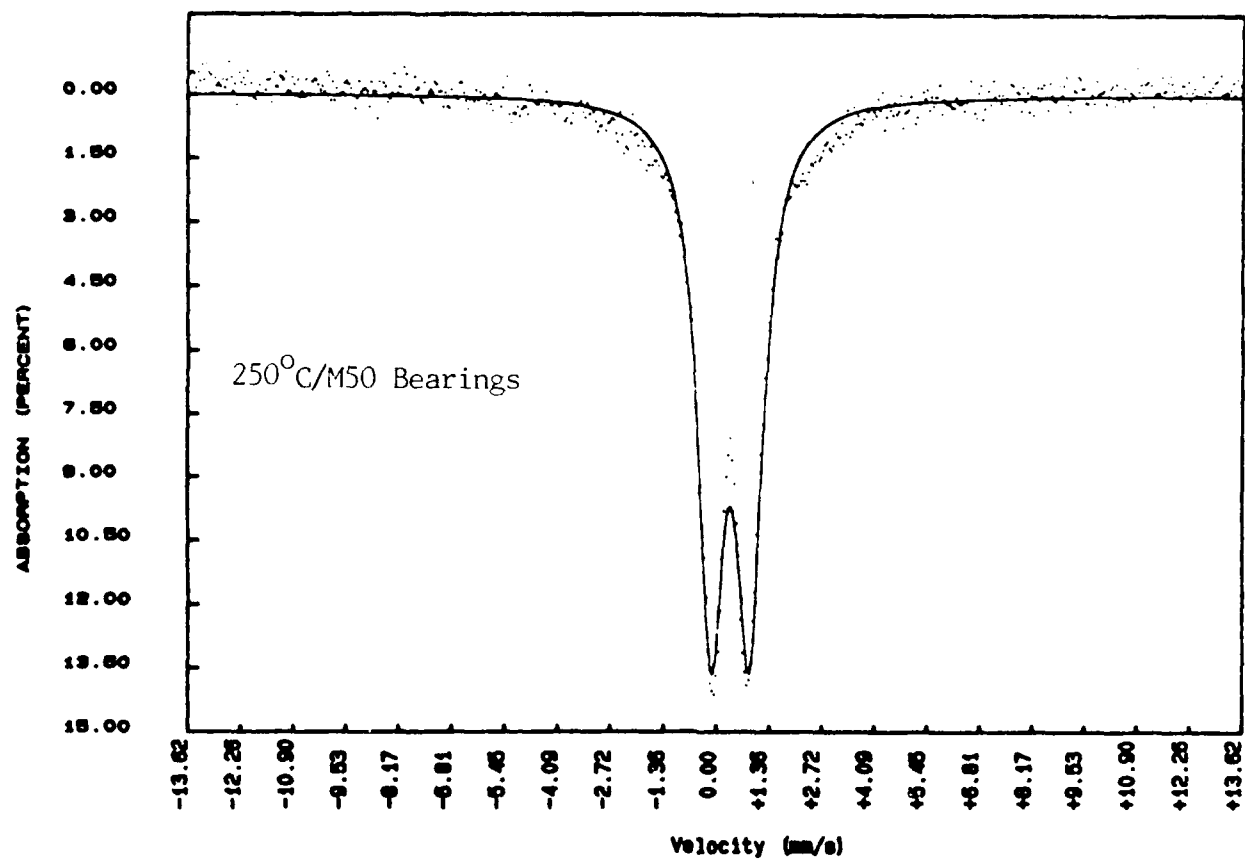


Figure 165. ^{57}Fe Mossbauer Spectra of Friction Polymer from Four-Ball Testing of 0-67-1 at 145 N Load

TABLE 103

⁵⁷FE MOSSBAUER PARAMETERS FROM FIVE FP SAMPLES

Test* Temp., °C	Bearing	Isomer Shift(s)(mm/sec)	Quadrupole Splitting (mm/sec)
150	52100	0.39 0.38 0.39	0.61 1.05
250	52100	0.37	0.94
150	M50	0.36 0.37 0.39	0.67 1.09 1.53
250	M50	0.36	1.00
315	M50	0.35 0.34 0.34	1.60 1.05 0.62

*The FP samples were collected from multiple tests run under the same test conditions in order to collect enough sample.

(Table 104) show that the bearing material does not have a great influence on the C/H ratio, but that as test temperature is increased, the C/H ratio increases to approximately that of oxidized polymer (HMW-2). Oxygen analysis of FP from four-ball test number 353 (150°C) indicates considerable oxygen uptake.

(2) FTIR Analysis

The FTIR spectra of the FP (Figures 166-168) show considerable differences as a function of temperature. All deposits show a carbonyl absorption that shifts to higher wavenumbers as the test temperature is increased. All deposits also show a broad hydroxyl absorption at about 3400 cm^{-1} but the 52100 FP samples show a decrease in the intensity of this absorption with increasing test temperature while the M50 FP samples are unaffected. Also, the M50 FP samples display a broad absorption at about 600 cm^{-1} that may be related to the higher iron content in these samples. Finally, the 150°C FP samples from both bearings display a broad absorption at about 1400 cm^{-1} which may be due to a carboxylate group. Other absorptions in all of the spectra are essentially identical to that of the fresh lubricant.

e. Spectrometric Analysis of wear deposits

(1) Introduction

The iron containing wear debris produced by polyphenyl ether fluids is mainly organic in content, and consequently, the ferrographic analysis of the wear debris is limited. One factor limiting the ferrographic analyses of the wear debris is that the optical measurements cannot distinguish organic polymers from iron debris particulates. Therefore, a detection technique based on X-ray fluorescence was used to study a representative ferrogram prepared from an O-67-1 four-ball wear test.

TABLE 104

ELEMENTAL ANALYSIS OF FP FROM VARIOUS FOUR-BALL TESTS

Four-Ball Test No.	Test Temp., °C	Bearing	% C	% H	% O	C/H Ratio
353	150	52100	59.0	4.21	23.9	14.0
381	250	52100	66.6	3.09	-	21.5
365	315	52100	69.9	3.06	-	22.8
468	150	M50	48.9	2.87	-	17.0
467	250	M50	47.0	2.18	-	21.6
481	315	M50	51.1	2.12	-	24.1
O-67-1 (Fresh) ¹	-	-	80.7	4.97	14.3	16.2
HMW-2 ²	320	-	77.0	3.64	15.2	21.2

¹Theoretical data²Acetonitrile insolubles from 168 h C&O test at 320°C (see Reference 2)

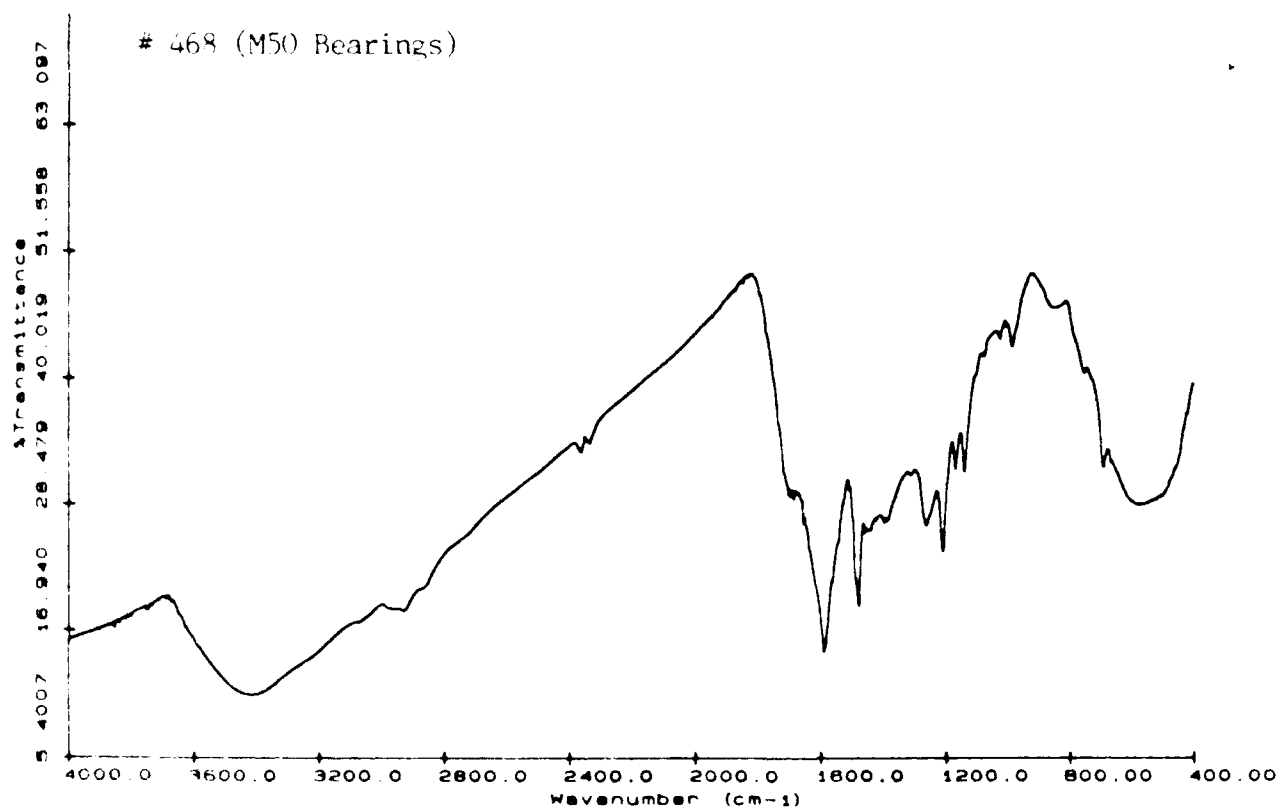
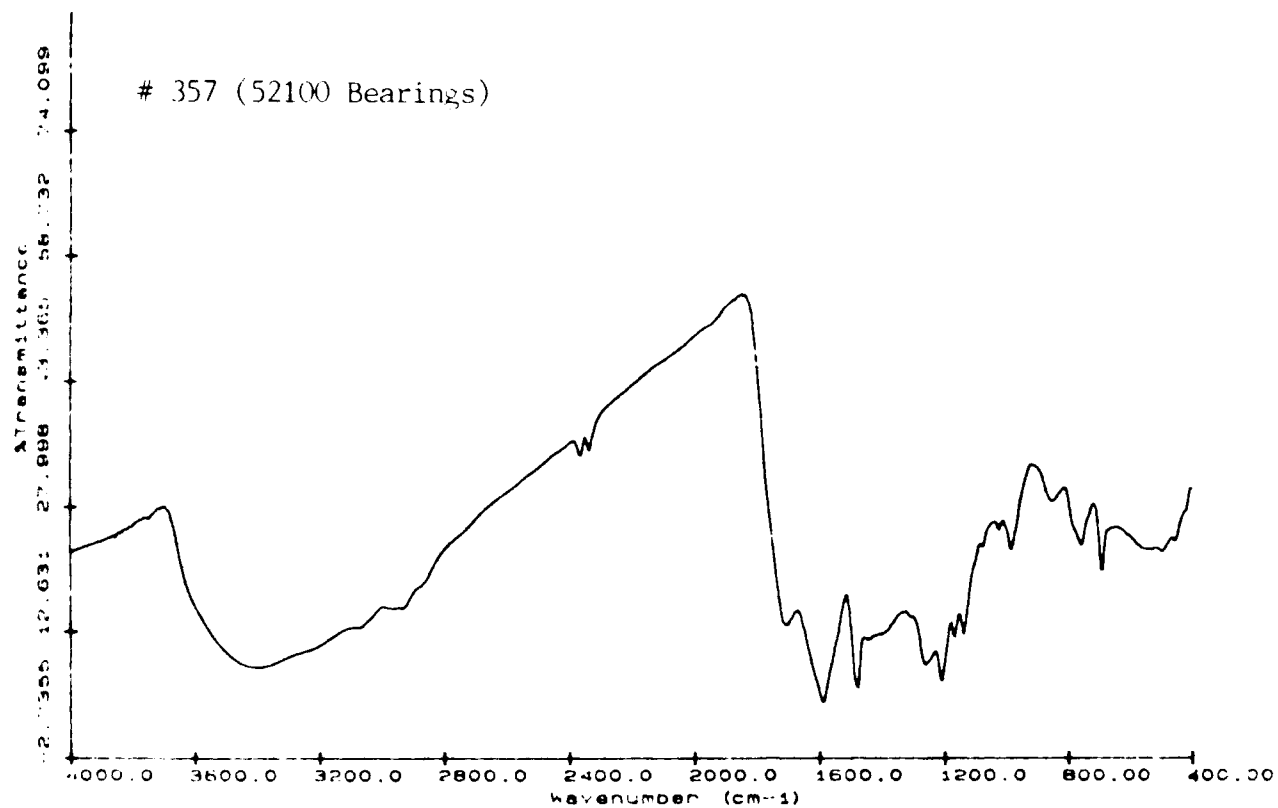


Figure 166. FTIR spectra of Friction Polymer from Four-Ball Testing of 0-67-1 at 150°C and 145 N Load

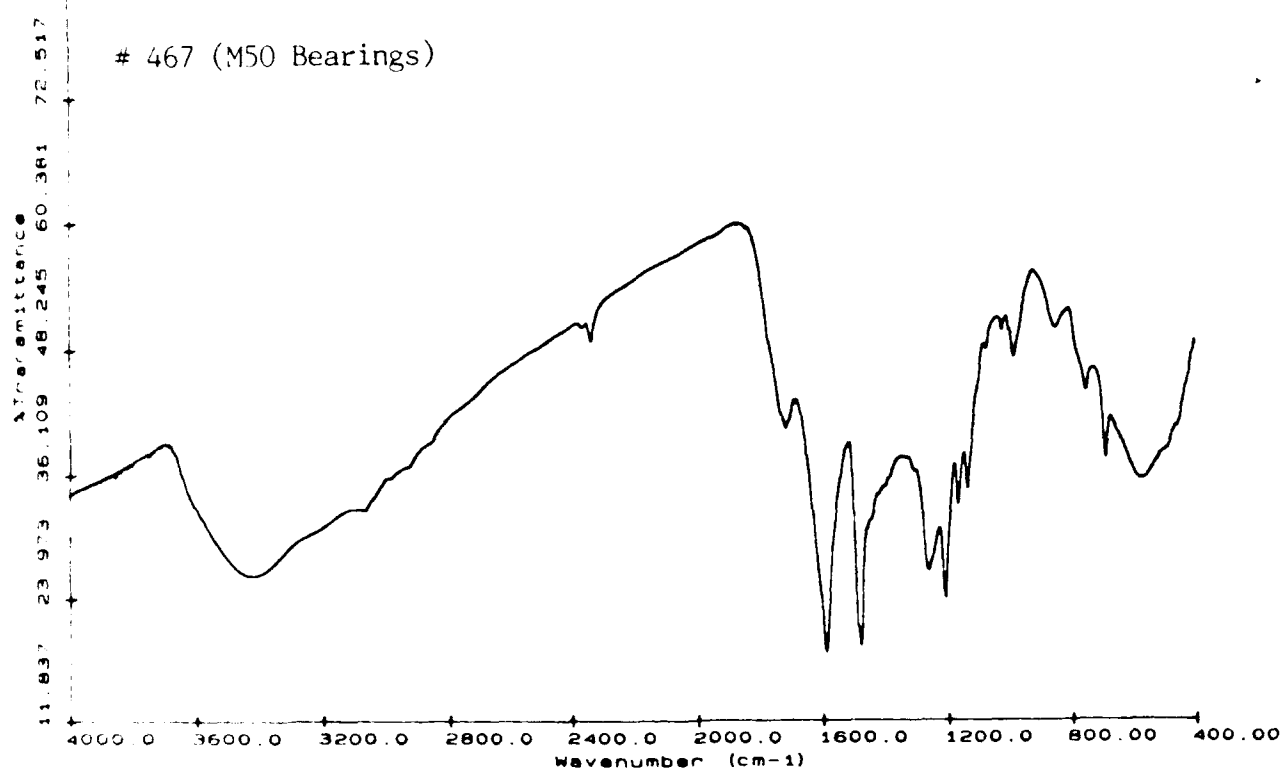
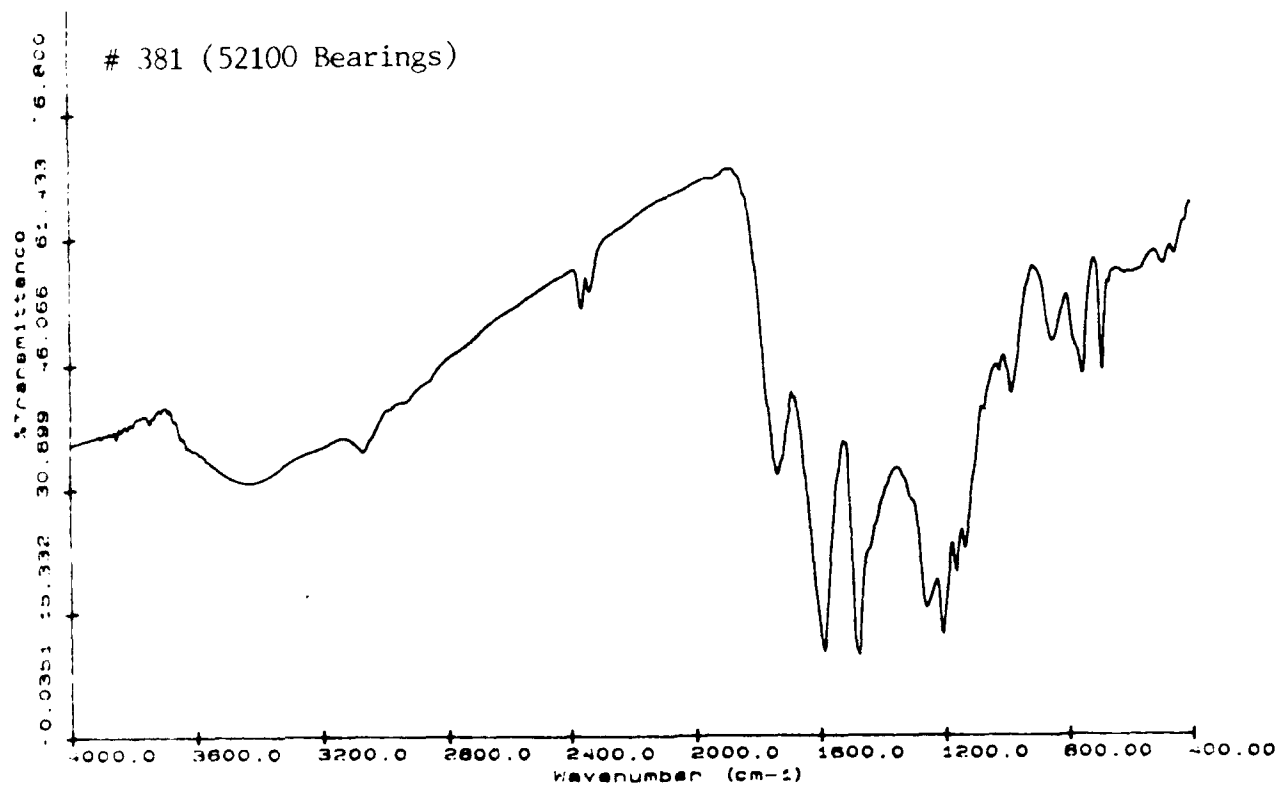


Figure 167. FTIR Spectra of Friction Polymer from Four-Ball Testing of 0-67-1 at 250°C and 145 N Load

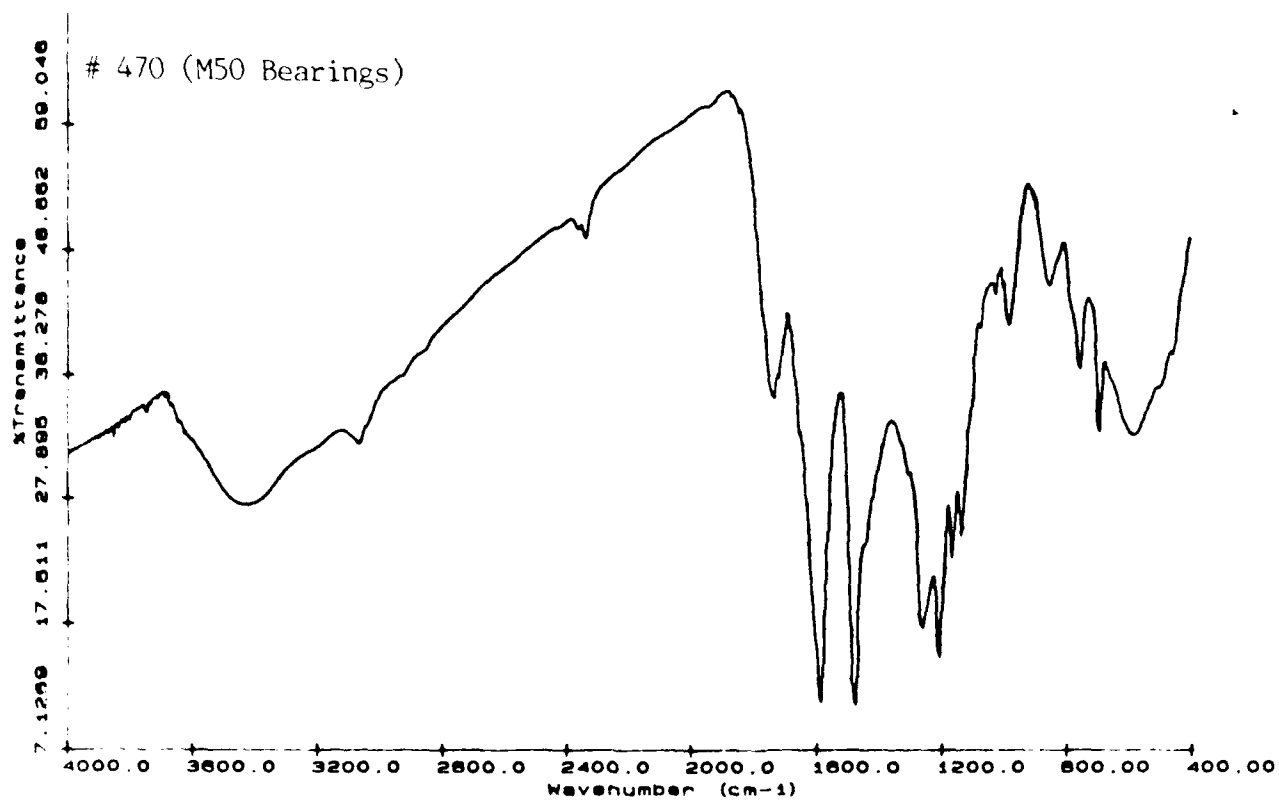
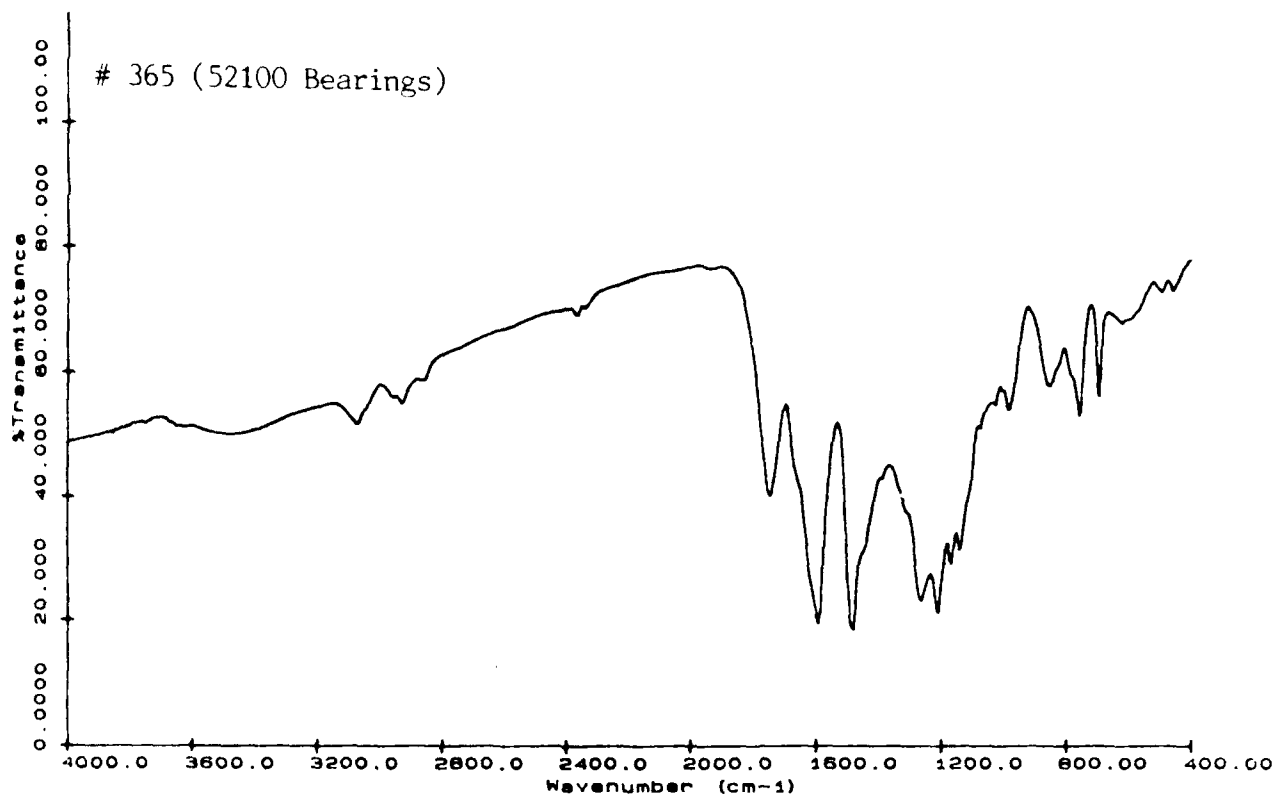


Figure 168. FTIR Spectra of Friction Polymer from Four-Ball Testing of 0-67-1 at 315°C and 145 N Load

The ferrogram was prepared on a graphite slide (instead of a glass slide to decrease background signal from the glass) using previously described techniques. A molybdenum X-ray source was used to excite 1 inch lengths of the entry and exit areas of the ferrographic slide and the emission spectrum of each area {counts versus energy (KeV)} was plotted as shown in Figure 169 using the X-ray fluorescence data acquisition system. The same areas of the slide were examined by SEM/EDS to examine the wear debris and to quantitate elemental compositions of the entry and exit areas as shown in Figure 170.

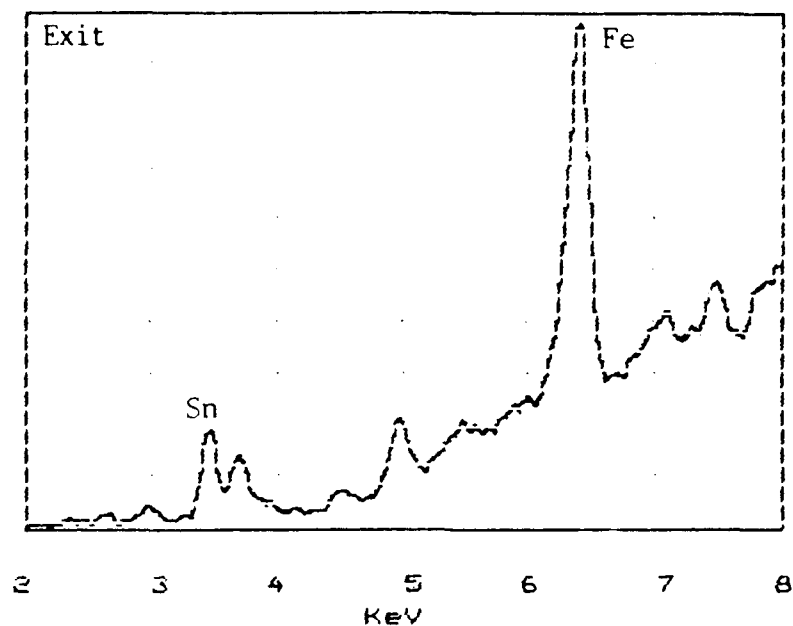
(2) X-Ray Fluorescence Analyses

The X-ray fluorescence spectra of the wear debris deposited on the entry and exit areas of the ferrographic slides in Figure 169 indicate that the wear debris contain tin (Sn) in addition to iron (Fe) and organic polymers (background from 4-8 KeV). The spectra in Figure 169 also show that the Fe/Sn and Fe/background ratios are higher for the entry area than for the exit area. The Sn/background ratio appears to be more constant than the Fe/background ratio but cannot be quantitated from Figure 169. The increase in background is an indication of decreasing Fe and Sn concentrations.

(3) SEM/EDS Analyses

The wear debris deposited in the entry and exit areas were examined by SEM/EDS and the elemental analyses of the wear debris are presented in Figure 170. As in previous examinations, the wear debris produced by polyphenyl ether fluids were polymeric in nature and were not suitable for photographing. The EDS elemental analyses in Figure 170 are in agreement with the X-ray fluorescence spectra in Figure 169, i.e., the Fe/Sn ratio is higher for the entry area than for the exit area. According to the EDS quantification system the Fe/Sn atomic ratio is exactly 2:1 in the entry

ENERGY DISPERSIVE SPECTROSCOPY
CFS= 908 BKGRND= 4



ENERGY DISPERSIVE SPECTROSCOPY
CFS= 908 BKGRND= 2

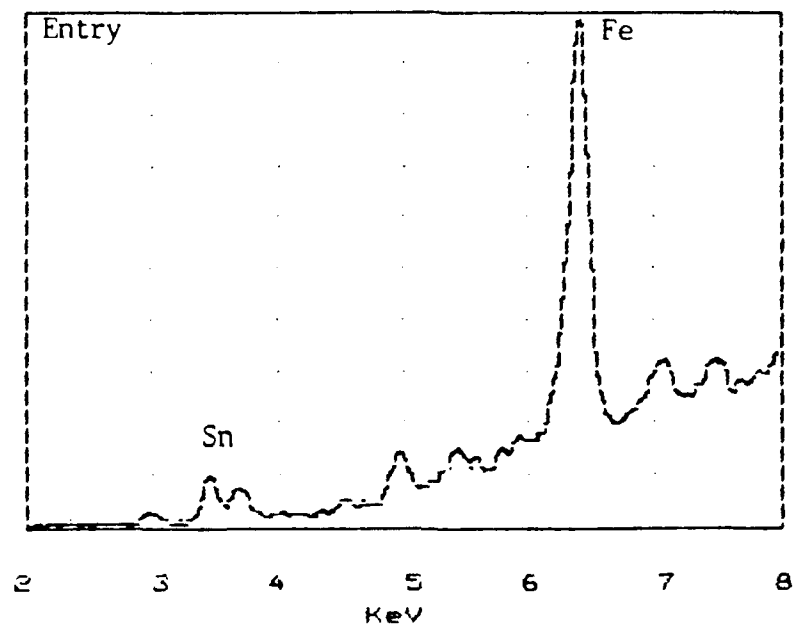


Figure 169. X-Ray Fluorescence Spectra of the
O-67-1 Wear Debris Collected on the
Entry and Exit Areas of a Ferrographic
Slide

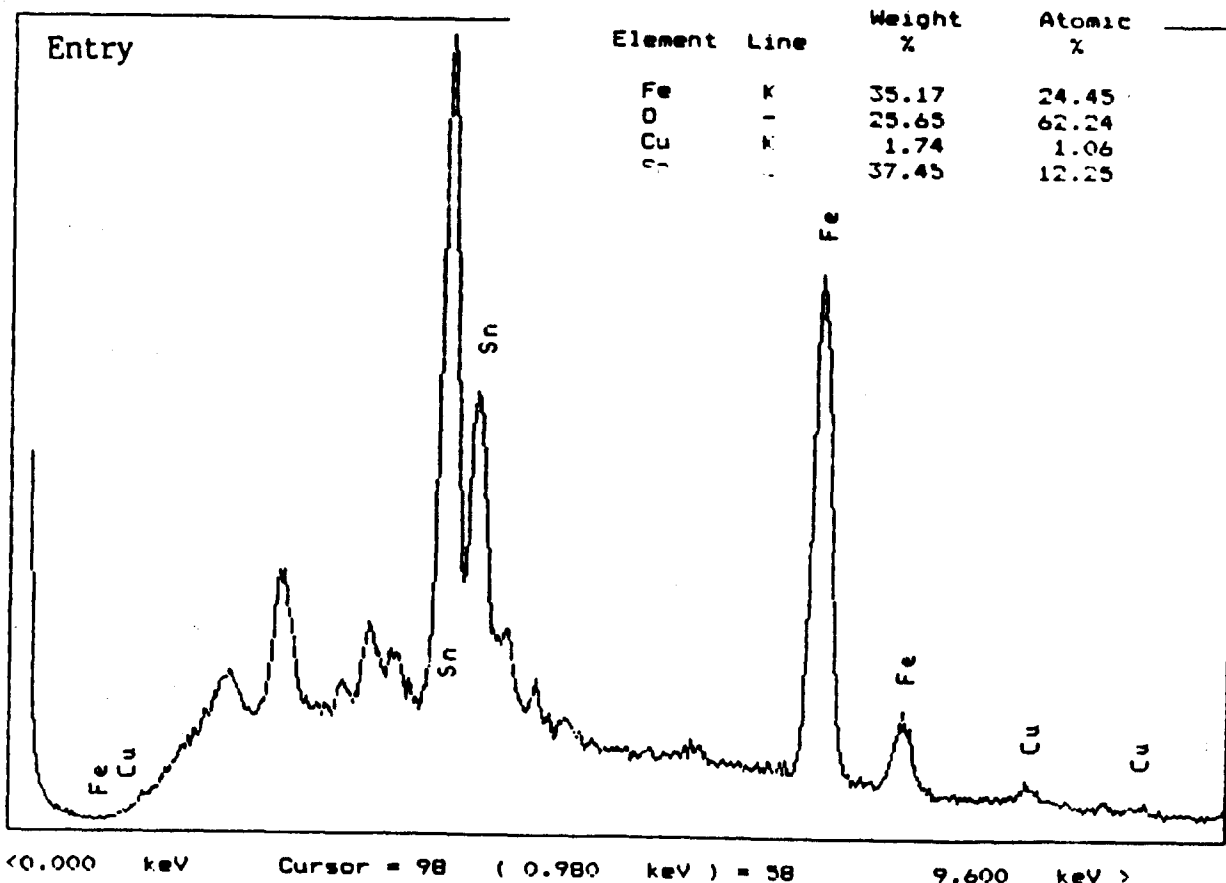
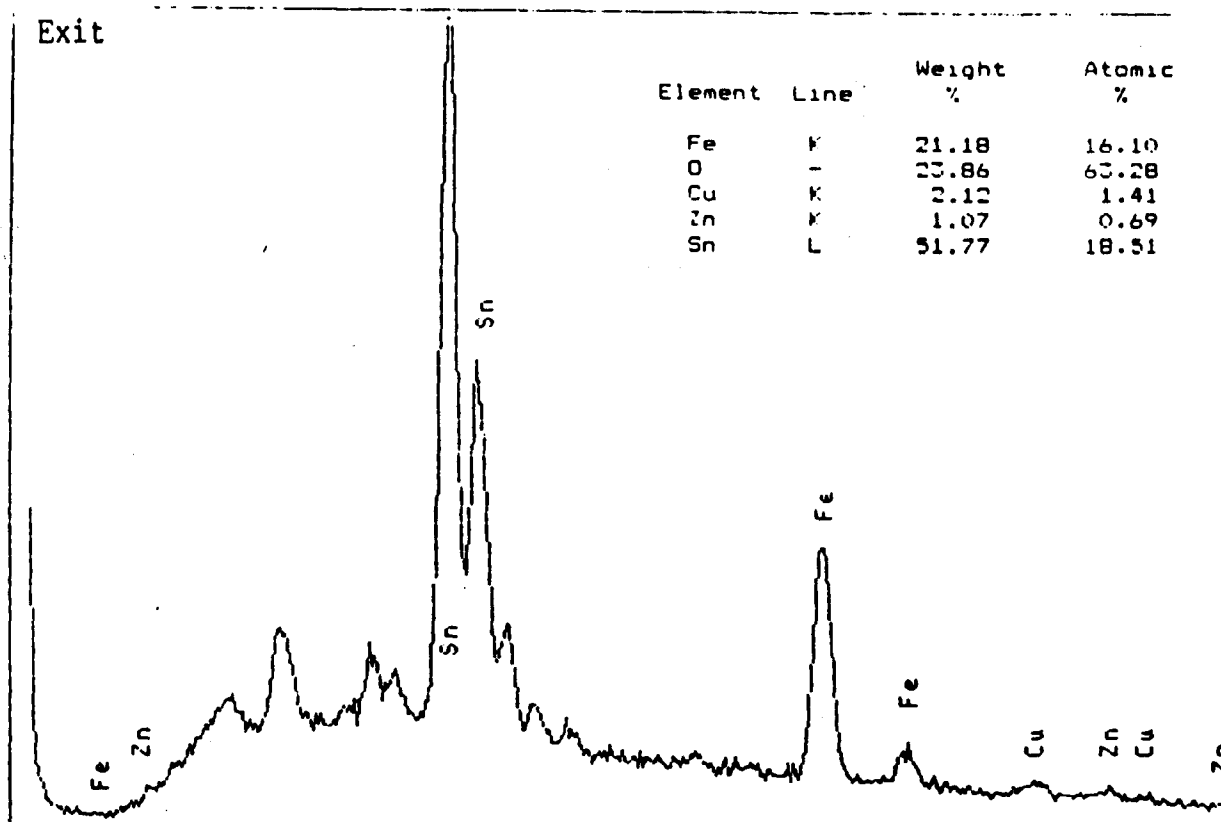


Figure 170. EDS Elemental Analyses of the O-67-1 Wear Debris Collected on the Entry and Exit Areas of a Ferrographic Slide

area and 1.1:1 in the exit area. Comparison of the spectra in Figure 170 shows that the Sn/polymer (background) ratio is higher for the entry area than for the exit area. Since the Fe/Sn ratio also is higher for the entry area than the exit area, the ratio of Fe/polymer ratio decreases at a faster rate than the Sn/polymer ratio when comparing the entry area to the exit area.

f. Analysis of Debris in Engine Tested PPEs

The analysis of FP in PPEs is of interest not only because of its involvement in the wear process but also because of its ability to lower the oxidative stability of the PPE lubricant. Oxidative destabilization of some engine tested PPE lubricants and improvement of some by 3 micron filtration have been reported (See Section II). The following analyses were made on various engine tested PPE lubes in order to determine if this destabilization is due to the presence of compounds similar to the friction polymer produced in sliding four-ball wear tests.

(1) Percent Filterable Insolubles

All engine tested PPE lubricants contained darkish particles that could be captured by filtration. The previously described method for determining percent FP in four-ball tested O-67-1 was used to determine the percent insolubles in various engine tested PPEs and the results are shown in Table 105. The percent insoluble material is fairly low, but was of a considerably different texture than the FP from four-ball testing. This filtrate was much finer, often plugging the filter, and could not be removed from the filter for further analysis. Therefore, further testing and analysis of these deposits were made by centrifugation of trichloroethylene solutions of the lubricant.

TABLE 105

% TRICHLOROETHYLENE INSOLUBLES IN VARIOUS ENGINE
STRESSED PPE LUBRICANTS

Lubricant	% Insolubles ¹
TEL-9028	0.070
TEL-9029	0.048
TEL-9030	0.029
TEL-9038	0.040
TEL-9039	0.088
TEL-9040	0.071
TEL-9069	0.016
TEL-9070-18	0.039
TEL-90025	0.040
TEL-90026	0.060

¹ Determined by filtration of 0.50 grams of lubricant through
a 0.22 micron filter

(2) FTIR Analysis

The FTIR spectra of isolated debris from the various engine tested PPE lubricants are all similar in that they contain the same absorptions as the basestock, plus a weak carbonyl absorption that varies from 1720 to 1740 cm^{-1} and a moderate to strong, broad hydroxyl absorption at 3450 cm^{-1} . It is unlikely that this material is the product of bulk oxidation as occurs in C&O tests since none of the engine stressed lubricants displayed any significant oxidative degradation. A typical spectrum of debris from an engine tested lubricant (Figure 171, TEL-9070-18) reveals its similarity to FP from four-ball testing (see Figure 168). But this spectrum is also similar to coke from a carbon seal from that same test engine stand (Figure 172). Since FTIR is not capable of precisely determining the source of the engine debris, all that can be noted is that this material is organic and is likely a product of the interaction of the lubricant with a hot surface.

(3) DSC Analysis

DSC was used to analyze debris isolated from two engine tested PPE, TEL-9030 and TEL-9040. These two lubricants were selected because they displayed the greatest improvement in C&O stability after 3 micron filtration. The thermograms (Figure 173) display some instability, as indicated by a broad exotherm that peaks at approximately the end of the temperature program (400°C), but do not display the same behavior as the FP from four-ball wear tests (Figure 28).

g. Conclusions

The production of insoluble particles during four-ball wear testing of polyphenyl ether is noted. This material, which is referred to as a friction polymer (FP) and had been previously reported to form in the

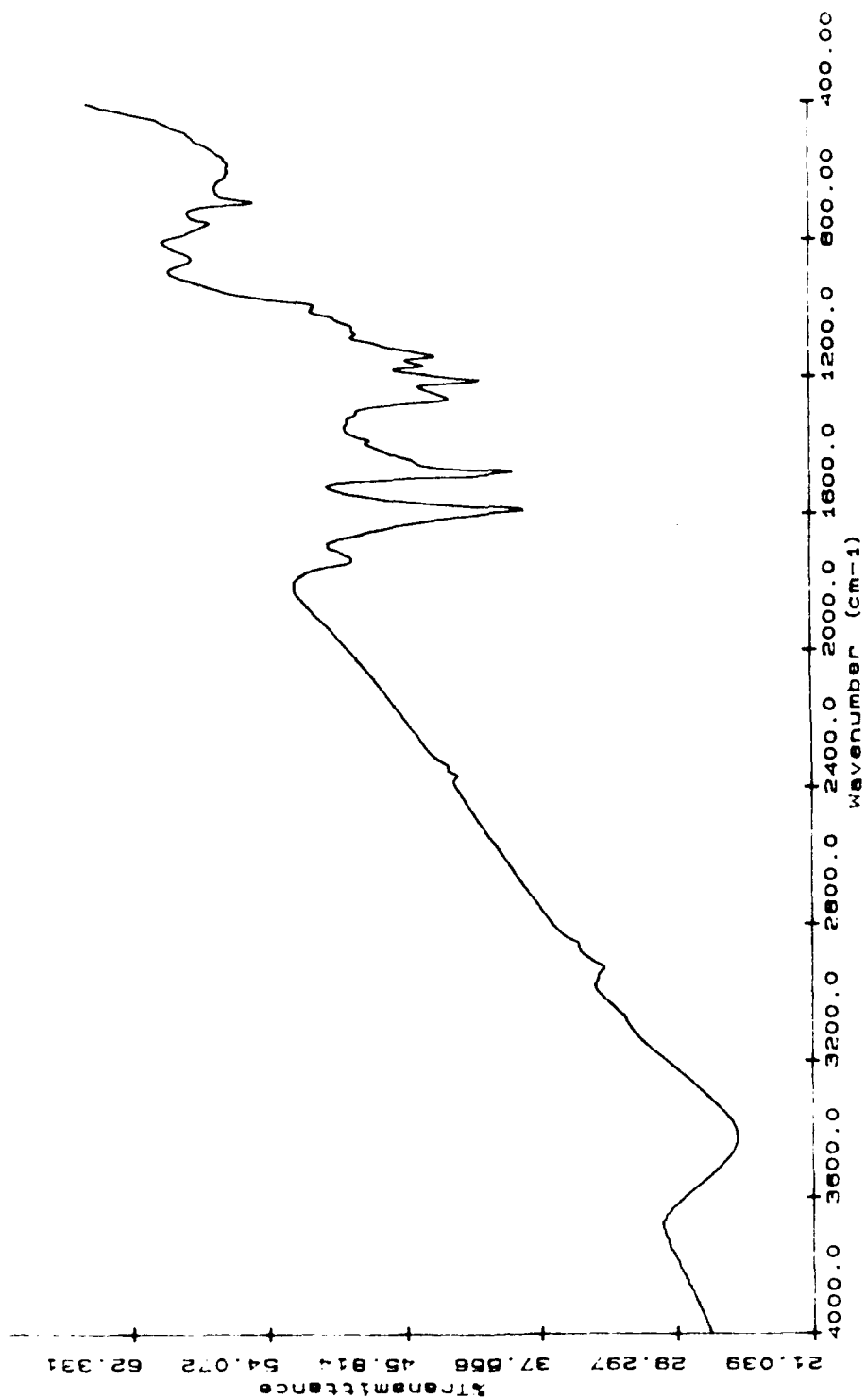


Figure 171. FTIR Spectrum of Isolated Debris from Engine Stressed PPE (TEL-9070-18)

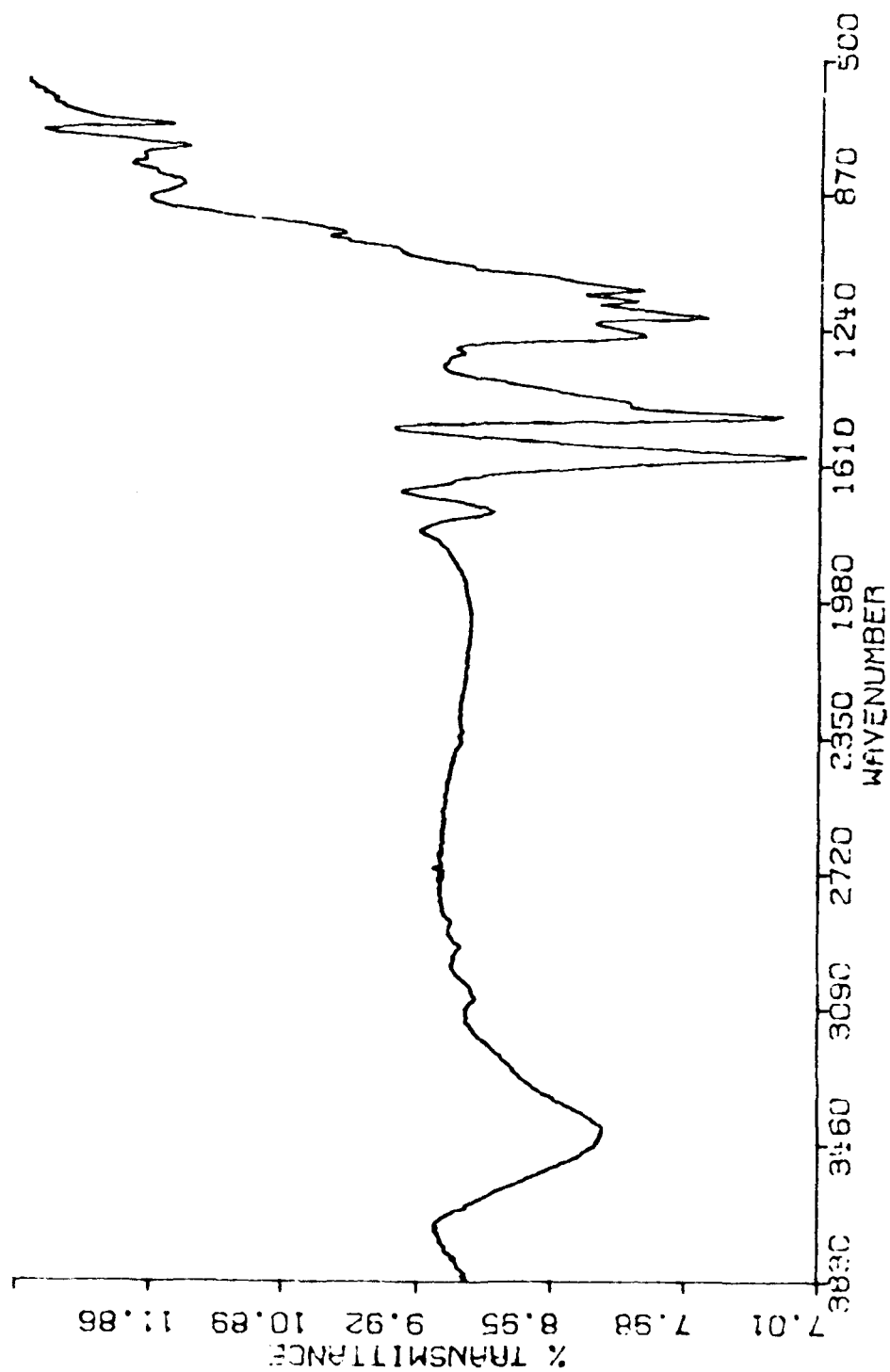


Figure 172. FTIR Spectrum of Carbon Seal Deposits from Engine Tested PPE (J58 FX-111 89)

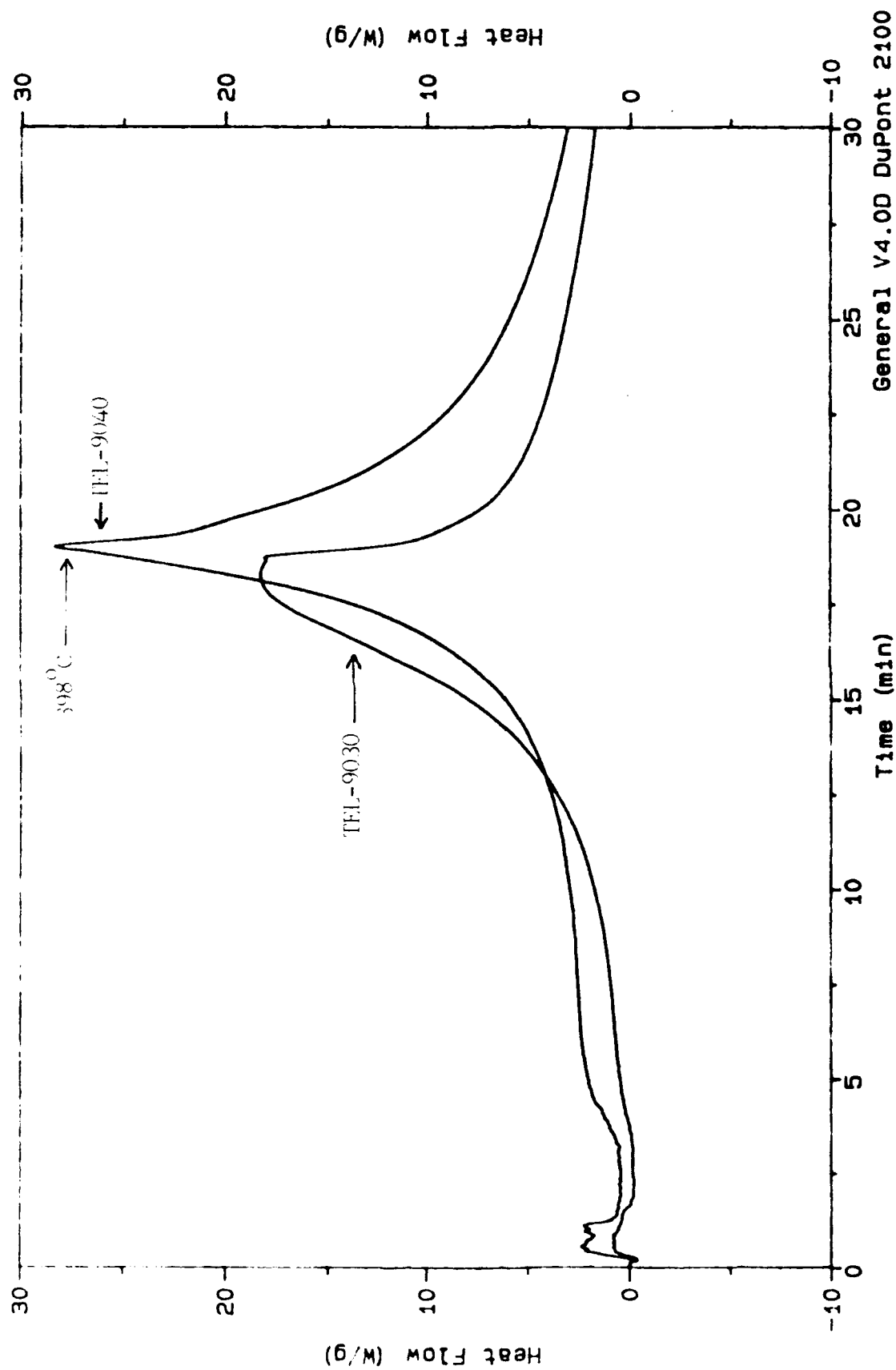


Figure 173. DSC Thermograms of Isolated Debris from Engine Stressed PPF Lubricants TEL-9030 and TEL-9040 [DSC Conditions: Ambient to 400°C at 20°C/Minute, Hold 20 Minutes]

metal-metal contact zone during wear testing of polyphenyl ether,^{28,43,44} was shown to be mostly organic (possibly polymeric) with various levels (2 to 22%) of iron. The most definitive analysis of the nature of the iron in the FP, by ⁵⁷Fe Mossbauer spectroscopy, indicates that all iron exists as high spin Fe(III), with no evidence of iron metal or oxide. Although specific compounds could not be identified, it is likely that the iron is chelated or perhaps exists as an organometallic. This work supports a previously proposed wear mechanism of polyphenyl ethers that involves corrosive attack and removal of iron by the lubricating film,²⁸ possibly involving exo-electron emission.³⁵

The corrosion/oxidation test instability of some four-ball tested PPE lubricants is most likely due to the thermal/oxidative instability of the FP that is produced. The relative stability of the FP, as determined by DSC and TGA, shows an approximate relationship to the acceleration in oxidation rates for the PPE lubricant from which they were isolated. It is theorized that the level of oxidative destabilization of any particular four-ball tested lubricant would be proportional to the concentration of the FP as well as its rate of decomposition.

Corrosion/oxidation testing of engine stressed PPEs indicates that an oxidative destabilization exists that is due to both low antioxidant (Sn) levels and insoluble debris in the lubricants. However, analysis of the debris indicated that it is not the same as the FP produced from four-ball wear tests.

APPENDIX A

LUBRICANT PERFORMANCE TEST DATA

Appendix A contains lubricant test data obtained during the development of improved methods for measuring lubricant performance and presented in Section II of this report. These test data are tabulated as follows:

- TABLE A-1. CORROSION AND OXIDATION DATA FOR TEL-9028, TEL-9029, TEL-9030, TEL-9038, TEL-9039 AND TEL-9040 LUBRICANTS (320°C, D 4871 TUBES, 10 L/H AIRFLOW)
- TABLE A-2. CORROSION AND OXIDATION TEST DATA FOR LUBRICANTS O-67-1, CB-1, TEL-9030 AND TEL-9040 (BEFORE AND AFTER 3 MICRON FILTERING) AT 320°C USING SQUIRES TUBES AND 25 ML SAMPLES
- TABLE A-3. SQUIRES OXIDATIVE TEST DATA
- TABLE A-4. CORROSION AND OXIDATION TEST DATA
- TABLE A-5. AFAPL STATIC COKER TEST DATA
- TABLE A-6. MCRT COKING TEST DATA
- TABLE A-7. LUBRICANT FOAMING TEST DATA

TABLE A-1

CORROSION AND OXIDATION DATA FOR
TEL-9028, TEL-9029, TEL-9030, TEL-9038, TEL-9039 AND TEL-9040 LUBRICANTS
(320°C, D 4871 TUBES, 10 L/H AIRFLOW)

Lubricant	Test Hours	Viscosity @ 40°C, cSt	Viscosity Chg @ 40°C, %	Viscosity @ 100°C, cSt	Viscosity Chg @ 100°C, %	Sn ppm	Refractive Index @ 20°C
TEL-9028 ¹	0	298.0 ²	-	12.95	-	96 ¹	1.6176 ¹
	48	342.5	14.9	13.81	6.6	115	
	72	366.2	22.9	14.22	9.8	106	
	96	398.0	33.6	14.79	14.1	99	
	120	455.3	52.7	15.48	19.5	112	
TEL-9028 ²	0	298.0	-	12.95	-	-	1.6300
	48	361.0	21.1	14.07	8.6	-	
	72	424.4	42.4	15.22	17.5	-	
TEL-9029	0	284.9	-	12.71	-	110	1.6307
	48	382.7	34.3	14.93	17.4	116	
	72	463.5	62.7	15.85	24.7	116	
TEL-9030	0	283.7	-	12.75	-	40	1.6303
	48	717.4	152.9	19.73	54.7	36	

Corrosion Test Data, mg/cm²

Lubricant	Aluminum	Silver	Mild Steel	M-50 Steel	Waspalloy	Titanium
TEL-9028 ¹	+0.04	-0.14	-0.30	+0.02	0.00	+0.02
TEL-9029	+0.02	+0.02	+0.04	+0.06	+0.02	+0.02
TEL-9030	+0.04	-0.16	+0.08	+0.04	0.00	0.00
TEL-9028 ²	+0.08	-0.68	+0.08	+0.02	+0.02	+0.04

¹As received with 15% tetrachloroethylene²After removal of tetrachloroethylene

TABLE A-1 (CONCLUDED)

Lubricant	Test Hours	Viscosity @ 40°C, cSt	Viscosity Chg @ 40°C, %	Viscosity @ 100°C, cSt	Viscosity Chg @ 100°C, %	Sn ppm	Refractive Index @ 20°C
TEL-9038	0	288.4	-	12.75	-	97	1.6301
	48	403.8	40.0	14.97	17.4	-	-
	72	682.1	136.5	19.25	51.0	-	-
TEL-9039 ¹	0	215.6	-	11.76	-	124	1.6287
	48	337.3	56.4	13.80	17.3	-	-
	72	514.8	138.8	16.38	39.3	-	-
TEL-9039 ²	0	298.1	-	12.92	-	-	1.6309
	48	338.6	13.6	13.71	6.1	-	-
TEL-9040	0	293.7	-	12.84	-	87	1.6301
	48	474.2	61.5	16.26	26.6	-	-
	72	>1300	>300	26.95	109.9	-	-

Corrosion Test Data, mg/cm ²					Waspaloy	Titanium
Lubricant	Aluminum	Silver	Mild Steel	M-50 Steel		
TEL-9038	+0.02	+0.44	+0.14	+0.10	+0.08	-0.02
TEL-9039 ¹	+0.06	-0.28	+0.04	+0.06	-0.02	+0.06
TEL-9032 ²	+0.02	+0.02	+0.06	+0.04	+0.02	+0.02
TEL-9040	+0.06	-0.22	+0.08	+0.10	+0.02	+0.02

¹As received with 1.9% trichloroethylene²After removal of trichloroethylene. "Squires" tube with 25 mL sample.

TABLE A-2

CORROSION AND OXIDATION TEST DATA FOR LUBRICANTS O-67-1, CB-1, TEL-9030
AND TEL-9040 (BEFORE AND AFTER 3 MICRON FILTERING) AT 320°C USING SQUIRES TUBES AND 25 ML SAMPLES

Lubricant	Test Hours	Viscosity @ 40°C, cSt	Viscosity Chg @ 40°C, %	Viscosity @ 40°C, % Chg of New O-67-1	Viscosity @ 100°C, cSt	Viscosity Chg @ 100°C, %	Viscosity @ 100°C % Chg of New O-67-1
New O-67-1	0 48	280.5 312.8	- 11.5	- -	12.61 13.11	- 4.6	- -
CB-1 ¹ Unfiltered	0 48	290.2 622.5	- 114.5	3.5 121.9	12.85 19.81	- 54.2	1.9 57.1
CB-1 ² Filtered (3 Micron)	0 48	288.1 326.9	- 13.5	2.7 16.5	12.68 13.42	- 5.8	0.6 6.4

¹ Heavy amount of sludge, varnish and coke deposits on C&O tube

² Very small amount of varnish at oil level on C&O tube

Corrosion Test Data, mg/cm ²					
Lubricant	Aluminum	Silver	Mild Steel	M-50 Steel	Waspaloy
CB-1 Unfiltered	+0.06	+0.04	+0.08	+0.06	+0.06
CB-1 Filtered	+0.06	+0.02	+0.08	+0.08	+0.08
					Titanium
					+0.06
					+0.08

TABLE A-2 (CONCLUDED)

Lubricant	Before Filtering		After Filtering	
	TEL-9030	TEL-9040	TEL-9030	TEL-9040
40°C Viscosity, cSt	717.4	474.2	381.1	336.2
% Change, 40°C Viscosity*	153.3	69.1	35.9	19.9
100°C Viscosity, cSt	19.73	16.26	14.48	13.61
% Change, 100°C Viscosity*	56.5	28.9	14.8	7.9
Iron, ppm	4	8	1	3
Tin, ppm	50	78	34	47
Sample Tube Deposits	Extremely high amt. of sludge, coke at oil level	Extremely high amt. of sludge, mod. coke, varnish	None	Very slight deposit above oil level
Blower Tube Deposits	Heavy amt. of sludge and brown residue	Heavy amt. of brown residue and coke	Slight Coke	Slight Coke

CORROSION TEST DATA

Lubricant	Wt. Chg. mg/cm ²					
	Al	Ag	MSt	M-50	Wasp.	Ti
TEL-9030	0.00	+0.06	+0.02	0.00	-0.02	-0.02
TEL-9040	0.00	-0.02	+0.02	+0.04	-0.02	0.00

*Percent change from new 0-67-1 oil

SQUIRES OXIDATIVE TEST DATA

LUBRICANT AND TEST TEMP.	LUBRICANT PROPERTY	New Oil	24	48	120	168	216	360
0-85-1 205 C	Weight Loss, %		7.1	13.8	32.7	42.8	51.6	ND
	COBRA Reading	8	36	63	109	119	110	110
	Total Acid No.	0.02	0.12	0.33	0.67	0.96	1.33	2.54
	Viscosity @100 C, cs	4.04	4.14	4.23	4.55	5.03	5.22	9.94
	Viscosity Change, %		2.5	4.7	12.6	24.5	29.2	146.0
	Toluene Insol, % wt	ND	ND	ND	ND	ND	ND	ND
	Visual Appearance of Deposits		None	Tacky Crystals	White Crystals	Crystals	Crystals	Crystals and Varnish
LUBRICANT AND TEST TEMP.	LUBRICANT PROPERTY	New Oil	24	68	116	168		
0-85-1 210 C	Weight Loss, %		9.4	26.1	44.8	50.7		
	COBRA Reading	8	50	97	123	113		
	Total Acid No.	0.02	0.33	1.00	1.70	2.90		
	Viscosity @100 C, cs	4.40	4.15	4.44	4.94	5.86		
	Viscosity Change, %		2.7	9.9	22.3	45.0		
	Toluene Insol, % wt	ND	ND	ND	ND	0.04		
	Visual Appearance of Deposits		White Deposits	Clear Deposit	Clear Deposits	Light Crystals		
LUBRICANT AND TEST TEMP.	LUBRICANT PROPERTY	New Oil	24	48	72	144		
0-85-1 215 C	Weight Loss, %		13.5	24.7	35.2	76.7		
	COBRA Reading	8	66	104	115	57		
	Total Acid No.	0.02	0.91	1.20	1.86	10.46		
	Viscosity @100 C, cs	4.04	4.23	4.46	4.73	ND		
	Viscosity Change, %		4.7	10.4	17.0	N/A		
	Toluene Insol, % wt	ND	ND	ND	ND	ND		
	Visual Appearance of Deposits		Clear Crystals	Clear Crystals	Clear Crystals	Clear Crystals		
			Sl. Varn.	Crystals	Crystals	Sl. Varn.		

SQUIRKS OXIDATIVE TEST DATA

LUBRICANT AND TEST TEMP.	LUBRICANT PROPERTY	New Oil	24	48	75	96	120	168
TEL-9076	Weight Loss, %		8.1	14.4	20.8	24.0	26.8	40.4
	CORRA Reading	2	133	185	188	196	>200	194
	Total Acid No.	0.26	0.60	0.74	1.08	1.21	1.43	2.28
210 C	Viscosity @100 C.c.s	4.04	4.40	4.55	4.71	4.84	4.92	5.44
	Viscosity Change, %		8.9	12.6	16.6	19.8	21.8	34.7
	Toluene Insol, % wt							
	Visual Appearance of Deposits		No deposits					
LUBRICANT AND TEST TEMP.	LUBRICANT PROPERTY	New Oil	168	192	241	241	241	241
TEL-9075 b	Weight Loss, %		41.2	48.6	67.8	67.8	67.8	67.8
(a)	CORRA Reading	2	NA	NA	NA	NA	NA	NA
210 C	Total Acid No.	0.26	2.52	2.6	13.47	13.47	13.47	13.47
	Viscosity @100 C.c.s	4.04	5.69	6.11	6.11	6.11	6.11	6.11
	Viscosity Change, %		40.8	51.2	51.2	51.2	51.2	51.2
	Toluene Insol, % wt							
	Visual Appearance of Deposits							
LUBRICANT AND TEST TEMP.	LUBRICANT PROPERTY	New Oil	24	48	92	92	92	92
TEL-9076	Weight Loss, %		11.7	20.9	59.8	59.8	59.8	59.8
	CORRA Reading		188	190	174	174	174	174
	Total Acid No.	.26	1.11	1.83	2.50	2.50	2.50	2.50
220 C	Viscosity @100 C.c.s	4.04	4.50	4.77	5.71	5.71	5.71	5.71
	Viscosity Change, %		11.3	18.1	41.3	41.3	41.3	41.3
	Toluene Insol, % wt							
	Visual Appearance of Deposits		None	NONE	SLIGHT	SLIGHT	SLIGHT	SLIGHT

(a) - continuation of TEL-9079 210 C

SQUIRES OXIDATIVE TEST DATA

LUBRICANT AND TEST TEMP.	LUBRICANT PROPERTY	New Oil	24	48	TEST HOURS
0-90-6	Weight Loss, %		13.1	23.8	92
	COBRA Reading	15	67	153	54.0
	Total Acid No.	.05	0.75	0.71	154
	Viscosity @100 C.cs	4.01	4.16	4.30	6.95
215 C	Viscosity Change, %		3.7	7.5	7.41
	Toluene Insol, % wt				84.8
	Visual Appearance of Deposits		None		
LUBRICANT AND TEST TEMP.	LUBRICANT PROPERTY	New Oil	24	48	TEST HOURS
0-90-6	Weight Loss, %		11.9	31.6	72
	COBRA Reading	15	72	103	60.3
	Total Acid No.	0.05	0.46	6.98	120
	Viscosity @100 C.cs	4.01	4.15	6.07	7.84
220 C	Viscosity Change, %		3.5	51.4	14.43
	Toluene Insol, % wt				259.8
	Visual Appearance of Deposits		NO COKE	LIGHT BRO	THICK LIQ.
				WN VARNIS	UID, LT.
LUBRICANT AND TEST TEMP.	LUBRICANT PROPERTY	New Oil	72	96	TEST HOURS
TEL-90003	Weight Loss, %		37.1	46.8	
	COBRA Reading		>200	>200	
	Total Acid No.	0.00	1.06	1.96	
	Viscosity @100 C.cs	3.94	6.06	6.88	
215 C	Viscosity Change, %		53.8	74.6	
	Toluene Insol, % wt				
	Visual Appearance of Deposits		None		SLT.VARN.

ACQUIRES OXIDATIVE TEST DATA

LUBRICANT AND TEST TEMP.	LUBRICANT PROPERTY	New Oil	28	52	79	104	128	148
TEL-90087 (a) 210 C	Weight Loss, %		NA	NA	30.5	36.5	42.7	45.6
	COBRA Reading	1.67	195	>200	>200	>200	>200	>200
	Total Acid No.	.00	.49	.63	1.10	1.27	1.46	1.62
	Viscosity @100 C.c.s.	4.02	4.61	4.97	5.47	5.85	6.33	6.94
	Viscosity Change, %		14.7	23.6	36.1	45.5	57.5	72.6
	Toluene Insol., % wt							
	Visual Appearance of Deposits							
LUBRICANT AND TEST TEMP.	LUBRICANT PROPERTY	New Oil	24	48	73	96	120	165
TEL-90087 225 C	Weight Loss, %		19.5	33.8	44.4	53.6	61.7	73.5
	COBRA Reading	1.67	24	197	>200	>200	>200	>200
	Total Acid No.	.00	.82	1.32	2.23	4.13	6.53	10.48
	Viscosity @100 C.c.s.	4.02	4.99	6.165	6.95	9.47	14.57	69.27
	Viscosity Change, %		24.1	53.3	72.9	135.6	262.4	1623
	Toluene Insol., % wt							
	Visual Appearance of Deposits							
LUBRICANT AND TEST TEMP.	LUBRICANT PROPERTY	New Oil	24	48	72	96	120	120
TEL-90087 210 C	Weight Loss, %		9.1	14.8	23.8	33.7		38.6
	COBRA Reading	8	58	82	97	111	116	122
	Total Acid No.	0.02	0.52	0.50	0.84	1.47	1.35	
	Viscosity @100 C.c.s.	4.04	4.18	4.27	4.42	4.63		
	Viscosity Change, %		3.55	5.7	9.41	14.7		
	Toluene Insol., % wt							
	Visual Appearance of Deposits		Clear crystals				CLEAR BWN CRYSTALS	

(a) - Same as 0-90-6 (lower temperatures of test)

SQUIRES OXIDATIVE TEST DATA

LUBRICANT AND TEST TEMP.	LUBRICANT PROPERTY	New Oil	96	TEST HOURS			
TEL-9022 (a) 215 C	Weight Loss, %		45				
	COBRA Reading	8	132				
	Total Acid No.		1.48				
	Viscosity @100 C.cs	4.04	5.16				
	Viscosity Change, %		27.7				
	Toluene Insol, % wt						
	Visual Appearance of Deposits						
LUBRICANT AND TEST TEMP.	LUBRICANT PROPERTY	New Oil	24	48	72	96	120
TEL-9031 210 C	Weight Loss, %		8.3	16.2	25.7	47.9	57.4
	COBRA Reading	10	59	87	99	122	108
	Total Acid No.	0.04	0.54	0.88	1.35	10.9	
	Viscosity @100 C.cs	4.01	4.12	4.32	4.43	8.55	
	Viscosity Change, %		2.77	7.7	10.5	114	
	Toluene Insol, % wt						
	Visual Appearance of Deposits		Clear crystals			NO CRYST. ; OIL LT. COLOR	
LUBRICANT AND TEST TEMP.	LUBRICANT PROPERTY	New Oil	TEST HOURS				
	Weight Loss, %						
	COBRA Reading						
	Total Acid No.						
	Viscosity @100 C.cs						
	Viscosity Change, %						
	Toluene Insol, % wt						
	Visual Appearance of Deposits						
(a) - Only one test time							

(a) - Only one test time

TABLE A-4

CORROSION AND OXIDATION TEST DATA

LUBRICANT SAMPLE SIZE TEST TEMP.	LUBRICANT PROPERTY	New Oil	48	TEST HOURS
CB-1 (a)	Viscosity @40C, cSt	290.2	622.5	
	40C Visc Change, %		144.5	
	Viscosity @100C, cSt	12.85	19.81	
	100C Visc Change, %		54.2	
31.41 grams	Total Acid Number	---		
320 C	% Insolubles	---		
	Visual Appearance of Deposits			
CORROSION DATA, Wt. Change mg/cm				
	Test Hrs.	Al	Ag	M-St
	48	0.06	0.04	0.08
				M-50
				0.06
				Wasp
				0.06
				Ti
				0.06
TEST HOURS				
LUBRICANT	LUBRICANT			
SAMPLE SIZE	PROPERTY	New Oil	48	
TEST TEMP.				
CB-1 (b)	Viscosity @40C, cSt	288.1	326.9	
	40C Visc Change, %		13.5	
	Viscosity @100C, cSt	12.68	13.42	
	100C Visc Change, %		5.8	
27.9 grams	Total Acid Number	---		
320 C	% Insolubles	---		
	Visual Appearance of Deposits		none	
CORROSION DATA, Wt. Change mg/cm				
	Test Hrs.	Al	Ag	M-St
	48	0.06	0.02	0.08
				M-50
				0.08
				Wasp
				0.06
				Ti
				0.08
TEST HOURS				
Test Variations				
5 micron filtered				

(a) - TUBE, HEAVY SLUDGE/BLOWER HEAVY DEPOSITS; COMPOSITE SAMPLE

(b) - tube, slight coke /blower, moderate deposits

CORROSION AND OXIDATION TEST DATA

LUBRICANT SAMPLE SIZE TEST TEMP.	LUBRICANT PROPERTY	New Oil	ET	48	TEST HOURS				
CB-2 (a) 29.2 grams 320 C	Viscosity @40C, cSt	280.5	284.4	340.0					
	40C Visc Change, %		1.5	21.3					
	Viscosity @100C, cSt	12.61	12.71	13.78					
	100C Visc Change, %		0.8	9.3					
	Total Acid Number								
	% Insolubles								
	Visual Appearance of Deposits								
<u>Test Variations</u>									
3 micron filtered									
					CORROSION DATA, Wt. Change mg/cm				
		Test Hrs.	Al	Ag	M-St	M-50	Wasp	Ti	
		48	0.06	0.04	0.08	0.10	0.04	0.06	
LUBRICANT SAMPLE SIZE TEST TEMP.	LUBRICANT PROPERTY	New Oil	ET	48	TEST HOURS				
CB-2 (b) 29.5 grams 320 C	Viscosity @40C, cSt	280.3	285.8	335.6					
	40C Visc Change, %		2.0	19.7					
	Viscosity @100C, cSt	12.61	12.76	13.68					
	100C Visc Change, %		1.2	8.5					
	Total Acid Number								
	% Insolubles								
	Visual Appearance of Deposits								
					CORROSION DATA, Wt. Change mg/cm				
		Test Hrs.	Al	Ag	M-St	M-50	Wasp	Ti	
		48	0.04	0.04	0.08	0.06	0.04	0.10	

(a) - VERY SLIGHT VARNISH ON BLOWER TUBE, ET=POST-ENGINE TEST DATA
 (b) - COMPOSITE SAMPLE

CORROSION AND OXIDATION TEST DATA

LUBRICANT SAMPLE SIZE TEST TEMP.	LUBRICANT PROPERTY	New Oil	ET	48	TEST HOURS
CB-3 (a) 30.6 grams 320 C	Viscosity @40C, cSt	280.3	292.8	348.3	
	40C Visc Change, %		4.5	24.3	
	Viscosity @100C, cSt	12.61	12.79	13.81	
	100C Visc Change, %				
	Total Acid Number				
	% Insolubles				
	Visual Appearance of Deposits				
	Test Variations				
3 micron filtered					
CORROSION DATA, Wt. Change mg/cm					
Test Hrs.		Al	Ag	M-St	Wasp
48		0.06	0.04	0.06	0.00
					Ti
					0.02
LUBRICANT					
SAMPLE SIZE	LUBRICANT	TEST HOURS			
TEST TEMP.	PROPERTY	New Oil	ET	48	
CB-3 (b) 30.6 grams 320 C	Viscosity @40C, cSt	280.3	294.7	340.8	
	40C Visc Change, %		5.1	21.6	
	Viscosity @100C, cSt	12.61	12.83	13.73	
	100C Visc Change, %		0.7	8.9	
	Total Acid Number				
	% Insolubles				
	Visual Appearance of Deposits				
	Test Variations				
CORROSION DATA, Wt. Change mg/cm					
Test Hrs.		Al	Ag	M-St	Wasp
48		0.02	0.00	0.08	0.04
					Ti
					0.047

(a) - (ET=ENGINE TEST), COMPOSITE SAMPLE
 (b) - COMPOSITE SAMPLE

CORROSION AND OXIDATION TEST DATA

LUBRICANT	LUBRICANT	TEST HOURS				
SAMPLE SIZE	PROPERTY	New Oil	48			
TEST TEMP.						
O-67-1 (a) 113.8 grams 320 C	Viscosity @40C, cSt	280.8	320.7			
	40C Visc Change, %		14.2			
	Viscosity @100C, cSt	12.64	13.33			
	100C Visc Change, %		5.4			
	Total Acid Number					
	% Insolubles					
	Visual Appearance of Deposits					
Test Variations						
48 hrs nitrogen, 48 hours air						
		Test Hrs.	Al	Ag	M-St	M-50 Wasp Ti
		48	0.06	-0.02	0.10	0.10 0.04 0.10
TEST HOURS						
O-67-1 (b) 120 grams 320 C	Viscosity @40C, cSt	New Oil	24	48	96	120 168
	40C Visc Change, %	280.8	312.6	328.0	358.4	367.3 401.8
	Viscosity @100C, cSt		11.3	16.8	20.0	27.6 30.8 43.0
	100C Visc Change, %	12.64	13.2	13.47	13.67	13.96 14.77
	Total Acid Number	0.00	0.00	0.00	0.00	0.00 0.00 0.00
	% Insolubles					
	Visual Appearance of Deposits					
CORROSION DATA, Wt. Change mg/cm						
		Test Hrs.	Al	Ag	M-St	M-50 Wasp Ti
		24	0.06	0.00	0.10	0.06 0.10
		48	0.02	0.02	0.08	0.06 0.08
		72	0.02	-0.04	0.06	-0.02 0.02
		96	0.08	0.04	0.16	0.06 0.06
		120	0.04	0.02	0.01	0.04 0.06
		168	0.04	-0.06	0.10	0.10 0.04
CORROSION DATA, Wt. Change mg/cm						
		Test Hrs.	Al	Ag	M-St	M-50 Wasp Ti
		24	0.06	0.00	0.10	0.06 0.10
		48	0.02	0.02	0.08	0.06 0.08
		72	0.02	-0.04	0.06	-0.02 0.02
		96	0.08	0.04	0.16	0.06 0.06
		120	0.04	0.02	0.01	0.04 0.06
		168	0.04	-0.06	0.10	0.10 0.04

(a) - RI @ 25 C = 1.6289 slight stain

(b) - RI @ 25 C = 1.6344 /RI @ 25 C = init 1.6290 fin 1.6289

CORROSION AND OXIDATION TEST DATA

LUBRICANT SAMPLE SIZE TEST TEMP.	LUBRICANT PROPERTY	New Oil	192	240	48	TEST HOURS
O-67-1 (a) 117 grams	Viscosity @40C, cSt	280.8	434.6	529.1	333.3	
	40C Visc Change, %		54.7	88.4	18.6	
	Viscosity @100C, cSt	12.64	15.26	16.78	13.43	
	100C Visc Change, %		20.7	32.7	6.3	
320 C	Total Acid Number					
	% Insolubles					
	Visual Appearance of Deposits					

CORROSION DATA, Wt. Change mg/cm

Test Hrs.	Al	Ag	M-St	M-50	Wasp	Ti
192	-0.10	0.00	0.10	0.00	0.00	0.00
240	0.00	-0.01	0.00	0.00	0.00	0.00
48	-0.06	-0.08	0.00	-0.02	-0.06	-0.20

LUBRICANT SAMPLE SIZE TEST TEMP.	LUBRICANT PROPERTY	New Oil	48(1)	48(2)	48(3)	TEST HOURS
O-67-1 (b) 36.0 grams	Viscosity @40C, cSt	280.8	317.2	318.5	318.1	
	40C Visc Change, %		12.9	13.4	13.2	
	Viscosity @100C, cSt	12.64	13.38	13.37	13.28	
	100C Visc Change, %		5.9	5.8	5.1	
320 C	Total Acid Number					
	% Insolubles					
	Visual Appearance of Deposits		none			

Test Variations

Squires Tube	48(1)=3L/H, 48(2)=7L/H, 48(3)=10L/h	Test Hrs.	Al	Ag	M-St	M-50	Wasp	Ti
		48(1)	0.00	0.00	+0.10	+0.10	0.00	-0.10
		48(2)	0.00	0.00	+0.10	0.00	-0.10	0.00
		48(3)	0.00	0.00	-0.40	-0.80	-0.12	-0.08

(a) - RI @ 25 C i= 1.6290 48h= 1.6289

(b) - RI @ 25 C=1.6297/slight stain

CORROSION AND OXIDATION TEST DATA

LUBRICANT SAMPLE SIZE TEST TEMP.	LUBRICANT PROPERTY	New Oil	24	48	72	96	168
O-67-1	Viscosity @40C, cSt	280.8	308.5	322.0	337.7	353.0	419.2
	40C Visc Change, %		9.9	14.7	20.3	25.7	49.3
	Viscosity @100C, cSt	12.61	13.11	13.42	13.68	13.97	
	100C Visc Change, %		4.0	6.4	8.5	10.8	19.8
168.1 grams	Total Acid Number						
320 C	% Insolubles	---					
	Visual Appearance of Deposits		none				
<u>Test Variations</u> Sampled from top of can-B							
CORROSION DATA, Wt. Change mg/cm							
Test Hrs.	Al	Ag	M-St	M-50	Wasp	Ti	
24	0.02	0.02	0.10	0.06	0.10	0.12	
48	-0.02	0.02	0.08	0.10	0.04	0.00	
72	0.04	-0.06	0.06	0.06	0.08	0.04	
96	0.06	-0.08	0.14	0.08	0.06	0.02	
168	0.04	-0.08	0.10	0.06	0.00	0.02	
<u>TEST HOURS</u>							
LUBRICANT	LUBRICANT						
SAMPLE SIZE	PROPERTY	New Oil	---	48			
TEST TEMP.		280.8		304.9			
O-67-1	Viscosity @40C, cSt			8.5			
	40C Visc Change, %			13.20			
	Viscosity @100C, cSt	12.64		4.4			
	100C Visc Change, %						
66.1 grams	Total Acid Number						
320 C	% Insolubles						
	Visual Appearance of Deposits		none				
<u>TEST HOURS</u>							
<u>Test Variations</u> Squires Tube							
CORROSION DATA, Wt. Change mg/cm							
Test Hrs.	Al	Ag	M-St	M-50	Wasp	Ti	
48	0.02	-0.02	0.08	0.02	0.00	-0.04	

CORROSION AND OXIDATION TEST DATA

LUBRICANT	LUBRICANT	TEST HOURS			
SAMPLE SIZE	PROPERTY	New Oil	---	48	
TEST TEMP.					
O-67-1	Viscosity @40C, cSt	280.8		425.0	
	40C Visc Change, %			51.3	
	Viscosity @100C, cSt	12.64		15.69	
	100C Visc Change, %			24.1	
38.7 grams	Total Acid Number				
320 C	% Insolubles				
	Visual Appearance				
	of Deposits				
Test Variations					
Squires Tube					
wear metal added					
CORROSION DATA, Wt. Change mg/cm					
Test Hrs.	Al	Ag	M-St	M-50	Ti
48	0.00	0.02	0.02	0.06	0.04

CORROSION AND OXIDATION TEST DATA

LUBRICANT	LUBRICANT PROPERTY	New Oil	24	48	72	TEST HOURS
O-67-1	Viscosity @40C, cSt	280.8	301.5	306.2	317.8	
	40C Visc Change, %		7.4	9.0	13.2	
	Viscosity @100C, cSt	12.61	12.97	13.27	13.36	
	100C Visc Change, %		2.9	5.2	5.9	
320 C	Total Acid Number	---				
	% Insolubles	---				
	Visual Appearance of Deposits		none			
CORROSION DATA, Wt. Change mg/cm						
	Test Hrs.	Al	Ag	M-St	M-50	Ti
	72	0.06	0.10	0.10	-0.04	-0.02
LUBRICANT	LUBRICANT PROPERTY	New Oil	48	72	96	TEST HOURS
O-67-1 (a)	Viscosity @40C, cSt	298.0	342.5	366.2	398.0	
	40C Visc Change, %		22.1	30.6	41.9	
	Viscosity @100C, cSt	12.95	13.81	14.22	14.78	
	100C Visc Change, %		9.7	12.8	17.2	
320 C	Total Acid Number	---				
	% Insolubles	---				
	Visual Appearance of Deposits		none			
CORROSION DATA, Wt. Change mg/cm						
	Test Hrs.	Al	Ag	M-St	M-50	Ti
	120	0.04	-0.14	-0.30	0.02	0.02

(a) - slt.coke on test&air tubes /40C visc. as received was 50.55

CORROSION AND OXIDATION TEST DATA

LUBRICANT SAMPLE SIZE TEST TEMP.	LUBRICANT PROPERTY	TEST HOURS				
O-67-1 119.6 grams 320 C	Viscosity @40C, cSt	New Oil	168			
	40C Visc Change, %	285.1	392.3			
	Viscosity @100C, cSt	12.85	14.75			
	100C Visc Change, %	14.8				
	Total Acid Number					
	% Insolubles					
	Visual Appearance of Deposits		slight varnish above oil			
CORROSION DATA, Wt. Change mg/cm						
	Test Hrs.	Al	Ag	M-St	M-50	Wasp
	168	0.02	-0.04	0.04	0.04	0.02
						Ti
						0.04
LUBRICANT SAMPLE SIZE TEST TEMP.	LUBRICANT PROPERTY	TEST HOURS				
O-67-1 30.45 grams 320 C	Viscosity @40C, cSt	New Oil	48			
	40C Visc Change, %	280.8	324.3			
	Viscosity @100C, cSt	15.67				
	100C Visc Change, %					
	Total Acid Number					
	% Insolubles					
	Visual Appearance of Deposits					
CORROSION DATA, Wt. Change mg/cm						
	Test Hrs.	Al	Ag	M-St	M-50	Wasp
	48	0.02	-0.02	0.04	0.00	0.04
						Ti
						0.00
LUBRICANT SAMPLE SIZE TEST TEMP.	LUBRICANT PROPERTY	TEST HOURS				
25% Trichloroethylene added	Viscosity @40C, cSt	New Oil	48			
	40C Visc Change, %	280.8	324.3			
	Viscosity @100C, cSt	15.67				
	100C Visc Change, %					
	Total Acid Number					
	% Insolubles					
	Visual Appearance of Deposits					
CORROSION DATA, Wt. Change mg/cm						
	Test Hrs.	Al	Ag	M-St	M-50	Wasp
	48	0.02	-0.02	0.04	0.00	0.04
						Ti
						0.00

CORROSION AND OXIDATION TEST DATA

LUBRICANT	LUBRICANT	TEST HOURS				
SAMPLE SIZE	PROPERTY					
TEST TEMP.						
O-67-1 (a) 30.3 grams 320 C	New Oil	48				
	Viscosity @40C, cSt	324.6				
	40C Visc Change, %	15.5				
	Viscosity @100C, cSt					
	100C Visc Change, %					
25% Trichloroethylene added	Total Acid Number					
	% Insolubles					
	Visual Appearance					
	of Deposits					
	Test Variations					
CORROSION DATA, Wt. Change mg/cm						
Test Hrs.	Al	Ag	M-St	M-50	Wasp	Ti
48	0.02	0.02	0.04	0.02	0.00	0.00
O-67-1 (b) 111.2 grams 320 C	New Oil	24	48	72	76	
	Viscosity @40C, cSt	315.7	386.7	555.9	610.7	
	40C Visc Change, %	12.4	37.7	97.9	117.4	
	Viscosity @100C, cSt					
	100C Visc Change, %					
Moist Air	Total Acid Number	0.10	0.11	0.23	0.23	
	% Insolubles					
	Visual Appearance					
	of Deposits					
	Test Variations					
CORROSION DATA, Wt. Change mg/cm						
Test Hrs.	Al	Ag	M-St	M-50	Wasp	Ti
24	0.1	-0.32	0.04	0.04	0.06	

(a) - no silver coupon
(b) - TEST 1

CORROSION AND OXIDATION TEST DATA

LUBRICANT	LUBRICANT	TEST HOURS
SAMPLE SIZE	PROPERTY	
TEST TEMP.		
O-67-1	Viscosity @40C, cSt	New Oil 95
(a)	40C Visc Change, %	280.8 379.8
119.1 grams	Viscosity @100C, cSt	35.2
320 C	100C Visc Change, %	
	Total Acid Number	
	% Insolubles	
	Visual Appearance of Deposits	
Test Variations		
Moist Air	CORROSION DATA, Wt. Change mg/cm	
	Test Hrs.	Al AG M-St M-50 Wasp Ti
	95	0.06 0.06 0.06 0.04 -0.18 -0.02
LUBRICANT	LUBRICANT	TEST HOURS
SAMPLE SIZE	PROPERTY	
TEST TEMP.		
O-67-1	Viscosity @40C, cSt	New Oil 25 48 72
120 grams	40C Visc Change, %	280.8 311.7 324.2 342.0
320 C	Viscosity @100C, cSt	11.0 15.4 21.7
	100C Visc Change, %	
	Total Acid Number	
	% Insolubles	
	Visual Appearance of Deposits	
Test Variations		
Moist Air	CORROSION DATA, Wt. Change mg/cm	
	Test Hrs.	Al AG M-St M-50 Wasp Ti
	72	0.04 -0.3 0.02 0.02 0.00 0.02

(a) - TEST 2

CORROSION AND OXIDATION TEST DATA

LUBRICANT SAMPLE SIZE TEST TEMP.	LUBRICANT PROPERTY	TEST HOURS						
		New Oil	24	74	96	145	168	
O-67-1 (a) 144.1 grams 320 C	Viscosity @40C, cSt	281.8	288.5	289.8	291.2	293.7	292.7	
	40C Visc Change, %		2.4	2.8	3.34	4.2	3.85	
	Viscosity @100C, cSt							
	100C Visc Change, %							
	Total Acid Number							
Nitrogen	% Insolubles							
	Visual Appearance of Deposits							
	Test Variations							
CORROSION DATA, Wt. Change mg/cm								
Test Hrs.	Al	Ag	M-St	Wasp	Ti			
413	0.14	0.12	0.18	0.14	0.14	0.14	0.14	0.30

LUBRICANT SAMPLE SIZE TEST TEMP.	LUBRICANT PROPERTY	TEST HOURS						
		New Oil	190	242	337	413		
O-67-1 (b) 144.1 grams 320 C	Viscosity @40C, cSt	281.8	293.7	294.3	297.6	297.1		
	40C Visc Change, %		4.22	4.44	5.60	5.41		
	Viscosity @100C, cSt							
	100C Visc Change, %							
	Total Acid Number							
Nitrogen	% Insolubles							
	Visual Appearance of Deposits							
	Test Variations							
CORROSION DATA, Wt. Change mg/cm								
Test Hrs.	Al	Ag	M-St	Wasp	Ti			
413	0.14	0.12	0.18	0.14	0.14	0.14	0.14	0.30

(a) - TEST 1

(b) - CONTINUED FROM TEST 1

LUBRICANT SAMPLE SIZE TEST TEMP.	LUBRICANT PROPERTY	New Oil	24	48	72	96
O-67-1	Viscosity @40C, cSt	280.8	310.8	324.2	338.2	349.9
(a)	% 40C Visc Change,		10.7	15.5	20.4	24.6
116.0 grams	Viscosity @100C, cSt	12.6	13.15	13.47	13.73	13.89
	% 100C Visc Change,		10.7	15.5	20.4	24.6
320 C	Total Acid Number					
	% Insolubles					
	Visual Appearance of Deposits					
<u>Test Variations</u>						
from top of hand shaken can B						
Test Hrs.	Al	Ag	M-St	M-50	Wasp	Ti
24	0.02	0.02	0.10	0.06	0.10	0.12
48	-0.02	0.02	0.08	0.10	0.04	0.0
72	0.04	-0.06	0.06	0.06	0.08	0.04
96	0.06	-0.08	0.14	0.08	0.06	0.02
LUBRICANT SAMPLE SIZE TEST TEMP.	LUBRICANT PROPERTY	New Oil	48	TEST HOURS		
O-67-1	Viscosity @40C, cSt	281.8	294.6			
(b)	% 40C Visc Change,		4.54			
117.1 grams	Viscosity @100C, cSt	12.61	12.75			
	% 100C Visc Change,		1.11			
320 C	Total Acid Number					
	% Insolubles					
	Visual Appearance of Deposits					
<u>Test Variations</u>						
Nitrogen						
Test Hrs.	Al	Ag	M-St	M-50	Wasp	Ti
48	0.0	0.0	0.0	0.0	-0.1	-0.1

(a) - 48H-118g 72H-120g 96H-116g
(b) - 48 HOUR TEST

CORROSION AND OXIDATION TEST DATA

LUBRICANT	LUBRICANT	TEST HOURS					
SAMPLE SIZE	PROPERTY	New Oil	48	96	168	216	264
TEST TEMP.	Viscosity @40C, cSt	280.3	315.9	340.1	381.0	417.6	489.0
0-67-1	40C Visc Change, %		12.7	21.3	35.9	49.0	74.5
	Viscosity @100C, cSt	12.61	13.32				
121.5 grams	100C Visc Change, %		5.6				
	Total Acid Number						
320 C	% Insolubles						
	Visual Appearance of Deposits						
Test Variations							
No Condensate Return							
CORROSION DATA, Wt. Change mg/cm							
Test Hrs.	Al	Ag	M-St	M-50	Wasp	Ti	
264	0.04	-0.02	0.12	0.12	0.04	0.06	
LUBRICANT	LUBRICANT	TEST HOURS					
SAMPLE SIZE	PROPERTY	New Oil	48				
TEST TEMP.	Viscosity @40C, cSt	280.8	341.3				
0-67-1	40C Visc Change, %		21.5				
(a)	Viscosity @100C, cSt	12.64	13.61				
35.00 grams	100C Visc Change, %		7.6				
	Total Acid Number						
327 C	% Insolubles		none				
	Visual Appearance of Deposits						
Test Variations							
Squires Tube							
CORROSION DATA, Wt. Change mg/cm							
Test Hrs.	Al	Ag	M-St	M-50	Wasp	Ti	
48	0.00	0.00	0.02	0.00	-0.02	-0.02	

(a) - RI @ 25 C 1.6297 NEW= 1.6290

CORROSION AND OXIDATION TEST DATA

LUBRICANT SAMPLE SIZE TEST TEMP.	LUBRICANT PROPERTY	New Oil	48	TEST HOURS				
O-67-1 (a) 117.7 grams 327 C	Viscosity @40C, cSt	280.3	356.2					
	40C Visc Change, %		27.0					
	Viscosity @100C, cSt							
	100C Visc Change, %							
	Total Acid Number							
	% Insolubles							
	Visual Appearance of Deposits							
CORROSION DATA, Wt. Change mg/cm								
	Test Hrs.	Al	Ag	M-St	M-50	Wasp	Ti	
	48	0.039	0.039	0.00	0.00	-0.019	-0.019	
LUBRICANT SAMPLE SIZE TEST TEMP.	LUBRICANT PROPERTY	New Oil	72	96	120	TEST HOURS		
O-77-6 (b) 120 grams 290 C	Viscosity @40C, cSt	276.2	350.6	398.3	484.4			
	40C Visc Change, %		26.9	44.2	75.4			
	Viscosity @100C, cSt	12.52	13.91	14.86	16.26			
	100C Visc Change, %		11.1	18.7	29.9			
	Total Acid Number	---						
	% Insolubles							
	Visual Appearance of Deposits							
CORROSION DATA, Wt. Change mg/cm								
	Test Hrs.	Al	Ag	M-St	M-50	Wasp	Ti	
	120	0.00	-0.04	0.04	0.02	0.00	-0.02	

(a) - R.I @ 25C 1.6307 NEW= 1.6290

(b) - RI @ 24 C = 1.6290

CORROSION AND OXIDATION TEST DATA

[illegible]

(a) - slight coke on blower tube

CORROSION AND OXIDATION TEST DATA

LUBRICANT	LUBRICANT	TEST HOURS			
SAMPLE SIZE	PROPERTY	New Oil	24	48	
TEST TEMP.					
O-77-6	Viscosity @40C, cSt	276.2	354.1	844.1	
	40C Visc Change, %		28.2	205.6	
	Viscosity @100C, cSt	12.52	13.97	21.32	
	100C Visc Change, %		11.6	70.3	
116.6 grams	Total Acid Number	---			
	% Insolubles				
	Visual Appearance			NO COKE	
	of Deposits			ON TUBE,	
310 C				BLOWER	
CORROSION DATA, Wt. Change mg/cm					
	Test Hrs.	Al	Ag	M-St	M-50
	48	0.02	0.08	0.08	0.08
				Wasp	Ti
					0.04
TEST HOURS					
LUBRICANT	LUBRICANT	TEST HOURS			
SAMPLE SIZE	PROPERTY	New Oil	48		
TEST TEMP.					
O-77-6	Viscosity @40C, cSt	276.2	534.5		
	40C Visc Change, %		93.5		
	Viscosity @100C, cSt	12.52	17.05		
	100C Visc Change, %		37.9		
37.60 grams	Total Acid Number				
	% Insolubles				
	Visual Appearance				
	of Deposits				
320 C					
CORROSION DATA, Wt. Change mg/cm					
	Test Hrs.	Al	Ag	M-St	M-50
	48	-0.16	-0.12	+0.02	-0.06
				Wasp	Ti
					-0.06
Test Variations					
Squires Tube					

(a) - RI @ 25 C INITIAL 1.6290, 48 HRS 1.6302

CORROSION AND OXIDATION TEST DATA

LUBRICANT	LUBRICANT	TEST HOURS				
SAMPLE SIZE	PROPERTY	New Oil	24			
TEST TEMP.						
O-77-6 (a) 120 grams 320 C	Viscosity @40C, cSt	279.5	565.3			
	40C Visc Change, %		102.2			
	Viscosity @100C, cSt	---	---			
	100C Visc Change, %					
	Total Acid Number					
	% Insolubles					
	Visual Appearance of Deposits					
CORROSION DATA, Wt. Change mg/cm						
	Test Hrs.	Al	Ag	M-St	M-50	Wasp
	24	0.08	0.04	0.10	0.06	0.10
						Ti
						0.06
O-77-6 (b) 144.8 grams 320 C	Viscosity @40C, cSt	279.1	300.9	315.7	330.3	370.0
	40C Visc Change, %		7.8	13.1	18.3	32.6
	Viscosity @100C, cSt	---	---	---	---	---
	100C Visc Change, %					
	Total Acid Number	---	---	---	---	---
	% Insolubles					
	Visual Appearance of Deposits					
CORROSION DATA, Wt. Change mg/cm						
	Test Hrs.	Al	Ag	M-St	M-50	Wasp
	72	-0.04	-0.06	0.02	-0.02	-0.02
						Ti
						-0.02
Test Variations						
Relative 50% Additive A added						

(a) - 48 hrs oil too thick to test

(b) - ccke on blower slight stain tube

CORROSION AND OXIDATION TEST DATA

LUBRICANT	LUBRICANT	TEST HOURS					
SAMPLE SIZE	PROPERTY	New Oil	168	192	216	240	
TEST TEMP.	Viscosity @40C, cSt	279.1	436.0	475.3	540.1	617.4	
0-77-6	40C Visc Change, %		56.2	70.3	93.5	121.2	
(a)	Viscosity @100C, cSt	---					
140 grams	100C Visc Change, %						
	Total Acid Number						
320 C	% Insolubles						
	Visual Appearance						
	of Deposits						
Test Variations							
Relative 50% Additive A added							
	Test Hrs.	Al	Ag	M-St	M-50	Wasp	Ti
	192	0.10	0.04	0.16	0.12	0.04	0.04
	240	-0.08	-0.12	-0.02	-0.02	-0.06	-0.06
TEST HOURS							
LUBRICANT	LUBRICANT	New Oil	48	72	144	168	192
SAMPLE SIZE	PROPERTY	279.5	318.0	332.5	380.7	406.2	427.6
TEST TEMP.	Viscosity @40C, cSt		13.8	19.0	36.2	45.3	53.0
0-77-6	40C Visc Change, %						
	Viscosity @100C, cSt	---					
139.2 grams	100C Visc Change, %						
	Total Acid Number	---					
320 C	% Insolubles						
	Visual Appearance						
	of Deposits						
Test Variations							
Relative 100% Additive A added							
	Test Hrs.	Al	Ag	M-St	M-50	Wasp	Ti

(a) - coke on blower tube

LUBRICANT	LUBRICANT	TEST HOURS			
SAMPLE SIZE	PROPERTY	New Oil	216	240	
TEST TEMP.					
O-77-6	Viscosity @40C, cSt	279.5	460.1	494.0	
	40C Visc Change, %		64.6	76.7	
	Viscosity @100C, cSt	---			
139.2 grams	100C Visc Change, %				
	Total Acid Number	---			
	% Insolubles				
320 C	Visual Appearance				
	of Deposits				
Test Variations					
Relative 100% Additive A added					
		CORROSION DATA, Wt. Change mg/cm			
		Test Hrs.	Al	Ag	M-St
		240	-0.08	-0.16	-0.04
					M-50
					Wasp
					Ti
					-0.12
TEST HOURS					
LUBRICANT	LUBRICANT	New Oil	48	48	
SAMPLE SIZE	PROPERTY				
TEST TEMP.					
O-77-6	Viscosity @40C, cSt	280.4	368.4	365.8	
	40C Visc Change, %		31.4	30.9	
	Viscosity @100C, cSt				
30.15 grams	100C Visc Change, %				
	Total Acid Number				
	% Insolubles				
320 C	Visual Appearance				
	of Deposits				
Test Variations					
25% Trichloroethylene added					
		CORROSION DATA, Wt. Change mg/cm			
		Test Hrs.	Al	Ag	M-St
		48	0.0	0.06	0.04
		48	0.0	-0.02	0.06
					M-50
					Wasp
					Ti
					0.02
					0.0
					0.02

CORROSION AND OXIDATION TEST DATA

LUBRICANT SAMPLE SIZE TEST TEMP.	LUBRICANT PROPERTY	New Oil	24	48	TEST HOURS				
O-77-6 144 grams 320 C	Viscosity @40C, cSt	278.7	449.3	4223.					
	40C Visc Change, %		61.2	1415.					
	Viscosity @100C, cSt	---							
	100C Visc Change, %								
	Total Acid Number	---							
	% Insolubles								
	Visual Appearance of Deposits								
Test Variations									
417 ppm of 1-5 um Sn powder added									
		Test Hrs.	Al	Ag	M-St	M-50	Wasp	T1	
		48	0.08	0.16	0.24	0.28	0.12	0.12	
TEST HOURS									
LUBRICANT SAMPLE SIZE TEST TEMP.	LUBRICANT PROPERTY	New Oil	72	144	240				
O-77-6 (a) 144 grams 320 C	Viscosity @40C, cSt	285.4	341.5	387.4	491.7				
	40C Visc Change, %		19.6	35.7	72.3				
	Viscosity @100C, cSt	---							
	100C Visc Change, %								
	Total Acid Number	---							
	% Insolubles								
	Visual Appearance of Deposits								
TEST HOURS									
CORROSION DATA, Wt. Change mg/cm									
		Test Hrs.	Al	Ag	M-St	M-50	Wasp	T1	
		240	0.10	-0.10	0.14	0.12	0.08	0.08	
CORROSION DATA, Wt. Change mg/cm									
Test Variations									
Relative 250% Additive A added									
		Test Hrs.	Al	Ag	M-St	M-50	Wasp	T1	
		240	0.10	-0.10	0.14	0.12	0.08	0.08	

(a) - heavy coke and inside blower

CORROSION AND OXIDATION TEST DATA

LUBRICANT SAMPLE SIZE TEST TEMP.	LUBRICANT PROPERTY	New Oil	72	144	240	TEST HOURS				
O-77-6 144 grams 320 C	Viscosity @40C, cSt	279.5	322.5	359.2	457.6					
	40C Visc Change, %		15.4	28.5	63.7					
	Viscosity @100C, cSt	---	---	---	---					
	100C Visc Change, %	---	---	---	---					
No Metal Specimens Relative 100% Additive A	Total Acid Number	---								
	% Insolubles	---								
	Visual Appearance of Deposits		none							
	Test Variations									
LUBRICANT SAMPLE SIZE TEST TEMP.	LUBRICANT PROPERTY	Test Hrs.	Al	Ag	M-St	M-50	Wasp	Ti	CORROSION DATA, Wt. Change mg/cm	
O-77-6 144 grams 320 C	Viscosity @40C, cSt	279.7	24	48						
	40C Visc Change, %		421.4	3461.						
	Viscosity @100C, cSt	---	50.7	1137.						
	100C Visc Change, %	---	---	49.61						
529 ppm SnO2 added	Total Acid Number	---	---	---						
	% Insolubles	---								
	Visual Appearance of Deposits		none							
	Test Variations									
CORROSION DATA, Wt. Change mg/cm										
Test Hrs.		Al	Ag	M-St	M-50	Wasp	Ti			
48		0.06	0.16	0.18	0.18	0.08	0.10			

CORROSION AND OXIDATION TEST DATA

LUBRICANT SAMPLE SIZE TEST TEMP.	LUBRICANT PROPERTY	New Oil	48	TEST HOURS				
0-77-6 30.25 grams 320 C	Viscosity @40C, cSt	280.5	371.4					
	40C Visc Change, %		32.45					
	Viscosity @100C, cSt							
	100C Visc Change, %							
	Total Acid Number							
	% Insolubles							
	Visual Appearance of Deposits							
Test Variations								
25% Tetrachloroethylene added								
		Test Hrs.	Al	Ag	M-St	M-50	Wasp	T1
		48	0.02	0.32	0.02	0.02	0.00	0.00
TEST HOURS								
0-77-6 (a) 36.5 grams 327 C	Viscosity @40C, cSt	New Oil	48					
	40C Visc Change, %	276.2	472.2					
	Viscosity @100C, cSt	12.52	70.9					
	100C Visc Change, %		15.75					
	Total Acid Number	0.00	25.7					
	% Insolubles	---	0.00					
	Visual Appearance of Deposits		---					
TEST HOURS								
		New Oil	48					
		276.2	472.2					
		12.52	70.9					
		100C Visc Change, %	15.75					
		Total Acid Number	25.7					
		% Insolubles	---					
		Visual Appearance of Deposits	none					
TEST HOURS								
CORROSION DATA, Wt. Change mg/cm								
		Test Hrs.	Al	Ag	M-St	M-50	Wasp	T1
		48	-0.04	-0.02	0.02	0.00	-0.04	-0.020
CORROSION DATA, Wt. Change mg/cm								
Squires Tube								
		Test Hrs.	Al	Ag	M-St	M-50	Wasp	T1
		48	-0.04	-0.02	0.02	0.00	-0.04	-0.020

(a) - RI @25 C = 1.6321 new= 1.6290

CORROSION AND OXIDATION TEST DATA

LUBRICANT	LUBRICANT	TEST HOURS				
SAMPLE SIZE	PROPERTY	New Oil	48	144	240	312
TEST TEMP.	Viscosity @40C, cSt	291.2	308.8	334.4	362.5	381.9
TEL-8039	40C Visc Change, %		6.0	14.8	24.5	31.1
(a)	Viscosity @100C, cSt	12.77	13.05	13.49	13.92	14.06
140 grams	100C Visc Change, %		2.2	5.6	9.0	12.1
	Total Acid Number	00.00	00.09	---	---	---
320 C	% Insolubles					
	Visual Appearance					
	of Deposits					
CORROSION DATA, Wt. Change mg/cm						
	Test Hrs.	Al	Ag	M-St	M-50	Wasp
	312	0.00	0.02	0.24	0.10	0.00
						Ti
						0.04
LUBRICANT	LUBRICANT	TEST HOURS				
SAMPLE SIZE	PROPERTY	New Oil	336	360	384	408
TEST TEMP.	Viscosity @40C, cSt	291.2	393.9	401.3	412.7	421.7
TEL-8039	40C Visc Change, %		35.3	37.8	41.7	44.8
(b)	Viscosity @100C, cSt	12.77	14.53	14.69	14.87	
140 grams	100C Visc Change, %		13.8	15.0	16.4	17.1
	Total Acid Number	---				
320 C	% Insolubles					
	Visual Appearance					
	of Deposits					
CORROSION DATA, Wt. Change mg/cm						
	Test Hrs.	Al	Ag	M-St	M-50	Wasp
	408	-0.02	-0.04	0.16	0.04	-0.04
						Ti
						0.00

(a) - RI 1.6283@26.8 C; 1.6284 @26.8C; 1.6294 @25.9C; 1.6299 @25.8C

(b) - RI 1.6301@26 C; 1.6201@26.4 C; 1.6300@26.8 C; 1.6301,27 C

CORROSION AND OXIDATION TEST DATA

LUBRICANT	LUBRICANT	TEST HOURS					
SAMPLE SIZE	PROPERTY	New Oil	24	48	72	96	120
TEST TEMP.							
TEL-8039	Viscosity @40C, cSt	291.2	312.3	336.2	353.7	376.0	393.7
(a)	40C Visc Change, %		7.2	15.4	21.5	29.0	35.2
135.9 grams	Viscosity @100C, cSt	12.77	13.27	13.53	13.97	14.25	
	100C Visc Change, %		3.9	6.0	9.4	11.6	14.4
330 C	Total Acid Number	---					
	% Insolubles						
	Visual Appearance						
	of Deposits						

CORROSION DATA, Wt. Change mg/cm

Test Hrs.	Al	Ag	M-St	M-50	Wasp	Ti
-----------	----	----	------	------	------	----

LUBRICANT	LUBRICANT	TEST HOURS					
SAMPLE SIZE	PROPERTY	New Oil	168	192			
TEST TEMP.							
TEL-8039	Viscosity @40C, cSt	291.2	421.3	433.7			
(b)	40C Visc Change, %		44.7	48.9			
135.9 grams	Viscosity @100C, cSt	12.77	14.94	15.05			
330 C	100C Visc Change, %		17.0	17.8			
	Total Acid Number	---					
	% Insolubles						
	Visual Appearance						
	of Deposits						

CORROSION DATA, Wt. Change mg/cm

Test Hrs.	Al	Ag	M-St	M-50	Wasp	Ti
192	0.02	0.10	0.16	0.06	0.02	0.02

(a) - RI @24 h 1.6289/48 1.6292/192 1.6309

(b) - RI @192 h 1.6309 @25 C

CORROSION AND OXIDATION TEST DATA

LUBRICANT	LUBRICANT	TEST HOURS						
SAMPLE SIZE	PROPERTY	New Oil	48	144	240	264	312	
TEST TEMP.								
TEL-8040 (a) 140 grams 320 C	Viscosity @40C, cSt	287.9	310.7	335.8	363.0	366.2	382.2	
	40C Visc Change, %		7.9	16.6	26.1	27.2	32.8	
	Viscosity @100C, cSt	12.79	13.09	13.56	13.95	14.01		
	100C Visc Change, %		2.3	6.0	9.1	9.5	11.3	
	Total Acid Number	00.00	00.30					
	% Insolubles							
	Visual Appearance of Deposits							
CORROSION DATA, Wt. Change mg/cm								
	Test Hrs.	Al	Ag	M-St	M-50	Wasp	Ti	
	312	0.04	0.24	0.30	0.08	0.02	0.04	
LUBRICANT	LUBRICANT	TEST HOURS						
SAMPLE SIZE	PROPERTY	New Oil	336	360	384	408		
TEST TEMP.								
TEL-8040 (b) 140 grams 320 C	Viscosity @40C, cSt	287.9	407.0	412.3	424.6	433.0		
	40C Visc Change, %		41.4	43.2	47.5	50.4		
	Viscosity @100C, cSt	12.79	14.76	14.83	15.01			
	100C Visc Change, %		15.4	15.9	17.4	18.8		
	Total Acid Number	---						
	% Insolubles							
	Visual Appearance of Deposits							
CORROSION DATA, Wt. Change mg/cm								
	Test Hrs.	Al	Ag	M-St	M-50	Wasp	Ti	
	408	-0.04	0.02	0.02	0.08	0.00	0.00	

(a) - RI @ 0 h 1.6278@26.8 C 312 hrs 1.6301@25.8 C

(b) - RI @ 312 hrs 1.6301@26.2 C 408hrs 1.6303 @27.0 C

LUBRICANT SAMPLE SIZE TEST TEMP.	LUBRICANT PROPERTY	TEST HOURS					
		New Oil	24	48	72	96	120
TEL-8040	Viscosity @40C, cSt	287.9	310.9	327.6	341.3	355.6	367.5
	40C Visc Change, %		8.0	13.8	18.5	23.5	27.6
	Viscosity @100C, cSt	12.79	13.18	13.53	13.73	13.90	
	100C Visc Change, %		3.0	5.8	7.3	8.7	10.2
119.7 grams	Total Acid Number	---					
	% Insolubles						
330 C	Visual Appearance						
	of Deposits						
CORROSION DATA, Wt. Change mg/cm							
		Test Hrs.	Al	Ag	M-St	M-50	Wasp
							T1
LUBRICANT SAMPLE SIZE TEST TEMP.	LUBRICANT PROPERTY	TEST HOURS					
		New Oil	168	192			
TEL-8040	Viscosity @40C, cSt	287.9	388.3	399.4			
	40C Visc Change, %		34.9	38.7			
	Viscosity @100C, cSt	12.79	14.41	14.54			
	100C Visc Change, %		12.7	13.7			
119.7 grams	Total Acid Number	---					
	% Insolubles						
330 C	Visual Appearance						
	of Deposits						
CORROSION DATA, Wt. Change mg/cm							
		Test Hrs.	Al	Ag	M-St	M-50	Wasp
		192	0.04	0.18	0.24	0.10	-0.04
							T1
							0.00

CORROSION AND OXIDATION TEST DATA

LUBRICANT SAMPLE SIZE TEST TEMP.	LUBRICANT PROPERTY	New Oil	120	218	288	337	TEST HOURS
TEL-8085 (a)	Viscosity @40C, cSt	287.3	337.5	362.7	383.0	399.1	
	40C Visc Change, %		17.5	26.2	33.3	38.9	
132.9 grams	Viscosity @100C, cSt	12.76	13.62	14.01	14.41	14.61	
	100C Visc Change, %		6.7	9.8	12.9	14.5	
320 C	Total Acid Number	---					
	% Insolubles	---					
	Visual Appearance of Deposits		none				
CORROSION DATA, Wt. Change mg/cm							
	Test Hrs.	Al	Ag	M-St	M-50	Wasp	Ti
	337	0.18	0.18	0.34	0.24	0.18	0.20
LUBRICANT SAMPLE SIZE TEST TEMP.	LUBRICANT PROPERTY	New Oil	48	96	168	216	240
TEL-8035 (b)	Viscosity @40C, cSt	287.3	306.7	327.0	362.5	390.2	408.0
	40C Visc Change, %		6.8	13.8	26.2	35.8	42.0
133 grams	Viscosity @100C, cSt	12.76	13.03	13.39	14.02	14.50	
	100C Visc Change, %		2.1	4.9	9.9	13.6	15.7
330 C	Total Acid Number	---					
	% Insolubles						
	Visual Appearance of Deposits						
CORROSION DATA, Wt. Change mg/cm							
	Test Hrs.	Al	Ag	M-St	M-50	Wasp	Ti
	240	0.00	-0.04	0.26	0.14	0.04	0.06

(a) - Amber - clear

(b) - sample was partly cloudy when test was initiated

CORROSION AND OXIDATION TEST DATA

LUBRICANT	LUBRICANT PROPERTY	TEST HOURS				
SAMPLE SIZE	TEST TEMP.	New Oil	24	48	72	96
TEL-8085	Viscosity @40C, cSt	287.3	309.1	331.2	354.6	377.6
	40C Visc Change, %		7.6	15.2	23.4	31.4
	Viscosity @100C, cSt	12.67	13.12	13.50	13.75	14.27
	100C Visc Change, %		2.8	5.8	7.8	11.8
134.3 grams	Total Acid Number	---				
	% Insolubles					
	Visual Appearance of Deposits					
CORROSION DATA, Wt. Change mg/cm						
	Test Hrs.	Al	Ag	M-St	M-50	Wasp
	96	0.00	-0.06	0.20	0.10	0.00
						Ti
						0.02
LUBRICANT	LUBRICANT PROPERTY	TEST HOURS				
SAMPLE SIZE	TEST TEMP.	New Oil	120	218	288	337
TEL-8087	Viscosity @40C, cSt	280.5	324.3	346.7	365.0	377.6
	40C Visc Change, %		15.6	23.6	30.1	34.6
	Viscosity @100C, cSt	12.58	13.36	13.74	14.08	14.31
	100C Visc Change, %		6.2	9.2	11.9	13.8
132.9 grams	Total Acid Number	---				
	% Insolubles	---				
	Visual Appearance of Deposits		none			
CORROSION DATA, Wt. Change mg/cm						
	Test Hrs.	Al	Ag	M-St	M-50	Wasp
	337	0.18	0.20	0.38	0.24	0.16
						Ti
						0.18

(a) - Yellow - cloudy

CORROSION AND OXIDATION TEST DATA

LUBRICANT	LUBRICANT	TEST HOURS				
SAMPLE SIZE	PROPERTY	New Oil	24	48	72	
TEST TEMP.	Viscosity @40C, cSt	280.5	300.0	309.8	316.0	
TEL-8087	40C Visc Change, %		7.0	10.4	12.6	
(a)	Viscosity @100C, cSt	12.58	12.97	13.26	13.20	
140 grams	100C Visc Change, %		3.1	5.4	4.9	
320 C	Total Acid Number	---				
	% Insolubles	---				
	Visual Appearance	none				
	of Deposits					
CORROSION DATA, Wt. Change mg/cm						
	Test Hrs.	Al	Ag	M-St	Wasp	Ti
	72	0.06	0.30	0.08	-0.02	-0.04
LUBRICANT	LUBRICANT	TEST HOURS				
SAMPLE SIZE	PROPERTY	New Oil	24	48	72	96
TEST TEMP.	Viscosity @40C, cSt	280.5	314.6	339.3	366.9	390.4
TEL-8037	40C Visc Change, %		12.1	21.1	30.7	39.2
	Viscosity @100C, cSt	12.58	13.19	13.60	14.13	14.51
140.5 grams	100C Visc Change, %		4.8	8.1	12.3	15.3
340 C	Total Acid Number					
	% Insolubles					
	Visual Appearance					
	of Deposits					
CORROSION DATA, Wt. Change mg/cm						
	Test Hrs.	Al	Ag	M-St	Wasp	Ti
	96	-0.02	-0.10	0.22	0.08	-0.02

(a) - no drop out of additive noted after 2 weeks

CORROSION AND OXIDATION TEST DATA

LUBRICANT	LUBRICANT	TEST HOURS							
SAMPLE SIZE	PROPERTY	New Oil	24	48	72	96	122	144	
TEST TEMP.	Viscosity @40C, cSt	280.3	301.7	312.8	326.6	346.5	360.9	384.1	
TEL-8092	40C Visc Change, %		7.6	11.6	16.5	23.6	28.8	37.0	
(a)	Viscosity @100C, cSt	---							
144.8 grams	100C Visc Change, %								
	Total Acid Number	---							
320 C	% Insolubles								
	Visual Appearance								
	of Deposits								
CORROSION DATA, Wt. Change mg/cm									
	Test Hrs.	Al	Ag	M-St	M-50	Wasp	Ti		
	72	0.00	-0.08	0.04	0.02	-0.04	-0.04		
LUBRICANT	LUBRICANT	TEST HOURS							
SAMPLE SIZE	PROPERTY	New Oil	168	192	216	240			
TEST TEMP.	Viscosity @40C, cSt	280.3	411.4	434.1	455.2	495.3			
TEL-8092	40C Visc Change, %		46.8	54.9	62.4	76.7			
(b)	Viscosity @100C, cSt	---							
136.3 grams	100C Visc Change, %								
	Total Acid Number	---							
320 C	% Insolubles								
	Visual Appearance								
	of Deposits								
CORROSION DATA, Wt. Change mg/cm									
	Test Hrs.	Al	Ag	M-St	M-50	Wasp	Ti		
	192	0.08	0.06	0.16	0.10	0.06	0.08		
	240	-0.06	-0.14	-0.02	-0.06	-0.10	+0.00		

(a) - 24-144 hrs coke on blower tube

(b) - 168-240 hrs coke on blower

CORROSION AND OXIDATION TEST DATA

LUBRICANT	LUBRICANT	TEST HOURS							
SAMPLE SIZE	PROPERTY	New Oil	24	48	72	96	120	144	
TEL-8092 (a) 133.6 grams	Viscosity @40C, cSt	280.3	312.2	331.3	356.1	385.5	431.6	484.4	
	40C Visc Change, %		11.4	18.2	27.0	37.5	54.0	72.8	
	Viscosity @100C, cSt	12.55	13.21	13.59	14.11	14.63		16.23	
	100C Visc Change, %		5.3	8.3	12.4	16.6	22.3	29.3	
	Total Acid Number	---							
330 C	% Insolubles								
	Visual Appearance of Deposits								
CORROSION DATA, Wt. Change mg/cm									
Test Hrs.	Al	Ag	M-St	M-50	Wasp	Ti			
144	0.00	0.02	0.08	0.02	0.00	0.02			
LUBRICANT	LUBRICANT	TEST HOURS							
SAMPLE SIZE	PROPERTY	New Oil	24	48	72				
TEL-8092 136.2 grams	Viscosity @40C, cSt	280.3	328.1	375.2	478.8				
	40C Visc Change, %		17.0	33.9	70.8				
	Viscosity @100C, cSt	12.55	13.52	14.45	16.00				
	100C Visc Change, %		7.7	15.1	27.5				
	Total Acid Number	---							
340 C	% Insolubles								
	Visual Appearance of Deposits								
CORROSION DATA, Wt. Change mg/cm									
Test Hrs.	Al	Ag	M-St	M-50	Wasp	Ti			
72	0.00	-0.04	0.10	0.06	0.00	-0.02			

(a) - RI @ 24 h 1.6285 @ 26.3 C / @ 48 h 1.6290 @ 26.4 C

LUBRICANT	SAMPLE SIZE	LUBRICANT	TEST HOURS
TEST TEMP.	PROPERTY	New Oil	24
TEL-90001 (a) 125.4 grams 320 C	Viscosity @40C, cSt	235.4	+++++
	40C Visc Change, %		+++++
	Viscosity @100C, cSt	16.25	
	100C Visc Change, %		
	Total Acid Number		
	% Insolubles		
	Visual Appearance		
	of Deposits		
CORROSION DATA, Wt. Change mg/cm			
Test Hrs.	Al	Ag	M-St
24	0.10	-5.78	0.08
			Wasp
			Ti
			0.12
LUBRICANT	LUBRICANT	TEST HOURS	
SAMPLE SIZE	PROPERTY	New Oil	24
TEST TEMP.		195.4	238.9
TEL-90024 (b) 342.6 grams 320 C	Viscosity @40C, cSt	313.7	375.7
	40C Visc Change, %	60.5	92.3
	Viscosity @100C, cSt		
	100C Visc Change, %		
	Total Acid Number	0.13	0.37
	% Insolubles		
	Visual Appearance		
	of Deposits		
CORROSION DATA, Wt. Change mg/cm			
Test Hrs.	Al	Ag	M-St
24	0.04	-0.10	0.00
			Wasp
			Ti
			0.02

(a) - OIL TOO THICK TO TEST AFTER 24 HRS.
(b) - COKE ON BLOWER AND ABOVE OIL LEVEL

CORROSION AND OXIDATION TEST DATA

LUBRICANT	LUBRICANT	TEST HOURS			
SAMPLE SIZE	PROPERTY	New Oil	48		
TEST TEMP.					
TEL-90025	Viscosity @40C, cSt	288.3	329.8		
(a)	40C Visc Change, %		14.4		
29.02 grams	Viscosity @100C, cSt				
	100C Visc Change, %				
320 C	Total Acid Number		0.033		
	% Insolubles				
	Visual Appearance		NO COKE		
	of Deposits				
CORROSION DATA, Wt. Change mg/cm					
	Test Hrs.	Al	Ag	M-St	M-50
	48	0.02	0.06	0.06	0.02
					Ti
					0.02

(a) - USED ENGINE OIL

LUBRICANT SAMPLE SIZE TEST TEMP.	LUBRICANT PROPERTY	New Oil	48	TEST HOURS
TEL-90025 (a) 30 grams	Viscosity @40C, cSt	289.3	330.2	
	40C Visc Change, %		14.1	
	Viscosity @100C, cSt			
	100C Visc Change, %			
	Total Acid Number		0.196	
320 C	% Insolubles			
	Visual Appearance of Deposits		NO COKE	
<u>Test Variations</u>				
3 micron filtered				
		CORROSION DATA, Wt. Change mg/cm		
	Test Hrs.	Al	M-St	Wasp
	48	0.04	0.10	0.02
			0.04	0.04
				Ti
				0.06
LUBRICANT SAMPLE SIZE TEST TEMP.	LUBRICANT PROPERTY	New Oil	48	TEST HOURS
TEL-90026 (b) 31 grams	Viscosity @40C, cSt	289.3	342.2	
	40C Visc Change, %		18.3	
	Viscosity @100C, cSt			
	100C Visc Change, %			
	Total Acid Number		0.10	
320 C	% Insolubles			
	Visual Appearance of Deposits		SLIGHT COKE AND SLUDGE	
		CORROSION DATA, Wt. Change mg/cm		
	Test Hrs.	Al	M-St	Wasp
	48	0.0	0.06	0.0
			0.02	0.06
				Ti
				0.06

467

CORROSION AND OXIDATION TEST DATA

LUBRICANT	LUBRICANT	TEST HOURS			
SAMPLE SIZE	PROPERTY	New Oil	48		
TEST TEMP.	Viscosity @40C, cSt	292.1	344.5		
TEL-90026	40C Visc Change, %		17.9		
(a)	Viscosity @100C, cSt				
29.6 grams	100C Visc Change, %				
320 C	Total Acid Number		0.10		
	% Insolubles				
	Visual Appearance		SLIGHT		
	of Deposits		COKE AND		
			SLUDGE		
<u>Test Variations</u>					
3 micron filtered		CORROSION DATA, Wt. Change mg/cm			
		Test Hrs.	Al	Ag	M-St
		48	0.02	0.04	0.06
					M-50
					Wasp
					Ti
					0.0
<u>TEST HOURS</u>					
LUBRICANT	LUBRICANT	New Oil	24	48	72
SAMPLE SIZE	PROPERTY	1468	1613	1681	1699
TEST TEMP.	Viscosity @40C, cSt		9.9	14.6	15.7
TEL-90026	40C Visc Change, %				20.4
	Viscosity @100C, cSt				30.9
123.9 grams	100C Visc Change, %				
310 C	Total Acid Number				
	% Insolubles				
	Visual Appearance				
	of Deposits				
<u>CORROSION DATA, Wt. Change mg/cm</u>					
		Test Hrs.	Al	Ag	M-St
		144	0.00	-0.04	0.02
					M-50
					Wasp
					Ti
					0.02

(a) - USED ENGINE OIL

CORROSION AND OXIDATION TEST DATA

LUBRICANT	LUBRICANT PROPERTY	New Oil	48	72	92	TEST HOURS
SAMPLE SIZE	Viscosity @40C, cSt	1468	1780	1828	1935	
TEST TEMP.	40C Visc Change, %	21.2	24.5	31.7		
TEL-90028	Viscosity @100C, cSt					
122.1 grams	100C Visc Change, %					
320 C	Total Acid Number					
	% Insolubles					
	Visual Appearance of Deposits					
CORROSION DATA, Wt. Change mg/cm						
Test Hrs.	Al	Ag	M-St	M-50	Wasp	Ti
92	-0.06	-0.08	0.00	0.00	-0.04	-0.02
LUBRICANT	LUBRICANT PROPERTY	New Oil	24	48	TEST HOURS	
SAMPLE SIZE	Viscosity @40C, cSt	195.4	299.9	SOLID		
TEST TEMP.	40C Visc Change, %	53.5	N/A			
TEL-90059	Viscosity @100C, cSt					
(a)	100C Visc Change, %					
134.9 grams	Total Acid Number					
310 C	% Insolubles					
	Visual Appearance of Deposits		COKE RING	HEAVY COKE		
CORROSION DATA, Wt. Change mg/cm						
Test Hrs.	Al	Ag	M-St	M-50	Wasp	Ti
48	0.08	-0.98	0.04	0.04	0.04	0.38

(a) - HEAVY COKING

CORROSION AND OXIDATION TEST DATA

LUBRICANT SAMPLE SIZE TEST TEMP.	LUBRICANT PROPERTY	New Oil	24	48	70.	119	TEST HOURS
TEL-90059 (a)	Viscosity @40C, cSt	195.4	241.9	371.1	397.3	---	
	40C Visc Change, %		23.8	89.9	103.3		
117.1 grams	Viscosity @100C, cSt						
	100C Visc Change, %						
320 C	Total Acid Number	.01	.16	0.59	1.45		
	% Insolubles						
	Visual Appearance of Deposits						
CORROSION DATA, Wt. Change mg/cm							
	Test Hrs.	Al	Ag	M-St	M-50	Wasp	Ti
	24	2.7	1.06	-43.86	-63.0	0.30	-6.84
LUBRICANT SAMPLE SIZE TEST TEMP.	LUBRICANT PROPERTY	New Oil	24	27	TEST HOURS		
TEL-90059	Viscosity @40C, cSt	195.4	320.2	375.5			
	40C Visc Change, %		63.9	92.2			
119.4 grams	Viscosity @100C, cSt						
	100C Visc Change, %						
330 C	Total Acid Number						
	% Insolubles						
	Visual Appearance of Deposits			COKE RING AT TOP OF TUBE			
CORROSION DATA, Wt. Change mg/cm							
	Test Hrs.	Al	Ag	M-St	M-50	Wasp	Ti
	27	0.02	-0.04	-0.04	0.06	-0.02	0.08

(a) - TOTAL COKE IN TUBE WHITE RING AT TOP OF TUBE AT END OF TEST

CORROSION AND OXIDATION TEST DATA

LUBRICANT	LUBRICANT	TEST HOURS				
SAMPLE SIZE	PROPERTY	New Oil	24	48	72	
TEST TEMP.						
TEL-90063	Viscosity @40C, cSt	215.4	233.5	326.2	N/A	
	40C Visc Change, %		8.4	51.4	N/A	
	Viscosity @100C, cSt					
	100C Visc Change, %					
140.8 grams	Total Acid Number	0.02	0.27	2.87	N/A	
310 C	% Insolubles					
	Visual Appearance of Deposits		NONE	HEAVY COK E, FROST ON GLASS	SOLID OIL	
CORROSION DATA, Wt. Change mg/cm						
	Test Hrs.	Al	Ag	M-St	M-50	Ti
	72	0.02	-7.56	0.14	0.14	0.16
LUBRICANT						
SAMPLE SIZE						
TEST TEMP.						
TEL-90063	Viscosity @40C, cSt	New Oil	24	48	50	
	40C Visc Change, %	215.4	237.7	452.6	N/A	
	Viscosity @100C, cSt		10.4	110.1	N/A	
	100C Visc Change, %					
139.6 grams	Total Acid Number	0.02	0.162	4.858	N/A	
320 C	% Insolubles					
	Visual Appearance of Deposits		DK. BROWN STR. SMEL L	BLACK W/ RESIDUE D	TEST TERMINATE	
CORROSION DATA, Wt. Change mg/cm						
	Test Hrs.	Al	Ag	M-St	M-50	Ti
	50	0.04	-4.52	0.04	0.02	0.0

CORROSION AND OXIDATION TEST DATA

LUBRICANT	LUBRICANT	TEST HOURS				
SAMPLE SIZE	PROPERTY	New Oil	24			
TEST TEMP.						
TEL-90063 (a) 67.61 grams 330 C	Viscosity @40C, cSt	215.4	276.7			
	40C Visc Change, %		28.5			
	Viscosity @100C, cSt	10.81	13.64			
	100C Visc Change, %		26.1			
	Total Acid Number	0.02	0.65			
	% Insolubles					
	Visual Appearance of Deposits					
CORROSION DATA, Wt. Change mg/cm						
	Test Hrs.	Al	Ag	M-St	M-50	Wasp
	24	0.02	-0.66	0.02	0.02	-0.02
						Ti
						0.04
TEST HOURS						
TEL-90102 (b) 32.4 grams 320 C	Viscosity @40C, cSt	New Oil	48			
	40C Visc Change, %	282.9	407.7			
	Viscosity @100C, cSt		44.08			
	100C Visc Change, %	12.77	15.17			
	Total Acid Number	NA	18.79			
	% Insolubles	NA	NA			
	Visual Appearance of Deposits	M-St adn	M-50			
		black				
CORROSION DATA, Wt. Change mg/cm						
	Test Hrs.	Al	Ag	M-St	M-50	Wasp
	48	0.04	0.0	0.14	0.10	0.08
						Ti
						0.04

(a) - INITIAL OIL APPEARED DARK

(b) - blk. deposits located at half in. from oil surface

CORROSION AND OXIDATION TEST DATA

LUBRICANT	LUBRICANT	TEST HOURS				
SAMPLE SIZE	PROPERTY	New Oil	48	72		
TEST TEMP.	Viscosity @40C, cSt	298.0	361.0	424.4		
TEL-9028	40C Visc Change, %		21.1	42.4		
(a)	Viscosity @100C, cSt	12.95	14.07	15.22		
123.5 grams	100C Visc Change, %		8.6	17.5		
320 C	Total Acid Number					
	% Insolubles					
	Visual Appearance of Deposits					
Test Variations						
Solvent evaporated before testing						
		CORROSION DATA, Wt. Change mg/cm				
		Test Hrs.	Al	Ag	M-St	M-50
		72	0.08	-0.68	0.08	0.02
						0.04
						Wasp
						Tl
LUBRICANT						
SAMPLE SIZE	LUBRICANT	TEST HOURS				
TEST TEMP.	PROPERTY	New Oil	48	72		
TEL-9029	Viscosity @40C, cSt	284.9	382.7	463.5		
(b)	40C Visc Change, %		34.3	62.7		
115 grams	Viscosity @100C, cSt	12.71	14.93	15.85		
320 C	100C Visc Change, %		17.4	24.7		
	Total Acid Number	---				
	% Insolubles	---				
	Visual Appearance of Deposits		none			
CORROSION DATA, Wt. Change mg/cm						
		Test Hrs.	Al	Ag	M-St	M-50
		72	0.02	0.02	0.04	0.06
						0.02
						0.02
						Tl

(a) - USED ENGINE OIL

(b) - tube, coke at oil level/blower, mod. coke in - residue out

LUBRICANT	LUBRICANT PROPERTY	TEST HOURS
SAMPLE SIZE	New Oil	48
TEST TEMP.	283.7	717.4
TEL-9030	Viscosity @40C, cSt	152.9
(a)	40C Visc Change, %	19.73
118.1 grams	Viscosity @100C, cSt	54.7
	100C Visc Change, %	---
320 C	Total Acid Number	---
	% Insolubles	none
	Visual Appearance	
	of Deposits	
CORROSION DATA, Wt. Change mg/cm		
	Test Hrs.	Al Ag M-St Wasp Ti
	48	0.04 -0.16 0.08 0.04 0.00
LUBRICANT	LUBRICANT PROPERTY	TEST HOURS
SAMPLE SIZE	New Oil	48
TEST TEMP.	280.3	381.1
TEL-9030	Viscosity @40C, cSt	35.9
(b)	40C Visc Change, %	14.48
32.7 grams	Viscosity @100C, cSt	14.8
	100C Visc Change, %	---
320 C	Total Acid Number	---
	% Insolubles	---
	Visual Appearance	
	of Deposits	
CORROSION DATA, Wt. Change mg/cm		
	Test Hrs.	Al Ag M-St Wasp Ti
	48	0.00 0.06 0.02 0.00 -0.02
3 micron filtered		

(a) - tube,sludge coke at oil level/blower,coke & sludge in & out
(b) - USED ENGINE OIL

CORROSION AND OXIDATION TEST DATA

LUBRICANT	LUBRICANT PROPERTY	New Oil	48	72	TEST HOURS
SAMPLE SIZE	Viscosity @40C, cSt	288.4	403.8	682.1	
TEST TEMP.	40C Visc Change, %		40.0	136.5	
TEL-9038	Viscosity @100C, cSt	12.75	14.97	19.25	
(a)	100C Visc Change, %		17.40	51.0	
124.1 grams	Total Acid Number				
320 C	% Insolubles				
	Visual Appearance of Deposits			RI@23C @ 25C 1.6292 1.6286	
CORROSION DATA, Wt. Change mg/cm					
	Test Hrs.	Al	Ag	M-St	M-50 Wasp Ti
	72	0.02	0.44	0.14	0.10 0.08 -0.02
LUBRICANT	LUBRICANT PROPERTY	New Oil	48	TEST HOURS	
SAMPLE SIZE	Viscosity @40C, cSt	298.1	338.6		
TEST TEMP.	40C Visc Change, %		13.6		
TEL-9039	Viscosity @100C, cSt	12.92	13.71		
(b)	100C Visc Change, %		6.1		
29.9 grams	Total Acid Number	---			
320 C	% Insolubles	---			
	Visual Appearance of Deposits				
CORROSION DATA, Wt. Change mg/cm					
	Test Hrs.	Al	Ag	M-St	M-50 Wasp Ti
	48	0.02	0.02	0.06	0.04 0.02 0.02
Test Variations					
Solvent evaporated before testing					

(a) - HEAVY SLUDGE AND POLYMERIC GLOBS AT END OF TEST
 (b) - tube, stain/blower, varnish

CORROSION AND OXIDATION TEST DATA

LUBRICANT SAMPLE SIZE TEST TEMP.	LUBRICANT PROPERTY	New Oil	48	TEST HOURS				
TEL-9039	Viscosity @40C, cSt	215.6	337.3					
(a)	40C Visc Change, %		13.15					
36.03 grams	Viscosity @100C, cSt	11.76	13.80					
320 C	100C Visc Change, %		6.80					
	Total Acid Number	---						
	% Insolubles	---						
	Visual Appearance of Deposits							
CORROSION DATA, Wt. Change mg/cm								
	Test Hrs.	Al	Ag	M-St	M-50	Wasp	Ti	
	48	0.02	0.06	0.10	0.06	0.04	0.08	
LUBRICANT	LUBRICANT	TEST HOURS						
SAMPLE SIZE	PROPERTY	New Oil	48	72				
TEST TEMP.		217	386.0	514.8				
TEL-9039	Viscosity @40C, cSt		78.0	137.2				
(b)	40C Visc Change, %							
116.7 grams	Viscosity @100C, cSt	12.01	14.63	16.38				
320 C	100C Visc Change, %		21.8	227.2				
	Total Acid Number							
	% Insolubles							
	Visual Appearance of Deposits							
CORROSION DATA, Wt. Change mg/cm								
	Test Hrs.	Al	Ag	M-St	M-50	Wasp	Ti	
	48	0	0	0	0	0	0	
	72	0.06	-0.28	0.04	0.06	-0.02	0.06	

(a) - sediment in squires tube (Initial w/solvent)
 (b) - COKE/VARN @ OIL LEVEL GLOBLETS IN TUBE/ BRN RES. IN TUBE

CORROSION AND OXIDATION TEST DATA

LUBRICANT	LUBRICANT	TEST HOURS
SAMPLE SIZE	PROPERTY	
TEST TEMP.		
	New Oil	48
TEL-9040	Viscosity @40C, cSt	336.2
(a)	40C Visc Change, %	19.9
30.8 grams	Viscosity @100C, cSt	13.61
320 C	100C Visc Change, %	7.9
	Total Acid Number	
	% Insolubles	
	Visual Appearance	SLIGHT
	of Deposits	COKE ON SLIGHT LEVEL
		BLOWER DEPOSIT
Test Variations		
3 micron filtered	CORROSION DATA, Wt. Change mg/cm	
	Test Hrs.	Al Ag M-St M-50 Wasp Ti
	48	0.00 -0.020 0.02 0.04 -0.02 0.00
LUBRICANT	LUBRICANT	TEST HOURS
SAMPLE SIZE	PROPERTY	
TEST TEMP.		
	New Oil	48 72
TEL-9040	Viscosity @40C, cSt	293.7 474.2 1380
(b)	40C Visc Change, %	61.5 369.9
118.7 grams	Viscosity @100C, cSt	12.84 16.26 26.95
320 C	100C Visc Change, %	26.6 109.9
	Total Acid Number	
	% Insolubles	
	Visual Appearance	RI@ 23C RI@ 25C
	of Deposits	1.6295 1.6289
CORROSION DATA, Wt. Change mg/cm		
	Test Hrs.	Al Ag M-St M-50 Wasp Ti
	72	0.06 -0.22 0.08 0.10 0.02 0.02

(a) - USED ENGINE OIL

(b) - HEAVY SLUDGE/POLYMERIC MAT./BRN.RES ,COKE (MOD-HEAVY)

CORROSION AND OXIDATION TEST DATA

LUBRICANT	LUBRICANT	TEST HOURS									
SAMPLE SIZE	PROPERTY	New Oil	24	48	72	96	120	144			
TEL-9050	Viscosity @40C, cSt	214.3	227.0	237.4	249.9	266.7	285.4	309.2			
(a)	40C Visc Change, %		5.9	10.8	16.6	24.5	33.2	44.3			
139.6 grams	Viscosity @100C, cSt	10.88	11.37	11.89	12.58	13.38		15.20			
	100C Visc Change, %		4.5	9.3	15.6	23.0	32.0	39.7			
290 C	Total Acid Number	0.10	0.08	0.20	0.26	0.28	0.51	0.36			
	% Insolubles										
	Visual Appearance		none								VARNISH
	of Deposits										AND COKE
CORROSION DATA, Wt. Change mg/cm											
	Test Hrs.	Al	Ag	M-St	M-50	Wasp	Ti				
	144	0.00	0.06	0.06	0.02	0.06	0.04				
LUBRICANT	LUBRICANT	TEST HOURS									
SAMPLE SIZE	PROPERTY	New Oil	24	48	54						
TEL-9050	Viscosity @40C, cSt	214.3	239.4	304.3	336.1						
(b)	40C Visc Change, %		11.7	42.0	57.2						
142.1 grams	Viscosity @100C, cSt	10.88	11.91	14.64	---						
	100C Visc Change, %		9.5	34.6	---						
295 C	Total Acid Number	0.10	0.56	1.85	2.22						
	% Insolubles	---									
	Visual Appearance		none		HEAVY						
	of Deposits				COKE						
CORROSION DATA, Wt. Change mg/cm											
	Test Hrs.	Al	Ag	M-St	M-50	Wasp	Ti				
	54	0.10	-3.94	0.12	0.12	0.10	0.12				

(a) - RI 1.5111 @ 24 C/tube, varnish/ blower, coke in tube

(b) - tube, heavy coke above oil level/blower, heavily coked

CORROSION AND OXIDATION TEST DATA

LUBRICANT SAMPLE SIZE TEST TEMP.	LUBRICANT PROPERTY	New Oil	72	96	TEST HOURS
TEL-9050 (a) 141.2 grams 280 C	Viscosity @40C, cSt	214.3	261.8	292.5	102
	40C Visc Change, %		22.2	36.5	300.1
	Viscosity @100C, cSt	10.88	13.25	14.46	40.0
	100C Visc Change, %		21.8	32.9	14.76
	Total Acid Number	0.10	0.53	0.98	35.7
	% Insolubles				0.87
	Visual Appearance of Deposits	none			VARNISH AND COKE
CORROSION DATA, Wt. Change mg/cm					
Test Hrs.	Al	Ag	M-St	M-50	Wasp
102	0.04	-3.02	0.06	0.14	0.00
					-0.02
LUBRICANT SAMPLE SIZE TEST TEMP.	LUBRICANT PROPERTY	New Oil	24	48	TEST HOURS
TEL-9050 (b) 140.9 grams 280 C	Viscosity @40C, cSt	214.3	230.7	243.8	72
	40C Visc Change, %		7.7	13.8	296.8
	Viscosity @100C, cSt	10.88	11.58	12.46	38.5
	100C Visc Change, %		6.4	14.5	14.36
	Total Acid Number	0.10	0.22	0.72	32.0
	% Insolubles				1.12
	Visual Appearance of Deposits	None			1.34
					COKE
CORROSION DATA, Wt. Change mg/cm					
Test Hrs.	Al	Ag	M-St	M-50	Wasp
					Ti

(a) - tube, dk brn var above oil level/blower, heavy coke below spec

(b) - re-check of TEL-9050 a at 280 C

CORROSION AND OXIDATION TEST DATA

LUBRICANT SAMPLE SIZE TEST TEMP.	LUBRICANT PROPERTY	New Oil	24	48	TEST HOURS
TEL-9050 (a)	Viscosity @40C, cSt	214.3	299.4	297.8	343.7
	40C Visc Change, %		39.7	39.0	60.4
	Viscosity @100C, cSt	10.88	14.25	14.28	15.75
141.5 grams	100C Visc Change, %		8.9	31.3	44.8
	Total Acid Number	0.10	0.35	1.72	2.14
300 C	% Insolubles				
	Visual Appearance of Deposits		non		55.5 hours MOD. COKE COKE ON ON SIDES B. TUBE OIL LEVEL
CORROSION DATA, Wt. Change mg/cm					
	Test Hrs.	Al	Ag	M-St	Wasp
	55.	0.12	-3.78	0.12	0.14
					0.10
LUBRICANT SAMPLE SIZE TEST TEMP.	LUBRICANT PROPERTY	New Oil	48	TEST HOURS	
WT 359 (b)	Viscosity @40C, cSt	304/c	377.6		
	40C Visc Change, %		34.5		
	Viscosity @100C, cSt	13/c	14.49		
24.3 grams	100C Visc Change, %		14.9		
	Total Acid Number	---			
320 C	% Insolubles	---			
	Visual Appearance of Deposits		none		
CORROSION DATA, Wt. Change mg/cm					
	Test Hrs.	Al	Ag	M-St	Wasp
	48	0.00	-0.02	0.08	-0.02
					0.02

(a) - tube, coke above oil level/blower, considerable amt. of coke

(b) - same comment as (a) plus (c) WT 417 similar to WT 359

CORROSION AND OXIDATION TEST DATA

LUBRICANT	LUBRICANT	TEST HOURS
SAMPLE SIZE	PROPERTY	
TEST TEMP.		
WT 362	Viscosity @40C, cSt	New Oil 48
(a)	40C Visc Change, %	368.9
29.5 grams	Viscosity @100C, cSt	31.3
	100C Visc Change, %	14.28
	Total Acid Number	13.2
320 C	% Insolubles	---
	Visual Appearance	none
	of Deposits	
CORROSION DATA, Wt. Change mg/cm		
	Test Hrs.	Al Ag M-St M-50 Wasp Ti
	48	0.04 0.00 0.06 0.02 -0.02 0.02
LUBRICANT	LUBRICANT	TEST HOURS
SAMPLE SIZE	PROPERTY	
TEST TEMP.		
WT 382	Viscosity @40C, cSt	New Oil 48
(b)	40C Visc Change, %	280.5 323.8
30.4 grams	Viscosity @100C, cSt	15.4
	100C Visc Change, %	13.33
	Total Acid Number	5.7
320 C	% Insolubles	---
	Visual Appearance	
	of Deposits	
CORROSION DATA, Wt. Change mg/cm		
	Test Hrs.	Al Ag M-St M-50 Wasp Ti
	48	0.04 0.02 0.08 0.08 0.02 0.04

(a) - tube, slight residue/blower, coke in - slight residue out

(b) - tube, slight stain/blower, slight varnish (0-67-1)

CORROSION AND OXIDATION TEST DATA

LUBRICANT SAMPLE SIZE TEST TEMP.	LUBRICANT PROPERTY	New Oil	48	TEST HOURS				
WT 386 (a)	Viscosity @40C, cSt	280.5	325.3					
	40C Visc Change, %		16.0					
22.87 grams	Viscosity @100C, cSt	12.61	13.47					
	100C Visc Change, %		6.8					
320 C	Total Acid Number	---						
	% Insolubles	---						
	Visual Appearance of Deposits							
CORROSION DATA, Wt. Change mg/cm								
Test Hrs.	Al	Ag	M-St	M-50	Wasp	Ti		
48	0.04	-0.08	0.02	0.06	0.00	0.00		
LUBRICANT SAMPLE SIZE TEST TEMP.	LUBRICANT PROPERTY	New Oil	48	TEST HOURS				
WT 401 (b)	Viscosity @40C, cSt	280.5	343.7					
	40C Visc Change, %		22.5					
29.8 grams	Viscosity @100C, cSt	12.61	13.79					
	100C Visc Change, %		9.4					
320 C	Total Acid Number							
	% Insolubles							
	Visual Appearance of Deposits							
CORROSION DATA, Wt. Change mg/cm								
Test Hrs.	Al	Ag	M-St	M-50	Wasp	Ti		
48	0.00	0.00	0.04	0.02	0.00	0.00		

(a) - sample bareley covered top specimen (0-67-1)

(b) - slight coke on blower tube wear test #401

CORROSION AND OXIDATION TEST DATA

LUBRICANT SAMPLE SIZE TEST TEMP.	LUBRICANT PROPERTY	TEST HOURS				
		New Oil	---	48		
WT 388 30 grams 320 C	Viscosity @40C, cSt	280.5		306.0		
	40C Visc Change, %			9.0		
	Viscosity @100C, cSt	12.61		13.47		
	100C Visc Change, %			6.8		
	Total Acid Number					
	% Insolubles					
	Visual Appearance of Deposits					
CORROSION DATA, Wt. Change mg/cm						
	Test Hrs.	Al	Ag	M-St	M-50	Wasp
						Ti

TABLE A-5

AFAPL STATIC COKER TEST DATA

(Specimen Type Used : 1- Shim Stock, 2 - SS-302, 3 - Quartz, 4 - Brass, 5 - Pyrex, 6 - Aluminum)

Test #	Oil	Specimen	Temp, C	Time, Min	Size, in	Specimen eq/g Residue	Average	Std Dev	Seal eq/g Residue	Average	Std Dev	Total eq/g Residue	Average	Std Dev	Description of coke
1	0-77-6	1	375	180	0.12	30.74			0.6831						lt brown small dep
2	0-77-6	1	375	180	0.22	16.2			0.0						lt brown small dep
3	0-77-6	1	375	180	0.18	21.2			0.0						lt brown small dep
4	0-77-6	1	375	180	0.13	34.48	28.6		6.8	0.330		0.342			lt brown small dep
5	0-77-6	1	375	180	0.35	9.1									lt brown thin dep
6	0-77-6	1	375	180	0.38	8.4									lt brown thin dep
7	0-77-6	1	375	180	0.35	10.1									lt brown thin dep
8	0-77-6	1	375	180	0.33	8.7	9.1		0.7						lt brown thin dep
9	0-77-6	1	375	180	0.26	16.5			0.0						lt brown deposit
10	0-77-6	1	375	180	0.19	24.2			0.0						lt brown deposit
11	0-77-6	1	375	180	0.15	21.3			0.0						lt brown deposit
12	0-77-6	1	375	180	0.13	37.7	24.93		9.09	0.0	0.0				lt brown deposit
13	0-77-6	1	375	180	0.5				6.49						brown thin stain
14	0-77-6	1	375	180	0.5				3.92						brown thin stain
15	0-77-6	1	375	180	0.5				6.06						brown thin stain
16	0-77-6	1	375	180	0.5		6.5		0.4	5.85	1.33				brown thin stain
17	0-77-6	1	375	180	0.75	4									brown slight stain
18	0-77-6	1	375	180	0.75	4.7									brown slight stain
19	0-77-6	1	375	180	0.75	4.7									brown slight stain
20	0-77-6	1	375	180	0.75	5	4.6		0.4						brown slight stain
21	0-77-6 24H 320C	1	375	180	0.75	17.1			8.59						blk flak dk brn var
22	0-77-6 24H 320C	1	375	180	0.75	16.6			13.82						blk flak dk brn var
23	0-77-6 24H 320C	1	375	180	0.75	24.6			14.17						blk flak dk brn var
24	0-77-6 24H 320C	1	375	180	0.75	25.6	21		4.8	13.75	4.02				blk flak dk brn var
25	0-67-1	1	425	180	0.19	30.9									brown slight stain
26	0-67-1	1	425	180	0.25	24.4									brown slight stain
27	0-67-1	1	425	180	0.26	24									brown slight stain
28	0-67-1	1	425	180	0.22	33	28.1		4.6						brown slight stain
29	---	1	425	180											
30	---	1	425	180											
31	---	1	425	180											
32	---	1	425	180											
33	WATER TEST 370	1	425	180	0.2	43									lt brown small dep
34	WATER TEST 370	1	425	180	0.19	49.6									lt brown small dep
35	WATER TEST 370	1	425	180	0.19	41.3									lt brown small dep
36	WATER TEST 370	1	425	180	0.2	46.3	0.5		0.46						lt brown small dep
37	---	2	475	180											
38	---	2	425	180											

Test #	Oil	Spectraen	Temp, C	Time, Min	Size, µL	Specimen eq/g		Seal eq/g		Total eq/g		Description of coke	
						Average	Std Dev	Average	Std Dev	Average	Std Dev		
39	---	2	425	180									
40	---	2	425	180									
41	0-67-1	2	425	180	0.25								
42	0-67-1	2	425	180	0.25								
43	0-67-1	2	425	180	0.25								
44	0-67-1	2	425	180	0.25								
45	0-67-1	2	425	180	1	0.2						no coke or varnish	
46	0-67-1	2	425	180	1	0.2						no coke or varnish	
47	0-67-1	2	425	180	1	0.2						no coke or varnish	
48	0-67-1	2	425	180	1	0.2	0.2	0.0				no coke or varnish	
49	0-67-1	2	400	180	1	0.1						no coke or varnish	
50	0-67-1	2	400	180	1	0.1						no coke or varnish	
51	0-67-1	2	400	180	1	0.2						no coke or varnish	
52	0-67-1	2	400	180	1.5	0.1	0.13	0.05				no coke or varnish	
53	0-67-1	1	400	180	1	3.51		3.51				no dep, iron oxide	
54	0-67-1	1	400	180	1	3.54		3.54				no dep, iron oxide	
55	0-67-1	1	400	180	1	3.65	3.6	0.07	3.65	3.56	0.08	no dep, iron oxide	
56	---	1	400	180	1							no dep, iron oxide	
57	---	1	400	180									
58	---	1	400	180									
59	---	1	400	180									
60	---	1	375	180		2.4							
61	---	1	375	180		2.3							
62	---	1	375	180		2.7	2.47	0.21					
63	0-67-1	2	375	180	1							no dep, spec bronz	
64	0-67-1	2	375	180	1							no dep, spec bronz	
65	0-67-1	2	375	180	1							no dep, spec bronz	
66	0-67-1	2	375	180	1							no dep, spec bronz	
67	0-67-1	2	375	180	1	0.08							
68	0-67-1	2	375	180	1	0							
69	0-67-1	2	375	180	1	0							
70	0-67-1	2	375	180	1	0.08	0.04	0.04					
71	0-67-1 168H 320	2	375	180	1	10.92		1.62				brn stain and dep	
72	0-67-1 168H 320	2	375	180	1	9.58		1.68				brn stain and dep	
73	0-67-1 168H 320	2	375	180	1	9.1		1.65				brn stain and dep	
74	0-67-1 168H 320	2	375	180	1	9.52	9.87	0.53	1.63	1.64	0.03	brn stain and dep	
75	0-67-1 168H 320	2	375	180	0.5	9.23		3.30				brn coke to varnish	
76	0-67-1 168H 320	2	375	180	0.5	9.23		3.37				brn coke to varnish	

Test #	Oil	Specimen	Temp, C	Time, Min	Size, mL	Specimen ag/g			Seal ag/g			Total ag/g			Description of coke		
						Average	Std Dev	Residue	Average	Std Dev	Residue	Average	Std Dev	Residue			
77		0-67-1 168H 320	2	375	180	8.98		3.48	0.25	3.37	3.38	0.07			brn coke to varnish		
78		0-67-1 168H 320	2	375	180	8.7		3.37							brn coke to varnish		
79		0-67-1 168H 320	2	375	180	5.28		0.4							hard brown varnish		5.69
80		0-67-1 168H 320	2	375	180	3.56		2.4							hard brown varnish		5.94
81		0-67-1 168H 320	2	375	180	4.08		1.6							hard brown varnish		5.71
82		0-67-1 168H 320	2	375	180	4.04	4.24	0.73			1.3	0.89			hard brown varnish	0.48	5.54
83		0-67-1 168H 320	2	375	180	6.6		7.17							dk to lt brn deposit		13.8
84		0-67-1 168H 320	2	375	180	6.8		6.24							dk to lt brn deposit		13.2
85		0-67-1 168H 320	2	375	180	6.8		4							dk to lt brn deposit		13.3
86		0-67-1 168H 320	2	375	180	1.9		11.5			7.23	3.14			dk to lt brn deposit	0.26	13.43
87		0-67-1 240H 320	2	375	180	17.1		4.19							dk brn hard varnish		22
88		0-67-1 240H 320	2	375	180	8.4		5.13							non-uniform dep		13.5
89		0-67-1 240H 320	2	375	180	13.3		10.2							dk brn hard varnish		23.6
90		0-67-1 240H 320	2	375	180	15.6	15.32	7			7.4	2.7			dk brn hard varnish	4.66	20.43
91		0-67-1 240H 320	2	375	180	19.05		10.28							dk brn heavy var		29.33
92		0-67-1 240H 320	2	375	180	20.67		8.73							dk brn heavy var		29.41
93		0-67-1 240H 320	2	375	180	16.06		12.25							dk brn heavy var		28.32
94		0-67-1 240H 320	2	375	180	16	17.95	2.3			10.4	1.44			dk brn heavy var	1.4	26.36
95		0-67-1 240H 320	2	375	180	10.4		8.4							dk brn var, coke		18.8
96		0-67-1 240H 320	2	375	180	10		8.36							dk brn var, coke		18.4
97		0-67-1 240H 320	2	375	180	8.2	9.5	1.0			8.6	0.4			dk brn var, coke	0.7	17.2
98		0-67-1 240H 320	2	375	180	8		18.29							brown hard varnish		26.3
99		0-67-1 240H 320	2	375	180	10.4		13.08							brown hard varnish		23.5
100		0-67-1 240H 320	2	375	180	6		24.4							brown hard varnish		30.4
101		0-67-1 240H 320	2	375	180	7.7	8.0	1.6			17.7	5.0			brown hard varnish	3.0	22.7
102		0-67-1 168H 320	2	375	180	2.6		13.56							dk brn hard var, coke		16.1
103		0-67-1 168H 320	2	375	180	3.1		13.06							dk brn hard var, coke		16.1
104		0-67-1 168H 320	2	375	180	3.2		13.84							dk brn hard var, coke		17
105		0-67-1 168H 320	2	375	180	2	2.7	0.5			13.0	0.98			dk brn hard var, coke	1.3	13.6
106		TEL-9040	2	375	180	0.5		1.3							golden no deposit		1
107		TEL-9040	2	375	180	0.5		1.52							golden no deposit		1.1
108		TEL-9040	2	375	180	0.5		1.17							golden no deposit		0.8
109		TEL-9040	2	375	180	0.5	0.5	0.1			1.22	0.25			golden no deposit	0.18	0.7
110		TEL-9039	2	375	180	0.5		0.54							golden no deposit		0.5
111		TEL-9039	2	375	180	0.5	0.183								golden no deposit		0.8
112		TEL-9039	2	375	180	0.5	0.182								golden no deposit		0.6
113		TEL-9039	2	375	180	0.5	0.409	0.14			0.47	0.09			golden no deposit	0.15	0.8
114		CB-1 48H 320C	2	375	180	24.7		3.6							brn-blk flakey coke		28.3

Test #	0.1	Specimen	Temp, C	Size, Min	Size, Max	Specimen wt/g	Average	Std Dev	Residue	Seal wt/g	Average	Std Dev	Residue	Total wt/g	Average	Std Dev	Description of coke
115		CB-1 48H 320C	2	375	180	0.5	20.8			6.3			27.1				brn-blk flakey coke
116		CB-1 48H 320C	2	375	180	0.5	22			9.2			31.2				brn-blk flakey coke
117		CB-1 48H 320C	2	375	180	0.5	20.5	22.0	1.9	6.1	6.4	2.30	27.1	28.4	1.9		brn-blk flakey coke
118		CB-1 30H	2	375	180	0.5	1.7			0.57			2.3				varbrn-blk coke
118		48H 320	2	375	180	0.5	1.9			1.16			3.1				varbrn-blk coke
119		CB-1 30H	2	375	180	0.5	1.5			2.08			3.6				varbrn-blk coke
119		48H 320	2	375	180	0.5	2	1.8	0.2	1.47	1.9	1.75	3.5	3.1	0.5		varbrn-blk coke
120		CB-1 30H	2	375	180	0.5	0.2			1.24			1.41				slight brn deposit
120		48H 320	2	375	180	0.5	0.4			1.62			1.8				slight brn deposit
121		CB-1 30H	2	375	180	0.5	0.2			1.84			2.02				slight brn deposit
121		48H 320	2	375	180	0.5	0.2	0.25	0.1	1.77	1.6	0.27	1.77	1.75	0.25		slight brn deposit
122		TEL-9028	2	375	180	0.5	0.6			0			0.96				golden no coke
123		TEL-9028	2	375	180	0.5	1			0.38			1.36				golden no coke
124		TEL-9028	2	375	180	0.5	0.9	0.83	0.21	0.19	0.24	0.18	1.12	1.15	0.2		golden no coke
125		TEL-9028	2	375	180	0.5	0.18			0.37			0.56				golden no deposit
126		TEL-9029	2	375	180	0.5	0.16			0.5			0.67				golden no deposit
127		TEL-9029	2	375	180	0.5	0.0			0.17			0.35				golden no deposit
128		TEL-9029	2	375	180	0.5	0.0	0.2	0	0.66	0.4	0.2	0.66	0.6	0.14		golden no deposit
129		TEL-9030	2	375	180	0.5	0.2			1.56			1.73				golden slight var
130		TEL-9030	2	375	180	0.5	0.3			1.67			2				golden slight var
131		TEL-9030	2	375	180	0.5	0			1.5			1.32				golden slight var
132		TEL-9030	2	375	180	0.5	0.5	0.3	0.2	1.53	1.56	0.07	2.03	1.8	0.33		golden slight var
133		TEL-9030	2	375	180	0.5	0.36			0			0.72				slight orange powder
134		TEL-9038	2	375	180	0.5	0.68			0.51			1.18				slight orange powder
135		TEL-9038	2	375	180	0.5	0.69			0.34			1.19				slight orange powder
136		TEL-9038	2	375	180	0.5	0.37	0.5	0.18	0.55	0.4	0.25	0.92	1	0.22		slight orange powder
137		TEL-9038	2	375	180	0.5	0.2			0.0			0.2				slight orange powder
138		MEAN TEST 397	2	375	180	0.5	0.2			0.0			0.3				slight orange powder
139		MEAN TEST 397	2	375	180	0.5	0.2			0.0			0.3				slight orange powder
140		MEAN TEST 397	2	375	180	0.5	0.2			0.1			0.2				slight orange powder
141		MEAN TEST 397	2	375	180	0.5	0.2	0.2	0	0.0	0.04	0.09	0.2	0.04	0.09		slight orange powder
142		MEAN TEST 397	2	375	180	0.5	0.2			0.0			0.2				slight orange powder
143		MEAN TEST 397	2	375	180	0.5	0.2			0.0			0.2				slight orange powder
144		MEAN TEST 397	2	375	180	0.5	0.2			0.0			0.2				slight orange powder
145		MEAN TEST 397	2	375	180	0.5	0.2			0.0			0.2				slight orange powder
146		MEAN TEST 397	2	375	180	0.5	0.2			0.0			0.2				slight orange powder
147		MEAN TEST 397	2	375	180	0.5	0.2			0.0			0.2				slight orange powder
148		MEAN TEST 397	2	375	180	0.5	0.2			0.0			0.2				slight orange powder

Test #	Oil	Specimen	Temp, C	Time, Min	Size, mL	Specimen oil/g			Seal oil/g			Total oil/g			Description of coke		
						Average	Std Dev	Residue	Average	Std Dev	Residue	Average	Std Dev	Residue			
149	WEAK TEST 352	2	375	180	0.5	0.5	0.6	0.27							slight orange powder		
150	0-67-1	2	375	180	0.5	0.17			0.69			0.86			golden dep near seal		
151	0-67-1	2	375	180	0.5	0.5			0.68			1.19			golden dep near seal		
152	0-67-1	2	375	180	0.5	0.16			0			0.17			golden dep near seal		
153	0-67-1	2	375	180	0.5	0.28	0.19					0	0.34	0.40	golden dep near seal	0.56	
154	0-77-6	2	350	360	0.5	1.53			0.85						no deposit		
155	0-77-6	2	350	360	0.5	0			0.84			0.84			no deposit		
156	0-77-6	2	350	360	0.5	0.51			0.51			1.03			no deposit		
157	0-77-6	2	350	360	0.5	0	1	2.07	0.33	0.63	0.26	0.33			no deposit		
158	0-67-1	2	350	360	0.5	0.68			0.68			0.8			no deposit		
159	0-67-1	2	350	360	0.5	0.34			0.0			0.2			no deposit		
160	0-67-1	2	350	360	0.5	0.17			0.0			0.1			no deposit		
161	0-67-1	2	350	360	0.5	0	0.39	0.26	0.0	0.17	0.34	0	0.47	0.6	no deposit		
162	0-67-1 240H 320	2	350	360	0.5	17.29			6.70			24			brn to blk coke		
163	0-67-1 240H 320	2	350	360	0.5	23.56			5.82			29.2			brn to blk coke		
164	0-67-1 240H 320	2	325	360	0.5	22.57			7.58			30.2			brn to blk coke		
165	0-67-1 240H 320	2	325	360	0.5	22.23	21.41	2.8	10.55	7.61	2.12	32.8	29.1		brn to blk coke	3.7	
166	0-67-1 240H 320	2	325	360	0.5	13.48			36.03			49.7			brn-blk non-unif coke		
167	0-67-1 240H 320	2	325	360	0.5	18.92			25.99			44.9			brn-blk non-unif coke		
168	0-67-1 240H 320	2	325	360	0.5	17.29			28.53			45.8			brn-blk non-unif coke		
169	0-67-1 240H 320	2	325	360	0.5	20.57	17.57	3.03	23.80	28.59	5.32	44.4	46.2		brn-blk non-unif coke	2.4	
170	0-67-1 240H 320	2	325	540	0.5	15.92			29.07			45			brn-blk non-unif coke		
171	0-67-1 240H 320	2	325	540	0.5	17.78			24.03			41.8			brn-blk non-unif coke		
172	0-67-1 240H 320	2	325	540	0.5	17.66			28.71			46.4			brn-blk non-unif coke		
173	0-67-1 240H 320	2	325	540	0.5	16.93	17.07	0.85	27.65	27.36	2.30	44.6	44.5		brn-blk non-unif coke	1.9	
174	0-67-1 240H 320	2	350	540	0.5	19			6.21			25.2			brn - blk var coke		
175	0-67-1 240H 320	2	350	540	0.5	19.2			8.37			27.6			brn - blk var coke		
176	0-67-1 240H 320	2	350	540	0.5	17.7			8.04			25.8			brn - blk var coke		
177	0-67-1 240H 320	2	350	540	0.5	17.4	18.3	0.89	9.07	7.92	1.22	26.5	26.3		brn - blk var coke	1	
178	0-77-6	2	325	540	0.5	0.34									no deposit		
179	0-77-6	2	325	540	0.5	0									no deposit		
180	0-77-6	2	325	540	0.5	0									no deposit		
181	0-77-6	2	325	540	0.5	0.34	0.3	0							no deposit		
182	0-67-1	2	325	360	0.5	0.16			0.68			0.8			no deposit		
183	0-67-1	2	325	360	0.5	0.33			0.67			0.7			no deposit		
184	0-67-1	2	325	360	0.5	0			0.51			0.5			no deposit		
185	0-67-1	2	325	360	0.5	0.17	0.16	0.13	0.52	0.60	0.09	0.5	0.63		no deposit	0.15	
186	0-77-6	2	325	360	0.5	0			0.0			0.0			no deposit		

Test #	Oil	Specimen	Temp, C	Time, Min	Size, mL	Specimen mg/g		Seal mg/g		Total mg/g		Description of coke		
						Average	Std Dev	Residue	Average	Std Dev	Residue			
187	0-77-6	2	325	360	0.5	0.16		0.0			0.0		no deposit	
188	0-77-6	2	325	360	0.5	0.17		0.0			0.0		no deposit	
189	0-77-6	2	325	360	0.5	0.16	0.2	1.00	0.25	0.5	1.2	0.3	0.6	no deposit
190	0-77-6	2	300	360	0.5	0.17		1.20			1.37		slight residue	
191	0-77-6	2	300	360	0.5	0.33		1.17			1.51		slight residue	
192	0-77-6	2	300	360	0.5	0.27		2.73			2.20		slight residue	
193	0-77-6	2	300	360	0.5	0.16	0.23	2.66	1.94	1.07	2.83	2.17	0.85	slight residue
194	TEL-9050	2	350	360	0.75	0.82		8.30			9.13		tetlon seals used	
195	TEL-9050	2	350	360	0.75	0.68		7.14			7.83		tetlon seals used	
196	TEL-9050	2	350	360	0.75	0.84		2.67			3.51		tetlon seals used	
197	TEL-9050	2	350	360	0.75	1.12	0.89	3.77	5.47	2.68	4.98	6.36	3.15	tetlon seals used
198	0-67-1 240H320C	2	350	180	0.5	15.2		32.58			32.58		dkbrn non-unif var	
199	0-67-1 240H320C	2	350	180	0.5	17.59		37.65			37.64		dkbrn non-unif var	
200	0-67-1 240H320C	2	350	180	0.5	16.15		24.67			40.82		dkbrn non-unif var	
201	0-67-1 240H320C	2	350	180	0.5	16.92	16.47	25.15	30.01	6.25	42.07	38.3	4.2	dkbrn non-unif var
202	0-67-1 240H320C	2	325	180	0.5	21.21		31.46			52.67		dkbrn non-tak var	
203	0-67-1 240H320C	2	325	180	0.5	26.29		23.06			49.35		dkbrn non-tak var	
204	0-67-1 240H320C	2	325	180	0.5	17.14		36.87			54.01		dkbrn non-tak var	
205	0-67-1 240H320C	2	325	180	0.5	14.68	19.83	34.88	31.56	6.10	49.57	51.4	2.3	dkbrn non-tak var
206	0-67-1 240H320C	2	300	180	0.5	13		50.35			63.35		dkbrn non-unif var	
207	0-67-1 240H320C	2	300	180	0.5	15.83		45.34			61.17		dkbrn non-unif var	
208	0-67-1 240H320C	2	300	180	0.5	15.87		45.35			61.22		dkbrn non-unif var	
209	0-67-1 240H320C	2	300	180	0.5	13.83	14.63	39.63	45.17	4.38	53.46	61.1	5.5	dkbrn non-unif var
210	0-77-6 120H290C	2	350	180	0.5	25.6		17.07			43.3		dkbrn non-tak var	
211	0-77-6 120H290C	2	350	180	0.5	22.6		21.59			44.2		dkbrn non-tak var	
212	0-77-6 120H290C	2	350	180	0.5	23.6		14.71			38.4		dkbrn non-tak var	
213	0-77-6 120H290C	2	350	180	0.5	32.5	26.1	12.46	16.61	3.95	44.9	42.7	2.9	dkbrn non-tak var
214	0-77-6 120H290C	2	375	180	0.5	18.4		16.86			35.3		dk brn var silt flak	
215	0-77-6 120H290C	2	375	180	0.5	16.8		15.63			32.4		dk brn var silt flak	
216	0-77-6 120H290C	2	375	180	0.5	17.2		12.48			29.7		dk brn var silt flak	
217	0-77-6 120H290C	2	375	180	0.5	17.2	17.4	13.87	14.71	1.93	31.1	32.1	2.4	dk brn var silt flak
218	0-77-6 120H290C	2	400	180	0.5	10.11		2.76			12.86		librn-blk ver flak c	
219	0-77-6 120H290C	2	400	180	0.5	9.89		1.17			11.15		librn-blk ver flak c	
220	0-77-6 120H290C	2	400	180	0.5	13.63		2.63			16.26		librn-blk ver flak c	
221	0-77-6 120H290C	2	400	180	0.5	9.58	10.82	6.65	3.03	2.34	16.22	14.2	2.5	librn-blk ver flak c
222	0-77-6 120H290C	2	325	180	0.5	21.84		28.74			50.58		dk brown varnish	
223	0-77-6 120H290C	2	325	180	0.5	19.18		30.17			49.35		dk brown varnish	
224	0-77-6 120H290C	2	325	180	0.5	17.9		33.71			51.2		dk brown varnish	

Test #	Specimen	Temp, C	Time, Min	Size, µl	Specimen wt/g	Seal wt/g	Average	Std Dev	Residue	Total wt/g	Average	Std Dev	Description of coke
225	0-77-6 120H 290	2	325	180	0.5	14.86	18.4	2.8	32.56	47.43	31.30	2.26	1.6 dk brown varnish
226	0-77-6 120H 290	2	300	180	0.5	31.17			16.06	47.23			dk brn non-uni var
227	0-77-6 120H 290	2	300	180	0.5	19.73			38.96	58.69			dk brn non-uni var
228	0-77-6 120H 290	2	300	180	0.5	18.21	23.04	7.08	38.77	56.98	31.26	13.17	6.18 dk brn non-uni var
229	0-77-6 120H 290	2	300	180	0.5								
230	0-77-6 120H 290	2	425	180	0.5	7.1			3.83	11			dk brn flakey var
231	0-77-6 120H 290	2	425	180	0.5	3.1			2.11	5.2			dk brn flakey var
232	0-77-6 120H 290	2	425	180	0.5	5.4			4.46	10.2			dk brn flakey var
233	0-77-6 120H 290	2	425	180	0.5	3.2	4.7	1.9	2.82	6	3.31	1.04	2.9 dk brn flakey var
234	0-77-6 120H 290	2	425	360	0.5								no visible deposit
235	0-77-6 120H 290	2	425	360	0.5								no visible deposit
236	0-77-6 120H 290	2	425	360	0.5								no visible deposit
237	0-77-6 120H 290	2	425	360	0.5		0.2	0					no visible deposit
238	0-77-6 120H 290	2	425	120	0.5	5.5			6.12	11.6			dk brn flakey var
239	0-77-6 120H 290	2	425	60	0.5	10.5			11.27	21.8			dk brn flakey var
240	0-77-6 120H 290	2	425	60	0.5	10.5	10.5	0	6.34	16.8	19.3		3.5 dk brn flakey var
241	0-77-6 120H 290	2	425	120	0.5	6.2	5.9	0.5	7.98	14.2	12.9		1.8 dk brn flakey var
243	0-77-6 120H 290	2	425	300	0.5	0.2			0.34	0.5			so blk coke flakes
244	0-77-6 120H 290	2	425	240	0.5	0			0.33	0.3			so blk coke flakes
245	0-77-6 120H 290	2	425	240	0.5	0	0	0	0.49	0.5			0.1 so blk coke flakes
246	0-77-6 120H 290	2	425	300	0.5	0.7	0.5	0.4	1.66	1.7			0.8 so blk coke flakes
247	TEL-9089	2	375	180	0.5	2.2			3.05	5.25			lt brn-golden stain
248	TEL-9089	2	375	180	0.5	0.2			1.90	2.06			lt brn-golden stain
249	TEL-9089	2	375	180	0.5	0.7			3.09	2.05			lt brn-golden stain
250	TEL-9089	2	375	180	0.5	0.3	0.9	0.9	1.02	1.36	2.27	1.00	1.74 lt brn-golden stain
251	0-67-1 240H 320	2	325	180	0.5	26.7			20.37				forgot weights
252	0-67-1 240H 320	2	325	180	0.5	17.9			28.85				forgot weights
253	0-67-1 240H 320	2	325	180	0.5	15.9			29.63				forgot weights
254	0-67-1 240H 320	2	325	180	0.5	8	17.31	7.68	27.98		26.71	4.28	forgot weights
255	0-67-1 240H 320	2	325	180	0.5	15.3			30.30	45.6			dk brn splitchy dep
256	0-67-1 240H 320	2	325	180	0.5	15.6			37.29	52.8			dk brn splitchy dep
257	0-67-1 240H 320	2	325	180	0.5	13.8			37.07	50.8			dk brn splitchy dep
258	0-67-1 240H 320	2	325	180	0.5		14.9	1			49.7	3.7	dk brn splitchy dep
259	0-67-1 240H 320	2	400	180	0.5	6.15			3.85	10			dk brn var to coke
260	0-67-1 240H 320	2	400	180	0.5	9.44			2.31	11.75			dk brn var to coke
261	0-67-1 240H 320	2	400	180	0.5	7.7			6.56	14.51			dk brn var to coke
262	0-67-1 240H 320	2	400	180	0.5	9.68	8.24	1.65	3.68	13.36	4.1	1.78	1.96 dk brn var to coke
263	0-67-1 240H 320	2	425	180	0.5								

Test #	Oil	Specimen	Temp, C	Time, Min	Size, µL	Specimen mg/g		Seal mg/g		Average		Std Dev	Total mg/g		Average		Std Dev	Description of coke	
						Residue		Residue					Residue						
264	0-67-1	240H 320	2	425	180	0.5	1.58			3.56			5.14					dk brn var to coke	
265	0-67-1	240H 320	2	425	180	0.5	1.99			3.98			5.97					dk brn var to coke	
266	0-67-1	240H 320	2	425	180	0.5	2.79	2.12	0.61	3.02	3.52	0.48	5.81	5.64	0.43			dk brn var to coke	
267	0-67-1	240H 320	4	375	180	0.5	2.61			1.21			3.81					gold/grey-brn stain	
268	0-67-1	240H 320	4	375	180	0.5	3.35			0.56			3.91					gold/grey-brn stain	
268	0-67-1	240H 320	4	375	180	0.5	3.59			1.60			5.19					gold/grey-brn stain	
270	0-67-1	240H 320	4	375	180	0.5	2.69	3.06	0.48	1.66	1.26	0.51	4.35	4.31	0.62			gold/grey-brn stain	
271	0-67-1	0	4	375	180	0.5	2.8			1.75			4.6					golden, grey circ aid	
272	0-67-1	0	4	375	180	0.5	2.5			2.12			4.6					golden, grey circ aid	
273	0-67-1	0	4	375	180	0.5	3			2.16			5.1					golden, grey circ aid	
274	0-67-1	0	4	375	180	0.5	1.9	2.6	0.5	1.87	1.98	0.20	3.7	4.5	0.6			golden, grey circ aid	
275	0-67-1	0	5	375	180	0.5	0.6			1.32			1.9					no visible deposit	
276	0-67-1	0	5	375	180	0.5	0.3	0.5	0.2	1.52	1.42	0.14	1.9	1.9	0			no visible deposit	
277	0-67-1	0	6	375	180	0.5	1			1.03			2.4	1.9	0			no visible deposit	
278	0-67-1	0	6	375	180	0.5	0.3	0.7	0.5	1.17	1.17	1.1	1.5	2	0.6			no visible deposit	
279	0-67-1	240H 320	6	375	180	0.5	14.58			7.45			22.04					hard lt-dk brn var	
280	0-67-1	240H 320	6	375	180	0.5	14.92	14.8	0.2	5.62	6.50	1.29	20.54	21.3	1.1			hard lt-dk brn var	
281	0-67-1	240H 320	5	375	180	0.5	18.04			14.15			32.18					hard lt-dk brn var	
282	0-67-1	240H 320	5	375	180	0.5	18.64	18.3	0.4	14.36	14.26	0.15	33	32.6	0.6			hard lt-dk brn var	
283	0-77-6	120H 290	4	375	180	0.5	2.69			2.69			2.69					silt rust-grey dep	
284	0-77-6	120H 290	4	375	180	0.5	6.94			3.74			10.68					silt rust-grey dep	
285	0-77-6	120H 290	4	375	180	0.5	4.14			4.14			4.14					silt rust-grey dep	
286	0-77-6	120H 290	4	375	180	0.5	3.95	4.9	1.8	3.95	3.63	0.65	3.95	3.37	3.60			silt rust-grey dep	
287	0-77-6	120H 290	6	375	180	0.5	18.78			13.07			31.85					ltbrn - blk var, coke	
288	0-77-6	120H 290	6	375	180	0.5	13.91	16.34	3.44	7.93	10.50	3.63	21.84	26.84	7.07			ltbrn - blk var, coke	
289	0-77-6	120H 290	5	375	180	0.5	20.92			11.89			32.81					ltbrn - blk var, coke	
290	0-77-6	120H 290	5	375	180	0.5	22.87	21.89	1.38	13.46	12.68	1.11	36.33	34.57	2.48			ltbrn - blk var, coke	
291	MEW 0-77-6		4	375	180	0.5				0.27								gray in aid, golden	
292	MEW 0-77-6		4	375	180	0.5	1.36			1.34			2.04					gray in aid, golden	
293	MEW 0-77-6		4	375	180	0.5	1.0887			4.04			3.13					gray in aid, golden	
294	MEW 0-77-6		4	375	180	0.5	1.65	1.3665	0.281	2.32	1.99	1.60	2.85	2.67	0.56			gray in aid, golden	
295	MEW 0-77-6		6	375	180	0.5	0.341			0.5106			0.85					no visible deposit	
296	MEW 0-77-6		6	375	180	0.5	0.347	0.344	0.004	0.0	0.2553	0.36	0.34	0.595	0.361			no visible deposit	
297	MEW 0-77-6		5	375	180	0.5	0			0.0			0					no visible deposit	
298	MEW 0-77-6		5	375	180	0.5	0	0	0	0.0	0.0	0.0	0	0.0	0.0			no visible deposit	
299	MEW 0-77-6		2	375	180	0.5	0.2			0.3551			0.8					golden no deposit	
300	MEW 0-77-6		2	375	180	0.5	0.2			0.0								golden no deposit	
301	MEW 0-77-6		2	375	180	0.5	0.2			0.0								golden no deposit	

Test #	Oil	Specimen	Temp, C	Time, Min	Size, ml	Specimen wt/g			Seal wt/g			Total wt/g			Average Std Dev			Description of coke		
							Average	Std Dev	Residue		Residue	Average	Std Dev	Residue		Residue				
302	NEW 0-77-6	2	375	180	0.5	0.2	0.2	0	0.0			0.084	0.17					golden no deposit		
303	0-67-1 168H 320	2	375	180	0.5	6.1								6.1				hard dark varnish		
304	0-67-1 168H 320	2	375	180	0.5	5.5								5.5				hard dark varnish		
305	0-67-1 168H 320	2	375	180	0.5	7.1								7.1				hard dark varnish		
306	0-67-1 168H 320	2	375	180	0.5	6.9	6.4	0.74						6.9				hard dark varnish	0.74	
307	0-67-1 240H 320	2	375	180	0.5	8.8								24.47				hard dark varnish		
308	0-67-1 240H 320	2	375	180	0.5	9								21.3				hard dark varnish		
309	0-67-1 240H 320	2	375	180	0.5	9								21.1				hard dark varnish		
310	0-67-1 240H 320	2	375	180	0.5	9.7	9.125	0.395						19.72	21.65			hard dark varnish	2	
311	0-77-6 120H 290	2	300	180	0.5	19								60.66				hard dark varnish		
312	0-77-6 120H 290	2	300	180	0.5	18.9								57.3				hard dark varnish		
313	0-77-6 120H 290	2	300	180	0.5	13.9								61.1				hard dark varnish		
314	0-77-6 120H 290	2	300	180	0.5	14.6	16.6	2.7						53.5	5.82			hard dark varnish	3.5	
315	NEW 0-77-6	2	300	180	0.5													slight tarnish		
316	NEW 0-77-6	2	375	180	0.5	0.209								0.209				slight tarnish		
317	NEW 0-77-6	2	375	180	0.5	0.329								0.329				slight tarnish		
318	NEW 0-77-6	2	375	180	0.5	0.421	0.3	0.1						0.421	0.3			slight tarnish	0.1	
319	NEW 0-77-6	4	375	180	0.5	1.3								1.3				tarnish with grey		
320	NEW 0-77-6	4	375	180	0.5	1.1								1.1				tarnish with grey		
321	NEW 0-77-6	4	375	180	0.5	1.7								1.7				grey no tarnish		
322	NEW 0-77-6	4	375	180	0.5	1.2	1.3	0.3						1.2	1.03			grey no tarnish	0.3	
323	NEW 0-77-6	6	375	180	0.5	0.3								0.3						
324	NEW 0-77-6	6	375	180	0.5	0.0	0.2	0.1										oil on ring no dep		
325	NEW 0-77-6	5	375	180	0.5															
326	NEW 0-77-6	5	375	180	0.5															
327	TEL-90001	2	375	180	0.5															
328	TEL-90001	2	375	180	0.5	16.2								16.06				blk and oil		
329	TEL-90001	2	375	180	0.5	11.4								15.09				blk and oil		
330	TEL-90001	2	375	180	0.5	12.9	13.5	2.5						15.10	15.42	29		blk and oil	3.2	
331	0-67-1	2	375	180	0.5	13.37								0.0101						
332	0-67-1	2	375	180	0.5	1.134								0.0255						
333	0-67-1	2	375	180	0.5	1.314								0.0021						
334	0-67-1	2	375	180	0.5	2.019	1.489	0.4677						0.0039						
335	TEL-90028	2	375	180	0.5	0.3								0.3						
336	TEL-90028	2	375	180	0.5	0.2								2.1						
337	TEL-90028	2	375	180	0.5	0								2.2						
338	TEL-90028	2	375	180	0.5	0.3	0.2	0.1						1.8	1.6					2.03
339	TEL-90024	2	375	180	0.5	0.1								0.1						

Test #	0.1	Specimen	Temp, C	Time, Min	Size, in.	Specimen Residue	Average	Std Dev	Seal Residue	Average	Std Dev	Total Residue	Average	Std Dev	Description of coke
340	TEL-90024	2	375	180	0.5	0.4						0.4			
341	TEL-90024	2	375	180	0.5	0.5						0.5			
342	TEL-90024	2	375	180	0.5	0.8	0.5	0.3				0.8	0.5	0.3	LIGHT POWDER RESIDUE
343	0-67-1	2	375	varies	2.54g							3.97			
344	0-67-1	2	375	varies	2.52g							10.12			
345	0-67-1	2	375	varies	2.37g							0.88			
346	0-67-1	2	375	varies	2.54g							1.36	2.07	1.66	< MOD. TESTS
347	0-67-1	2	325	varies	2.40g							2.9954			SAMPLE INJECTED
348	0-67-1	2	325	varies	2.42g							2.2332			OVER ENTIRE
349	0-67-1	2	325	varies	2.39g							0.2504			TEST CYCLE >
350	0-67-1	2	325	varies	2.40g							3.1617	2.16	1.33	
351	0-67-1	2	425	varies	2.37g							---			
352	0-67-1	2	425	varies	2.41g							---			
353	0-67-1	2	425	varies	2.38g							0.965			
354	0-67-1	2	425	varies	2.33g							1.9238	1.44	0.6779	---
355	0-67-1	2	400	varies	2.38g							1.005			
356	0-67-1	2	400	varies	2.35g							0.2973			
357	0-67-1	2	400	varies	2.38g							1.1747			
358	0-67-1	2	400	varies	2.35g							---	0.825	0.465	---
359	0-67-1	2	400	varies	4.41g							1.744			
360	0-67-1	2	400	varies	4.37g							1.303			
361	0-67-1	2	400	varies	4.35g							0.2531			
362	0-67-1	2	400	varies	4.41g							0.885	1.1	0.765	---
363	WEAR TEST #10	2	375	180	0.5	0.3						---			
364	WEAR TEST #10	2			0.5							---			
365	WEAR TEST #10	2			0.5	0.6			0.3			0.9			
366	WEAR TEST #10	2			0.5	0.7	0.53	0.2		1	1.14	0.7	0.8	0.1	OIL WITH SLIGHT COKE
367	TEL-90059	1	400	180	0.5	3.7			---			3.4			
368	TEL-90059	1			0.5	4.5			2.07			6.6			
369	TEL-90059	1			0.5	4			1.17			5.2			
370	TEL-90059	1			0.5	4.2	4.1	0.3	0.98	1.058	0.848	5.2	5.1	1.3	
371	TEL-90025	1	375	180	0.5	5.88			---			5.88			
372	TEL-90025	1	375		0.5	5.326	5.603	0.39	---			5.236	5.56	0.453	
373	TEL-90026	1	375		0.5	4.716						4.716			
374	TEL-90026	1	375		0.5	4.759	4.738	0.03	---			4.759	4.737	0.03	
375	TEL-90059	2	375	180	0.5	1.069			0			1.069			
376	TEL-90059	2			0.5	0.9599			0			0.9599			
377	TEL-90059	2			0.5	1.178			0			1.178			

Test #	Oil	Specimen	Temp, C	Time, Min	Size, ml	Specimen mg/g			Seal mg/g			Total mg/g			Description of coke		
							Average	Std Dev	Residue		Average	Std Dev	Residue				
378	TEL-90059	2			0.5	1.1903	1.0993	0.107	0			1.1903	1.0993	0.1077	LIGHT YELLOW		
379	TEL-90026	2	375	180	0.5	0.525						0.525					
380	TEL-90026	2			0.5	0.1709	0.3479	0.25	---			0.1709					
381	TEL-90025	2			0.5	0.1772						0.1772					
382	TEL-90025	2			0.5	0.5541	0.3657	0.266	---			0.5541	0.3568	0.21	YELLOW/BRN STAIN		
383	TEL-90025	2	375	180	0.5	0.3822						0.3733					
384	TEL-90025	2			0.5	0.3875						1.5489					
385	TEL-90025	2			0.5	0.3932						1.1795					
386	TEL-90025	2			0.5	0.1949	0.3395	0.096	---			1.1691	1.1177	0.4036	YELLOW TARNISH		
387	TEL-90026	2	375	180	0.5	0.2823						0.2023					
388	TEL-90026	2			0.5	0						0.2077					
389	TEL-90026	2			0.5	0						0.1891					
390	TEL-90026	2			0.5	0.1923	0.0986	0.1139	---			0.192	0.1978	0.0087	LIGHT BRN STAIN		
391	TEL-9030	2	375	180	0.5	0.54						0.54					
392	TEL-9030	2			0.5	0.19						0.19					
393	TEL-9030	2			0.5	0.64						0.64					
394	TEL-9030	2			0.5	0.52	0.47	0.19	---			0.52	0.47	0.19			
395	TEL-9040	2	375	180	0.5	0.4029						0.4029					
396	TEL-9040	2			0.5	0.3559						0.7118					
397	TEL-9040	2			0.5	0.382						0.382					
398	TEL-9040	2			0.5	0.2064	0.3368	0.89	---			0.2064	0.4258	0.2101	SLIGHT TARNISH		
399	TEL-90063	2	350	360	0.5	0						0.74					
400	TEL-90063	2			0.5	0.14						0.56					
401	TEL-90063	2			0.5	0						0.43					
402	TEL-90063	2			0.5	0	0.035					0.28	0.5	0.2	LIGHT GOLDEN BRN		
403	TEL-90018	2	375	180	0.5	0.3812						0.3812					
404	TEL-90018	2			0.5	0.3771						0.3771					
405	TEL-90018	2			0.5	0.1738						0.1738					
406	TEL-90018	2			0.5	0.1888	0.2812	0.1444				0.1888	0.2802	0.1144	LIGHT GOLDEN BRN		
407	TEL-91001	2	400	180	0.5	0.4334						0.4334					
408	TEL-91001	2			0.5	0.2756						0.2756					
409	TEL-91001	2			0.5	0.1404						0.1404					
410	TEL-91001	2			0.5	0.14	0.2473	0.1395				0.14	0.2473	0.1395	LIGHT GOLDEN VARN		
411	0-64-20 48H 320	2	400	180	0.5	0.39						0.3979					
412	0-64-20 48H 320	2			0.5	0.27						0.2755					
413	0-64-20 48H 320	2			0.5	0.26						0.2667					
414	0-64-20	2			0.5	0	0.23	0.1643				0.1364	0.2691	0.1068	LIGHT GOLDEN VARN		
415	TEL-90103	2	300	180	0.5	14.5037						17.894			dk varn		

TABLE A-6

MCRT COKING TEST DATA

(Vial Type Used : 1 - 7.5 cm Glass Vial, 2 - 3.5 cm Glass Vial, 3 - 7.5 cm SS-304 Vial, 4 - 3.5 cm SS-304 Vial, 5 - 19 mm X 70 mm Glass Vial)

Test:	Oil Sample	Temp. C	Hrs	Size Grams	Vial Type	Gas Type	2 Res	Sid. Dev.	Residue Description	Coke Color
1 :	0-86-2	275	30	0.5	2	AIR	17.21	0.41		
2 :	0-86-2	275	30	0.5	2	AIR	19.32	0.69		
3 :	0-86-2	282	30	0.5	2	AIR	15.42	0.49		
4 :	0-86-2	275	30	0.5	2	AIR	17.14	0.5		
5 :	0-86-2	275	30	0.5	2	AIR	19.07	0.8		
6 :	0-86-2	265	30	0.5	2	AIR	40.77	1.94	liq&coke	----
7 :	0-86-2	265	30	0.5	2	AIR	44.08	1.34	liq&coke	---
8 :	0-86-2	290	30	0.5	2	AIR	16.46	0.39	hard varn	
9 :	0-86-2	290	30	0.5	2	AIR	16.29	0.66		
10 :	0-86-2	300	30	0.5	2	AIR	17.97	0.3		
11 :	0-86-2	300	30	0.5	2	AIR	17.54	0.56		
12 :	0-86-2	310	30	0.5	2	AIR	15.3	0.37		
13 :	0-86-2	310	30	0.5	2	AIR	16.56	0.75		
14 :	0-86-2	310	30	0.5	2	AIR	15.59	0.36		
15 :	0-86-2	310	30	0.5	2	AIR	16.33	0.27		
16 :	0-67-1 240H 0320C	350	30	0.5	1	AIR	47.23	1.33	liq&hd varn	
17 :	0-67-1 240H 0320C	350	60	0.5	1	AIR	16.26	1.02	hard varn	drk brown
18 :	0-67-1 240H 0320C	350	90	0.5	1	AIR	13.03	0.89	hard residue	drk brown
19 :	0-67-1 160H 0320C	400	30	0.5	2	AIR	2.16	0.26	varn	drk brown
20 :	0-67-1 160H 0320C	400	30	0.5	1	AIR	13.73	1.35	varn	drk brown
21 :	0-67-1 240H 0320C	425	30	0.5	2	AIR	2.52	0.6	suspect temp	
22 :	0-67-1 240H 0320C	425	30	0.5	1	AIR	13.04	1.15	hard coke	black
23 :	0-67-1 240H 0320C	400	30	0.5	2	AIR	6.59	0.16	varn/flak	drkbrown
24 :	0-67-1 240H 0320C	400	30	0.5	1	AIR	16.74	1.01	flaky coke	
25 :	0-67-1 160H 0320C	400	30	0.5	2	AIR	4.05	0.15	varn	drk brown
26 :	0-67-1 160H 0320C	400	30	0.5	1	AIR	14.02	1.35	varn	drk brown
27 :	0-67-1 192H 0320C	350	30	0.5	2	AIR	16.35	2.14	tacky	drk brown
28 :	0-67-1 192H 0320C	350	30	0.5	1	AIR	42.20	0.57	visc. oil	
29 :	0-67-1 192H 0320C	400	30	0.5	1	AIR	14.68	1.51	varn	drk brown
30 :	0-67-1 192H 0320C	400	30	0.5	2	AIR	2.50	0.41	varn	drkbrown
31 :	0-67-1	400	30	0.5	2	AIR	1.45	0.05	varn	drk brown
32 :	0-67-1	400	30	0.5	1	AIR	11.34	1.69	varn	drk brown
33 :	0-67-1	425	30	0.5	1	AIR	7.54	1.06	hard coke	black
34 :	0-67-1	425	30	0.5	2	AIR	0.69	0.27	hard coke	black
35 :	0-67-1 160H 0320C	425	30	0.5	2	AIR	1.07	0.17	hard coke	black
36 :	0-67-1 160H 0320C	425	30	0.5	1	AIR	9.01	1.5	hard coke	dark
37 :	0-67-1	400	30	0.5	2	AIR	2.65	0.13	varn	drk brown
38 :	TEL-9030	400	30	0.5	2	AIR	2.47	0.76	hard varn	drk
39 :	WEAR TEST 369	400	30	0.5	2	AIR	0.05	0.02		lite orange
40 :	WEAR TEST 367	400	30	0.5	2	AIR	0.06	0.04	powder	lite orange
41 :	WEAR TEST 370	400	30	0.5	2	AIR	0.39	0.09	no varn	red Fe.3s
42 :	TEL-9020	400	30	0.5	2	AIR	2.03	0.09	coke	white filo
43 :	TEL-9029	400	30	0.5	2	AIR	1.24	0.4	coke/varn	
44 :	TEL-8085	400	30	0.5	2	AIR	0.12	0.02	residue	white
45 :	TEL-8087	400	30	0.5	2	AIR	0.08	0.03	res.,slt. coke	white,yellow
46 :	TEL-9030	400	30	0.5	2	AIR	1.45	0.11		drk,dull brown
47 :	TEL-9030	400	30	0.5	2	AIR	2.7	1.35	DATA SUSPECT	
48 :	TEL-9039	400	30	0.5	2	AIR	3.87	0.35	flaky coke	black
49 :	TEL-9040	400	30	0.5	2	AIR	4.30	0.94	hard varn	drk brn to blk
50 :	0-67-1 240H 0320C	400	60	0.5	2	AIR	0.54	0.24	particals	black
51 :	TEL-9020	400	30	0.5	2	AIR	2.09	0.93	varn	brown
52 :	WEAR TEST 302	400	30	0.5	2	AIR	2.17	0.54	flaky varn	drk brown
53 :	TEL-9030	400	30	0.5	2	AIR	3.87	0.72	flaky	drk brown

Test	Oil Sample	Temp C	Hrs	Size Grass	Vial Type	Gas Type	% Res	Std. Dev.	Residue Description	Coke Color
54	WEAR TEST 378	400	30	0.5	2	AIR	0.96	0.71	loose coke	black
55	CB-1	400	30	0.5	2	AIR	0.1	0.02	pouder	orng,red FE.Ox
56	CB-1	400	30	0.5	2	AIR	2.11	0.31	hard coke/varn	drkbrown
57	WEAR TEST 370	400	30	0.5	2	AR	1.78	0.15	flaky coke	drkbrown, grey/w
58	WEAR TEST 400	400	30	0.5	2	AIR	0.31	0.33	coke	drkbrn wht dep
59	0-67-1	400	30	0.5	2	AR	0.08	0.02	residue	wht, grey/brn
60	WEAR TEST 399	580	1	0.5	2	AIR	0.62	0.12	particals	black, amber
61	WEAR TEST 399	400	30	0.5	2	AIR	0.13	0.04	partic/resid	orang/amber
62	0-67-1 100PPM Fe	400	30	0.5	2	AIR	2.41	0.27	hard varn	drkbrown hvy co
63	CB1 o/c 320C 48H	400	30	0.5	2	AIR	1.22	0.37	part., nonmag.	amber to black
64	WEAR TEST 401--	=	=	=	=	=	=	=	=	=
64	320C 48H	400	30	0.5	2	AIR	0.68	0.23	varn	drkbrown to bla
65	WEAR TEST 399	400	30	0.5	2	AR	2.89	0.19	coke/part	grey/black part
66	CB1 o/c 48H 320C	400	30	0.5	2	AIR	1.2	0.17	hard varn	drkbrown to blk
67	CB1 o/c 48H ---	=	=	=	=	=	=	=	=	=
67	FILTERED 3uM	400	30	0.5	2	AIR	1.04	0.2	varn	dk. brn. & white
68	WEAR TEST 405	400	30	0.5	2	AIR	2.14	0.45	varn/flkcoke	brn to blk
69	WEAR TEST 405	400	30	0.5	2	AR	5.26	0.35	hard varn	drkbrn to blk
70	0-77-6	400	30	0.5	2	AIR	3.78	0.47	brd/brittle/flk	black
71	0-77-6	400	30	0.5	2	AR	0.07	0.02	hard varn	drk brn/blk
72	WEAR TEST 378	400	30	0.5	2	AIR	1.56	0.67	loose coke	black
73	TEL-9028	400	30	0.5	2	AR	0.5	0.1	res. & hard varn	brn. & black
74	TEL-9050	400	30	0.5	2	AIR	2.83	0.07	hard flaky	black
75	TEL-9029	400	30	0.5	2	AR	0.1	0.02	part. & varn.	brn grey brn
76	WEAR TEST 346	400	30	0.5	2	AIR	0.04	0.02	Fe 8x	red
77	TEL-9030	400	30	0.5	2	AR	0.21	0.11	res/varn	grey-brown
78	WEAR TEST 347	400	30	0.5	2	AIR	2.43	0.61	hard flaky varn	black
79	TEL-9030	400	30	0.5	2	AR	0.06	0.02	residue//varn	grey brn// dark
80	WEAR TEST 364	400	30	0.5	2	AR	1.98	0.78	flaky//	drk brn to blk
81	TEL-9038	400	30	0.5	2	AR	0.1	0.02	res//varn	grey brn//xxxx
82	WEAR TEST 364	400	30	0.5	2	AIR	1.5705	0.83	brittle flaky v	brn to blk
83	TEL-9039	400	30	0.5	2	AR	0.3	0.04	hard varn//resi	drkbrn//greybl
84	WEAR TEST 358	400	30	0.5		AIR	0.65	0.36	loose coke	black
85	TEL-9040	400	30	0.5	2	AR	0.11	0.06	hard varn//resi	blkbrn//greybrn
86	WEAR TEST 380	400	30	0.5	2	AIR	0.11	0.04	iron oxide	red
87	0-67-1 o/c ---	=	=	=	=	=	=	=	=	=
87	168H 320C	400	30	0.5	2	AR	2.31	0.23	hard varnish	black
88	0-67-1 o/c ---	=	=	=	=	=	=	=	=	=
88	168H 320C	400	30	0.5	2	AR	4.21	0.47	hard varnish	dkbrn to black
89	WEAR TEST 379	400	30	0.5	2	AIR	3.14	0.57	loose coke	black
90	CB1 o/c 48H 320C	400	30	0.5	2	AR	8.2	0.11	hard dull varn	dkbrn to black
91	WEAR TEST 404	400	30	0.5	2	AIR	0.31	0.25	loose coke	blk& bri orange
92	WEAR TEST 383	400	30	0.5	2	AIR	0.11	0.02	depos/loosepart	orange/dkorange
93	0-77-6	425	30	0.5	2	AIR	0.97	0.25	brdsemi-loose c	black
94	0-77-6	375	30	0.5	2	AIR	1.88	0.37	hard varnish	dk brown
95	0-77-6	425	30	0.5	1	AIR	9.03	1.77	brittle coke	black
96	0-77-6	375	30	0.5	1	AIR	20.24	1.29	var/viscous oil	
97	0-77-6	400	30	0.5	1	AIR	13.71	1.59	hard varnish	black
98	0-67-1	375	30	0.5	2	AIR	1.72	0.21	hard varnish	black
99	WEAR TEST 400	400	30	0.5	2	AIR	0.36	0.31	flakey coke	dk brown
100	0-67-1	375	30	0.5	2	AIR	1.72	0.2	dark varnish	black
101	0-67-1	375	30	0.5	1	AIR	20.89	1.01	var/viscous oil	black
102	0-67-1	350	30	0.5	2	AIR	19.88	1.96	var/viscous oil	black

Test	Oil Sample	Temp C	Hrs	Size Grams	Vial Type	Gas Type	Z Res	Std. Dev.	Residue Description	Coke Color
: 103 :	0-77-6	350	30	0.5	2	AIR	24.53	1.56	var/viscons oil	black
: 104 :	TEL-9050	350	30	0.5	2	AIR	4.19	0.13	soft solid dep	brn to black
: 105 :	TEL-9050	350	30	0.5	1	AIR	14.11	1.79	soft waxy flak c	lt to dk brown
: 106 :	0-77-6 72H 0290C	400	30	0.5	2	AIR	6.09	0.36	var/hard flak c	
: 107 :	0-77-6 120H 0290C	400	30	0.5	2	AIR	9.72	0.72	var/hard flak c	
: 108 :	TEL-9050 24H 0290C	400	30	0.5	2	AIR	3.72	0.09	hvar/ltvar/flak	dk/lt/dk
: 109 :	TEL-9050 120H 0290	400	30	0.5	2	AIR	5.79	0.34	hard flak c	black
: 110 :	0-77-6	400	60	0.5	1	AIR	9.83	1.45	var/hard coke	
: 111 :	0-67-1	400	60	0.5	1	AIR	7.76	1.58	varnish	lt brn/black
: 112 :	0-67-1	400	30	0.25	2	AIR	0.41	0.13	hard varnish	black
: 113 :	0-77-6	400	30	0.25	2	AIR	0.53	0.14	hard varnish	black
: 114 :	0-67-1 168H 0320C	400	30	0.25	2	AIR	2.43	0.73	hard var/loose	dk brown
: 115 :	0-67-1 168H 0320C	400	30	0.25	2	AIR	1.96	0.41	hard var/loose	dk brown
: 116 :	0-77-6	375	60	0.5	1	AIR	17.81	2.48	var/hard coke	black
: 117 :	0-77-6	375	60	0.5	1	AIR	16.8	1.87	var/hard coke	black
: 118 :	WEAR TEST 411	400	30	0.25	2	AIR	0.1	0.08	iron oxide	red
: 119 :	WEAR TEST 413	400	30	0.25	2	AIR	0.07	0.03	Fe ox/varnish	red/yell-brn
: 120 :	WEAR TEST 414	400	30	0.5	2	AIR	0.11	0.03		
: 121 :	WEAR TEST 417	400	30	0.5	2	AIR	0.09	0.04		
: 122 :	WEAR TEST 411	400	30	0.5	2	AIR	0.04	0.02		
: 123 :	WEAR TEST 413	400	30	0.5	2	AIR	1.62	0.76		
: 124 :	WEAR TEST 414	400	30	0.5	2	AIR	0.88	0.42		
: 125 :	WEAR TEST 415	400	30	0.5	2	AIR	1.82	1.59		
: 126 :	WEAR TEST 379	400	30	0.5	2	AIR	4.15	0.79		
: 127 :	TEL-9050	400	30	0.5	2	AIR	2.39	0.68		
: 128 :	TEL-9050	400	30	0.25	1	AIR	1.43	0.17		
: 129 :	TEL-9050	400	30	0.5	1	AIR	5.29	0.18		
: 130 :	0-67-1	350	60	0.5	1	AIR	25.83	1.49	oil w/varn.	dark
: 131 :	0-67-1	375	60	0.5	1	AIR	6.9	0.5	varnish	dark
: 132 :	0-77-6	350	60	0.5	1	AIR	25.04	0.74	var/viscons oil	black
: 133 :	0-77-6 120H 0290C	400	30	0.25	2	AIR	1.67	0.5	hard part.	black
: 134 :	0-67-1	375	60	0.5	1	AIR	6.78	0.67		
: 135 :	0-67-1 196H 0320C	400	30	0.5	2	AIR	2.68	0.25	hard varn.	brown
: 136 :	0-67-1	350	90	0.5	1	AIR	4.33	0.95	brdvarn.&flacky	
: 137 :	0-77-6	350	90	0.5	1	AIR	4.72	0.85	hard varn.	
: 138 :	0-77-6	400	30	0.5	1	AR	0.28	0.05	hard varn.	dark brown
: 139 :	0-67-1	400	30	0.5	1	AR	0.53	0.13	hard varn.	brown
: 140 :	0-67-1	375	60	0.5	1	AIR	5.49	0.42	hard varn.	brown
: 141 :	TEL-9050	400	30	0.5	2	AR	0.8	0.03		
: 142 :	0-77-6	350	90	0.5	4	AIR	0.13	0.15	slt. varn.	
: 143 :	0-77-6	350	60	0.5	3	AIR	27.43	1.79	viscous	
: 144 :	0-77-6	350	30	0.5	4	AIR	14.55	0.88	deposits	dark
: 145 :	0-67-1	350	30	0.5	4	AIR	19.4	0.89	hard deposits	dark
: 146 :	0-67-1	400	30	0.5	2	AIR	2.44	0.48	hard varn.	dark brown
: 147 :	0-77-6	375	60	0.5	1	AIR	8.55	0.54	hard varn.	dark
: 148 :	0-77-6	375	30	0.5	4	AIR	2.0075	0.26		
: 149 :	0-77-6	375	30	0.5	4	AIR	1.46	0.92	hard varn.	
: 150 :	0-77-6	400	30	0.5	4	AIR	2.65	0.85	hard varn.	dark brown
: 151 :	0-67-1	375	30	0.5	4	AIR	0.69	0.2	brdvarn.&flacky	
: 152 :	0-67-1	400	30	0.5	4	AIR	0.71	0.42	hard varn.&ash	dark&white
: 153 :	0-77-6	425	30	0.5	4	AIR	0.02	0.02		
: 154 :	0-67-1	425	30	0.5	4	AIR	0.1	0.06	coke & ash	
: 155 :	WEAR TEST 397 CD-1	400	30	0.5	2	AR	0.127	0.02	coke/Fe ox	black/red

Test	Oil Sample	Temp C	Hrs	Size Grans	Vial Type	Gas Type	Res	Std. Dev.	Residue Description	Coke Color
: 156 :	0-67-1 W/100PPMFe	400	30	0.5	2	AR	0.058	0.04	coke/residue	black/white
: 157 :	0-77-6	350	30	0.5	4	AIR	15.75	1.41	viscous oil	black
: 158 :	0-77-6	450	20	0.5	1	AIR	6.1	1.12	hard coke	black
: 159 :	0-77-6	475	10	0.5	1	AIR	4.155	0.7	hard coke	black
: 160 :	0-77-6	500	5	0.5	1	AIR	1.687	0.51	hard coke	black
: 161 :	0-77-6	375	30	0.5	4	AIR	8.657	1.15	hard coke	black
: 162 :	0-77-6	525	2.5	0.5	1	AIR	0.255	0.23	hard coke	black
: 164 :	0-77-6	400	30	0.5	4	AIR	5.233	0.68	hard coke	black
: 165 :	0-77-6	550	1.15	0.5	1	AIR	0	0	no deposit	
: 166 :	0-77-6	350	30	0.5	4	AIR	14.99	0.97		
: 167 :	0-77-6	425	30	0.5	4	AIR	0.2	0.1	coke	black
: 168 :	0-67-1	350	30	0.5	2	AIR	20.74	0.85	var/viscous oil	dark/black
: 169 :	0-67-1	350	30	0.5	4	AIR	19.67	1.25	var/viscous oil	dark/black
: 170 :	TEL90001	400	30	0.5	2	AIR	27.33	3.39	hard coke	black
: 171 :	CB-2 FILTERED	400	30	0.5	2	AIR	2.19	0.25	VARNISH	DARK
: 172 :	CB-2	400	30	0.5	2	AIR	1.56	0.26	VARNISH	DARK
: 173 :	CB-3	400	30	0.5	2	AIR	3.18	1.02	VARNISH	DARK BROWN
: 174 :	CB-3 FILTERED	400	30	0.5	2	AIR	0.2924	0.01	VARNISH	DARK
: 175 :	0-77-6	400	30	0.5	2	AIR	3.59	0.71	hard black coke	
: 176 :	NEW 0-77-6	375	30	0.5	4	AIR	5.76	1.12		
: 177 :	0-67-1 CAN D	350	30	0.5	4	AIR	16.97	1.19	dk viscous oil	
: 178 :	0-77-6 CAN G	350	30	0.5	4	AIR	19.73	1.29	dk oil/varnish	
: 179 :	0-67-1 CAN D	350	30	0.5	4	AIR	17.16	1.08	dk viscous oil	
: 180 :	0-67-1 CAN D	350	30	0.5	4	AIR	19.71	1.14	dk viscous oil	
: 181 :	0-67-1 CAN D	350	30	2.5	5	AIR	68.39	1.21	dk viscous oil	
: 182 :	0-67-1 CAN D	425	2	2.5	5	AIR	81.64	0.36	dk viscous oil	
: 183 :	0-67-1 CAN D	375	20	2.5	5	AIR	59.029	0.65		
: 184 :	0-67-1 CAN D	400	10	2.5	5	AIR	58.58	0.33		
: 185 :	0-67-1 CAN D	350	15	2.5	5	AIR	85.07	0.31		
: 186 :	0-67-1 CAN D	350	20	2.5	5	AIR	80.87	0.42		
: 187 :	0-67-1 CAN D	375	9	2.5	5	AIR	80.9	0.18		
: 188 :	0-67-1 CAN D	375	15	2.5	5	AIR	69.76	0.37		
: 189 :	0-67-1 CAN D	400	7	2.5	5	AIR	68.95	0.43		
: 190 :	0-67-1 CAN D	400	5	2.5	5	AIR	79.05	3.62		
: 191 :	0-67-1 CAN D	425	1	2.5	5	AIR	90.47	0.43		
: 192 :	0-67-1 CAN D	425	0.5	2.5	5	AIR	95.53	0.61		
: 193 :	TEL-90024	400	30	0.5	2	AIR	1.87	0.06	BLACK COKE	
: 194 :	TEL-90028	400	30	0.5	2	AIR	24.5	2.51	HRD BRK BRN VAR	
: 195 :	WT 476	400	30	0.5	2	AIR	3.97	0.45	HRD BLK VARN CO	
: 196 :	TEL-90024	350	20	2.5	5	AIR	51.47	0.34		
: 197 :	TEL-90024	350	10	2.5	5	AIR	73.08	0.47		
: 198 :	TEL-90024	325	30	2.5	5	AIR	66.916	0.5		
: 199 :	TEL-90024	350	5	2.5	5	AIR	85.54	0.23		
: 200 :	TEL-90024	325	10	2.5	5	AIR	87.706	0.12		
: 201 :	TEL-90024	325	20	2.5	5	AIR	77.809	0.2		
: 202 :	TEL-90024	375	2	2.5	5	AIR	85.51	0.35		
: 203 :	TEL-90024	375	5	2.5	5	AIR	68.42	0.71		
: 204 :	TEL-90024	400	0.5	2.5	5	AIR	NA	NA		
: 205 :	TEL-90024	400	1	2.5	5	AIR	84.29	0.39		
: 206 :	0-77-6	300	20	2.5	5	AIR	95.867	0.26		
: 207 :	0-77-6	300	30	2.5	5	AIR	93.525	0.26		
: 208 :	0-77-6	325	20	2.5	5	AIR	76.526	0.18		
: 209 :	0-77-6	325	15	2.5	5	AIR	92.976	0.18		

Test	Oil Sample	Temp C	Hrs	Size Grains	Vial Type	Gas Type	2 Res	Std. Dev.	Residue Description	Coke Color
: 210 :	0-77-6	350	10	2.5	5	AIR	88.515	0.29		
: 211 :	0-77-6	350	20	2.5	5	AIR	79.45	0.45		
: 212 :	0-77-6	375	5	2.5	5	AIR	87.64	0.26		
: 213 :	0-77-6	375	10	2.5	5	AIR	78.05	0.41		
: 214 :	0-67-1	425	1	2.5	5	AR	91.74	0.24		
: 215 :	TEL-90025	400	30	0.5	2	AIR	6.86	0.43	flacky varn.	dark
: 216 :	TEL-90026	400	30	0.5	2	AIR	5	1.37		
: 217 :	TEL-90026	400	30	0.5	2	AIR	7.33	0.39		
: 218 :	TEL-9030 FILTERED	400	30	0.5	2	AIR	3.88	0.77		
: 219 :	TEL-90025 FILTERED	400	30	0.5	2	AIR	5.025	0.71	varn.	lt.to dk.brown
: 220 :	TEL-90063	400	30	0.5	2	AIR	1.299	0.06	heavy coke&varn	
: 221 :	TEL-90059	400	30	0.5	2	AIR	1.69	0.07	varn.	
: 222 :	WEAR TEST 427	400	30	0.5	2	AIR	3.3	0.45	flackycoke&varn	
: 223 :	WEAR TEST 428	400	30	0.5	2	AIR	3.45	0.78		
: 224 :	WEAR TEST 494	400	30	0.5	2	AIR	2.58	0.12	varn.&coke	dark
: 225 :	WEAR TEST 412	400	30	0.5	2	AIR	0.13	0.03		
: 226 :	WEAR TEST 475	400	30	0.5	2	AIR	0.34	0.6	residue&powder	red-brn-Fe2O3
: 227 :	TEL-90028	400	30	0.5	2	AIR	25.43	0.71	coke&varn.	
: 228 :	WEAR TEST 477	400	30	0.5	2	AIR	0.13	0.01	fil&powder	lt.grey-ZnO
: 229 :	TEL-90087	275	30	0.5	2	AIR	22.75	0.44	coke	
: 230 :	TEL-9040 FILTERED	400	30	0.5	2	AIR	3.15	0.5	varn.	lt.brn. to dark
: 231 :	TEL-9071	400	30	0.5	2	AIR	1.16	0.11	slt. varn.	
: 232 :	TEL-90018	400	30	0.5	2	AIR	27.55	1.69	flacky coke	
: 233 :	0-90-6	275	30	0.5	2	AIR	15.72	0.39	thick varn	
: 234 :	0-67-1	400	30	0.63	2	AIR	3.68	0.51	varn.&coke	dark
: 235 :	TEL-90103	275	30	0.5	2	AIR	22.64	0.51	crystal coke	dark
: 236 :	TEL-90104	275	30	0.5	2	AIR	18.25	0.74	crystal coke	dark
: 237 :	0-64-20	400	30	0.5	1	AIR	13.58	0.3	thk. flake varn	dark
: 238 :	0-64-20	400	30	0.5	2	AIR	6.66	0.23	coke deposits	dark
: 239 :	TEL-91005	275	30	0.5	2	AIR	24.31	0.34	uniform	flacky
: 240 :	TEL-91003	275	30	0.5	2	AIR	24.01	0.28	on sides	heavy&flacky
: 241 :	TEL-90104	275	30	0.5	2	AIR	16.24	0.28		blk. uniform
: 242 :	TEL-90103	275	30	0.5	2	AIR	26.82	1.04	flacky	on top&bottom
: 243 :	0-85-1	275	30	0.5	2	AIR	16.38	0.32	blk. uniform	
: 244 :	0-90-6	275	30	0.5	2	AIR	16.08	0.26	blk. uniform	
: 245 :	9-86-2	275	30	0.5	2	AIR	10.42	0.58	varnish	dark
: 246 :	0-64-20	400	30	0.5	2	AIR	6.67	0.3	bottom circle	blk,little varn
: 247 :	0-91-13	275	30	0.5	2	AIR	25.06	0.6	black varn.coke	

TABLE A-7
LUBRICANT FOAMING TEST DATA

STATIC FOAM TEST
VARIABLE AIR FLOW
DIFFUSER 13/16" SPARGER
(5 um PORE SIZE)

SAMPLE No.	TEST TEMP C	AIRFLOW cc/min	AERATION TIME		VOLUME			FOAM COLLAPSE TIME sec.
			@ AIRFLOW min.		OIL ml	OIL & FOAM ml	FOAM ml	
C-67-1 (13/16 in. SPARGER)	200	100	10		240	245	5	
		250	10		240	250	10	
		500	10		247	260	13	
		750	10		255	270	15	
		1000	10		265	280	15	
		1100	10		265	285	20	4
O-67-1 MINI TEST	200	100	10		38	40	2	
		250	10		42	48	6	
		500	10		42	50	8	
		750	10		28	54	26	6
		1000	10		24	58	34	
O-67-1 (11/16 in. SPARGER)	200	100	10		36	38	2	
		250	10		36	44	8	
		500	10		36	48	12	
		750	10		34	54	20	
		1000	10		24	56	32	5
TEL-9029 MINI TEST	200	150	10		40	48	8	
		250	5		42	50	8	
		500	5		44	54	10	
		750	5		48	62	14	
		1000	5		50	66	16	6
TEL-9030 MINI TEST	200	150	10		38	42	4	
		250	5		38	44	6	
		500	5		38	48	10	
		750	5		40	53	13	
		1000	5		40	60	20	<8
TEL-9028 (14X TRIC) MINI TEST	200	150	10		38	42	4	
		250	10		38	44	6	
		500	10		40	48	8	
		750	5		40	50	10	
		1000	10		40	55	15	3
TEL-9038 MINI TEST	200	150	5		38	42	4	
		250	5		38	44	6	
		500	5		40	48	8	
		750	5		42	52	10	
		1000	5		44	54	10	<7
TEL-9039 MINI TEST	200	150	5		38	42	4	
		250	5		38	42	4	
		500	5		40	46	6	
		750	5		42	48	6	
		1000	5		44	52	8	3
TEL-9040 MINI TEST	200	150	10		36	42	6	
		250	10		36	44	8	
		500	10		38	47	9	
		750	10		38	50	12	
		1000	10		40	55	15	<7

STATIC FOAM TEST
VARIABLE AIR FLOW
DIFFUSER 13/16" SPARGER
(5 um PORE SIZE)

SAMPLE No.	TEST TEMP C	AIRFLOW cc/min	AERATION TIME @ AIRFLOW min.	VOLUME			FOAM COLLAPSE TIME sec.
				OIL ml	OIL & FOAM ml	FOAM ml	
TEL-9050	200	150	10	15	72	57	
MINI TEST	(25ml)	250	10	16	102	86	
		500	10	5	160	155	
		750	10	5	160	155	
		1000	10	5	182	177	
		500	5	5	170	165	15
0-67-1	200	150	10	37	41	4	
CaO 24h		250	10	38	43	5	
320 C		500	10	39	47	8	
MINI TEST	(25ml)	750	10	41	50	9	
		1000	10	41	53	12	2
0-67-1	200	150	10	39	42	3	
CaO 24h		250	10	39	43	4	
320 C		500	10	40	46	6	
MINI TEST	(25ml)	750	5	41	49	8	
		1000	10	42	52	10	1
TEL-9069	200	150	10	38	46	8	
A21729		250	10	39	49	10	
MINI TEST	(25ml)	500	10	40	52	12	
		750	10	41	59	18	
		1000	10	40	69	29	16
TEL-9069-8	200	150	10	38	44	6	
A21744		250	5	39	47	8	
MINI TEST	(25ml)	500	10	40	52	12	
		750	10	42	57	15	
		1000	10	43	64	21	10
TEL-90001	200	150	5	15	62	47	
WT 444		250	5	12	99	87	
MINI TEST	(25ml)	500	10	10	150	140	
		750	10	10	128	118	
		1000	10	10	105	95	15
TEL-90018	200	150	10	39	41	2	
MINI TEST	(25ml)	250	5	37	44	9	
		500	10	32	44	12	
		750	10	20	46	26	
		1000	10	16	52	36	1
TEL-90024	200	150	10	17	80	63	
MINI TEST	(25ml)	250	10	10	125	115	
		500	10	5	210	205	19.5
0-77-6	80	250	10	9	109	100	
ASTM STONE	(25ml)	500	10	8	112	104	
		750	10	8	109	101	
		1000	5	8	107	99	
TEL-90070	80	500	10	11	74	63	8.8
		1000	20	10	112	102	7.4
TEL-90071	80	500	5	15	70	55	7.5

STATIC FOAM TEST
VARIABLE AIR FLOW
DIFFUSER 13/16" SPARGER
(5 mm PORE SIZE)

SAMPLE No.	TEST TEMP C	AIRFLOW cc/min	AERATION TIME		VOLUME			FOAM COLLAPSE TIME sec.
			at AIRFLOW min.		OIL ml	OIL & FOAM ml	FOAM ml	
TEL-90071		1000	15		<10	118	108	7.9
TEL-90072	80	500	5		17	65	48	3
		1000	5		<10	115	105	4.5
TEL-90070	80	500	5		215	240	25	4.8
ASTM STONE		1000	5		216	260	44	5.4
TEL-90071	80	500	5		211	245	34	5.2
ASTM STONE		1000	5		211	260	49	4.9
TEL-90072	80	500	5		215	250	35	6
ASTM STONE		1000	5		215	270	55	6
O-77-6	100	250	15		50	455	405	
FTM3213 (200ML)		500	1		0	550	550	
		1000	20		0	465	465	47
O-77-6	100	250	1	OF	OF		550	81
(13/16 in. (200ML)		500	1	OF	OF		550	
SPARGER)		1000	1.5	OF	OF		550	129
O-77-6	80	500	2		520	520	520	102
FTM3213 (200ML)		1000	25		0	460	460	74
O-77-6	80	250	2	OF	OF		525	
(13/16 in. (200ML)		750	5		0	440	440	
SPARGER)		1000	5		0	460	460	
		1200	5		0	460	460	
O-77-6	80							
(13/16 in. (200ML)		500	1		0	480	480	137
SPARGER)		1000	5		0	445	445	120
O-77-6	80	500	5		13	88	75	55
MINI TEST (25ml)		700	5		10	114	104	
		1000	15		8	130	122	65
O-77-6	80	200	15		10	85	75	37
ASTM STONE (25ml)		500	5		8	90	82	
		700	5		6	88	82	40
		1000	5		5	96	91	
O-77-6	100	500	10		14	74	60	27
MINI TEST (25ml)		1000	5		10	138	128	38
O-77-6	100	200	10		38	54	16	
MINI TEST (25ml)		500	5		16	72	56	
		700	5		15	86	71	
		1000	10		10	130	120	54
O-77-6	100							
MINI TEST (25ml)		1000	10		12	80	68	
O-77-6	100	200	10		16	102	86	86
ASTM STONE (25ml)		500	10		10	114	104	
		700	10		8	118	110	100
		1000	20		8	128	120	140
O-77-6	80	200	5		11	126	115	
MINI TEST (25ml)		500	5		8	146	138	190
		1000	15		7	152	145	197

STATIC FOAM TEST
VARIABLE AIR FLOW
DIFFUSER 13/16" SPARGEE
(5 mm PORE SIZE)

SAMPLE No.	TEST TEMP C	AIRFLOW cc/min	AERATION TIME @ AIRFLOW min.	VOLUME			FOAM COLLAPSE TIME sec.
				OIL ml	OIL & FOAM ml	FOAM ml	
0-77-6	80	200	5	12	100	88	
ASTM STONE (25ml)		500	5	8	110	102	
		1000	20	8	100	92	198
0-77-6	80	200	5	10	90	80	
ASTM STONE (25ml)		500	10	8	90	92	54
		1000	10	6	108	102	216
0-77-6	80	200	5	14	88	74	
MINI TEST (25ml)		500	10	12	92	80	48
		1000	10	10	96	86	53
0-77-6	80	200	5	12	106	94	
MINI TEST (25ml)		500	10	10	120	110	
		1000	25	6	146	140	194
0-77-6	80						
MINI TEST (25ml)		1000	2	8	110	102	
0-77-6	80	200	5	9	152	143	
MINI TEST (25ml)		500	5	7	160	153	
		1000	5	6	160	154	>300
0-77-6	80	200	5	12	136	124	
MINI TEST (25ml)		500	10	8	146	136	
		1000	15	8	152	144	>300
TEL-90087	80	500	30	214	255	41	4
		1000	50	220	285	65	5
TEL-91035	80	500	5	45	261	216	4.7
FTN3213 (200ML)		1000	15	30	365	335	7.8
TEL-91035	80	500	5	12	70	58	4.3
MINI TEST (25ml)		1000	15	10	74	64	4.5
TEL-91036	80	500	5	12	52.2	40.2	3
MINI TEST (25ml)		1000	15	10	53	43	3.3
TEL-91036	80	500	5	50	265	215	4.6
FTN3213 (200ML)		1000	15	35	405	370	9.8
TEL-91003	80	500	5	20	38	18	2.8
MINI TEST (25ml)		1000	15	16	42	26	2.9
TEL-91003	80	500	5	40	245	205	5.5
FTN3213 (200ML)		1000	15	25	250	225	5.6
TEL-91005	80	500	5	50	260	210	5.6
FTN3213 (200ML)		1000	15	35	325	290	5.9
TEL-91005	80	500	5	40	262	222	5.2
FTN3213 (200ML)		1000	15	25	325	300	6.1
TEL-91005	80	500	5	16	56	40	3.2
MINI TEST (25ml)		1000	15	12	54	42	3.2
TEL-90103	80	500	5	20	48	28	2.2
MINI TEST (25ml)		1000	15	12	60	48	2.7
TEL-90104	80	500	25	50	250	200	4.3
FTN3213 (200ML)		1000	25	45	350	305	9.5
0-85-1	80	500	5	235	240	5	3.6
FTN3213 (200ML)		1000	5	250	258	8	3.4

STATIC FOAM TEST
VARIABLE AIR FLOW
DIFFUSER 13/16" SPARGER
(5 um PORE SIZE)

SAMPLE No.	TEST TEMP C	AIRFLOW cc/min	ABRATTION TIME @ AIRFLOW min.	VOLUME			FOAM COLLAPSE TIME sec.
				OIL ml	OIL & FOAM ml	FOAM ml	
O-90-6	80	500	10	235	240	5	3.4
FTM3213	(200ML)	1000	20	246	254	8	3.4
O-85-2	80	500	5	36	40	4	
MINI TEST	(25ml)	1000	15	26	44	18	2.9
TEL-90104	80	500	5	40	46	6	2
MINI TEST	(25ml)	1000	15	42	50	8	2.4
O-86-2	80	500	5	226	232	6	2
FTM3213	(200ML)	1000	15	235	243	8	2
O-85-1	80	500	5	38	44	6	
MINI TEST	(25ml)	1000	15	40	48	8	2.2
O-90-6	80	500	5	38	43	5	
MINI TEST	(25ml)	1000	15	42	48	6	2.3
TEL-91002	80	500	15	238	243	5	
FTM3213	(200ml)	1000	10	252	261	9	10.1
TEL-91002	80	500	15	35	44	9	
MINI TEST	(25ml)	1000	10	40	46	6	3
TEL-91001		500	20	41	50	9	2
ASTM STONE	(25ml)	1000	5	N/A	68	49	3.5
O-91-13		500	5	36.5	42.1	5.6	1.5
MINI TEST	(25ml)	1000	5	40	48	8	1.9

APPENDIX B

IMPROVING SAMPLE INTRODUCTION FOR TOTAL WEAR METAL DETERMINATION BY ATOMIC EMISSION SPECTROSCOPY

1. INTRODUCTION

Among the diagnostic techniques used in monitoring the level of metallic contamination in used engine oils, spectrometric oil analysis (SOA) has been the most commonly used. Since its application in the early 1940's, considerable cost savings have been achieved in reducing maintenance and repairs and improving machine operational reliabilities for both industry and U.S. military. The rotating disk atomic emission (RDE) spectrometer is an analytical technique used primarily in SOA. This technique has limitations in providing accurate metal content and analyzing wear metal particles.⁴⁷ Previous work⁴⁸⁻⁵¹ has shown that the RDE analytical capability can be improved by modifying its sample introduction system. Our previous paper on improving the wear metal detection of SOA⁵² has dealt with developing a sample introduction system that would ensure total transport of all the metallic wear debris to the source and eliminate matrix interference. Modification of the electrode surface geometry and increasing the electrode surface density have improved the spectrometer particle detection.

In this work, the RDE parameters were optimized using the modified electrode geometry and surface density. A reliable ashing technique was developed to improve repeatability and accuracy. Used oil samples containing real metallic wear debris were analyzed and comparative data were established to illustrate the improved capability of this technique in detecting wear.

2. EXPERIMENTAL

a. Instrumentation

The atomic emission spectrometer used in this study utilizes an RF discharge AC spark excitation source, and a collimating lens installed in the optical path between the analytical gap and the entrance slit to condense the light reaching the entrance slit. The rotating disk electrode (RDE) determinations were made using medium density graphite disks and rods (density = 1.75 g/cc). The reversible polarity pin stand electrodes (PSE) were also medium density graphite, with the top (counter) electrodes having a geometry cut to a 160° angle. The bottom electrode tips were carved into a variety of cup-like shapes using an in-house fabricated sharpener which utilized bits of various dimensions.⁵²

b. Procedure

The sample electrodes were coated with paraffin wax and air dried before pipetting the oil standards and samples onto the surface. Following application of the oil, the electrodes were placed in the pre-heated chamber of a commercially available residue tester⁵³ for ashing of the lubricant matrix. The tester allows selection of ash times and chamber purge gases. After ashing, the PSE electrodes were placed in a desiccator to cool for subsequent analysis. Analyses of the samples containing particles were accomplished under the following conditions:

Spectrometer Parameters

Spark Intensity:	90%
Electrode Gap Setting:	3 mm
Bottom Electrode (Cup-Tip):	0.82 mm Deep
Argon Flow:	2 L/min
Exposure Time:	20 s
Preburn Time:	0 s
Exhaust Setting:	15 SCF/h

Ashing Parameters

Ashing Temperature:	450°C
Ashing Gas:	Air
Ashing Time:	6 min
Sample Size:	5 μL

c. Standards and Samples

The standards used in this study were prepared from organo-metallic (aryl alkyl sulfonate concentrates) by diluting with ester based gas turbine engine lubricating oil to the desired concentration. Dry iron powder (0-45 microns) was sized using a sonic sifter and then suspended in ester oil at the desired concentration. Wear metal generated from a pin-on-disk wear test²¹ was isolated from the test lubricant by diluting with petroleum ether, centrifuging and decanting the liquid layer repeatedly. After the solvent was allowed to evaporate, the wear metal was sized with the sonic sifter and resuspended in ester oil. Real used oil samples were obtained from operating jet engines and filtered through a 3-micron pore size filter.

To determine the actual iron concentration in the samples, flame atomic absorption-acid dissolution method⁵⁴ (ADM) and graphite furnace atomic absorption (Portable Wear Metal Analyzer or PWMA)⁵⁵ were used. The PWMA is a particle size independent technique which makes use of a small sample size in the range of less than one microliter to 100 microliters. Our previous work⁵⁶ indicated that the accuracy and repeatability of this technique suffers when nonhomogeneous samples like particles in oils are analyzed. Microliter size sampling makes it very difficult to obtain a representative aliquot of the sample. Nevertheless, the PWMA results are included to provide credence to the RDE and PSE methods.

3. RESULTS AND DISCUSSION

a. Optimization Techniques

In order to determine the linearity of the calibration curve produced by the PSE method, calibration standards were analyzed over the range of 0 to 100 ppm Fe, using 0.5 mm deep cup tip electrodes as described previously⁵² and actual concentration plotted against signal intensity to produce the

curve shown in Figure B-1. For comparison, Figure B-1 also shows the calibration curve produced from using the 0.82 mm deep cup tip. The signal intensity decreased significantly at concentrations greater than 80 ppm for the 0.5 mm. However, the same decrease was also observed for the 0.82 mm electrode but at a lesser magnitude. Knowing the linear dynamic range of atomic emission spectroscopy, this decrease is not totally understood. However, the large sample volume of 25 microliters coupled with the dynamic activity of the spark in the analytical gap where some of the analyte is blasted off could contribute to this decrease. The initial sample size employed for the preliminary work and for this curve was 25 microliters. The PSE method is very sensitive even at low concentrations due to direct detection of iron without sample matrix interference. The use of a collimating lens condensed emitted light on the entrance slit and provided increased repeatability of signal, and the effect of sample size on signal intensity was investigated. Sample sizes of 1 to 5 microliters produced larger emission signals than sample sizes of 10 microliters or larger. Figure B-2 shows that the emission signal increased with concentration for the 10, 20, 25 and 50 microliter sample sizes. However, these sample sizes were not optimum because the data clearly show smaller sizes of 1 to 5 microliters significantly enhance the signal. Reduced emission signals for larger sample volumes could be due to the sample boiling over during the ashing process. The data also show that signal increases with sample size in the range of 1 to 5 microliters. The signal for the 5 microliters is approximately four times that of the 1 microliter at the 100 ppm level. As little as 1 microliter of sample can produce a linear working curve up to 100 ppm. The 5 microliter size provided the optimum balance between signal intensity, linearity and repeatability, and was chosen for all subsequent

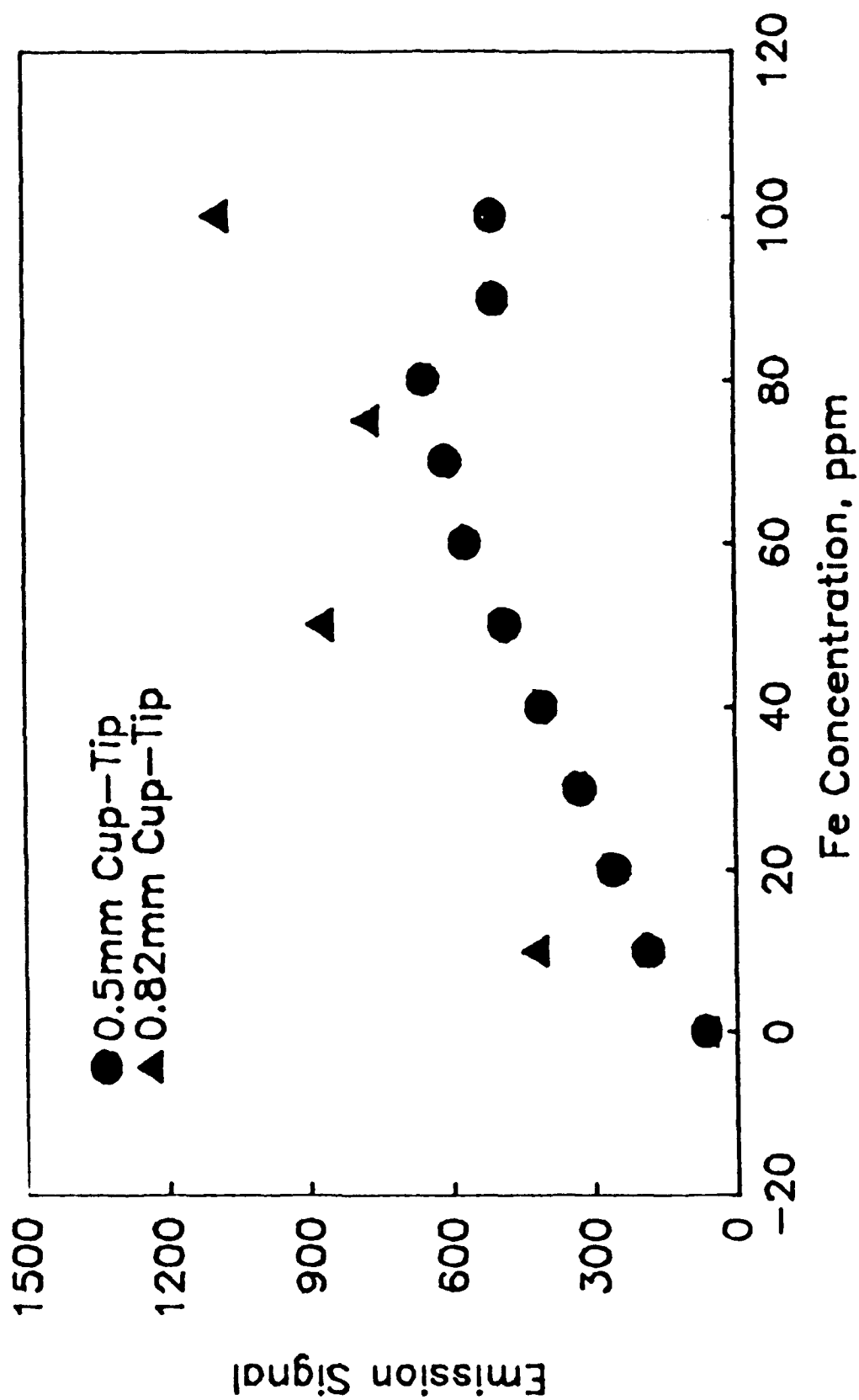


Figure B-1. Calibration Curve for Fe Using 25 μ L of Dissolved Organo-Metallic Single Element Standard, Ashing for 6 min. at 450°C in Air.

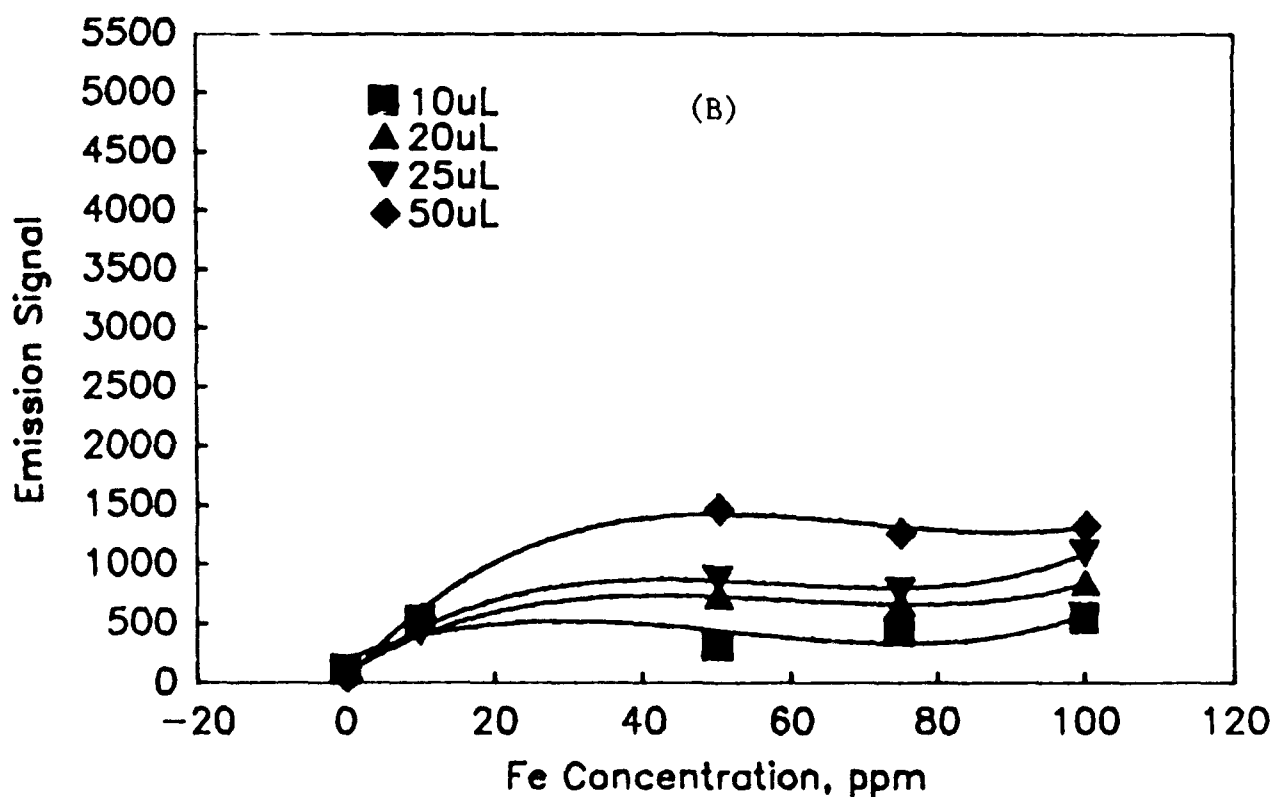
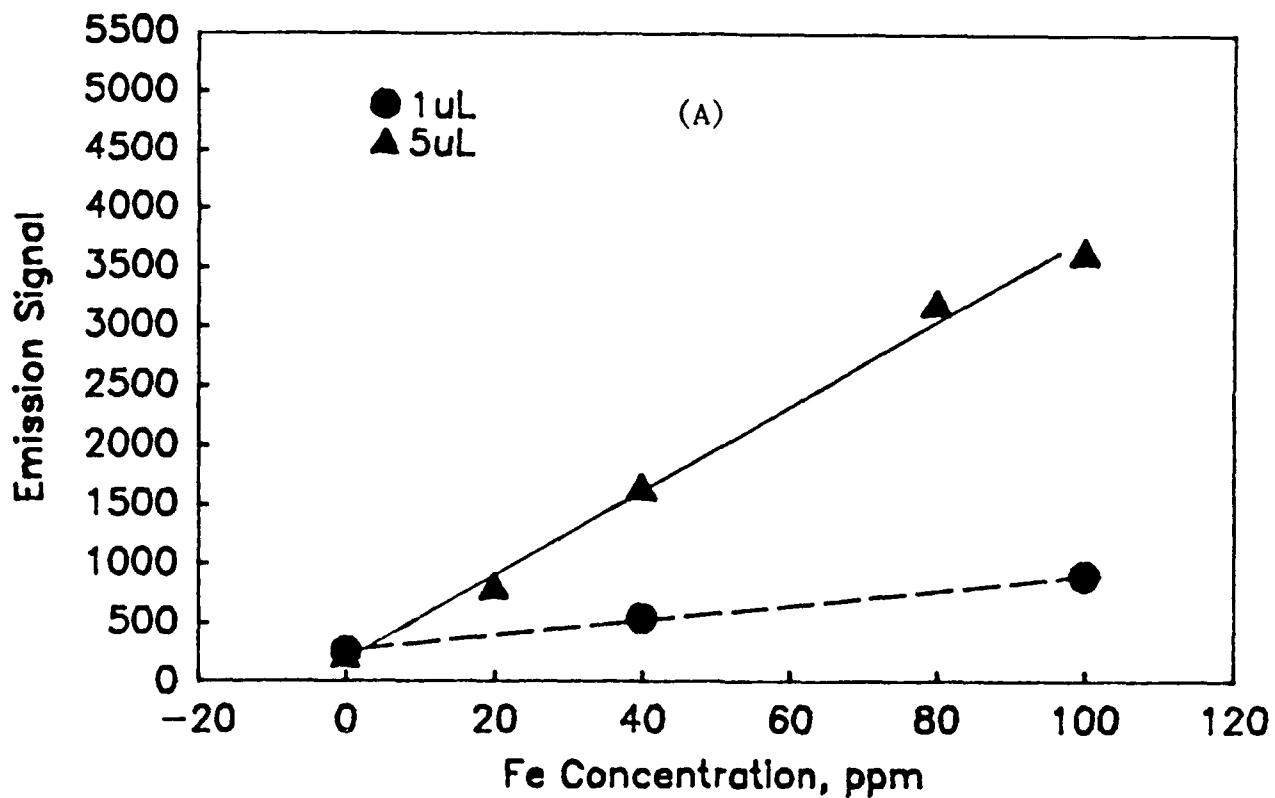


Figure B-2. Effect of Sample Size on Emission Signal at Various Concentrations of Fe Organo-Metallic Standard Using 0.82 mm Deep Cup-Tip Electrodes.

analyses.

The optimization of spark discharge rate, analytical gap distance, and exhaust flow yielded data showing a 90% spark, 3 mm gap, and 15 SCF/hour exhaust rate to be best for this type of analysis. The various conditions investigated are shown in Table B-1. Higher spark intensity (95%) was tried previously⁵² but 90% seems to be optimum for this work.

In employing a sensitive analysis method such as PSE, care must be taken to avoid any source of contamination and/or any variation in the ashing procedure. These two factors can greatly influence the results and therefore the use of a commercial residue tester greatly enhanced the repeatability of the results. The use of a standard muffle furnace resulted in temperature variations within the furnace and heat loss due to insertion and removal of the samples. Using the residue tester, the temperature program was selected to ramp to 450°C and dwell for 6 minutes, which was found to be adequate for ashing the oil matrix. Either air or argon can be used to ash the samples, and as shown in Figure B-3, ashing under air yields the best calibration curve.

The final parameter to be optimized was the configuration of the bottom electrode which contains the sample. Earlier work⁵² had shown a "cup-tip" configuration provided the best signal. This is due to the small rise in the center which attracts the spark and directs the sparking action toward the center. Table B-2 shows how certain configurations differ in producing acceptable signal intensity response. Although the conical cut had shown promise, this shape produced poor repeatability ($\pm 25\%$) for the 100 ppm sample. Therefore, the 0.82 mm deep cut electrode was chosen and employed for the study of detecting large particles in lubricating oil.

TABLE B-1

EFFECT OF SPARK DISCHARGE INTENSITY, ANALYTICAL GAP
DISTANCE AND EXHAUST FLOW FOR 100 PPM FE STANDARD

Emission Signal	Spark Intensity (%)	Gap (mm)	Exhaust Damper (SCF/H)
1342	90	2	30
2494 + 17%*	90	3	30
1296	90	4	30
1270	90	6	30
2644 + 0.08 %*	90	3	15
2638 + 12.4%*	90	3	10
1208	85	3	30
1257	82	3	30

*Ashed using residue tester in air

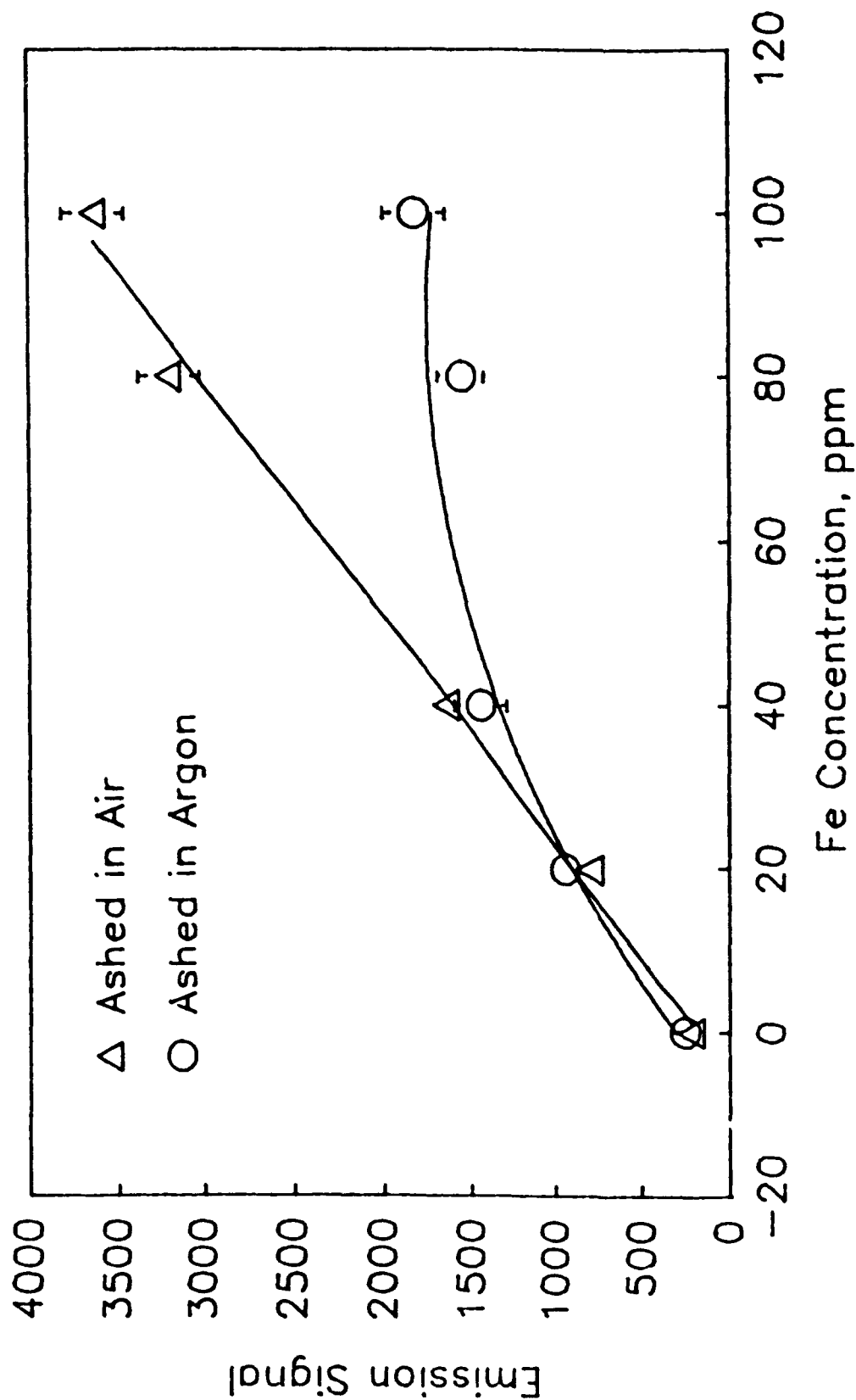


Figure B-3. Effect of Ashing in Air Versus Argon on Emission Intensity for Fe Organo-Metallic Standards Using 0.82 mm Cup-Tip Electrodes.

TABLE B-2

EFFECT OF BOTTOM ELECTRODE GEOMETRY
ON SIGNAL INTENSITY USING 5 μ L SAMPLES

Sample	Configuration					
	0.5 mm Regular Cup-Tip	0.82 mm Deep Cup-Tip	0.5 mm Cup (No Tip)	Conical Cut	0.005" Shallow Cup	Ultra Carbon
0	256	215	-	265	265	-
10	-	-	780	-	-	-
20	-	793	-	-	-	-
40	1600	1639 (1862)	-	1574	902	2178
50	-	-	2393	-	-	-
75	-	-	1898	-	-	-
80	2445	3195	-	-	-	-
100	3088	3632	1685	5042	1598	3117
MFR-2-A-1, 10 μ m (26 ppm)	-	768 (1057)	-	1035	817	956

b. Analysis of Particles in Oil

The only optimization parameter investigated extensively using particles was that of exposure time. This is an important feature of the analysis because the sparking action must be of sufficient duration to vaporize all the metallic particles in the analytical gap for efficient excitation of the elements. Figure B-4 shows the effect of exposure time on the emission signal using various sizes of Fe powder. Error bars from replicate analyses were determined only for the 20 second burn time. Considering the magnitude of the error involved, it is clearly shown that the 20 second burn time is sufficient and no improvement in the signal is realized if exposure times longer than 20 seconds were used. Furthermore, our previous work⁵² showed that even a 10 second burn time was sufficient for the analysis of the same size particles. After each burn, the electrodes were burned a second time to assure that complete vaporization of the metal had occurred.

c. Iron Powder Suspensions

The results of the iron powder suspensions are shown in Table B-3. The basestock oil, trimethylolpropane triheptanoate, is of very low viscosity and high volatility, and during the RDE analysis the fluid was vaporized by the heat before it could actually be delivered to the analytical gap. The formulated MIL-L-7808 oil did not exhibit this problem and was easily picked up by the rotating disk. The PSE method allows direct deposition of sample on the electrode and therefore delivery to the sparking zone is not limited by the viscosity or hindered by volatility. However, the detection of smaller particles (0-5 and 5-10 microns) was not as efficient as that of the larger particles. Two factors influencing efficiency are particle size and concentration. The PSE method detected 30-40% of the large particles and

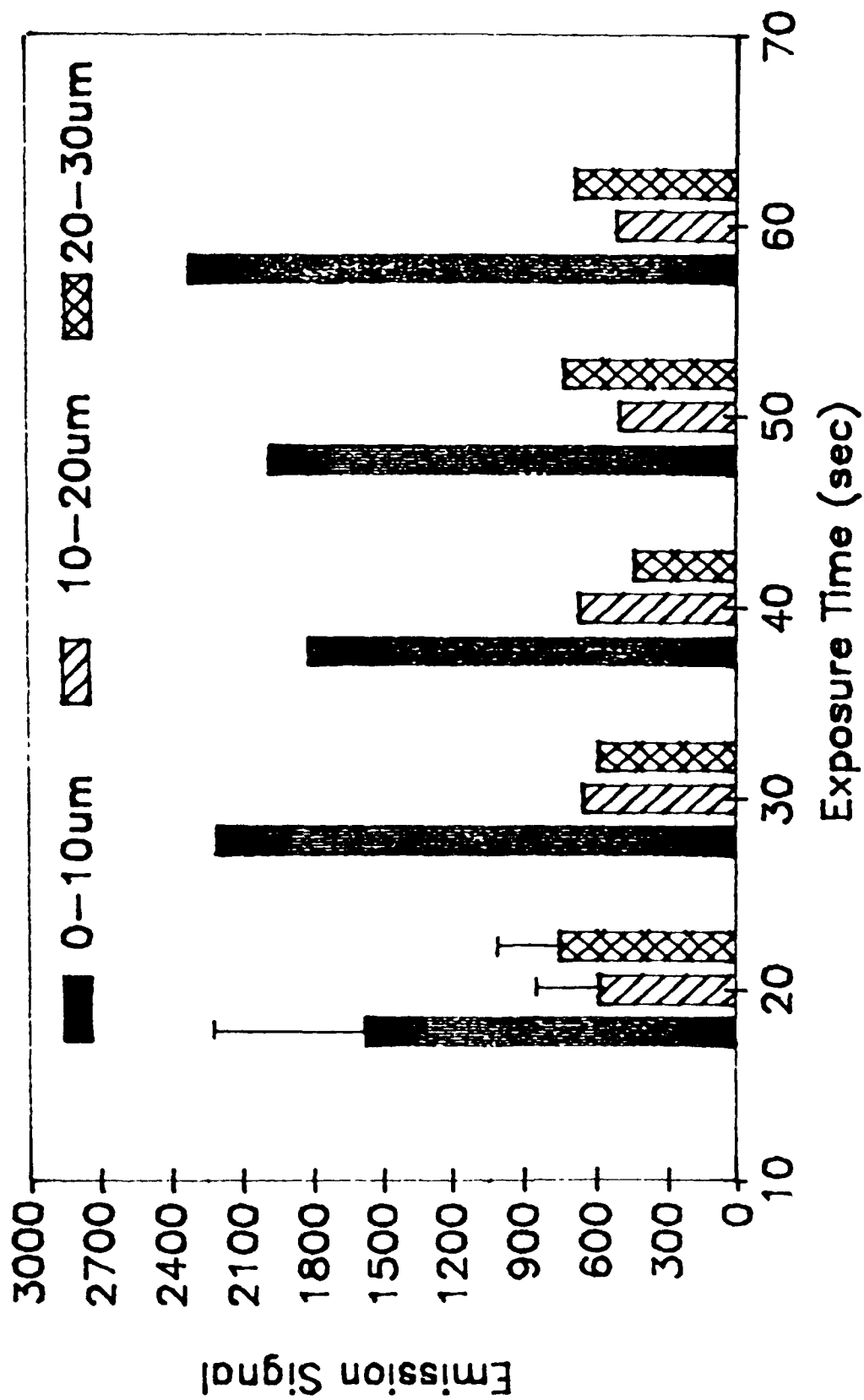


Figure B-4. Effect of Exposure Time on Particle Analysis Using Various Sizes of Fe Powder.

TABLE B-3

COMPARISON OF FE SIGNAL INTENSITY
USING RDE VERSUS PSE METHOD

	Signal Intensity	
	RDE	PSE
Air Force Mineral Oil Stds.		
0 ppm	165	ND *
3 ppm	226	ND
50 ppm	1062	ND
100 ppm	1860	ND
MIL-L-7808/Conostan Stds.		
0 ppm	156	252
20 ppm	1252	1355
40 ppm	2436	2133
70 ppm	4078	2752
90 ppm	ND	4328
	(r = 0.9999)	(r = 0.9802)
Iron Powder/TMP		
0-5 μ m (40 ppm) ***	152 (0) **	517 (5) **
5-10 μ m (30 ppm)	152 (0)	462 (4)
10-20 μ m (10 ppm)	148 (0)	412 (3)
20-30 μ m (10 ppm)	ND	446 (4)
Wear Metal/MIL-L-7808		
0-10 μ m (11 ppm)	292 (3)	624 (8)
10-20 μ m (6 ppm)	184 (1)	416 (3)
20-30 μ m (9 ppm)	173 (0.4)	421 (3)
0-10 μ m (81 ppm)	1305 (20)	1678 (33)
10-20 μ m (41 ppm)	372 (4)	742 (11)
20-30 μ m (62 ppm)	353 (4)	902 (14)

*ND = Not Determined

**ppm Based on calibration curve

***Actual ppm based on AA-ADM or PWMA

only 13% of the total small particle concentration, but the large particle concentration was one fourth to one third less than that of the small particle concentration. It is expected that higher concentrations (> 20 ppm) of large particles would be detected less efficiently by PSE than lower ones (< 20 ppm). Traditionally, this concentration effect has not been seen using RDE; however, the particle size limitation of RDE has been well documented.⁴⁷⁻⁵¹

d. Wear Metal Suspensions

The wear metal suspensions studied at two concentration levels and three particle size levels also show a dependence on concentration and particle size for increased detection efficiency (Table B-3). For RDE, the lower concentration samples of smaller particle size (0-10 microns) yielded a 27% efficiency of detection and that of larger particles (10-20 and 20-30 microns), yielded a 17% and 4% efficiency of detection, respectively. At higher concentrations the PDE efficiency was 25% for 0-10 micron particles and 10% and 6% for 10-20 micron and 20-30 micron particles, respectively. In comparison, for low Fe concentration, the PSE method detected 72% of the smaller particles, 50% at the 10-20 micron size and 33% at the 20-30 micron size. For higher concentrations, PSE detected 41% of the smaller particles. Whereas RDE is very efficient in detecting small particles, PSE shows greater efficiency in detecting larger particles. Although this greater efficiency is hampered by increasing element concentration, PSE still detected 27% of the 10-20 micron particles, and 23% of the 20-30 micron particles.

e. Actual Operating Engine Wear Samples

To demonstrate the potential of the PSE method for detecting large wear particles that may be missed by RDE, several field samples were obtained and a portion filtered through a three-micron rated pore size filter. The -1

suffix designates a pre-filtered sample and -2 denotes the post filtered sample. Table B-4 shows the actual concentrations by AA-ADM and the comparative PWMA, PSE and RDE values. The PWMA data are included because PWMA analyzes a small size sample and makes use of a graphite surface for analysis similar to the PSE technique. Our previous work⁵⁶ showed that the graphite furnace technique is particle size independent and should give results similar to the ADM technique. The PWMA results are, in general, comparable to the ADM except for samples having particles < 3 microns which is due primarily to a sampling problem mentioned in the Experimental Section. For those samples having an actual concentration of 10 ppm or less, PSE equaled or exceeded the efficiency of RDE by as much as 26-67%. For the sample containing the largest wear particles (MFR-4-A-1 = 56% above 3 microns), PSE detected 72% of the iron and RDE detected only 22%. For the MFR-2-A-1 and A-2 samples which contained extremely fine wear (41-67% one micron) RDE detected 54-77% of the iron and PSE only detected 32 to 61% of the iron. These data indicate that the PSE technique is more advantageous specifically for large wear and does not necessarily result in better detection when dealing with extremely small particles (as in normal wear). However, most abnormally operating engines would be expected to contain a mixture of normal, small rubbing wear and abnormal, large cutting and severe wear which RDE can only partially detect.

4. CONCLUSIONS

1. Even though PSE is not suited as a routine analytical technique at its early stages of development, it offers increased efficiency of detection when dealing with large particles, especially at lower concentrations.
2. At high concentrations, PSE loses efficiency but still is superior to RDE in detecting abnormal wear.

TABLE B-4

RESULTS OBTAINED BY AA-ADM AND PWMA SHOWING
IMPROVED PARTICLE DETECTION OF LARGE PARTICLES
USING PSE VERSUS RDE TECHNIQUE FOR
ACTUAL OPERATING ENGINE SAMPLES

Sample	PPM Fe			
	RDE	PSE	PWMA	AA-ADM
MFR-2-A-1				
(8 μm)	35	16	32	50
(5 μm)	31	15	31	46
MFR-2-A-2				
(10 μm)	20	16	33	26
(3 μm)	15	11	38	28
MFR-4-A-1	7	23	40	32
MFR-4-A-2	0	2	2	1
MFR-6-A-1	5	10	10	9
MFR-6-A-2	4	5	5	7
MFR-10-A-1	2	5	3	3
MFR-10-A-2	1	3	2	1
MFR-18-A-1	3	6	2	6
MFR-18-A-2	1	4	1	3

3. PSE has the disadvantage of being more time consuming and requiring more equipment (i.e., ash tester), but the procedure could be modified to allow "in situ" ashing of the sample matrix, eliminating the 6 minutes ash time.
4. When monitoring an oil for abnormal wear, PSE is very sensitive to trend changes as is RDE, but offers the increased particle detection capability necessary to determine problems indicated by the production of large wear particles.

APPENDIX C

DETERMINATION OF THE ALPHA PARAMETER BY THE LOWER BALL WEAR SCAR

1. INTRODUCTION

In Section VI.3., a four-ball wear model was developed to calculate scar wear volumes on all of the specimens in a four-ball test. The calculation is based on an approximated surface profile of the wear surfaces perpendicular to the wear tracks of the scar. Since the lower ball surfaces match the upper ball surface, an approximate scar profile applies to all of the test specimens. The weighting function, alpha, predicts the scar profile and can be calculated from the scar length (chord length) and the scar width. As seen in Figures 102 and 151 the shapes of lower ball wear scars vary tremendously, and the widest points of some scars are not at the mid-point of the chord length. By characterizing a scar only by the largest distance across its width, no distinction can be made between an odd shaped scar such as in Figure 151 from a simpler geometric form such as a circle or an ellipse. In order to be able to quantify the dimensions of lower ball wear scars, a procedure for measuring a scar width at various points along its chord length was developed in order to transform unusual scar shapes into an ellipse of equivalent area. With the simplified geometry of an ellipse, the elliptical width is the equivalent width of the original scar shape and can be used to calculate alpha.

2. DETERMINING THE ELLIPTICAL WIDTH

The profile of a lower ball scar can be quite rough (Figure 109), and if there is substantial variation in the roughness along the chord length, unusual scar shapes are formed. In order to approximate the profile parameter, alpha, from the scar shape, an appropriate scar width must be

determined. Figure C-1 shows the evolution of an unusual scar geometry into an ellipse whose width is an average of the widths at distinct points around the original scar. The individual equivalent widths are calculated by taking the equation of an ellipse:

$$\frac{x^2}{(\frac{w}{2})^2} + \frac{y^2}{(\frac{c}{2})^2} = 1 \quad C1$$

and solving it in terms of the width (see Figure C-2).

$$W = \frac{2cX}{\sqrt{c^2 - 4Y^2}} \quad C2$$

Widths are measured on the scar at various distances along the chord as shown in Figure C-3. These lengths (x_i for width and y_i for chord position) are then converted into coordinates, X and Y, to correspond to Equations C1 and C2. The equivalent elliptical width for the scar is then averaged from the individual equivalent widths:

$$\bar{W} = \sum_{i=1}^N \frac{w_i}{N} \quad C3$$

where N is the number of points measured (N = 5 for the scar of Figure C-3).

The points at which the individual equivalent widths are calculated do not have to be chosen at random. A scar can easily be divided into various sections, and the measurements that are taken in each section depend upon the section shape. Figure C-4 shows five common types of sections. The first two, (a) and (b), are the relatively smooth upper and lower portions of the scar. One measurement is taken at the open end of this type of section. The closed ends are uniquely determined by the chord. The next section, (c), has straight edges and two elliptical widths are calculated, one at the lower end of the section and one at the upper end of the section. The last two sections, (d) and (e), have curved edges, one in which the edge has an

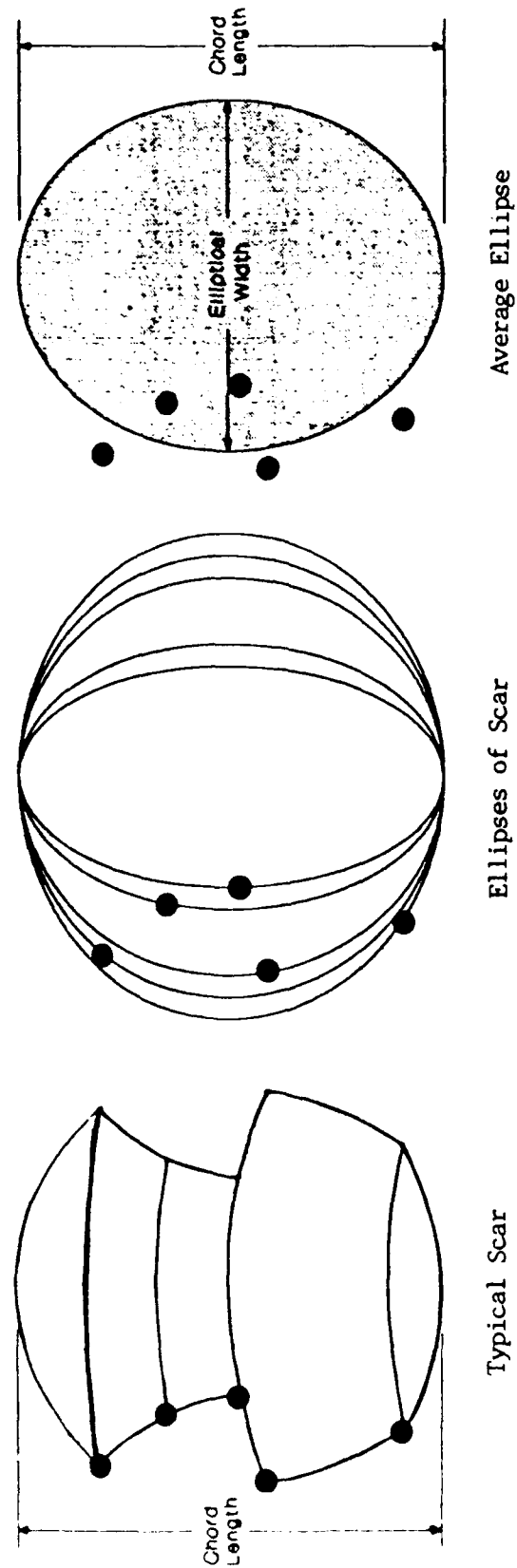
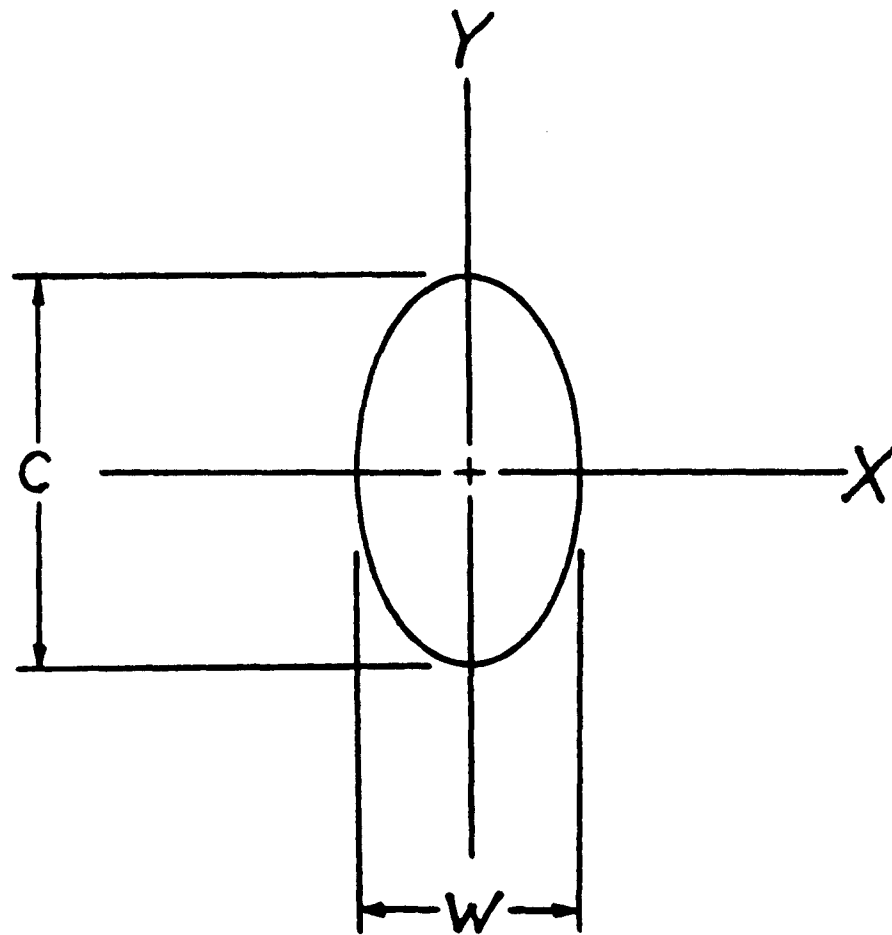


Figure C-1. Evolution of a Lower Ball Wear Scar into an Equivalent Ellipse



$$\frac{X^2}{\left(\frac{W}{2}\right)^2} + \frac{Y^2}{\left(\frac{C}{2}\right)^2} = 1$$

$$W = \frac{2cX}{\sqrt{c^2 - 4Y^2}}$$

Figure C-2. Equation of an Ellipse Solved in Terms of Width

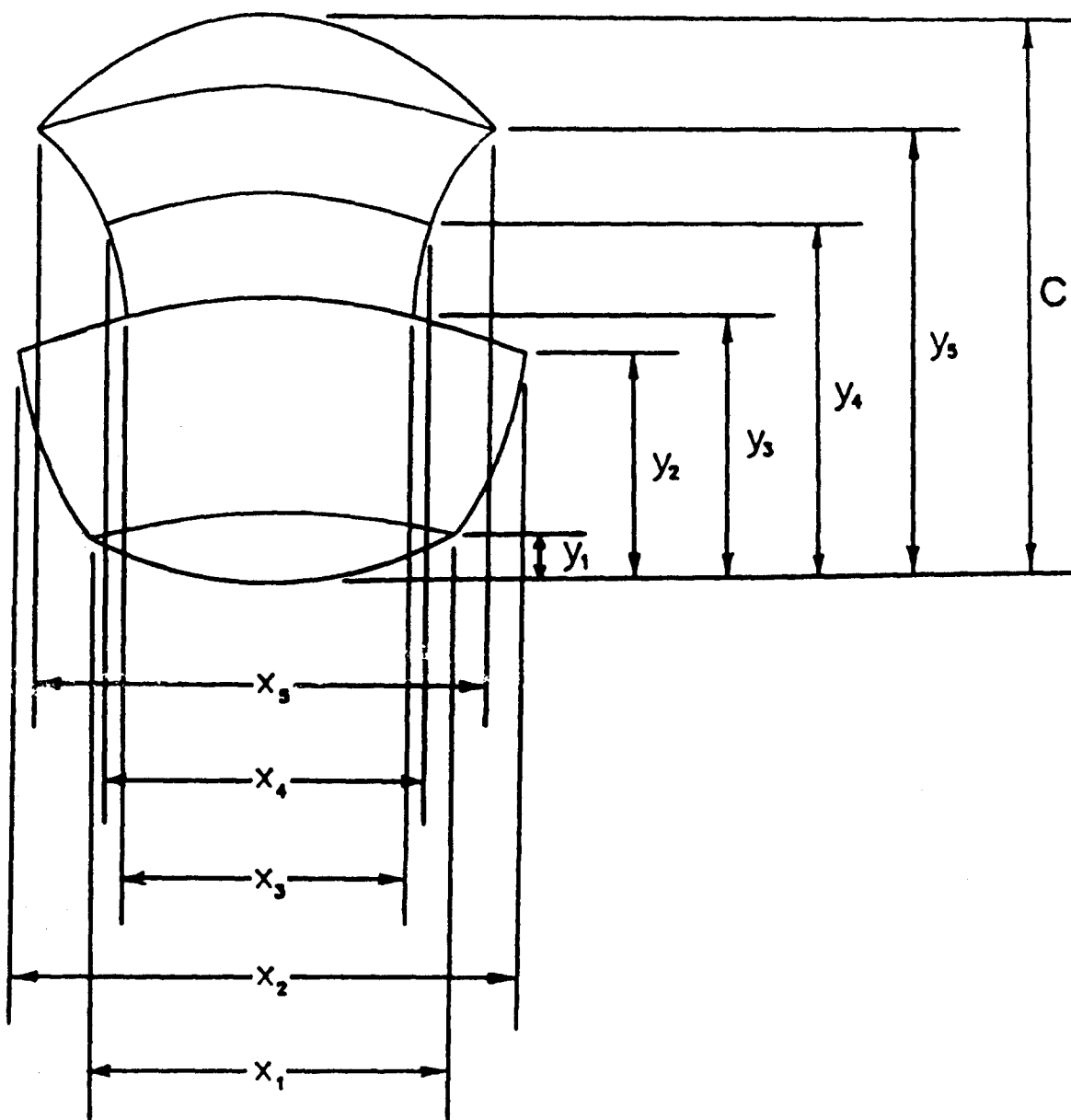
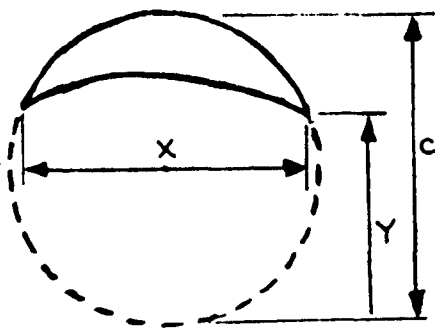
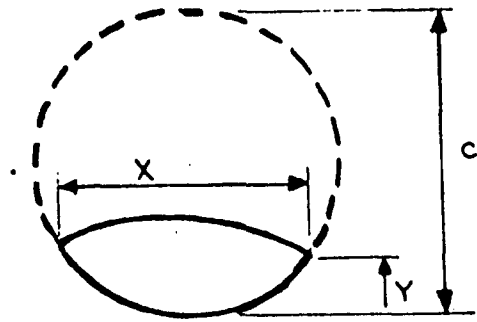


Figure C-3. Width and Length Measurements (x_i, y_i) Taken on an Odd-Shaped Lower Ball Wear Scar



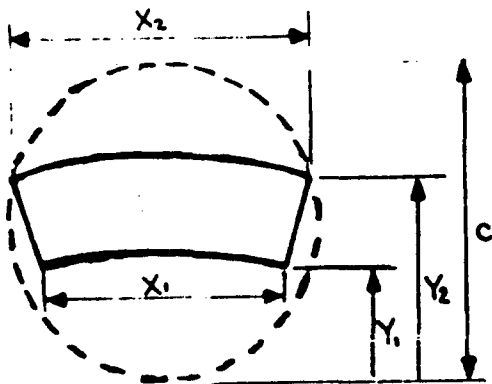
Top Cap

(a)



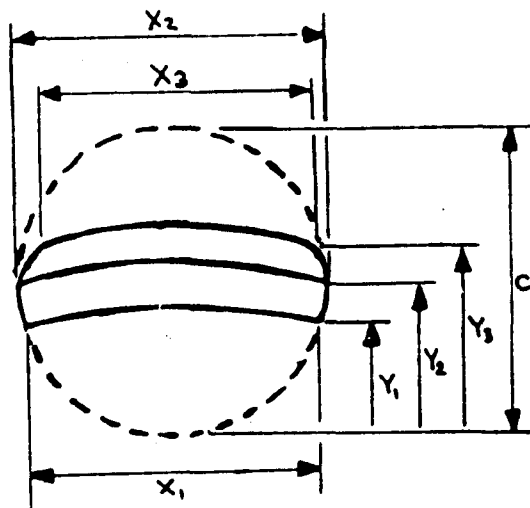
Bottom Cap

(b)



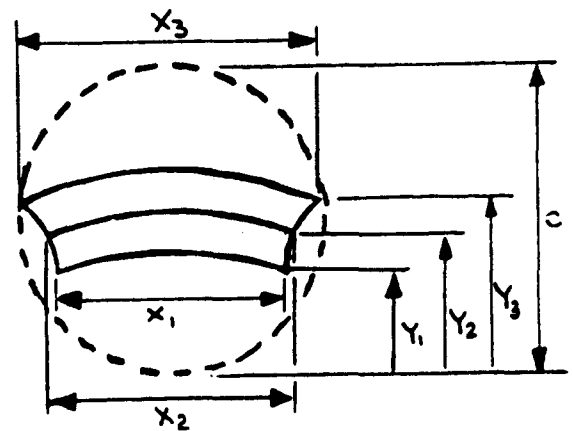
Flat Edge

(c)



Outward Edge Curvature

(d)



Inward Edge Curvature

(e)

Figure C-4. Measurements Taken on Various Scar Sections

outward curvature and one in which the edge has an inward curvature. Three sets of coordinates are taken in these types of sections. Measurements are made at the upper and lower ends of the section and at some distinct point (i.e. maximum or minimum) between the section ends. The average of the elliptical widths from each section results in an ellipse with a semi-major axis equal to $c/2$ and a semi-minor axis equal to $w/2$. This equivalent ellipse is used to approximate the scar shape.

3. CALCULATION OF ALPHA FROM CHORD LENGTH AND ELLIPTICAL WIDTH

a. The Gamma Parameter

The scar equation developed in Section VI.3 d. (Equation 8) can be rewritten from the form:

$$\left(x - \frac{ah}{2\alpha-1}\right)^2 + \left(y - \frac{ak}{2\alpha-1}\right)^2 = R^2 - \left(1 - \frac{\alpha}{2\alpha-1}\right)\left(\frac{ah^2}{2\alpha-1} + \frac{ak^2}{2\alpha-1}\right) \quad C4$$

to a condensed version:

$$(x - \gamma h)^2 + (y - \gamma k)^2 = R^2 - \gamma(1 - \gamma)(h^2 + k^2) \quad C5$$

where γ is defined as:

$$\gamma = \frac{\alpha}{2\alpha - 1} \quad C6$$

Referring to Figure 110, gamma is a measure of the distance from the center of the scar equation to the center of the lower ball. Where alpha is a dimensionless profile parameter, gamma is a dimensionless radius of curvature parameter. When $\alpha = 1$, $\gamma = 1$, and the radius of curvature of the scar equation is the radius of the top ball. When $\alpha = 0$, $\gamma = 0$, and the radius of curvature corresponds to the radius of the bottom ball. At $\alpha = 0.5$, the radius of curvature is infinitely long because the scar profile is a plane, and $\gamma = \infty$. Solving Equation C5 in terms of gamma gives:

$$\gamma = \frac{R^2 - x^2 - y^2}{h(h - 2x) + k(k - 2y)} \quad C7$$

b. Locating a Point on the Scar Profile

The gamma parameter of Equation C6 can be solved by finding the x-y coordinates of one point along the scar surface. Since an elliptical width can be calculated to approximate the scar shape, the x-y coordinates can be conveniently chosen to correspond to a width measurement taken half-way along the scar chord. Let point q be located on the scar surface at the same y-coordinate as a point mid-way along the scar chord (see Figure 110). The y-coordinate at q, y_c , is the average of the y-coordinates of points p1 and p2:

$$y_c = \frac{1}{2}(y_1 + y_2) \quad C8$$

or

$$y_c = \frac{k}{2} \quad C9$$

A second description of the upper ball surface can now be defined in the x-z plane at this y-coordinate. This plane will be referred to as the plane of rotation, and the following relationship defines the distance from the scar surface to the center of rotation of the top ball:

$$(x - h)^2 + z^2 = r_t^2 \quad C10$$

where r_t is a function of y. An expression for the x-coordinate at q, x_c , can be derived from the x-z plane of Figure 110:

$$x_c = h - r_t \quad C11$$

To solve for x_c , the unknown radius, r_t , must be calculated. To do

so, recall that the equation of the lower ball surface is given by:

$$x^2 + y^2 + z^2 = R^2 \quad C12$$

and at y_c , the equation can be expressed as:

$$x^2 + z^2 = R^2 - \left(\frac{k}{2}\right)^2 \quad C13$$

The coordinates at points p3 and p4 correspond to the endpoints of the elliptical width, w. By using the coordinates of p3 (which lies both on the lower ball surface and on the plane of rotation), a second equation may be generated which allows r_t to be calculated. Since the distance from p3 to p4 is w, the z-coordinate at p3 is:

$$z_3 = \frac{w}{2} \quad C14$$

Solving for x_3 by substituting z_3 into Equation C13 gives:

$$x_3 = \sqrt{R^2 - \left(\frac{k}{2}\right)^2 - \left(\frac{w}{2}\right)^2} \quad C15$$

Substituting this relation for x_3 into Equation C10 along with the value of z_3 :

$$\left[\sqrt{R^2 - \left(\frac{k}{2}\right)^2 - \left(\frac{w}{2}\right)^2} - h\right]^2 + \left(\frac{w}{2}\right)^2 = r_t^2 \quad C16$$

and

$$r_t = \sqrt{\left[\sqrt{R^2 - \left(\frac{k}{2}\right)^2 - \left(\frac{w}{2}\right)^2} - h\right]^2 + \left(\frac{w}{2}\right)^2} \quad C17$$

Finally, Equation C17 can be used along with Equation C11 to determine x_c :

$$x_c = h - \sqrt{\left[\sqrt{R^2 - \left(\frac{k}{2}\right)^2 - \left(\frac{w}{2}\right)^2} - h\right]^2 + \left(\frac{w}{2}\right)^2} \quad C18$$

so that, in summation, the coordinates of point q are given by Equations C18

and C9.

c. Solving for the Alpha Parameter

The scar curvature is described by the x-y coordinates of a point q along the scar surface at $z = 0$. Now that the coordinates (x_c, y_c) of point q have been solved for, these values can be expressed solely in terms of the measured variables c and w (chord length and elliptical width) and the constants R and h (radius and horizontal position). In order to express the coordinates of q in terms of only known quantities, the relation between chord length and upper ball vertical position must be used. This relation (Equation 1 of Section VI.3.c.) can be manipulated into either the form:

$$R^2 - \left(\frac{k}{2}\right)^2 = \left(\frac{c}{2}\right)^2 + \left(\frac{h}{2}\right)^2 \quad C19$$

or

$$\frac{k}{2} = \sqrt{R^2 - \left(\frac{c}{2}\right)^2 - \left(\frac{h}{2}\right)^2} \quad C20$$

so that the coordinates of q in terms of c, w, h, and R are:

$$\left\{ h - \sqrt{\left[\sqrt{\left(\frac{c}{2}\right)^2 + \left(\frac{h}{2}\right)^2} - \left(\frac{w}{2}\right)^2 - h\right]^2 + \left(\frac{w}{2}\right)^2}, \sqrt{R^2 - \left(\frac{c}{2}\right)^2 - \left(\frac{h}{2}\right)^2} \right\} \quad C21$$

With (x_c, y_c) , the weighting function, gamma, can be calculated from Equation C7. With gamma, alpha can finally be calculated by manipulating Equation C6 into the form:

$$\alpha = \frac{\gamma}{2\gamma - 1} \quad C22$$

4. COMPARISON OF PROFILED AND CALCULATED ALPHA VALUES

The scar surfaces on 52100 balls from a series of tests run under the same conditions (1200 rpm, 145 N, and 150°C lubricated with O-67-1) at varying test times were profiled, and a curvature was approximated. From

this curvature, an alpha was calculated. The lower ball scars were also measured optically using the method described in Section 2. From the chord length and the equivalent elliptical width, alpha was determined. Table C-1 compares the profiled alpha values to the alpha values calculated from optical measurements.

Table C-1

PROFILED ALPHA PARAMETER COMPARED TO CALCULATED ALPHA PARAMETER FOR FOUR-BALL TESTS OF 0-67-1 ON 52100 BALLS AT 150°C (145 N, 1200 RPM)

Test	Duration (hours)	Profiled	Calculated	Error
368	0.5	0.957	0.866	-0.091
362	1.0	0.955	0.858	-0.097
366	1.5	0.815	0.773	-0.042
363	2.0	0.870	0.838	-0.032
367	2.5	0.702	0.664	-0.038
369	3.0	0.905	0.857	-0.048
393	5.0	0.823	0.739	-0.084
389	10.0	0.674	0.632	-0.042
357	20.0	0.692	0.783	+0.091

5. CONCLUSION

The error associated with the alpha values calculated from chord length and elliptical width varies for the different durations of the four-ball tests of the oil 0-67-1. A deviation from alpha of ± 0.050 is reasonable considering the approximating procedure for determining an equivalent elliptical width. Larger errors in estimating alpha adversely effect volume calculations (see Figure 115). The inconsistency of error for the tests chosen for this analysis can be explained at least partially by how the alpha values were chosen. The calculated alpha values are an average of the individual alpha values of the three lower balls of each test while the profiled alpha values were made on only a single lower ball of each test. Depending on which of the three balls of each test was profiled and the variation of the calculated alpha values for each lower ball set, the error

may either be greater or worse than the value given. Additionally, another error is introduced by the approximation of the scar curvature from the surface profiles so that the profiled alpha values are not necessarily correct.

In conclusion, the scar measuring procedure developed to predict the profile parameter, alpha, is a valid method for describing the scar surface. Furthermore, the difficulty in accurately approximating a curve fit through a wear scar profile makes the expedient method of determining alpha from the scar shape an attractive option. Unfortunately, both methods introduce an uncertainty into wear volume calculations.

REFERENCES

1. Saba, C.S., Smith, H.A., Keller, M.A., Jain, V.K. and Kauffman, R.E., "Lubricant Performance and Evaluation," Interim Technical Report AFWAL-TR-87-2025, DDC No. AD A183881, June 1987.
2. Saba, C.S., Smith, H.A., Keller, M.A., Kauffman, R.E. and Jain, V.K., "Lubricant Evaluation and Performance," Final Technical Report AFWAL-TR-89-2008, DDC No. AD A208925, April 1989.
3. Smith, H.A., Centers, P.W. and Craig, W.R., "Foaming Characteristics of MIL-L-7808 Turbine Lubricants," Report No. AFAPL-TR-75-91, November 1975.
4. Rhine, W.E., Saba, C.S., Kauffman, R.E., Brown, J.R. and Fair, P.S., "Evaluation of Plasma Source Spectrometers for the Air Force Oil Analysis Program," AFWAL TR-82-4017, February 1982.
5. Jones, Jr., W.R. and Lowenthal, S.H., "Analysis of Wear Debris from Full-Scale Bearing Fatigue Tests Using the Ferrograph," ASLE Trans., 24, p 323 (1980).
6. Arneson, M.C., Chambers, K.W., Smith, I.M. and Swiddle, J.E., "Probe for Determining the Concentration of Ferromagnetic Particles in Water at High Temperature and Pressure," Power Industry Research, 1, p 87 (1981).
7. Chambers, K.W. et al., "An Intelligent Sensor System for Equipment Health Monitoring of Ferromagnetic Wear Debris Concentration in Fluids," AGARD-CPP-448, Engine Condition Monitoring-Technology and Experience, 1988.
8. Campbell, P., "On-line Monitoring of Ferromagnetic Debris Concentration," Proceedings of the 44th Meeting of the Mechanical Failures Prevention Group, Virginia Beach, VA, April 3-5, 1990.
9. Westcott, V.C. and Seifert, W.W., "Investigation of Iron Content of Lubricating Oil Using a Ferrograph and an Emissions Spectrometer," Wear, 23, p 239 (1973).
10. Blumberg, W.E., Eisinger, J., Lamola, A.A. and Zuckerman, D.M., "Zinc Protoporphyrin Level in Blood Determined by a Portable Hematofluorometer: A Screening Device for Lead Poisoning," J. Lab. Clin. Med., 89, p 712 (1977).
11. Eisinger, J. and Flores, J. "Front-Face Fluorometry of Liquid Samples," Anal. Biochem., 94, p 15 (1979).

12. Keller, M.A. and Saba, C.S., "Monitoring of Ester Base Lubricants by Dielectric Constant," Lub. Eng., 45, pp 347-351 (1989).
13. Morgan, S.O., Trans. Am. Electrochem. Soc., 65, p 109 (1934).
14. Kauffman, R.E. and Rhine, W.E., "Development of a Remaining Useful Life of a Lubricant Evaluation Technique. Part I: Differential Scanning Calorimetric Techniques," Lub. Eng., 44, pp 154-161 (1988).
15. Martynova, N.V., Ermakova, N.G., Popova, L.A. and Dintses, A.I., "Rapid Method for Determination of Thermal-Oxidative Stability of Lubricating Oils," Translated from Khim. Teknol. Topliv Masel, 12, pp 44-46 (1972).
16. Lucas, P.C. and Porter, R.S., "Hydroperoxides from Phenyl Ring Reactions of Photo-oxidized Polystyrene," Polymer Degradation and Stability, 22, pp 175-184 (1988).
17. Kauffman, R.E., "Development of a Remaining Useful Life of a Lubricant Evaluation Technique. Part III: Cyclic Voltammetric Methods," Lub. Eng., 45, pp 709-716 (1989).
18. Doblhofer, K. and Armstrong, R.D., "Membrane-Type Coatings on Electrodes: A Review," Electrochimica Acta, 33, pp 453-460 (1988).
19. Reed, R.A., Geng, L. and Murray, R.W., "Solid State Voltammetry of Electroactive Solutes in Polyethylene Oxide Polymer Films on Microelectrodes," J. Electroanal. Chem., 208, pp 185-193 (1986).
20. Oldham, K.B., "Theory of Microelectrode Voltammetry Without Electrolyte," J. Electroanal. Chem., 250, pp 1-23 (1988).
21. Voitik, R.M. and Heerdt, L.R., "Wear and Friction Evaluation of Gear Lubricants by Bench Test," Lubri. Eng., 40, p 719 (1984).
22. Wright, M.S., Jain, V.K. and Saba, C.S., "Wear Rate Calculation in the Four-Ball Wear Test," Wear, 134, pp 321-334 (1989).
23. Bos, A., "Wear in the Four-Ball Apparatus: Relationship Between the Displacement of the Upper Ball and the Diameter of the Wear Scars on the Lower Balls," Wear, 41, pp. 191-194 (1977).
24. Feng, I. M., "A New Approach in Interpreting the Four-Ball Wear Results," Wear, 5, pp 275-288 (1962).
25. Willermet, P.A. and Kandah, S.K., "Wear Assymetry - A Comparison of the Wear Volumes of the Rotating and Stationary Balls in the Four-Ball Machine," ASLE Trans., 26, pp 173-178 (1983).
26. Boresi, A.P. and Sidebottom, O.M., Advanced Mechanics of Materials,

John Wiley and Sons, Inc., New York (1985), pp 602-608.

27. Bisson, E.E. and Anderson, W.J., Advanced Bearing Technology, NASA SP-38, Washington, D.C.(1964), page 322.
28. Jones, Jr., W.R., "Ferrogaphic Analysis of Wear Debris From Boundary Lubrication Experiments with a Five Ring Polyphenyl Ether," ASLE Trans., 18, pp 153-162 (1975).
29. Gong, D., Zhang, P. and Xue, Q., "Studies on Relationship Between Structure of Chlorine-Containing Compounds and Their Wear and Extreme-Pressure Behavior," Lub. Eng., 46, pp 566-572 (1990).
30. Munroe, R. G., "Temperature Considerations in the Study of Surfaces Using a Four-Ball Wear Apparatus," J. App. Phys., 57, pp. 4950-4953 (1985).
31. Hermance, H.W. and Egan, T.F., "Organic Deposits on Precious Metal Contacts " Bell System Tech. J., 27, pp 739-766 (1958).
32. Fein, R.S. and Kreuz, K.C., "Chemistry of Boundary Lubrication of Steel by Hydrocarbons," ASLE Trans., 8, pp 29-38 (1965).
33. Stinton, H.C., Spikes, H.A. and Cameron, A., "A Study of Friction Polymer Formation," ASLE Trans., 25, pp 355-360 (1982).
34. Glaeser, W.A., "The Nature of Wear Debris Generated During Lubricated Wear-in," ASLE Trans., 26, pp 517-522 (1983).
35. Goldblatt, I.L., "Model for Lubrication Behavior of Polynuclear Aromatics," Ind. Eng. Chem. Prod. Res. Develop., 10, pp 270-278 (1971).
36. Chaikin, S.W., "On Friction Polymer," Wear, 10, pp 49-60 (1967).
37. Campbell, W.E. and Lee, R.E., "Polymer Formation on Sliding Metals in Air Saturated with Organic Vapors," ASLE Trans., 5, pp 91-103 (1962).
38. Tabor, D. and Willis R.R., "The Formation of Silicone Polymer Films on Metal Surfaces at High Temperatures and Their Boundary Lubricating Properties," Wear, 13, pp 413-442 (1969).
39. Furey, M.J., "The Formation of Polymeric Films Directly on Rubbing Surfaces to Reduce Wear," Wear, 26, pp 369-392 (1973).
40. Furey, M.J., Kajdas, C., Ward, T.C. and Hellgeth, J.W., "Thermal and Catalytic Effects on Tribo-polymerization as a New Boundary Lubrication Mechanism," Wear, 136, pp 85-97 (1990).
41. Lauer, J.L. and Dwyer, S.R., "Continuous High Temperature Lubrication of Ceramics by Carbon Generated Catalytically,"

42. Graham, E.E. and Klaus, E.E., "Lubrication from the Vapor Phase at High Temperatures," ASLE Trans., 29, pp 229-234 (1986).
43. Spar, C. and Damasco, F., "High Temperature Fluid Lubrication," ASLE Trans., 7, pp 211-217 (1964).
44. Loomis, W.R., "Evaluation of Five Bearing-Separator Materials and Polyphenyl Ether Lubricants for use in Space Power Generation Systems," NASA-TN-D2663 (1965).
45. Kauffman, R.E., Saba, C.S., Rhine, W.E. and Eisentraut, K.J. "Quantitative Multielement Determination of Metallic Wear Species in Lubricating Oils and Hydraulic Fluids," Anal. Chem., 54, p 975 (1982).
46. Kauffman, R.E., Saba, C.S., Rhine, W.E. and Eisentraut, K.J., "Chemical Nature of Wear Debris," ASLE Trans., 28, p 400 (1985).
47. Eisentraut, K.J., Newman, R.W., Saba, C.S., Kauffman, R.E. and Rhine, W.E., "Spectrometric Oil Analysis," Anal. Chemistry, 56 (9), 1087A (1984).
48. Rhine, W.E., Saba, C.S. and Kauffman R.E., "Spectrometer Sensitivity Investigations on the Spectrometric Oil Analysis Program," NAEC-92-169, 22 April 1983.
49. Rhine, W.E., Saba, C.S. and Kauffman, R.E., "Metal Particle Detection Capabilities of Rotating-Disk Emission Spectrometers," Lubr. Eng. 42, (12) 755 (1986).
50. Kauffman, R.E., "Particle Size and Composition Analyses of Wear Debris Using Atomic Emission Spectrometry," Lubr. Eng., 45 (3), 147 (1989).
51. Kauffman, R.E., "Techniques to Improve the Wear Metal Detection Capabilities of Rotating-Disk Emission Spectrometers," Lubr. Eng., 46 (3), 173 (1990).
52. Saba, C.S., "Improving the Wear Metal Detection of Spectrometric Oil Analysis," Lubr. Eng., 46 (5), 310 (1990).
53. Bochartz, W., "Carbon Residue Studies with a Microcarbon Residue Tester," Lubr. Eng., 43 pp 473-478 (1987).
54. Kauffman, R.E., Saba, C.S. and Rhine, W.E., "Quantitative Multielement Determination of Metallic Wear Species in Lubrication Oils and Hydraulic Fluids," J. Anal. Chem., 54, pp 975-979 (1982).
55. Quinn, M.J., "New Device for Analysis of Metal Particles in Oil," Wear, 120, pp 369-381 (1987).

56. Saba, C.S., Rhine, W.E. and Eisentraut, K.J., "Determination of Wear Metals in Aircraft Lubricating Oils by Atomic Absorption Spectrometry Using a Graphite Furnace Atomizer," Applied Spectroscopy, 39 (4), 689 (1985).